Lecture Notes in Physics

328

G. Wegner (Ed.)

White Dwarfs

Proceedings of IAU Colloquium No. 114
Held at Dartmouth College, Hanover,
New Hampshire, USA, August 15–19, 1988

Springer-Verlag
Berlin Heidelberg New York London Paris Tokyo

Editor

Gary Wegner
Department of Physics and Astronomy
Dartmouth College, Wilder Laboratory
Hanover, NH 03755, USA

ISBN 3-540-51031-1 Springer-Verlag Berlin Heidelberg New York
ISBN 0-387-51031-1 Springer-Verlag New York Berlin Heidelberg

Printed in Germany

Printing: Druckhaus Beltz, Hemsbach/Bergstr.
Binding: J. Schäffer GmbH & Co. KG., Grünstadt
2158/3140-543210

FOREWORD

The colloquium on white dwarfs reported in this book was held at Dartmouth College 14 - 19 August 1988 and was jointly sponsored by Dartmouth College and the International Astronomical Union as IAU Colloquium Number 114. Over the years, there have been a number of international meetings devoted to white dwarfs, and the proceedings of such gatherings document the steady increase in our knowledge of these objects. Perhaps the beginning can be placed with the International Colloquium on Novae and White Dwarfs held in Paris in 1939 (Shaler 1941), followed by IAU Colloquium No. 42 (Luyten 1971) which took place in St. Andrews and IAU Colloquium No. 53 in Rochester (Van Horn & Weidemann 1979). There have been a number of other conferences on white dwarfs. These include the European Workshops beginning with the 1974 Kiel meeting, and the Delaware workshops, the first taking place in 1980. Numerous other meetings on related subjects such as faint blue stars and planetary nebulae have also taken place. Each meeting has been typified by the unusually good relations and comaraderie of the people who work on white dwarfs.

The Dartmouth meeting resulted from the Delaware workshop held in Montreal in June 1983 when I promised to host a meeting in Hanover. However, in early 1986 when I was planning it, Brian Warner suggested to me that another IAU colloquium on white dwarfs was due and that it would coincide nicely with the Baltimore General Assembly in 1988. The first step was to form a Scientific Organizing Committee and the following people kindly consented to serve as members: F. D'Antona (Italy), G. Fontaine (Canada), D. Koester (U. S. A.), J. Liebert (U. S. A.), J. Pringle (U. K.), G. Shaviv (Israel), H. M. Van Horn (U. S. A.), G. Vauclair (France), B. Warner (South Africa), R. Wehrse (F. R. G.), V. Weidemann (F. R. G.), and G. Wegner (U. S. A., Chairman).

Next, endorsement for the colloquium had to be obtained from commissions of the IAU. The present meeting was held with the sponsorship of the following IAU Commissions: 29 (Stellar Spectra), 35 (Stellar Constitution), and 36 (Theory of Stellar Atmospheres).

The Local Organizing Committee consisted of: F. I. Boley (Chairman), G. Wegner, R. K. McMahan, J. R. Thorstensen, and D. Mook. A number of other people worked very hard to make the meeting happen. Kay Wegner and Josef Wegner handled most of the details of the mailings, printing programs, finances, and organization of social activites. The Dartmouth Conference Center was responsible for the dormitory arrangements. Several others helped in ways crucial at the time: Steve Swanson, Ralph Gibson, Fred Ringwald, Robert Hamwey, May Suzuki,

Connie Elder, and Judy Lowell. Prof. John Cummins delivered the after dinner speech, "Ripples: A View from the Outside", which was enjoyed by all present at the banquet held at the Dartmouth Outing Club. The United States Park Service gave a special tour of the Saint Gaudens Historical Site for our delegates. We are most grateful to all of those named above for their efforts in our behalf.

Both the IAU and Dartmouth College provided financial support for this meeting. In this respect, we wish to acknowledge these organizations and in particular Associate Dean of Science P. Bruce Pipes of Dartmouth for his endorsement of the conference. As a result, the colloquium was attended by 115 registered participants from 17 nations and it was possible to give 18 persons partial support for either travel or local expenses. There were 44 oral papers given in Dartmouth's Cook Auditorium and 58 poster presentations, available for viewing during the week in Alumni Hall and discussed during the oral sessions. We are grateful for the following individuals who conducted valuable and insightful reviews of the posters: F. Wesemael (Canada), H. M. Van Horn (U. S. A.), K.-H. Böhm (U. S. A.) and B. Warner (South Africa).

The accompanying volume contains the numerous new and original contributions presented at IAU Colloquium No. 114. We are thankful to the firm of Springer-Verlag for undertaking to publish them. The amount of material exceeded our original expectations and consequently there were problems with keeping the book at a manageable size. As a result, we have not published the abstracts of some of the longer papers and have omitted the often lively discussions following the presentations also in the interest of conciceness. Nevertheless, it is hoped that none of the main parts of the material have become lost and that this volume will remain a reminder of a pleasant meeting and a tribute to all those people who have contributed to the field of white dwarfs.

Gary Wegner
Dartmouth College
December 5, 1988

TABLE OF CONTENTS

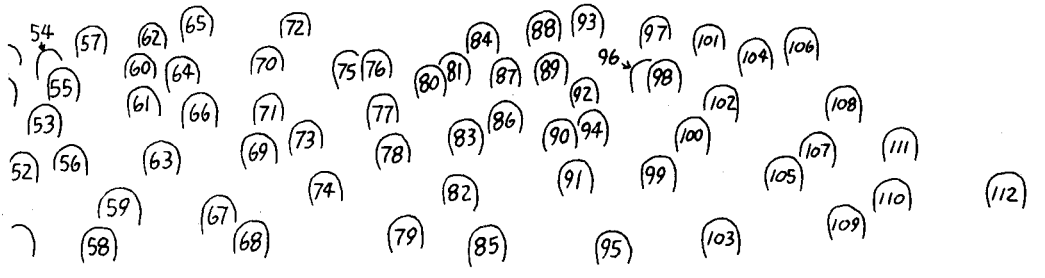

LIST OF PARTICIPANTS

(Numbers refer to above diagram)

Maria Arévalo - (Inst. Astro. Canarias, Spain) [33]
Martin Barstow - (University of Leicester, U.K.) [74]
Pierre Bergeron - (Univ. of Montréal, Canada) [64]
Willy Benz - (Harvard Univ., U.S.A.) [44]
G. Bisnovaty-Kogan (Space Research Inst., Acad.of Sci., U.S.S.R.) [1]
Karl-Heniz Böhm - (University of Washington, U.S.A.) [102]
Forrest Boley - (Dartmouth College, U.S.A.) [65]
Howard Bond - (Space Telescope Science Inst., U.S.A.) [3]
Paul Bradley - (University of Texas, U.S.A.) [87]
Angela Bragaglia- (Univ. of Bologna, Italy) [49]
Pierre Brassard - (Univ. of Montréal, Canada) [54]
Clyde Bryja - (Univ. of Minnesota, U.S.A.) [87]
Irmela Bues - (Univ. Erlangen-Nürnberg, F.R.G.) [27]
Gilles Chabrier - (Univ. of Rochester, U.S.A.) [57]
Pierre Chayer - (Univ. if Montréal, Canda) [50]
Chuck Claver - (Univ. of Texas, U.S.A.) [75]
J.C. Clemens - (Univ. of Texas, U.S.A.)
John Cummins - (Orange County Comm. College, U.S.A.) [26]
Conard C. Dahn - (U.S. Naval Observatory, U.S.A.) [66]
Francesca D'Antona - (Osservatorio Astronomico di Roma, Italy) [95]
Doris Daou - (Univ. of Montréal, Canada) [55]

Jean Dupuis - (Univ. of Montréal, Canada) [56]
E.V. Ergma - (Astro. Council, Academy of Sciences, U.S.S.R.) [15]
G.G. Fahlman (Univ. of British Columbia, Canada) [18]
Lilia Ferrario - (Australian National University, Australia) [34]
David Finley - (Univ. of California, Berkeley, U.S.A.) [106]
Gilles Fontaine - (University of Montréal, Canada) [88]
Diana Foss - (Steward Observatory, Univ. of Arizona, U.S.A.) [13]
Carl Fristrom - (Univ. of Delaware, U.S.A.) [16]
Jeanne Geczi - (Univ. of Delaware, U.S.A.) [9A]
C.V. Goodall - (Univ. of Manchester, U.K.) [63]
A.D. Grauer - (Univ. of Arkansas, U.S.A.) [111]
Laura Greggio - (Univ. of Bologna, Italy) [42]
Izumi Hachisu - (Keio University, Japan) [59]
Gordon Hammond - (Univ. of South Florida, U.S.A.) [48]
Robert Hamway - (Dartmouth College, U.S.A.)
John Heise - (Lab. for Space Research, Netherlands) [4]
Butler P. Hine - (NASA,Ames Research Center, U.S.A.) [76]
Ted von Hippel - (Univ. of Michigan, U.S.A.) [92]
J.B. Holberg - (Univ., of Arizona, U.S.A.) [10]
Icko Iben - (Univ. of Illinois, U.S.A.) [12]
Jordi Isern - (C.S.I.C., Spain) [110]
Naoki Itoh - (Sophia Univ., Japan) [40]
Stefan Jordan - (Univ. of Kiel, F.R.G.) [14]
Mariko Kato - (Keio University, Japan) [58]
Steven Kawaler - (Yale University, U.S.A.) [70]
S.O. Kepler - (Fed. Univ. of Rio Grande de Sol, Brazil) [94]
Ken Kidder - (L.P.L. Univ. of Arizona, U.S.A.) [20]
J. Davy Kirkpatrick - (Univ. of Arizona, U.S.A.) [89]
Detlev Koester - (Louisiana State Univ., U.S.A.) [5]
Attay Kovetz - (Tel Aviv University, Israel) [82]
J.P. Lasota (Obs. de Paris, France) [28]
Berit E. Laüglo (Univ. of Trondheim, Norway) [25]
Pierre LaCombe - (Univ. of Montréal, Canada) [52]
Robert Lamontagne - (Univ. of Montréal, Canada) [60]
Carlos Lázaro - (Inst. Astro, Canarias, Spain)
James Liebert - (Univ. of Arizona, U.S.A.) [90]
James MacDonald - (Univ. of Delaware, U.S.A.) [17]
John McGraw - (Steward Observatory, Univ. of Arizona, U.S.A.) [99]
Robert McMahan - (Harvard-Smithsonian Cen. for Astro., U.S.A.)
Italo Mazzitelli - (Inst. Astrofisica Spaziale, Italy) [31]
Romas Mitalas - (Univ. of Western Ontario, Canada) [39]
R. Mochkovitch - (Inst. d'Astro de Paris, France) [62]
David Muchmore - (Univ. of Montréal, Canada) [61]
Ed Nather - (Univ. of Texas, U.S.A.) [68]
Lorne Nelson - (Canadian Inst. Theor. Astrophysics, Canada) [22]
Erlend Østgaard- (Univ. of Trondheim, Norway) [78]
Frits Paerels - (Lab. for Space Research, Netherlands) [2]
Marie Pageau - (Univ. of Montréal, Canada) [21]
Claude Pelletier - (Univ. of Montréal, Canada) [47]
Eric R. Peterson - (Univ. of Washington, U.S.A.) [35]

M. Politano - (Univ. of Illinois, U.S.A.) [41]
Elizabeth Poulin - (Univ. of Montréal, Canada)
Judith Provencal - (Univ. of Texas, U.S.A.) [81]
D. Prialnik (Tel Aviv University, Israel) [30]
Pat Purnell-Grauer - (Little Rock, Arkansas, U.S.A.) [107]
N.C. Rana - (Tata Institute of Fundamental Research, India) [51]
Alak Ray - (Tata Institute of Fundamental Research, India) [101]
Oded Regev - (Columbia Univ., U.S.A. & Technion, Israel)
Alvio Renzini - (Univ. of Bologna, Italy) [8]
Harvey Richer - (Univ. of British Columbia, Canada) [109]
Fred Ringwald - (Dartmouth College, U.S.A.) [86]
Hans Ritter - (Univ. of München, F.R.G.) [100]
Edward Robinson - (Univ. of Texas, U.S.A.) [77]
Eric Rubenstein - (Columbia University, U.S.A.) [23]
Maria Teresa Ruiz - (Univ. of Santiago, Chile) [37]
R.A. Saffer - (Univ. of Texas, U.S.A.) [19]
Didier Saumon - (Univ. of Rochester, U.S.A.) [84]
Gary Schmidt - (Univ. of Arizona, U.S.A.) [83]
Detlef Schönberner - (Univ. of Kiel, F.R.G.) [11]
Harry Shipman - (Univ. of Delaware, U.S.A.) [43]
Giora Shaviv (Israel Inst. of Tech., Israel) [91]
Edward M. Sion - (Villanova Univ., U.S.A.)
Jan-Erik Solheim - (Univ. of Tromso, Norway) [69]
S. Starrfield - (Ariz. St. Univ. & Los Alamos Nat. Lab., U.S.A.) [7]
K. Aa. Strand - (Washington D.C., U.S.A.)
Mayumi Suzuki - (Dartmouth College, U.S.A.) [96]
Steve Swanson - (Dartmouth College, U.S.A.) [80]
Paula Szkody - (Univ. of Washington, U.S.A.) [32]
Peter Thejll - (Univ. of Delaware, U.S.A.) [93]
John Thorstensen - (Dartmouth College, U.S.A.) [73]
James Truran - Univ. of Illinois, U.S.A.) [9]
D. Tytler - (Columbia University, U.S.A.) [6]
Hugh M. Van Horn - (Univ. of Rochester, U.S.A.) [97]
Gérard Vauclair - (Toulouse Observatory, France) [53]
Stephane Vennes - (Univ. of Montréal, Canada)
Brian Ventrudo - (Univ. of Western Ontario, Canada) [36]
Richard Wade - (Steward Obs., Univ. of Arizona, U.S.A.) [67]
Brian Warner - (Univ. of Cape Town, South Africa) [108]
Ron Webbink - (Univ. of Illinois, U.S.A.) [38]
Gary Wegner - (Dartmouth College, U.S.A.) [79]
Kay Wegner - (Dartmouth College, U.S.A.) [85]
Rainer Wehrse - (Univ. of Heidelberg, F.R.G.) [105]
Volker Weidemann - (Univ. of Kiel, F.R.G.) [103]
Klaus Werner - (Univ. of Kiel, F.R.G.) [24]
François Wesemael - (Univ. of Montréal, Canada) [46]
Barbara Whitney - (Univ. of Wisconsin, U.S.A.) [71]
D.T. Wickramasinghe - (Australian National Univ., Australia) [104]
Don Winget - (Univ. of Texas, U.S.A.) [112]
Michael Wolff - (Naval Research Lab, U.S.A.) [45]
Matt Wood - (Univ. of Texas, U.S.A.) [72]
Kinwah Wu -(Louisiana State Univ., U.S.A.) [29]

MASS DISTRIBUTION AND LUMINOSITY FUNCTION OF WHITE DWARFS

Volker Weidemann and Jie W. Yuan
Institut f. Theoretische Physik u. Sternwarte
der Universität Kiel, D-2300 Kiel 1, F.R. Germany

1. The white dwarf mass distribution

Ever since Graham's Strömgren photometry (1972) demonstrated the existence of a single well defined cooling sequence of DA white dwarfs the question of the mass dispersion (or the width of the number-mass distribution) has been in the foreground of my studies (Weidemann, 1970, 1977).

Indeed it turned out that the shape of the white dwarf mass distribution provides strong constraints on the theory of stellar evolution with mass loss, a fact which will be demonstrated again in the following lecture. It therefore seems worthwhile to dwell in some detail on the methods of its determination. For the benefit of the non-specialists I shall first present some of the historical results and then continue to discuss the present situation.

After my demonstration (1970) that Strömgren photometry was highly superior to Johnson (UBV) photometry, due to the fact that the narrow bands are essentially line-free, and after understanding the S-shape of the line-free DA-sequence as caused by the effects of Balmer depression and H minus opacity as compared to black-body energy distribution it was possible to use calculated two-color diagrams for the determination of surface gravity, with the highest sensitivity around 12000 K. It turned out that the g-distribution - and via the mass-radius relation therefore also the mass distribution - is fairly narrow, around $M \approx 0.6\ M_{\odot}$.

Observationally, the next step was the use of Oke's multichannel spectrophotometer with which Greenstein secured reliable energy distributions for hundreds of white dwarfs at the Hale 5 m telescope (see Greenstein, 1976, 1984).

The Kiel group - to which Greenstein kindly provided most of his observations - was able to evaluate the data, and it turned out that Schulz's idea to bin the monochromatic fluxes into wider filters reduced observational and instrumental scatter and thereby provided more reliable g-determinations (see Koester, Schulz, Weidemann, 1979, Fig.6). KSW used

a weighted least square method to incorporate Strömgren and Johnson colors and Balmer line data, as available, and thus were able to weight their results. Aside from mass distributions derived from surface gravity they also determined radii for stars with known distances and thus obtained mass distributions for M(R).

The difference in the shape and width of the distributions obtained was demonstrated in Fig. 7 to 10 of KSW. The "most" reliable distribution showed a shape which was expected from synthetic calculations for stellar evolution with mass loss as I had shown a few years earlier (Weidemann, 1977, Fig. 2), using a Salpeter initial mass function (IMF) and semi-empirical relations between initial and final mass, derived from white dwarf in open clusters of known age or calculated by stellar evolution with wind mass loss according to the Reimers formula.
By variation of IMFs, star formation histories in the Galaxy, and initial-final mass relations Koester and Weidemann (1980) demonstrated how one is able to constrain these essential parameters for models of galactic evolution and estimates of the mass given back to the interstellar medium by the shape of the white dwarf mass distribution. It therefore seemed worth every effort to improve its empirical determination. That this was still necessary could be seen e.g. by the non-agreement of M(g) and M(R) determinations in KSW (Fig.11).
We thus embarked on the evaluation of the remaining multichannel spectra and concentrated on the most g-sensitive temperature range 16000 > T_{eff} > > 8000 K with improved model atmospheres and least square fits to the whole energy distribution (Weidemann, Koester, 1984) (WK 84). A specific goal was the determination of better parameters for the ZZ Ceti stars. The resulting mass distribution for 70 DA stars is reproduced in Fig. 1. It seems still the most reliable one up to the present time.
Before we go on with its discussion let us consider results obtained for non-DA stars.

For the DB stars Oke's multichannel observations were evaluated in Kiel by the same methods. The results were published by Oke et al. 1984 (OWK) and for the first time demonstrated convincingly that the masses of DA and DB stars are very similar. The same holds for the cooler non-DA stars of type DC and DQ, for which masses were determined from effective temperatures obtained with new model atmospheres and from radii in case of known distances. The resulting distributions are shown in Fig. 2 (reproduced from Weidemann, 1987a).

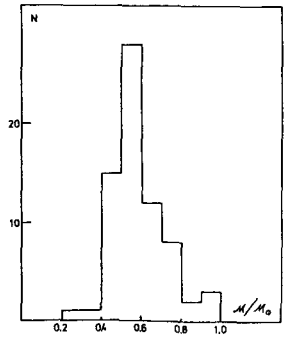

Fig.1. Mass distribution for 70 DA stars, M(g). WK 84.

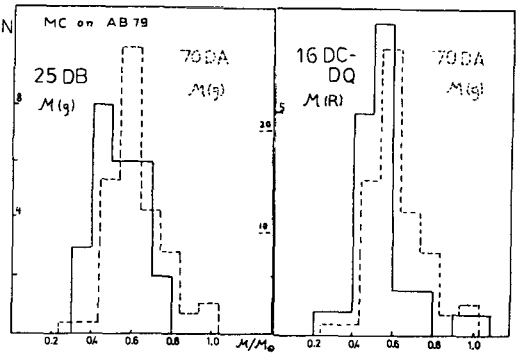

Fig.2. Mass distribution for non DA stars. ---: DA stars for comparison (see text).

A side remark is necessary which at the same time is important for future improvements. Oke's multichannel data were calibrated on AB 79 (Oke and Gunn, 1983) whereas the DA studies used the earlier calibration of Hayes and Latham (1975).

AB 79 seemed superior in the DB case as demonstrated by Fig. 2 and 6 in OWK. If so the DA results should also be corrected. The difference amounts to an average increase of about 0.04 $M_\odot$ as compared to KSW and WK 84. This implies that the average mass of DA's goes up to 0.62 $M_\odot$ from 0.58 $M_\odot$. The average masses are compared in Table 3 of Weidemann, 1987a. We may thus conclude that the non-DA masses could in the average be somewhat smaller, although this seems not to be significant. The recent study of the kinematics of DA and DB stars by Sion et al. (1988) also reaches the conclusion that there are no significant differences between both spectral types.

Sion et al. determined masses M(R) via radii from effective temperatures and distances. I took their Fig. 3 and compare both histograms (normalized to equal area). Although the temperature ranges show little overlap (13000-16000 K) the similarity is striking, and the distribution appears even somewhat narrower than the one of WK 84. However we may not fall into a trap: Sion et al. derived the masses from radii, M(R) with the M-R-relation, with radii from T_{eff} and distances using single valued T_{eff}(color) and M_V(color) relations (from Shipman, 1979 and Greenstein, 1984), where the first is calculated for log g = 8 ($\triangleq$ M = 0.58 $M_\odot$) and the second from an empirical mean fit to observational data for stars with known parallaxes.

This implies to assign to a given color an average radius which corresponds of course to the average mass. With other words: had Sion et al. not included many stars with independently determined T_{eff} and g or M(R) or M_V from parallaxes the distribution would only reflect the deviation

of the empirical M_V-color relation (e.g. Greenstein 1984, 1985) from a calculated M_V-color relation for M = ⟨M⟩. The difference is, as expected, minute. Greenstein (1985), however, used his empirical studies of multi-channel data to estimate also the width of the distribution and finds with $\sigma(M_V) = 0^m.25$ corresponding to a mass range from -0.10, +0.14 $M_\odot$ in essential agreement with WK 84 (see Table 5 of Greenstein, 1985). It is remarkable that this refers to the M(R) distribution of 52 white dwarfs of different spectral types, (omitting a few deviating objects like EG 11, L870-2, which has recently been shown to be a close binary by Saffer et al., 1988). Thus there can be little doubt that the distribution is at least as narrow as shown in Fig. 1.

However, several questions arise at this point:

1) how does this distribution compare with the distribution of progenitors: central stars of planetary nebulae, or core masses of stars leaving the AGB?
2) how can one understand the observed distribution in terms of models of galactic and stellar evolution?
3) how to improve the results observationally and theoretically?

We address each question in turn in the next sections.

2. Comparison with M-distributions of white dwarf progenitors.

Today it is generally accepted that the immediate progenitors of white dwarfs are in the large majority central stars of planetary nebulae (CPN). Schönberner (1981) has first demonstrated how one can use evolutionary post-AGB tracks and kinematical ages in order to determine CPN masses in cases where distances are known. The luminosity in the plateau phase equals that of a star with the same core-mass in the AGB phase. The rate of evolution along the tracks is determined by burning of the remaining hydrogen fuel. After its exhaustion follows a fast decline of luminosity. As can be seen from the time marks along the tracks, planetary nebulae (PN) are not excited for CPN with $M < 0.55\ M_\odot$, since those stars evolve too slowly. In the course of time some exceptions have become apparent, which I shall not discuss, instead I refer to the literature, e.g. to the forthcoming Proceedings of the IAU Symposium No. 101 in Mexico City, Oct. 1987. A survey of the methods has also been given in my Tucson lecture last year (Weidemann, 1987a).

The main results of the Schönberner method (see Schönberner and Weidemann, 1983) is a confirmation of the narrow highly peaked M-distribution around 0.6 $M_\odot$, (see Fig. 5, below).

However there are two differences: one expected, one unexpected. The first is the absence of CPN below 0.55 $M_\odot$, the second is the steeper decrease towards the high mass tail. Part of it is certainly due to selection effects which discriminate against high mass CPN which pass the high luminosity phase very quickly, but part of it may be due to the possibility that the white dwarf distribution is in reality also narrower and appears broadened due to observational errors. Indeed, the post-AGB luminosity is so extremely sensitive to mass that a distribution could be determined with comparatively higher accuracy, if only distances of PN were better known, or the ensemble on the plateau phase were more complete. Unfortunately both is not the case, and it appears that progress can be made only if one either goes to extragalactic PN's or concentrates on low luminosity CPN's which are hard to find and to observe.
Both ways have been entered now. Ford et al. (1988) find evidence for a steep high mass tail above 0.6 $M_\odot$ with $\sigma \leq 0.05$ $M_\odot$ by observations of [OIII] luminosities for local group galaxies and comparison with evolutionary calculations, whereas a similar small scatter around 0.6 $M_\odot$ has been derived for the Magellanic Clouds. Barlow (1988) combines these MC results to find (0.597 $\pm$ 0.023) $M_\odot$ for 17 CPN.
A different claim was made by Heap and Augensen (1987) which evaluated IUE UV fluxes instead of M_V by the Schönberner method to derive a broader M-distribution with a maximum at 0.65 $M_\odot$. However I have shown (Weidemann, 1988) that the discrepancies completely disappear if larger distances are applied, for which there is other evidence. For details I refer to my paper.

A third possibility to derive a progenitor M-distribution is a comparison of AGB luminosity functions with synthetic evolutionary calculations. This method has been applied to the LMC AGB luminosity function of Reid and Mould (1985). First results were presented at the Calgary Workshop 1986 (Weidemann, 1987b) and a detailed explanation of the method has been published in my recent paper (Weidemann, 1987c).
The results are sensitive to the location of the start-TP-AGB relation in the initial mass-luminosity plane.
If thermal pulses start early - as shown by recent evolutionary calculations - the derived M-distribution of stars leaving the AGB becomes very narrow, intermediate between the extremely small (selection effect dominated) CPN distribution and the comparatively wider white dwarf distribution.
A final possibility lies in the evaluation of IRAS sources the luminosity distribution of which in the Galaxy, according to Habing (1988), peakes at log $L/L_\odot$ = 4000 (corresponding to an AGB core mass of 0.57 $M_\odot$). Habing

concludes that the M-distribution is very similar to that of the white dwarfs which is taken as support for the hypothesis that the IRAS point sources are the immediate predecessors of white dwarfs.

3. Mass distributions calculated with galactic evolution models

Yuan (1987a) has updated our galactic evolution program, which considers single pool models specified by a given IMF, star formation rate, SFR(t), total age, and initial-final mass relation. Changes compared to our earlier calculations (Koester and Weidemann, 1980, WK 84) concerned mainly incorporation of newer IMFs and $M_f(M_i)$-relations, and normalization to a smaller present white dwarf birth rate of $1 \cdot 10^{-12}$ WD/pc^{3}yr, revised downwards by a factor of two in view of the results of Fleming, Liebert and Green (1986).

The variety of $M_f(M_i)$-relations is shown in Fig. 3. For the discussion of $M_f(M_i)$-relations I refer to my lecture at the Mt. Porzio Workshop (Weidemann, 1987d) and the following publication (Weidemann, 1987c). Resulting white dwarf M-distributions become wider as steeper the relations are and begin at smaller masses for lower values of M_f for M_i = 1 (about the galactic turn-off).

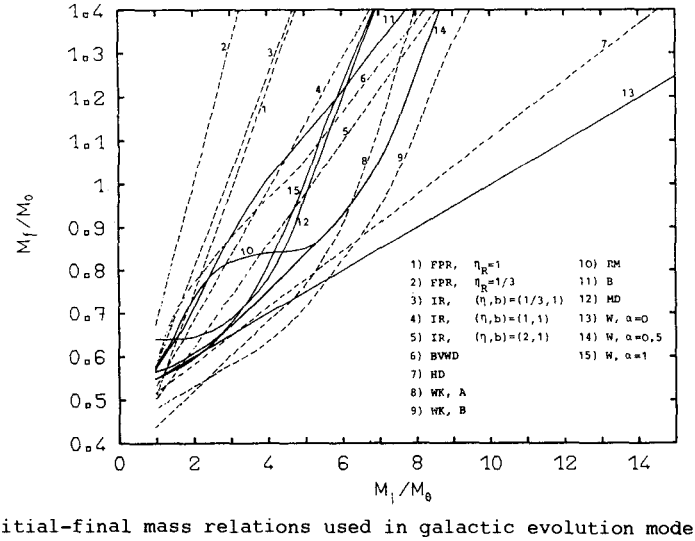

Fig.3. Initial-final mass relations used in galactic evolution model calculations (Yuan,1987a). 1),2): Fusi-Pecci, Renzini (1976); 3)-5): Iben, Renzini (1983); 6): Weidemann (1977); 7): Hills, Dale (1973); 8),9): Weidemann, Koester (1983); 10): Reid, Mould (1985); 11): Bedijn (1986); 12): Mazzitelli, D´Antona (1987a); 13)-15): Weidemann (1987d).

Relations 8), 9) and 13) to 15) are based on observations of white dwarfs in open clusters mainly by Koester and Reimers (for details see Weidemann,Koester,1983, or Weidemann,1987c). For stellar evolution with intermediately strong overshooting, characterized by a parameter $\alpha_c = 0.5$ the upper mass limit for white dwarf production is about $M_i \approx 8\ M_\odot$. Calculated M-distributions are broadened by a Gaussian with $\sigma = 0.05\ M_\odot$ in order to account for observational errors. An essential result is reproduced in Fig. 4 (the influence of different IMFs turned out to be minor) which shows two distributions compatible with the observational histogram.

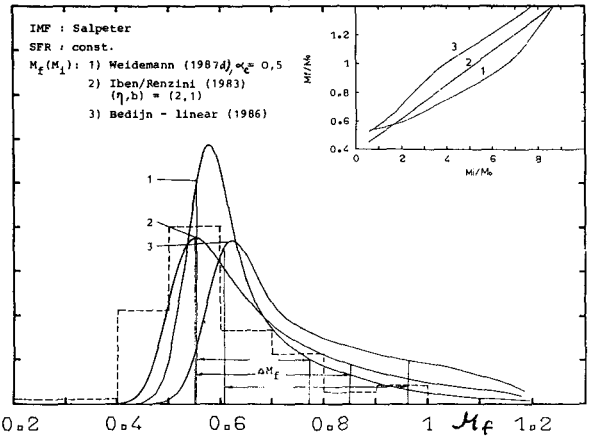

Fig.4. Mass distribution as calculated with galactic evolution model for different $M_f(M_i)$ relations (see insert);
1): Weidemann (1987d) α_c=0.5;
2): Iben, Renzini (1983) for (η,b)=(2,1), (η: Reimers wind loss factor, b: PN efficiency parameter);
3): Bedijn (1986) linearized relation derived from mass loss calculations for AGB evolution for OH/IR stars;
ΔM_f measures the 2σ (67%) width;
---: DA distribution.

The left side indicates that either $M_f(M_i = 1)$ should be assumed smaller, since relation 1 starts at $M_f = 0.55\ M_\odot$ implying that there are no white dwarfs with smaller masses, which is probably not true. The fraction of white dwarfs born below the PN visibility limit is at present unknown, it is composed of stars leaving the AGB below it and of stars which do not reach the AGB at all (horizontal branch stars, which enter the white dwarf region via sdO and sdB channels). The fraction of the latter should not be larger than 10%, although a firm estimate can be only be made for the extreme horizontal branch stars, with $0.45 < M_c < 0.50\ M_\odot$, for which Heber (1986) finds 2%.

In this context it is worthwile to mention that the mass of 40 Eri B, for a long time considered to be well established by stellar dynamics, $(0.43 \pm 0.02)M_\odot$, is probably more around $0.50\ M_\odot$ as indicated by recent redshift observations of Wegner (1980, 1987) and Koester (1988).

The fraction of white dwarfs entering below the PN limit of $0.55\ M_\odot$ cannot be too large since otherwise the discrepancies between PN and WD birth rates, amounting to a factor of three (see Fleming et al., 1986) would become unbearable, although some remedy can be found by increased PN distances (Weidemann, 1988) and hidden white dwarfs in binaries.

On the other hand there is evidence for differential mass loss at a given M_i, thus the unique M_i/M_f-relations have to be replaced by some kind of strip (see Fig. 1 in Weidemann, 1987d). However, it is evident from the calculations that such a strip must be of restricted width in order to remain compatible with the observed narrow M-distributions.
As far as the results of Yuan's calculations are concerned it is impressive to show that one can rule out the $M_f(M_i)$-relation proposed by Mazzitelli and D'Antona (1986b) which begins at $M_f = 0.64\ M_\odot$ for $M_i = 1\ M_\odot$, although its slow increase results in an acceptable distribution, as far as its width is concerned.
The calculated M-distributions as presented comprise all white dwarfs above log $L/L_\odot = -3.7$ corresponding to a cooling age of $2 \cdot 10^9$ yrs, down to $T_{eff} = 6000$ K (Koester and Schönberner, 1986). Of course it is easy to obtain also the M-distribution at white dwarf birth which is identical to the M-distribution of CPN. Fig. 5 thus gives the predicted CPN M-distribution for a model which fits the white dwarf data well. It is unfolded and indeed appears compatible with the observed distribution.

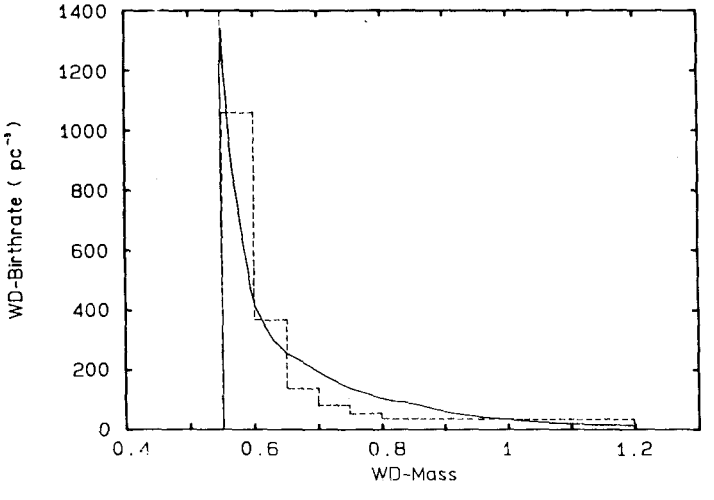

Fig.5. Predicted present WD birthrate or birthrate of CPN, for galactic evolution model with IMF from Salpeter, SFR = const and $M_f(M_i)$ from Weidemann (1987c) for $\alpha_c = 0.5$.
---: CPN mass distribution as derived from observations with the Schönberner method (local ensemble), cf. Weidemann (1988).

Yuan (1987b) has used the evolutionary tracks for CPN (Schönberner, 1981, 1983, Wood and Faulkner, 1986) to indicate the expected density of CPN in the HR-diagram, which is shown in Fig. 6.
It is evident that the true M-distribution can only be found by observing faint CPN since selection effects favor the observation of low mass CPN. A similar approach has been recently presented by Shaw (1988). However we have here included also 20% helium-burning CPN, which are found at higher luminosities (cf. Iben, 1984) so that the observed fraction at log $L/L_\odot \approx 3$ should be about 50%. Since WC type CPN are less frequent (17 - 20%, Schönberner, 1986, Barlow, 1987) it appears that the 20% fraction assume

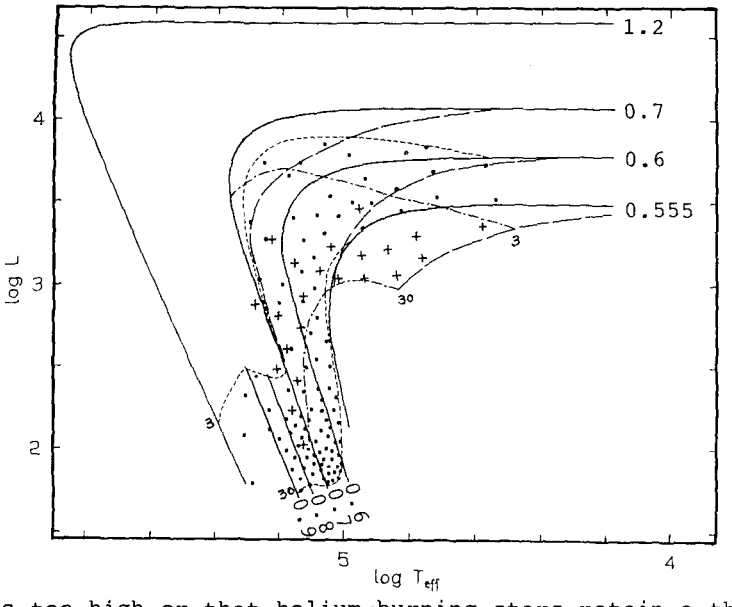

Fig.6. Expected density distribution of CPN in HR-diagram (Yuan,1987b) with evolutionary tracks from Paczynski (1970), Wood and Faulkner (1986), and Schönberner (1981, 1983).
. : for hydrogen burning;
+ : for 20% helium burning CPN added;
——: evolutionary tracks for H-burning CPN;
– – –: for He-burning CPN.

Time interval 3000 to 30000 yrs indicated by
--- for H-burning CPN,
-·- for He-burning CPN.

is too high or that helium-burning stars retain a thin hydrogen atmosphere. PG 1159 objects, from their approximate location in the HR-diagram are probably helium-burning stars, which explains their relative frequency (see Weidemann, 1987a).

If we take all uncertainties into account we may close this section with the statement that M-distributions of white dwarfs and planetary nebulae can be well understood within a comparatively simple model of galactic evolution.

4. Possibilities of improvement

As far as the observations is concerned, it is now possible to attain spectroscopy and photometry at higher signal to noise (see Greenstein, 1986) and higher resolution with modern detectors. High quality spectra - like that of the DB star GD 358 (Koester et al., 1985) - enable more reliable analysis. In the case of DA stars, one should improve the g/T_{eff} determination by the analysis of high resolution line profiles, and by careful calibration, providing better M(g). With Hipparcos coming up it can also be envisaged to obtain much better parallaxes, which are essential in order to determine M(R) and to check on the mass-radius relation. The present situation is still completely unsatisfactory, as shown in Fig. 7, which gives the position of those DA stars whithin the WK 84 ensemble for which parallaxes are available. Some progress has recently been made by redshift determinations of high accuracy. (Wegner, 1987,

Koester, 1987). I shall skip this since we shall hear more about it in Prof. Wegner's lecture (this volume).

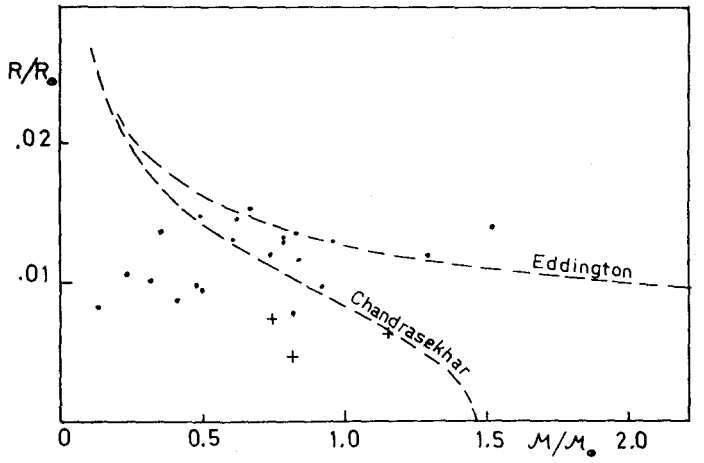

Fig.7. Mass and radii derived for 21 stars with known distances out of 70 DA with well determined surface gravities (Weidemann and Koester,1984), M = M(R,g). If not for Sirius B, at $1M_{\odot}$, and three higher mass stars in NGC 2516 (WK 83 indicated by crosses, Chandrasekhar would come out only marginally vs. Eddington.

In this context I should like to mention that the ongoing search for close double degenerates has yielded first results (cf. Saffer and Liebert, and the Bologna group, Bragaglia et al., this Conference). The smaller masses found for L 870-2 (EG 11) are in line with predictions by Iben and Tutukov (1986) for a secondary peak in the number-mass distribution around 0.2 - 0.3 $M_{\odot}$, although the frequency of these objects is evidently smaller than first estimated.
I shall not go into details but refer to the other contributions concerning binarity at this Conference.

On the theoretical side much improvement is needed in the field of stellar evolution which enters directly or indirectly many of our conclusions, e.g. concerning the presence of overshooting, the onset of the thermal-pulsing AGB and mass loss mechanisms. Also models of galactic evolution should be extended to include different populations, and dependence on different locations in the Galaxy. Such population synthesis models have already been published (cf. Bienaymé et al., 1987) and white dwarf results shall appear if the proposed HST parallel survey - in which we participate - becomes reality.

Population II results are still too meager as to reach any conclusion. The local fraction should be of the order of a few percent (see Sion et al., 1988). The exciting possibility to observe white dwarfs in globular clusters (first claimed by Richer and Fahlmann, this Conference) and to determine their masses will be also provided by the HST (see Renzini and Fusi Pecci, 1988).

A final word should be said about selection effects. These have been shown to be extremely important in the case of CPN (see Heap and Augensen, 1987), and could have been influential also in the white dwarf case. This has been emphasized by Shipman (1979), taken up by Guseinov et al. (1983), but shown to be practically unimportant due to the very fact that the true M-dispersion is evidently narrow (Koester, 1984). But it is clear that for and with further improvements also selection effects have to be more carefully taken into account.

5. The white dwarf luminosity function

Since this topic has been covered recently by Liebert, Dahn and Monet (1988) and will be dealt with again in Liebert's following lecture (this Conference) I shall restrict myself to a few remarks and to the presentation of some relevant results obtained with the Kiel galactic evolution program.

The discussion during the last years centered on three questions, which are closely connected, namely first: how is the shape of the LF at the cool end? Second: does the observed downturn of the LF reflect the finite age of the galactic disk and third: how reliable is the cooling theory, especially what is the influence of miscibility in the solid phase?

To begin with the last question: the most recent contribution by Barrat, Hansen and Mochkovitch (1988) finds that the influence of a minor phase separation at crystallization on the WD LF is moderate and does increase the estimates of the age of the galactic disc from the downturn of the LF by Winget et al. (1987) by only 0.50 to 0.75 Gyrs. However, for the second question, if the LF downturn measures the age of the galactic disk, there remain controversial statements. The calculations of Mazzitelli and D'Antona, 1986a, predicted, and Larson's bimodal SFR (1986) needed a large number of WDs cooled down below invisibilty in order to explain the local missing mass.

On the other hand, it is important to notice that the population synthesis model by Bienaymé et al. (1987) can explain the dynamical constants without the introduction of local missing mass, a result confirmed also by studies of the Cambridge group as recently presented at the Bologna ESO-CERN Conference by Lynden-Bell (1988).

Whereas Larson's hypothesis seems thus weakened the question of the extension of the cooling curves remains still important: as Winget and Van Horn (1987) have demonstrated the raw ages of WDs cooled down to $\log L/L_{\odot} = -4.5$ range from 5 to 13 Gyrs according to different models and physical assumptions.

The Winget et al. (1987) conclusion for the galactic age must therefore be viewed with caution (especially as recent detailed studies of globular clusters by Buonanno et al. (1988) yield again a large age for the Galaxy, of 19 $\pm$ 3 Gyrs).
Its derivation has another weakness which lies in the fact that for the model calculations a constant WD birth rate (weighted by the DA M-distribution) has been assumed down to some time interval of 0.3 Gyrs after the beginning of the Galactic disk, which is estimated to be a mean pre-white dwarf lifetime.
Yuan 's calculations with our galactic evolution program however show that the results change significantly if the time dependence of the WD birth rate is taken into account.

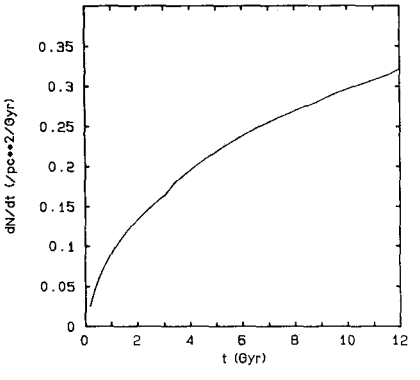

Fig.8. White dwarf birth rate increase as function of time. Galactic evolution model with IMF Salpeter, SFR = const, $M_f(M_i)$ from Weidemann (1987c), α_c=0.5.

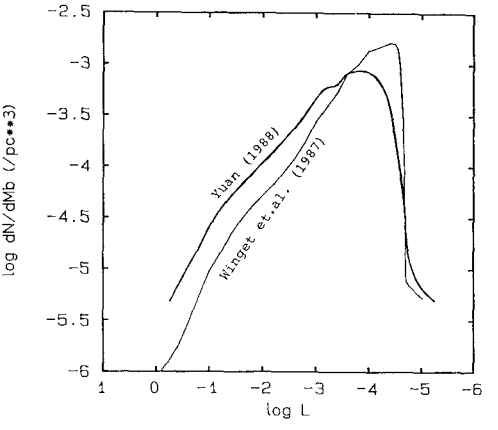

Fig.9. Luminosity function as calculated with galactic evolution model, compared to Winget et al. modelling (see text).

Whereas Fig.8 demonstrates how the WD birth rate increases gradually, Fig.9 shows the corresponding LF to run smoother and to display not such a steep downturn than in the Winget et al. approach (keeping all other parameters as in their publication).
However it might be also interesting to show how the LF changes with other assumptions: on IMF - we can rule out the Larson model; on SFR - we can demonstrate that it is not possible to conclude from the WD LF on SFR(t) except in extreme cases of star bursts; on $M_f(M_i)$ - the differences are minor; on cooling curves and galactic age - it will be difficult to disentangle the effects, since longer or shorter cooling times can be nearly compensated by larger or smaller galactic ages.

As always we thus have to conclude what is almost trivial: we need improvements as well on the observational side of very cool degenerates (cf. Ruiz and Anguita at this Conference) as on the interpretation of cool atmospheres and especially on cooling theory.

References

Barlow, M.J.: 1987, Mon.Not.Roy.Astr.Soc. **227**, 161

Barlow, M.J.: 1988, in IAU Symp. No. 131, Planetary Nebulae eds. Torres-Peimbert et al., in press

Barrat,J.L.,Hansen,J.P.,Mochkovitch,R.: 1988, Astron. Astrophys. **199**, L15

Bedijn, P.J.: 1986, preprint

Bienaymé, O., Robin, A.C., Crézé, M.: 1987, Astron. Astrophys. **180**, 94

Buonanno, R., Corsi, C.E., Fusi Pecci, F.: 1988, Astron. Astrophys. submitted (ESO preprint No. 594)

Fleming, T.A., Liebert, J., Green, R.F.: 1986, Astrophys. J. **308**, 176

Ford, H.C., Ciardullo, R., Jacoby, G.H., Hui, X.: 1988, in IAU Symp. No. 131, Planetary Nebulae, eds. Torres-Peimbert et al. in press

Fusi Pecci, F., Renzini, A.: 1976, Astron. Astrophys. **46**, 447

Greenstein, J.L.: 1976, Astron. J. **81**, 323

Greenstein, J.L.: 1984, Astrophys. J. **276**, 602

Greenstein, J.L.: 1985, Publ. Astr. Soc. Pac. **97**, 827

Greenstein, J.L.: 1986, Astrophys. J. **304**, 334

Graham, J.A.: 1972, Astron. J. **77**, 144

Guseinov,O.H., Novruzova,H.I., Rustamov,Y.S.: 1983, Ap. Space Sci. **96**, 1

Habing, H.J.: 1988, Astron. Astrophys. **200**, 40

Hayes, D.S., Latham, D.W.: 1975, Astrophys. J. **197**, 593

Heap, S.R., Augensen, H.J.: 1987, Astrophys. J. **313**, 268

Heber, U.: 1986, Astron. Astrophys. **155**, 33

Hills, J.G., Dale, T.M.: 1973, Astrophys. J. **185**, 937

Iben, I., Jr.: 1984, Astrophys. J. **277**, 333

Iben, I., Jr., Renzini, A.: 1983, Ann. Rev. Astron. Astrophys. **21**, 271

Iben, I., Jr., Tutukov, A.V.: 1986, Astrophys. J. **311**, 753

Koester, D.: 1984, Astrophys. Space Sci. **100**, 471

Koester, D.: 1987, Astrophys. J. **322**, 852

Koester, D.: 1988, to be published

Koester, D., Schulz, H., Weidemann, V.: 1979, Astron. Astrophys. **76**, 262

Koester, D., Weidemann, V.: 1980, Astron. Astrophys. **81**, 145

Koester, D., Vauclair, G., Dolez, N., Oke, J.B., Greenstein, J.L., Weidemann, V.: 1985, Astron. Astrophys. **149**, 423

Koester, D., Schönberner, D.: 1986, Astron. Astrophys. **154**, 125

Larson, R.B.: 1986, Mon. Not. Roy. Astr. Soc. **218**, 409

Liebert, J., Dahn, C.C., Monet, D.G.: 1988, Astrophys. J., in press

Lynden-Bell, D.: 1988, The Third ESO-CERN Symposium on Astronomy Cosmology and Fundamental Physics, Bologna, in press
Mazzitelli, I., D'Antona, F.: 1986a, Astrophys. J. **308**, 706
Mazzitelli, I., D'Antona, F.: 1986b, Astrophys. J. **311**, 762
Oke, J.B., Gunn, J.E.: 1983, Astrophys. J. **266**, 713
Oke, J.B., Weidemann, V., Koester, D.: 1984, Astrophys. J. **281**, 276
Reid, N., Mould, J.: 1985, Astrophys. J. **299**, 236
Renzini, A., Fusi Pecci, F.: 1988, Ann. Rev. Astron. Astrophys. in press (ESO preprint No. 565)
Saffer, R.A., Liebert, J., Olszewski, E.W.: 1988, Astrophys. J. (Nov.)
Schönberner, D.: 1981, Astron. Astrophys. **103**, 119
Schönberner, D.: 1983, Astrophys. J. **272**, 708
Schönberner, D.: 1986, Astron. Astrophys. **169**, 189
Schönberner, D., Weidemann, V.: 1983, in Planetary Nebuale, D. Flower ed., Reidel Dordrecht, p. 359
Shaw, R.A.: 1988, in IAU Symp. No. 131, Planetary Nebulae S. Torres-Peimbert, M. Peimbert, J. Kaler eds. Reidel, in press
Shipman, H.L.: 1979, Astrophys. J. **228**, 240
Sion,E.M., Fritz,M.L., McMullin,J.P., Lallo,M.D.: 1988, Astron. J.
Wegner, G.: 1980, Astron. J. **85**, 1255
Wegner, G.: 1987, in IAU Coll. No. 95. Second Conf.on Faint Blue Stars, A.G.D.Philip,D.S.Hayes,J.Liebert eds., L.Davis press, p. 649
Weidemann, V.: 1970, in IAU Symp. No. 42 White Dwarfs, W.J. Luyten ed., D. Reidel, p. 81
Weidemann, V.: 1977, Astron. Astrophys. **59**, 411
Weidemann, V.: 1987a, IAU Coll.95, Second Conference on Faint Blue Stars. A.G.D.Philip, D.S.Hayes, J.W.Liebert eds., L. Davis press, p. 19
Weidemann, V.: 1987b, in Late Stages of Stellar Evolution. S. Kwok, S.R. Pottasch, eds. Reidel, p. 347
Weidemann, V.: 1987c, Astron. Astrophys. **188**, 74
Weidemann, V.: 1987d, in 6th European Workshop on White Dwarfs. Mem. Soc. Astr. Ital. **58**, 33
Weidemann, V.: 1988, Astron. Astrophys. submitted
Weidemann, V., Koester, D.: 1983, Astron. Astrophys. **121**, 77
Weidemann, V., Koester, D.: 1984, Astron. Astrophys. **132**, 195
Winget, D.E.,Van Horn, H.M.: 1987,IAU Coll.95,Second Conf.on Faint Blue Stars,A.G.D.Philip,D.S.Hayes,J.Liebert, eds. L.Davis press, p.363
Winget, D.E., Hansen,C.J., Liebert, J., Van Horn, H.M., Fontaine,G., Nather,R.E.,Kepler,S.O.,Lamb,D.Q.:, 1987, Astrophys. J. **315**, L77
Wood, P.R., Faulkner, D.J.: 1986, Astrophys. J. **307**, 659
Yuan, J.W.: 1987a, Diplomarbeit, Univ. Kiel
Yuan, J.W.: 1987b, Poster (Weidemann), IAU Symp. 101, Planetary Nebulae

THE LUMINOSITY FUNCTION OF WHITE DWARFS IN THE LOCAL DISK AND HALO

James Liebert
Steward Observatory, University of Arizona
Tucson, Arizona 85721

Conard C. Dahn and David G. Monet
U. S. Naval Observatory
Flagstaff, Arizona 86002

I. INTRODUCTION

The luminosity function (LF) and total space density of white dwarfs in the solar neighborhood contain important information about the star formation history of the stellar population, and provide an independent method of measuring its age. The first empirical estimates of the LF for degenerate stars were those of Weidemann (1967), Kovetz and Shaviv (1976) and Sion and Liebert (1977). The follow-up investigations made possible by the huge Luyten Palomar proper motion surveys, however, added many more faint white dwarfs to the known sample. While the number of known cool white dwarfs grew to nearly one hundred, these did not include any that were much fainter intrinsically than the coolest degenerates found from the early Luyten, van Biesbroeck and Eggen-Greenstein lists.

In an analysis of a fainter sample, Liebert et al. (1979) first discussed the evidence that there was a paucity of white dwarfs fainter than $M_v \sim +16$ with respect to the predictions of theoretical cooling models allowing cooling ages greater than 10 Gyrs. Taken at face value, the result implied that the bulk of star formation in the disk began less than 10 Gyrs ago, an effective age for the disk billions of years younger than the ages estimated for globular clusters and the galactic halo (Liebert 1980). These results also implied that degenerate dwarfs are a relatively minor contributor to the local mass density of the galactic disk.

The last several years have brought considerable improvements in both the theoretical calculations and the observational data base. Iben and Tutukov (1984) presented new evolutionary models and rediscussed the published observational data, offering alternative explanations for an apparent paucity of very faint degenerate stars. Winget et al. (1987) combined a new set of theoretical calculations with a preliminary version of the observational data base reported here and reported a direct estimate of the age of the galactic disk of 9.3 ± 2 billion years. However, Winget

and Van Horn (1987) discussed in considerable detail the sensitivity of this number – which basically represents the cooling time of a model to reach a luminosity near $\log(L/L_{\odot}) \sim -4.5$ – to various physical parameters in the models. The use of different parameters explains the discrepancies between their conclusion and the result of D'Antona and Mazzitelli (1986).

The improved observational data base is documented in detail in (Liebert, Dahn and Monet 1988; hereafter LDM). While this paper includes a brief review of that work, we now can incorporate new parallax data and considerably improved absolute magnitude estimates for several stars in the sample. Thus Figure 1 is an updated observational LF, which supersedes that appearing in LDM. After the brief review and presentation of updated results in Section II, a discussion of the sources of error and incompleteness is given in Section III. The kinematics of the sample based on the derived tangential velocities is also discussed. Section IV features a preliminary look at the LF yielded by the sparse population of local halo white dwarfs, as defined from a kinematic criterion.

II. THE LHS 8TENTHS SAMPLE

The sample used in LDM consists of the 43 spectroscopically confirmed white dwarfs contained in the LHS Catalogue (Luyten 1979) which have (1) proper motions (μ) $\geq$ 0.″800 yr^{-1}, (2) locations in the sky north of $\delta = -20°$, and (3) $M_v \geq 13.0$. Available astrometric, photometric and spectroscopic data for each star in the sample are summarized in Table 1 of LDM and the notes. Absolute magnitudes were calculated for each star, usually based on an available trigonometric parallax. Space densities were calculated using the $1/V_{max}$ method similar to the application of Schmidt (1975). In this presentation, new or updated trigonometric parallaxes are substituted for six stars. These stars, with the improved absolute parallax values and mean errors in parentheses, are: LHS239/240 (0.″0525 ± 0.″0011), LHS342 (0.″0374 ± 0.″0022), LHS483 (0.″0577 ± 0.″0015), LHS542 (0.″0322 ± 0.″0037), LHS2364 (0.″0416 ± 0.″0022) and LHS2673 (0.″0284 ± 0.″0033).

For a dwindling minority without trigonometric values, photometric parallaxes were assigned based on new determinations of the relationships between absolute visual magnitude, effective temperatures and broad band BVI colors. Particular attention was given to estimating the bolometric correction (BC), necessary to place the stars in bolometric luminosity intervals for comparison with theoretical predictions.

For the hotter DA stars, the available tabulations of BCs for hydrogen-rich atmosphere calculations show considerable scatter about what is expected to be a monotonic functional dependence on the effective temperature (T_{eff}). Matt Wood has kindly pointed out to us that the mean M_{bol} bin centers for the hot white dwarfs listed in Table 4 of LDM differ slightly (i.e., up to approximately a symbol diameter) from the corresponding points plotted in Figures 3 and 4 of that paper. This discrepancy resulted from inadvertently using preliminary values for the mean M_{bol} numbers in the figures rather than those finally adopted and presented in Table 4 of LDM. These preliminary values were based on slightly different smoothings of the model BC values used in estimating a functional relationship between BC and T_{eff} from that finally adopted for hot DA

white dwarfs. Figure 1 includes the hot white dwarf LF from the Palomar Green Survey now plotted with a luminosity scale entirely consistent with Table 4 of LDM.

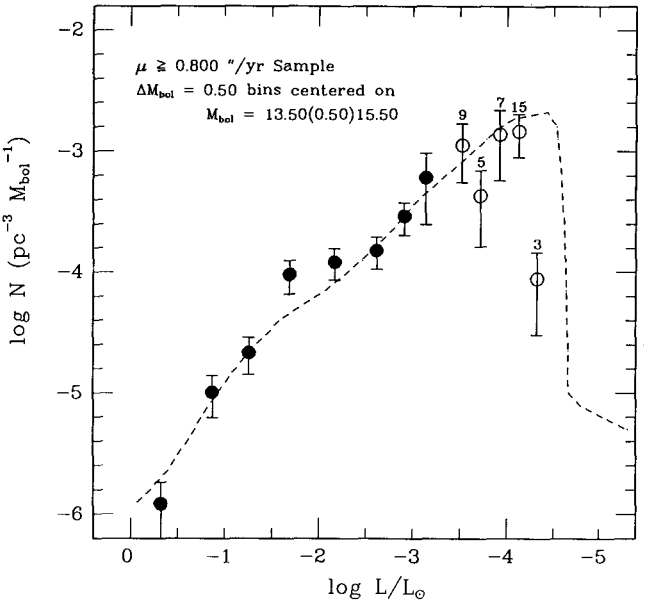

Figure 1. Luminosity function for disk white dwarfs, using blackbody BCs and updated from Fig. 3c of LDM by incorporating new trigonometric parallaxes. Numbers of WDs in each bin are listed above the tops of the bins.

For the cooler white dwarfs, the problem is that BCs for the more accurate calculations of the energy distributions of stars with helium-rich atmospheres are not generally available. In one approach, BCs were estimated by applying the value for the blackbody corresponding to the derived T_{eff} consistent with the measured value of M_v. Arguments were given that the blackbody BCs probably overestimate the corrections for helium atmosphere white dwarfs. For several well-studied cases, these imply larger radii and smaller masses than the means for DA white dwarfs. It is implausible that the older white dwarfs should have a smaller mean mass than that for the hotter DA stars. On the other hand, a conservative lower limit to the luminosities of the coolest stars in the sample (and an upper limit to the derived cooling ages for a given set of models) is provided by assuming no BCs at all! This was the alternative approach, and it was argued that the LFs presented from both methods bound the uncertainty due to the BCs.

III. THE DISK WHITE DWARF LUMINOSITY FUNCTION: SOURCES OF ERROR AND INCOMPLETENESS

While the observed maximum and apparent cutoff in the white dwarf LF derived from this sample has already been used to infer an age for the local galactic disk population (Winget et al. 1987), there are several ways in which the function is likely to be incomplete. Each of these

is discussed below, and underscores our caution that the empirical LF is not necessarily accurate enough yet to infer many details about the star formation history of the disk population.

(a) Possible existence of stars much fainter than $M_v \sim +16$.

It is asserted in LDM that this sample and others discussed in that paper show that there is a sharp drop in the LF at M_v fainter than 16.5. Note that the preliminary trigonometric parallax reported for the southern proper motion star ER8 by M. T. Ruiz at this meeting indicates that this star also lies near this empirical luminosity limit. The space densities of stars at $M_v \sim 17-17.5$ must be reduced by more than an order of magnitude from the peak. However, there is very little search volume available from this sample to test the numbers of stars at $M_v > +18$, if such objects avoid low mass main sequence stellar companions. The constraints these results place on a bimodal star formation hypothesis (e.g., Larson 1986) are discussed in LDM.

(b) Unidentified members of binary systems.

Two kinds of unresolved binaries may hide white dwarfs from this census. First, there are those white dwarfs with bright nondegenerate companions (the "Sirius B" type). Insofar as close binaries tend to have mass ratios near unity, there could be a fair fraction of A–K dwarfs, subgiants and giants with white dwarf companions. It is still controversial as to what fraction of G stars, for example, are binary; however, it is often impossible to distinguish a lower luminosity main sequence companion from a degenerate companion for single-lined spectroscopic binaries. For wide binaries the incidence of white dwarf–nondegenerate pairs appears to be rather small (Greenstein 1986). However, the frequency of binaries with an evolved component and their period distribution are certainly not well determined. In the solar neighborhood, the census of stars within 5.2 pc of the Sun (cf. van de Kamp 1971), often regarded as a nearly complete sample, contains two single white dwarfs, two with distant, low luminosity nondegenerate companions, and two white dwarfs (Sirius B and Procyon B) with close, bright companions which could not be found by the usual techniques.

Secondly, there are now known to be unresolved binary white dwarfs, such as L870–2 (Saffer, Liebert and Olszewski 1988). The frequency of such objects is not well determined, especially for periods longer than several hours (see Robinson and Shafter 1987). However, the frequency of progenitor binaries with the required small separations is surely small enough that the effect of unresolved degenerate pairs is unlikely to exceed (conservatively) 10%.

(c) Allowance for low velocity stars.

While the $1/V_{max}$ method as applied by Schmidt (1975) is designed to define a correct, effective search volume based on the limits of both apparent magnitude and proper motion, there may be significant numbers of white dwarfs missed which have small tangential velocities(v_{tan}), despite the minimum ages (set by the cooling times) of at least 1 Gyr and the well known increase in space motions with stellar age. This problem is clearly worse for the brighter stars

near $M_v \sim +13$, which are found at greater distances and are also likely to have a younger mean age, than for the critical stars near the faint end used in defining the turnover of the LF.

It is instructive to consider the distribution of v_{tan} with M_v for this sample (Figure 2). Here we also include stars in the LHS Eight Tenths Sample brighter than $M_v = +13$, although these were not included in the determination of the disk LF since the Palomar Green Survey is a much superior sample. While there hotter stars of low velocity, no cool stars are present with $v_{tan} <$ 40 km s^{-1}. For an earlier sample (Liebert 1978), we compared the distribution of tangential velocities for the known cool white dwarfs near the Sun with those of a strictly color-selected sample of nearby M dwarf stars – the Gliese/McCormick sample – and with the van de Kamp 5 pc sample of K–M dwarfs. The comparison suggested that a correction factor of up to 100% for missing low velocity white dwarfs was possible, if the white dwarfs have the same mean age as the low mass main sequence stars. However, as each white dwarf with $M_v > +13$ has a minimum age of at least 1 Gyr, and a nuclear-burning lifetime before that, the mean age of this sample is likely to be significantly older. Moreover, if cool, low velocity white dwarfs were present in comparable numbers to those constituting the known sample, it seems improbable that not a single representative of this group with $v_{tan} < 40$ km s^{-1} would have been found.

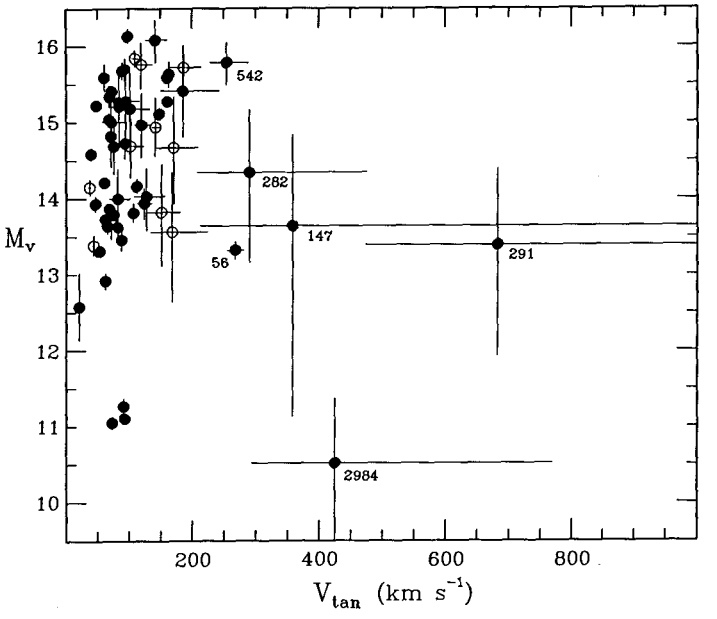

Figure 2. The distribution of tangential velocities (v_{tan}) against absolute visual magnitude (M_v) with error bars shown. Filled circles are data points from this paper, for LHS stars with $\mu \geq 0''.8$. Open circles are a new set of data presented in the following paper (Dahn et al. 1989), for LHS stars with $0''.700 \leq \mu \leq 0''.799$ yr^{-1}.

Finally, the nice matchup between these bins derived from the proper motion sample (open circles in Figure 1) with the kinematically-unbiased hot star sample (filled circles) and the model slope of Winget et al. (1987) suggests that the effect is not substantial even for the brighter intervals of the proper motion sample. Thus, it is unclear as to what correction needs to be

applied for the missing low velocity stars to define better the shape of the empirical LF. It is clear that the omission of significant numbers of low velocity stars could distort the true shape.

(d) Possible scale height inflation.

Some authors have suggested (Iben and Tutukov 1984; Garcia-Berro et al. 1988) that substantial numbers of cool white dwarfs could be missing from the solar neighborhood due to a greatly increased scale height associated with their larger mean age than that of a typical sample of stars in the solar neighborhood. This effect could be especially important if carbon and oxygen separate in the core, releasing additional energy and slowing the cooling rate by 1.6 Gyr per 0.1 $M_\odot$ of deposited oxygen (Garcia-Berro et al. 1988). Later calculations (Barrat, Hansen and Mochkovitch 1988) indicate that the effect on the white dwarf cooling rate is much more modest, adding only ~ 1 Gyr to the cooling ages.

However, we have a potential empirical test as well: If there were a population of old, dispersed white dwarfs with a scale height 6.6 times that of the typical old disk (Garcia-Berro et al., p. 146), we may expect the sample in the solar neighborhood to reflect this in the mean motions, which should scale approximately as $v_{tan} \sim z$ for a harmonic law. Thus, the mean tangential velocity should "inflate" by a factor of 6 between $M_v = +13$, a luminosity too high for oxygen settling, and $M_v = +15-16$. An examination of Figure 2 suggests a modest indication of an increasing v_{tan} between $M_v \sim +13$ and $+16$, as expected for the increasing mean age of the sample without the inclusion of gravitational settling in the cooling curve. However, the difference in mean velocity among the magnitude bins is not statistically significant. There is little evidence in this data set for the effect of scale height inflation amongst the coolest white dwarfs.

In summary then, it is difficult to quantify the various effects discussed above into a statement about how incomplete the empirical LF reported here might be. The effect of excluded binaries should not exceed the space density of luminous stars plus 10% of the white dwarfs themselves. We argued that the incompleteness due to low velocities is at most a factor of two for the coolest stars, but is likely to be much less. The effect of scale height inflation in pulling stars out of the plane is also likely to be modest. The total mass density of white dwarfs in the solar neighborhood derived from this sample (using a mean mass of 0.6 $M_\odot$) is only 0.002 $M_\odot$ pc^{-3}. It is possible that this density could be as much as doubled by correcting for these effects.

IV. A PRELIMINARY LUMINOSITY FUNCTION FOR WHITE DWARFS OF THE LOCAL HALO

Several of the white dwarfs in this sample clearly have high enough space velocities to be considered interlopers from the halo population. In fact Schmidt (1975) first applied the $1/V_{max}$ method to estimating the local density of halo stars from a bright proper motion sample. This sample included only one white dwarf. He assumed (1) that such a population would have a mean $v_{tan} = 250$ km s^{-1}, based on Oort's (1965) studies of metal-poor RR Lyrae stars; (2) that all stars

with velocities above this value were assignable to the halo population; but (3) that stars falling in the lower half of the distribution would be counted as disk population members. Thus, the density derived from the assigned stars should be corrected upwards by a factor of two.

Depending on the possible existence of a "thick disk" population (Gilmore and Reid 1983), or of an extended non-gaussian, high-velocity tail to the velocity distribution of old disk stars, the Schmidt (1975) assumptions may be too simplified. However, even for an assumed scale height of order 1 kpc, few hypothetical "thick disk" stars would be expected to have tangential velocities reaching 250 km s^{-1}. For a first look at the luminosity function of local halo white dwarfs, let us simply adopt the same prescription, so that comparisons may be made with the total LF of visible halo stars derived by Schmidt in exactly the same way.

Six white dwarfs in this sample have $v_{tan} > 250$ km s^{-1} and are assignable to the halo sample; five of these are fainter than $M_v = +13$. None of the other stars have estimated tangential velocities exceeding 200 km s^{-1}, although some error bars overlap with those of the assigned halo sample. In Figure 3, the LF derived from these six stars is displayed with the disk LF binned in unit M_v intervals, applying the blackbody BC values to both disk and halo degenerate stars.

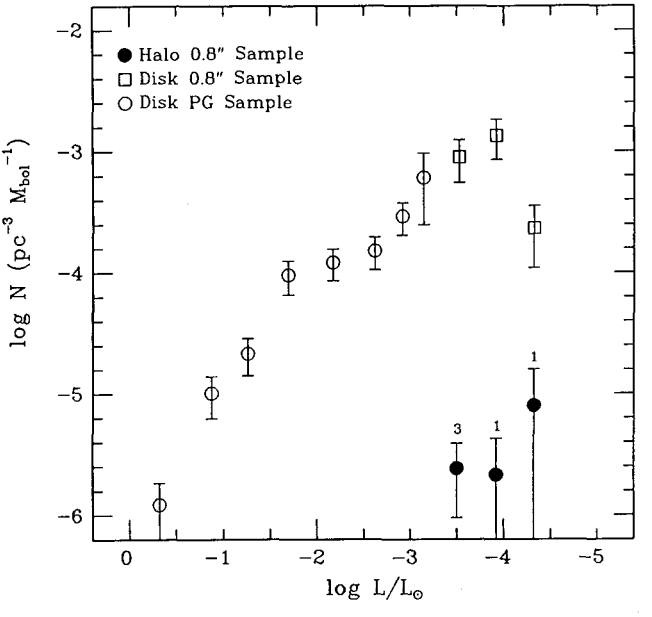

Figure 3. Luminosity functions for the local disk and halo, binned in one bolometric magnitude intervals with blackbody BCs applied.

The total space density of the designated halo sample is 1.3 ($\pm$ 0.6) $\times$ 10^{-5} pc^{-3}, with poisson error bars. Let us compare this with the subset of Schmidt's (1975) Table 2 with $v_{tan} > 250$ km s^{-1}. These add up to total number densities of nondegenerate and degenerate stars of 5.75 $\times$ 10^{-5} and 3.69 ($\pm$ 3.69) $\times$ 10^{-5} pc^{-3}, respectively. The former was derived from 17 main sequence stars with assigned masses between 0.25 and 0.75 $M_\odot$ for which Schmidt assumed the LF was reasonably complete, except for the correction for the low velocity part of the distribution. The latter number was based on one white dwarf star, so that our new result should be an improvement.

If the local halo LF may be approximated as a Salpeter (1955) power law, a comparison of the white dwarf density with that for nondegenerate stars can give a measure of the slope. We shall again follow Schmidt in assuming that the latter applies to the main sequence only in mass range 0.25–0.75 $M_{\odot}$. The white dwarf density should include stars above the appropriate halo turnoff mass of $\sim 0.8–0.9 M_{\odot}$. Since we can make no claims to be complete for white dwarfs as faint as $M_v \sim +15$, this white dwarf LF may not provide a complete census for masses up to the mass limit for the production of neutron stars. The exercise thus yields an upper limit to the power law slope for the local halo mass function.

The ratio of the number density of degenerate stars from this work to nondegenerate stars, as defined above from Schmidt (1975) is 0.22 ± 0.11. For Salpeter mass distributions of the form

$$\xi(M) \sim M^{-\alpha}$$

the *number* ratios of stars for the $0.8–60 M_{\odot}$ and $0.25–0.75 M_{\odot}$ mass intervals are 0.12 for $\alpha = 2$ and 0.49 for $\alpha = 1$, respectively. Our white dwarf space density thus indicates that the local halo mass function slope is not steeper than 2 over this wide range of mass, and may well be considerably flatter, as inferred from proper motion data by Reid (1984). We note that there are contrasting claims for power law slopes in deep CCD analyses of the main sequences of various globular clusters.

The Schmidt prescription leads to a total space density of local halo white dwarfs of $2.6 (\pm 1.2) \times 10–5$ pc^{-3}. This result is two orders of magnitude lower than that derived previously for the white dwarfs of the disk population, before any corresponding correction for the missed low velocity stars. Neither number includes a correction for missed binaries. This ratio for the dying stars compares with ratios derived for main sequence stars of 1/253 from Hartwick, Cowley and Mould (1984), 1/600 by Dawson (1984), or 1/200 by Chiu (1980). The degenerate star ratio, if complete, ought to be somewhat lower since a larger effective interval of the mass function has formed white dwarfs in the halo population.

This first sampling indicates that more extended proper motion samples complete for higher proper motions and to fainter absolute magnitudes may achieve a meaningful description of the local LF for halo white dwarfs. It is curious that one halo star already shows up in the somewhat-sparse faintest magnitude bin, giving that interval a correspondingly high (but precarious) space density. We permit ourselves two premature remarks: First, the halo LF may obviously form a peak at lower luminosity if this is an older population than the local disk. Secondly, the theoretical LF calculations of Iben and Laughlin (1988) assuming a delta function or "impulse" star formation 10^{10} years ago lead us to anticipate a steeper slope prior to the peak in the halo LF.

We thank Matt Wood for pointing out the discrepancy in the hot star luminosity scale discussed in Section 2 here. This work was supported by the National Science Foundation through grant AST 88-40482.

REFERENCES

D'Antona, F. and Mazzitelli, I. 1986, *Astron. Astrophys.*, **162**, 80.

Barrat, J. L., Hansen, J. P. and Mochkovitch, R. 1988, *Astron. Astrophys.*, **199**, L15.

Chiu, L.-T. G. 1980, *Astron. J.*, **85**, 812.

Dahn, C. C., Monet, D. G. and Harris, H. C. 1989, following paper in these proceedings

Dawson, P.C. 1986, *Astrophys. J.*, **311**, 984.

Garcia-Berro, E., Hernanz, M., Mochkovitch, R. and Isern, J. 1988, *Astron. Astrophys.*, **193**, 141.

Gilmore, G. and Reid, N. 1983, *Mon.Not.R.A.S.*, **202**, 1025.

Greenstein, J. L. 1986, *Astron. J.*, **92**, 859.

Hartwick, F. D. A., Cowley, A. P. and Mould, J. R. 1984, *Astrophys.J.*, **286**, 269.

Iben, Jr., I. and Tutukov, A. V. 1984, *Astrophys. J.*, **282**, 615.

Kovetz, A. and Shaviv, G. 1976, *Astron. Astrophys.*, **52**, 403.

Larson, R. B. 1986, *Mon.Not.R.A.S.*, **218**, 409.

Liebert, J. 1978, *Astron. Astrophys.*, **70**, 125.

Liebert, J. 1980, *Ann. Rev. Astr. Ap.*, **18**, 363.

Liebert, J., Dahn, C. C., Gresham, M. and Strittmatter, P. A. 1979, *Astrophys. J.*, **233**, 226.

Liebert, J., Dahn, C. C. and Monet, D. G. 1988, *Astrophys. J.*, **332**, 891.

Luyten, W. J. 1979, *LHS Catalogue*, (Univ. of Minnesota: Minneapolis), 2nd Ed.

Oort, J.H. 1965, in *Galactic Structure*, ed. A. Blaauw and M. Schmidt, (Univ. of Chicago: Chicago), p. 455.

Reid, N. 1984, *Mon.Not.R.A.S.*, **206**, 1.

Robinson, E. L. and Shafter, A. W. 1987, *Astrophys. J.*, **322**, 296.

Saffer, R. A., Liebert, J. and Olszewski, E. 1988, *Astrophys. J.*, **334**, in press.

Schmidt, M. 1975, *Astrophys. J.*, **202**, 22.

Sion, E.M. and Liebert, J. 1977, *Astrophys. J.*, **213**, 468.

van de Kamp, P. 1971, *Ann. Rev. Astr. Ap.*, **9**, 103.

Weidemann, V. 1967, *Zs. f. Astrophys.*, 67, 286.

Winget, D.E., Hansen, C.J., Liebert, J., Van Horn, H.M., Fontaine, G., Nather, R.E., Kepler, S.O. and Lamb, D.Q. 1987, *Astrophys.J. (Letters)*, **315**, L77.

Winget, D.E. and Van Horn, H.M. 1987 in *The Second Conference on Faint Blue Stars*, IAU Coll. 95, eds. A.G.D. Philip, D.S. Hayes and J. Liebert, (L. Davis Press: Schenectady NY) p. 363.

TWO NEW LATE-TYPE DEGENERATES: IMPLICATIONS FOR THE WHITE DWARF LUMINOSITY FUNCTION

Conard C. Dahn, David G. Monet and Hugh C. Harris
U. S. Naval Observatory
Flagstaff, Arizona 86002

I. INTRODUCTION

Recent preliminary USNO CCD parallax solutions for over 100 fields have yielded relative parallaxes with formal errors less than 0.″0030 for approximately 60 faint ($15.9 \leq V \leq 20.3$) stars. The stars observed include a variety of late-type dwarfs, extreme subdwarfs, and degenerates. Among the latter are the well-known, spectroscopically confirmed degenerates LP543−32/33 (= LHS239/240), LP131−66 (= LHS342), LP754−16 (= LHS483), LP702−7 (= LHS542), LP374−4 (= LHS2364), and LP322−800 (= LHS2673), all of which have $M_v \geq 15.0$. In addition, two "new" (in terms of previously lacking both spectroscopic confirmations and absolute luminosity estimates) late-type degenerates were identified — LP53−7 (= LHS1405) and LP550−178 (= LHS2288) — both with proper motions in the range $0.''700 \leq \mu \leq 0.''799$ yr^{-1}.

The white dwarf luminosity function (WDLF) presented by Liebert et al. (1988) and updated slightly in Liebert et al. (1989) employed a $1/V_{max}$ solution for the 43 degenerates contained in the LHS Catalogue (Luyten 1979) which have $\mu \geq 0.''800$ yr^{-1}, $\delta \geq -20°$, and $M_v \geq 13.0$ (hereafter, referred to as the ">8tenths" sample). The most important feature of the derived WDLF is an apparent sharp falloff for $\log(L/L_\odot) < -4.4$, corresponding to approximately $M_{bol} > 15.6$ or $M_v > 16.5$. The identification of LHS1405 and LHS2288 as two new degenerates with $M_v \geq 15.0$ among the LHS stars with $0.''700 \leq \mu \leq 0.''799$ yr^{-1} and $\delta \geq -20°$ (hereafter, the "7tenths" sample) raises the possibility of augmenting the >8tenths sample and thereby improving the statistics of the WDLF determination near the apparent falloff. Success will depend, of course, on the completeness achieved in distinguishing degenerates from non-degenerates within the 7tenths sample.

II. THE 7TENTHS SAMPLE

The LHS Catalogue contains a total of 320 stars within the 7tenths sample. Astrometry, photometry and/or spectroscopy are available in the published literature to establish reliable degenerate versus non-degenerate discriminations for 212 of these objects. Unpublished data, either obtained at USNO or communicated privately to us by various colleagues (e.g., P. Hintzen,

J. Liebert, and R. Probst), establish the nature of an additional 37 stars. Basic data for the eleven stars regarded as established degenerates are collected in Table 1, where an asterisk indicates that a specific explanation is included in the following text. The adopted parallaxes given to four decimal places indicate trigonometric determinations and the values quoted for LHS1341,

TABLE 1

Established White Dwarfs in the 7Tenths Sample

LHS WD	P.M. Vtan	Pi m.e.	V m.e.	B−V m.e.	V−I m.e.	n,n,n Sp.	M_V m.e.
1038	0.718	0.0908	14.36	0.42	0.57	4,4,1	14.15
0009+501	37	0.0037	0.01	0.01		DA8	0.09
1244	0.712	0.0329	17.10	0.82		4,4,-	14.69
0121+401	103	0.0055	0.02	0.06		DC9	0.36
1341	0.799	0.0268	17.8*				14.9
0203+184	141	0.0010	0.3				0.3
1405	0.727	0.0316	18.34		1.23	2,-,2	15.84
0222+648	109	0.0014	0.01		0.03		0.10
1433	0.708	0.020p	17.05	0.37	0.91	1,1,1	13.6p
0239+167	168	0.005					0.5
1693	0.765	0.024p	16.92*				13.8p
0437+093	151	0.004				DA8	0.4
1822	0.793	0.022p	17.96*				14.7p
0600+735	171	0.004				DC9	0.4
2288	0.735	0.0187	19.36		1.20	1,-,1	15.72
1034+078	186	0.0024					0.27
2542	0.706	0.0470	15.32*	0.38		*	13.68
1214+032	71	0.0034				DAs	0.16
2696	0.777	0.031p	18.30		1.37	1,-,1	15.7p
1310+027	119	0.004					0.3
3501	0.790	0.0864	13.71	0.30		3,3,-	13.39
1953−011	43	0.0031	0.05	0.01		DA6	0.09

LHS1405, and LHS2288 are from preliminary USNO CCD solutions. A "p" denotes photometrically derived parallaxes and M_v values. The broadband photometric data (with V−I on the Kron-Cousins system) were obtained either with a single channel photometer on the 61–in reflector (by Dahn) or with a CCD on the 40–in reflector (by Harris). The numbers of individual V, B−V, and V−I observations are specified by n,n,n. The data adopted for LHS1693 and LHS1822 were derived from Greenstein's (1984) MCSP results. The V magnitude for LHS1341 was estimated from unpublished calibrations of m_{pg} and m_R obtained from the LHS Catalogue. Photometric deconvolution of LHS2541/2, a close red dwarf/white dwarf binary, was adopted from Dahn et al. (1976). Where available, spectral types from the McCook and Sion (1987) compilation are included.

Two potential degenerates, the unseen companion responsible for the periodic radial velocity variations reported by Dearborn et al. (1986) for G77−61 (= LHS1555) and LP424−15 (= LHS1986 = WD0807+190), have been explicitly excluded. While the former may well turn

out to be a cool white dwarf, there is presently insufficient information to even roughly estimate its absolute magnitude. However, it is known from astrometry of G77−61 that the system possesses space velocity components characteristic of the halo population so that the star will make essentially zero contribution to the disk WDLF estimated by the $1/V_{max}$ method. Regarding LP424−15, the only reference to the degenerate nature of this star is that presented by McCook and Sion which is erroneous and no other evidence suggesting a WD — either published or unpublished — could be located.

At this time 71 stars within the 7tenths sample lack the necessary astrometry, photometry, and/or spectroscopy to establish their nature. Figure 1 shows the number distributions of reduced proper motion, H_r, for both the >8tenths and the 7tenths samples. Since the >8tenths sample

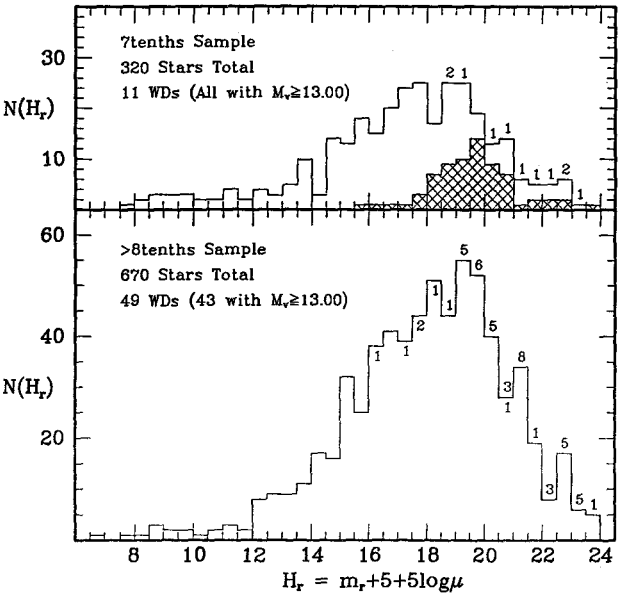

Figure 1. Frequency distributions of reduced proper motion, H_r, for both the 7tenths and >8tenths samples. Numbers of WDs with either $M_v \geq 13.0$ or $M_v < 13.0$ in each bin are given either above or below the bin tops, respectively. The crosshatch area indicates the 71 unobserved stars.

is complete — that is, the degenerate versus non-degenerate status has been observationally established for *all* of the >8tenths stars — a comparison of the two distributions should provide an indication of the likelihood of having unidentified WDs among the unobserved sample. Figure 1 reveals that 20 of the 43 cool WDs found in the >8tenths sample have reduced proper motions within the range $18.0 \leq H_r \leq 21.0$ — just the range within which the 7tenths sample is seriously incomplete. Consideration of the Luyten color classes of the unobserved stars, however, yields a much more encouraging picture. Table 2 gives the numbers of degenerates and nondegenerates within the relevant H_r bins for the various Luyten color classes. The majority of the unobserved 7tenths stars with $18.0 \leq H_r \leq 21.0$ (40 of the total 56) have m color classes. Based upon the complete >8tenths sample, m color class degenerates are known to be extremely rare. [In fact, a total of only 3 degenerates are presently recognized among this color class: LP701−29 (= LHS69),

TABLE 2

Numbers of >8Tenths and 7Tenths Stars by Luyten Color Class

H_r Bin Center	Luyten Color Class a	a–f	f	f–g	g	g–k	k	k–m	m	m+
				The >8Tenths Sample (Degenerates/Non-Degenerates)						
18.25	1/0						0/2	0/12	0/22	0/1
18.75						0/3	0/3	0/3	0/27	
19.25	2/0			1/0	1/0		0/2	0/5	0/36	
19.75	3/0		2/0				1/3	0/9	0/34	
20.25		1/0	1/0			2/0	1/1	0/4	0/29	0/1
20.75	2/0				1/0		0/2	1/2	0/20	
				The 7Tenths Sample (Degenerates/Non-Degenerates/Unknowns)						
18.25							0/0/1	0/4/2	0/6/4	
18.75	2/0/0						0/1/1	0/1/3	0/11/5	0/1/0
19.25	1/0/0	0/0/1					0/2/0	0/3/2	0/9/7	
19.75							0/0/1	0/0/2	0/5/11	
20.25						1/0/0	0/1/2	0/1/0	0/1/7	
20.75		1/0/0					0/1/0	0/1/1	0/4/6	

the unique, highly-blanketed degenerate (Dahn et al. 1978) with $H_r = 22.0$; LP131–66 (= LHS342; Liebert et al. 1979) with $H_r = 22.6$; and LP550–358 (= LHS2288), one of the newly established late-type degenerates reported in this study, with $H_r = 23.4$. Note that all three fall well outside of the H_r range of serious incompleteness for our 7tenths sample.] The data contained in Table 2 suggests that the 15 unobserved stars with k or k–m colors might include one or possibly two additional degenerates. One unobserved star that is almost assuredly a degenerate is the a–f

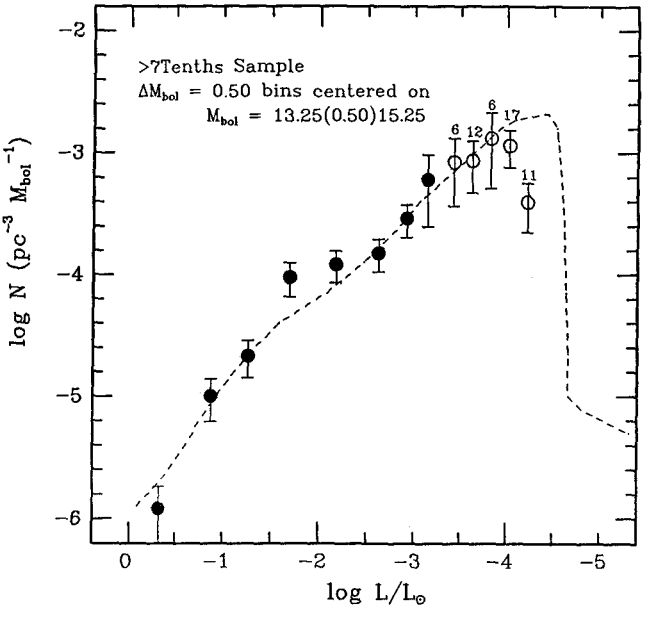

Figure 2. The derived WDLF employing the >7tenths sample degenerates. Filled circles represent the Fleming et al. (1986) data as presented in Liebert et al. (1988) and the dashed curve is the theoretical function of Winget et al. (1987, their Fig. 1). The open circles give the present results where the numbers of stars within each bin are indicated above the error bars.

color object LP737−47 (= LHS2712) with $H_r = 19.4$. Since this star is relatively bright ($V \sim 15.0$ according to our unpublished calibrations of the LHS Catalogue m_{pg} and m_R values) it might have a relatively small value of V_{max} and therefore make a significant contribution to the space density at whatever M_{bol} bin it turns out to occupy. However, based on the blueness of the a–f color class this star most likely has $M_v < 14.2$ and thus will *not* affect the cool end of the WDLF. In summary, the arguments presented above suggest that the degenerates listed in Table 1 comprise a very nearly complete subsample of the 7tenths stars — at least for $M_v < 16.3$.

III. THE WDLF FROM THE >7TENTHS SAMPLE

The 7tenths and >8tenths degenerates together are now referred to as the >7tenths sample. A $1/V_{max}$ analysis identical to that used by Liebert et al. (1988) was performed on the >7tenths degenerates with $M_v \geq 13.0$ and the results are presented in Figure 2. Comparing Figure 2 with the results of Liebert et al. (1989) indicates that the present results are fully consistent with the results from the smaller but fully complete sample, at least over the range $-3.3 \geq \log(L/L_\odot) \geq -4.3$. Since the 7tenths subsample is observationally incomplete for the m color class (which includes degenerates with $M_v > 16.3$ if they exist at densities detectable within the solar neighborhood), the total absence of stars below $\log(L/L_\odot) \sim -4.3$ is based primarily on the Liebert et al. (1988, 1989) results. However, the continued failure to detect such stars within the 7tenths sample does add to the evidence supporting a real turnover in the WDLF at the faint end.

REFERENCES

Dahn, C. C., Harrington, R. S., Riepe, B. Y., Christy, J. W., Guetter, H. H., Behall, A. L., Walker, R. L., Hewitt, A. V., and Ables, H. D. 1976, *Publ. U. S. Naval Observ.*, Second Series, Vol. XXIV, Part III.

Dahn, C. C., Hintzen, P. M., Liebert, J. W., Stockman, H. S., and Spinrad, H. 1978, *Astrophys. J.*, **219**, 979.

Dearborn, D. S. P., Liebert, J., Aaronson, M., Dahn, C. C., Harrington, R., Mould, J. and Greenstein, J. L. 1986, *Astrophys. J.*, **300**, 314.

Fleming, T. A., Liebert, J., and Green, R. F. 1986, *Astrophys. J.*, **308**, 176.

Greenstein, J. L. 1984, *Astrophys. J.*, **276**, 602.

Liebert, J., Dahn, C. C., Gresham, M., Hege, E. K., Moore, R. L., Romanishin, W., and Strittmatter, P. A. 1979, *Astrophys. J.*, **229**, 196.

Liebert, J., Dahn, C. C., and Monet, D. G. 1988, *Astrophys. J.*, **332**, 891.

Liebert, J., Dahn, C. C., and Monet, D. G. 1989, previous paper in these preceedings

Luyten, W. J. 1979, *LHS Catalogue*, (Univ. of Minnesota: Minneapolis), 2nd Ed.

McCook, G. P., and Sion, E. M. 1987, *Astrophys. J. Suppl.*, **65**, 603.

Winget, D. E., Hansen, C. J., Liebert, J., Van Horn, H. M., Fontaine, G., Nather, R. E., Kepler, S. O., and Lamb, D. Q. 1987, *Astrophys. J. (Letters)*, **315**, L77.

PRE-WHITE DWARF EVOLUTION: UP TO PLANETARY NEBULAE

Italo Mazzitelli
Istituto di Astrofisica Spaziale del CNR
Via E. Fermi 21, 00044 Frascati, Italy

ABSTRACT. The main evolutionary phases having some interest for the formation of the remnant white dwarf are discussed, starting from the core helium burning phase, in the attempt of evaluating a theoretical relation between initial main sequence mass and final white dwarf mass. Several difficulties, mainly due (but not only) to uncertainties in the theory of mass loss, have been met, so that only a fiducial bona fide correlation can be drawn. The mass function of population I white dwarfs has probably a secondary maximum at $M \simeq 0.9 - 1\ M_\odot$.

1. INTRODUCTION

In a review of this kind it is very difficult to correctly quote all the researchers who, in the last thirty years, have contributed to our present understanding of the pre-white dwarf stellar evolution. In the following, several results will be given for granted, without explicit quotations, apart from a few cases; it is however to be noted that the most of the discussion will be based upon works by Schönberner, Iben, Becker, Lattanzio, the Padua group (Bertelli, Bressan, Chiosi and coworkers), Packzynski, Wood, Faulkner, D'Antona and myself and, in general, upon the results by people who afforded the risk to plug their hands in the mess of numerical computations. Our thanks to those people who have the courage to do the dirty job, which can be always easily criticized, but which is at the very ground of most improvements in astrophysical knowledge, at the same level as the observational activity.

In principle, the stellar evolution through the WD state could be studied without a previous understanding of the preceeding evolutionary phases (D'Antona 1988). A parametrical approach in which total mass and chemical distribution in the interior can be arbitrarily chosen, is however almost meaningless when the comparison

to the observational data is tried (Mazzitelli and D'Antona 1987), since the initial choice of parameters severely affects the following evolution. For this reason, in the last ten years a number of attempts have been performed to follow the whole stellar evolution from the main sequence to the white dwarf stage (Schönberner 1979, 1981, 1983, 1987a Iben et al. 1983, Iben 1984, Iben and Tutukov 1984, Mazzitelli and D'Antona 1986a Wood and Faulkner 1986), to determine the proper, physically correct choice for the initial white dwarf parameters. In the following, I will try to summarize our present level of understanding of the evolutionary processes having some influence upon the star when it reaches its white dwarf stage. I will limit the discussion to Population I stars, since at present the vast majority of observational informations upon white dwarfs is relative to the solar environment. Since in any case I am left with a mammoth task, I will further restrict the subject, trying to focus my attention upon only one of the various aspects relevant for the understanding of the white dwarfs properties, that is: the relation between initial main sequence mass (M_{in}) and the final white dwarf mass (M_{fin}). Of course, a number of questions cannot yet be solved by theory alone, and I will be forced, in some cases, to take advantage from the observations in the tuning of some free parameters, especially for what concerns the mass loss and/or envelope ejection mechanisms; nevertheless I will always try to stay on the theoretical, modelistic side of the subject, as my intention is to give clues about the theoretical relatively safe conclusions which can be raised, and on those which are still subject to debate, for which there is still room for substantial revisions.

2. STARS EXPERIENCING THE CENTRAL HELIUM FLASH

Let me start by fixing boundaries and internal subdivisions to the range of initial masses which can give rise to white dwarfs.It is very hard to expect disk white dwarfs coming from Population I stars having mass smaller than the solar one, since the pre-white dwarf evolutionary life of the Sun is just of the order of the galactic age. On the other side, there is still no agreement about the maximum initial mass which can die as a white dwarf. In fact, most of the recent computations (Castellani et Al., 1985) seem to show that a star of initial mass about 7 $M_\odot$ ignites carbon off-center in a degenerate core leading, perhaps, to the distruction of the star. Detailed hydrodynamic computations of this carbon ignition are still far from our reach (Iben 1982) but, as we will see, the possibility of a

quiescent carbon burning with the formation of neon-magnesium white dwarfs of mass larger than 1.05-1.1 $M_\odot$ cannot be excluded, at least on the observational ground, so that the upper limiting mass for the formation of white dwarfs can be shifted up to about 9 $M_\odot$ (Iben 1987). In the following I will limit my discussion to stars which do not reach the carbon ignition, but this last possibility has to be taken seriously into account.

The range 1 to 7 $M_\odot$ can be further divided into three subranges, namely:

i) stars undergoing the central helium flash ($M < 2.4\ M_\odot$);

ii) stars gently igniting Helium, and not undergoing the second dredge-up ($M = 2.4 \div 4.5\ M_\odot$, Becker and Iben 1979);

iii) stars undergoing the second dredge-up ($M > 4.5\ M_\odot$).

Let me start from the first mass range. There seems to be at present a general agreement about the relation between the total mass of the star and the core mass at which the helium flash takes place. The results by Rood (1972), Sweigart and Gross (1978), Lattanzio (1986) and Mazzitelli (1988) all agree within about 0.03 $M_\odot$, and the agreement between the last two authors is even better than 0.015 $M_\odot$. This small difference can perhaps be of some significance when studying the details in the HR diagram of the horizontal branch evolution (Caputo et Al 1984), but it is of no matter at all in the more general framework of the pre-white dwarf evolution. Also, agreement exists about the total and core mass for which a non degenerate helium core firstly ignites. Broadly speaking, a core mass about 0.48 $M_\odot$ can be assumed for degenerate ignition in the whole range 1.0 to 2.4 $M_\odot$ for a solar metal abundance and X=0.7, and a core mass about 0.34 $M_\odot$ for the star of 2.5 $M_\odot$ which ignites in non-degenerate conditions (Figure 1). Most unfortunately, if we allow for massive convective overshooting in main sequence (Roxburgh 1978, Maeder and Mermilliod 1981), the whole picture is dramatically modified. In fact, for those stars having a non negligible convective core in main sequence ($M > 1.5\ M_\odot$), overshooting enlarges the core in such a way that, at the central hydrogen exaustion, a helium core about 0.33-0.35 $M_\odot$ is already present (Bertelli et Al 1986), which can gently ignite helium without degenerating. This leads to substantially lower core masses at helium ignition in the mass range 1.5 - 2.5 $M_\odot$, and much larger core masses for $M > 2.5\ M_\odot$, since a general feature of the stellar evolution is that mass of the non degenerate helium core at the helium ignition increases almost linearly with the total mass of the star. Massive overshooting has been recently criticized, on apparently sound bases (Renzini 1987, Baker and Kuhfuss 1987);

nevertheless, this possibility cannot at present be 'a priori' excluded, and I will briefly come back on this subject.

Going on to the central helium burning phase, up to the first thermal pulse, people working in stellar evolution well know the still open debate about the existence of large scale mixing mechanisms, such as semiconvection, overshooting on different scales, and breathing pulses or helium spikes (Robertson and Faulkner 1972, Sweigart and Renzini 1979, Castellani et al. 1985). All these mechanisms strongly affect the horizontal branch evolution, especially for Pop II stars. Luckily enough, it can be shown that, at least for Pop I stars in which a powerful hydrogen burning shell is present in any case, all the core mixing mechanisms have little influence upon the final hydrogen exausted core mass at the first thermal pulse.

Let me define M_H the hydrogen exausted core mass, and M_{He} the helium exausted core mass. Without taking too seriously the following mathematics, we can write in a first approximation:

1) $$\mathrm{Ln}\ L_H = C_1 M_H + C_2$$

which is a "Red Giant" relation between the shell hydrogen luminosity and the core mass. We can write also:

2) $$\mathrm{Ln}\ L_{He} = C_3 M_H + C_4$$

which is instead a "helium main sequence" relation between helium luminosity and helium core mass. Moreover, we can obviously write:

3) $$dM_H/dt = C_5 L_H$$

4) $$dM_{He}/dt = C_6 L_{He}$$

where the various coefficients C_n can be derived, partly from the models, partly from the first principles. Defining t = 0 the beginning time of central helium burning, and t' the time of the first thermal pulse, from 4) and 2) one can write

5) $$M_{He}' = \int_0^{t'} C_7 \exp(M_H)\, dt$$

where M_{He}' is the helium exausted mass at the first thermal pulse. Moreover, from 3) and 1):

6) $$dt = dM_H / C_8 \exp(M_H)$$

and, substituting 6) in 5) with the proper changing of the integration boundaries:

$$M_{He}' = \int_{M_1}^{M_{He}'} C_9 \exp(M_H)\, dM_H$$

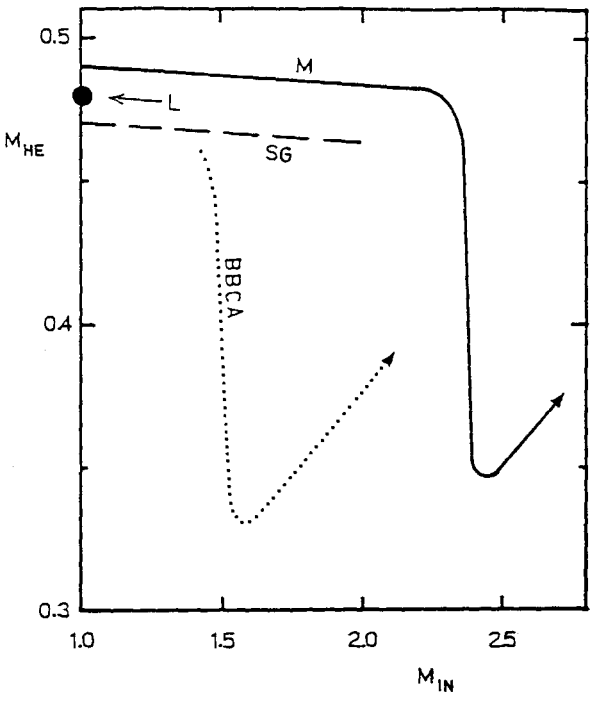

Figure 1: core mass at the central helium ignition for stars at helium flash. The continuous line (M) is relative to computations for the present paper; the point L is from Lattanzio (1987); the dashed line (SG) is extrapolated from Sweigart and Gross (1978) and the dotted line (BBCA) is from Bertelli, Bressan, Chiosi and Angerer (1986), for models with extensive convective overshooting in main sequence.

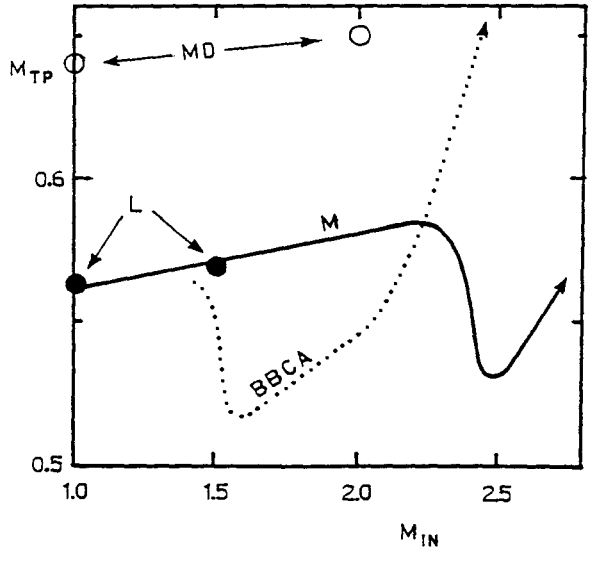

Figure 2: Core mass at the first thermal pulse for the same range of initial masses as in Figure 1. The values labelled MD are from Mazzitelli and D'Antona (1986).

being M_1 the hydrogen-exausted mass at the beginning of central helium burning, and the upper boundary having been put M_{He}' instead of M_H' (the hydrogen exausted core mass at the first thermal pulse), since the two values are coincident within 1 - 2 hundreths of solar mass. One has finally:

$$C_{10} \exp(M_{He}') - C_{11} M_{He}' = C_{10} \exp(M_1)$$

that is: as long as 1) to 4) are verified, the final core mass at the first thermal pulse is a function of the initial core mass only, and not of the details of the helium-burning phase. In more plain words, as long as the luminosity of helium burning follows its main sequence like relation outlined in eq. 2), it is of no importanca at all where helium is burned (at the center, in a convective core or in a thick shell). The problem is rather to understand if eq 2) holds also in thick shell, and this seems to be the case according to the numerical models, at least for stars with masses not larger than 3 $M_\odot$, in which hydrogen and helium burning shells can coexist before the thermal pulses phase.

The behavior of the core mass at the first thermal pulse versus the total mass is shown in Figure 2 (Lattanzio 1986, 1987). As can be seen, almost all the stars undergoing the helium flash give rise to cores in the range 0.57 - 0.58 $M_\odot$ unless, of course, mass loss during the first rise on the red giant branch has not already reduced the total mass of the star below these values. This is possible especially for stars of 1.0 - 1.2 $M_\odot$ with large mass loss rates, which can then die as low mass white dwarfs, possibly in the range 0.50 - 0.55$M_\odot$.

Very different is the case if massive overshooting is present; definitely smaller core masses are found in the range 1.5 - 2.2 $M_\odot$, and much larger core masses for larger total masses (Bertelli et al. 1986). It is however to be recalled that these large differences are due to the differences in core mass at the beginning of the helium burning phase since, as shown before, the core mass at the first thermal pulse is quite insensitive to the behavior of central convection and, in any case, semiconvection and/or breathing pulses have the effect of mixing matter well beyond the formally convective core, almost in the same amount of large overshooting.

In Figure 2, also two values of core mass from Mazzitelli and D'Antona 1986b are shown, and labeled as "upper limits". Care has to be taken with the chemical evolution scheme when performing this kind of computations, since the helium depletion during each time step is proportional to the third power of the helium abundance and, during the time step itself, the helium abundance decreases. In our

computations of 1986, an algorithm was present which tended to overcorrect for this effect, giving rise to lower depletion rates and larger final core masses. In all the other computations, including the present ones and those by Lattanzio (1986, 1987), the abundance variation during the time step is instead computed according to the starting helium abundance, which causes an overestimate of the depletion and gives rise to lower core masses. It is to be expected that a better algorithm would lead to core masses somewhere in between the present values and those by Mazzitelli and D'Antona 1986.

Going ahead through the thermal pulse phase, it can be useful to note that the current calibration for the recurrency period of the thermal pulses versus the core mass (Paczynski 1975) probably gives smaller values than those presently found by several authors with updated input physics (Sweigart 1971, Gingold 1974, Iben 1975 and 1982, Schonberner 1979, Fujimoto 1979, Sackmann 1980, Wood and Zarro 1981, Lattanzio 1986, Mazzitelli 1987). Part of the difference is also due to the fact that Paczynski tuned the relation by computing a very few thermal pulses for each core mass, and all the computations show that at least for the first 10 - 12 pulses, the interpulse period increases. It is then recommended to multiply by a factor 2 - 3 the interpulse periods deduced by the Paczynski relation. This means, in turn, that the total number of thermal pulses experienced by a star during its asymptotic giant branch life is not very large; in the following we will see that it can be of the order of 30-40 in some cases but, for the more frequent cases, it can hardly exceed 10-20. Since the star at the first pulses is underluminous with respect to the equilibrium conditions, the following relations between asymptotic giant branch luminosity and core mass are suggested, holding also for the first pulses. Given a present core mass M_c, and a core mass M' at the first pulse, the steady interpulse luminosity and the peak surface luminosity at the pulse are respectively:

$$\text{Log } L_{steady}/L_\odot = 3.15 + 1.33M_c - 0.3\exp(M'-M_c)/0.015$$

and

$$\text{Log } L_{peak}/L_\odot = 3.25 + 1.5M_c - 0.4\exp(M'-M_c)/0.015$$

The asymptotic branch phase is ultimately truncated by the loss of the hydrogen rich envelope by stellar wind or superwind (Renzini 1981). Most unfortunately, no complete theory based upon the first principles exists to be included in stellar evolution codes. For the wind, the empirical calibration by Reimers (1975) can be of some

utility; for the superwind, only qualitative estimates of orders of magnitude, and indirect evidences exist. The main classes of mass loss mechanisms presently under investigation, upon which Linsky (1987) and Holzer (1987) have given extensive theoretical reviews, are:

-thermally driven winds, that is: steady state radial flow from the chromosphere. The gas density at the critical point (defined as the point where the outflow gas speed exceeds the sound speed) is however too low in all the cases to account for the observed mass loss rates. One has to invent mechanisms to increase the critical density, either by lifting matter in the corona, or shifting the critical point closer to the surface.

-Radiatively driven winds, that is: radiation pressure on ions or, mainly, on circumstellar dust grains. Also in this case the mechanism seems not to work efficiently enough, since the stellar atmosphere theory predicts the grains to be very close to the surface, with greenhouse effect, melting of the grains, cooling, new grains formation and so on, but little or no wind.

-Periodic shock waves in pulsating stars, that is: periodic lifting of gas and grains due to pulsationally driven shock waves, with period shorter than the gravitational return time, so that in the end matter ejection occurs. This is probably the more clearly understood mechanism up today, but if it works for Mira variables, what about non-Miras?

-Alfven waves, that is: the same as before, but driven by hydromagnetic waves. Unfortunately, our present understanding of stellar magnetohydrodynamics is so poor that this mechanism is little more than a free parameter in the theory.

In summary, what we expect is heating and lifting of the atmosphere due to gravitational or hydromagnetic waves, so that the thermally and radiatively driven winds are largely powered. This gives no indication at all about the ignition of the superwind, so that the best the theory can say is that, if the maximum white dwarf mass which can be given birth from a given initial mass is computed according the Reimer's mass loss rate during the asymptotic giant branch evolution, and the minimum white dwarf mass is of course the core mass at the first thermal pulse, the superwind will give rise to a white dwarf mass somewhere in between these two limiting values. This situation is illustrated in Figure 3. The total number of thermal pulses ranges between 5 and 30, and this is relevant when computing the expected enrichment in carbon and s-elements due to the third dredge-up.

As a result of the termination of the asymptotic giant branch phase during a continuous (wind or superwind) mass loss, the chances

are that the blueward excursion for an object in this mass range begins during the interpulse phase, when a steady hydrogen burning shell is powering the star. In fact, from the computations it turns out that about 90% of the total mass lost from the star during a complete thermal pulse cycle is lost during the steady hydrogen burning phase. If it is so, the planetary nebulae nuclei should be hydrogen burners, according to Schönberner (1987), taking also into account the complex picture outlined by Iben (1984) who follows also the case in which a final thermal pulse can take place during the blueward excursion, or the case in which, by chance, the blueward excursion itself begins during a thermal pulse. In practice, according to the above results, and considering that the initial mass function for main sequence stars is peaked around the lower limits, it is to be expected that more than 80% of the white dwarfs have their origin in this way, and more than 70% of them die with a still thick hydrogen envelope, apart of course from the possible depletion of surface hydrogen due to wind in the luminous blue region of the HR diagram.

3. STARS GENTLY IGNITING HELIUM

Let me now go ahead to the second mass range that is: stars gently igniting helium at the center, and not undergoing the second dredge-up. For these stars, the relation between core mass at the helium ignition and initial mass is not flat any more as it was for the first mass range, but the core mass steeply increases, almost linearly with total mass. Of course, also the envelope mass linearly increases and, in principle, this would mean that such stars should experience a larger and larger number of thermal pulses before wind or superwind can stop the asymptotic giant branch evolution. Actually, not only the observations (Iben 1981), but also some theoretical considerations suggest that the game is played in a different way. In fact, when the core mass increases due to the ongoing thermal pulses, both the steady interpulse and peak-of-the-pulse surface luminosities increase, the latter with a 3/2 power of the core mass. At a given point we see from the models that, at the peak of the surface luminosity during a thermal pulse, when the hydrogen shell is completely turned off, several processes occur in the envelope, mainly:

-the hydrogen rich envelope is cooled, lifted and expanded;

-the temperature at the base of the convective envelope drops to a few in 10^5 ^oK, and Hydrogen recombines in almost the whole envelope;

-the total energy of the envelope (including the dissociation and ionization energy) becomes larger than the gravitational binding

energy (of course this does not necessarily mean that the ejection of the envelope is unavoidable, since one has to estimate the conversion efficiency into kinetic energy);

-the radiation pressure at the H-He interface dominates by orders of magnitude (it can be easily more than 99% of the total pressure);

-in the helium rich layers just behind the base of the convective envelope, the mean free path of a photon begins to be a non negligible fraction (some hundreths) of the local stellar radius, so that the radiation field is not isotropic any more, but there is a net radiation flux toward the external layers.

In these conditions, not only the evolutionary computations begin to become very hard, since the specific heat of matter is higly non linear with respect to the thermodynamical quantities, but also the approximation of local isotropy of the energy flux is no longer valid and the numerical results obtained in this hypotesis can be no longer reliable.

In practice, several authors, working in different structural or evolutionary frameworks, have found that a sudden loss of the hydrogen rich envelope it is to be expected at the peak of a thermal pulse, when the core mass ranges between 0.8 and 0.9 $M_\odot$. I can quote the hydrodynamic computations by Kutter and Sparks (1974) for a structure with a helium core powering the luminosity and a turned off hydrogen envelope, the results by Tuchman et Al. (1978) and Barkat and Tuchman (1979) showing that the envelope of a Mira variable at the maximum is unbound and can be ejected beyond a given luminosity, the difficulties met by Faulkner and Wood (1984) in computing advanced thermal pulses, which lead the same Wood and Faulkner (1986) to hypotize the reaching of an "Eddington - like" luminosity at the base of the envelope, and a similar result by myself (Mazzitelli 1987) in the computation of a long run of thermal pulses, with the ratio between mean free path of photons and local radius exponentially increasing from the peak of one pulse to the other.

As can be seen, the effects quoted above are completely different from each other, and seem to have nothing in common; actually, at the very base of all of them there is the enormous lifting and cooling of the hydrogen rich envelope, which causes recombination, large increase in opacity, and the storage of a large amount of energy in the envelope itself. In spite of the uncertainties in the theory, we can reasonably safely conclude that, in these conditions, a detachment of the hydrogen rich envelope is very likely at the maximum surface luminosity at the peak of a thermal pulse, when the core mass is about 0.85 $M_\odot$ (depending on the total mass) and the steady interpulse

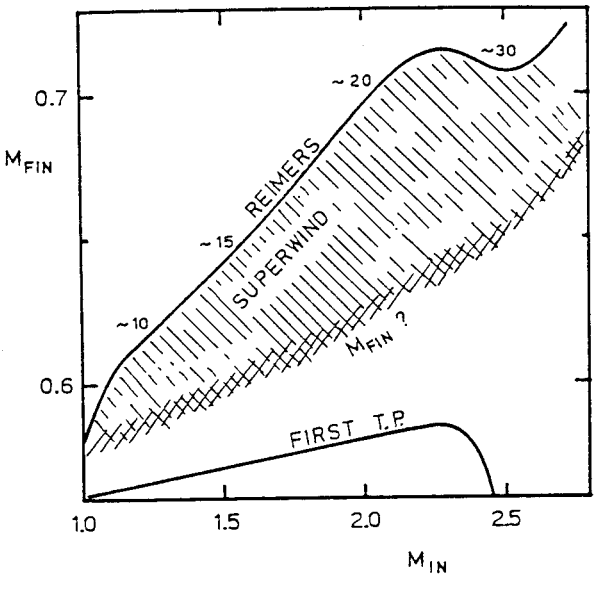

Figure 3: the relation between M_{in} and M_{fin} according to the normal wind (Reimers) and the superwind. The approximate numbers of thermal pulses experienced by stars of various masses are also shown.

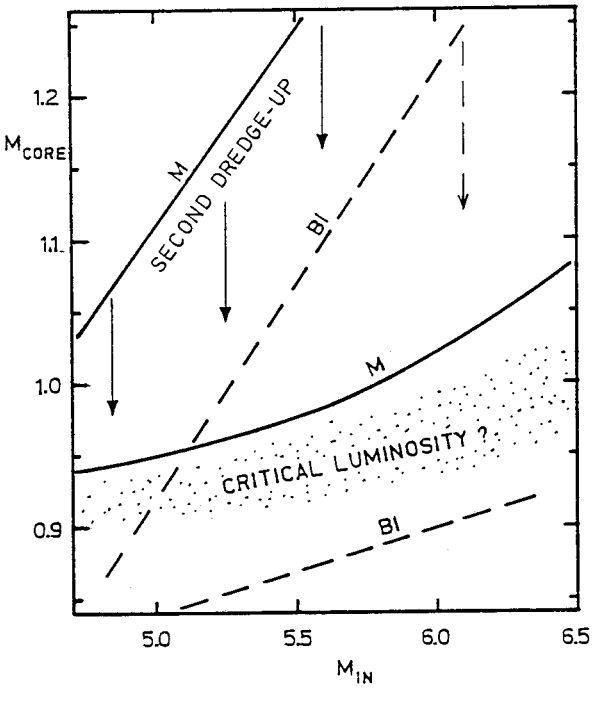

Figure 4: the core mass before and after the second dredge-up are shown for the computations by Becker and Iben (1979, BI dashed lines), and for the present computations (M continuous lines). Also the expected region where the envelope is ejected for critical luminosity is shown.

luminosity is around Log $L/L_\odot$ = 4.3, and this is the mechanism terminating the asymptotic giant branch phase for these stars. Note that, if this is the real occurrence, we can expect very thin hydrogen envelopes upon the white dwarfs originated in this way: in fact, if the hydrogen opacity is the triggering mechanism for the envelope ejection, almost no hydrogen (probably enough for an optical atmosphere, but not for hydrogen burning in the blue) should be left at the surface of the star. We further expect a steep slope in the $M_{fin} - M_{in}$ relation for masses in the range 2.5 - 4 $M_\odot$, since also the mass at the beginning of the helium burning phase sharply increases with total mass. For $M_{in} > 4\ M_\odot$ we then expect a much flatter behaviour, since, for these stars, the evolution in asymptotic giant branch terminates for core masses in a relatively narrow range (0.8 to 0.9 $M_\odot$). Also note that the total number of thermal pulses experienced by these stars reaches a maximum of the order of 50 around 3 - 3.5 $M_\odot$, then fastly decreases to a very few or no thermal pulses at all for larger masses.

4. STARS EXPERIENCING THE SECOND DREDGE-UP

I will finally discuss the last mass range, that is stars experiencing the second dredge-up (Becker and Iben 1979). The core masses before and after the dredge-up as a function of the total mass are shown in Figure 4, where both the results by Becker and Iben and a set of results computed by myself for the present talk are collected. There are some differences due, only in part, to updating of the input physics. One major difference, which unfortunately throws a shade upon the reliability of all these results, is that at the maximum deepening of surface convection during the second dredge-up, all the convective region, down to the base just above the helium burning shell, is largely overadiabatic. This could not be found with previous computer codes, in which the overadiabaticity is considered only in the external subatmospheric layers, but I have found it in the present computations since, being the code a full Raphson-Newton up to the base of the optical atmosphere, overadiabatic convection had to be included all through the structure (in these computations, the ratio of mixing length to pressure scale height is 1.0). As an example, for the star of 6.5 $M_\odot$, an average overadiabatic gradient about 0.2 was found down to the bottom of the convective envelope, around 1.1 $M_\odot$. When recalling that these envelopes are highly dominated by radiation pressure, so that the adiabatic gradient is very close to 0.25, the

consequences of such large overadiabaticity can be easily understood, at least from the side of the reliability of the models. Lacking any better physical treatment than the mixing length theory, we are forced to assume that the stellar models be reliable at least as long as overadiabatic convection is present in thin subatmospheric layers only; it is however hard to believe that a theory which can be responsible for large scale density inversions along more than 80% of a stellar structure can provide physically sound models, to be compared to the observations. In my opinion this is presently another of the boundaries within which the theory of stellar evolution has to be forced.

In the hope that all the models dealing with this phase are not completely meaningless, let me go on to the discussion of the evolution to white dwarf for this mass range. Actually, the general structure of the star at the maximum deepening of the second dredge-up closely resembles the structure at the peak of a thermal pulse. Also in this case the hydrogen rich envelope is cold and enormously expanded (the density at the base of the envelope can be 10^{-6} or 10^{-7} g/cc) and so on, so that it is likely that the envelope itself be blown up without even igniting the first thermal pulse or, since the helium remnant layer above the helium burning shell is, at the maximum penetration of surface convection, still of several hundreths of $M_\odot$, very few thermal pulses can occurr, due to thermal adjustment of the helium layer. The possibility that stars in this mass range die without previously going through a long run of thermal pulses has already been indicated for instance by Iben (1987), on the ground that asymptotic giant branch stars of this kind are by far undernumerous.

Unfortunately, if this is true, we are left with a severe problem. In fact, white dwarfs with masses larger than 1.05 - 1.1 $M_\odot$ were thought to be originated by asymptotic giant branch stars with initial core masses smaller than these values, but undergoing long runs of thermal pulses, and accreting mass upon the core up to the theoretical Chandrasekhar limit since, as already quoted at the beginning, a carbon - oxygen core born with a mass larger than 1.05 - 1.1 $M_\odot$ (depending on the carbon abundance) very fastly ignites. In the above outlined framework, there is no room for white dwarfs of mass larger than 1.05 - 1.1 $M_\odot$, unless they are formed after a violent but not catastrophyc phase of carbon burning, following degenerate ignition, and without the destruction of the structure. In this case, large mass white dwarfs should be formed by ^{22}Mg and ^{24}Mg, but no theoretical models showing this possibility are presently available so that the existence of these white dwarfs is still not explained.

5. CONCLUSIONS

In summary, the relation M_{fin} - M_{in} for the whole range of initial masses of interest is summarized in Figure 5, together with a recent semiempirical relation suggested by Weidemann (1987a). The agreement for low initial masses is quite good, but it is an artificial byproduct of the fact that, knowing almost nothing about the theoretical superwinds, I simply draw a bona fide band not far from the semiempirical calibration. For larger masses, there is a sistematic difference about 0.15 $M_\odot$ with respect to the calibration by Weidemann, but I do not think this disagreement be dramatic since, up today, due to the low statistics, the semiempirical relation is not easily tuned in this region. It is interesting to note that, if the relation follows indeed the band drawn in Figure 5, the mass distribution function of the observed white dwarfs has to show a peculiar behavior. After a peak around 0.6 $M_\odot$ and a sharp decrease up to 0.85 $M_\odot$, the mass function shows a flattening, if not a secondary (very low) peak around 0.9 $M_\odot$, to drop again for larger masses. Actually, this seems to be the case (Weidemann 1987b), although the statistics is too low to be reliable, and we will have to wait perhaps the Hubble Space Telescope for an answer. This theoretical prediction, which could be probably confirmed or ruled out by the observations in a few years, can be a reasonable conclusion for the review.

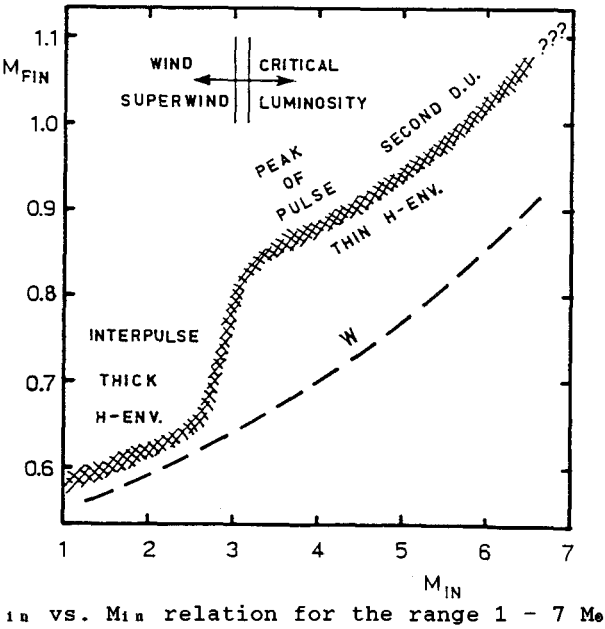

Figure 5: M_{fin} vs. M_{in} relation for the range 1 - 7 $M_\odot$, together with the semiempirical relation (dashed line) obtained by Weidemann (1987a).

REFERENCES

Baker, N. H., Kuhfuss, R. 1987, Astron. Astrophys. 185, 117.
Barkat, Z., Tuchman, Y. 1979, Astrophys. J. 237, 105.
Becker, S. A., Iben, I. Jr., 1979 Astrophys. J. 232, 831.
Bertelli, G., Bressan, A., Chiosi, C., Angerer, K. 1986, Astron. Astrophys. Suppl. 66, 191.
Caputo, F., Castellani, V., Di Gregorio, R., Tornambe', A. 1984 Astron. Astrophys. Suppl. 55, 463.
Castellani, V., Chieffi, A., Pulone, L., Tornambe', A., 1985a, Astrophys. J. Lett. 294, L31.
Castellani, V., Chieffi, A., Pulone, L., Tornambe', A., 1985b, Astrophys. J. 296, 204.
D'Antona, F., 1988, in this volume.
Faulkner, D.J., Wood, P.R. 1984, Proc. Astr. Soc. Australia, 5, 543.
Fujimoto, M. Y., 1979 Publ. Astron. Soc. Japan 31, 1.
Gingold, R. A., 1974 Astrophys. J. 193, 177.
Holzer, T.E. 1987, in IAU symposium No. 122, Circumstellar Matter, ed. I. Appenzeller and C. Jordan (D. Reidel Publ. Co.), 289.
Iben, I. Jr., 1975 Astrophys. J. 196, 525.
Iben, I. Jr., 1981, Astrophys. J. 246, 278.
Iben, I. Jr., 1982 Astrophys. J. 253, 248.
Iben, I. Jr., Kaler, J. B., Truran, J., W. and Renzini, A. 1983, Astrophys. J. 264, 605.
Iben, I. Jr. 1984, Astrophys. J. 277, 333.
Iben, I.Jr., Tutukov, A. V. 1984, Astrophys. J. 282, 615.
Iben, I. Jr. 1987, in Late Stages of Stellar Evolution, S. Kwok and S. R. Pottasch ed., (Reidel,Dordrecht), p. 175.
Kutter, G. S., Sparks, W. M. 1974, Astrophys. J. 192, 447.
Lattanzio, J. C. 1986, Astrophys. J. 311, 708.
Lattanzio, J. C. 1987, in Late Stages of Stellar Evolution, S. Kwok and S. R. Pottasch ed., (Reidel,Dordrecht), p. 235.
Linsky, J. L. 1987, in IAU symposium No. 122, Circumstellar Matter, ed. I. Appenzeller and C. Jordan (D. Reidel Publ. Co.), 271.
Maeder, A., Mermilliod, J. C. 1981, Astron. Astrophys. 93, 136.
Mazzitelli, I., D'Antona, F. 1986a, Astrophys. J. 308, 706.
Mazzitelli, I., D'Antona, F. 1986b, Astrophys. J. 311, 762.
Mazzitelli, I., D'Antona, F. 1987, in IAU Colloquium No. 95 The Second Conference On Faint Blue Stars, L.Davis Press p. 351.
Mazzitelli, I. 1987, in 6th European Workshop on White Dwarfs, Mem. Soc. Astron. Ital. 58, 117.
Mazzitelli, I. 1988, Astrophys, J. in press.
Paczynski, B. 1975, Astrophys. J. 202, 558.
Reimers, D. 1975, Mem. Soc. Roy. Sci. Liege, 6e Ser., 8, 369.
Renzini, A. 1981, in Physical Processes in Red Giants, I. Iben Jr. an A. Renzini Eds., Reidel, Dordrecht, p. 431.
Renzini, A. 1987, Astron. Astrophys. 188, 49.
Robertson, J. W., Faulkner D. J. 1972, Astrophys. J. 171, 309.
Rood, R. T. 1972, Astrophys. J. 177, 681.
Roxburgh, I. 1978, Astron. Astrophys. 65, 281.
Sackmann, I. J. 1980, Astrophys. J. 235, 960.
Schönberner, D. 1979, Astron. Astrophys. 79, 108.
Schönberner, D. 1981, Astron. Astrophys. 103, 119.
Schönberner, D. 1983, Astrophys. J. 272, 708.
Schönberner, D. 1987a, in IAU Colloquium No. 95 The Second Conference On Faint Blue Stars, L.Davis Press p. 201.
Schönberner, D. 1987b, in Late Stages of Stellar Evolution, S. Kwok and S. R. Pottasch ed., p. 337.
Sweigart, A. V. 1971, Astrophys. J. 168, 79.
Sweigart, A. V., Gross, P. G. 1978, Astrophys. J. Suppl. 36, 405.
Sweigart, A. V., Renzini, A. 1979, Astron. Astrophys. 71, 66.
Tuchman, Y., Sach, N., Barkat, Z. 1978, Astrophys. J. 219, 183.
Weidemann, V. 1987a, in Late Stages of Stellar Evolution, S. Kwok and S. R. Pottasch ed., p. 347.
Weidemann. V. 1987b, in IAU Colloquium No. 95 The Second Conference On Faint Blue Stars, L.Davis Press p. 19.
Wood, P. R., Faulkner, D. J. 1986, Astrophys. J. 307, 659.
Wood, P. R., Zarro, D. M. 1981, Astrophys. J. 247, 247.

EVOLUTION OF WHITE DWARFS: STARTING FROM PLANETARY NEBULAE

Francesca D'Antona

Osservatorio Astronomico di Roma
I-00040 MONTE PORZIO (Italy)

1.INTRODUCTION

The ultimate aim in the study of White Dwarf (WD) evolution is to understand properly the observed Luminosity Function (LF) of WDs, that is the number of WDs observed per unit magnitude interval. The complicated route to the interpretation of this scarne quantity (12 fiducial points in the recent update of Liebert et al. 1988) is schematically summarized in figure 1. Clearly, the main input to the LF are the evolutionary (cooling) times, but it is necessary to consider their non trivial dependence on galactic evolutionary inputs, namely the initial mass function of disk stars, their age distribution with time (ultimately: the disk age), and their evolutionary properties. Stellar evolution enters in the problem of cooling by two main routes: first, by determining the mass of the WD as a function of the inital stellar mass and chemistry, second by fixing the internal constitution of the WD remnant for each given mass, and the initial physical conditions at the start of WD evolution (mainly the temperature distribution, which is important for the first phases of evolution). Of course, there is no need of good evolutionary inputs to study "theoretical" WDs. In fact, historically, the first approach in the study of "cooling" (Mestel 1952, Schwarzschild 1958)) has been directly related to the stimulating physical properties of these objects, in which neutrino losses at the beginning (Vila 1966, Savedoff et al. 1969) and, in late stages, liquification and crystallization of the plasma (Brush,Sahlin and Teller 1966, Hansen 1973) long recognized to be dominated by coulomb interactions, (Kirzhnits 1960, Abrikosov 1960, Salpeter 1961), are the main features to be investigated (Mestel and Ruderman 1967, Van Horn 1968, Kovetz and Shaviv 1970).

While also the theory of heat conduction by degenerate electrons went on improving in the course of years (Marshak 1940, Mestel 1950, Hubbard and Lampe 1969, Canuto 1970, to end, recently, with Itoh et al. 1983. 1984), we may regard as a second approach, the stage in which it has been recognized that full consideration should be given

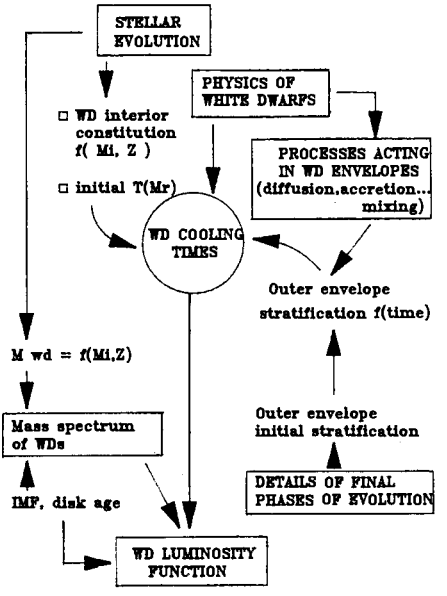

Figure 1: inputs for the determination of the luminosity function

to the envelope physics, (Bohm 1968, Van Horn 1971). The envelope is an incompletely ionized, strongly coupled, partially degenerate plasma, whose physics is much more complex than that of the interior, and this required long studies to assess properly the equation of state (Fontaine et al. 1974, Fontaine and Van Horn 1976, Fontaine, Graboske and Van Horn 1977, Magni and Mazzitelli 1979), while only one attempt has been made, as far as I am aware of, to compute opacities under these extreme conditions (Bohm et al 1977).

Together with the study of cooling properties through the central temperature - luminosity relations obtained by integration of envelope models (Koester 1972, Sweeney 1976), these years see the quantification of convection in the WD envelopes, and the study of possible transitions between hydrogen and helium dominated atmospheres by convective mixing (Baglin and Vauclair 1973, D'Antona and Mazzitelli 1974 and 1975, Vauclair and Reisse 1977) while the first insight is given to the role of additional problems like accretion of interstellar matter, gravitational settling, and radiative acceleration (Strittmatter and Wickramasinghe 1971, Koester 1976, Wesemael 1978, D'Antona and Mazzitelli 1979, Vauclair et al 1979).

In the seventies, two sets of complete models were evolved, by Lamb and Van Horn 1975 and Shaviv and Kovetz 1976. Only starting from 1984, a third approach to the study of WDs evolution begins, with a fundamental paper by Iben and Tutukov (1984): here and in the

following computations (Koester and Schönberner 1986, Mazzitelli and D'Antona 1986, Iben and Mc Donald 1985 and 1986) consideration is given to the construction of the WD, following all the burning phases up to the building up of the degenerate carbon- oxygen core, and simulating mass loss by stellar wind and/or superwind until the WD phase is reached. The starting models for the WD cooling reflects the result of the previous evolution. Iben and Tutukov (1984) first found out that the "evolutionary" remnant hydrogen layer on DA WDs can appreciably contribute to the energy generation at very low luminosity by proton- proton burning.

Nevertheless, the recent results also showed a large spread in the total evolutionary time of WDs according to the different authors: in practice, we (Mazzitelli and D'Antona 1986) had obtained cooling times down to $\log L/L_\odot \sim -4.5$ of the order of 5-7 10^9 yr, others had obtained times longer than 10^{10} yr. These differences have obvious consequences on the weight to be given to the interpretation of the luminosity function of WDs in terms of disk age (D'Antona and Mazzitelli 1978, Winget et al. 1987), and must be clarified.

Winget and Van Horn (1987) have shown that most of the differences between the results of different researchers can be attributed to the different physical and chemical inputs adopted. While we are still comparing our computations in the effort to understand whether this is certain, let us take advantage of this conclusion and realize that, although on the "physics" of WDs there is today broad agreement, the uncertainty in the inputs to be used (see Mazzitelli and D'Antona 1987 for an overview, and Mazzitelli 1988a for an update), is such that the cooling times are "evolutionary" uncertain by at least a factor two!

In practice, our times were shorter mainly for two reasons: i) our models are very oxygen rich, having been obtained by adopting the new reaction rates suggested by Kettner et al. (1982) for the $^{12}C+^{4}He$, and ii) we have chosen envelopes which at low T_{eff} are helium dominated and mostly deprived of metals down to the end of the evolution, adopting very low surface opacities (Cox and Tabor 1976 for $Z=10^{-5}$). Even if 3/4 of WDs show hydrogen dominated spectra, it seems (Greenstein 1986) that most of them are mixed at low T_{eff}, leading to helium dominated atmospheres and fast cooling. Unfortunately, how much Hydrogen is left on the surface (if any) and also how large is the helium layer remnant depend on the <u>details</u> of the final phases of evolution, as it has been shown both by stellar evolution computations (Schönberner 1983, 1987, Iben 1984, Mazzitelli and D'Antona 1986, Wood and Faulkner 1986) and by the theoretical inferences bases also on the

observations (Iben et al. 1983, Renzini 1987). This conclusion is however frustrating, as the final phases of pre-WD evolution, linked to the complex hydrodynamical problem of Planetary Nebula ejection, can be solved up today only parametrically, and the unknowns leave shadows on our global understanding of WD evolution. The fourth approach to the study of WDs is therefore the combination between what we may infer on the external layer composition by the predictions of stellar evolution, and what information we may extract from the observational evidences on WDs, interpreted through the knowledge of the processes acting on WD envelopes. In recent years, this has been the tentative approach of the Canadian group (e.g. Fontaine and Wesemael 1987). The ongoing discussion on the evolution of WDs is another tentative to follow this route.

I will concentrate on:

-the main phases of WD evolution;

-the outer envelope composition, its links to previous evolution, and its influence on the final fate of the WD;

-comparison of theoretical and observational luminosity functions;

-problems with building of cool WD models.

2.THE MAIN EVOLUTIONARY STAGES OF WHITE DWARFS

WD evolution can be divided into five main regimes according mainly to the stellar luminosity. Into these regimes the physical processes which play a major role are different, so as the information which we may derive from observations. These phases are illustrated mainly with the results of our models of 0.68M⊙ (Mazzitelli and D'Antona 1986) and of 0.564M⊙ (D'Antona and Mazzitelli 1989).

1st stage: $\log L/L_\odot > 0$; $\log T_{eff} > 4.7$: "mixed approach to WDs".

This phase includes the late CNO burning -if the remnant hydrogen layer is the maximum possible), the onset of diffusion of CNO elements, the main period in which neutrino losses are dominant and are counteracted by the residual gravitational contraction of the outer layers. Helium burning is never dominant in these stars, although it may have been playing a major role before.

The effect of diffusion of CNO in the interior has been selfconsistently investigated by Iben and McDonald 1985, and has two main effects: it lengthens this phase of evolution, as the reactions $^{12}C \rightarrow ^{14}N$ contribute energy for a longer time, but it leaves a smaller

hydrogen mass on top of the WD so that proton-proton burning at a later stage is less important. In any case, Iben and McDonald showed that diffusion induced nuclear burning can not reduce the mass of the evolutionary remnant by more than a factor two. If there are reasons to believe that in many cases the hydrogen remnant is orders of magnitude smaller, this can not be inputed to this mechanism.

The external layers are fully radiative, but convection in pure helium envelopes begins to appear just at log $T_{eff} \sim 4.70$, with scarce dependence on the gravity and on the treatment of convection.

Observationally, the hottest WDs appear at $T_{eff} > 10^5$K (the PG 1159 class (Wesemael, Green and Liebert 1985) followed by the hottest DAs (the DAOs) and by the DOs. The hottest WDs are helium dominated: while Fontaine and Wesemael (1987) suggest that most DAs appear at $T_{eff} \lesssim 80000$K, where gravitational separation had the time to bring to the surface the amount of hydrogen necessary to form the hydrogen atmosphere, we also know that the WDs of low mass with thick hydrogen layers have radii considerably larger than the corresponding one of helium atmosphere WDs, and, at large T_{eff}, the time of evolution of non DAs can be considerably longer than that of DAs (e.g. Iben and Tutukov 1984 and figure 2). If we consider, on the other hand, an already stratified hydrogen layer of much smaller mass (say $10^{-7}M_\odot$), the radius does not differ significantly from that of the WD in which no hydrogen is present at the surface (e.g. Koester and Schönberner 1986). In practice, PG 1159 WDs may be progenitors of some DA WDs with very thin hydrogen envelopes, as suggested by Fontaine and Wesemael 1987, but the lack of DAs at large T_{eff} may also mean that many DAs have thick ($\sim 10^{-4}M_\odot$) remnant hydrogen layers.

Several features conspire against a meaningfully simple assessment in this first stage:

i) The time of evolution in the PG1159 stage (at $T_{eff} \sim 10^5$yr) is of the order of 10^5yr from all evolutionary computations. Observers must take care in adopting these timescales when trying to derive information on the number of white dwarfs expected in the following evolutionary phases. Models built from non evolutionary starting models do not necessarily give the correct times at these first stages, although later on differences of a million year in the total cooling time becomes negligible. Furthermore, the evolutionary times show a somewhat large dependence on the evolutionary inputs (compare, in figure 2, the timescale for $0.68M_\odot$ and for $0.56M_\odot$). As an entire set of computations for the whole set of parameters to be explored is not yet available, it is difficult at present to say how many selection biases weigh on the interpretation of the hottest WDs;

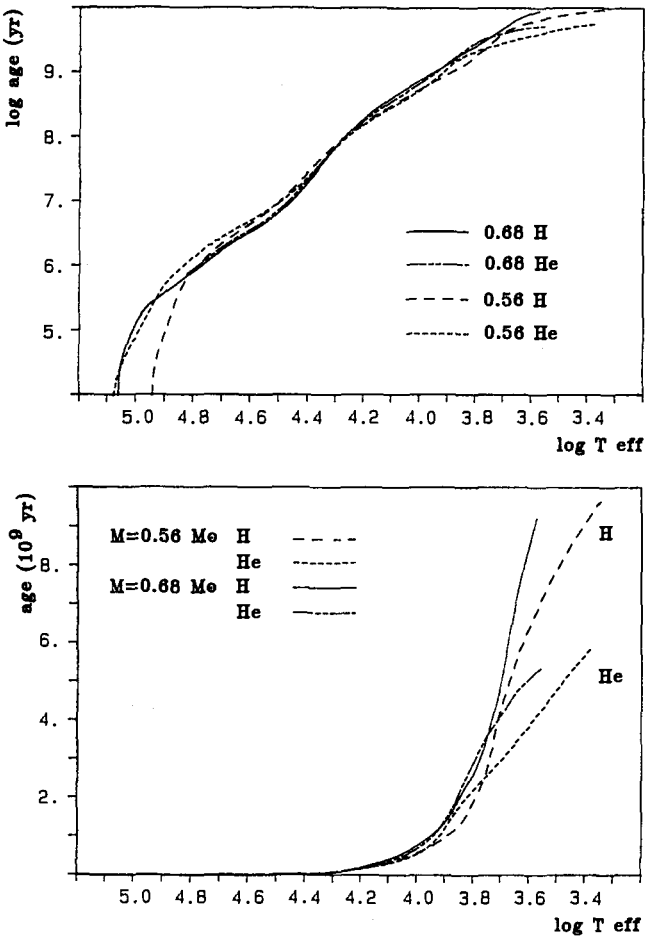

Figure 2: Logaritmic (upper part) and linear (lower part) behavior of evolutionary times with T_{eff} for the models of Mazzitelli and D'Antona 1986 and of D'Antona and Mazzitelli (1989).

ii) it is not easy to derive correct T_{eff} and gravities;

iii) the atmospheric chemical composition is not simply linked to the previous evolution, as radiation pressure, operating on the lines, is the dominant process for establishing a given pattern of abundances, regardless the initial compositions (Vauclair et al 1979, Vauclair 1987);

iv) mass loss is still operating: it is not easy to predict what happens to a given spectral type in the subsequent evolution: for instance, DAOs may become DAs when diffusion of helium sets in, or DBs if the remnant hydrogen is completely lost by wind.

2nd stage: $0 > \log L/L_\odot > -1.5$, $4.7 > \log T_{eff} > 4.3$: "end of neutrino cooling".

In this phase the deviations of the radius from a constant value begin to be negligible. Neutrino cooling decreases, while, possibly, nuclear burning by the p-p chain becomes important. Helium convection begins and becomes progressively more important when decreasing T_{eff}.

In the range $4.65 \lesssim \log T_{eff} \lesssim 4.5$ the HeII lines should be already visible, but there are no DBs (Wesemael et al 1985). The latter appear only at $\log T_{eff} = 4.5$. Pelletier et al (1986) suggest that DO evolve into DAs and, later on, the onset of He convection below the H-layer is able to mix this layer and leads to the appearence of DB stars. Hydrogen masses up to 10^{-15} of the total mass of the star can be mixed at $\log T_{eff} < 4.5$ (Pelletier et al 1986, Liebert, Fontaine and Wesemael 1987, D'Antona and Mazzitelli 1975). Actually, the statistic significance of the DB gap is given by the relative population of the range. The ratio of expected numbers of WDs is equal to the ratio of the relevant cooling times multiplied by the ratio of discovery probability. The ratio of the time spent in the range where DBs are predicted but are not seen ($45000 \gtrsim T_{eff} \gtrsim 30000$K) to the time spent in the DB phase (say $30000 \gtrsim T_{eff} \gtrsim 21000$K and $21000 \gtrsim T_{eff} \gtrsim 12000$K) in our models ranges from 1:9:60 for the $0.68 M_\odot$ evolution (Mazzitelli and D'Antona 1986) to 1:5.3:33 for the evolution of 0.56 and $0.6 M_\odot$. The latter values are consistent also with the ratios derived from Koester and Schönberner (1986) models (1:5:27). As the relative probability of discovery is 1:0.8:0.2 (Wesemael et al. 1985) we should expect from 10 to 17 DBs at $30000 \gtrsim T_{eff} \gtrsim 12000$K for each DB at larger T_{eff}. As in the Palomar Green survey there are 39 DBs, only 2 to 4 hot DBs are missing, and the DB gap can be considered at least partially due to observational selection effects. Wesemael et al (1985) expected from 6 to 7 hot DBs, based on Winget et. al. evolutionary times: this is a further indication that observers must be very careful in the use of evolutionary times at large T_{eff}, as they depend critically on the starting models. I conclude that <u>not necessarily</u> most of DBs come out from mixing of a very thin outer hydrogen layer.

3rd stage: $-1.5 > \log L/L_\odot > -3$ $4.3 > \log T_{eff} > 4.0$: "cooling".

The inner structure is dominated by "cooling", possibly with residual p-p burning if the hydrogen layer is thick. Helium convection in He-envelopes reaches its maximum depth around 10000K. In hydrogen envelopes convection sets in around $\log T_{eff} = 4.2$.

According to the available computations, this is the region where the evolutionary times do not differ too much for "details" of evolution and so this is the best place where to normalize the luminosity function.

From an observational point two interesting classes appear: the DBAs (DBs with hydrogen abundances of 10^{-3} - 10^{-5} -Shipman et al 1987) and the DQs (WDs with C_2 abundances from 10^{-3} to 10^{-7} -Koester et al. 1982, Wegner and Yackovich 1983, 1984). While DBAs are still not well explained -the trace hydrogen can be due to accretion of interstellar matter, and however can not be due to mixing of the hydrogen layer, unless our prediction on convection efficiency are wrong by about two orders of magnitude (see the full discussion by Shipman et al. 1987 and by Koester 1987)- DQs are tracers of previous evolution: carbon appears in the envelope as it is dredged up by the sinking helium convection.

The case of DQs is the best occasion we have to get information on the previous evolution from the WD surface composition. It was obvious even ten years ago that this carbon should come out from the regions of the WD where triple alpha processes had occurred. The first attempts to see whether this carbon could be picked up directly from the core failed: if the helium envelope was so small that helium convection could reach its base, also carbon would have been convective, and a pure carbon composition would have resulted at the surface (D'Antona and Mazzitelli 1979, Fontaine and Michaud 1979). Subsequently, Koester et al (1982) suggested that the appearence of carbon at the surface could be due to the encounter of the convective region with the region in which finite but small abundances of carbon are present due to the effect of diffusion from the core. Relevant computations have been done by Muchmore (1982, 1984), Fontaine et al (1984) and Pelletier et al (1986). As shown by Wegner and Yackovich (1983) the correlation between carbon abundance and T_{eff} predicted by this theory is successfully consistent with the observations. Unfortunately, the best fit is achieved for very small He-buffer layers ($\log M_{he}/M_t = -3.5$ -4.0), but stellar evolution predicts helium intershell remnants from 10^{-3} to 10^{-2} $M_\odot$ (e.g. Mazzitelli and D'Antona 1987). In fact, although there are several phases in which the sudden loss of the hydrogen envelope could keep the <u>pure</u> helium layer at a minimum, on top of the star remains a massive layer in which the carbon abundance is very large. D'Antona and Mazzitelli 1979 suggested that, instead of coming from the core itself of the WD, the Carbon could have been picked up by the helium convection from this region of the He intershell enriched in carbon during the thermal pulse phase.

This would solve the discrepancy between the evolutionary theory and the prediction of the diffusion-convection model, but is contradicted by the results by Muchmore (1984), which imply, at large T_{eff}, very fast settling of carbon even in the regions where it is not a trace element. The whole intershell region is never very small, and fast gravitational settling leaves about 70% of it as a pure helium layer at the top of the WD. This mass can not be smaller than $10^{-3} M_\odot$.

We must therefore look for mechanisms which skip from the WD the most of its helium, to reduce the layer to the $2 \times 10^{-4} M_\odot$ or less indicated by the interpretation of DQs. We can think about:

i) winds in the post planetary nebula phase: if the hot temperature domain is crossed during the stationary helium burning stage, a reasonable rate of $10^{-8} M_\odot$/yr acting for 5×10^4yr is able to do the job. But, if the helium mass is reduced below a percent of solar mass, the 3α reactions can no longer be sustained, the evolutionary times shorten, and the phase of large luminosity, where reasonably strong winds may act, finishes. A further argument against winds is the following: we should probably expect a much larger spread in carbon abundances in the DQs than actually observed.

ii) when a He-shell flash is ignited in the blue, it is very probable that at the peak of the pulse convection reaches the bottom of the hydrogen layer, bringing protons in the region of helium burning , with consequences which up today are predictable only by speculations. The explosive burning of hydrogen, occurring mostly at the base of the convective envelope, could be sufficient to expell the entire helium layer! This occurrence, foreseen by Renzini (1982) was tentatively investigated by Iben et al, 1983 and by Iben 1984 (see also Iben 1987). If any hydrogen is left, (according to Iben et al. 1983, $4 \times 10^{-5} M_\odot$, less than $10^{-6} M_\odot$ according to Iben 1984), it can easily be lost by wind, leading to expose helium and carbon rich layers. It is very easy that a last He-shell flash occurs in the blue mainly for low mass stars. It has been found for instance also in the computations by Caloi (1989) regarding the evolution of very blue horizontal branch stars. The indication that DQs have space velocities larger than the average sample of other spectral types (McMullin et al. 1987, Sion et al. 1988) may be in favour of the interpretation of DQs as a subclass of WDs having suffered a late He-shell flash with hydrogen mixing in their pre-WD life. In the framework of this interpretation, we may regard the extremely carbon rich nucleus of the planetary nebula NGC 246 (Husfeld 1987) as a possible progenitor.

I conclude with a caveat: remember that the results by Pelletier et al (1986) depend on many other parameters: they show that a

turbulent diffusion could modify substantially the situation, by allowing helium shell masses about a factor ten larger ($2x10^{-3}M_\odot$), in substantial agreement with the stellar evolution predictions. Although Pelletier et al. (1986) are not in favour of this interpretation, as the turbulence parameter should be adjusted with the effective temperature, let us remember that also the lithium depletion during main sequence evolution requires the same type of adjustment of turbulent diffusion with T_{eff}.

4th stage: $-3>\log L/L_\odot>-4.5$ $4.0>\log T_{eff}>3.6$: "crystallization".

In the interior crystallization sets in. In the outer hydrogen layer convection reaches its maximum depth at $\log T_{eff} \sim 3.7$. The WD with hydrogen or helium atmospheres become considerably different in their internal structure. If mixing of a "massive" ($10^{-5}M_\odot$) H-layer occurs, the evolution is delayed until the extra-thermal content of the WD is lost (D'Antona and Mazzitelli 1987).

This is probably the most important stage for our understanding of white dwarfs. The input physics of crystallization is assumed as more or less "standard" by all authors. The latest years have seen the interesting development of the idea that oxygen and carbon are not miscible in the solid phase (Stevenson 1980), and that "oxygen snow" settles at the center liberating gravitational energy which contributes to substantially lengthen the evolution. This idea, first developed by Mochkovitch (1983), has been carefully explored recently by Garcia-Barro et al. (1988a and 1988b). A recent new investigation of the crystallization properties of carbon oxygen mixtures indicates however that disordered crystallization, as first assumed by Kovetz and Shaviv 1970 is probably the best approach to the reality (Barrat, Hansen and Mochovitch 1988).

While the interior suffers the transformations which will ultimately lead to the reduction of its thermal energy like in a common crystal, the external layers begin to play a major role.

First of all, we begin to reach critical conditions at the surface. I discuss now these facts on the basis of our latest WD models (D'Antona and Mazzitelli 1989) referring to the evolution of a $1M_\odot$ pop.I star which becomes a white dwarf of $0.564M_\odot$ after losing mass simply by stellar wind during the first and second giant branch evolution. Our previous computations were done down to $\log L/L_\odot \sim -4.5$, as the opacity and e.o.s. employed were not extended enough to study lower luminosities. The e.o.s. has been recently updated by Mazzitelli (1988b) and for the opacities we decided to make extrapolations which

could allow us to perform wider computations, although we must still keep in mind that these must be considered only educated guesses.

If the metals are scarce, as they observationally are in WDs, the densities reached in the atmospheres at low temperature become so large that the photospere is out of the normal available radiative opacity tables (Cox and Stewart 1970, or analogous). At low temperature, large density, the helium is mostly atomic, and we must not worry for electron conduction. We selected one set of radiative opacities (the $Z=10^{-5}$ mixtures by Cox and Tabor 1976), and extrapolated them up to the pressure ionization boundary. At densities large enough that pressure ionization has set in, but at low temperature, the conductive opacities can be computed by the formulation by Itoh et al (1983 and 1984). The result is shown in figure 3.

Inspection of our models shows that, while the T_{eff} declines below 10000K, the structures begin to enter the pressure ionization domain: this has the effect of changing the slope of the relation T_{eff} - Tc in a way which depends on the assumed envelope composition (He, H, or H with large metal content, see as an example figure 10 in Mazzitelli and D'Antona 1986).

5th stage: $\log L/L_\odot < -4.5$, $\log T_{eff} < 3.6$: "Debye cooling".

What happens in the interior at this phase depends critically on the external opacities. After crystallization is completed, Debye cooling will sure set in, but at which luminosity it is still in the phase of debate, further it is not clear whether any stars had enough time to reach the stage of Debye cooling! In order to describe this stage we must therefore rely on models which are able to reach it in a time shorter than the age of the Universe. In our models, actually this happens.

The reasons why we had chosen for these models very low opacities was precisely to understand how short evolutionary times of "typical" WDs could be. Also the fact that these WDs are mainly composed of oxygen conspires to have them get an early crystallization in the interior, so that, by the time the stars are at $\log L/L_\odot = -4.5$ Debye cooling is already very efficient. The total evolutionary time down to $\log L/L_\odot = -5.3$ is 5.8×10^9 yr for the helium envelope models, 9.3×10^9 yr for the hydrogen atmosphere models (figure 2). The central temperature is 3×10^5 K at $\log L/L_\odot = -5.3$, while the relevant Debye temperature:

$$\vartheta_D = 3.48 \times 10^3 (Z/A) \rho^{1/2}$$

at center ($\rho_c = 3 \times 10^6$ g cm^{-3}) is a factor ten larger, and the specific

heat is reduced to $6x10^6$ cgs, while it is $2x10^8$ cgs in normal conditions. However, the temporal evolution of the surface luminosity does not show the signs of acceleration we would have primarily expected. The reasons for this behaviour are examined in the following sections.

The lower T_{eff} models have their photosphere at the boundary of pressure ionization! This interesting feature is by no means new: it had been found in the pure helium models computed by Bohm et al 1977.

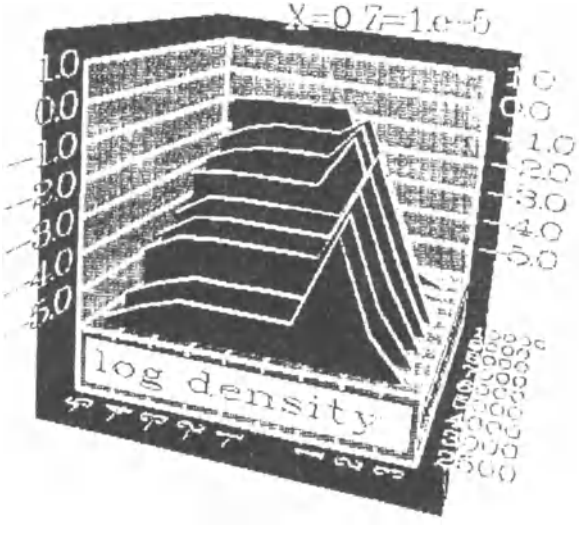

Figure 3: logarithm of the opacities adopted for the helium composition, as function of log ϱ (cgs) and T (K). The pressure ionization is assumed to occur at $0 < \log \varrho < 1$

If we look at the opacities adopted for the helium composition (figure 3), we see that these are so low when helium is not ionized that even the quite low electron conduction opacities which are adopted at log ϱ =1 are two orders of magnitude larger, a plausible explanation of the reason why the photosphere is reached just at this interface. The model having helium surface at log T_{eff}=3.46 resembles quite closely the model plotted by Böhm et al (1977) at logT_{eff}=3.48, even in the central temperature reached. It is interesting to notice that also in the coolest models with hydrogen envelopes the photosphere is reached at the boundary of pressure ionization. We can conclude that the effect of Debye cooling appears at the surface through the opacity of free electrons at the boundary of pressure ionization. This clearly deserves further, much more physically appropriate investigation.

3.THE LUMINOSITY FUNCTION OF WHITE DWARFS

The work on the luminosity function of WDs has seen the efforts of many careful researchers, starting from Luyten (1958) and Weidemann (1967), and ending with Fleming et al (1986), but I think every theoretician should be grateful to Liebert Dahn and Monet 1988 to have made two non simple efforts:

- to take the responsibility to assert that the number density at $\log L/L_\odot \simeq -4.5$ is no longer a lower limit, but a significant point with estimated error bars;

- to convert the observed magnitudes into theoretical values. The different M_V - M_{bol} relations adopted by Liebert et al. 1988 give also a clear hint of how much uncertain we must consider the very low luminosity points.

Let me take advantage of all the previous discussion on evolutionary times to make clear one point: if we want to compare the theoretical and observed LFs, we must find a reasonable way of normalization. It is clear that we must avoid normalization at large luminosities, where the evolutionary times are somewhat dependent on the previous evolution. Probably the best choice for normalization is the region of pure "cooling" at $-1.5 > \log L/L_\odot > -3$, which is safe from dramatic problems, at least if p-p nuclear burning does not play a very important role (as it seems from Iben and McDonald 1985). Further, probably this is also the region in which we may trust the observational points without entering in difficult problems as the drastic decrease of discovery probability (Lamb and Van Horn 1975, Iben and Tutukov 1985).

Let me further define the theoretical LF simply as

$$\log \varphi = \log (dt/ d\log L/L_\odot) + \text{constant}$$

Fit with observations is thus simply a vertical shift which determines the value of the constant. This approach is valid until we may consider the birth rate of WDs constant with time, namely, until the proper WD evolutionary times are not longer than -say- $5 \div 8 \times 10^9$ yr, otherwhise, proper account must be taken of the finite age of the disk in which WDs have been searched (D'Antona and Mazzitelli 1978).

In figure 4 I compare the LF obtained by our latest computed models of $0.56M_\odot$ with the observational LF. I further show the comparison with the previous LF obtained by the evolution of $0.68M_\odot$ WDs with helium or hydrogen envelopes (Mazzitelli and D'Antona 1986, D'Antona and Mazzitelli 1986). I show also the LF from the models of Winget and Van Horn for a disk age of 10^{10} yr, adopted by Liebert et

al. 1988 as a comparison. In figure 6b this LF is shifted, to achieve a better fit of the observational points in the "secure" region at logL/L⊙=-2. The overall shape of the LF is very reasonably fit by our models, particularly by those having helium envelopes, apart from the crucial point at log L/L⊙=-4.5. (The models used in D'Antona and Mazzitelli 1986 were extended only to logL/L⊙ =-4.3, and this problem was not so evident). In particular, there is a good agreement between the theoretical curve and the flattening shown by the observational

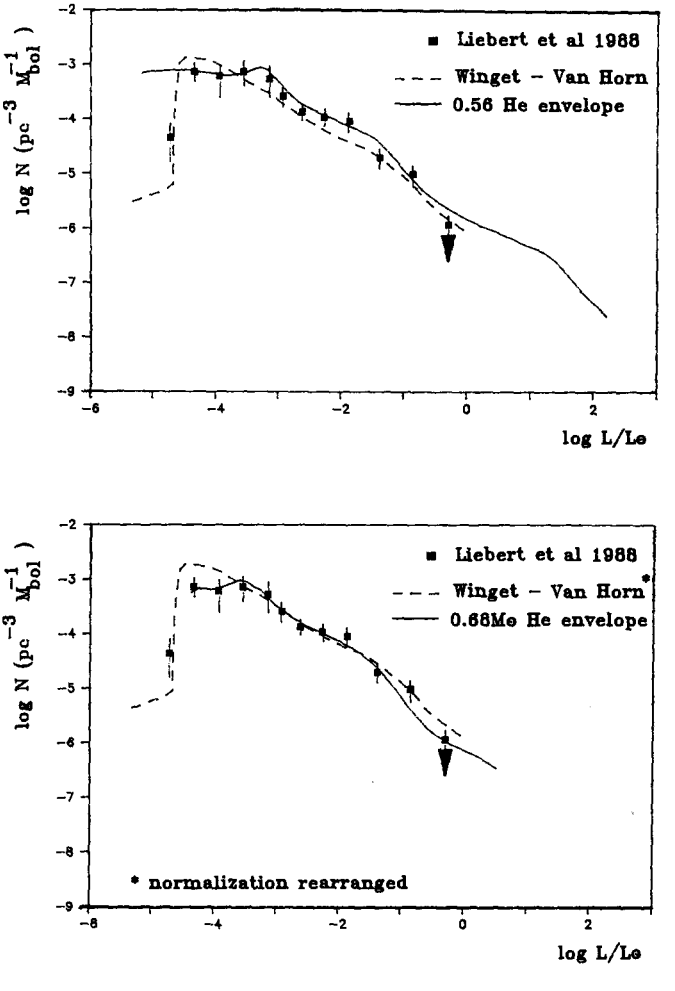

Figure 4:Comparison of observed and theoretical luminosity functions.

LF at logL/L⊙<-3.

Although the following exercize has already been done in many forms, let me derive the dependence of the luminosity function on th luminosity as a function of two quantities: the functional relation between the specific heat and the WD average (central) temperature:

$$C_p \propto T^k_c$$

where k=0 in the case of a gas, and k=3 in the the Debye phase; the second is the relation between central temperature and T_{eff}:

$$T_c \propto T_{eff}^n$$

Simple algebra and the fundamental relations:

$$L = 4 \pi R^2 \sigma T_{eff}^4$$

and

$$L = d E_{th} / dt$$

where the thermal energy is

$$E_{th} \propto T_c^{k+1}$$

provide

$$\varphi = dN/ d\log(L/L_\odot) \propto dt/d\log(L/L_\odot) \propto L^{(n(k+1)/4-1)}$$

in the case of k=0:

$$\varphi \propto L^{(n/4-1)}$$

in the Debye phase:

$$\varphi \propto L^{(n-1)}$$

We can derive the index n from our models. In the first phases, we have n 1.6, but, at logL/L⊙=-3, n suddenly increases to n=2.7 due to the discussed effects of e.o.s. and atmospheric opacities. Here the LF behaviour should change from $L^{-0.6}$ to $L^{-0.3}$. For this reason the helium atmosphere models, where the change of slope of the T_c - T_{eff} relation occurs earlier, seem more appropriate to reproduce the flattening of the LF. In the meantime k becomes larger than zero and the LF shows some decline. Had the n index remained the same, during Debye cooling the LF would have shown a <u>decrease</u> with the power 1.7 of the luminosity. In our models, however, n <u>decreases</u> to $n \simeq 1$, and <u>the LF remains flat</u>.

We see therefore that the results we have obtained are related in a crucial way to the input opacities adopted, which determine the dependence of T_{eff} on T_c. If we want that Debye cooling appears at the

surface with a sharp decrease of the LF, we need a steeper relation, which our (maybe naif) extrapolations do not indicate. It is clear that further exam of the physics in this difficult region begins to be really worthwhile.

As present models seem to reproduce very well the global shape of the LF, but are not able to explain the factor 10 deficit in the WDs at very low luminosity, although they reach Debye cooling very early, we must then investigate the other possibilities.

Both our models and the models by the Texas group (Winget and Van Horn 1987, Wood et al 1987) agree that simple increase of the low temperature opacities is able to increase substantially the evolutionary times so that the drop in the LF acquires the meaning that all WDs formed from the birth of the Universe (or at least of the disk) are still visible (Winget et al. 1987, Liebert et al 1988). To increase the ages we can think either that the metal abundances in the envelopes of cool WDs, although not perfectly determined, are somewhat larger than those we have assumed (see for a summary Koester 1987). Accretion of metals from interstellar clouds may be more and more relevant at later stages of evolution. It is also possible that hydrogen (although not seen in most of cool WDs) is present in cool WDs. Interestingly enough, if this is the case, the very drastic conditions we meet at the photospheric boundary are avoided, and we may also trust more the results (a similar situation is encountered when dealing with brown dwarfs, e.g. D'Antona and Mazzitelli 1985, D'Antona 1987). Finally, maybe that the interior composition of WDs may be not so substantially dominated by oxygen (although for the small masses it is difficult to believe that carbon is more than 20%).

Remember also that, although it helps in solving the factor ten discrepancy in the LFs at $\log L/L_\odot=-4.5$, prolonged cooling may create a problem with the space densities around $\log L/L_\odot=-4.3$, if the numbers given by Liebert et al. 1988 are to be taken at face value.

I conclude that, if the observational luminosity function is correct, we are left with two interesting alternatives: are the metals or hydrogen in the atmospheres of WDs sufficient to considerably prolongate the lifetime at low luminosity? Or is Debye cooling responsible for the drop in the luminosity function, and we are simply missing the correct $T_{eff} - T_c$ relation due to our poor understanding of high density atmospheres and envelope physics?

Acknowledgements: I thank dr. J.Greenstein for an illuminating discussion on the luminosity function at Debye cooling, Vittoria

Caloi, Gilles Fontaine and Detlev Koester for useful conversations and Italo Mazzitelli for a life-long cooperation.

REFERENCES

Abrikosov,A.A. 1960, Soviet Phys.-JETP, 12, 1254.
Baglin,A., Vauclair,G. 1973, Astron.Astrophys. 27,307.
Barrat,J.L.,Hansen,P,Mochkovitch,R. 1988, Astron.Astrophys.199,L15.
Bohm,K.H. 1968, Astrophys. Space Sci. 2,375.
Bohm,K.H., Carson,T.R.,Fontaine,G.,Van Horn,H. 1977, Astrophys.J. 217,521.
Brush,S.G., Sahlin,H.L., Teller,E. 1966, J.Chem.Phys. 45,2102.
Caloi,V. 1989, Astron. Astrophys., in press
Canuto,V. 1970, Astrophys.J. 159,641.
Cox,A.N.,Stewart,J.N. 1970, Astrophys.J. Suppl.Series 19,243.
Cox,A.N.,Tabor,J.E. 1976, Astrophys.J. Suppl.Series 31,271.
D'Antona,F., Mazzitelli,I. 1974, Astrophys. Space Sci. 27, 307.
D'Antona,F., Mazzitelli,I. 1975, Astron.Astrophys. 44, 253.
D'Antona,F., Mazzitelli,I. 1979, Astron.Astrophys. 74,161.
D'Antona,F., Mazzitelli,I. 1985, Astrophys.J. 296,502.
D'Antona,F., Mazzitelli,I, 1986, Astron. Astrophys. 162,80.
D'Antona,F. 1987, Astrophys. J. 320,653.
D'Antona,F., Mazzitelli,I, 1987, in "IAU Coll. 95, "The Second Conference on Faint Blue Stars", ed.A.G.DavisPhilip, D.S.Hayes and J.W.Liebert, L.Davis Press Inc. (Schenectady, New York), p.635.
Fleming,T.A., Liebert,J., Green,R.F. 1986, Astrophys.J. 308,176.
Fontaine,G., Van Horn,H.M., Bohm,K.H., Grenfell,J.C. 1974 Astrophys.J. 193,205.
Fontaine,G. Graboske,H.C., Van Horn,H.M. 1977, Astrophys.J. Suppl. Series 35,293.
Fontaine,G., Van Horn,H.M. 1976, Astrophys.J. Suppl.Series 31,467.
Fontaine,G., Michaud,G. 1979, Astrophys.J. 231,826.
Fontaine,G., Villeneuve,B., Wesemael,F., Wegner,G. 1984 Astrophys.J. 277,L61.
Fontaine,G., Wesemael,F. 1987, in "IAU Coll. 95, "The Second Conference on Faint Blue Stars", ed.A.G.DavisPhilip, D.S.Hayes and J.W.Liebert, L.Davis Press Inc. (Schenectady, New York), p.319.
Garcia-Berro,E.,Hernanz,M.,Mochkovitch,R.,Isern,J. 1988a, Astron.Astrophys. 193,141
Garcia-Berro,E.,Hernanz,M.,Isern,J.,Mochkovitch,R. 1988b, Nature 333,642.
Greenstein,J.L. 1986, Ap.J. 304,334.
Hansen, J.P. 1973, Phys.Rev. 8A,3096.
Hubbard,W.B., Lampe,M. 1969, Astrophys.J. Suppl. 18,297.
Husfeld,D. 1987, in "IAU Coll. 95, "The Second Conference on Faint Blue Stars", ed.A.G.DavisPhilip, D.S.Hayes and J.W.Liebert, L.Davis Press Inc. (Schenectady, New York), p.237.
Iben,I.Jr. 1984, Astrophys.J. 277,333.
Iben,I.Jr.,Kaler,J.B.,Truran,J.W.,Renzini,A. 1983, Astrophys.J. 264, 605.
Iben,I.Jr, Tutukov,A.N. 1984, Astrophys.J. 282,615.
Iben,I.Jr., McDonald,J. 1985, Astrophys.J. 296,540.
Iben,I.Jr., McDonald,J. 1986, Astrophys.J. 301,164.
Iben,I.Jr. 1987, in "Late Stages of Stellar Evolution", ed. S.Kwok and S.R. Pottasch, (D.Reide,Dordrecht), p.175.
Itoh,N.,Mitake,S.,Iyetomi,H.,Ichimaru,S. 1983, Astrophys.J. 273,774.
Itoh,N.,Kohyama,Y.,Matsumoto,J.,Seki,M. 1984, Astrophys.J. 285,758.
Kettner,K.V.,Becker,H.W.,Buchman,L.,Gorres,J.,Kravinkel,H.,Rolf,C. Schmalbrok,P.,Trauttvetter,H.P.,Vliekes,A. 1982, Z.Phys.308,73.
Kirzhnits,D.A. 1960, Soviet Phys.-JETP, 11,365.
Koester,D. 1972, Astron.Astrophys. 16,459.
Koester,D. 1976, Astron.Astrophys. 52, 415.
Koester,D.,Weidemann,V.,Zeidler-K.T.,E.M. 1982, Astron. Astrophys. 116,147
Koester,D., Schönberner,D. 1986, Astron.Astrophys. 154,125.

Koester,D. 1987, in "IAU Coll. 95, "The Second Conference on Faint Blue Stars", ed.A.G.DavisPhilip, D.S.Hayes and J.W.Liebert, L.Davis Press Inc. (Schenectady, New York), p.329.
Kovetz,A., Shaviv,G. 1970, Astron. Astrophys. 8, 398.
Lamb,D.Q., Van Horn,H.M. 1975, Astrophys.J. 200,306.
Liebert,J., Dahn,C.C.,Monet,D.G. 1988, Ap.J. in press.
Liebert,J., Fontaine,G.,Wesemael,F. 1987, Mem.S.A.It. 58,17.
Luyten,W.J. 1958, "On the frequency of White Dwarfs in Space" (Minneapolis: University of Minnesota Observatory).
Magni,G., Mazzitelli,I. 1979, Astron.Astrophys. 72,134.
Marshak,R.E. 1940, Ap.J. 92,321.
Mazzitelli,I. 1988a, in the present Colloquium.
Mazzitelli,I. 1988b, Astrophys.J., in press.
Mazzitelli,I., D'Antona,F. 1986, Astrophys.J. 308,706.
Mazzitelli,I., D'Antona,F. 1987, in "IAU Coll. 95, "The Second Conference on Faint Blue Stars", ed.A.G.DavisPhilip, D.S.Hayes and J.W.Liebert, L.Davis Press Inc. (Schenectady, New York), p.351.
McMullin,J.P.,Fritz,M.L.,Sion,E.M. 1987, in "IAU Coll. 95, "The Second Conference on Faint Blue Stars", ed.A.G.DavisPhilip, D.S.Hayes and J.W.Liebert, L.Davis Press Inc. (Schenectady, New York), p.645.
Mestel.L. 1950, Proc. Cambridge Phil. Soc. 46,331.
Mestel.L. 1952, M.N.R.A.S. 112,583.
Mestel,L., Ruderman,M.A. 1967, M.N.R.A.S. 136,27.
Mochkovitch,R. 1983, Astron.Astrophys. 122,212.
Muchmore,D. 1982, Bull.A.A.S. 13,810.
Muchmore,D. 1984, Astrophys.J. 278,769.
Pelletier,C.,Fontaine,G.,Wesemael,F.,Michaud,G. 1986, Astrophys.J.307,242.
Renzini,A. 1982, in IAU Symp. 99 "Wolf Rayet Stars" ed. C.De Loore and A.Willis (Dordrecht,Reidel), p.413.
Renzini,A. 1983, in IAU Symp. 103 "Planetary Nebulae", ed.D.R. Flower (Dordrecht, Reidel), p.267.
Renzini,A. 1987, in "Planetary Nebulae", IAU Symp.
Salpeter,E.E. 1961, Astrophys.J. 134,669.
Savedoff, M.P., Van Horn,H.M.,Vila,S.C. 1969, Ap.J. 155,221.
Schönberner,D. 1983, Ap.J. 272, 708.
Schönberner,D. 1987 in "Late Stages of Stellar Evolution", ed. S.Kwok and S.R. Pottasch, (D.Reidel,Dordrecht), p.337.
Schwarzschild,M. 1958, in Structure and Evolution of the Stars, Princeton University Press, Princeton.
Shaviv,G., Kovetz,A. 1976, Astron.Astrophys. 51,383.
Sion,E.M.,Fritz,M.L.,McMullin,J.P.,Lallo,M.D. 1988, Astron.J. in press.
Stevenson,D.J. 1980, J.Phys.Suppl. No3, 41,C2-53.
Strittmatter,P.A., Wickramasinghe,D.T. 1971, M.N.R.A.S. 152,47.
Sweeney,M.A. 1976, Astron.Astrophys. 49,375.
Vauclair,G., Reisse,C. 1977, Astron.Astrophys. 61,415.
Vauclair,G.,Vauclair,S., Greenstein,J.L. 1979, Astron.Astrophys.80,79.
Vauclair,G. 1987, in "IAU Coll. 95, "The Second Conference on Faint Blue Stars", ed.A.G.DavisPhilip, D.S.Hayes and J.W.Liebert, L.Davis Press Inc. (Schenectady, New York), p.341.
Van Horn,H.M. 1968, Ap.J. 151,227.
Van Horn,H.M. 1971, in "White Dwarfs", IAU Symp. 42, ed. W.Luyten (Dordrecht: Reidel), p.97.
Vila,S.C. 1966, Astrophys.J. 146, 437.
Wegner,G., Yackovich,F.H. 1983, Astrophys.J. 275,240.
Weidemann,V.1967, Zs. Ap. 67,286.
Wesemael,F. 1978, Astron.Astrophys. 72,104.
Wesemael,F., Green,R., Liebert,J. 1985, Astrophys.J. Suppl. 58,379.
Winget,D.E., Hansen,C.J., Liebert,J., VanHorn,H.M., Fontaine,G., Nather,R.E., Kepler,S.O., Lamb,D.Q. 1987, Astrophys.J. 315,L77.
Winget,D.E., Van Horn,H.M. 1987 in "IAU Coll. 95, "The Second Conference on Faint Blue Stars", ed.A.G.DavisPhilip, D.S.Hayes and J.W.Liebert, L.Davis Press Inc. (Schenectady, New York), p.363.
Wood,P.R., Faulkner,D.J. 1986, Astrophys.J. 307,659.
Wood,M.A., Winget,D.E., VanHorn,H.M. 1987, Faint Blue Stars", ed.A.G.Davis Philip, D.S.Hayes and J.W.Liebert, L.Davis Press Inc. (Schenectady, New York), p.639.

ON THE STRUCTURE OF PRE-WHITE DWARFs

D. Schönberner
Institut für Theoret. Physik u. Sternwarte
Universität, 2300 Kiel, Fed. Rep. Germany

R. Tylenda
Nicolaus Copernicus Astronomical Center
Acadamy of Sciences, Torun, Poland

White dwarfs (WD) are the final configurations of all stars up to initial masses between 5 and 9 M⊙. Two feeder channels for the creation of single WDs can be distinguished: Either evolution through the asymptotic giant branch (AGB) and the following planetary-nebula (PN) phase, or evolution from the horizontal branch through the hot subdwarf region. Prelimary estimates by Drilling and Schönberner (1985) and Heber (1986) indicate that the creation of WDs via the horizontal-branch channel is rather insignificant (few percent of the total WD birthrate) and can be neglected. Thus the evolution through the AGB determines the internal structure of single WDs, and the study of the PN stage serves to elucidate the inital conditions for the white-dwarf evolution.

Schönberner (1981) has presented the first evidences that hydrogen-burning post-AGB models of about 0.6 M⊙ explain well all observed properties of central stars of planetary nebulae (CPN). Although this case has been strengthened further, it remained debatable because of the well-known distance uncertanties. Therefore it is desirable to investigate the PN stage by distance-independent means. A first step into this direction has already been made by Schönberner (1986) and Szczerba (1987). Both anthors made a statistical study of the nebular line strength of He II 4686 Å relative to Hβ and came up with essentially the same results as Schönberner (1981).

In this communication we report on recent results of a similar study where the line ratio [OII] 3727 Å/ [OIII] 4959 Å has been used. We calculated the detailed photoionization in PN models of selected

evolutionary sequences computed by Schmidt-Voigt and Köppen (1987). Computational details will be given elsewhere (Schönberner and Tylenda, in preparation). The advantage of using [OII]/[OIII] instead of HeII/Hß is a greater sensitivity to changing degrees of ionization and an insensitivity to the spectral shape in the ultraviolet (HeII 4686 depends heavily on the 228 Å edge).

We concentrated our efforts on the later phases of the CPN evolution, viz. on the region above and below the turn-around point of the evolutionary tracks in the H-R diagram. Hydrogen-burning post-AGB models are expected to drop very rapidly in luminosity by more than a factor of 10, forcing the planetary to recombine. The [OII]/[OIII] line ratio will then vary accordingly. The following three sequences from Schmidt-Voigt and Köppen (1987) have been selected:

1. $M = 0.64\ M_\odot$, $M_{PN} = 0.19\ M_\odot$,
2. $M = 0.60\ M_\odot$, $M_{PN} = 0.27\ M_\odot$,
3. $M = 0.57\ M_\odot$, $M_{PN} = 0.30\ M_\odot$.

The CPN models are those of Schönberner (1981, 1983), with the evolutionary ages of both the CPNs and PNs taken as proposed there. Table 1 presents the results at some relevant points along these evolutionary sequences. It contains also one calculation for a low-luminosity 0.89 Mo post-AGB model of Wood and Faulkner (1986). The nebular masses are only mean values since these sequences assume mass accretion from the old AGB wind, and the expansion velocities vary between 25 and 40 km/s (see Schmidt-Voigt and Köppen, 1987, for details). A slighthy varying mass has only negligible influences on the nebular ionization.

It can be seen from the Table 1 that the rapid luminosity drop of the post-AGB models (0.64 and 0.60 Mo) forces the planetary to recombine, leading to a corresponding increase of I(3727)/I(4959). As the model's evolution slows down, the continuing nebular expansion leads to some reionisation as indicated by the decreasing line ratio. The ionization remains, however, rather low. In the extreme case of a slowly evolving model (0.57 Mo) together with a fast expanding nebula, recombination does not occur at all. The 0.89 Mo represents the other extreme, viz. the combination of a massive CPN with a massive PN.

Table 1: Properties of selected models

CPN model				PN model			
$M/M_\odot$	$L/L_\odot$	M_V	Age/yr	$M_{PN}/M_\odot$	R/pc	N_H/cm^{-3}	I(3727)/I(4959)
0.64	7675	1.8	3065	0.18	0.08	2300	0.013
	4210	4.2	4240		0.14	500	0.026
	2950	4.7	4440		0.15	420	0.045
	240	6.4	4740		0.16	340	1.9
	160	6.7	5545		0.19	215	2.8
	122	6.9	7870		0.27	75	1.8
	80	7.0	14430		0.49	12	1.0
	68	7.0	20000		0.67	4.5	0.61
0.60	5690	0.3	4780	0.27	0.16	300	0.021
	5145	1.9	6410		0.19	170	0.016
	1300	4.8	9300		0.33	53	0.055
	266	6.2	10530		0.37	37	0.35
	125	6.5	12220		0.43	24	0.89
	113	6.6	17580		0.61	8	0.55
0.57	3730	-0.2	8460	0.30	0.23	220	0.29
	3680	0.0	9250		0.29	90	0.11
	3580	0.7	10750		0.45	25	0.038
	3210	1.8	13750		0.78	5	0.013
0.89	55	8.1	30000	0.58	0.44	47	12

How do these computations compare with observations? To answer this question, we have chosen Kaler's (1983) sample of old PN because these correspond approximately to the models shown in Table 1. We have selected the objects with known [OII] and [OIII] lines (27 objects) and found them to fall into two distinct classes: one with $I(3727)/I(4959) \lesssim 0.1$ and bright central stars (6 objects), and the rest with $0.3 \lesssim I(3727)/I(4959) \lesssim 2$ and faint ($M_V > 5$) central stars (21 objects). All the oldest PN appear to have this low ionization. Inspection of Table 1 then clearly indicates that only PN models illuminated by hydrogen-burning post-AGB models of about 0.6 $M_\odot$ give a very good explanation of the observed ionization in old planetaries. More massive models, say with $M \gtrsim 0.7\ M_\odot$, give rise for too much OII during the low-luminosity stage (cf. 0.89 $M_\odot$ model of Table 1). Contrary, a low-mass model ($M \lesssim 0.57\ M_\odot$) does not fade fast enough as to allow for recombination in an expanding nebula.

Accepting these post-AGB models of ≈ 0.6 M$\odot$ as representative for most central stars, we have to face the following properties of pre-white dwarfs:

i) $M \approx 0.6$ M$\odot$;
ii) hydrogen-rich envelope of $M_e \approx 10^{-4}$ M$\odot$;
iii) helium inter-shell layer of $M_{is} \approx 10^{-2}$ M$\odot$.

Note that the residual hydrogen-rich envelope is determined by the shut-down of hydrogen burning. Should mass loss be important, the only effect would be a faster evolution toward this limiting envelope mass. More details on the influence of mass loss on the post-AGB evolution can be found in Schönberner (1987). The helium-rich intershell layer is a consequence of the interplay between the hydrogen-burning and the helium-burning shell and is determined by the stellar structure equations. Its mass is insensitive to even drastic changes of the energy generation rates (Despain and Scalo, 1976), although it varies by about a factor of 2 during one thermal pulse cycle.

References:

Despain, K.H., Scalo, J.M.: 1976, Astrophys. J. **208**, 789.
Drilling, J.S., Schönberner, D.: 1985, Astron. Astrophys. **146**, L23.
Heber, U.: 1986, Astron. Aastrophys. **155**, 33.
Kaler, J.B.: 1983, Astrophys. J. **271**, 188.
Schmidt-Voigt, M., Köppen, J.: 1987, Astron. Astrophys. **174**, 211.
Schönberner, D.: 1981, Astron. Astrophys. **103**, 119.
Schönberner, D.: 1983, Astrophys. J. **272**, 708.
Schönberner, D.: 1986, Astron. Astrophys. **169**, 189.
Schönberner, D.: 1987, Workshop "Late Stages of Stellar Evolution", S. Kwok, S.R. Pottasch, Eds., Reidel, Dordrecht, p. 337
Szczerba, R.: 1987, Astron. Astrophys. **181**, 365.
Wood, P.R., Faulkner, D.J.: 1986, Astrophys. J. **307**, 659.

TRANSPORT PROCESSES AND NEUTRINO EMISSION PROCESSES IN THE INTERIOR OF WHITE DWARFS

Naoki Itoh

Department of Physics, Sophia University
7-1, Kioi-cho, Chiyoda-ku, Tokyo 102 Japan

ABSTRACT. Recent developments in the studies of the transport processes and the neutrino emission processes in the interior of white dwarfs are reviewed. Special emphasis is placed upon the accuracy of the calculations. Ionic correlation effects play an essential role in the transport processes and the neutrino bremsstrahlung process. The Weinberg-Salam theory is the basis for the calculation of the neutrino emission processes.

1. INTRODUCTION

Transport processes and neutrino emission processes are the key elements in the calculation of the evolution of white dwarfs. Recent developments in plasma physics and high energy physics have made accurate calculations of the transport processes and the neutrino emission processes possible. In this paper we review the recent developments in the studies of the transport processes and the neutrino emission processes in the interior of white dwarfs.

2. TRANSPORT PROCESSES

Recent papers on the transport processes in the interior of white dwarfs include Flowers and Itoh (1976,1979,1981), Yakovlev and Urpin (1980), Raikh and Yakovlev (1982), Itoh et al. (1983), Mitake, Ichimaru, and Itoh (1984), Itoh et al. (1984c), Nandkumar and Pethick (1984), Itoh, Kohyama, and Takeuchi (1987).

2.1 Electrical and thermal conductivities of dense matter in the liquid metal phase

Essential ingredients that go into accurate calculations of the transport properties of the dense matter include the inter-ionic correlations brought about by the strong Coulomb coupling and the electron-ion interaction represented by the screening function of the electrons. Our understanding of such many-particle effects in the

Coulomb system has progressed remarkably during the period of those developments due mainly to the advancement in the Monte Carlo method and other theoretical means (see, e.g., Ichimaru 1982). In this section we take account of what we consider to be the most reliable results currently available on the description of those many-particle effects, and thereby present an accurate calculation of the electrical and thermal conductivities of dense matter limited by electron-ion scattering in the liquid metal phase.

We shall consider the case that the atoms are completely pressure-ionized. We further restrict ourselves to the density-temperature region in which electrons are strongly degenerate. This condition is expressed as

$$T \ll T_F = 5.930 \times 10^9 \left[\left[1 + 1.1018 (Z/A)^{2/3} \rho_6^{2/3} \right]^{1/2} - 1 \right] \ [\mathrm{K}], \qquad (1)$$

where T_F is the Fermi temperature, Z the atomic number of the nucleus, and ρ_6 the mass density in units of 10^6 g cm^{-3}. For the ionic system we consider the case that it is in the liquid state. The latest criterion corresponding to this condition is given by (Slattery, Doolen, and Dewitt 1982)

$$\Gamma \equiv \frac{Z^2 e^2}{a k_B T} = 2.275 \times 10^{-1} \frac{Z^2}{T_8} \left(\frac{\rho_6}{A} \right)^{1/3} < 178 , \qquad (2)$$

where $a = [3/(4\pi n_i)]^{1/3}$ is the ion-sphere radius, and T_8 the temperature in units of 10^8 K.

In the present calculation we restrict ourselves to the cases where the high-temperature classical limit is applicable to the description of the ionic system. Specifically we assume that the parameter

$$y \equiv \frac{\hbar^2 k_F^2}{2 M k_B T} = 1.656 \times 10^{-2} \frac{1}{A T_8} \left(\frac{Z}{A} \right)^{2/3} \rho_6^{2/3} \qquad (3)$$

is much less than unity, where k_F is the Fermi wave number of the electrons and M is the mass of an ion. In Figure 1, we show the parameter domain for the validity of the present calculation in the case of ^{56}Fe plasma.

For the calculation of the electrical and thermal conductivities we use the Ziman formula (1961) as is extended to the relativistically degenerate electrons (Flowers and Itoh 1976). On deriving the formula we retain the dielectric screening function due to the degenerate electrons. As to the explicit expression for the

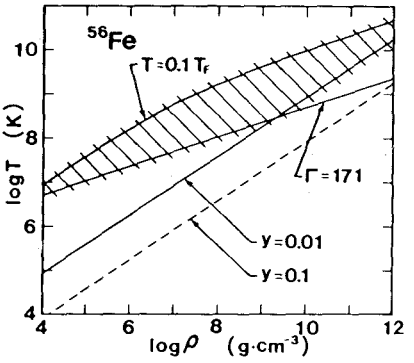

FIG.1. Parameter domain(shaded area) for the validity of the present calculation in the case of ^{56}Fe plasma.

dielectric function, we use the relativistic formula worked out by Jancovici (1962). The use of the relativistic dielectric function is an essential difference between the present work and that of Yakovlev and Urpin (1980). Yakovlev and Urpin set the dielectric function due to electrons equal to unity; this assumption is valid only in the high-density limit.

Working on the transport theory for relativistic electrons given by Flowers and Itoh (1976), we obtain the expression for the electrical conductivity σ :

$$\sigma = 8.693\times 10^{21}\ \frac{\rho_6}{A}\ \frac{1}{[1+1.018(Z/A)^{2/3}\rho_6^{2/3}]\langle S\rangle}\qquad [s^{-1}]. \qquad (4)$$

Here the scattering integral $\langle S\rangle$ is evaluated for $y \ll 1$ as

$$\langle S\rangle = \int_0^1 d\left(\frac{k}{2k_F}\right)\ \left(\frac{k}{2k_F}\right)^3\ \frac{S(k/2k_F)}{[(k/2k_F)^2\varepsilon(k/2k_F,0)]^2}$$

$$-\frac{1.018(Z/A)^{2/3}\rho_6^{2/3}}{1+1.018(Z/A)^{2/3}\rho_6^{2/3}}\int_0^1 d\left(\frac{k}{2k_F}\right)\ \left(\frac{k}{2k_F}\right)^5\ \frac{S(k/2k_F)}{[(k/2k_F)^2\varepsilon(k/2k_F,0)]^2}$$

$$\equiv \langle S_{-1}\rangle - \frac{1.018(Z/A)^{2/3}\rho_6^{2/3}}{1+1.018(Z/A)^{2/3}\rho_6^{2/3}}\ \langle S_{+1}\rangle\ , \qquad (5)$$

where $\hbar k$ is the momentum transferred from the ionic system to an electron, $S(k/2k_F)$ the ionic structure factor, and $\varepsilon(k/2k_F,0)$ the static dielectric screening function due to degenerate electrons. The first term in equation (5) corresponds to the ordinary Coulomb logarithmic term, and the second term is a relativistic correction term.

For the ionic liquid structure factor we use the results of the

improved hypernetted chain (IHNC) theory for the classical one-component plasma (Iyetomi and Ichimaru 1982).

For the thermal conductivity κ for relativistically degenerate electrons we analogously obtain the expression:

$$\kappa = 2.363\times 10^{17}\,\frac{\rho_6 T_8}{A}\,\frac{1}{[1+1.018(Z/A)^{2/3}\rho_6^{2/3}]\langle S\rangle}$$

$$[\mathrm{ergs\ cm^{-1}\ s^{-1}\ K^{-1}}]\ . \qquad (6)$$

where $\langle S\rangle$ is the same as that for electrical conductivity.

We have carried out the integrations in equation (5) numerically by using the IHNC structure factor of the classical one-component plasma and Jancovici's (1962) relativistic dielectric function for degenerate electrons. We have made calculations for the parameter ranges $2 \leqq \Gamma \leqq 160$, $10^{-4} \leqq r_S \leqq 0.5$, which cover most of the density-temperature region of the dense matter in the liquid metal phase of astrophysical importance.

In Figures 2,3,4, and 5 we compare the results of the calculation of $\langle S\rangle$ by Yakovlev and Urpin (1980) (dashed curves) with the present results (solid curves). For the ^{1}H matter and the ^{4}He

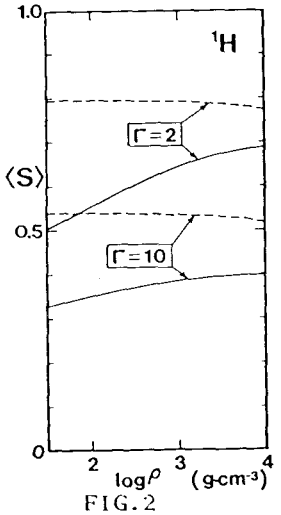

FIG.2

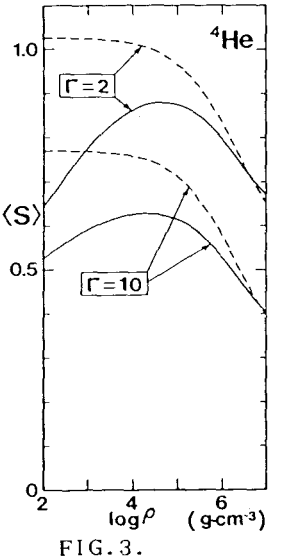

FIG.3.

FIG.2. Comparison of Yakovlev and Urpin's results(dashed curves) with the present results(solid curves) for the ^{1}H matter.

FIG.3. Same as FIG.2. for the ^{4}He matter.

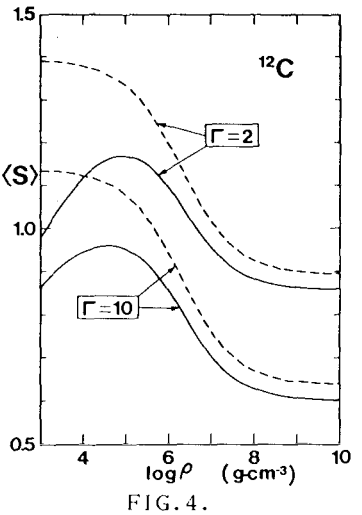

FIG.4.

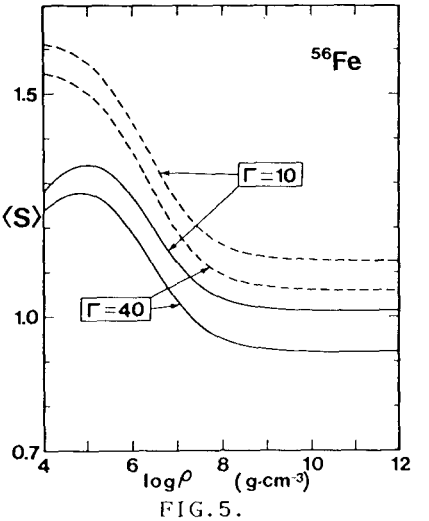

FIG.5.

FIG.4. Same as FIG.2. for the ^{12}C matter.

FIG.5. Same as FIG.2. for the ^{56}Fe matter.

matter Yakovlev and Urpin's results amount to an overestimation of ⟨S⟩ by 60% at low densities. For the ^{12}C matter their overestimation of ⟨S⟩ amounts to 40% at low densities. For the ^{56}Fe matter their overestimation is nearly 30% at low densities. At high densities Yakovlev and Urpin's results are reasonably close to the present ones. The large amount of the overestimation of ⟨S⟩ at low densities by Yakovlev and Urpin is due to their neglect of electron screening. At high densities, however, the effect of the screening due to electrons is relatively small. This is the main reason for their overestimation of the resistivity (underestimation of the conductivity) at low densities.

2.2 Electrical and thermal conductivities of dense matter in the crystalline lattice phase

In this section we deal with the electrical and thermal conductivities of dense matter in the crystalline lattice phase $\Gamma > 178$. The electrical conductivity σ and thermal conductivity κ are related to the effective electron collision frequencies ν_σ and ν_κ by

$$\sigma = \frac{e^2 n_e}{m^* \nu_\sigma} = 1.525 \times 10^{20} \frac{Z}{A} \rho_6 \left[1+1.018 \left(\frac{Z}{A}\rho_6\right)^{2/3}\right]^{-1/2} \times \frac{10^{18}\ s^{-1}}{\nu_\sigma}\ s^{-1}\ , \qquad (7)$$

$$\kappa = \frac{\pi^2 k_B^2 T\, n_e}{3m^* \nu_\kappa} = 4.146\times 10^{15}\frac{Z}{A}\,\rho_6\,[1+1.018\,(\frac{Z}{A}\rho_6)^{2/3}]^{-1/2}$$

$$\times T_8\,\frac{10^{18}\ s^{-1}}{\nu_\kappa}\quad \text{ergs cm}^{-1}\ \text{s}^{-1}\ \text{K}^{-1}\ , \qquad (8)$$

where n_e is the number density of electrons and m^* is the relativistic effective mass of an electron at the Fermi surface. In this section we are interested in the scattering of electrons by phonons. The collision frequencies ν_σ and ν_κ due to one-phonon processes can be calculated by the variational method (Flowers and Itoh 1976; Yakovlev and Urpin 1980; Raikh and Yakovlev 1982) as

$$\nu_{\sigma,\kappa} = \frac{e^2}{\hbar v_F}\,\frac{k_B T}{\hbar}F_{\sigma,\kappa} = 9.554\times 10^{16} T_8\,\{1+\frac{1}{1.018[(Z/A)\rho_6]^{2/3}}\}^{1/2}$$

$$\times F_{\sigma,\kappa}\ \ s^{-1}\ , \qquad (9)$$

$$F_{\sigma,\kappa} = \frac{2\gamma^2}{S^2}\int \frac{dS\ dS'}{k^4\,|\,\varepsilon(k,0)\,|^2}\ [1-(\frac{\beta k}{2k_F})^2]\ e^{-2W(k)}\,|\,f(k)\,|^2$$

$$\times \sum_{s=1}^{3}[k\cdot\hat{\varepsilon}_s(p)]^2(e^{z_s}-1)^{-2}e^{z_s}g_{\sigma,\kappa} \qquad (10)$$

In the above the integral is over the areas of the Fermi surface, k is the momentum transfer, $\hat{\varepsilon}_s(p)$ the polarization unit vector of a phonon with momentum p and polarization s, and

$$\gamma \equiv \frac{\hbar\omega_p}{k_B T} = 7.832\times 10^{-2}\,\frac{Z}{(AA')^{1/2}}\,\frac{\rho_6^{1/2}}{T_8} = 0.3443\,\frac{\rho_6^{1/6}}{A^{1/6}(A')^{1/2}Z}\,\Gamma\ , \qquad (11)$$

$$\beta \equiv \frac{\hbar k_F c}{E_F} = \{1+\frac{1}{1.018[(Z/A)\rho_6]^{2/3}}\}^{-1/2}\ , \qquad (12)$$

$$z_s \equiv \frac{\hbar\omega_s(p)}{k_B T}\ , \qquad (13)$$

$$g_\sigma = k^2\ , \qquad (14)$$

$$g_\kappa = k^2 - \frac{k^2 z_s^2}{2\pi^2} + \frac{3k_F z_s^2}{\pi^2}\ , \qquad (15)$$

ω_p being the ionic plasma frequency. The momentum conservation requires $k=\pm p+K$, where K is the reciprocal-lattice vector for the Brillouin zone to which k is confined. In equation (10) we have included the dielectric screening function due to relativistically

degenerate electrons $\varepsilon(k,0)$, the Debye-Waller factor $e^{-2W(k)}$, and the atomic form factor $f(k)$. Yakovlev and Urpin (1980) and Raikh and Yakovlev (1982) have used the Thomas-Fermi screening and set $e^{-2W(k)}=1$, $f(k)=1$.

The phonon spectra are modified by the screening due to electrons. The longitudinal optical phonon turns into an acoustic phonon in the long-wavelength limit, whereas the original transverse acoustic phonons are little affected by the electron screening (Pollock and Hansen 1973). Because the low-frequency transverse phonons play dominant roles in the resistivity of dense stellar matter, we neglect the effects of the electron screening on the phonon spectra and use the frequency moment sum rules for the pure Coulomb lattice.

As we consider the case in which the Fermi sphere is much larger than the Debye sphere, $(k_F/k_D)^3=Z/2 \gg 1$, Umklapp processes contribute to the scattering dominantly, and the vector k in equation (10) most probably falls in a Brillouin zone distant from the first zone. When we perform an integration within a single distant zone corresponding to the reciprocal-lattice vector K, we can make an approximation k=K in the integrand and carry out an integration over p within the first zone only.

Here we follow the semianalytical approach adopted by Yakovlev and Urpin (1980) and also by Raikh and Yakovlev (1982). We write

$$\sum_{s=1}^{3}[\mathbf{k}\cdot\hat{\boldsymbol{\varepsilon}}_s(\mathbf{p})]^2 z_s^n(e^{z_s}-1)^{-2}e^{z_s} \approx \frac{\pi n_k^2}{\gamma^2}\,G^{(n)}(\gamma)\,, \qquad (16)$$

$$G^{(n)}(\gamma) = \frac{\gamma^2}{3V_B\pi^n}\sum_{s=1}^{3}\int d\mathbf{p}\; z_s^n(e^{z_s}-1)^{-2}e^{z_s}\,, \qquad (17)$$

where n=0 or 2, and integration is carried out over the first Brillouin zone, whose volume is V_B. By the use of this approximation F_σ and F_κ in equation (10) are expressed as

$$F_\sigma = I_\sigma\, G^{(0)}(\gamma)\,, \qquad (18)$$

$$F_\kappa = I_\sigma\, G^{(0)}(\gamma) + I_\kappa^{(2)}\, G^{(2)}(\gamma)\,, \qquad (19)$$

$$I_\sigma = \int_{-1}^{\mu_{\max}} d\mu\; \frac{e^{-2W(q)}\,|f(q)|^2}{|\varepsilon(q,0)|^2}\,(1-\beta^2 q^2)\,, \qquad (20)$$

$$I_{\kappa}^{(2)} = \int_{-1}^{\mu_{max}} d\mu \; \frac{e^{-2W(q)}|f(q)|^2}{q^2|\varepsilon(q,0)|^2}(1-\beta^2q^2)\left(-\frac{1}{2}q^2+\frac{3}{4}\right) , \quad (21)$$

$$q = \left(\frac{1-\mu}{2}\right)^{1/2} , \quad (22)$$

$$q_{min} = \left(\frac{1-\mu_{max}}{2}\right)^{1/2} , \quad (23)$$

$$\mu_{max} = 1-0.3575Z^{-2/3} . \quad (24)$$

Here we have introduced a small momentum transfer cutoff q_{min} corresponding to the unavailability of Umklapp processes for $q<q_{min}$. The contributions of the normal processes are very much smaller than those of the Umklapp processes. For the choice of q_{min} we follow Raikh and Yakovlev (1982). Yakovlev and Urpin (1980) derived the asymptotic expressions of $G^{(0)}(\gamma)$ and $G^{(2)}(\gamma)$ for $\gamma \ll 1$ and $\gamma \gg 1$, and proposed the following analytic formulae for arbitrary γ, which fit the main terms of the asymptotic expressions:

$$G^{(0)}(\gamma)=u_{-2}\left[1+\left(\frac{3u_{-2}\gamma^2}{\pi^2c_2}\right)\right]^{-1/2}\approx 13.00(1+0.0174\gamma^2)^{-1/2} , \quad (25)$$

$$G^{(2)}(\gamma)=\frac{\gamma^2}{\pi^2}\left[1+\left(\frac{15}{4\pi^4c_2}\right)^{2/3}\right]^{-3/2}\approx\frac{\gamma^2}{\pi^2}(1+0.0118\gamma^2)^{-3/2}, \quad (26)$$

where $u_{-2}\approx 13.00$ (Pollock and Hansen 1973) and $c_2=29.98$ (Coldwell-Horsfall and Maradudin 1960) are the numerical constants that are characteristic of the phonon spectrum of the bcc Coulomb lattice. Raikh and Yakovlev (1982) calculated $G^{(0)}(\gamma)$ and $G^{(2)}(\gamma)$ numerically with the exact spectrum of phonons for $\gamma<100$. It has been confirmed that the fitting formulae (25) and (26) have an accuracy better than 10% even at $\gamma \sim 1$.

We have carried out the numerical integrations of equations (20) and (21) for ^{4}He, ^{12}C, ^{16}O, ^{20}Ne, ^{24}Mg, ^{28}Si, ^{32}S, ^{40}Ca, ^{56}Fe. Some of the results are presented in Figures 6-9. For comparison we have also included the case where we have neglected the effects of the Debye-Waller factor and set $e^{-2W}=1$. We also show the results of Raikh and Yakovlev (1982) which are

$$[I_{\sigma}]_{RY} = 2 - \beta^2 , \quad (27)$$

$$[I_{\kappa}^{(2)}]_{RY}= \ln Z - \beta^2 + 1.583 . \quad (28)$$

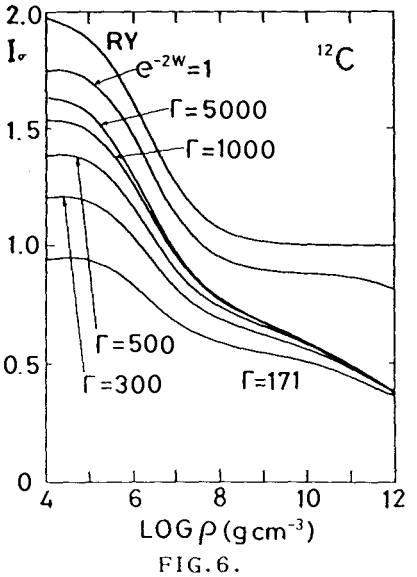

FIG.6.

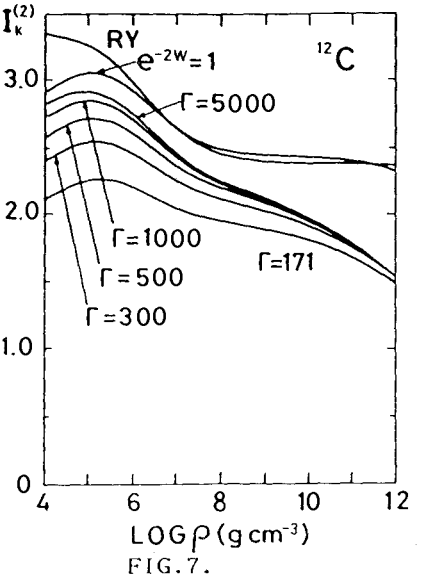

FIG.7.

FIG.6. I_σ for the ^{12}C matter. RY stands for the results of Raikh and Yakovlev(1982).

FIG.7. $I_\kappa^{(2)}$ for the ^{12}C matter.

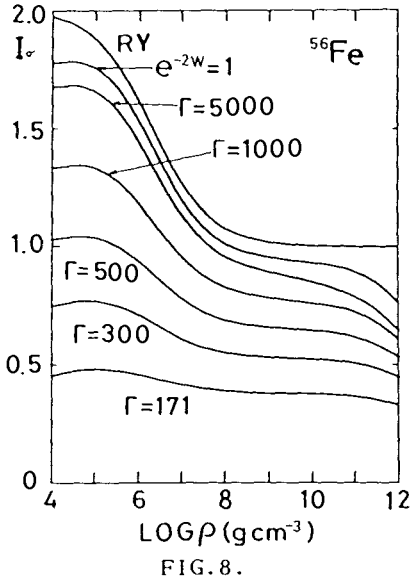

FIG.8.

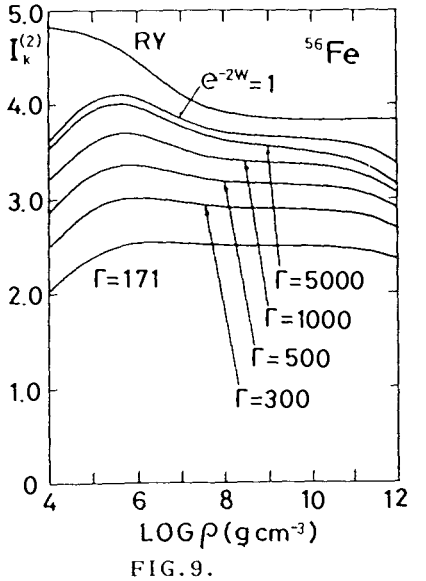

FIG.9.

FIG.8. I_σ for the ^{56}Fe matter.

FIG.9. $I_\kappa^{(2)}$ for the ^{56}Fe matter.

It is readily seen that the Debye-Waller factor reduces the resistivities (enhances the conductivities) by a factor of 2-4 near the melting temperature. This means that the results of Yakovlev and Urpin (1980) and those of Raikh and Yacovlev 1982) give too low conductivities by that factor. It is very interesting to observe that the present result is fortuitously rather close to the original Flowers-Itoh conductivity in the crystalline lattice phase near the melting temperature (Flowers and Itoh 1976,1981).

3. NEUTRINO EMISSION PROCESSES

Recent papers on the neutrino energy loss rates include Munakata, Kohyama, and Itoh (1985), Kohyama, Itoh, and Munakata (1986), Itoh, and Kohyama (1983), Itoh et al. (1984d), Itoh et al. (1984a), Itoh et al. (1984b), Munakata, Kohyama, and Itoh (1987), Schinder et al. (1987), and Itoh et al. (1988).

3.1 Photoneutrino process

The energy loss rate per unit volume per unit time due to the photoneutrino process is expressed as (Munakata, Kohyama, and Itoh 1985)

$$Q_{photo} = \frac{1}{2}\,[(C_V^2+C_A^2) + n(C_V'^2+C_A'^2)]\,Q^+_{photo} - \frac{1}{2}\,[(C_V^2-C_A^2) + n(C_V'^2-C_A'^2)]\,Q^-_{photo}\ , \tag{29}$$

$$C_V = 1/2 + 2\sin^2\theta_W\ ,\quad C_A = 1/2\ , \tag{30}$$

$$C_V' = 1 - C_V\ ,\quad C_A' = 1 - C_A\ , \tag{31}$$

$$\sin^2\theta_W = 0.23\ , \tag{32}$$

where θ_W is the Weinberg angle, and n is the number of the neutrino flavors other than the electron neutrino whose masses can be neglected compared with k_BT.

As in Munakata, Kohyama, and Itoh (1985) we have carried out Monte Carlo computations, using the method of importance sampling, to evaluate the five-dimensional integral which appears in Q^+_{photo} and Q^-_{photo}. In all the calculations of the photoneutrino process we used 50000 random points. Schinder et all. (1987) used 50000 random points for the calculations corresponding to the temperatures $T=10^8$, 10^9, 10^{10}, 10^{11} K, and they used 5000 random points for the other temperatures.

3.2 Pair neutrino process

The energy loss rate due to the pair neutrino process is expressed as (Munakata, Kohyama, and Itoh 1985)

$$Q_{pair} = \frac{1}{2}\left[(C_V^2+C_A^2) + n(C_V'^2+C_A'^2)\right] Q^+_{pair} + \frac{1}{2}\left[(C_V^2-C_A^2) + n(C_V'^2-C_A'^2)\right] Q^-_{pair} \quad . \qquad (33)$$

At high temperatures ($T>10^9$ K), the energy loss rate due to the pair neutrino process is independent of the density and dominates over the other processes.

3.3 Plasma neutrino process

Kohyama, Itoh, and Munakata (1986) have shown that the axial-vector contribution to the plasma neutrino energy loss rate is at most on the order of 0.01% of the vector contribution for $T \leqq 10^{11}$ K. Thus for practical purposes the axial-vector contribution can be safely neglected. Therefore the energy loss rate due to the plasma neutrino process is written as

$$Q_{plasma} = (C_V^2 + n\,C_V'^2)\,Q_V \quad . \qquad (34)$$

The expression for Q_V has been given by Beaudet, Petrosian, and Salpeter (1967) and also by Kohyama, Itoh, and Munakata (1986).

3.3 Bremsstrahlung neutrino process

The calculation of the neutrino energy loss rate due to the bremsstrahlung neutrino process has been carried out in the two different regions: the region in which electrons are strongly degenerate and the region in which electrons are partially degenerate.

In the first region we can take into account the ionic correlation accurately. The calculation of the bremsstrahlung neutrino energy loss rate based on the Weinberg-Salam theory which takes into account the ionic correlation fully has been reported by Itoh and Kohyama (1983), Itoh et al. (1984d), Itoh et al. (1984a), and Itoh et al. (1984b).

For the density-temperature region in which electrons are partially degenerate, Munakata, Kohyama, and Itoh (1987) have calculated the energy loss rate in the framework of the Weinberg-Salam theory.

3.4 Comparison of various neutrino processes

In Figures 10-14 we show the contributions of the various neutrino processes for the case of $\sin^2\theta_W=0.23$, n=2, and ^{56}Fe matter corresponding to the temperatures $T=10^7$, 10^8, 10^9, 10^{10}, 10^{11} K. In Figure 15 we show the most dominant neutrino process for a given density and temperature for the case of n=2 and ^{56}Fe matter. In Figure 16 we show the contours of the constant total neutrino energy loss

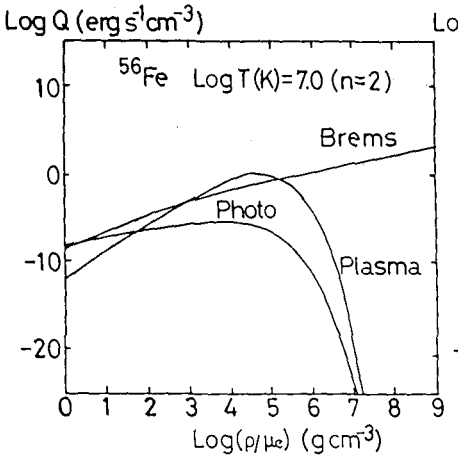

FIG.10.

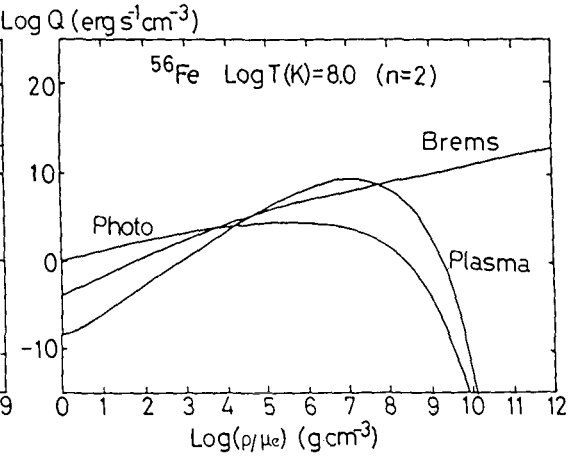

FIG.11.

FIG.10. Neutrino energy loss rates due to photo-, plasma, and bremsstrahlung processes for n=2, ^{56}Fe matter. $T=10^7$ K.
FIG.11. Same as FIG.10. but including pair neutrino process, for $T=10^8$ K.

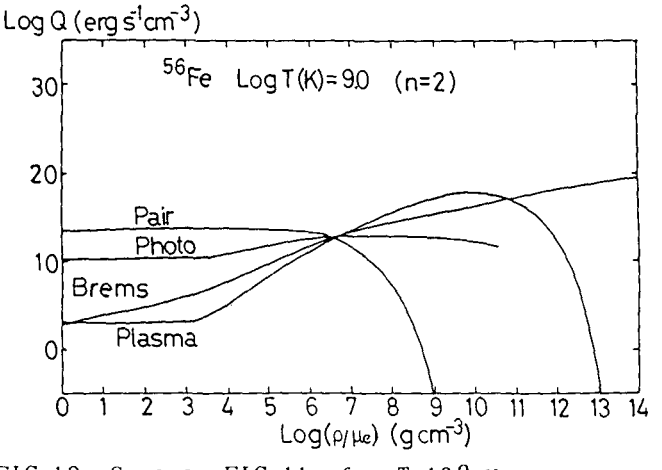

FIG.12. Same as FIG.11. for $T=10^9$ K.

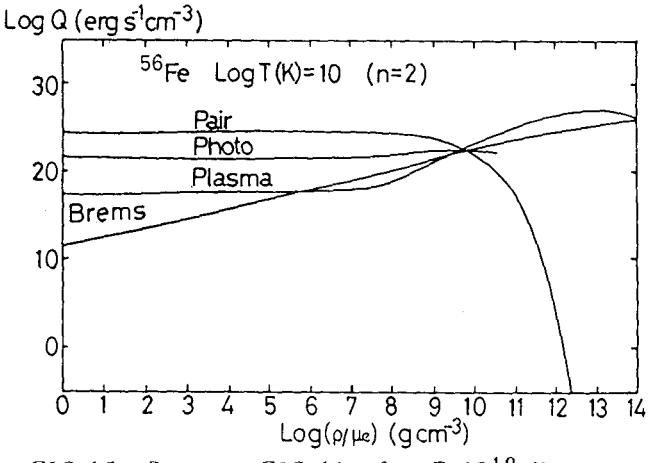

FIG.13. Same as FIG.11. for $T=10^{10}$ K.

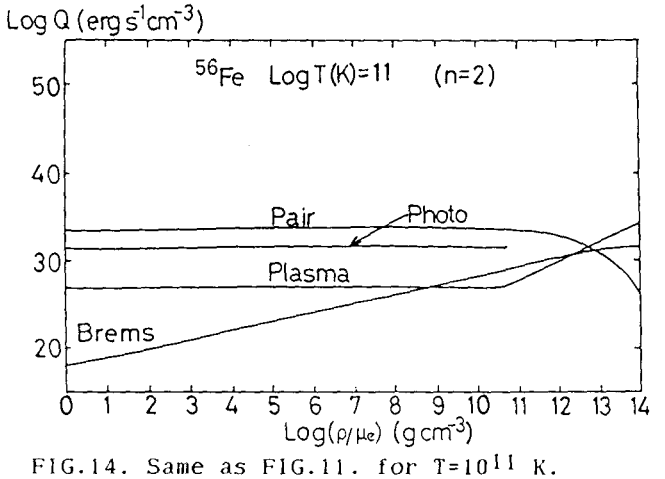

FIG.14. Same as FIG.11. for $T=10^{11}$ K.

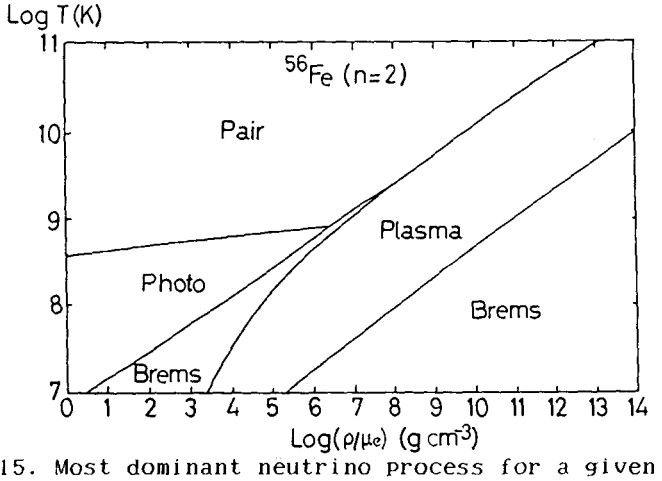

FIG.15. Most dominant neutrino process for a given density and temperature for the case of n=2 and ^{56}Fe matter.

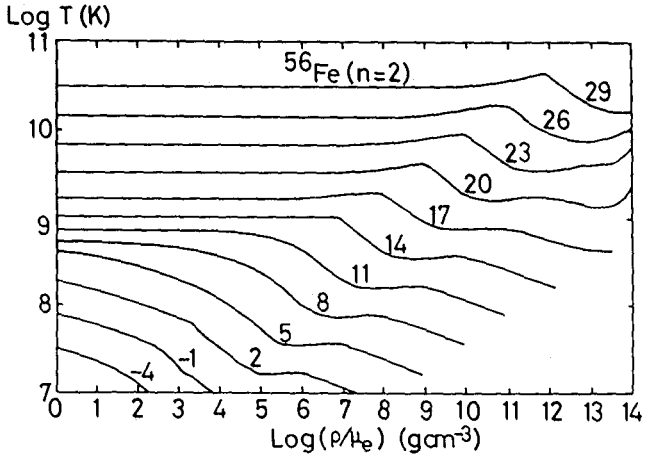

FIG.16. Contours of the constant total neutrino energy loss rates due to pair, photo-, plasma, and bremsstrahlung processes for the case of n=2 and ^{56}Fe matter, log Q (erg s^{-1} cm^{-3})=const.

rates due to pair, photo-, plasma, and bremsstrahlung processes for the case of n=2 and ^{56}Fe matter.

4. CONCLUDING REMARKS

The transport processes and the neutrino emission processes in the interior of white dwarfs determine the structure and evolution of white dwarfs. The recent developments in this field reviewed in this article are expected to elucidate the comparison of the observations of white dwarfs with the theoretical studies. It is interesting to quote the following:

> "Observe me well, Princess, before you give me your word," said the Yellow Dwarf.
>
> The classic fairy tales

I would make a parody of this as follows:

> "Observe me well, Astronomers, before you give me your word," said the White Dwarf.
>
> The modern fairy tales

REFERENCES

Beaudet,G., Petrosian,V., and Salpeter,E.E. 1967, Ap.J.,150,979.
Coldwell-Horsfall,R.A., and Maradudin,A.A. 1960, J.Math.Phys.,1,395.
Flowers,E., and Itoh,N. 1976, Ap.J.,206,218.

Flowers,E., and Itoh,N. 1979, Ap.J.,230,847.
Flowers,E., and Itoh,N. 1981, Ap.J.,250,750.
Ichimaru,S. 1982, Rev.Mod.Phys.,54,1017.
Itoh,N., Adachi,T., Nakagawa,M., Kohyama,Y., and Munakata,H. 1988, submitted to Ap.J.
Itoh,N., and Kohyama,Y. 1983, Ap.J.,275,858.
Itoh,N., Kohyama,Y., Matsumoto,N., and Seki,M. 1984a, Ap.J.,280,787.
Itoh,N., Kohyama,Y., Matsumoto,N., and Seki,M. 1984b, Ap.J..285,304; 322,584(1987).
Itoh,N., Kohyama,Y., Matsumoto,N., and Seki,M. 1984c, Ap.J., 285,758.
Itoh,N., Kohyama,Y., and Takeuchi,H. 1987, Ap.J.,317,733.
Itoh,N., Matsumoto,N., Seki,M., and Kohyama,Y. 1984d, Ap.J.,279,413.
Itoh,N., Mitake,S., Iyetomi,H., and Ichimaru,S. 1983, Ap.J.,273,774.
Iyetomi,H., and Ichimaru,S. 1982, Phys.Rev.,A25,2434.
Jancovici,B. 1962, Nuovo Cimento,25,428.
Kohyama,Y., Itoh,N., and Munakata,H. 1986, Ap.J.,310,815.
Mitake,S., Ichimaru,S., and Itoh,N. 1984, Ap.J.,277,375.
Munakata,H., Kohyama,Y., and Itoh,N. 1985, Ap.J.,296,197;304,580 (1986).
Munakata,H., Kohyama,Y., and Itoh,N. 1987, Ap.J.,316,708.
Nandkumar,R., and Pethick,C.J. 1984, M.N.R.A.S.,209,511.
Pollock,E.L., and Hansen,J.P. 1973, Phys.Rev.,A8,3110.
Raikh,M.E., and Yakovlev,D.G. 1982, Ap.Space Sci.,87,193.
Schinder,P.J., Schramm,D.N., Wiita,P.J., Margolis,S.H., and Tubbs,D. L. 1987, Ap.J.,313,531.
Slattery,W.L., Doolen,G.D., and Dewitt,H.E. 1982,Phys.Rev.,A26,2255.
Yakovlev,D.G., and Urpin,V.A. 1980, Soviet Astr.,24,303.
Ziman,J. 1961, Phil.Mag.,6,1013.

THE EFFECT OF COULOMB INTERACTIONS ON THE HELIUM FLASH

A. Harpaz
Department of Physics, The Technion, Haifa, and
University of Haifa, School of Education of the Kibbutz Movement, Oranim

A. Kovetz
Department of Geophysics and Planetary Sciences
and School of Physics and Astronomy
Raymond and Beverly Sackler Faculty of Exact Sciences, Tel Aviv University

ABSTRACT

Detailed evolutionary calculations show that Coulomb interactions between the charged particles of a stellar plasma reduce the core mass at which a low mass red giant undergoes the helium flash (contrary to a recent claim). This has implications for the determination of the rate of mass loss from red giants.

I. INTRODUCTION

The fact that Coulomb interactions between the charged particles of stellar plasmas result in a reduction of the pressure, at given density and temperature, has been known for a long time. Formulae for the pressure reduction in the case of a cold, dense, plasma were derived by Abrikosov (1960) and by Salpeter (1961), and the resulting reduction in the radii of white dwarfs was calculated by Hamada and Salpeter (1961). For the case of a finite temperature, several evaluations of the effect of Coulomb interactions on the equation of state were obtained in the 1970's (e.g., Grossman and Graboske, 1971; Shaviv and Kovetz, 1972; Hansen, 1973; Fontaine, Graboske and van Horn, 1977). The effect has been included in some calculations of stellar evolution, mainly cooling sequences of white dwarfs and low-mass main sequence stars (e.g., Lamb and van Horn, 1975; Shaviv and Kovetz, 1976; Iben and Tutukov, 1984; Vandenberg, Hartwick and Dawson, 1983).

Since the Coulomb correction is generally small (for example, Hamada-Salpeter white dwarf radii are typically about 7% less than Chandrasekhar's), its inclusion in stellar evolution calculations is not expected to lead to any dramatic effect. But there are some cases, besides white dwarfs and M-dwarfs, in which the effect is worth considering. One of these is the onset of the helium flash in the cores of red giants, which we consider in Section II. Others will be mentioned in the discussion (Section III).

II. THE EFFECT OF COULOMB CORRECTIONS ON THE HELIUM FLASH

While a low mass star is ascending the red giant branch (RGB), its growing helium core is continually contracting. This leads to higher and higher core temperatures (the so-called gravitational energy source).

Neutrino emission, mainly at the center, and radiative heat conduction lead to a temperature profile with an off-center maximum. When the core becomes sufficiently massive, the energy production due to helium burning exceeds the losses, and since the matter is degenerate, a flash occurs.

It is easy to determine the effect of the Coulomb correction on the core mass at the onset of the flash. If we imagine the Coulomb interaction being turned on at any instant, the pressure reduction will lead to sudden core contraction, and hence to higher temperature. It could trigger the flash in a core that would otherwise still need to grow somewhat. But since the processes leading to the flash proceed at a finite rate, and the Coulomb correction depends on density and temperature at each stage, a precise evaluation of the effect requires that it be turned on at an early stage. In order to demonstrate the effect, we have therefore carried out two parallel computations, with and without the correction.

We have evolved two 0.9 $M_\odot$ population II models (X = 0.7, Z = 0.001) through the main sequence and the RGB. In the first one (Model A) we used the Shaviv-Kovetz equation of state, which includes the Coulomb correction, and allowed for mass loss according to the Reimers formula

$$\dot{M} = -4\ 10^{-13}\ \eta\ LR/M \quad M_\odot/y \qquad (1)$$

with $\eta = 1$. (For other details regarding the method and the input physics, see Harpaz, Kovetz and Shaviv, 1987). When this model formed a core of 0.4 $M_\odot$, 7.154 10^9 years from the ZAMS, its total mass was M = 0.769 $M_\odot$, its central temperature was T_c = 74.5 10^6K, but helium burning still provided less energy (L_{He}) than was carried off by neutrinos (L_ν). The Coulomb parameter (ratio of $\langle Z^2\rangle e^2/\langle r\rangle$ to kT) was $\Gamma_c = 0.62$ at the center.

The second model (B) was evolved, again through the main sequence and the RGB, with the only difference that the Coulomb correction was switched off. Its evolution was somewhat slower than that of model A. For example, it took 7.329 10^9 years (from the ZAMS) to form a helium core of 0.4 $M_\odot$. Its total mass, central temperature and central Coulomb parameter at this stage were M = 0.7743$M_\odot$, T_c = 73.3 10^6K and Γ_c = 0.64.

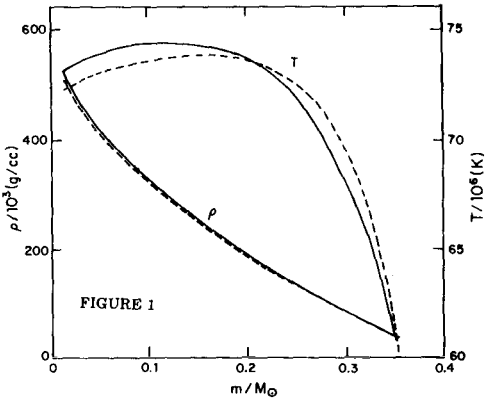

FIGURE 1

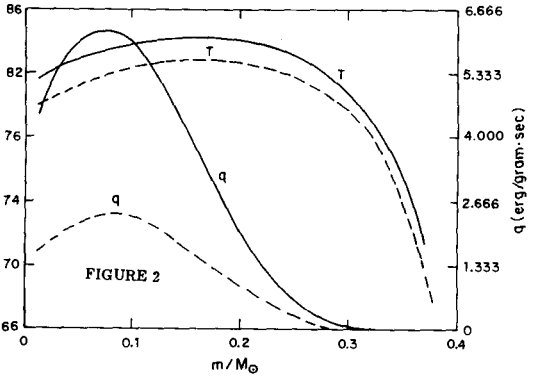

FIGURE 2

Figure 1 shows the density and temperature profiles in the central regions of models A and B when each one had a core of 0.40 $M_\odot$, and Figure 2 shows the temperature and nuclear production rate when each of the models has formed a core of 0.43 $M_\odot$. At this stage, L_{He} just exceeded L_ν for model A, but was still less than L_ν in model B. In all figures, solid lines apply to model A, and dashed lines to model B.

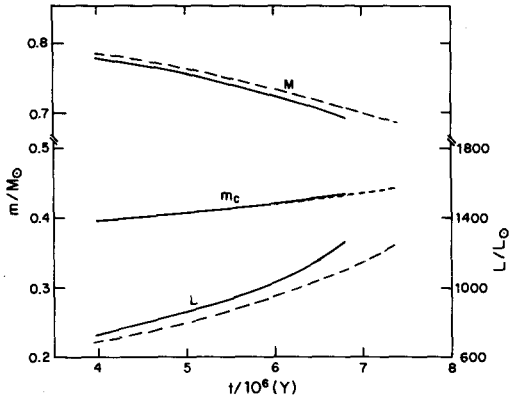

FIGURE 3

The helium burning in model A became a runaway at $M_c = 0.435\ M_\odot$, $M = 0.693\ M_\odot$, and its RGB evolution came to an end. Model B continued its evolution until it reached $M_c = 0.440\ M_\odot$, with $M = 0.690\ M_\odot$. Figure 3 shows the parallel evolution, represented by the total mass, the core mass and the luminosity, of the two models. Time for each model has been reset to zero when the core mass reached $0.175\ M_\odot$ (although the two models were not of the same age at this point).

III. DISCUSSION

The considerations of the preceding section have shown, and the results of two parallel calculations have demonstrated, that the Coulomb correction hastens the onset of the helium flash in low mass stars. These stars will therefore spend less time on the RGB, will lose a smaller amount of mass, and will leave the RGB at a smaller luminosity. They will arrive at the horizontal branch with smaller cores and more massive envelopes, and at an earlier time. The differences are all quite small, of the order of a few per cent (like the Hamada-Salpeter results for white dwarf radii), because the equation of state is dominated by the degenerate electrons.

We note that Mazzitelli and D'Antona, who included the Coulomb correction in an evolutionary calculation of a $1.0\ M_\odot$ population I model, obtained a higher (by about $0.05\ M_\odot$), rather than lower, core mass at the helium flash than did Sweigart and Gross (1978), who did not include the correction. Of course, small differences between results obtained with different computer codes, using different methods and different input physics, need not necessarily be due to a single correction in the equation of state. (Our Model B flash core mass happens to differ from that of Sweigart and Gross by less than $0.03\ M_\odot$). We are certainly not in a position to analyze differences between the results of Mazzitelli and D'Antona and those of Sweigart and Gross. But Mazzitelli and D'Antona claim that the correction should indeed lead to a higher core mass at helium flash: "At the flash conditions (typically $T = 10^8$K and $\rho = 10^6$ gcm^{-3}, at the ratio Γ of Coulombian to thermal energy is ~ 0.5, and the excess internal energy due to Coulombian effects can be 15%-20%; Hansen (1973). This means that our models which take into account Coulombian corrections need to contract more and thus reach larger total core masses before the flash may be ignited". Of course, at given T and ρ, the "excess internal energy" is negative, and if we understand correctly, what Mazzitelli and D'Antona are saying is that Coulomb interactions make the

matter colder, and therefore delay the onset of the flash. But the core of a red giant behaves pretty much like a star, which becomes hotter when it loses energy. This is essentially the argument we have used at the beginning of Section II.

Renzini (1977, 1981) used the results of evolutionary calculations carried out by Rood (1972), Tarbell and Rood (1975) and by Sweigart and Gross (1978) to obtain an upper limit on the parameter η in the mass loss formula (1). As he remarked, the very existence of horizontal and asymptotic giant stars in globular clusters proves that mass loss does not completely strip the RGB stars of their envelopes. This, he showed, meant that η could not be larger than about 0.6. But a detailed analysis of globular cluster HR-diagrams led him to place more stringent constraints on the envelope masses of horizontal branch stars. In this way he was able to show that η should not exceed $0.4 \pm 30\%$. Since the Coulomb correction (which had not been included in the calculations on which Renzini based his analysis) leads to higher total masses, and especially to higher envelope masses (0.258 in our Model A vs. 0.250 in our Model B), Renzini's method should lead to a slightly higher upper limit on η.

In conclusion, we should perhaps mention that there are other advanced stages in stellar evolution, in which the Coulomb correction may be worth considering. One is the onset of carbon burning, where changes similar to those we have considered may be expected. Another is the luminosity-core mass relation for thermally pulsating asymptotic giant branch stars.

REFERENCES

Abrikosov, A. A., 1960, Sov. Phys. JETP, **12**, 1254.

Fontaine, G., Graboske, H. C. and van Horn, H. M., 1977, Ap. J. Suppl., **35**, 293.

Grossman, A. S. and Graboske, H. C., 1971, Ap. J. **164**, 475.

Hamada, T. and Salpeter, E. E., 1961, Ap. J., **134**, 683.

Hansen, J.P., 1973, Phys. Rev. A., **8**, 3096.

Harpaz, A., Kovetz, A. and Shaviv, G., 1987, Ap. J., in press.

Iben, I. and Tutukov, A. V., 1984, Ap. J., **282**, 615.

Lamb, D. Q. and van Horn, H.M., 1975, Ap. J., **200**, 306.

Mazzitelli, I. and D'Antona, F., 1986, Ap. J., **311**, 762.

Reimers, D., 1975, Mem. Soc. Roy. Sci., Liege, 6e Ser., **8**, 369.

Renzini, A., 1977, Advanced Stages in Stellar Evolution, Ed. I. Iben, A. Renzini and D. N. Schramm, Geneva Observatory, Switzerland.

Renzini A., 1981, Effects of Mass Loss on Stellar Evolution, Ed. C. Chiosi and R. Stalio, Reidel Publishing Co., Dordrecht, Holland.

Rood, R. T., 1972, Ap. J., **177**, 681.

Salpeter, E. E., 1961, Ap. J., **134**, 669.

Shaviv, G. and Kovetz, A., 1972, Astron. and Astrophys., **16**, 72.

Shaviv, G. and Kovetz, A., 1976, Astron. and Astrophys., **51**, 383.

Sweigart, A. V. and Gross, P. G., 1978, Ap. J. Suppl., **36**, 405.

Tarbell, T. D. and Rood, R. T., 1975, Ap. J., **199**, 443.

Vandenberg, D. A., Hartwick, F. D. A. and Dawson, P., 1983, Ap. J., **266**, 747.

Equations Of State of Hydrogen-Helium and Carbon-Oxygen Mixtures

P. Godon, G. Shaviv, J. Ashkenazi* and A. Kovetz**

Department of Physics, Technion-Israel Institute of Technology 32000 Haifa, Israel

* Department of Physics, University of Miami, Coral Gables, FL 33124, U.S.A.
** Department of Physics and Astronomy and Department of Enviornmental Science
Tel-Aviv University, Ramat Aviv, Israel

The usual approach to the problem of the Equations Of State (EOS) for White Dwarfs and super giant Planets, under the conditions of high densities and low temperatures, faces two problems.

The first has to do with Pressure Ionization : the energy levels of the electrons in the case of extreme pressure ionization cannot be treated in the same way as the energy levels in a single isolated atom. The simple treatment of pressure ionization, in which the level of the continuum is reduced by an amount equal to the electrostatic energy, leads to problem because the number of energy levels, entering the Saha equation (partition functions), is not conserved, also the usual approach may lead to absurd results in which ions recombine as the density increases.

The second problem is the question of the microscopic separation of species in a mixture : is the prefered state a mixed crystal of two species or two separeted crystals (one of each specy) ?

The EOS in Astrophysics treats the electrons as a gas of free particles (1) (plane waves function) obeing the Fermi-Dirac statistics, where the ionic background forms a crystaline structure. At zero temperature the energy of the ions is then given by the Zero Point Oscillations (ZPO) (2) energy. At finite temperatures the phonons spectrum of the lattice (quasiharmonic approximation) is added to it.

Another approach to the problem of the EOS is by means of Solid State methods. The electrons individual energy levels form energy bands which take into account the conservation of the number of energy levels, and their wave function is a Bloch sum of a linear combinations of atomic orbitals (LCAO). The ions are sup-

posed to be fixed in the crystal lattice (Adiabatic approximation).

Since the astrophysical approach to the EOS cannot answer the above two questions, we resort to the solid state approach. In this contribution we report mainly on the results for the second problem.

The method we used in this work is the Linear Muffin-Tin Orbitals (LMTO) (3) method in which the wave functions are Bloch sums of Linear Orbitals defined by a Muffin-Tin (MT) potential. The MT potential is spherically symetric in spheres around the ions sites and of constant value in the interstitial regions. Then a variational method is used to derive the correct energy bands, their width, the density of state, etc...

It is of great interest to compare the results for the EOS obtained in the two methods. Such a comparison is shown in figure 1 and 2 for H/He. We note that the two methods yield the same EOS to within the accuracy of the methods (less than one percent).

We now turn to the second problem posed.

To answer the question of whether a H/He (or a C/O) mixture separates or not, we consider a volume V_* of the star, under pressure P_* and temperature T_*. We suppose that in this volume separated crystals of H and He have been formed. Let index 1 denote Hydrogen and 2 Helium. Then $V_* = V_1 + V_2, N = N_1 + N_2$ (number of particles in V_*). The most probable state for the coexistence of the two crystals in volume V_* is obtained by minimizing the free energy. This leads to the condition :

$P_1 = P_2 \quad ; \mu_1 = \mu_2$.

Where P_i is the pressure and μ_i the chemical potential (i=1,2). Let denote $P = P_1 = P_2$.

If $P \leq P_*$ then the pressure inside the volume V_* is not high enough to avoid separation of the mixed crystal. If $P \geq P_*$ then the separation process is stopped by the pressure inside V_*.

The results obtained, within the accuracy of the LMTO calculation (one percent), shows that the pressures P_* and P were equal. This leads us to conclude that there is no prefered state between a mixed crystal of two species and two separated crystals on a microscopic scale : microscopic separation does not require energy. Consequently the separation problem is a macroscopic problem that has to be treated within the frame work of the evolution of the star.

References

(1) A. Kovetz and G. Shaviv, Astron. Astrophys. **8**, 398-403 (1970).
G. Shaviv and A. Kovetz, Astron. Astrophys. **16**, 72-76 (1972).
(2) E. E. Salpeter, Astrophys. J., **134**, 669 (1961).
(3) O. K. Andersen, Phys. Rev. **B12**, 3060 (1975).
H. L. Skriver, *The LMTO Method*, Springer Verlag (1984).

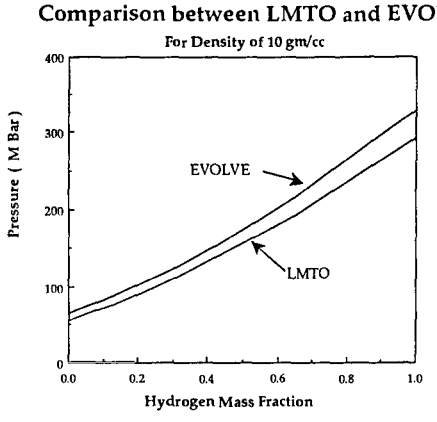

Fig.1 Comparison between the Astrophysical (Evolve) and the Solid State (LMTO) results for the pressure. We have omitted the ionic contribution (ZPO) in the LMTO (while it is included in Evolve).

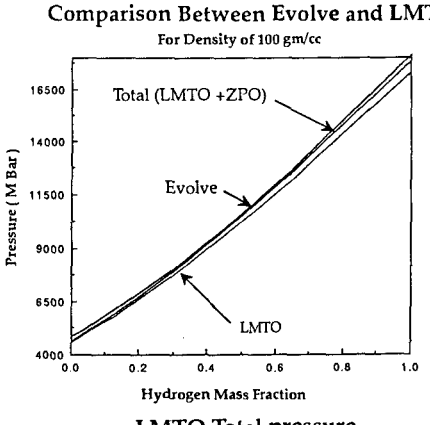

Fig.2 H-He mixture for a density of 100 gm/cc and T=0. We compare between the full EOS (ions + electrons) obtained by the two different methods. We see that the astrophysical results are good within a few percent.

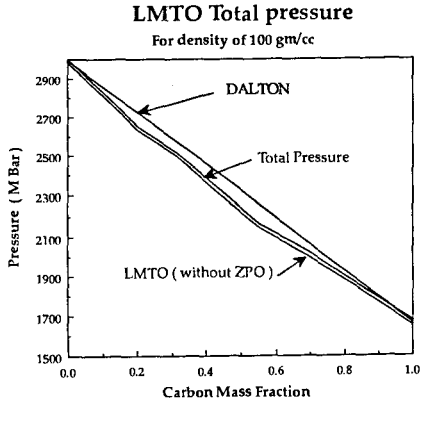

Fig.3 LMTO pressure for a C-O mixture, ρ = 100 gm/cc.

GRAVITATIONAL COLLAPSE OF MASS-ACCRETING WHITE DWARFS

J. Isern[1], R. Canal[2], D. García[3], M. Hernanz[3], and J. Labay[2]

[1]Centre d'Estudis Avançats de Blanes, CSIC
17300 Blanes (Girona), Spain
[2]Departament de Física de l'Atmosfera, Astronomia i Astrofísica
Universitat de Barcelona, 08028 Barcelona, Spain
[3]Universitat Politecnica de Catalunya
08028 Barcelona, Spain

1. INTRODUCTION

Massive star ($M \geq 10\ M_\odot$) core collapse is the standard mechanism for neutron star formation (see Brown 1988 for a recent review). It has long been realized (see, for instance, van den Heuvel 1988, and references therein) that the neutron stars found in different types of binary systems cannot come from such a standard mechanism. Those systems include wide binary radio pulsars, millisecond pulsars (not in wide binaries), galactic bulge X-ray sources (including QPO's), type I X-ray burst sources and X-ray transients, and γ-ray sources. Formation of those neutron stars is now widely attributed to the gravitational collapse of a white dwarf, growing above Chandrasekhar's limit by mass accretion from the current neutron star's companion in the binary system (Canal and Schatzman 1976; Canal and Isern 1979; Canal, Isern, and Labay 1980; Miyaji et al. 1980). Mass growth up to dynamical instability means that both explosive ejection of the accreted layers and explosive disruption of the whole star must be avoided. The former is associated with the nova phenomenon. The latter, with the occurrence of type I supernovae.

Concerning nova outbursts, the results as to the ranges of different parameters (initial mass and temperature of the star, mass accretion rate, chemical composition of both the star and the accreted material) allowing mass growth are so divergent, when the simplest hypotheses (spherical symmetry, no kinetic energy nor angular momentum deposition) are relaxed (see Sparks and Kutter 1987; Shaviv and Starrfield 1987) that those parameters should presently be regarded as almost free. Explosive ignition of electron-degenerate C+O cores has been studied by Nomoto, Thielemann, and Yokoi (1984), and Sutherland and Wheeler (1984). Ignition densities were in the range $\rho \cong (2\text{-}4)\times10^9$ g cm^{-3} and the cores were entirely fluid. Hydrodynamic burning

propagation leads to their complete disruption. Ignition at higher densities happens when the cores are cold and massive enough at the start of mass accretion (Hernanz et al. 1988). The range studied covers 6×10^9 g cm^{-3} $\leq \rho_{ign} \leq$ 1.5×10^{10} g cm^{-3} (for somewhat lower initial masses it covers the whole interval 2×10^9 g cm^{-3} $\leq \rho_{ign} \leq$ 1.5×10^{10} g cm^{-3}) and carbon ignition takes place in solid layers when $\rho_{ign} \geq 9.5 \times 10^9$ g cm^{-3}. Ignition would be delayed up to still higher densities if carbon and oxygen were inmiscible in solid phase (Stevenson 1980; Labay et al. 1985). Here we try to determine the critical ignition density corresponding to bifurcation between stellar explosion (either leading to complete disruption or leaving some white dwarf remnant) and gravitational collapse leading to neutron star formation and we analyze the physical processes involved. O+Ne+Mg cores have also been proposed as progenitors of neutron stars (Miyaji et al. 1980). Here we will briefly outline the uncertainties still involved as to their behaviour upon mass accretion.

2. DEGENERATE CARBON IGNITION AT VERY HIGH DENSITIES

Initially massive ($M \geq 1.2$ M$_\odot$) and cold ($T \leq 5 \times 10^7$K) C+O white dwarfs do ignite their thermonuclear fuel at higher densities than both less massive and hotter white dwarfs and intermediate mass (4 M$_\odot$ $\leq M \leq$ 8 M$_\odot$) red giant cores (see Hernanz et al. 1988, and references therein). This is due to the fact that pycnonuclear reaction rates (in the solid phase) are much lower than strongly screened thermonuclear rates (in the fluid phase) for C+O mixtures at a given density. Higher ignition densities also mean higher electron capture rates on the incinerated (NSE) material after thermonuclear runaway. When the surrounding layers are still solid at central carbon ignition, this equally means conductive burning propagation, typically at velocities of the order of 0.01 times the local velocity of sound c_s (it must be noted that conduction will dominate anyway close to the star's center, even in fluid layers: see Woosley and Weaver 1986). Both facts do favour electron captures (driving contraction and potentially leading to gravitational collapse) against thermonuclear burning propagation (driving hydrodynamical expansion, with potential disruption of the star). Solidification of a central core prior to the mass-accretion stage in the white dwarf's evolution would produce still more drastical effects if it were to lead to chemical separation of oxygen from carbon (Stevenson 1980; Mochkovitch 1983). Recent calculations by Barrat, Hansen, and Mochkovitch (1988) do indicate that carbon and oxygen are miscible in solid phase (nonetheless, these calculations

still involving fairly arbitrary approximations, chemical separation is not yet completely ruled out).

In previous papers (Canal and Isern 1979; Isern, Labay, and Canal 1984; Isern et al. 1988) we have already addressed the question as to the critical ignition density for collapse of a C+O white dwarf into a neutron star and its dependence on the still uncertain physics of thermonuclear burning propagation. In Table 1 we summarize the results from several calculations based on two deflagrating models taken from Hernanz et al.(1988).

TABLE 1

Model	ρ_{ign} (g cm^{-3})	v_{burn}/c_s	Outcome	t_{11} (s)
A	9.50×10^{9}	0.005	Collapse	1.47
B	1.09×10^{10}	0.005	Collapse	1.09
B	1.09×10^{10}	0.010	Collapse	0.93
B	1.09×10^{10}	0.100	Explosion	--

Burning front velocities in the two first rows of Table 1 are average values when using Woosley and Weaver's (1986) expression for conductive velocities. The other two values correspond to parametrization of burning propagation speed. t_{11} is the time elapsed between explosive ignition (at the indicated densities) and contraction to a central density of 10^{11}g cm^{-3}. When "collapse" is indicated as the outcome, the star is homologously contracting on a hydrodynamical time scale and its mass (due to electron captures) is above Chandrasekhar's mass. We see that, for ignitions at densities of the order of 10^{10}g cm^{-3}, the bifurcation between collapse and explosion is located between 0.01 and 0.1 times the local sound velocity. Concerning densities, for conductive burning, the minimum value for collapse is around 9.5×10^{9}g cm^{-3}. Comparison of Table 1 with Nomoto's (1986, 1987) recent results shows very big discrepancies. These are probably due to some mistake in the calculation of the burned mass (see, for instance, Nomoto's case D).

3. DEGENERATE OXYGEN IGNITION

O+Ne+Mg white dwarfs are also candidates to gravitational collapse upon mass accretion (Miyaji et al. 1980). Oxygen ignition is

triggered by electron captures on ^{20}Ne. But the exact density at which this happens depends on the adopted criterion for convective instability and on the treatment of semiconvection (Mochkovitch 1984; Miyaji and Nomoto 1987). Ignition at $\rho_{ign} \leq 9.5 \times 10^{9}$ g cm^{-3} is likely and the outcome (collapse or explosion) is still uncertain.

REFERENCES

Barrat, J.L., Hansen, J.P., Mochkovitch, R. 1988, Astron. Astrophys., 199, L15

Brown, G.E. 1988, Phys. Rept., 163, 1

Canal, R., Schatzman, E. 1976, Astron. Astrophys, 46, 229

Canal, R., Isern, J. 1979, in White Dwarfs and Variable Degenerate Stars, ed. H.M. Van Horn and V. Weidemann (Univ. Rochester Press, Rochester), p.52

Canal, R., Isern, J., Labay, J. 1980, Astrophys. J. (Letters), 241, L33

Hernanz, M., Isern, J., Canal, R., Labay, J., Mochkovitch, R. 1988, Astrophys. J., 324, 331

Isern, J., Labay, J., Canal, R. 1984, Nature, 309, 431

Isern, J., Canal, R., Garcia, D., Garcia-Berro, E., Hernanz, M., Labay, J. 1988, Adv. Space Res., in the press

Labay, J., Canal, R., Garcia-Berro, E., Hernanz, M., Isern, J. 1985, in Recent Results on Cataclysmic Variables, ed. J. Rahe (ESA SP-236)

Miyaji, S., Nomoto, K., Yokoi, K., Sugimoto, D. 1980, Pub. Astron. Soc. Japan, 32, 303

Miyaji, S., Nomoto, K. 1987, Astrophys. J., 318, 307

Mochkovitch, R. 1983, Astron. Astrophys., 122, 212

Nomoto, K. 1986, Progr. Part. Nucl. Phys., 17, 249

Nomoto, K. 1987, in The Origin and Evolution of Neutron Stars, ed. D.J. Helfand and J.-H. Huang (Reidel, Dordrecht), p. 281

Nomoto, K., Thielemann, F.K., Yokoi, K. 1984, Astrophys. J., 286, 644

Shaviv, G., Starrfield, S. 1987, Astrophys. J. (Letters), 321, L51

Sparks, W.M., Kutter, G.S. 1987 Astrophys. J., 321, 394

Stevenson, D.J. 1980, J. Phys. Suppl., No. 3, 41, C2-53

Sutherland, P.G., Wheeler, J.C., 1984, Astrophys. J., 280, 282

Van den Heuvel, E.P.J. 1988, Adv. Space Res., in the press

Woosley , S.E., Weaver, T.A. 1986, in Radiation Transport and Hydrodynamics, IAU Coll. No. 89, ed. D. Mihalas, K.H. Winkler. Dordrecht: Reidel

THE TEMPERATURES OF WHITE DWARFS IN ACCRETING BINARIES

Paula Szkody
Department of Astronomy, University of Washington
Seattle, Washington 98195

Edward M. Sion
Department of Astronomy and Astrophysics, Villanova University
Villanova, Pennsylvania 19085

I. Introduction

Through the use of accreting binary systems, it is possible to study the effects of the deposition of matter and energy on the surface of a white dwarf. The observed atmospheric properties of composition and temperature obtained from direct observation of the spectral lines and the continuum flux can be used to compare with those of single white dwarfs to understand the consequences of mass accretion on binary evolution.

Cataclysmic variables provide one of the best targets for this type of study because a) the primaries are all white dwarfs b) the level and the timescale of the accretion cover a large range from the high rate, relatively steady novalike accretors to the dwarf novae systems which are modulated on short timescales in a quasi-periodic manner. Unfortunately, due to the mass transfer process, an accretion disk builds up to the point where its radiation overwhelms the white dwarf light in most cases. Thus, to study the effects on the stellar primary, systems must be found which have low mass transfer rates (generally the short orbital period systems (Patterson 1984)) and/or high inclinations (since most of the disk flux emerges perpendicular to the plane of the disk). The best identification of the white dwarf emerges from IUE spectra which show a broad Lyman α absorption profile (in contrast to the normal emission lines from a disk at quiescence). The shape of this profile provides a sensitive indicator of the temperature and gravity. In some cases, broad absorption lines are also evident in the optical Balmer lines, although the broad emission lines from the disk usually make these difficult to detect. The steeply falling flux distribution of a white dwarf throughout the optical region, combined with a flat disk distribution usually means that the white dwarf contributes a minor amount to the optical flux. However, in the ultraviolet, the rising energy distribution of the white dwarf easily dominates the falling energy distribution of a low accretion rate disk (Mateo and Szkody 1984). White dwarfs are generally acknowledged to be prominent in the dwarf novae U Gem (Panek and Holm 1984), VW Hyi (Mateo and Szkody 1984) and Z Cha (Marsh, Horne and Shipman 1987) and suggested in EK TrA and WZ Sge (Verbunt 1987). In addition, the white dwarf has been seen in some novalike systems which sporadically turn off their mass transfer, (resulting in the disappearance of most of the disk and the resulting appearance of the white dwarf). This has been the case in TT Ari (Shafter *et al.* 1985) and

some limits have been determined for MV Lyr (Szkody and Downes 1982) and V794 Aql (Szkody, Downes and Mateo 1988). Several magnetic white dwarfs have also been seen when the mass transfer ceases in the AM Her systems (summarized in Szkody, Downes and Mateo 1988).

The temperatures for the white dwarfs in cataclysmic variables (regarded as upper limits) range from 9000K to more than 50000K, with a mean temperature of 25000K compared to 12000K for single white dwarfs (Sion 1986; 1987). In looking at the temperature as a function of the orbital period of the cataclysmic variables (Sion 1986,1987; Szkody, Downes, and Mateo 1988), it appears that there is a positive correlation in these parameters. If the orbital period is related to mass accretion rate as suggested by Patterson (1984), then the implication is that long term accretion has a heating effect on the underlying white dwarf.

To better understand the accretion interaction with the white dwarf, a few studies have been undertaken of the white dwarf following an outburst. This includes VW Hyi (Verbunt *et al.* 1987) and U Gem (Kiplinger, Sion and Szkody 1988). Both of these investigations have shown a decreasing ultraviolet flux after the optical flux has reached quiescence, which could be interpreted as a decreasing accretion rate or a cooling of the outer layers of the white dwarf following heating by the outburst. The indications from the U Gem study is that the white dwarf cools for several months. In both cases, the next outburst interrupted the monitoring sequence (after 14 days in VW Hyi and after 108 days in U Gem). Perhaps the best candidate for a long term study is the dwarf nova WZ Sge which has an outburst recurrence time of 33 yrs and has a prominent white dwarf which is evident in the ultraviolet and optical. Many spectra have been obtained with IUE and exist in the archive following the 1978 outburst. Holm (1988) has reported on the results up through 1981 and Hassall (1987) reported on the spectrum through 1986. We report on the results through May 1988 in section II and discuss the general implications from all 3 systems in section III.

II. WZ Sge

This dwarf nova has very large amplitude outbursts at long intervals. The last outburst occurred on Dec. 1, 1978 when the system reached V=7.8. A light curve compiled by the AAVSO (Bortle 1979) shows that optical quiescence (V $\sim$ 15) was reached in April, 1979 (about 126 days after outburst). Holm (1988) shows IUE spectra from outburst (a flat disk distribution) through Nov. 23, 1981 (distribution similar to DA white dwarfs). He finds that the April 25, 1980 spectrum matches a 15400K white dwarf, while the Nov. 23, 1981 spectrum matches a 14500K white dwarf. We obtained additional SWP and LWP exposures on July 5, 1987 and May 1, 1988 and extracted exposures from the archive obtained on Nov. 3, 1986. We then extracted IUE spectra of DA white dwarfs of known temperature from the archive: 40 Eri B (T=16325), Wolf 485A (T=14000) and G8-8 (T=13000) for comparison. We then used the flux at 1500A to normalize WZ Sge to each of the single white dwarfs and determine the best fit in temperature. Our results along with those of Holm (1988) are summarized in Table 1 and Figure 1 shows a representative fit of the May, 1988 spectrum of WZ Sge with Wolf 485A.

TABLE 1 Temperature fits of SWP Spectra

Date	1500A Flux (x E-14)	Best T (K)
April 25, 1980	9.0	15400
Nov. 23, 1981	6.5	14500
Nov. 3, 1986	2.0	13500
July 5, 1987	3.5	14000
May 1, 1988	2.2	13500

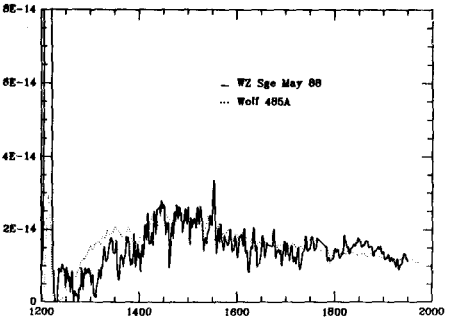

From these results, it appears that the UV flux reached some sort of equilibrium value about the end of 1986. The small excursions of brightness (as seen in July, 1987) may be fluctuations in the accretion rate (they cannot be due to orbital variations since the IUE exposures are all long *i.e.*, 180 min SWP and 120 min LWP as compared to the binary orbit of 82 min). This means that the UV flux continued to decrease for 8 yrs after outburst (while the optical flux reached quiescence in 126 days). If the underlying white dwarf has provided a dominant amount of the UV flux since the disk reached quiescence (April, 1979), then the outer layers of the white dwarf cooled by several thousand degrees.

The question remains as to whether we are indeed viewing the white dwarf and what portion of it has been heated. Holm (1988) points out 2 possible problems: 1) if the April 1980 IUE flux is fit with a 15400K white dwarf, then the optical flux would imply a V magnitude of 14.6, slightly above the normal quiescent value and 2) the equivalent widths of the absorption features do not change much between Jan. 1979 (outburst) and Nov. 1981. Point 1 cannot be proven true or false in terms of the observed values, because the AAVSO detection limits are near 14.6. To investigate Point 2, we measured the equivalent widths in the spectra after 1981.

Figure 1 shows that the May, 1988 spectra differ from Wolf 485A primarily in the spectral region from 1250 to 1400A. This is the area of the Si II and III absorption lines, although it is difficult to measure the equivalent widths accurately due to the correct positioning of the continuum level in this area. Our measurements for the absorption lines are summarized along with Holm's measurement in Table 2. The values for U Gem (Kiplinger, Sion and Szkody 1988) are also listed for comparison.

TABLE 2 Equivalent Widths of Absorption Features

Date	Nov.81	Nov.86	July 87	May 88	U Gem
Si II 1265	3.0	5.7	–	12.4	0.6
Si III 1300	6.3	6.0	7.7	10.6	2.7
C II 1335	3.9	–	–	–	0.8
Si IV 1400*	5.4	4.6	hit	6.5	4.4
Si II 1530	3.5	3.4	3.1	3.5	–

*This feature may be the broad 1400A feature seen in single white dwarfs (Nelan and Wegner 1985)

The Si II 1265 and Si III 1300 values are somewhat uncertain due to the poor signal in the continuum. These features also appear to be slightly redward of the correct wavelengths (Si II is at 1270 and 1535, Si III at 1310) in the May 88 spectra (but this is probably an instrumental effect). However, it is apparent that there is an increase of the equivalent widths in Si II 1265 and Si III 1300, consistent with an increasing contribution of a cooling white dwarf. The May 1988 equivalent width of Si II is consistent with a solar composition photospheric feature from a 13500K white dwarf (Henry, Shipman and Wesemael 1985). The Si II 1530 feature might not show this effect due to the difficulties of measuring with some residual disk emission at C IV 1550. For T < 20,000K, the expected Si IV equivalent width in white dwarfs is less than 2A, so the measured absorption feature at 1400A is most likely the H_2 quasi-molecule (Wegner 1984; Nelan and Wegner 1985). If photospheric, this feature confirms that we are dealing with high density material (log g > 6). Despite the fact that some accretion heating might be occurring, we expect this feature to maintain a similar equivalent width because it is more gravity than temperature sensitive.

To check the consistency of a T=13500K white dwarf dominating the quiescent flux of WZ Sge, we can compare the UV and optical fluxes from a white dwarf model (H. Shipman, private communication) with that of WZ Sge. The model gives a flux difference of a factor of 5.8 from 1300 to 5400 A. Using the May 88 observed flux at 1300A (8×10^{-15}) results in a V mag of about 16. This is below the quiescent magnitude range of 15.2-15.5 and allows for some disk contribution, especially if the white dwarf does not contribute 100% of the 1300A flux.

We can also determine the size of our proposed white dwarf via ($R^2 = Fd^2/4\pi H$) and compare with estimates from optical solutions. For a 13500K white dwarf, Shipman's models give H at 1300A = 5.5×10^7 ergs/cm^2/s/A. Using a distance of 83 pc for WZ Sge and the observed 1300A flux, the corresponding radius comes out to be 8.7×10^8 cm. The radial velocity solution of Gilliland, Kemper and Suntzeff (1986) results in a mass of 0.5 - 1.2 solar masses for the white dwarf. Our radius is consistent with the lower masses in this range, although Gilliland, Kemper and Suntzeff find that the secondary must be degenerate if the mass is low (for a main sequence secondary, the white dwarf mass must be near 1.1 solar masses, which would be a radius of 5×10^8 cm).

In summary, the indications are that a 13500K $\pm$ 500K white dwarf contributing most of the UV flux is consistent with the observed parameters of WZ Sge. However, the increase in temperature of this star to 15500K is not enough to account for the factor of 4 increase in the 1500A flux between 1988 and 1980 (Table 1). White dwarf models give a flux increase of about 3 for this temperature difference. Thus, there must also be some contribution from the hot disk or a larger emitting area to account for the April 1980 fluxes.

III. Summary

Table 3 summarizes the basic features of the 3 systems studied after accretion episodes.

Table 3

Object	Orb. P (min)	Mass WD	Outburst Interval	WD T (K)	Opt.Min Reached	UV Min Reached	WD Cooling
VW Hyi	107	(0.6)	28 d	18000	4 d	>14 d	–
U Gem	255	0.8	118 d	30000	16 d	>103 d	40000-30000
WZ Sge	82	1.1	33 yrs	13500	126 d	2894 d	15500-13500

The data on these 3 cataclysmic variables support a dominant contribution from a white dwarf to the ultraviolet flux. The temperature of the white dwarf is a rising function of the orbital period of the system. After an outburst, presumably originating in increased accretion of solar composition material onto the white dwarf, the disk quickly returns to its quiescent emission levels (as evidenced by the rapid optical decline) but the UV flux takes a much longer time to return to its pre-outburst value. This slowly declining UV emission may represent the cooling of a white dwarf whose outer layers have been heated by the outburst. This is supported by the continuum distribution and the Lyman α profile fitting of the fluxes to DA white dwarfs. However, the total amount of flux change and the metallic absorption line fitting presents some difficulties with such a simple picture. In U Gem, a hotter area near the white dwarf must be invoked to account for the He II absorption lines seen. In WZ Sge, some disk component or larger area must also account for emission during part of the decline.

We gratefully acknowledge Harry Shipman for providing some fluxes for cool white dwarfs. NASA grant NSG 5395 provided support of this project.

Bortle, J. 1979, *AAVSO Circ.* 110.
Gilliland, R. C., Kemper, E. and Suntzeff, N. 1986, *Ap. J.*, **301**, 252.
Hassall, B. J. M. 1987, poster presentation at Aspen Workshop.
Henry, R. B. C., Shipman, H. L. and Wesemael, F. 1985, *Ap. J. Suppl.*, **57**, 145.
Holm, A. V. 1988, in *A Decade of UV Astronomy with the IUE Satellite*, ESA SP-281, in press.
Kiplinger, A., Sion, E. M. and Szkody, P. 1988, *Ap. J.* submitted.
Marsh, T. R., Horne, K. D. and Shipman, H. L. 1987, *M.N.R.A.S.*, **225**, 551.
Mateo, M. and Szkody, P. 1984, *A. J.*, **89**, 863.
Nelan, E. P. and Wegner, G. 1985, *Ap. J.*, **289**, L31.
Panek, R. J. and Holm, A. V. 1984, *Ap. J.*, **277**, 700.
Patterson, J. 1984, *Ap. J. Suppl.*, **54**, 443.
Shafter, A. W., Szkody, P., Liebert, J., Penning, W. R., Bond, H. E. and Grauer, A. D. 1985, *Ap. J.*, **290**, 707.
Sion, E. M. 1986, *P.A.S.P.*, **98**, 821.
Sion, E. M. 1987, *I.A.U. Coll.* 95, eds. A. G. D. Phillip, D. S. Hayes and J. Liebert, L. Davis press, p. 413.
Szkody, P. and Downes, R. A. 1982, *P.A.S.P.*, **94**, 328.
Szkody, P., Downes, R. A. and Mateo, M. 1988, *P.A.S.P.*, **100**, 362.
Verbunt, F. 1987, *A. Ap. Suppl.*, **71**, 339.
Verbunt, F., Hassall, B. J. M., Pringle, J. E., Warner, B. and Marang, F. 1987, *M.N.R.A.S.*, **225**, 113.
Wegner, G. 1984, *A. J.*, **89**, 1050.

WHITE DWARF EVOLUTION IN REAL TIME: WHAT PULSATING WHITE DWARFS TEACH US ABOUT STELLAR EVOLUTION

Steven D. Kawaler
Center for Solar and Space Research, Yale University

Carl J. Hansen
J.I.L.A., University of Colorado

The variable white dwarfs repeatedly force theory to conform to their observed properties so that further progress can be made in understanding the structure and evolution of all white dwarfs. We use the term "understanding" in a loose sense here because, as we will show, both observational constraints and interpretation of the observations *vis-à-vis* theory contribute to uncertainties in our understanding at this time. In any case, recent progress in this field (sometimes called white dwarf seismology) has provided some fascinating insights into the evolutionary and structural properties of white dwarfs and their progenitors. This short review is our attempt to describe recent progress made in the interaction of theory with observations.

Because of space limitations, we do not include as many references as we would like. Instead, we offer the following list of texts and reviews that we have found useful: Cox (1980), Unno *et al.* (1979), Winget and Fontaine (1982), Van Horn (1984), Kawaler (1987), Winget (1988) and, finally, the forthcoming extensive review by Van Horn *et al.* (1989). The first two references are texts that contain most the material necessary for understanding the theory of nonradial pulsations as applied to stars in general, and in particular, the variable white dwarfs

1. The Observations and Some Matters of Theory

There are white dwarfs aplenty in this part of the Galaxy — some 25% of all stars near the Sun consist of these fascinating beasts. Among that plenitude there is a small subset which are obviously variable. Although they are usually dim and rather shy, they probably constitute the most populous class of variable star in the Universe. So much for those big, fat, yellow and red variables you hear so much about! Thus far, thirty-one of these white dwarf variables ("WDVs") have been discovered. We include in this total those variables that are well on their way to becoming white dwarfs. There are three major subclasses categorized primarily by effective temperature and spectral features. These are: the ZZ Ceti variables, or DAVs, ($T_{eff} \approx$ 12000K, DA hydrogen atmosphere), the DBVs ($T_{eff} \approx$ 27000K, DB helium atmosphere), and the DOV composite class consisting of very hot DO white dwarfs (the "PG 1159" stars)

and the nuclei of planetary nebulae ($T_{eff} \approx 10^5$K with considerable uncertainty, HeII, CIV and, perhaps OVI spectral features — but no Balmer lines).

All these variables are multiperiodic, with periods ranging between $100s \leq \Pi \leq 1000s$. Periods less than about 100*s* are not found in any of these stars; it is possible that periods longer than 1000*s*, currently found in the pulsating planetary nebula nuclei ("PNNs"), could exist in the cooler variables. The problem of detecting long periods using Earth-based observations stems from the possible confusion of variations in sky transparency with those of the star, and the requirement of adequate phase coverage and cycle counts to unambiguously determine the periods present. Reliable decoding of the pulsation spectra of for these "long period" objects requires multi-site observing techniques such as those to be described by Ed Nather at this meeting.

The following two subsections will briefly review the photometric properties of the variable white dwarfs along with some pertinent theory. We shall try to emphasize those properties which must be attacked and explained by theory before we all can agree that we understand what is really going on inside these stars.

(a) "Simple" Variables

The threshold for detectability of a statistically significant amplitude in a power spectrum, that is, a pulsation period, for WDVs is now about one millimagnitude in visible light — and this requires long, clean observing run(s). The maximum amplitude observed in any WDV is close to 500 mmag. Among the ZZ Ceti variables, there appears to be a loose correlation between average amplitude, complexity of light curve, and effective temperature. The trend is that cooler ZZ Ceti stars near the red edge of the observed instability strip tend to have numerous high power peaks in their Fourier power spectra whereas variables nearer the blue edge are characterized by spectra showing only a few modest signals (Winget and Fontaine 1982). For the hotter variables the situation is unclear and we shall return to those after discussing the "simple" DAV variables.

Possibly the best-studied DAVs are ZZ Ceti (a.k.a. R548), G117-B15A, G226-29, and GD385. All of these variables pulsate at relatively low amplitude. The power spectrum of ZZ Ceti contains two pairs (doublets) of peaks of average amplitude 5 mmag with periods of 213.132605, 212.768427, and 274.250814, 274.774562*s*, with uncertainties of around 4μs (Stover *et al.* 1980). The price paid for this remarkable precision was 58 observing runs spaced over nine years, and an exacting analysis of the data. Another result of that analysis is an upper limit on the secular rate of change of period of one signal of $\dot{\Pi} \leq 2\times10^{-13} ss^{-1}$. The significance of such measurements will be discussed shortly.

Another simple pulsator is GD385 (Kepler 1984). It has only three signals. Two of them make up a doublet with periods of 256.127*s* and 256.332*s*, while the third (a singlet) is at a frequency twice that of the average of the frequencies in the doublet. GD385 is similar in one respect to ZZ Ceti , but why isn't the singlet a doublet and what causes the near doubling of frequency? A similar pattern is seen in G226-29; Kepler *et al.* (1983) show that only three signals are present in this star. The triplet has a mean frequency (period) of 9.15 mHz (109.3*s*) and the three signals are spaced evenly in frequency by

Δf=1.614 $\times 10^{-2}$mHz within observational error. In addition, the amplitudes are symmetric about the center signal making GD385 perhaps the "neatest" of the well-studied low amplitude WDVs.

G117-B15A is an example of organized confusion. Kepler *et al.* (1982) have reported six well-resolved signals whose frequencies are related to each other by various sums and differences and mysterious factors of 3/4 (see their Table 4) — a theoreticians delight and nightmare. With all this going on, the star is remarkably steady in another respect; the strongest signal (at 215.2*s* period and 44 mmag amplitude) is found to be constant, with an upper bound of $9.9\times10^{-15} ss^{-1}$ on $\dot{\Pi}$ (Kepler *et al.* 1988).

None of the hot pulsators match the simplicity of the above stars except perhaps the DOV PG 1707+427, discovered by Bond *et al.* (1984, see also Grauer *et al.*, these proceedings). A first inspection of the power spectrum of PG 1707 reveals only two peaks — one at 447.9*s* and a much smaller one at 334.6*s*. Grauer *et al.*, however, find that the stronger peak varies in amplitude by as much as a factor of three between runs. Their analysis indicates that this peak is possibly composed of two (or more?) signals spaced very closely in frequency and these beat against each other to produce variations in the amplitude of the light curve. The individual signals are not resolvable in a single run. PG 1707 appears to be unique among the hot pulsators — the rest of these variables all show much more complex behavior (as do many DAVs).

(b) "Complex" Variables

There is a prejudice (probably well-founded) among theoreticians in the WDV community that associates low amplitude behavior with simplicity and sinusoidality of signal. This prejudice may be reinforced by the fact that we theorists can only handle such "linear" signals in our calculations; nonlinear calculations of nonradial pulsations of white dwarfs are intractable at present (whereas they have been part of the arsenal of tools used for many years in the study of purely radially pulsating Cepheids). But not all WDVs are linear pulsators and, in fact, most are probably not. Before discussing those observations which clearly indicate nonlinear behavior in WDVs, it is useful to review some results from linear theory that may carry over to the nonlinear regime.

If the dynamic behavior of a WDV is primarily governed by the mechanical response of the star to small (linear) perturbations of pressure, density, etc., (however produced) then the system acts like a coherent collection of springs or pendulums. And, as in a mechanical system, the star responds by pulsating in a ensemble of normal modes, each with a well defined frequency. For a WDV these modes are most certainly (we think!) gravity modes (*g*-modes), where the restoring force for displaced fluid is buoyancy. Also, as in a vibrating mechanical system (such as ocean waves), the modes differ in wavelength and in the geometry of crests, troughs, and nodal points (in three dimensions). It is a characteristic of *g*-modes that the lower frequency modes are the more complex in structure. In the simplest case, a particular mode is conveniently labeled by three indices that describe the nodal structure: in the radial direction the index is *k*, and in the two angular directions (θ and φ in spherical coordinates) these are *l* and *m* (from spherical harmonics... see, not one equation!).

One result from theory is that for nonrotating, nonmagnetic (theorist-style) stars, modes with sufficiently large k , but fixed l and m , are spaced equally in period for successive integer values of k; i.e., $\Pi \propto k$. Is this kind of period spacing seen in real stars? And what if it is not? Well, first of all, the preceding discussion has to do with what modes are *possible* in a WDV; not all (or any) may be present. Some guidance comes from a "nonadiabatic" analysis of pulsations which looks into the linear response of a potential variable with respect to *thermal* effects; i.e., is the star "stable" or "unstable" in certain modes? It may be that all, none, or some of a set of modes in a sequence of equally spaced modes are actually present. A nonadiabatic analysis may indicate this but, to warn the reader, such analyses are difficult and full of pitfalls. We shall review some of the nonadiabatic successes and failures later on.

The prototype DOV, PG 1159-035 (a.k.a. GW Vir), discovered by McGraw *et al.* (1979), is a multiperiodic, large amplitude, pulsator as seen in the optical (Winget *et al.* 1985) and X-ray (Barstow *et al.* 1986). One of us (Kawaler 1988a) has examined the power spectra from extensive optical observations of this star and concludes that some eight signals spanning periods from 390*s* to 833*s* yield a statistically significant mean period spacing of either 21.0±0.3*s* or 8.8±0.1*s*. A comparison with evolutionary models then yields the happy result that the first (second) figure corresponds to a set of l=1 (l=3) modes in a $0.6M_{\odot}$ white dwarf — a mass that is nearly the average for all single white dwarfs (Kawaler 1986; and see Weidemann and Koester 1984, and Oke *et al.* 1984 for traditional determinations of WD masses). However, some modes in the succession of k are never seen (missing intermediate modes), and some modes are not always present in all runs — they come and go.

Linear theory, at its present stage of development, cannot always adequately explain why some modes in a sequence are present and some not. The coming and going of modes is even more sinister. Is the star really in the process of stopping in its tracks and then starting again, or, as is the case with some of the simple pulsators, do some of these modes consist of finely spaced multiplets that periodically beat down the signal? A case can be made for either of these possibilities (and more). Rotation or magnetic fields (see below) can split signals into multiplets, but testing this idea requires long observation to resolve the splitting. Intrinsic appearance and disappearance of normal modes is not out of the question; energy could be transferred in a nonlinear way between widely separated modes, thus extinguishing one and reinforcing another. Present-day theory, at the level needed, is of no help here.

Both rotation and magnetic fields destroy the spherical symmetry of a star and cause a single pulsation mode to split in frequency into a multiplet. Slow, uniform, rotation splits a mode evenly in frequency. The triplet observed in G226-29 (see above) probably falls into this category. So may the two doublets in ZZ Ceti — although Jones *et al.* (1989) make a strong argument that a weak magnetic field of around 10^5 G may be responsible. Direct evidence for splitting is virtually absent in almost all other WDVs. However, stars do rotate, and white dwarfs probably rotate slowly for the most part, and there is no theoretical reason why they should not have magnetic fields of some sort. Hence, *we expect fine splitting of signals to be present in most WDVs — the problem of detecting that splitting is one of resolution.*

The DBV class of variable white dwarfs was predicted and then discovered by Winget and his collaborators (Winget *et al.* 1982a; Winget *et al.* 1982b). The class prototype is GD358 whose power spectrum shows tightly clumped groups of signals in the period ranges 550–950*s*, 300–420*s*, and on to higher frequencies, with pulsation amplitudes of as high as 300 mmag. In the discovery runs, Winget *et al.* (1982a) found that the peaks in each clump were spaced evenly in frequency by $\Delta f = 1.86 \times 10^{-4} s^{-1}$, leading them to suggest that GD358 was rotating with a period of around $(\Delta f)^{-1} \sim 1.5$ hours. Subsequent observations by J.A. Hill (1986) make this interpretation doubtful. He finds that the spacing varies with run length (typically 2--6 hours) and that not all signals are reproducible. This sounds familiar; beating is probably taking place and run lengths are not long enough to resolve the details. H. Saio, of the University of Tokyo, has suggested that perhaps the signals from GD358 are evenly spaced in period rather than frequency. As has been discussed here, the two types of spacing arise from different underlying causes and tell us quite different things about the star. P.W. Jones and one of us (CJH) have examined data kindly provided by Hill and find (unfortunately and paradoxically enough) that equal spacing in period or frequency are statistically equally likely. Sigh!

Other stars that have been extensively observed show problems similar to the above. PG 1159 has been discussed previously (and will be brought up again in a different context) and K1-16 (a PNN) is another example. The latter, discovered by Grauer and Bond (1984), is a very complex pulsator whose pulsation spectrum has not been completely deciphered. Grauer informs us that the best that can be said for it is that bands of power are definitely present. Since K1-16 may be the hottest and fastest evolving of the WDVs, it is essential that we find out what's going on. At the other end of the temperature and evolution scale, much the same might be said for HL Tau 76 — which is the first discovered WDV (Landolt 1968)!

Many of the WDVs show evidence for nonlinearities besides just high amplitudes and temporal changes in amplitude. A striking feature that is often present are signals whose frequencies are linear combinations of the frequencies other signals; i.e., if signals at f_1, f_2, and f_3 are seen, then, for example, f_3 might be equal to f_1+f_2 to the limits of resolution. At this level we might question what constitutes a normal mode for the star. GD358 may fall into this class. Jones and CJH, following a suggestion by Hill, have found that the second group of signals in the power spectrum from that star consist exclusively of linear combinations of signals in the first group. (This shows up clearly in long runs only.) Could it be that the star is excited to initially produce only the first group of modes but, through nonlinear coupling of undetermined origin, then goes on to produce all the rest of what is seen? If so, then simple linear seismological theory only tells part of the story.

Other evidence of a striking nature for nonlinearities comes from (at least) four other WDVs. The best documented is from GD154 (a DAV; Robinson *et al.* 1978) and PG 1351+489 (a DBV; Winget *et al.* 1987, Hill 1986). At first glance, the power spectra from most runs of these two stars look straightforward. There is one strong peak at low frequency — call it f_o — followed by a dribble of lower power peaks at higher frequencies. Closer examination, however, reveals the following: either the higher frequency peaks are exact harmonics of f_o ($2f_o$, $3f_o$, *etc.*), or they are very close to odd half-integer multiples of f_o ($\frac{3}{2}f_o$, $\frac{5}{2}f_o$, etc.). The harmonics are probably due to the periodic, but nonsinusoidal,

shape of the light curve. The other signals are right out of a textbook on nonlinear dynamics. And, just so things don't look too simple, their exact frequencies are: $1.53f_0$, $2.53f_0$, etc., for GD154, and $1.47f_0$, $2.47f_0$, etc., for PG 1351. In addition, apparently just for spite, the $1.53f_0$ signal in GD154 occasionally is the strongest, and $1.47f_0$ sometimes disappears in PG 1351. What gives?

PG 1351 is perhaps the best studied of the DBVs — and, as was once thought, for good reason. Because of the stability of its main peak (at 489.5*s*), researchers at UT (Austin) and CU (Boulder) have attempted to detect a secular change in period of that peak. The data should be sufficient to have done this but the analysis has not yet yielded a consistent result — for unknown reasons — and we blame the star (or our imagination) . Perhaps the nonlinear behavior introduces effects that defeat the analysis. Goupil *et al.* (1988), for example, have suggested that PG 1351 is on its way to chaos. We have examined some of their observational arguments for this conclusion and find that, while tentative, the suggestion has merit and deserves further study.

Well, there you have it. The range of behavior of the WDV pulsations is large indeed, ranging from simple "linear" pulsators with pulsation spectra that are well described by linear theory to stars which undergo complex light variations that border on non-periodic. In all of these pulsators, however, the observed pulsation characteristics do show, to some degree, underlying regularity that can be attributed to linear normal mode pulsation. In the remainder of this paper, we will describe how these regularities allow us to determine structural and evolutionary properties of white dwarf stars. Clearly, we only understand the tip of the iceberg; in working from the fundamental behavior alone we are ignoring the rich complexity that one day will provide even more detailed information about the workings of the white dwarf stars.

2. Physical Interpretation of White Dwarf Pulsation Spectra

As introduced in the previous section, the fundamental nature of the variable white dwarfs is that they are nonradial *g*-mode pulsators. The periods are much longer than the radial pulsation periods one expects from white dwarfs (i.e. 1-10 seconds) and they are multi-periodic. These facts, taken together, are the sole evidence for *g*-mode pulsation. Parameters relevant to *g*-mode pulsation reflect the physical conditions of the host star in an averaged sense; it is this line of thought that leads us to the exploitation of the pulsations in seismological inquiry. These "solid" seismological results are rooted in simple linear adiabatic pulsation theory; other more tentative conclusions can be drawn from the actual existence of observable pulsations. Since the pulsation modes are self-excited, there must be some interesting physics happening to drive the pulsations. Using techniques for examining nonadiabatic pulsations that have been developed over the past 60 years in the study of those yellow and red variables, we can make additional claims about the interior conditions that must exist in these stars.

(a) Mass and Composition from Period Spacings

Normal modes for *g*-mode pulsation are, in limiting cases, equally spaced in period for successive values of *k*. In practice, the mode spacing is not uniform for realistic models of stratified white dwarfs.

In this case, subsurface zones of rapidly changing composition such as the hydrogen-helium interface can "trap" certain modes in the outer layers, so that they are not global modes in a true sense. As shown in Kawaler (1987), this trapping effect can, in DOV models, cause the spacing to vary from mode to mode by up to 25% for low order modes, with the deviation decreasing as k increases. At the observed periods of around 500s, the deviation is less than about 10%, or 2-3s, in the models. In the theorists dream case where each mode in a series were present, we could use the departures from uniform spacings to diagnose the compositional structure of the outer layers of WDVs. The mean spacing over several modes, however, is uniform even in these models. In real stars, where not all modes are present, the spacings look even more uniform than we have the right to expect based on the models!

The period spacing for g-modes in DOVs is very insensitive to the internal composition or exact luminosity. In essence, for standard DOV models, the spacing is most sensitive to total stellar mass for two orders of magnitude in luminosity surrounding the observed DOV stars. Thus, the identification of period spacings in PG 1159 and PG 0122 (Hill, Winget and Nather 1987) have allowed their masses to be measured. In the near future, the resolution of the pulsation spectra of additional DOV star promises to give us a statistically significant (in the astronomer's sense: 5 objects is a respectable sample in this game) sample of white dwarf masses at the hot end of the cooling sequence.

At the cooler temperatures relevant to the DAV and DBV stars, the period spacings are sensitive to the composition of the outer layers as well as to the mass and luminosity of the star. In the DOVs, the whole star contributes about equally to setting the pulsation periods; since white dwarfs differ chemically only in the outermost layers comprising less than 1% of the mass, the DOV period spacings are very insensitive to the precise composition of the outer layers. In cool white dwarfs, the mass motions for each normal mode are large only in the outer, non-degenerate regions. These additional dependencies could result in correspondingly large differences in the fundamental period spacings from star to star. However, the pulsation spectra of some DBVs and DAVs do show surprising systematics (G. Fontaine, private communication) that are currently under investigation.

(b) Rotation Rate and Magnetic Field Strength from Frequency Splittings

As mentioned above, another property of nonradial oscillations is that pulsation modes with the same l and k, but with different values of m all have the same frequency in the absence of effects which remove spherical symmetry. Some processes which can lift this degeneracy include rotation and global magnetic fields. Slow rotation and weak magnetic fields both result in uniform frequency spacing of modes with successive m. By "slow" we mean that the rotation period is much longer than the pulsation periods (i.e. the rotational kinetic energy is smaller than the kinetic energy associated with the pulsation), and by "weak" we mean that the field doesn't affect the equilibrium structure of the star. As mentioned above, it is often difficult to unambiguously determine frequency spacing; even when successful, it is unclear whether rotational effects or magnetic fields are responsible for the splitting. In any case, this facet of seismological study has begun to yield measurements of rotation periods (i.e. 17.2 hours for G226-29) and magnetic field strengths (Jones *et al.* 1989) for a variety of white dwarfs.

(c) Evolutionary Time Scale from Rates of Period Change

Since the normal modes of g-mode pulsation depend on the global properties of the star, as the star evolves the periods of the normal modes will change. As indicated in the first section, the pulsation periods of WDVs can be measured to extraordinary accuracy; thus we can hope to measure the change in these periods in a relatively short time. The time scale for white dwarf cooling increases quickly with decreasing temperature. The DOV stars cool on time scales of 10^6 years or less, while the DAVs cool a thousand times more slowly. Theoretical computations of the rate of period change for DOV models indicate expected period *increases* of about $10^{-11} ss^{-1}$ (Kawaler, Hansen, and Winget 1985) for modes with periods of about 500s. Winget, Hansen and Van Horn (1983) show that cooling tends to increase WDV periods while contraction leads to period decrease with time. The models show a period increase; since they have already reached the constant-radius white dwarf cooling curve, their evolution is dominated by cooling effects.

Using data spanning 5 years, Winget *et al.* (1985) measured a secular period change for the dominant mode of PG 1159 of the same magnitude as expected from theoretical models; however, they found the period to be *decreasing* with time. The negative $\dot{\Pi}$ indicates that contraction dominates cooling in the evolution of the pulsation properties of PG 1159. While it is possible that the luminosity of PG 1159 is much higher than we think, and it is still approaching the white dwarf cooling track, the models say that it would then be difficult to match the magnitude of $\dot{\Pi}$. Rotation may play a role here, though. If PG 1159 rotates (and why shouldn't it ... it has never been very obliging to us simple-minded theorists!) then conservation of angular momentum requires that it spin up as it contracts. Thus if the 516s mode has a non-zero value of m, then its period will change in response to the spin-up. Computations of this effect indicate that it can account for the observations if the rotation period is fairly, but not unreasonably, short... say a few hours.

While rotation can explain the observed sign discrepancy between the simple models and the observations, it is possible that other factors (i.e. nonadiabatic effects, magnetic fields) are also at work. In particular, modes that are trapped near the surface by composition transition regions will be more sensitive to envelope conditions than the more global untrapped modes. The contraction of a hot white dwarf is really a surface effect. Since the degeneracy of the core is much higher than the envelope, it is already about as small as it is going to get. Modes with significant amplitude in the degenerate core will therefore be affected by cooling only. Those modes with small core amplitudes but large envelope amplitudes will be much more sensitive to changes in the envelope; and it is there where most of the radius change occurs. Thus trapped modes will show period decreases at cooler effective temperatures than the untrapped modes. The fact that trapped modes are also more easily excited suggests that the 516s mode of PG 1159 could be one of these modes; the observed secular decrease of its period supports this idea. Despite these possible complications, since the effects of cooling, contraction, and spin-up all occur on comparable time scales, we can say that the current agreement in the size of $\dot{\Pi}$ between PG 1159 and the models confirms the evolutionary status and input physics of models of PG 1159 stars. This means that we are able to calibrate the neutrino emission rates relevant to hot white dwarfs to about a factor of two, since plasmon neutrinos play an important role in the cooling of white dwarf interiors.

The expected rate of period change for DBV stars is about $10^{-13} ss^{-1}$ (Kawaler *et al.* 1986a). Since DBV stars are much cooler than DOV stars, contraction is unimportant throughout the star. Thus the periods of DBV stars must increase with time if evolutionary effects are the only factor. Though smaller than the $\dot{\Pi}$ for DOVs, the quality of its measurement increases, as often sung by Ed Nather, "as time *squared* goes by." However, as detailed in the first section, the best candidate for this measurement, PG 1351, has thwarted attempts to obtain consistent results. The DAV white dwarfs cool on a time scale of a few billion years; Winget (1981) computes a rate of period change for these stars as about $2\times10^{-15} ss^{-1}$, or only a factor of 5 smaller than the upper limit determined by Kepler *et al.* (1988) for G117-B15A. As Winget (1988) points out, this upper limit already has told us that the core composition of G117-B15A cannot be heavier than oxygen; otherwise the models show that it would have a cooling rate, and thus a rate of period change, higher than the observed limit. In effect, the two star photometer has been used as a mass spectrometer in constraining the interior composition of G117-B15A.

(d) Thermal Structure and Composition from Nonadiabatic Considerations

The culprit responsible for driving the pulsations we see in DBV and DAV stars is the partial ionization zone in their outer layers. The cyclical ionization of the dominant species, when it occurs at the proper depth, can cause pulsational instability in modes with the observed periods. We will not go into further detail with respect to the driving in these cool white dwarfs here; we refer the reader to the reviews by Winget and Fontaine (1982), Winget (1988), and Starrfield (1987, and these proceedings) for further discussions. The important facet of all this is that resonances between the thickness of the surface layers of different composition and the nodal structure of the pulsation modes leads to an effective mode selection mechanism. That is, trapped modes are preferentially excited in the DAV and DBV stars.

The success of the partial ionization mechanism in explaining the excitation of DAV and DBV pulsations led Starrfield, Cox, and their collaborators to suggest that the DOV stars are driven by the same process operating in carbon and/or oxygen (Starrfield *et al.* 1983, 1984, 1985). They find, using static C/O envelopes appropriate to PG 1159 and K1-16, that excitation of modes with the correct periods can occur. However, further work by Starrfield (1987) shows that the effect disappears when the helium content of the surface layers increases beyond only 20% or so. This helium "poisoning" suggest to them that not only are the DOV stars hydrogen deficient, but that they are helium deficient as well!

Unfortunately, avoiding this helium poisoning problem removes one of the desirable features of the driving mechanism. Without composition gradients, there is no obvious way for the star to select only a few modes in which to pulsate. Indeed Starrfield *et al.* find that while modes with the correct period are unstable, many more modes are unstable in the models than are seen in the DOV stars. The possibility remains that nonlinear interactions, or the interaction between pulsation and convection, could select only a few modes... but who knows?

Another possible mechanism for driving the DOV pulsations is associated with nuclear burning. Currently, all standard evolutionary models of PNNs and hot white dwarfs have active nuclear burning shells. Sienkiewicz (1980), and Kawaler *et al.* (1986b) show that nuclear burning drives low-k g-mode

pulsation in models appropriate to planetary nebula nuclei. In models with helium-rich surfaces, the unstable periods are a factor of 2-5 shorter than the periods observed in the pulsating PG 1159 stars. It is possible that nuclear burning is responsible for the observed pulsations, but only if some additional physics left out of Kawaler *et al.*'s models is responsible for lengthening the observed periods. For example, the inclusion of mass loss in a self-consistent way into the structure of the the models and also into the stability analysis could provide a stabilizing influence. On the other hand, it could also lengthen the unstable periods to a degree where the pulsations of the DOV stars could be ascribed to modes driven by nuclear burning.

Recently, one of us (SDK) has investigated the pulsation properties of hydrogen-burning PNN models, finding that they too are unstable to short period *g*-mode pulsation. In particular, if the standard PNN models are correct, the hottest PNN should be pulsating with periods of about 50 to 200*s* (Kawaler 1988b). Extensive ground-based optical surveys of the best PNN candidates have been carried out by Hine (1988), and Hine and Nather (1987). Despite detection limits of order 0.5 mmag, as compared with the observed amplitudes of several mmag seen in the DOV stars, Hine and Nather have found no such pulsators. It is possible that the observed stars are, in fact, pulsating, but the amplitudes in the optical are too small to have been detected. If this is the case, then time series X-ray photometry will provide a much more stringent test of the pulsational stability of these objects.

A likely explanation for the important null result of Hine and Nather (1987) is that the standard PNN models used in the vibrational stability analysis are somehow in error. The precise structure of PNNs and PWDs depend sensitively on their prior evolutionary history. Models of PNNs based on this picture suggest that most PNNs have hydrogen-burning shells; this conclusion is based on the fact that models which burn hydrogen show the correct time scales of evolution across the H-R diagram (Schönberner 1987, and references therein). Similar models which burn helium evolve too slowly across through the region of the H-R diagram populated by planetary nebulae.

The null result of Hine and Nather (1987) indicates that current models which contain nuclear-burning shells are inadequate for detailed study of the pulsation and evolution of PNN and hot white dwarfs. For example, if nuclear burning were extinguished in a prior evolutionary stage, then the PNN would remain vibrationally stable. Models which do not contain burning shells but which evolve through the H-R diagram with acceptable time scales can, in principle, be constructed (D'Antona *et al.* 1987). Models of PNN evolution that satisfy the observational constraint that they are pulsationally stable result in white dwarfs with thin surface hydrogen layers. Such hot white dwarfs would be formed with total hydrogen masses less than $10^{-5}M_{\odot}$. However, because the tail of the hydrogen distribution reaches deep into the interior, a small fraction of hydrogen remains even if a large amount of mass is lost from the surface. This scenario for PNN evolution satisfies the pulsation constraint, and results in very few hot hydrogen rich white dwarfs; the surface hydrogen mass fraction falls below 0.1 when mass loss has reduced the total amount of hydrogen remaining to below $10^{-6}M_{\odot}$. The appearance of a hydrogen-rich spectrum in hot white dwarfs would occur only after gravitational settling of heavy elements has floated sufficient hydrogen to the surface, by which time the white dwarf would have cooled to a lower temperature. It is perhaps significant that the luminosity function of hot hydrogen-rich white dwarfs

shows a sharp drop above 70,000K (Fleming, Liebert, and Green 1987). This temperature may provide a clue to total amount of hydrogen that remains at the surface of a cooling PNN. Clearly, the chemical evolution of white dwarf surfaces depends strongly on the initial thickness of the surface hydrogen layer (Fontaine and Wesemael 1987); the lack of observed pulsations in hot PNNs is an important clue to how much hydrogen hot white dwarfs have when they are born.

3. Conclusions

The frontier of stellar evolution represented by the white dwarfs is being pushed back thanks to observational mapping of the pulsation properties of the WDVs over the past 20 years; it is worthwhile to note that the most important tools in all this work have been modest 1-meter class telescopes. Using the observed pulsation spectra of the WDVs, pulsation theory has been able to determine some important quantities describing white dwarfs, such as rotation velocities and total masses. The evolutionary time scale for hot white dwarfs has been measured; it is just a matter of time before the more gradual changes in cooler white dwarfs are also detected. With a little additional work on both observational and theoretical sides, we may soon measure moderate magnetic fields in WDVs. We will also soon be able to quantitatively determine the compositional structure of their outer layers as modelling progresses. Even the lack of observed pulsations in the hottest white dwarfs is leading to re-evaluation of models of their structure. All of this success is rooted in the analysis of the basic pulsation spectra; the rich observed variations on this "linear" theme promise to provide additional detailed information on white dwarf structure and evolution. The WDVs are garden variety white dwarfs that have simply been caught in the act of pulsation; they are currently in one of the relatively brief phases of their evolution in which they are vibrationally unstable. By studying the properties of the pulsators, then, one is sampling the properties of all white dwarfs.

REFERENCES

Barstow, M.A., Holberg, J.B., Grauer A.D., and Winget, D.E. 1986, *Ap. J.*, **306**, L25.
Bond, H.E., Grauer, A.D., Green, R.F., and Liebert, J. 1984,*Ap. J.*, **279**, 751.
Cox, J.P. 1980, *Theory of Stellar Pulsation*, (Princeton University Press: Princeton).
D'Antona, F., Mazzitelli, I., and Sabbadin, F. 1987, in *Planetary and Proto-Planetary Nebulae: From IRAS to ISO*, ed. A. Preite Martinez, (Dordrecht: Reidel) p. 121.
Goupil, M.J., Auvergne, M., and Baglin, A. 1988, *Astr. Ap.*, **196**, L13.
Grauer, A.D., and Bond, H.E. 1984, *Ap. J.*, **277**, 211.
Fleming, T.A., Liebert, J., and Green, R.F. 1987, *Ap. J.*, **308**, 176.
Fontaine, G. and Wesemael, 1987, in *IAU Colloquium #95, The Second Conference on Faint Blue Stars*, eds. A.G.D. Philip, D.S. Hayes, and J. W. Liebert (Schenectady: L. Davis Press), p. 319.
Hill, J.A. 1986, M.A. Dissertation, University of Texas (Austin).
Hill, J.A., Winget, D.E., and Nather, R.E. 1987, in *AU Colloquium #95, The Second Conference on Faint Blue Stars*, eds. A.G.D. Philip, D.S. Hayes, and J. W. Liebert (Schenectady: L. Davis Press), p. 627.
Hine, B.P. 1988, Ph. D. thesis, University of Texas at Austin.
Hine, B.P. and Nather, R.E. 1987, in *IAU Colloquium #95, The Second Conference on Faint Blue Stars*, eds. A.G.D. Philip, D.S. Hayes, and J. W. Liebert (Schenectady: L. Davis Press), p. 619.
Jones, P.W., Pesnell, W.D., Hansen, C.J., and Kawaler, S.D. 1989, *Ap. J.*, January 1, in press.
Kawaler, S.D. 1986, Ph.D Dissertation, University of Texas (Austin).
Kawaler, S.D. 1987, in *I.A.U. Colloquium #95, The Second Conference on Faint Blue Stars*, eds. A.G.D. Philip, D.S. Hayes, and J.W. Liebert, (Schenectady: L. Davis Press), p. 297.
Kawaler, S.D. 1988a, in *I.A.U. Colloquium #123, Advances in Helio- and Asteroseismology*, eds. J. Christensen-Dalsgaard and S. Frandsen, (Dordrecht: Reidel), p. 329.
Kawaler, S.D. 1988b, *Ap. J.*, in press (1 November).

Kawaler, S.D., Hansen, C.J., and Winget, D.E. 1985, *Ap. J.*, **295**, 547.
Kawaler, S.D., Winget, D.E., Iben, I. Jr., and Hansen, C.J. 1986a, *Ap. J.*, **302**, 530.
Kawaler, S.D., Winget; D.E., Hansen, C.J., and Iben, I. Jr. 1986b, *Ap. J. (Lett.)*, **306**, L41.
Kepler, S.O. 1984, *Ap. J.*, **278**, 754.
Kepler, S.O., Robinson, E.L., Nather, R.E., and McGraw, J.T. 1982, *Ap. J.*, **254**, 676.
Kepler, S.O., Robinson, E.L., and Nather, R.E. 1983, *Ap. J.*, **271**, 744.
Kepler, S.O., Winget, D.E., Robinson, E.L., and Nather, R.E. 1988, in *I.A.U. Colloquium #123, Advances in Helio- and Asteroseismology*, eds. J. Christensen-Dalsgaard and S. Frandsen, (Dordrecht: Reidel), p. 325.
Landolt, A.U. 1968, *Ap. J.*, **153**, 151.
McGraw, J.T., Starrfield, S.G., Liebert, J., and Green, R.F. 1979, in *IAU Colloquium 53, White Dwarfs and Variable Degenerate Stars*, eds. H.M. Van Horn and V. Weidemann (Rochester: University of Rochester), p. 377.
Oke, J.B., Weidemann, V., and Koester, D. 1984, *Ap. J.*, **281**, 276.
Robinson, E.L., Stover, R.J., Nather, R.E., and McGraw, J.T. 1978, *Ap. J.*, **220**, 614.
Schönberner, D. 1987, in *Late Stages of Stellar Evolution*, eds. S. Kwok and S.R. Pottasch, (Dordrecht: Reidel), p. 175.
Starrfield, S. 1987, in *I.A.U. Colloquium #95, The Second Conference on Faint Blue Stars*, eds. A.G.D. Philip, D.S. Hayes, and J.W. Liebert, (Schenectady: L. Davis Press), p. 307.
Starrfield, S., Cox, A., Hodson, S., and Pesnell, W.D. 1983, *Ap. J. (Lett.)*, **268**, L27.
Starrfield, S., Cox, A., Kidman, R., and Pesnell, W.D. 1984, *Ap. J.*, **281**, 800.
Starrfield, S., Cox, A., Kidman, R., and Pesnell, W.D. 1985, *Ap. J. (Lett.)*, **293**, L23.
Stover, R.J., Hesser, J.E., Lasker, B.M., Nather, R.E., and Robinson, E.L. 1980, *Ap. J.*, **240**, 865.
Unno, W., Osaki, Y., Ando, H., and Shibahashi, H. 1979, *Nonradial Oscillations of Stars*, (University of Tokyo Press: Tokyo).
Van Horn, H.M. 1984, in *Theoretical Problems in Stellar Stability and Oscillations*, eds. A Noels and M Gabriel (Universite de Liège: Cointe-Ougree, Belgium), p. 307.
Van Horn, H.M., Winget, D.E., and Hansen, C.J. 1989, *Rev. Mod. Phys.*, in preparation.
Weidemann, V., and Koester, D. 1984, *Astr. Ap.*, **132**, 195.
Winget, D.E. 1981, Ph. D. Dissertation, University of Rochester.
Winget, D.E. 1988, in *I.A.U. Colloquium #123, Advances in Helio- and Asteroseismology*, eds. J. Christensen-Dalsgaard and S. Frandsen, (Dordrecht: Reidel), p. 305.
Winget, D.E., and Fontaine, G. 1982, in *Pulsations in Classical and Cataclysmic Variable Stars*, eds. J.P. Cox and C.J. Hansen (Boulder: Joint Institute for Laboratory Astrophysics), p. 46.
Winget, D.E., Van Horn, H.M., Tassoul, M., Hansen, C.J., Fontaine, G., and Carroll, B.W. 1982a, *Ap. J.*, **252**, L65.
Winget, D.E., Robinson, E.L., Nather, R.E., and Fontaine, G. 1982b, *Ap. J.*, **262**, L11.
Winget, D.E., Hansen, C.J., and Van Horn, H.M. 1983, *Nature*, **303**, 781.
Winget, D.E., Kepler, S.O., Robinson, E.L., Nather, R.E., and O'Donoghue, D. 1985, *Ap. J.*, **292**, 606.
Winget, D.E., Nather, R.E., and Hill, J.A. 1987, *Ap. J.*, **316**, 305.

THE WHOLE EARTH TELESCOPE

R. Edward Nather
The University of Texas at Austin

ABSTRACT

The history of our galaxy and the detailed history of star formation in the early universe is written in the white dwarf stars. Recently we have learned how to reach beneath their exposed surfaces by observing white dwarfs that are intrinsic variables. We use the stellar equivalent of seismology to probe their interiors, and thus to unravel the history they hold inside. We have designed and placed into operation an observational technique that uses the whole earth as a telescope platform, defeating the effects of daylight which, until now, had seriously limited the length of a single light curve, and therefore the amount of information we could hope to extract from it. This paper describes our new telescope and presents preliminary results from our first observing run in March, 1988.

TELESCOPE DESCRIPTION

The Multi-Mirror telescope at the University of Arizona, and other multi-mirror designs in various stages of development, collect their mirrors closely in space so they can cooperate to increase the brightness of their optical images. Our new telescope, in contrast, has its several mirrors distributed in longitude around the earth, so they can cooperate in time rather than in space, to increase the resolution (rather than the intensity) of the spectra they obtain. Rather than the traditional spectra in wavelength, we obtain spectra in frequency — power spectra or amplitude spectra — from the time-series data recorded for a single object. We study the regular changes in light level of close binaries and the intrinsic periodic oscillations of white dwarf stars.

The resolution in frequency is determined primarily by the length of the light curve. We use existing telescopes equipped with high speed photometers to obtain light curves of our target objects with as few gaps as possible: as the object is setting for one observer it is rising for another located farther west. The distributed nature of our telescope allows it to remain in darkness as the earth turns on its axis, and thus to keep a single object under continuous study for days, rather than hours.

Figure 1 shows the locations of the different existing optical telescopes we used in March, 1988, for our first observing run using this technique, and Figure 2 lists the observers involved. The overall operation was coordinated in real time from our command post in Austin, Texas, using telex machines and long distance telephone calls for communication. We operate the process as if we were operating a single telescope, so we have come to think of it that way. It may not have the largest light-gathering power in the world — it had the equivalent of a single 3.8m mirror on its first run — but it certainly has the largest telescope mounting (hence its name). And unlike some other telescope designs, additional mirrors can be added quite easily.

In a curious way this is an invisible telescope: it was there all the time, unnoticed, and it disappears again in between scheduled operations. It's very hard to run because administrative overhead is large — planning and coordination of observations and observing techniques, as well as data reduction and analysis. Uniformity of instrumentation is difficult to arrange. The telescope is also difficult to fund because no single monument exists that can be named after a donor; almost all the cost lies in the instrumentation and in operating expenses. But its power to gather scientific data of unprecedented value makes it unlikely that it will return permanently to its earlier, invisible state.

FIRST LIGHT

Figure 3 shows a graph of the time-series photometric coverge during our first operation of the Whole Earth Telescope in March, 1988. Additional spectroscopic coverage of the primary target, PG1346+082, was obtained at the the M.M.T. telescope in Arizona, the 1.8m telescope in Sutherland,

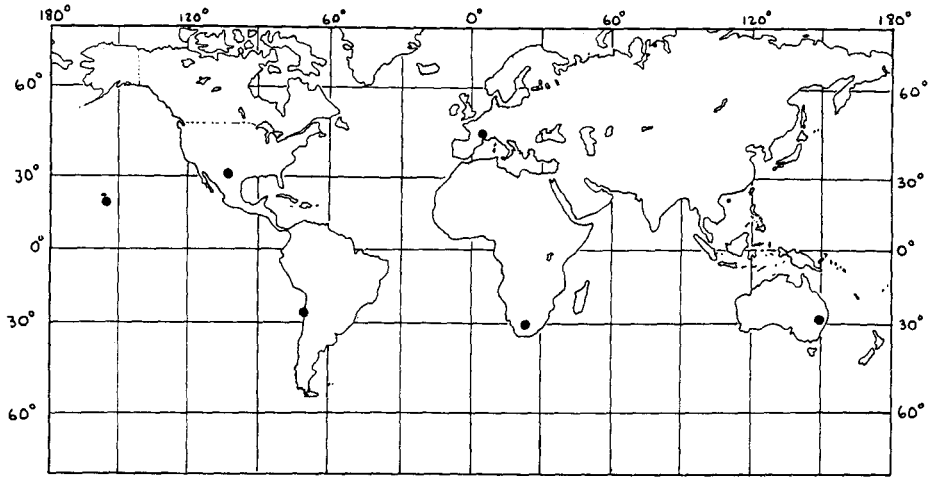

Figure 1: The Whole Earth Telescope. The observatories involved are denoted by the •.

South Africa and the I.U.E. satellite in space. The star rose about three hours after twilight and the early part of the run had more moonlight than was desirable, but these disadvantages were more than offset by unprecedented luck with the weather: most of the sites were photometric most of the time. We give priority to targets which can be seen from observatories in either hemisphere, both to increase coverage and to minimize data loss from atmospheric opacity (clouds). We are unlikely to be this lucky with the weather again and do not require it, but we will not complain if it happens.

Our primary target object, PG1346+082, was one we had studied extensively from a single observatory (Wood *et al.* 1987) but were not satisfied we understood it. Our working model for the system describes it as a close pair of interacting stars, both of which are degenerate. Mass is being stripped from the less massive of the pair by Roche lobe overflow, forms an accretion disk around its orbital companion, and accretes in episodic fashion much like a dwarf nova. The material is pure helium: hydrogen is notable by its total absence. We believe we are seeing revealed the inner core of a star that was once much more massive, burned hydrogen to helium on the main sequence but never initiated helium burning, and later collapsed to form a helium-core white dwarf when hydrogen burning could no longer be sustained. The average rate of mass transfer in the system is set by the effects of gravitational radiation, which removes orbital momentum and forces the two objects to interact.

The episodic nature of the accretion process causes the system to vary from magnitude 17.2, when accretion flow is minimal, to magnitude 13 when it is at a maximum. It behaves much like a yo-yo (or a computer): it's sometimes up but mostly down. We had hoped it would stay near maximum brightness most of the time, because we were convinced our smallest telescope — the 0.6m on Mauna Kea in Hawaii — would be unable to gather useful data should the object stay near minimum. We were wrong. Our observer there got accurate offset measurements from a bright guide star when PG1346 was at magnitude 14, and set on it "blind" for the subsequent nights of the run when it was much fainter. To our astonishment the data were quite usable, if somewhat noisy, a tribute to the dark sky and excellent seeing that permitted use of a very small isolating aperture.

THE SPECTRAL WINDOW

If a star exhibits a single, pure sine wave modulation in brightness, then the Fourier transform of its light curve will show a single delta function at its frequency of modulation — if we can watch it for an infinite amount of time. We can't, of course, so all real light curves have some finite length, and their Fourier transforms show a spike with some finite width for each periodicity present. The shorter the run, the poorer is our ability to resolve two periodicities close together in frequency.

WHOLE EARTH TELESCOPE XCOV-I MARCH 1988

Dramatis Personae

PHOTOMETRIC OBSERVATIONS

Texas, Command Central
D. E. Winget
J. C. Clemens
C. F. Claver
Hawaii, Mauna Kea Observatory
B. P. Hine
Australia, Siding Spring & Mt. Stromlo Observatories
A. D. Grauer
Lilia Ferrario
South Africa, Sutherland Observatory
Brian Warner
Darragh O'Donoghue
Peter Martinez
France, Haute-Province Observatory
Gerard Vauclair
Michel Chevreton
Chile, Cerro Tololo Interamerican Observatory
Greg Henry
S. O. Kepler
Texas, McDonald Observatory
R. E. Nather
M. A. Wood

DATA REDUCTION AND ANALYSIS

Judi Provencal
D. E. Winget
S. O. Kepler
Brian Warner
C. F. Claver

Figure 2: Participants in XCOV-1.

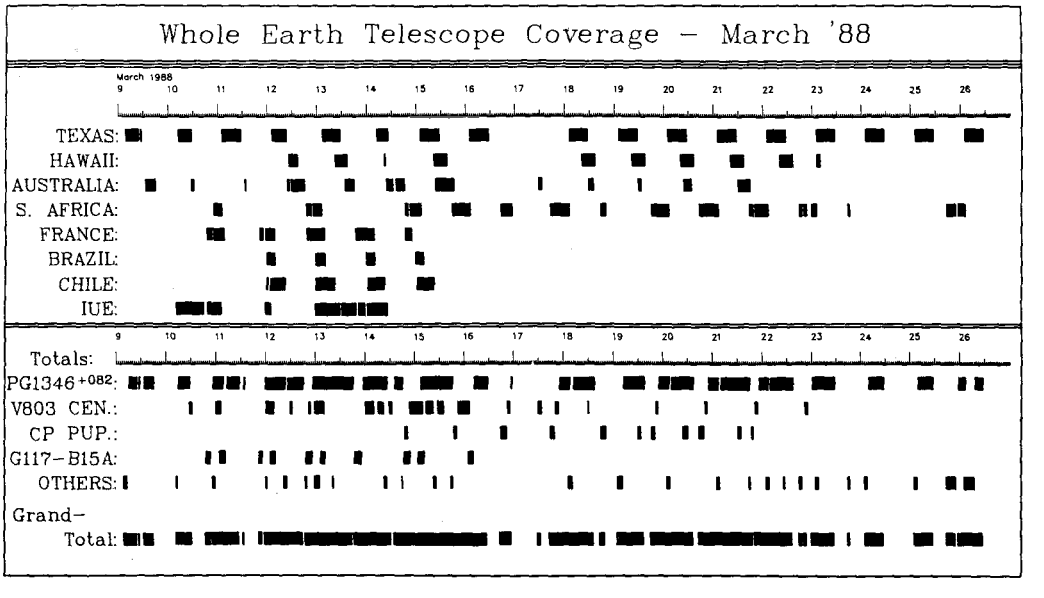

Figure 3: Whole Earth Telescope Coverage

If a long light curve is sampled — that is, if it extends over several successive nights but is interrupted by daylight — then each single periodicity present becomes a forest of spikes in the power spectrum, each one representing a difference of one oscillation cycle from its nearest neighbor. We call this the "alias forest" and it is inevitable if data are obtained only from a single observatory. We can easily calculate the pattern of spikes we can expect for a single, noise-free sine wave by sampling it in just the way our data run was sampled, and then obtaining the Fourier transform of this artifical data. The result is not a pretty sight.

OBSERVATIONAL RESULTS

Figure 4 shows the product of such an exercise for the McDonald data on PG1346, sampled in just the way the original data were taken (Figure 3 shows the data intervals and the daytime gaps

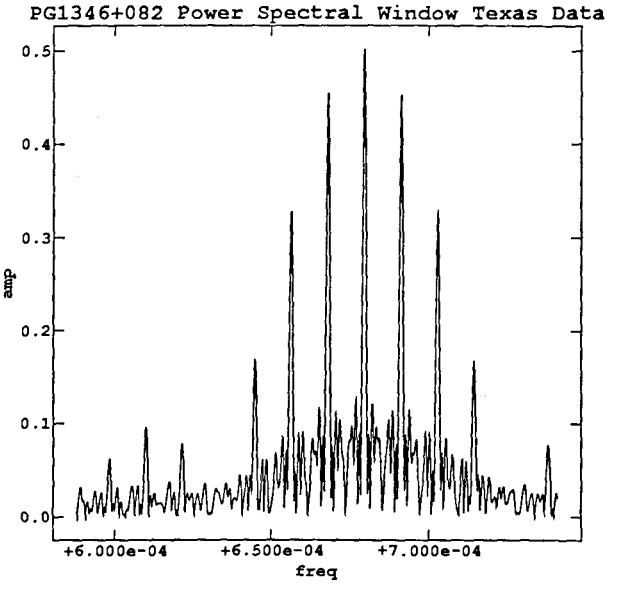

Figure 4: Power spectrum of a sine wave (Texas data only).

between them). Each separate periodicity present in the data will generate this ugly pattern, centered on its own frequency, and piled on top of all the others. While we might be able to identify two or three such patterns jumbled together, separating the multiple periodicities generated by g-mode pulsations is hopeless, particularly in the presence of the inevitable noise of measurment. Figure 5 shows a small portion of the time-series spectrum of PG1346, obtained by using only the data from the Texas observations. The small arrow indicates a periodicity of 1471s, the ninth largest of the group.

Figure 6 shows the spectral window for the complete data set. Ideally, it should contain only a single spike, and it would were our coverage complete. The flanking alias peaks arise because of a periodic gap in coverage at about −6h in longitude — we had not yet established collaboration with astronomers in India. We now have, and hope to reduce this effect on our next run, planned for November 1988. While flanking peaks can arise if one or another observatory is cloudy for part of the run, the most damaging gaps are those which appear regularly throughout the whole data set.

Figure 7 shows the same portion of the time-series spectrum, this time using the combined data from all of the observing sites. Note that the 1471s periodicity is now clearly the most prominent and other periodicities — marked with arrows — can be identified from the simpler patterns they generate in the spectrum. The large number of periodicities which are clearly well above the noise level was a real surprise. Unmarked peaks arise from combinations of the flanking alias peak patterns, so the

interpretation is still a bit tentative. What is clear, though, is that far more than three periods are present in the system in this narrow range of frequencies.

Rotational effects in a binary system can be invoked to explain observed periodicities, but only a few of them. They might arise as rotation of one or both objects on their own axes, if they present non-uniform surfaces to our view, or they might arise from the orbital motion of the pair. Distortions from obscuration or other effects can produce harmonics but will not introduce new, incommensurate periods. The large number of observed peaks in this preliminary data suggest immediately that we are

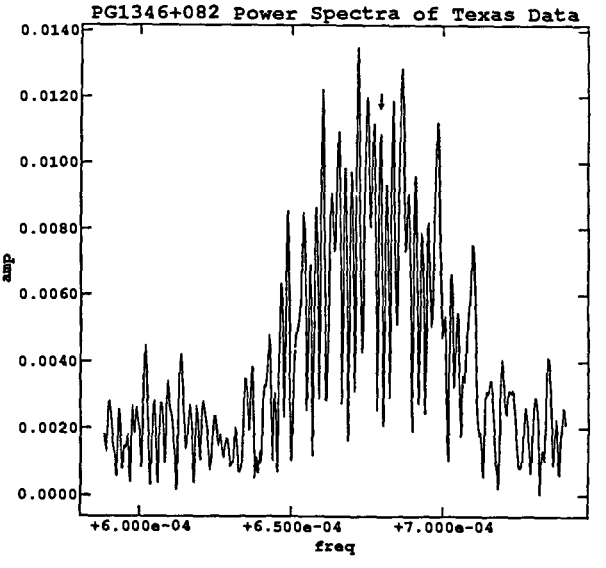

Figure 5: Power spectrum of PG1346+082 (Texas data only).

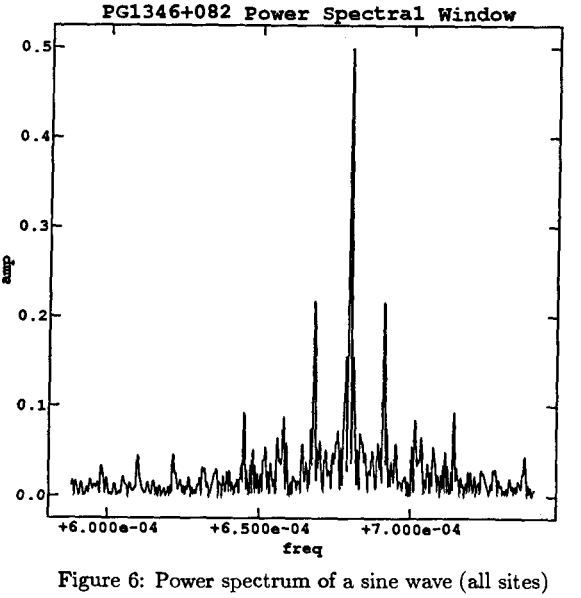

Figure 6: Power spectrum of a sine wave (all sites)

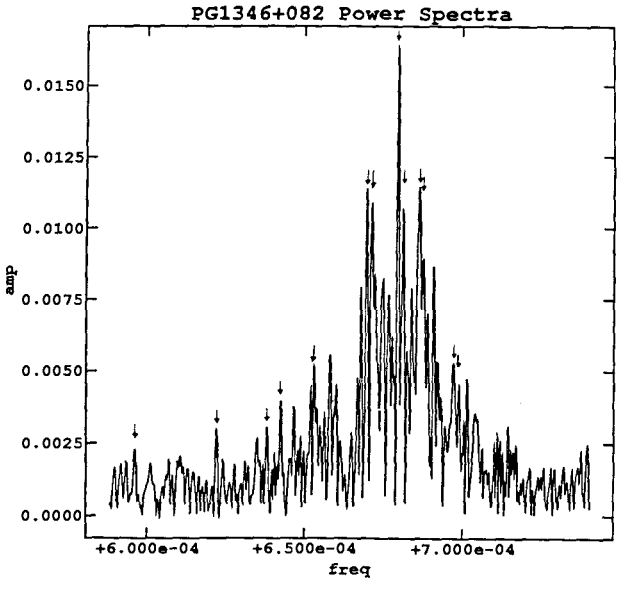

Figure 7: Power spectrum of PG1346+082 (all sites)

seeing g-mode pulsations from the surface of the more massive white dwarf.

This conclusion is quite plausible. The surface temperature of the accreting object lies comfortably within the instability strip for white dwarfs with atmospheres of helium (the DBV stars), and PG1346 spends most of its time in the low state, where light from a bright accretion disk would not drown out the modulation from g-mode oscillations. This wealth of oscillations was not seen by Wood *et al.* in PG1346 during its high state. The "flickering" they reported at minimum will need to be re-examined, however: beating among many periodicities might mimic the flickering seen in mass transfer binaries. It's just possible that mass transfer shuts off completely when PG1346 is at minimum light.

If this picture is correct, then PG1346+082 is the first known object to combine both g-mode pulsations in the accreting object and mass transfer from a degenerate donor — the two mechanisms we have identified that allow us to probe the internal structure of white dwarfs, and attempt to extract from them details about the early history of our galaxy, back when the universe was young.

CONCLUSIONS

Our results presented here are preliminary; a great deal more information can be extracted from the data in hand. We removed all of the slow excursions in brightness so we could better examine the rapid periodicities, and we have not examined all regions of the spectrum where signal power is evident. We have found that the harmonic structure is unexpectedly rich in detail (Provencal *et al.*, these proceedings) and may offer opportunities for exploring the structure of the (pure helium) accretion disk from modulations induced in it.

The development of instruments or techniques that can reveal new things, or can measure known things in a new way, has historically been the path to astronomical discovery and new astrophysical insight. We believe the Whole Earth Telescope is such a development.

REFERENCES

1. Wood, M.A., Winget, D.E., Nather, R.E., Hessman, F.V., Liebert, James, Kurtz, D.W., Wesemael, F. and Wegner, G. 1987, Ap. J., **313**, 757.

THE EFFECTS OF TIME DEPENDANT CONVECTION ON WHITE DWARF RADIAL PULSATIONS

S. Starrfield

Theoretical Division, T-6, MSB288
Los Alamos National Laboratory, Los Alamos, NM 87545
and Department of Physics Arizona State University, Tempe, AZ 85287

and

A. N. Cox
Theoretical Division, T-6, MS B288
Los Alamos National Laboratory, Los Alamos, N.M. 87545

ABSTRACT

We have investigated the effects of relaxing the normal assumption of frozen in convection on studies of radial instabilities in $0.6M_{\odot}$ carbon-oxygen white dwarfs with either pure hydrogen layers overlying pure helium layers or $0.6M_{\odot}$ carbon-oxygen white dwarfs with pure helium surface layers. In this paper we assume that convection can adjust to the pulsation at a rate determined by the time scale of a convective eddy. Using this assumption in our analysis stabilizes most of the modes in both the DA and DB radial instability strips. We also find that the blue edge of the DA radial instability strip, assuming frozen in convection, is between 12,000K and 13,000K. The blue edge for the DB radial instability strip (frozen in convection) is between 32,000K and 33,000K.

I. INTRODUCTION

The first member of the ZZ Ceti class of nonradially pulsating white dwarfs, HL Tau 78, was discovered by Arlo Landolt in 1964. Since its periods and those of other members of the class, discovered later, were much longer than the radial pulsation periods of white dwarfs, it was proposed by both Chanmugam (1972) and Warner and Robinson (1972) that these stars were pulsating in nonradial g^+ modes.

However, the first discovery of an excitation mechanism in DA dwarfs was found for the radial modes of very short period (Cox, Hodson, and Starrfield 1980). In this case the driving was the normal κ and γ effects that are well known from studies of Cepheids and RR Lyrae variables. At that time we did not have a nonradial analysis code available to us and were unable to test our stellar models for nonradial instabilities. This problem was solved by Winget, Van Horn, and Hansen (1981) who used the Saio and Cox (1980) method to analyze both DA and DB dwarfs for instability and found that they were unstable in the same T_e range that we had found radial instabilities.

After that time much of the theoretical work on the DA and DB instability strips was done in order to understand the cause of the driving in the nonradial g^+ modes which are observed in these stars (recent reviews can be found in Starrfield 1987; Winget 1988).

Further work on the radial instability was done by Saio, Winget, and Robinson (1983), Starrfield *et al.*(1983), and Cox *et al.*(1987; hereafter CSKP). In all cases they found that low order radial modes were unstable both in the DA and the DB nonradial instability strips. However, none of the observational studies of either these variables or stars close, in T_e, to these variables found any sign of a radial instability (Robinson 1984; and references therein).

This is an important confrontation between theory and observations since the same white dwarf models are used both in the radial and nonradial studies and, in addition, the same radial analysis methods are used in studies of Cepheids and RR Lyr variables where they have proved to be very successful. Therefore, we have continued to search for a physical mechanism that could damp out the radial instability but would not completely stabilize the nonradial modes.

II. METHOD OF ANALYSIS AND IMPORTANCE OF CONVECTION

One such mechanism is the interaction between pulsation and convection. In our nonradial analyses of the DAV (ZZ Ceti) and DBV classes of variable stars (CSKP), we identified and described the importance of a new driving mechanism for stellar pulsations: convection blocking. This mechanism depends upon the fact that a surface convective region cannot react instantaneously to a change in the energy flow from pulsation and when it carries most of the energy it can block the changing flow of radiation from below and drive pulsations analogous to the κ-effect. This pulsation-convection interaction must be occurring since the pulsational motion of the zones changes the temperature gradient within the convective region so that the flow of energy (through the region) will vary in a very complex fashion. Time dependant convection (TDC) will actually drive pulsations if the period of pulsation is shorter than the convective eddy time scale. If the pulsation period is of the same order or longer than the convective eddy time scale, then convection should damp pulsations.

In an attempt to simulate TDC, we have now added the method of Cox, Brownlee, and Eilers (1966; see also Cox and Giuli 1968) to the Los Alamos linear, nonadiabatic, analysis (LNA) code (CSKP). Their technique removes the assumption of frozen-in convection (the normal assumption in both the radial and nonradial studies of white dwarfs) but also assumes that convection cannot adjust instantaneously to a perturbation. There will be some lag in the adjustment which depends on the ratio of the convective eddy time scale to the pulsation period. They write the perturbation in the convective flux in terms of a constant part plus a time varying part which is assumed to exhibit sinusoidal variations. When this technique is included, it is found that if the pulsation period is much shorter than the convective eddy time scale (the mixing length divided by the convective velocity in the Böhm-Vitense 1958 theory), it becomes difficult for the convective region to adjust to the pulsation and the flow of energy allowed by convection lags the pulsation. In the most extreme case we again find convection blocking and the lag is sufficient to drive rather than damp the instability. Here, we are concerned mostly with a lag that is almost 90 degrees out of phase with the pulsation. Finally, we note that we cannot add the procedure as described by Cox, Brownlee, and Eilers (1966) directly into our nonradial analysis code because it is unable to specify the amount of horizontal energy flow.

In the analysis reported in this paper we use the above LNA code with both TDC and non-TDC (NTDC). We have described this program and our models in some detail elsewhere (CSKP) and will not include that discussion here. We searched in T_e from 9000K to 14,000K for the DA radial instability strip and from 24,000K to 35,000K for the DB radial instability strip. We use various values of l/H_p and find that, as expected, our hottest blue edges require efficient convection (Fontaine, Tassoul, and Wesemael 1984).

III. RESULTS AND DISCUSSION

Our principle result is that for most of the unstable modes found in studies with NTDC, the assumption of TDC stabilizes the modes. There are a few fundamental or very high order modes

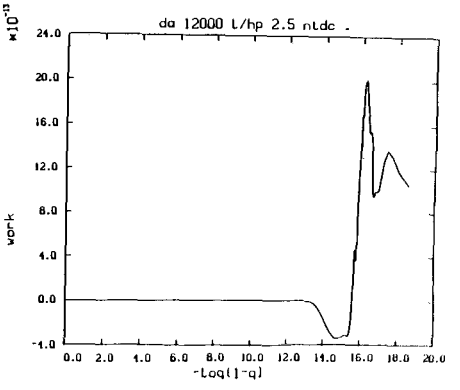

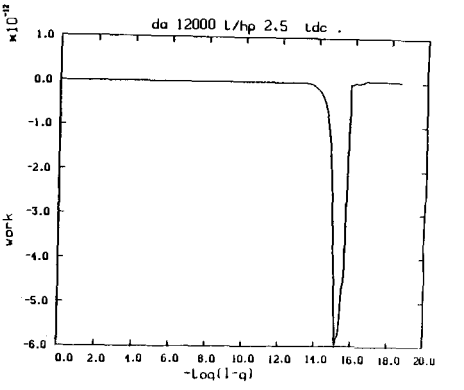

Figure 1a. This is the work plot for the ninth overtone in a DA dwarf with T_e = 12,000K, $1/H_p$ = 2.5, and frozen-in convection (NTDC) assumed. Peak driving occurs at the bottom of the convective region which has a temperature of 33,000K. The period of this mode is 1.43s and it is unstable.

Figure 1b. This is the work plot for the same model in which time dependant convection (TDC) is assumed. All of the driving has disappeared and this mode is stable. Note the difference in scales of the abscissae between the two plots.

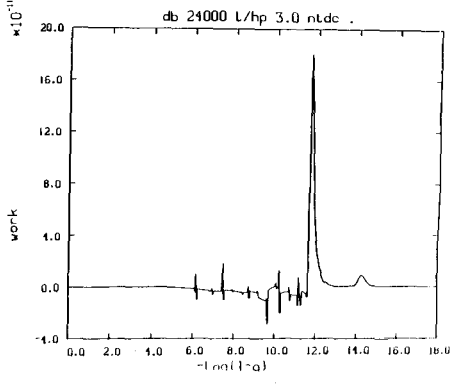

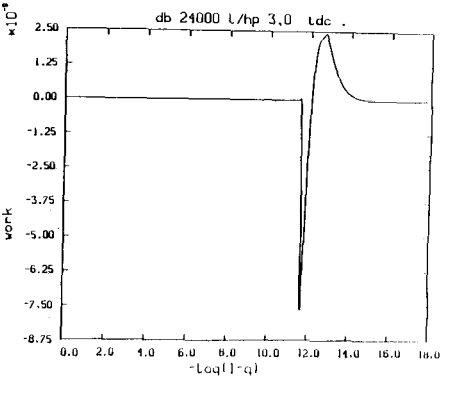

Figure 2a. This is the work plot for the ninth overtone in a DB dwarf with T_e = 24,000K, $1/H_p$ = 3.0, and frozen-in convection (NTDC) assumed. The sharp spikes occur at tabular points and the work sums to zero. The period of this mode is 1.34s, peak driving occurs at a depth where the temperature is 270,000K, and it is unstable.

Figure 2b. The work plot for the same model in which time dependant convection (TDC) is assumed. Again, note the difference in scales of the two abscissae. The masses of the zones increase inwards so that there is more damping than driving in this model and it is stable.

where TDC *causes* an instability but this is because the deepest zone of the convective region has a large convective time scale. This driving may disappear when we include more zones.

We found that the analyses done with NTDC produced a DA radial instability strip that extended from below 9000K (we did not search any cooler in T_e) to 12,000K. The models at 13,000K and 14,000K were stable except for 3 very high order modes at 13,000 (TDC) that were probably driven by only one zone. The models with $l/H_p = 2.5$ were, in general, more unstable than the models with smaller values of l/h_p. Figure 1 shows two work plots for the 9th overtone in a 12,000K model. The differences are obvious.

For the DB instability strip, we found that models with frozen in convection (NTDC) were unstable for T_e's from 24,000 (we did not go cooler) to 32,000K ($l/H_p = 3.0$). Models hotter than this were stable. We were surprised to find that the instability strip extends to this high an T_e since the blue edge for the nonradial instability strip is at ~27,000K. Figure 2 shows two work plots for the 9th overtone in a 24,000K model and it is clear that TDC has stabilized this mode. Some modes at 33,000K and 35,000K were unstable when we analyzed the envelopes assuming TDC. As in the DA's, they seemed to be driven by the deepest convective zone layers.

We gratefully acknowledge discussions with W.D. Pesnell and E. M. Sion. S. Starrfield thanks G. Bell, S. Colgate, M. Henderson, and J. Norman for the hospitality of the Los Alamos National Laboratory and a generous allotment of computer time. This work was partially supported by NSF grant AST85-16173 to Arizona State University and by the DOE.

REFERENCES

Böhm-Vitense, E., *Zs. Ap.*, **46**, 108, (1958).

Chanmugam, G., *Nature Phys. Sci.*, **236**, 83, (1972).

Cox, A. N., Brownlee, R. R., and Eilers, D. D., *Astrophys. J.*, **144**, 1024 (1966).

Cox, A. N., Hodson, S. W., and Starrfield, S., in *Nonradial and Nonlinear Stellar Pulsations*, ed. H. A. Hill and W. Dziembowski, Berlin, Springer-Verlag, p. 453, (1980).

Cox, A. N., Starrfield, S., Kidman, R. B., and Pesnell, W. D., *Astrophys. J.*, **317**, 303, (1987).

Cox, J. P., and Giuli, R. T., *Principles of Stellar Structure*, New York, Gordon and Breach, (1968).

Fontaine, G., Tassoul, M., and Wesemael, F., in *Proc. 25th Liége Internat. Astrophys. Coll.*, ed. A. Noels and M. Gabriel, p. 328, (1984).

Robinson, E. L. *Astron. J.*, **89**, 1732, (1984).

Saio, H., and Cox, J. P., *Astrophys. J.*, **236**, 549, (1980).

Saio, H., Winget, D. E., and Robinson, E. L., *Astrophys. J.*, **265**, 982, (1983).

Starrfield, S., in *Stellar Pulsation: A Memorial to John P. Cox*, ed. A. N. Cox, W. M. Sparks, and S. Starrfield, Berlin, Springer-Verlag, p. 332, (1987).

Starrfield, S., Cox, A. N., Hodson, S. W., and Clancy, S. P., *Astrophys. J.* , **269**, 645, (1983).

Warner, B., and Robinson, E. L., *Nature Physical Science*, **329**, 2, (1972).

Winget, D. E., in *Advances in Helio and Asteroseismology* ed. J. Christensen-Dalsgaard and S. Frandsen, Dordrecht, Reidel, p. 305, (1988).

Winget, D. E., Van Horn, H. M., and Hansen, C. J., *Astrophys. J. Letters*, **245**, L33, (1981).

PG 1707+427: The DOV Star with the Simplest Fourier Transform

Albert D. Grauer
Department of Physics and Astronomy
University of Arkansas at Little Rock

James Liebert
Steward Observatory
University of Arizona

Richard Green
Kitt Peak National Observatory
National Optical Astronomy Observatories

PG 1707+427 was identified in the Palomar-Green survey (Green Schmidt and Liebert, 1986) as an object with a significant ultraviolet excess. Observations by Bond and Grauer in 1982 showed it to be a pulsating variable (Bond, Grauer, Green and Liebert, 1984). Fourier transforms of the discovery time-series photometric runs revealed power in PG 1707+427's light curves in two bands with periods near 450-s and 333-s. The longer period peak was observed to have a variable amplitude while the other one appeared relatively constant in strength. Wesemael, Green and Liebert (1985) placed PG 1707+427 in the spectroscopic class of PG 1159-035 (DOV) pulsating variables.

McGraw, Starrfield, Liebert and Green (1979) found that PG 1159-035 pulsates. It is the prototype of the DOV class of variable stars. These authors and others (Winget, Hansen and Van Horn, 1983) suggested that the internal structural evolution of such a star can be measured through careful observation of its pulsational periods. Winget, Kepler, Robinson, Nather and O'Donoghue (1985) have been able to measure an evolutionary rate of period change for PG 1159-035.

In 1987 the authors began to gather time-series photometric data on PG 1707+427 to determine if any stable periods suitable for the measurement of dP/dt exist in its power spectrum. The 1.3-m telescope at Kitt Peak National Observatory and Steward Observatory's 1.5-m telescope on Mt. Bigelow and 1.5-m telescope on Mt. Lemmon were used. The two-star photometer of the University of Arkansas at Little Rock was used for all of the observations. An Apple II microcomputer

recorded the 1987 data. It was replaced in 1988 by an IBM PC clone type computer with an interface board designed by Chris Clemens (1988). PG 1707+427 and a nearby comparison star were observed simultaneously with two separate photomultipliers. No filters were used with the blue-sensitive (3200-6500 A) bialkali photocathodes to increase the count rates. The effective wavelength of the photomultiplier-tube-atmosphere combination is slightly bluer than Johnson B with a peak response occuring between 3700 and 4000 A. To date more than 114 hours of observations on 30 nights have been recorded. The purpose of this paper is to report on the preliminary results of this effort.

A 3.1-h run on 23 May 1987 coupled with a 6.4-h time-series data set obtained on the following night revealed several important facts concerning PG 1707+427. The Fourier transform (Deeming, 1975) calculated from each night's data contained only two peaks with periods near 448-s and 335-s. The amplitude of the shorter period component was approximately the same on both nights while that of the longer period one was significantly different for these two data sets. When the transform of both nights data combined was calculated the main (448-s) peak appeared to be unresolved. However CLEAN (Roberts, Lehar and Dreher 1987) found this peak to have a 447.107-s and a 449.026-s component whose beat period is 1.2 days. Future observations showed a remarkable similarity between this calculation and what is actually happening in PG 1707+427's light curves.

Thirty time-series data sets were obtained for PG 1707+427 in May, June and October of 1987 and May and June of 1988. The Fourier transforms of every one of the individual nights show only two peaks near 448-s and 335-s. The amplitude of the 448-s period peak varies by more than a factor of three while that of the shorter period one is similar from night-to-night. For example, semi-amplitudes of the 448-s peak on 9 May and 11 May of 1988 were 29.2 and 9.2 millimagnitudes respectively.

The amplitude of the 448-s period peak was calculated for each of the nineteen nights obtained in May and June of 1988. For those data sets longer than 6-hr in duration, transforms of both the first and second half of the data set were also calculated. A total of 29 Fourier transform amplitudes for the 448-s peak were fitted to a sine wave using a least squares technique. The beat period so obtained is 1.30218-d. The same sine wave fits both the May and June 1988 data.

For the May 1988 data set, simple inspection of the multi-night transform and CLEAN show the main peak to have a 447.163-s and a 448.942-s component whose beat period is 1.306-d.

The light curves have been analyzed individually and in blocks of nights by using a non-linear least squares fit to a sine wave. The two components constituting the main peak in the power spectrum have been found to have phase coherence for over one year. These components have periods of 447.163854-s and 448.947344-s. It appears that it will be possible to have a sufficient time base to measure dP/dt for this star in the near future.

ACKNOWLEDGEMENTS

This work was supported in part by NSF grant AST-8712249 (ADG). The authors would like to thank the Directors and Staff of Kitt Peak National Observatory and Steward Observatory for telescope time and assistance. Pat Purnell-Grauer helped to make this research effort possible.

REFERENCES

Bond, H.E., Grauer, A.D., Green, R.F. and Liebert, J.W. 1984, Ap. J., 279, 751
Clemens, Chris 1988, private communications.
Deeming, T.J. 1975, Ap. Space Sci., 36, 137.
Green, R.F., Schmidt, M. and Liebert, J.W. 1986, Ap. J. Suppl., 61, 305.
McGraw, J.T. Starrfield, S.G., Liebert, J. and Green, R.F. 1979, in IAU Colloquium No. 53, White Dwarfs and Variable Degenerate Stars, ed. H. Van Horn and V. Weidemann (Rochester: University of Rochester), p. 377
Roberts, D.H., Lehar, J. and Dreher, J.W. 1987, A.J., 93, 968.
Wesemael, F., Green, R.F., and Liebert, J.W. 1985, Ap. J. Suppl., 58, 379.
Winget, D.E., Hansen, C.J., and Van Horn, H.M. 1983, Nature, 303, 781.
Winget, D.E., Kepler, S.O., Robinson, E.L., Nather, R.E. and O'Donoghue, D. 1985, Ap. J., 292, 606.

OBSERVATIONS OF COLD DEGENERATE STARS

Maria Teresa Ruiz[1,2] Claudio Anguita[1] and Jose Maza[3]
Departamento de Astronomia, Universidad de Chile

1 Abstract.

Spectrophotometry, BVRI CCD photometry and CCD trigonometric parallaxes of the southern DC stars vB3, ER8 and ESO 439-26 are presented. These stars should be considered among the lowest luminosity degenerates known, with absolute visual magnitudes of 15.4, 16.2 and 17.2 respectively.

2 Introduction.

Recently the study of cold DC type white dwarfs has received considerable attention. These old stars can provide crucial information about the star formation history of the Galaxy, the age of the galactic disk (Winget et al. 1987) and also give observational constraints necessary to tne formulation of cooling theories of white dwarfs.

One of the controversial issues related to these very low luminosity degenerates is their number density, that is the trend of the White Dwarf's Luminosity Function at its faint end. There is also the question of their bolometric magnitudes, which provides information about sizes and masses of WDs. In both cases it is important to obtain their distances and apparent magnitudes with accuracy.

Motivated by the importance of cold DC stars, we included a few of them in a CCD parallax program of faint southern nearby stars presently under way at our institution (Anguita and Ruiz, 1988).

3 Observations.

Good signal-to-noise spectrophotometry of vB3, ER8 and ESO439-26 was obtained in March 1988 at La Silla (ESO) using the 3.6m telescope and EFOSC (ESO Faint Objects Spectrograph and Camera) with the B300 grism covering tne spectral range between 3800 Å and 6900 Å with about 20 Å resolution. The spectra thus obtained are shown in Figures 1, 2 and 3.

---

1 Visiting Astronomer, Cerro Tololo Interamerican Observatory (NOAO).
2 Visiting Astronomer, La Silla Observatory (ESO).
3 Visiting Astronomer, Las Campanas Observatory, (Carnegie).

TABLE 1

	vB3	ER8	ESO439-26
V	16.59	17.05	20.34
B-V	+1.20	+1.40	+1.3
V-R	+0.63	+0.73	+0.37
R-I	+0.57	+0.60	+0.44
Parallax (")	0.0575±0.0031	0.0676±0.0033	0.0240±0.0090
Distance (pc)	17.4±1	14.8±0.8	41.7^{+25}_{-10}
M_V	15.4±0.1	16.2±0.1	$17.2^{+.7}_{-1}$
μ ("/year)	1.7015±0.0063	2.1812±0.0020	0.3972±0.0140
μα cosδ ("/year)	-0.2796	-2.1805	-0.3960
μδ ("/year)	+1.6784	-0.0542	+0.0307
v_t (km/s)	140±8	153±8	78^{+45}_{-25}

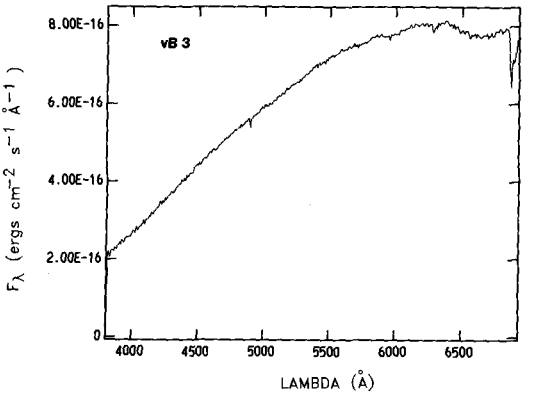

Figure 1. Spectrum of vB3 taken with the ESO 3.6m telescope. The integration time was 1 hour.

CCD photometry of vB3 has been published by Kunkel et al. (1984) their results together with our CCD photometry for ER8 and ESO439-26 obtained in March 1988 at Las Campanas 1m telescope equipped with a TI chip, is summarized in Table 1.

The CCD parallaxes and proper motions obtained by Anguita and Ruiz (1988) using the CTIO 1.5m telescope and an RCA chip are also given in Table 3.

Figure 4 is a finding chart for ESO439-26, its 1986.1 coordinates for the equinox 1950.0 are: $\alpha=11^h\ 36^m\ 33^s.4$ and $\delta=-28°\ 35'\ 39''$. This star was found during a search for faint nearby stars (Ruiz et al. 1988).

3. Results.

The spectra in Figures 1, 2 and 3 look very similar with a smooth continuum showing a broad shallow absorption near 6600 Å, this feature

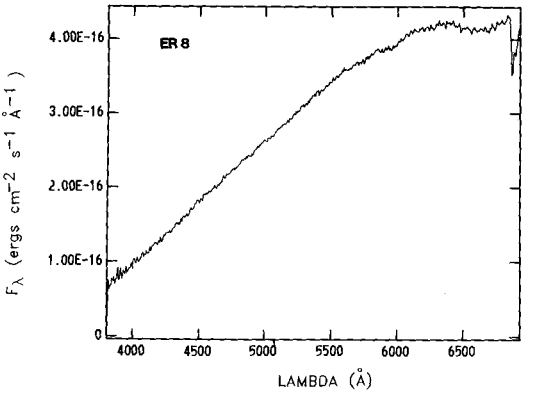

Figure 2. Spectrum of ER8 taken with 1 hour of integration.

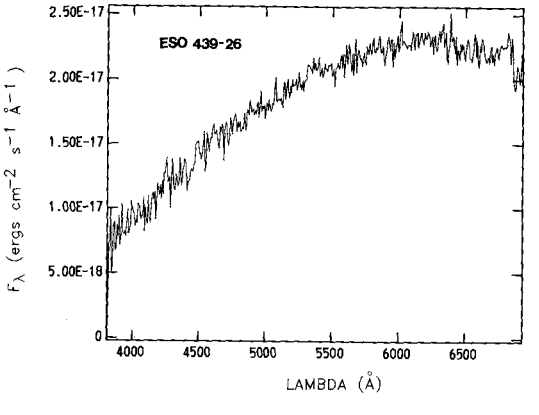

Figure 3. Spectrum of ESO439-26 taken with 3 hours of integration.

was also observed in the DC star ESO439-163 (see Ruiz and Maza this volume). Other faint non DC stars observed during the same run did not show the broad shallow feature, suggesting that it might be real and not an artifact of the observing or reduction procedures. The identification of the 6600 Å feature with Hα is tempting; however a definite ID should await the fitting of an appropriate model atmosphere to the observed spectra.

The CCD photometry given in Table 1 show that the spectral distribution of these cold degenerates differ from one another. It is clear that even when their B-V colors are similar (like ESO439-26 and ER8) their V-R and R-I colors are different and so are their bolometric corrections, which do not correspond to that of a black body at a given temperature. The bolometric corrections for these stars are probably close to 0.0 (Liebert et al. 1988), therefore an estimate of their luminosities can be obtained from the visual absolute magnitudes in Table 1, taking BC=0.0. They turn out to be:

$$L\ (vB3) = 5.5 * 10^{-5}\ L_\odot$$

$$L\ (ER8) = 2.6 * 10^{-5}\ L_\odot$$

$$L\ (439\text{-}26) = 1.0 * 10^{-5}\ L_\odot$$

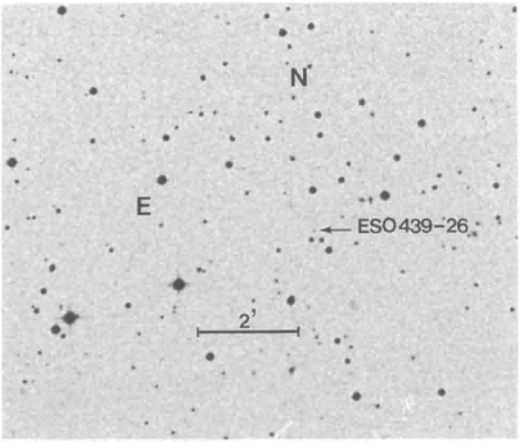

Figure 4. Finding chart for the star ESO439-26.

The large differences observed in the luminosities are partly due to differences in their BC and partly the consequence of a different evolutionary history suggesting that isolated white dwarfs like ER8 and ESO439-26 are more massive than those members of a binary like vB3, giving some weight to the bimodal star formation hypothesis (Larson, 1986).

This research received partial support from FONDECYT, grant #359/87-88.

References.

Anguita, C. and Ruiz, M.T., 1988, in preparation.

Kunkel, W.E., Liebert, J. and Boroson, T.A., 1984, Pub. A.S.P., 96, 891.

Larson, R.B., 1986, M.N.R.A.S., 218, 409.

Liebert, J., Dahn, C.C., and Monet, D.G., 1988, Ap. J. September 1 issue.

Ruiz, M.T., Maza, J., Mendez, R., and Wischnjewsky, M., 1988. "The ESO Messenger", September issue.

Winget, D.E., Hansen, C.J., Liebert, J., Van Horn, H.M., Fontaine, G., Nather, R.E., Kepler, S.O., and Lamb, D.Q., 1987, Ap. J. Lett., 315, L77.

TWO NEW FAINT COMMON PROPER MOTION PAIRS

María Teresa Ruiz[1] and José Maza[2]
Departamento de Astronomía, Universidad de Chile

1 Abstract

Spectrophotometry of the common proper motion pairs ESO439-162/163 and ESO440-55a/55b shows that the first is formed by an m_V=18.8 magnetic DQ white dwarf and an m_V=19.8 DC9 wnite dwarf separated by 23". ESO440-55a/55b has an m_V=20.2 red dwarf (ST=M5.1) component and a DZ7 white dwarf with m_V=19.3, their angular separation being 5".4. The proper motion of the pairs is μ=0.38±0.03"/year and μ=0.22±0.04"/year respectively.

2 Observations

As a result of a search program for faint nearby stars, done using glass copies of the ESO R Survey plates, (Ruiz et al, 1988) we have found several common proper motion pairs not previously catalogued. Figure 1 and 2 are finding charts for ESO439-162/163 and ESO440-55a/55b. Spectrophotometry of the above pairs revealed that both contained WD components. The spectra were obtained at La Silla (ESO) in March 1988 using the 3.6m telescope equipped with EFOSC (Faint Objects Spectrograph and Camera) and a CCD RCA detector. With a 2" slit the resolution was about 20 Å, the night was photometric with a seeing of 1".5. Three flux standards and He-Ar lamps were observed during the night for flux and wavelength calibrations. The spectrograph was rotated in order to obtain the spectra of both components of each pair at the same time. The spectra are shown in Figures 3a, 3b, 4a and 4b. Integration times were 3 hours for ESO439-162/163 and 2 hours in the case of ESO440-55a/55b.

CCD photometry for ESO439-162/163 was obtained in March 1988 at Las Campanas (Carnegie) with the 1m telescope and a TI chip. The results are given in Table 1, where B, V are in the Johnson system and R, I in the Kron-Cousins system.

---

1 Visiting Astronomer, European Southern Observatory (La Silla).
2 Visiting Astronomer, Las Campanas Observatory (Carnegie).

TABLE 1

CCD Photometry of ESO439-162/163

	V	B-V	V-R	R-I
ESO439-162	18.77	0.82	0.53	0.31
ESO439-163	19.84	1.14	0.80	0.13

No CCD photometry is yet available for ESO440-55a/55b therefore the apparent magnitudes have been estimated from the spectra in Figures 4a and 4b. For ESO440-55a we get an apparent visual magnitude $m_V \approx 19.3$ and for ESO440-55b and $m_V \approx 20.2$.

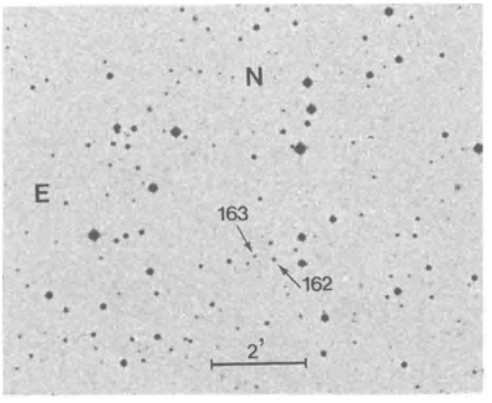

Figure 1. Finding chart for ESO439-162/163. The 1986.1 coordinates (equinox 1950.0) of ESO 439-162 are; $\alpha=11^h27^m24\overset{s}{.}0$ and $\delta=-31°06'19''$.

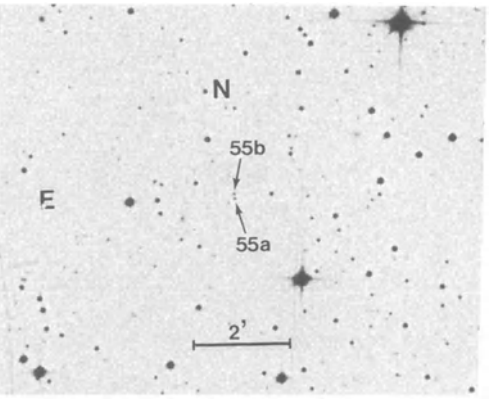

Figure 2. Finding chart for ESO 440-55a/55b. The 1979.2 coordinates (equinox 1950.0) of ESO440-55a are: $\alpha=12^h04^m03\overset{s}{.}2$ and $\delta=-31°20'30''$.

3 Results

a)ESO439-162/163: This pair formed by a magnetic DQ white dwarf (439-162) and a cold DC white dwarf (439-163) has a proper motion $\mu=0.38\pm0.03$("/year) in the direction $\Theta=233°$, the separation between the stars is 23". If we assume that the absolute visual magnitude of the cold DC star ESO439-163 is $M_V \approx 17$ then its distance would be 35 pc, at such distance their separation would be 1.2×10^{16} cm.

The star ESO439-162 has a remarkable spectrum showing broad absorption troughs, similar only to those observed in LP790-29 whose spectral features have been identified by Liebert et al. (1978) as due to C_2 Swan bands distorted by a strong ($B \geq 10^8$G) magnetic field. In ESO439-162 the absorptions observed at 4590 Å, 4992 Å, 5411 Å and 5912 Å correspond

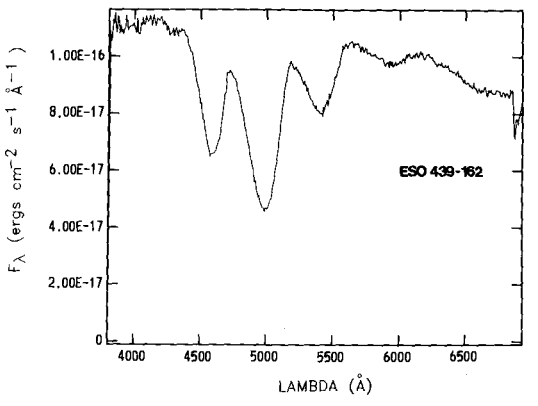

Figure 3a. Spectrum of ESO439-162. The integration time was 3 hours.

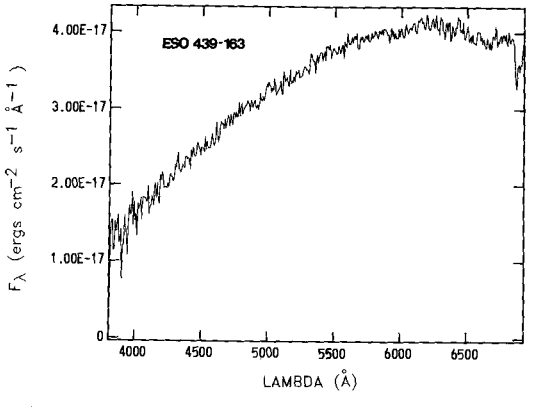

Figure 3b. Spectrum of ESO439-163 taken with an integration time of 3 hours.

to those normally (B≈0) at 4700 Å, 5160 Å, 5585 Å and 6100 Å respectively due to the Swan band of C_2. The observed displacement in wavelength of the absorptions are produced by a magnetic field B∿10^8G.

The companion star ESO439-163, has a smooth spectrum typical of DC white dwarfs with a spectral distribution that can be fitted by a 4000K black body, while that of ESO439-162 corresponds (with some imagination) to a black body at 6300K. This difference in temperature and magnitude reflects a large difference in their cooling ages (of 10^9 years or more), which would suggest that the mass of the progenitor of ESO439-162 must have been significantly less than that of its cold DC companion, contradicting the idea that the progenitors of magnetic white dwarfs are Ap stars, which have masses > $2M_\odot$ (Angel et al. 1981).

b) ESO440-55a/55b: This pair, formed by a DZ7 white dwarf and an M5.1 red dwarf, share a common proper motion μ=0.22±0.04 ("/year) in the direction θ=273°. The components have an angular separation of 5".4.

The absolute visual magnitude of an M5.1 dwarf is M_V∿14.8 (Wing and Dean, 1983) which suggests a distance to ESO440-55b, given its m_V ≈ 20.2, of 120 pc.

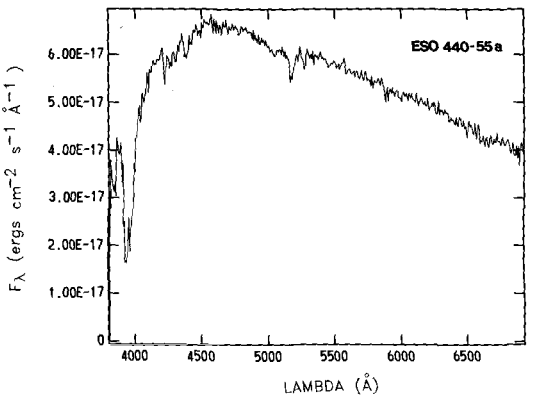

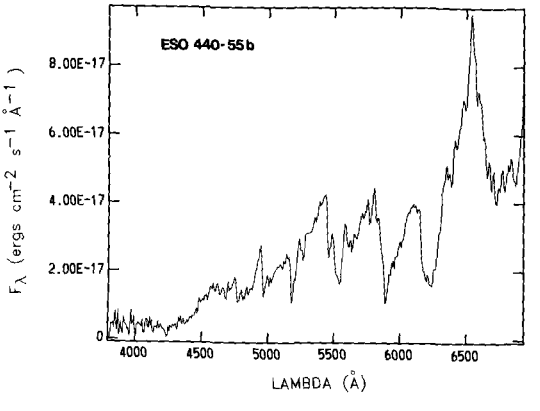

Figures 4a and 4b, Spectra of ESO440-55a and ESO440-55b respectively, taken with an integration time of 2 hours.

The star ESO440-55a has a DC type spectrum with lines of CaII (H and K), CaI (4227 Å), MgI (3839 Å, 5173 Å + 5184 Å) and FeI (4384 Å, 5270 Å and 5456 Å) no H or He lines are present. The spectrum can be fitted by a BB at T≈7000 K, at a distance of 120 pc its absolute visual magnitude would be $M_V \approx 13.9$.

The mechanism most commonly invoked for the presence of metals in the atmospheres of DZ stars is that of accretion from interstellar clouds, however in order to explain the peculiar abundances in their atmospheres a selective mechanism which inhibits the accretion of H has to exist, up to now all of those proposed work efficiently for $T \geq 11000 \pm 1000$K (Liebert et al. 1987) and for DZ stars as cold as ESO440-55a there is no satisfactory explanation for the presence of metals in their atmospheres.

We would like to thank Dr. James Liebert for very helpful comments. This research received partial support from FONDECYT grant #359-87/88.

References

Angel,J.R.P., Borra,E., and Landstreet,J.D., 1981, Ap.J.Suppl., 45, 457.

Liebert,J., Angel,J.R.P., Stockman,H.S., and Beaver,E.A., 1987, Ap.J., 225, 181.

Liebert,J., Wehrse,R., and Green,R.F., 1987, Astron. Astrophys. 175, 173.

Ruiz,M.T., Maza,J., Mendez,R., and Wischnjewsky,M., 1988, "The ESO Messenger" September issue.

Wing,R. and Dean,C.A., 1983, "IAU Colloq. N°76", ed. A.G.D. Philip and A.R. Upgren, pg. 385.

Cluster analysis of the hot subdwarfs in the PG survey.

by Peter Thejll[1], Darryl Charache, Harry L. Shipman
Department of Physics and Astronomy, University of Delaware,
Newark, DE 19716.

Introduction

The Palomar Green survey (Green et al., 1986) of faint blue, high galactic-latitude objects, turned up several interesting new classes of objects, such as gravitational lenses (Weyman et al., 1980), the ultra hot star H1504+65 (Nousek et al., 1986), and the PG 1159-035 variables (McGraw et al., 1979). The PG survey forms a mainstay in the investigations of late stages of stellar evolution. Work (Flemming et al., 1986) has already cast light on the important question of the space density of DA's and continuing work is seeking values for similar population parameters for the subdwarfs: Evolutionary links between the subdwarf stage and white dwarfs will thereby be illuminated.

Astrophysics shares certain traits with botany and zoology - the collection and counting of different types of objects. The reason is straightforward; it is hoped that different types of stars represent different evolutionary stages or that the relative distribution over the classes of objects will give insight into evolutionary rates etc. In biology it has happened that nearly identical specimens from the same species were 'classified' as representing a new species - only to turn out to be the male or the female of the species. The same might happen in the astrophysical beastiary if too fine distinctions are made between objects - notably if the distinctions are based on data of low quality.

If the subdivisions are objectively defined and if the data is of such a quality that the categories are significantly different from each other then one may be able to use the characteristics of these classes to study evolution. The key is to choose objective criteria for subdividing the spectra. No matter how important the chosen criteria for subdivision are, nothing will be learned if the data is of such low quality that the groupings are sensitive to noise in the data. Cluster analysis, carried out properly, offers the means for such a robust subdivision.

Using cluster analysis

Cluster analysis consists of certain arithmetic steps carried out on numerical data. The clusters are found as algorithms look for similarity between data points based on a 'distance' between the objects. The rules for calculating the distance and the rules for deciding on the degree of similarity are chosen from a large set of possible methods. One problem with using cluster analysis is that the results can depend on the method used. The best

[1]This research was supported by the Danish Research Academy, grant no. 880070, the NSF grants AST-8720, AST-8515747 and NASA grant NAG 5-972.

choice is one that gives results that are *similar* to those of other methods. You should not choose a method that gives results *different* from most other methods - the information would be artefacts of the method and not consequences of the data.

There is furthermore the question of how many clusters to subdivide the data into. Most clustering programs will give a dendrogram, or a tree, showing the interrelations of the data points. On a dendrogram (Figure 1) you can see how closely related any two classes are by how far up the tree they are joined by a horizontal branch - the higher, the less related are the two groups. At one end of the tree all objects fall into two groups and at the other end they fall into individual groups with one member in each. Where should one 'cut' the dendrogram? If the data was noise free one could choose the cut anywhere one wished purely from considerations of the ultimate needs of the user; any degree of smoothing or enhancement of details could be furnished. When the data is noisy, however, it becomes meaningless to cut the tree at a level so low that, given typical noise, many of the objects might as well be in other clusters. Usually the user wants as much detail as possible so the cutoff point is defined by the level at which noise does not significantly alter the memberships of the clusters.

The Data

We used values for the equivalent widths of the lines H_γ at 4340 A, HeI at 4387 A, HeI at 4471 A, HeII at 4542 A, HeII at 4686 A and HeI at 4713 A. These values were obtained from spectra taken of the subdwarfs with the 90 inch telescope at Kitt Peak by Dr. Richard Green (Kitt Peak) and Dr. James Liebert (Steward Observatory) during several years. Between the spectra quality varies: The best are few and have very little noise, there are about as many of low quality with barely visible lines while the majority have medium quality and often allow the determination of the weakest lines' equivalent width to within 50% or so. The equivalent widths were obtained partly at Kitt Peak and at Steward Observatory using software that did the calculations from files of the spectra on

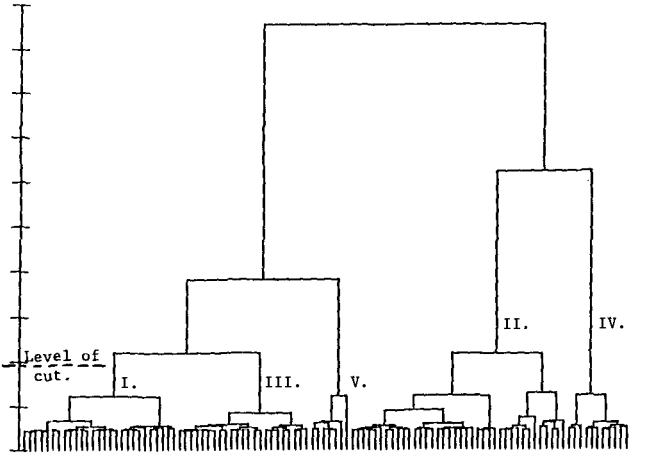

Figure 1: A dendrogram of the average equivalent widths of the Hydrogen, Helium I and Helium II lines in the spectra of 106 hot, helium rich spectra. If the tree is cut at the level shown 5 groups appear. This is the lowest level at which the tree can be cut, given the typical noise in the data. The tree should not be cut lower so that group II breaks into two classes. The dendrogram was produced using Euclidean distances between the data points and clustered by Wards method.

magnetic tapes and partly at University of Delaware, using a hand digitizer and photocopies of plots of the spectra. Although distortions are introduced by this procedure the errors are in no cases as large as the noise inherent to the observational data.

The spectra we have form a subset of the complete survey of subdwarfs in the PG catalog. Some of the spectra were clearly from high gravity objects with line widths of a hundred Angstroms, some were of medium gravity and some were from objects originally classified as white dwarfs in the PG survey before higher quality spectra were obtained. We choose to apply cluster analysis to all Helium rich objects of medium gravity. This is 106 stars out of 121. Liebert and Green have taken pains to obtain spectra of good quality from as many of the 'sdO-like' stars in the PG survey as possible; there should be no selection effects in the subset we have. There are about 220 sdO's in the PG catalog: Applying a correction for the white dwarfs reclassified as sdO's, we see that our subset of 106 sd's is about 50% of all the subdwarfs in the volume of stars surveyed. As has been pointed out (Green et al., 1986) the survey is *complete* for subdwarfs - the observed cone stretches outside the galaxy and has not missed any subdwarfs.

It became clear that we should average all lines from similar ionic species to avoid dominance of line types that appear often - like HeI lines. Therefore we averaged all Hydrogen lines, all HeI lines and all HeII lines and used these averages for the cluster analysis.

The Results

We applied cluster analysis, using the CLUSTAN program (Wishart, 1982), to the above data. Distances were calculated using the Euclidean formula and clustering was done by Wards method. Based on our experience with the methods available in CLUSTAN we feel confident in stating that, given spectra of the available quality, the following 5 groups represent natural divisions of the subdwarf stars in the PG survey.

GROUP	ABUNDANCE	FEATURES
I	(26 %)	**H> HeI and HeII.** H = 5 +/- 1 A, HeI and HeII = 1 +/- 1 A.
II	(36 %)	HeII = 3 +/- 1 A, H = 2 +/- 1 A, HeI = 1 +/- 1 A.
III	(22 %)	H = 3 +/- 1 A, HeII = 1 +/- 1 A, HeI nearly absent.
IV	(10 %)	**HeI >> H and HeII.** HeI = 4 +/- 1 A, H and HeII nearly absent.
V	(7 %)	**H >> HeI > HeII.** H = 9 +/- 1 A, HeI = 2 +/- 1 A, HeII nearly absent.

Here H represents the average of visible Balmer lines, often the β,δ lines and always the γ line. HeI is the average of 4387 and 4471 and sometimes 4026 and 4713. HeII is the average of 4686 and 4542. The given deviations are +/- 1 standard deviation of the mean and do not define upper and lower limits.

We used our scheme to classify sdO's for which NLTE analysis has been published (Hunger et al., 1981) and found preliminary group characteristics for groups **I** and **II**: Group **I** has $T_{eff} \approx$ 38 000K +/- 1500K, log(g) $\approx$ 5.9 +/- 0.5 and composition y $\approx$ 0.1 +/- 0.05. Group **II** has $T_{eff} \approx$ 48 000K +/- 5000K, log(g) $\approx$ 5.6 +/- 0.5 and y $\approx$ 0.4 +/- 0.15.

Discussion

The above groups only coincide with the PG classes to some extent. Notably group **V** is like the sdOA's and group **IV** is like the sdOD's. The stars in these two groups have spectra that all are very similar. The stars in the three

other groups all show evidence of temperature differences. Group **I** is dominated by Hydrogen lines but shows a sequence of additional He lines: HeII only, HeII+HeI and HeI only. Since the H lines are similar between these three subgroups composition must be fairly constant and T_{eff} varies. Groups **II** and **III** show the same pattern.

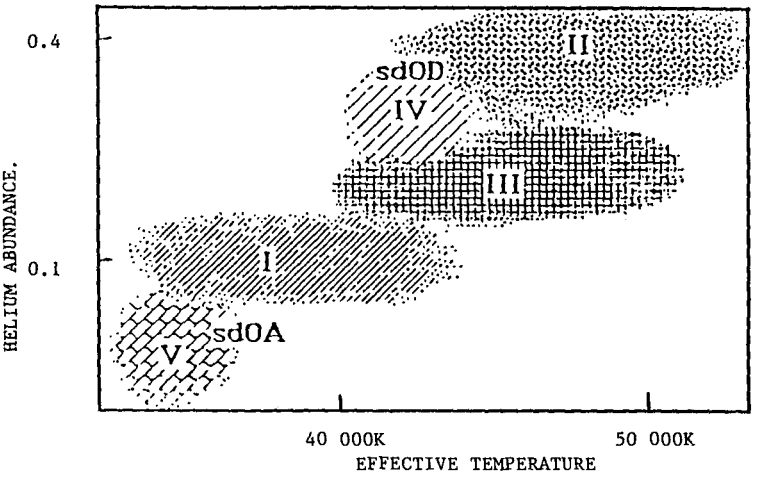

Figure 2: T_{eff} vs. Helium abundance for the five clusters found in the cluster analysis of the subdwarfs. Groups **IV** and **V** are well defined while groups **I**,**II** and **III** show a range of temperatures at roughly constant composition.

References

Green,R., Schmidt, M., and Liebert, J. The Palomar-Green Catalog of Ultraviolet-Excess stellar objects. *Astrophysical Journal Supplement Series*, 1986, *61*, 305-352.

Weyman, R.J., Latham, D., Angel, J.R.P., Green, R.F., Liebert, J.W., Turnshek, D.A., Turnshek, D.E., and Tyson, J.A. The triple QSO PG1115+08: another probable gravitational lens. *Nature*, 1980, *285*, 641.

Nousek, J.A., Shipman, H.L., Holberg, J.B., Liebert, J.W., Pravdo, S., White, N.E., and Giommi, P. H1504+65: An Extraordinary Hot Compact Star Devoid of Hydrogen and Helium. *Astrophysical Journal*, 1986, *309*, 230-240.

McGraw, J.T., Starrfield, S.G., Liebert, J., and Green, R. PG1159-035: A New, Hot, non-DA Pulsating Degenerate. In H. Van Horn and V. Weidemann. (Eds.), *Proceedings of IAU Colloquium No. 53: White Dwarfs and Variable Degenerate Stars.* IAU, 1979.

Flemming, T.A., Liebert, J., Green, R.F. The luminosity function of DA white dwarfs. *Astrophysical Journal*, 1986, *308*, 176-189.

Wishart, D. *CLUSTAN User Manual* (Third ed.). Inter-University/Research Councils Series, Report No 47, 1982.

Hunger, K., Gruschinske, J., Kudritzki, R.P., Simon, K.P. NON-LTE Analysis of Subluminous O-stars. IV Spectral Photometry and NLTE Analysis of 11 Subluminous Stars. *Astronomy and Astrophysics*, 1981, *95*, 244-249.

AN UNSUCCESSFUL SEARCH FOR WHITE DWARF COMPANIONS TO NEARBY MAIN SEQUENCE STARS

Harry L. Shipman and Jeanne Geczi
Physics and Astronomy Department, University of Delaware
Newark, Delaware 19716

ABSTRACT

Many of the nearest white dwarf stars (e.g., Sirius B and Procyon B) are in such binaries and would have remained undiscovered if they were even a little bit further away. White dwarfs which are sufficiently hot (T(eff) > 10,000 K) would, if present in binary systems with a relatively cool (F, G, K, or M) main-sequence secondary, be visible in IUE images as a hot companion to the main sequence star. We systematically examined 318 IUE images of 280 different G, K, and M stars which had been observed for other purposes. No previously undiscovered white dwarf stars were found.

Understanding the evolution of the stellar population of the Milky Way Galaxy requires that we have a reasonably good knowledge of the space density of its stellar constituents. However, cursory examination of the stars within a few parsecs indicates that there is a potential, major uncertainty in that we do not know how many white dwarf stars remain undiscovered because they are binary companions to main sequence stars and would be hidden in the same way that Sirius B and Procyon B would be even if they were at modestly greater distances. To be more specific, the four white dwarf stars within five parsecs of the sun are Sirius B (d=2.7 parsecs), Procyon B (3.5), van Maanen 2 (4.2), and 40 Eri B (4.9). The nearest two of these objects (Sirius B and Procyon B) would undoubtedly be missed by a photometric or proper-motion survey relying on wide-field images like Schmidt plates. It is these surveys which discover most white dwarfs and which are the basis for statistical arguments. Even 40 Eri B, 1 arc min from 40 Eri A, might well be overlooked in such a survey were it 50 pc away rather than 5. The potential presence of such white dwarf companions to main sequence stars was illustrated clearly when a CCD search for brown dwarf companions to nearby stars accidentally uncovered a previously unknown white dwarf

component in a binary system (Skrutskie, Forrest, and Shure 1985).

An easy way to search for binary white dwarfs is to restrict one's attention to those which are hot enough to show a continuum in the IUE spectral region. In fact, several such companions have been discovered (Bohm-Vitense 1980, Schindler et al 1982, Stencel et al. 1984) though in a few cases the reality of the companion is in dispute (Imhoff 1985). Since we did not discover any undiscovered companions we don't need to worry about whether some of our discoveries are scattered light masquerading as an ultraviolet continuum.

Based in the IUE observing log, we selected a number of spectra of G, K, and M-type main sequence stars which were sufficiently well exposed (exposure time > 15 min) so that a white dwarf with T(eff) > 10,000 K would in fact be visible. Examination consisted of visual inspection of the photowrites. Tests indicated that visual inspection is sufficient to detect a continuum at DN = 20 or so, depending on the quality of the image.

We did not discover any new white dwarf stars. We examined 108 G stars, 118 K stars, and 54 M stars. For the G stars, we examined SWP images only since a significant continuum is present in the LWP spectral region. For the K and M stars we examined both SWP and LWP images, if they were available. A total of 318 IUE images were examined.

We did find two cases in which an ultraviolet continuum was present, but in both cases the explanations were straightforward. As it turned out, the well-known interacting binary V 471 Tauri was not delected from the list of stars to be searched before the search was undertaken. The hot white dwarf companion in this close binary system was, in fact, recognized. Another "false alarm" was Walker 92 (SWP 11044) a pre-main sequence star in the open cluster NGC 2264 investigated by Simon, Cash, and Snow (1985). We examined this star on the Palomar Sky Survey and found that the star is superposed on an H II region. We thus confirm Simon, Cash, and Snow's conculsion that the ultraviolet continuum comes from nebular emission. We analyzed a number of test cases to determine just how hot a white dwarf would have to be in order to be detectable by our search technique. We assumed that a white dwarf would have a typical radius of 0.012 solar radii, estimated the distance to the target by whatever information was available, and used unpublished models by Shipman to determine the minimum temperature of a detectable white dwarf star. Temperatures of 9,000 to 10,000 K were typical; for the remainer of this paper a white dwarf with T(eff) > 10,000 K is called a "hot" white dwarf.

The minimum temperature of white dwarfs detectable in our search is fortuitously close to the minimum temperature of white dwarfs detectable in the Palomar-Green survey for high latitude blue objects (Fleming, Liebert, and Green, 1986, hereafter FLG). As a result, the cleanest way of determining what our negative result means is to compare our results with FLG. Counting statistics

dictate that if we found zero stars, a 3 sigma upper limit to the average number of hot white dwarf companions in a similar sized sample of G,K, and M stars is 5. Thus the space density of hot white dwarf companions to G,K, and M stars is constrained to be (a 3 sigma upper limit)

$$n_{comp} < (5/280)\ n_{GKM}\ 1/f_{aper} \qquad (1)$$

where n_{GKM} is the space density of G, K, and M stars of spectral types similar to those in our sample and f_{aper} is the fraction of the total number of binary companions which fall within the IUE aperture.

Evaluating the right hand side of (1) is reasonably straightforward. We adopt n_{GKM} = 0.103 stars pc^{-3} from Wielen's luminosity function (Philip and Upgren 1983). The evaluation of f_{aper} is a bit more indirect but under the circumstances its uncertainty is immaterial to our results. Most of the stars in our sample are reasonably bright, near 6th magnitude, and are approximately 10 pc away. The IUE large aperture at a distance of 10 pc is 10 AU x 20 AU, so we could detect all white dwarfs within 150 AU of the primary. Although we do not know the distribution of the semimajor axes of white dwarfs in binary systems, there is reason to believe that main sequence-white dwarf pairs should have separations which exceed their initial separation by a ratio M_{ms}/M_{wd} (Shipman, MacDonald, and Sion 1988), and so we are catching all white dwarf companions which initially had semimajor axes < 100 AU. Based on current statistics of binary separations (e.g., Greenstein 1986a,b), our search strategy is sensitive to the vast majority of conceivable companions, as was expected before the search was undertaken. Inspection of the figures in Greenstein's paper suggests that $0.8 < f_{aper} < 0.95$.

The numbers worked out in the previous paragraph suggest, using a conservative value of f_{aper} = 0.8, that a 3 sigma upper limit to the space density of hot white dwarf companions to main sequence stars is

$$n_{comp} < 2.2 \times 10^{-3} \text{ stars } pc^{-3}. \qquad (2)$$

When this project was designed, the accepted value of the space density of white dwarfs was the higher value of Green (1980), about twice the value in FLG of 0.6 stars pc^{-3} (this number allows for both DA and non-DA stars, assuming a ratio of DA/non-DA of 4:1). Because of this revision in the space density of white dwarfs, the results of our survey are less meaningful than they might be; all we can say is that the density of undiscovered white dwarfs in binaries is less than 3.5 times the density of single white dwarfs. The upper limit is inversely proportional to the number of stars examined, and a search with about 4 times the

scope which we performed could discover or rule out the proposition that the number of undiscovered white dwarfs in binaries equals the number of single white dwarfs.

Based on a total mass density in single white dwarfs of 5.7 X 10^{-3} solar masses pc^{-3} (FLG), we can use our results to demonstrate that the total space density of white dwarf stars, including those which are binary companions of main sequence stars, is less than 3.5 times the density in single white dwarfs, or less than 0.025 solar masses pc^{-3}. While this is not a very tight upper limit, it confirms results cited by earlier authors (Liebert, Dahn, and Sion 1983) that white dwarfs cannot be sought as a possible constituent of the missing mass in the galactic disk, if the missing mass exists.

We thank the National Science Foundation (grant AST 87-20530) and NASA (NAG 5-972) for financial support. This research was conducted under the auspices of the Science and Engineering Scholars Program of the University of Delaware Honors Program.

REFERENCES

Bohm-Vitense, E. 1980, Ap.J.(Letters) 239, L79.

Fleming, T.A., Liebert, J., and Green, R.F. 1986, Ap.J. 308, 176. (FLG)

Green, R.F. 1980, Ap.J. 238, 685.

Greenstein, J.L. 1986a, A.J. 92, 859.

Greenstein, J.L. 1986b, A.J. 92, 867.

Liebert, J., Dahn, C., and Sion, E. 1983, in IAU Colloquium 76: Nearby Stars and the Stellar Luminosity Function, A.G.D. Philip and A.R. Upgren, eds., (Schenectady, NY: L. Davis Press), 103.

Philip, A.G.D., and Upgren, A.R. 1983, in IAU Colloquium 76: Nearby Stars and the Stellar Luminosity Function, A.G.D. Philip and A.R. Upgren, eds., (Schenectady, NY: L. Davis Press), 471.

Schindler, M., Stencel, R.E., Linsky, J.L., Basri, G.S., and Helfand, D. 1982, Ap.J. 263, 269.

Shipman, H.L., MacDonald, J., and Sion, E.M. 1988, A.J., submitted.

Simon, T., Cash, W., and Snow, T.P. 1985, Ap.J. 293, 542.

Skrutskie, M.F., Forrest, W.J., and Shure, M.A. 1985, in Astrophysics of Brown Dwarfs, M. Kafatos, R. Harrington, and S. Maran, eds., (Cambridge: Cambridge University Press), 82.

Stencel, R.E., Neff, J.A., and McClure, R.D. 1984, in Future of Ultraviolet Astronomy Based on Six Years of IUE Research, NASA CP-2349, 400.

THE BOLOGNA/ESO SEARCH FOR DOUBLE DEGENERATES

Angela Bragaglia, Laura Greggio, and Alvio Renzini
Dipartimento di Astronomia, Università di Bologna, CP 596, I-40100 Bologna
and
Sandro D'Odorico
European Southern Observatory, D-8046 Garching b. München

In 1984 a program has been set up for a systematic search of double degenerates (DD) among spectroscopically confirmed white dwarfs. For each WD at least two CCD spectra are obtained, which are then cross-correlated in order to get a radial velocity difference, if any. For this purpose we have used the *ESO Faint Object Spectrograph and Camera* (EFOSC) attached at the ESO 3.6m telescope. Exposure times are typically in the range 5–15 min, and the typical error in the radial velocity difference (Δv_r) is ~ 20 km s^{-1}.

Until now we had two observing runs, respectively in September 1985 and January 1988, for a total of 5 usable nights. For 20 WDs we have obtained more than one spectrum. Among them we have singled out two DD candidates. The first object (WD0957–666) has shown Δv_r values up to ~ 220 km s^{-1} and three other spectra were kindly taken for us in April 1988 by Stefano Cristiani. These also showed Δv_r's up to ~ 140 km s^{-1}. Another object (WD0954–710) exhibits a $\Delta v_r \simeq 70$ km s^{-1}. The two DD candidates will be observed again in the next observing run in order to confirm their binarity and in case determine the periods.

Two other objects turned out to be WD+red dwarf pairs whose binary nature was already known from multicolor photometry. One of them (WD0034–211) shows an emission core in all the Balmer lines. For the other (WD0419–487) we have been able to obtain the Δv_r's separately for the WD and the RD components. From them, and from the spectroscopic mass of the WD ($0.29 M_\odot$) we then estimate the RD to be $\sim 0.15 M_\odot$. Subject to the decision of the time allocation committee, we plan to keep searching for DDs and to obtain periods for every candidate pair. More information can be obtained in Bragaglia et al. (*The Messenger*, **52**, 35, 1988).

Far Ultraviolet Observations of Hot DA White Dwarfs

David Finley, Gibor Basri, † *and Stuart Bowyer* ‡

Space Sciences Laboratory, University of California, Berkeley
† Astronomy Department, University of California, Berkeley
‡ Astronomy Department and Space Sciences Laboratory,
University of California, Berkeley

ABSTRACT

Far ultraviolet (FUV) fluxes have been used for determining the effective temperatures of a number of DA white dwarfs hotter than 20,000 K. The spectra were obtained with the International Ultraviolet Explorer (IUE). The analysis consisted of comparing the observed FUV fluxes with model fluxes scaled to the V-band flux. After suitable corrections were performed for the time-dependent sensitivity degradation of the IUE, it was found that the available flux calibrations for the IUE were insufficiently accurate for precise temperature determinations. Accordingly, we used seven white dwarfs for which accurate, independent temperature determinations have been made from line profile analyses to improve the accuracy of the IUE flux calibration. The correction to the original calibration was as great as 20% in individual 5-Å wavelength bins, while the average over the IUE wavelength range was 5%. We present both our IUE flux correction and the temperatures obtained for the hot white dwarfs.

Introduction

Accurate temperature determinations for hot DA white dwarfs are necessary for several reasons. Temperatures are needed for deriving the luminosity function of DA's; the luminosity function then serves to check calculations of cooling rates for these stars. Trace element abundances in DA's result from temperature-dependent processes. Successful confrontation of observational abundance determinations with theory requires that the effective temperatures be known with sufficient accuracy. Also, the upper temperature limit for DA's needs to be determined with reasonable precision, because this limit will help constrain post main sequence evolutionary calculations. Additionally, upcoming extreme ultraviolet (EUV) photometric survey missions (Bowyer 1983, Pye and Page 1987) are likely to discover hundreds of very hot DA white dwarfs (Finley 1988). Non-EUV measurements will be required to make the accurate temperature determinations necessary for interpretation of the EUV photometric data for these stars (Finley 1988).

Three basic types of measurements are available for determining temperatures of hot white dwarfs: optical continua (from photometry), FUV continua, and line profiles. Optical photometry is insufficiently accurate for the hotter (>25,000 K) white dwarfs. Line profiles and FUV continua give results of comparable accuracy. We present here our temperature determinations based on FUV continuum measurements.

Observations and Data Reduction

We conducted a program of observations of hot DA white dwarfs with the International Ultraviolet Explorer satellite (IUE). A description of the IUE instrumentation is presented in Boggess *et al.* (1978a,b). Our observations consisted primarily of low dispersion exposures using the SWP and LWR cameras. Additionally, a number of spectra obtained from the IUE data archives are included in the results presented here. In processing the data, the SWP spectra were truncated shortward of 1320 Å to avoid the wing of the $L\alpha$ line. An extended wavelength baseline was obtained by including the V-band flux, which was calculated per the relation $f(5490\text{Å}) = 3.61\times10^{-9}/10^{0.4m_V}$ erg/cm^2 sec Å.

Data Analysis Technique

The IUE data were analyzed by comparing observed fluxes with model fluxes that were calculated with Basri's white dwarf model atmosphere code (Malina, Bowyer, and Basri 1982). Based on Auer's complete linearization method, this is an LTE, hydrogen line–blanketed atmosphere code, which omits convective energy transport. The atmosphere code was used to generate a grid of models at different effective temperatures between 20,000 K and 100,000 K, while log g and n(He)/n(H) were held fixed at 8 and 1×10^{-6}. The

variation of log g within the white dwarf range was found to have an insignificant effect on the FUV flux. Inferred temperatures based on FUV fluxes vary by only ±3 K at 30,000 K if log g is allowed to vary from 7 to 9, for the case of n(He)/n(H) = 1×10^{-6}. Over the allowable range of n(He)/n(H) for DA white dwarfs, 0 to $\lesssim 10^{-2}$, the variation of the helium fraction has a relatively small effect on the continuum flux. Variations in this range change the average FUV flux (relative to the visible) by at most ~3%. Furthermore, it is not possible to solve separately for both T_{eff} and n(He)/n(H), because variations in n(He)/n(H) produce effects on the continuum flux which are indistinguishable from the effects of temperature variations. The shape of the continuum does vary with n(He)/n(H), but only at the level of ≲0.1%. Consequently, there was no advantage to performing the analysis with n(He)/n(H) as a free parameter.

The effective temperatures were obtained by comparing the stellar FUV/visible flux ratios to the model FUV/visible flux ratios. The calculated stellar-to-model ratio at each wavelength is defined as

$$\delta(\lambda_j) = -2.5 \log \left[\frac{f(\lambda_j)/f(\lambda_V)}{H(T_{eff},\lambda_j)/H(T_{eff},\lambda_V)} \right], \quad (1)$$

where f is the measured stellar flux, while H is the Eddington flux. The λ_j are the IUE data wavelength points, and λ_V = 5490 Å. The stellar effective temperatures were found by calculating the model effective temperatures which gave

$$S = \sum \delta(\lambda_j) = 0. \quad (2)$$

Temperature Determinations

The nominal IUE fluxes were corrected for the time-dependent sensitivity variations of the IUE cameras per the prescription of Bohlin (Bohlin and Grillmair 1988a,b), giving fluxes corresponding to the "May 1980" IUE flux calibration (Bohlin and Holm 1980). If desired, the fluxes may be transformed to the 1986 IUE calibration (Bohlin 1986) or the proposed 1988 IUE calibration (Bohlin 1988). However, none of those calibrations give fluxes for white dwarfs which are in reasonable agreement with model atmosphere predictions based on effective temperatures determined from hydrogen line profile measurements. At 60,000 K, for example, the 1980 calibration would give an inferred temperature of only 52,500 K based on the IUE continuum flux. Correspondingly, the 1986 and 1988 calibrations would give temperatures of 53,500 K and 46,900 K, respectively. These inferred temperatures are inconsistent with the line profile temperatures at the 2 to 4 σ level.

The inconsistency between line profile and FUV continuum flux temperatures was removed thus: we used spectra from seven hot white dwarfs for which accurate temperatures were available to derive flux corrections for the IUE calibration. The temperatures for those stars, based on IUE Lα profiles, were obtained by Holberg, Wesemael, and Basile (1986, hereafter referred to as HWB). Given their quoted uncertainties, these are the most accurate hot DA white dwarf temperature measurements presented to date. The errors quoted by HWB are ±3,500 K at 60,000 K; ±1,500 K at 40,000 K; and ±300 K at 20,000 K.

Time-corrected fluxes (SWP + LWR) for WD0050-332, 0501+527, 0549+158, 1254+223, 1620-391, 2111+498, and 2309+105 were used to obtain the flux correction. For each star, a model was calculated at the temperature presented by HWB. Next, the $R_i(\lambda_j)$ values were calculated for the individual stars per

$$R_i(\lambda_j) = \frac{f(\lambda_j)/f(\lambda_V)}{H(T_{eff},\lambda_j)/H(T_{eff},\lambda_V)}. \quad (3)$$

Then the flux correction was calculated per

$$COR(\lambda_j) = \sum_i [R_i(\lambda_j)\, ID_i(\lambda_j)] / \sum_i ID_i(\lambda_j). \quad (4)$$

ID_i is the data quality flag for each spectrum (1 ≡ good data, 0 ≡ bad data).

The resulting flux correction to the 1980 IUE photometric calibration, binned over 5-Å intervals, is plotted in Figure 1. The correction factor at each wavelength is the value by which a nominal flux must be divided to produce the correct flux. The 1980 IUE flux calibration (relative to the predicted white dwarf fluxes) is seen to give fluxes as much as 15% high and as much as 20% low. Averaged over wavelength, the IUE fluxes per the 1980 calibration are low by 5%, which is within the stated overall accuracy for the IUE flux calibration of ±10%. The uncertainty in the correction is dominated by the uncertainties in the V magnitude and line profile temperature determinations for the stars used to calculate the correction. The resulting overall uncertainty in the flux correction, averaged over the IUE wavelength range, was 1.3%.

After applying the flux corrections to the spectra, the effective temperatures were then calculated for all the stars. The temperatures derived from the IUE fluxes are presented in Table 1, along with the temperatures given in HWB, and the temperatures which we have calculated from optical colors. The optical photometric temperatures were based on the multichannel (u-v) color, or on Johnson (U-V) or Stromgren (u-y) colors

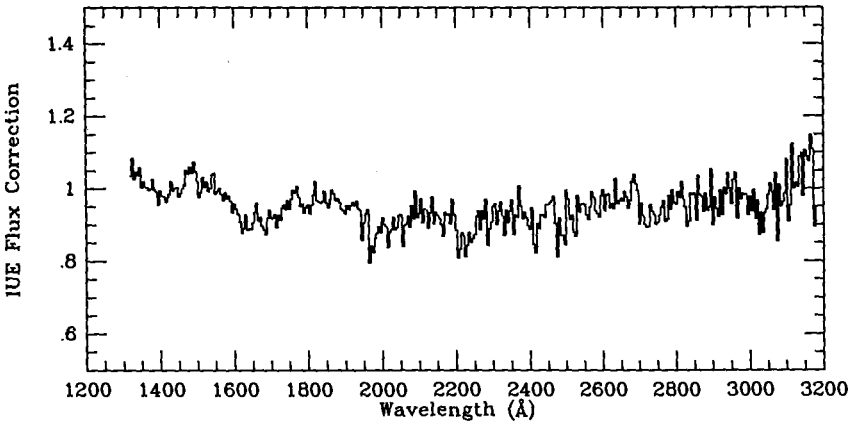

Figure 1. Correction to IUE initial epoch calibration. The correction is based on seven observations of different DA white dwarfs, and is binned into 5 Å intervals. The spectra used were from WD 0050-332, 0501+527, 0549+158, 1254+223, 1620-391, 2111+498, and 2309+105 (1982/142 observation).

temperatures were based on the multichannel (u-v) color, or on Johnson (U-V) or Stromgren (u-y) colors which were transformed to the equivalent $(u\text{-}v)_{MC}$ value. It was necessary to adjust the $(u\text{-}v)_{MC}$ or $(u\text{-}v)_{MC}$-equivalent colors blueward by $0^m.044$ to achieve consistency with the line profile and FUV continuum temperatures.

Table 1: Temperatures of stars derived from different measures.

WD Name	IUE Continua		Line Profiles			Optical Photometry	
	T_{eff}[a]	Error[b]	T_{eff}	Error	Ref.	T_{eff}	Error
0004+330 (GD2)	46.33	$^{+3.44}_{-2.94}$	--	--	--	54.8	$^{+18.2}_{-10.0}$
0050-432 (GD659)	34.15	$^{+1.64}_{-1.37}$	36.85	±1.39	HWB	33.21	$^{+1.49}_{-1.21}$
0346-011 (GD50)	39.10	$^{+2.21}_{-1.90}$	47.5	±2.5	K	39.66 31.23	$^{+6.54}_{-4.07}$ $^{+1.96}_{-1.48}$
0501+527 (G191-B2B)	66.37	$^{+8.76}_{-7.13}$	62.25	±3.52	HWB	68.7	$^{+15.3}_{-10.4}$
0549+158 (GD71)	34.03	$^{+1.62}_{-1.35}$	33.30	±0.83	HWB	37.26	$^{+3.31}_{-2.43}$
0644+375 (EG50)	21.76	$^{+0.29}_{-0.29}$	--	--	--	22.61	$^{+0.34}_{-0.33}$
0651-020 (GD80)	35.50	$^{+2.47}_{-1.96}$	--	--	--	36.27	$^{+4.48}_{-2.90}$
1031-114 (EG70)	25.67	$^{+0.36}_{-0.34}$	--	--	--	24.91	$^{0.49}_{-0.48}$
1033+464 (GD123)	28.38	$^{+4.81}_{-2.30}$	--	--	--	"27.2"	
1254+223 (GD153)	40.67	$^{+2.65}_{-2.22}$	42.375 42	±1.48 ±2	HWB K	41.14	$^{+3.23}_{-2.59}$
1403-077 (PG)	45.98	$^{+8.18}_{-5.78}$	--	--	--	40.89	$^{+7.28}_{-4.53}$
1615-154 (EG118)	31.76	$^{+0.85}_{-0.76}$	--	--	--	30.63	$^{+0.65}_{-0.58}$
1620-391 (CD-38°10980)	24.83	$^{+0.39}_{-0.39}$	24.50	±0.14	HWB	24.26	$^{+0.47}_{-0.46}$
2111+498 (GD394)	37.36	$^{+2.32}_{-1.91}$	36.125	±0.94	HWB	36.66	$^{+2.43}_{-1.91}$
2309+105 (GD246)	50.30[c] 52.69[d]	$^{+4.25}_{-3.57}$ $^{+4.74}_{-3.98}$	53.60	±2.94	HWB	62.8	$^{+9.3}_{-7.1}$

[a]Temperatures are given in 10^3 K. [b]Errors are 1σ uncertaintics. [c]Based on 1982/142 observations. [d]Based on 1979/355 observations.
References: HWB = Holberg, Wesemael, and Basile (1986). K = Kahn *et al.* 1984.

The line profile and FUV continuum temperatures are consistent for all the objects analyzed, with the exception of WD0346-011, as can be seen in Figure 2a. The optical photometric and IUE temperatures are also consistent, as shown in Figure 2b, except for WD0346-011. (The lower of the two optical temperatures is based on Greenstein's photometry [Greenstein 1974], which may be more accurate than the measurements which give the higher optical temperature [Kondo *et al.* 1982]. The WD photometry of Kondo *et al.* appears to have a somewhat higher dispersion than is generally seen in WD work). The absence of systematic trends in the correlation between the FUV continuum temperatures and the other measurements confirms that any possible errors in the models which affect the continuum differently from the lines are not present at more than the ~1% level.

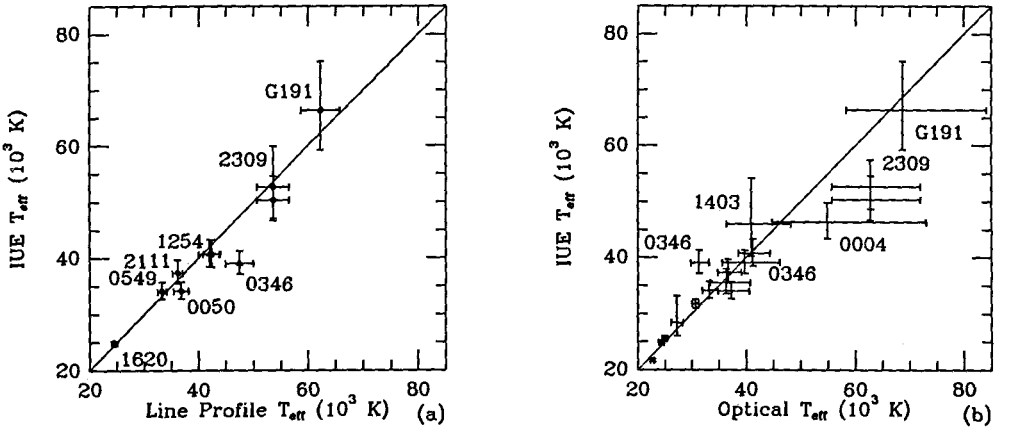

Figure 2. (a) Temperatures derived from IUE fluxes *vs.* published temperatures calculated from line profile fitting of Hβ (open triangles) or *L*α (open squares).
(b) Temperatures derived from IUE fluxes *vs.* temperatures based on optical photometry.

Results

G191-B2B. At 66,400 K (+8,800/-7,100), G191-B2B is among the hottest known DA white dwarfs. It has a well-determined parallax of 0.021 ±0.002 (Routly 1972). This places it at a distance of 47.6 pc ±5 pc. Taking T_{eff} = 66,380 K and m_V = 11.79, we have $f_V/H_V = 8.58\times10^{-22}$. The derived radius is then 0.0170 $R_\odot$. This value is the same as that predicted by the evolutionary models of Koester and Schönberner (1986) for a 0.6 $M_\odot$ white dwarf with a hydrogen envelope of 10^{-4} $M_\odot$. Therefore, G191-B2B may provide an example of a DA white dwarf with a relatively massive remnant hydrogen envelope.

This possible large hydrogen envelope mass would rule out the interpretation offered by Vennes *et al.* (1987) for the *EXOSAT* photometric observations of DA white dwarfs. The *EXOSAT* data indicate that the short wavelength flux is strongly cut off by some absorber within the stellar atmosphere. Vennes *et al.* suggest that the observed EUV fluxes may result from very thin hydrogen layers overlying the helium. Under their interpretation, the observational results for G191-B2B could be satisfied if the mass of the hydrogen envelope were $\sim10^{-14.6}$ of the stellar mass, which is inconsistent with the observed radius and the evolutionary models.

WD0346-011. The inconsistent temperatures for this star may be due to the presence of a faint companion; the presence of such a companion is consistent with the optical colors. However, the apparent temperature discrepancies may occur because the star is not a normal DA. WD0346-011 may be a member of a class of white dwarfs currently comprising one object: WD1302+597 (GD323). GD323 has Balmer line profiles consistent with a T_{eff} of 40,000 K, but the optical and FUV continua are better fit with a T_{eff} of only 30,000 K (Liebert *et al.* 1984). Liebert, Fontaine, and Wesemael (1987) point out that the predominantly helium channel of the white dwarf sequence is totally depopulated between 30,000 K and 45,000 K, and they suggest that GD323 is in transition between DA and DB at the cool end of the helium gap. Perhaps WD0346-011 is undergoing a similar transition at the hot end of the gap.

WD1033+464. This star is composite; hence the optical temperature included in Table 1 is only nominal. The companion, which contributes ≤15% of the light at 5490 Å, is probably an M dwarf. The contribution of the companion to the combined light of the system is ≤1% at 3571 Å. Therefore, the flux at that wavelength was used as the visible flux point for the IUE temperature analysis.

Non-DA Objects. Two of the stars in our observing program are currently classified as DA but were shown on the basis of the IUE spectra to belong to other spectral classes. The two stars in question are WD (or PG) 1247+553 (GD319), and WD 1544+008 (EG113, BD+01 3129B). 1247+553 is evidently an sdB, while 1544+008 appears to be a helium-rich subdwarf. Of the stars whose spectra were obtained from the archive, 0109-264 (GD691) is also an sdB, while 0823+316 appears to be a very hot hydrogen-poor object. (Analysis of 0823+316 using pure H models yields T_{eff} >100,000 K.)

Conclusions

Line profile measurements and IUE FUV fluxes (when the latter are suitably corrected) provide very accurate temperatures for hot DA white dwarfs. In most instances, the FUV continuum measurements are equivalent to line profile measurements for the purpose of temperature determinations. When the optical photometry is suitably adjusted, the optical photometric temperatures are consistent with the corrected IUE temperatures and the line profile temperatures. The presence of significant variations between the three measurements in one of the instances discussed demonstrates the value of correlating the information available in many wavelength bands to identify abnormal stars. FUV spectra are also useful for discriminating between DA white dwarfs and other stellar types.

Acknowledgements

This work was supported by NASA grant NAS5-29298. Many of the spectra used were obtained from the IUE Archives via the National Space Sciences Data Center (NSSDC).

References

Boggess, A., *et al.* 1978a, *Nature,* **275,** 372.
Boggess, A., *et al.* 1978b, *Nature,* **275,** 377.
Bohlin, R., and Holm, A. 1980, NASA IUE Newsletter No. 10, 37.
Bohlin, R. C. 1986, *Ap. J.*, **308,** 1001.
Bohlin, R. 1988, in preparation.
Bohlin, R., and Grillmair, C. 1988a, *Ap. J. Suppl.*, Vol. 66, in press.
Bohlin, R., and Grillmair, C. 1988b, in preparation.
Bowyer, S. 1983, *Adv. Space Res.* **2,** 157.
Finley, D. S. 1988, Ph.D. thesis, University of California, Berkeley.
Greenstein, J. L. 1974, *Ap. J.*, **189,** L131.
Holberg, J. B., Wesemael, F., and Basile, J. 1986, *Ap. J.*, **306,** 624.
Kahn, S. M., Wesemael, F., Liebert, J., Raymond, J. C., Steiner, J. E., and Shipman, H. L. 1984, *Ap. J.*, **278,** 255.
Koester, D., and Schönberner, D. 1986, *Astron. Astrophys.*, **154,** 125.
Kondo, M., Watanabe, E., Yutain, M., and Noguchi, T. 1982, *Pub. Astr. Soc. Japan,* **134,** 541.
Liebert, J., Wesemael, F., Sion, E. M., and Wegner, G. 1984, *Ap. J.*, **277,** 692.
Liebert, James, Fontaine, G., and Wesemael, F. 1987, *Memorie della Societa Astronomica Italiana,* **58,** 17.
Malina, R. F., Bowyer, S., and Basri, G. 1982, *Ap. J.*, **262,** 717.
Pye, J. P., and Page, C. G. 1987, *Astronomy from Large Databases: Scientific Objectives and Methodological Approaches,* Proc. European Southern Observatory No. 28, F. Murtagh and A. Heck, eds., Garching, 447.
Routly, P. M. 1972, *Publ. U. S. Naval Obs., Second Series,* **20,** Part 3.
Vennes, S., Pelletier, C., Fontaine, G., and Wesemael, F. 1987, *Proc. IAU Colloquium 95: The Second Conference on Faint Blue Stars,* A. G. D. Philip, D. S. Hayes, and J. Liebert, eds., L. Davis Press, Schenectady, NY, p. 665.

FAR-ULTRAVIOLET SPECTROPHOTOMETRY OF TWO DO WHITE DWARFS FROM *VOYAGER*

E. Poulin and F. Wesemael
Département de Physique, Université de Montréal

J.B. Holberg
Lunar and Planetary Laboratory, University of Arizona

G. Fontaine
Département de Physique, Université de Montréal

While the observed number of hot, helium-rich degenerates is noticeably larger than that of their hydrogen-rich counterparts, the calibration of their effective temperatures has been comparatively much less trustworthy. The spectroscopic classification scheme introduced three years ago by Wesemael, Green, and Liebert (1985, hereafter WGL), and the crude temperature domains associated with each class remain, to this date, the only comprehensive effort at defining a temperature scale for DO stars. The current uncertainty in this is perhaps best epitomized by two objects, HD149499B and PG1034+001. The former belongs to a binary system which also contains a K0 V primary, 2" away. The temperature determined for the degenerate secondary ranges from 85,000±15,000 K (Wray, Parsons, and Henize 1979) to 55,000±5000 K (Sion, Guinan, and Wesemael 1982, hereafter SGW). PG1034+001, on the other hand, is the prototype of the so-called hot DO spectroscopic class; WGL assign an uncertain temperature of 80,000±20,000 K to this object.

The large uncertainty associated with these temperature determinations is perhaps not overly surprising. For these hot stars, measured energy distributions — even from the *IUE* — sample only the Rayleigh-Jeans tail, and thus cannot constrain effectively the temperature. Furthermore, the optical spectrum of hot, high-gravity helium-rich stars tends to be rather sparse, with apparently HeII λ4686 the only transition not broadened out of existence. Of course, the case of HD149499B is not helped by the presence of its companion, which tends to outshine the degenerate star at optical wavelengths (Wegner 1978). The situation is not desperate, however, as the ultraviolet spectrometers on board the *Voyager* probes have recently made it possible to sample the energy distribution of both these bright objects nearer its peak by extending observations to regions shortward of Lyα. We report here on a preliminary analysis of far-ultraviolet data (900–1200 Å) on both objects obtained with *Voyager 2* which should, eventually, provide tighter constraints on the atmospheric parameters of these stars.

HD149499B and PG1034+001 were observed with the ultraviolet spectrometers on board the *Voyager 2* spacecraft. Coverage extends from ~950 Å to 1200 Å at a resolution of 25 Å. Additional details of these observations will be provided elsewhere. The calibrated *Voyager 2* spectra, augmented with archival *IUE* low-dispersion observations longward of 1150 Å are shown in Figure 1. The normalization at 1950 Å reveals that the energy distribution of PG1034+001 is clearly steeper than that of HD149499B. This is already an important result, which suggests that HD149499B and PG1034+001 cannot *both* have effective temperatures near 80,000 K (see above): either HD149499B is cooler or PG1034+001 is hotter than that value, or both.

The issue of an absolute temperature calibration is somewhat more delicate as it requires input from suitable model atmosphere calculations. We use here a improved grid of LTE, pure-helium models at log g=8.0 based on earlier work (Wesemael 1981). However, rather than to present preliminary fits to the complete energy distribution of both stars, we first consider here the consistency of previous temperature determinations with the new *Voyager* data.

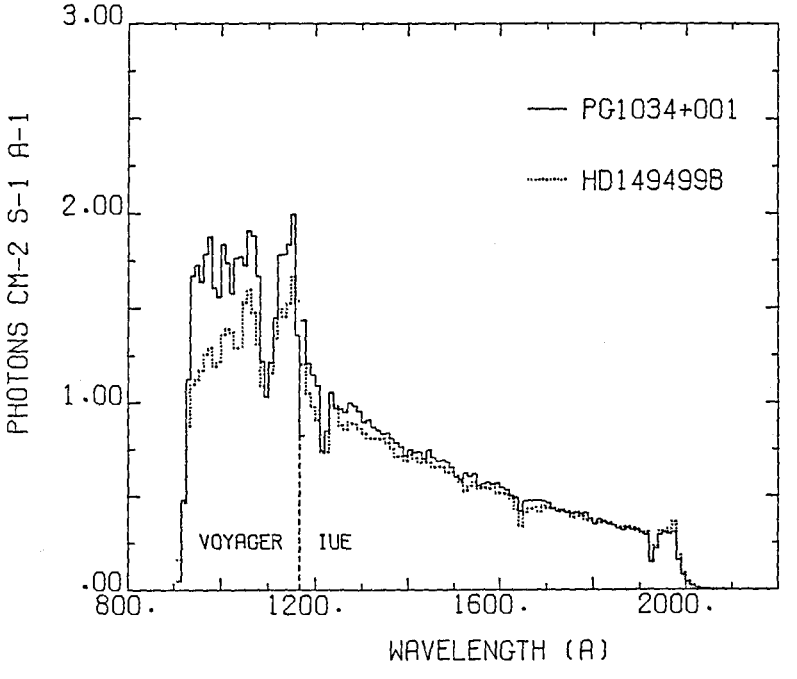

Fig.1 The far-ultraviolet spectra of HD149499B and PG1034+001. Both sets of data are normalized at 1950 Å.

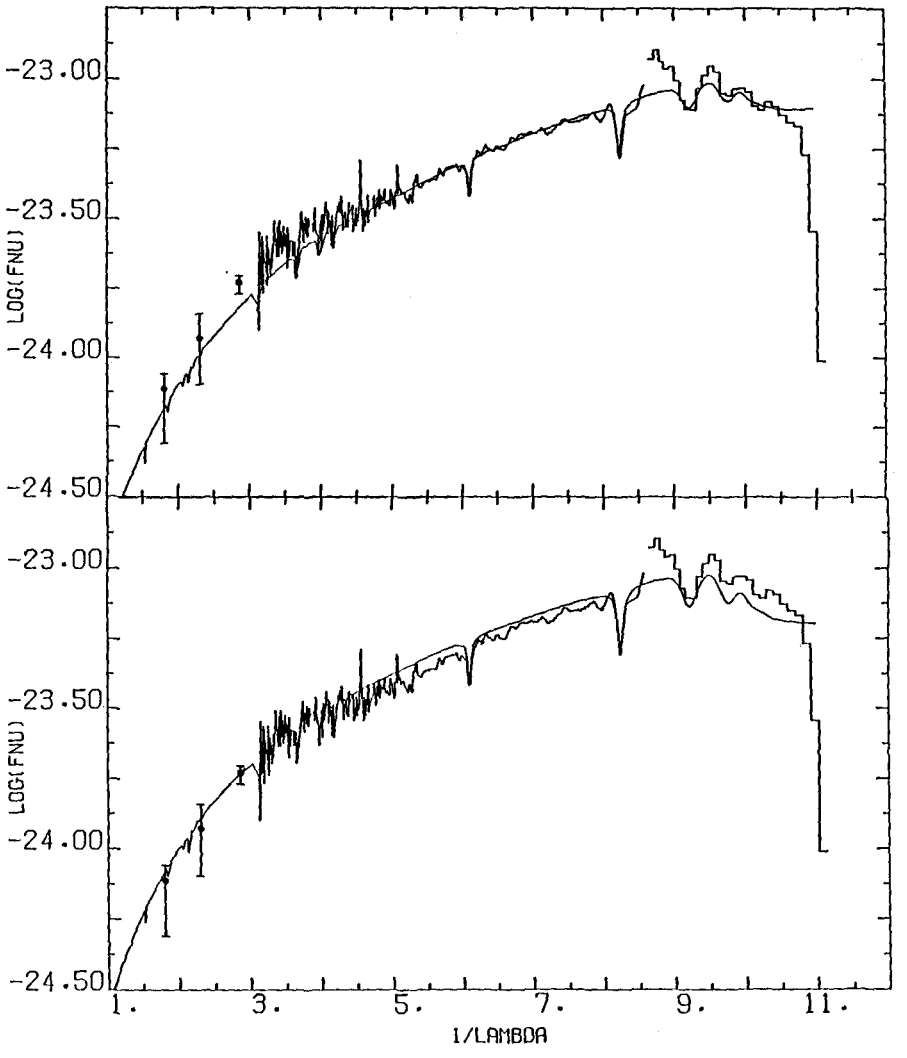

Fig.2 Preliminary fits to the energy distribution of HD149499B obtained by normalizing at 1900 Å (T_e=80,300 K; top panel) and at U (T_e=54,200K; bottom panel).

Figure 2 shows the composite energy distribution of HD149499B. The *Voyager 2* and *IUE* data are now augmented with the broad-band data discussed by Wegner (1978). The large error bar at V reflects the fact that the visual magnitude difference between the primary and white dwarf remains uncertain. We adopt here $\Delta V=2.95$ based on Rossiter's (1955) estimates, but take into account in the error the independent estimate of Holden (1977; $\Delta V=3.5$). At B, the error is dominated by the uncertain spectral type of the primary, which we take here to be K0 ± one subclass. Furthermore, the contribution of the primary to the light longward of ~2800 Å has been subtracted as well from the *IUE* data, following the procedure of SGW. The bottom panel shows the preliminary fit we obtain by normalizing at U, as was done by SGW. No reddening is included in our fits to this nearby object (d~34 pc; Ianna, Rhode, and Newell 1982). Our fit to the *IUE* is comparable to that achieved by SGW, although the model fluxes appear somewhat low in the *Voyager* range. The effective temperature is 54,200 K, in agreement with that determined by SGW. The top panel shows an alternate fit to the data, obtained by normalizing at 1900 Å and by *ignoring* the LWR and broad-band optical data. This fit, at 80,300 K, provides better agreement with the far-ultraviolet data, but appears inconsistent both with the long-wavelength *IUE* data and with the U magnitude, presumably the most accurate among the derived colors of the secondary.

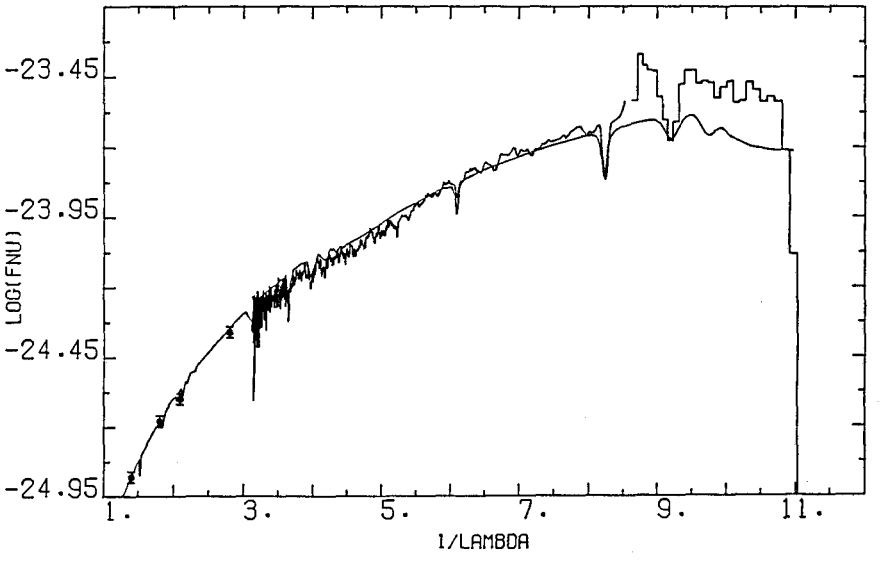

Fig.3 The energy distribution of PG1034+001, together with a model at 80,000 K, E(B-V)=0.02, the values derived by WGL.

Figure 3 shows similar data for PG1034+001. The optical photometry, from Green, Schmidt, and Liebert (1986), is again shown together with low-dispersion *IUE* data and *Voyager* flux points. Superposed on this is a model at 80,000 K, normalized at V, and reddened by a color excess of E(B-V)=0.02. These are the values derived by WGL on the basis of *IUE* and optical data only. Not unexpectedly, the agreement is quite good above 1200 Å, but the fit becomes marginal in the *Voyager* range. The suggested temperature appears hotter than this nominal value, but the competing influences of effective temperature and small amounts of reddening must be fully understood before a value of the effective temperature can be derived.

We are grateful to R. Lamontagne for his help with parts of this investigation. This work was supported in part by the NSERC Canada. One of us (GF) was supported by a E.W.R. Steacie Memorial Fellowship.

Green, R.F., Schmidt, M., and Liebert, J. 1986, *Ap. J. Suppl.*, **61**, 305.
Holden, F. 1977, *Pub.A.S.P.*, **89**, 588.
Ianna, P.A., Rhode, J.R., and Newell, E.B. 1982, *Ap. J.(Letters)*, **259**, L71.
Rossiter, R.A. 1955, *Pub.Obs.Univ.Michigan*, **11**, 1.
Sion, E.M., Guinan, E.F., and Wesemael, F. 1982, *Ap. J.*, **255**, 232(SGW).
Wegner, G. 1978, *M.N.R.A.S.*, **187**, 17.
Wesemael, F. 1981, *Ap. J. Suppl.*, **45**, 177.
Wesemael, F., Green, R.F., and Liebert, J. 1985, *Ap. J. Suppl.*, **58**, 379(WGL).
Wray, J.D., Parsons, S.B., and Henize, K.G. 1979, *Ap. J.(Letters)*, **234**, L187.

A Spectrophotometric Atlas of White Dwarfs Compiled from the IUE Archives

Steven R. Swanson (Dartmouth College, U.S.A.)
Gary Wegner (Dartmouth College, U.S.A.)

INTRODUCTION

In the past ten years, more than 775 low resolution spectra of white dwarfs have been taken with the *International Ultraviolet Explorer* satellite (*IUE*). This wealth of information has yielded many new discoveries in the field of white dwarf research; a few of which include: the λ1400 and λ1600 quasi-molecular features discovered in hydrogen rich DA white dwarfs (Greenstein 1980; Wegner 1982, 1984; Nelan and Wegner 1985; and Koester et. al. 1985), strong C I lines in some DQ white dwarfs (Koester, Weidemann, and Vauclair 1980; Wegner 1981a,b), and the absence of these same lines in hotter DB white dwarfs by Wegner and Nelan (1987) which may indicate convective mixing (Pelletier et al. 1986).

In this study, spectra from the *IUE* archives will be re-processed and corrected for changes which have occured in data reduction procedures over the past ten years. For example, all SWP (short wavelength primary) spectra processed before November 4, 1980 at Goddard Space Flight Center (GSFC) and March 10, 1981 at VILSPA, used an intensity transfer function (ITF) which was in error. This resulted in reduced absolute fluxes. Another major correction is due to the gradual degradation of the LWR (long wavelength redundant) camera over time, but which was not noticed until after many spectra were affected. Therefore, in order to create a relatively homogeneous set of data, reprocessing of most of the spectra is necessary. Of the 775 spectra which will be used in this study, there are 528 spectra of DA white dwarfs (354 of those are SWP), 195 spectra of DB white dwarfs (117 of those are SWP), and 51 spectra of other types of white dwarfs which include DZ and DQ types. These spectra comprise approximately 200 different stars. One of the results of this study will be the detection of the spectra which have been misclassified in the *IUE* merged log. Once these spectra have been reprocessed, an atlas will be published of the resultant merged spectra as well as tables of the flux values.

This large database will then be used to do a statistical study on the mass distribution of the white dwarfs and also their luminosity function. Several studies on these topics have been done using visual data only (Koester, Schulz, and Weidemann 1979; Shipman 1979; and Fleming, Green, and Liebert 1986). The mass distribution and the luminosity function of white dwarfs are very strongly tied to theories concerning the origin and cooling of white dwarfs, and many detailed calculations have been done to predict these properties (e.g. Iben and Tutukov 1986). By using a model atmosphere program to study the UV spectral energy distribution, the effective temperature (T_{eff}) and the surface gravity (log(g)) can be obtained. When these parameters are combined with trigonometric parallaxes, values of the radii can be obtained. Currently, aproximately 57 of the white dwarfs in the archives have trigonometric parallaxes.

DATA ANALYSIS

The first step in the reprocessing of the archived data is to examine the quality of the data, and reject very noisy spectra. Then the remaining data are re-extracted from the two-

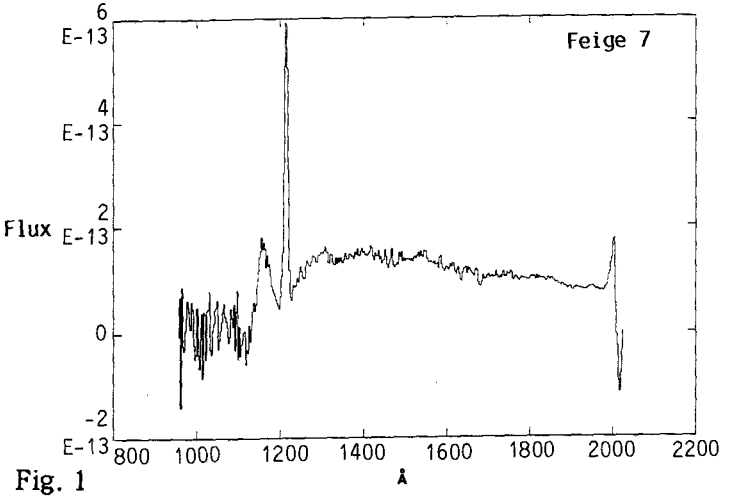

Fig. 1

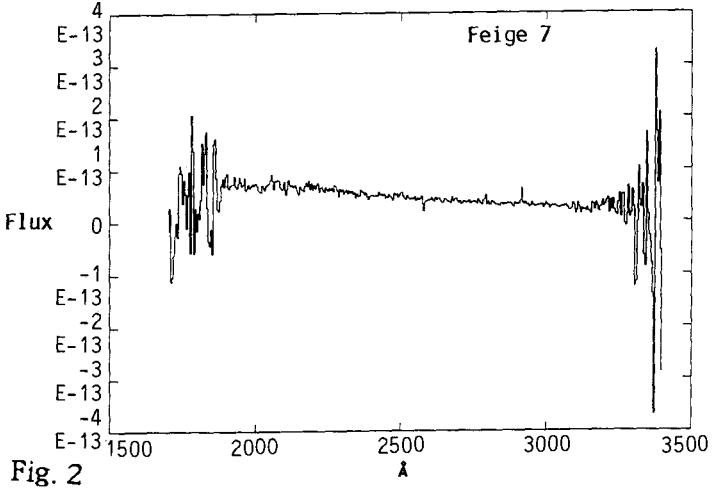

Fig. 2

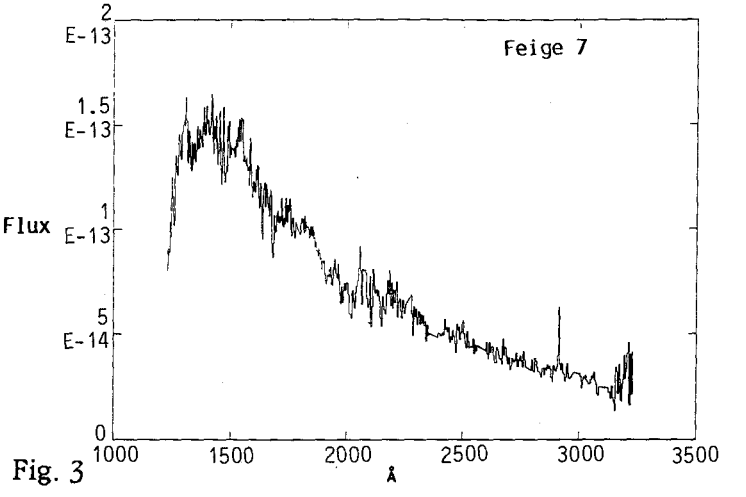

Fig. 3

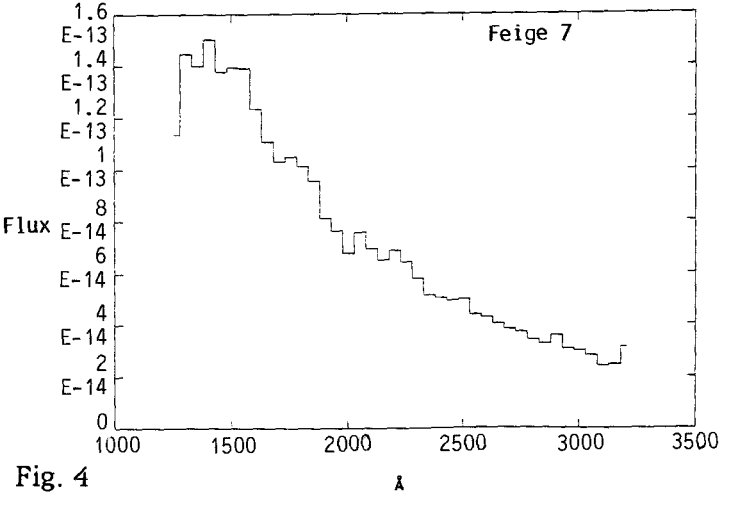

Fig. 4

dimensional data files. The re-extraction is necessary in order to apply the ITF correction for early SWP spectra and the LWR camera degradation correction. In this way, the finished spectra will be a homogeneously reduced database. The extraction of the one-dimensional spectra will be done using one of two techniques. The first uses a rectangular extraction slit, which is most accurate for the high signal to noise spectra. The rectangular method is the standard extraction technique for *IUE* spectra, and is the fastest method to use. The second method is a gaussian slit extraction. This is more time consuming, but results in more accurate fluxes for for lower quality data.

The one-dimensional spectra are then corrected for cosmic ray hits, blemishes, and reseau calibration points. Figures 1 and 2 show typical SWP and LWR spectra respectively, before the noisy ends have been trimmed off. Next all exposures of the same star are summed for each wavelength region and the resultant SW and LW spectra are merged, giving an effective spectral range of about 1200 Å to 3400 Å (see Fig. 3). The final step in the re-reduction will be to bin these spectra in 50Å bins for the final atlas (Fig. 4 shows an example of a final atlas spectrum).

When the above study has been finished, the model atmosphere program LUCIFER (Nelan 1985, McMahan 1986) will be used to analyse the UV spectra (and combined optical spectra where available). With this program T_{eff} and log(g) will be determined for each star.

CONCLUSION

This study will result in a homogeneous photometric set of ultraviolet energy distributions for a large number of white dwarfs. The resulting atlas should prove to be very useful to the astronomical community. Also the statistical study of the mass distribution and the luminosity function of white dwarfs using this ultraviolet data will be a valuable compliment to the similar studies which have been done in the optical wavelengths.

REFERENCES

Auer, L. H. and Mihalas, D. 1970, *M.N.*, **149**, 65.
Fleming, T., Liebert, J., and Green, R. F. 1986, *Ap. J.*, **308**, 176.
Greenstein, J. L. 1980, *Ap. J. (Letters)*, **241**, L89.
Grenfell, T. C. 1974, *Astr. Ap.*, **31**, 303.
Iben, I. and Tutukov, A. V., 1986, *Ap. J.*, **311**, 753.
Koester, D., Weidemann, V., Zeidler-K.T., E.-M., and Vauclair, V. 1985, *Astr. Ap.*, **142**, L5.
Koester, D., Weidemann, V., and Vauclair, G. 1980, *Astr. Ap.*, **83**, L13.
Koester, D., Schulz, H., and Weidemann, V. 1979, *Astr. Ap.*, **76**. 262.
Liebert, J., Wesemael, F., Hansen, C. J., Fontaine, G., Shipman, H. L., Sion, E. M., Winget, D. E., and Green, R. F. 1986, *Ap. J.*, **309**,
McMahan, R. K. 1986, Ph.D. Thesis, Dartmouth College.
Nelan, E. P. 1985, Ph.D. Thesis, Dartmouth College.
Nelan, E. P., and Wegner, G. 1985, *Ap. J. (Letters)*, **289**, L31.
Pelletier, C., Fontaine, G., Wesemael, F., Michaud, G., and Wegner, G. 1986, *Ap. J.*, **307**, 242.
Shipman, H. L. 1979, *Ap. J.*, **228**, 240.
Sion, E. M. 1986, *P.A.S.P.*, **98**, 821.
Wegner, G. 1981a, *Ap. J. (Letters)*, **245**, L27.
Wegner, G. 1981b, *Ap. J. (Letters)*, **248**, L129.
Wegner, G. 1982, *Ap. J. (Letters)*, **261**, L87.
Wegner, G. 1984, *A. J.*, **89**, 1050.
Wegner, G. and Nelan, E. P. 1987, *Ap. J.*, in press.
Zeidler-K. T., E.-M., Weidemann, V., and Koester, D. 1986, *Astr. Ap.*, **155**, 356.

SCALEHEIGHTS OF LOW MASS STARS FROM THE LUMINOSITY FUNCTION OF THE LOCAL WHITE DWARFS

N.C. Rana
Tata Institute of Fundamental Research
Homi Bhabha Road, Bombay 400005, India

It is shown that a combination of the observed luminosity function of the local white dwarfs and the theoretical cooling rates of a typical white dwarf suggests an approximately constant rate of formation of the white dwarfs. This rate is found to be about a factor of three lower than the observed birthrate of their immediate progenitors. This discrepancy is here interpreted as a three-fold increase in the scaleheight of the white dwarfs due to dynamical interaction with stars, molecular clouds; an average white dwarf being much more aged than an average progenitor. Since the low mass stars on an average are even slightly more long-lived than these white dwarfs, one can place a lower bound on the scaleheights of the low mass stars to be given by the required scaleheights of the white dwarfs, which is, according to the present work, 660 pc in the solar neighbourhood.

The Figure 1 shows the cooling curves for 0.6 $M_\odot$ white dwarfs with surface composition ranging from DA (with hydrogen envelope) to DB (helium rich envelope) types.

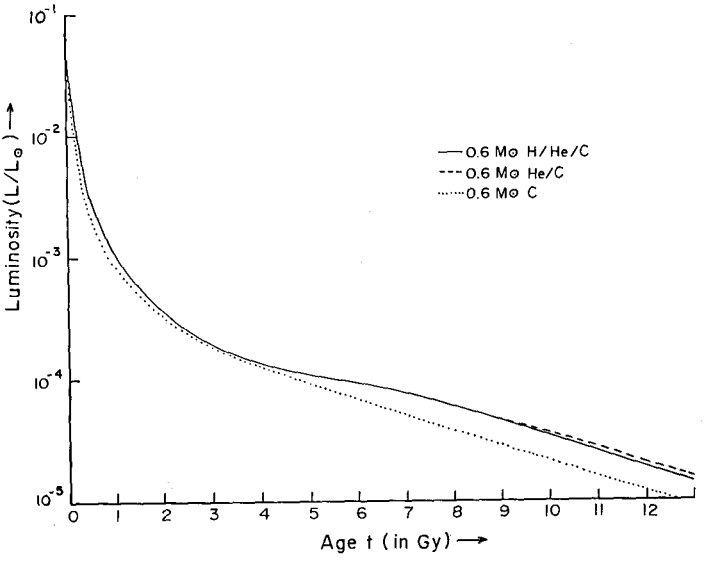

Figure 1. Theoretical cooling curves for white dwarfs of mass 0.6$M_\odot$.

In Table 1, the observed luminosity function of the local white dwarfs has been taken from Winget et al (1987). Combining this data with the cooling rates derived from Figure 1, the past history of the rate of formation of white dwarfs per unit volume of space in the solar neighbourhood (expressed in units of pc^{-3} Gy^{-1}) is determined and shown in the last column of Table 1. The average rate seems to have remained

Table 1

Luminosity function and birthrates of the white dwarfs in the solar neighbourhood

$\log (L/L_0)$	M_{Bol}	$\log [\phi(M_{Bol},T_d)]$; ϕ in $pc^{-3}M_{Bol}^{-1}$	$\frac{d \log (L/L_0)}{dt}$	Look back time $(T_d - t)$ in Gy	Birthrate of white dwarfs log [C(t)]; C(t) in pc^{-3} Gy^{-1}
-0.50	6.00	-5.81 ± 0.13	79(52)*	0.0044(0.0084)*	$-3.51^{+0.15}_{-0.30}$
-0.93	7.07	-4.96 ± 0.07	25(20)	0.015(0.022)	$-3.16^{+0.10}_{-0.15}$
-1.46	8.39	$-4.79^{+0.08}_{-0.09}$	7.1(7.6)	0.059(0.068)	$-3.54^{+0.12}_{-0.10}$
-1.95	9.62	$-4.10^{+0.09}_{-0.06}$	2.6(3.7)	0.180(0.164)	$-3.29^{+0.25}_{-0.10}$
-2.36	10.64	$-3.79^{+0.15}_{-0.08}$	1.6(2.1)	0.39(0.28)	$-3.19^{+0.25}_{-0.10}$
-2.70	11.49	$-3.73^{+0.10}_{-0.09}$	1.0(1.1)	0.65(0.52)	$-3.33^{+0.13}_{-0.10}$
-3.04	12.34	$-3.51^{+0.09}_{-0.13}$	0.57(0.63)	1.10(0.90)	-3.36 ± 0.13
-3.58	13.69	$-3.14^{+0.13}_{-0.30}$	0.28(0.27)	2.50(2.35)	$-3.29^{+0.13}_{-0.30}$
-4.04	14.84	$-3.27^{+0.25}_{-0.60}$	0.075(0.14)	5.95(5.00)	-4.00 ± 0.60
-4.40	15.74	$-2.92^{+0.14}_{-0.18}$	0.125(0.135)	9.55(7.92)	-3.42 ± 0.20
-4.66	16.39	$-4.20^{+0.45}_{-0.50}$	0.125(0.125)	11.6(10.05)	-4.70 ± 0.50

*The quantities in the parenthesis are for He/C $0.6M_\odot$ WDs.

fairly constant over the life-span of the disc with the value given by

$$\log < C > = -3.28 \pm 0.15$$

This can readily be compared with the observed rate of formation of the immediate progenitors (C_p) of the white dwarfs, such as planetary nebulae, stars on the AGB or HB of the HR diagram. Various authors have estimated this number to be roughly agreeing within a factor of 5 or so, with the lowest of the values given by Drilling and Schönberner (1985):

$$\log C_p = -2.78.$$

Even though it is the lowest of the estimates, it matches exactly with the predicted value, provided Rana (1987)'s IMF is taken. So I consider the above one to be a reasonable estimate.

Now obviously, there is a discrepancy between $<C>$ and C_p, at least by a factor of 3. The observed average rate of formation of the white dwarfs per unit volume is at least a factor of three less than that of their immediate progenitors.

We interpret this discrepancy to be arising due to longer life as well as stay of an average white dwarf than an average progenitor star. According to Wielen (1977), a longer stay of any object, be it a star or a cloud in the disc, makes the object increase its velocity dispersion with time, which means that the vertical amplitude of oscillation or its so-called scaleheight also increases with time. If we take the population average of the lifetime of the possible progenitors of the observed white dwarfs to be a measure of the average lifetime of the progenitors, then this lifetime is much shorter than the average age of the white dwarfs in the disc. So one could naturally expect that the white dwarfs would have a larger scaleheight than their progenitors. In fact, the ratio between $<C>$ and C_p may be interpreted as the inverse of the ratio between the respective scaleheights of their distributions.

In Table 2, the data on the mass function of the stars in the solar neighbourhood are taken from Rana (1987). The population average of the scaleheights of the progenitor stars of the white dwarfs is estimated to be

$$< H >_{*pg} = \int_{m_1}^{m_2} H(m)\, n(m)\, dm \Big/ \int_{m_1}^{m_2} n(m)\, dm = 220 \text{ pc},$$

where $m_1 = 0.95\ M_\odot$ and $m_2 = 8\ M_\odot$. Hence, we claim that the scaleheight of the vertical distribution of the local white dwarfs is at least 660 pc, that is, three times that of their immediate progenitors.

Now since on an average a low mass star lives slightly longer than an average white dwarf, the scaleheight distribution of the former should in general be somewhat larger than that of the white dwarfs. Therefore, we expect that the average scaleheight of the low mass stars that can outlive the disc would be given by

$< H >_{\text{low mass*}} \gtrsim 660$ pc.

Table 2

Basic data on the mass functions, lifetimes and the scaleheights distribution of main sequence stars in the solar neighbourhood.

Stellar mass (in $M_\odot$)	Present day mass function ϕ_{ms} (in $M_\odot$ pc^{-2})	Total life-time T_t (in Gy)	Main sequence lifetime (in Gy)	Scaleheight (in pc)	Initial mass function (in $M_\odot$ pc^{-2})	Volume density mass function (in pc^{-3})
log m	log ϕ_{ms}(log m)	log T_t	log T_{ms}	log(2H)	log ξ(log m)	log n(log m)
1.08	-2.91	-1.63	-1.70	2.27	-0.13	-2.40
0.92	-2.40	-1.40	-.1.50	2.30	0.18	-2.12
0.73	-1.89	-0.98	-1.10	2.33	0.29	-2.04
0.54	-1.28	-0.42	-0.61	2.38	0.41	-1.97
0.39	-0.43	-0.07	-0.27	2.46	0.92	-1.54
0.26	+0.15	0.35	0.15	2.59	1.08	-1.51
0.16	0.78	0.68	0.48	2.76	1.38	-1.38
0.06	1.32	1.05	0.85	2.97	1.55	-1.42
-0.02	1.62	1.35	1.15	3.01	1.62	-1.39

Both these conclusions about the scaleheight distributions can be tested once the more deep sky surveys of the low mass stars and the white dwarfs become available. It may be mentioned that Van der Kruit (1986)'s model of the galaxy and the IRAS image of the local disc suggest the scaleheight of the local disc stars to be in the range of 500-600 pc. With such a large scaleheight for the low mass stars and the white dwarfs, the problem of the local dark matter can also be satisfactorily resolved.

References

Drilling, J.S., and Schönberner, D., 1985, Astron. Astrophys. 146, L23.
Rana, N.C., 1987, Aston. Astrophys. 184, 104.
Van der Kruit, P.C., 1986, Astron. Astrophys. 157, 230.
Winget, D.E., Harsen, C.J., Leibert, J., Van Horn, H.M., Fontaine, G., Nather, R.E., Kepler, S.O., and Lamb, D.Q., 1987, Astrophys. J. 315, L77.

ROSAT - AN ALL-SKY X-RAY AND EUV SURVEY OF WHITE DWARFS

M.A.Barstow

X-ray Astronomy Group, Physics Department, University of Leicester

University Road,Leicester, LE1 7RH, UK

ABSTRACT

The West German astronomy satellite *ROSAT* comprises two imaging telescopes - an X-ray instrument covering the energy band 0.15-2keV and an EUV instrument (provided by the UK) covering the range 0.02-0.21keV. A primary aim of the mission is to perform a sensitive all-sky survey with both telescopes (two 'colours' in the EUV) in the first 6 months. This will be followed by a least one year of pointed observations at specific targets. This paper briefly describes the *ROSAT* instrumentation and discusses the likely impact of the survey on white dwarf studies.

1. INTRODUCTION

ROSAT is a West German X-ray astronomy mission led by the Max Planck Institut für Extraterrestriche Physik. The satellite comprises two instruments, a large Wolter I imaging X-ray telescope (XRT) covering an energy range 0.15-2keV (80-6Å) and a wide field EUV telescope spanning the band ≈0.02-0.21keV (620-60Å). The latter instrument, the Wide Field Camera (WFC), is being provided by the UK. The US will provide a high resolution imaging detector (HRI) for the XRT focal plane (in addition to the German imaging proportional counter - PSPC) and the launch, on a Delta rocket in early 1990. The major objective of the mission is to perform the first imaging all-sky surveys in both X-ray and EUV bands during the initial six months of operation. After this a minimum of one year of pointed observations are planned, with possible extensions for up to two years depending on the lifetime of the satellite. During the survey the XRT will employ the energy sensitive PSPC at its focus and the WFC will image the sky in two wavebands by use of selected filters. Two more filters will be available to extend the WFC spectral coverage to lower energies during the pointed observations. Experience with the *Einstein* and *EXOSAT* satellites has shown how important soft X-ray observations are in the study of hot white dwarfs (WDs) (eg. Paerels et al., 1987; Petre et al., 1986) particularly in determining the concentrations of trace elements such as He and CNO (eg. Paerels et al., 1987; Barstow, 1988). A sensitive all-sky survey in soft X-ray and EUV bands will provide an unprecedented database with which to pursue these studies. This paper gives brief descriptions of the XRT and WFC instruments and discusses their sensitivities in the context of white dwarf observations.

2. DESCRIPTION OF THE XRT AND WFC

Both these instruments have been described in detail in a number of papers (eg. Trumper, 1984: XRT; Barstow and Pounds, 1988: WFC). Consequently, this discussion is restricted to the important details and scientific performance.

The XRT consists of a nest of four Wolter I grazing incidence telescopes having an intrinsic resolution of a few ″, with a focal plane assembly of two PSPCs and one HRI which are mounted on a carousel. The PSPC (Pfefferman et al, 1986) has a relatively large 2° field of view with an on-axis resolution of 30 ″ FWHM and an average over the field of view of 2 ′. Its nominal energy range is 0.1-2keV (6-80Å) and the spectral resolution of $< 45\%$ FWHM at 1keV allows four distinguishable 'colour' bands. The HRI (Pfefferman et al, 1986) is a microchannel plate (MCP) detector,

similar to that flown on *Einstein* but with a CsI photocathode to enhance the quantum efficiency. It has a resolution of 1.7″ FWHM but poor energy resolution. A filter of aluminised Parylene N protects the detector from geocoronal radiation and ions.

The WFC has a nest of three Wolter-Schwarzchild type I mirrors with two identical MCP detectors mounted on a turret mechanism in the focal plane. The mirror grazing angles chosen ($\approx 7.5°$) allow the collecting area to be optimised while retaining a wide (5.0°diam.) field of view and a low energy reflectivity cutoff at 0.21keV (60Å). An on-axis resolution of 2.3″ HEW is expected degrading to 4.4″ HEW at the edge of the field as a result of inherent optical aberrations. Hence, the average survey resolution will be 3.5″ HEW. The MCP detector has a CsI photocathode to enhance its quantum efficiency but has no intrinsic energy resolution. A filter wheel assembly mounted near the focal plane contains a number of filters which can be selected to define wavelength pass bands, suppress geocoronal radiation and prevent detection of UV radiation from hot O/B0 stars.

The XRT and WFC spectral bands and respective sensitivities are summarised in table I. In the context of WD studies the PSPC can be taken to have a single energy band (44-80Å) since in general no significant flux is observed below 44Å and the PSPC energy resolution is poorest in this region.

3. OBSERVING HOT WHITE DWARFS

Our current understanding of the formation and evolution of WDs has recently been reviewed by Sion (1986). It is clear that many problems concerning the relationships between different groups of objects remain to be understood, in particular between H-rich and He-rich WDs and their progenitors. There is evidence that He-rich WDs contain significant quantities of CNO but their abundances are not well determined. The combination of *ROSAT* XRT and WFC is an ideal tool for such studies. Figure 1 illustrates this, comparing the instrument bands (3 in the survey and up to 5 in pointed mode) with some typical WD spectral models. This indicates that the instruments are much more sensitive to H dominated stars than He-rich ones, as might be expected given the relatively high opacity of He at soft X-ray energies. The ability of *ROSAT* to observe WDs has been quantified by convolving model WD spectra with the instrument response for each bandpass. A minimum detectable temperature limit can be estimated for each bandpass, as a function of absorbing column density, as illustrated in figure 2 for pure H and pure He atmospheres.

To assess the potential of the sky survey requires an estimate of the number of WDs that we might expect to see. Fleming, Liebert and Green (1986; hereafter FLG) present a summary of space densities for DA and DO/DB WDs subdivided by temperature. Their estimated scale height is 250pc. If the volume accessible to *ROSAT* is known for each band, calculating the number of stars is simple. However, this depends on assumptions made about the ISM and WD radii. A good indication of the effect of the ISM can be obtained by assuming that it is uniform with a mean density of 0.07 atoms cm^{-3}, although in reality there are large line of sight variations with viewing direction (eg. Paresce, 1984). Based on this assumption the maximum distances at which WDs could be detected were determined for each bandpass as a function of temperature. WD radii were assumed to be $0.0125R_{\odot}$. These distances and the respective column densities are summarised in table II for the temperatures corresponding to the centre of the ranges for which FLG tabulate space densities. To account for WDs in binary systems their densities are multiplied by a factor of 2 in this calculation. The expected numbers of DA WDs in the volumes defined are also listed in table II. It is not possible to perform a similar calculation for DO/DB WDs. The temperatures to which *ROSAT* is sensitive are

TABLE I. *ROSAT* XRT+PSPC & WFC Filters - Wavebands and Sensitivity

Instrument	Detector or Filter Type [a]	Survey (S) or Pointed (P)	FOV Diam. (deg.)	'Mean' Wavelength (Å)	Bandpass (Å) (at 10% of peak efficiency)	Point-source Sensitivity[b] (μJy)	(HZ43^{-1})
XRT	PSPC	S + P	2.0	60	44–80	0.47	6000
WFC	C/Lexan/B (×2)	S + P	5	100	60–140	1.0	2400
	Be/Lexan (×2)	S + P	5	140	112–200	1.4	4800
	Al/Lexan	P	2.5	180	150–220	7.3	1300
	Sn/Al	P	2.5	600	530–720	220	160

[a] Provisional. [b] For 5σ significance, exposure time of 2000s (a typical value for each filter for the survey and for pointed observations) and 'typical' background. The right hand column expresses the sensitivity in terms of the flux from the white dwarf HZ43, the brightest known EUV source.

Figure 1. White dwarf model atmospheres for a 60000K star comprising [1] pure H, [2] He/H=10^{-4} and [3] pure He. The solid vertical lines indicate the mean wavelengths of each band.

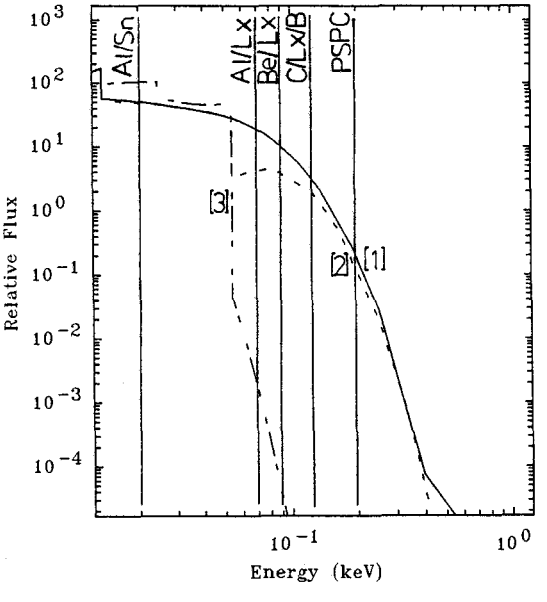

Figure 2. The minimum WD temperature to which each *ROSAT* band is sensitive as a function of photon energy and wavelength

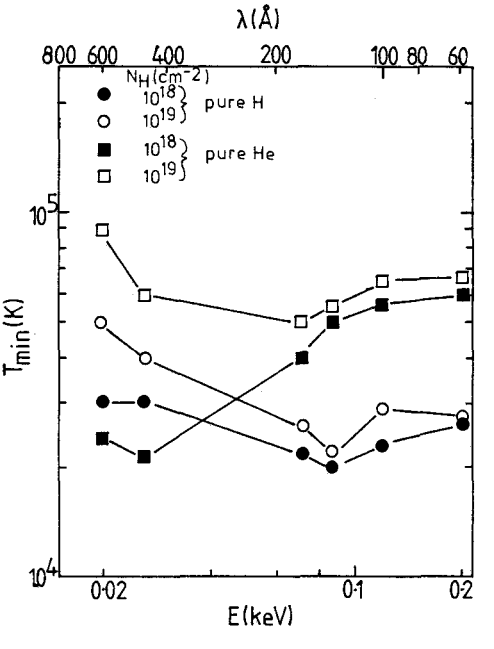

TABLE II. Numbers of DA WDs detected in each *ROSAT* band with maximum distances and values of $N_H^{[a]}$.

		XRT PSPC	WFC C/Lexan/B	Be/Lexan	Al/Lexan	Al/Sn
30000K	d(pc)	175	78	104	55	< 30
	$N_H(cm^{-2})$	3.6×10^{19}	1.6×10^{19}	2.2×10^{19}	1.0×10^{19}	$< 10^{18}$
60000K	d(pc)	1240	554	350	175	40
	$N_H(cm^{-2})$	2.6×10^{20}	1.0×10^{20}	7.4×10^{19}	3.7×10^{19}	8.0×10^{18}
No of DA WDs		5500	2200	1400	200	< 10

[a] For ISM with constant volume number density of neutral hydrogen of 0.07 cm^{-3} (Paresce 1984).

generally in the upper range considered by FLG, where the space density is very low. Within the volumes accessible very few stars would be seen. However, it is known that hot DO stars exist with temperatures substantially in excess of 80000K (FLG's upper limit). *ROSAT* could see such objects up to distances of 1kpc and N_H values of $2.0 \times 10^{20} cm^{-2}$.

4. CONCLUSION

The survey bands of *ROSAT* are capable of detecting hot WDs at distances of more than 1kpc and column densities above $1-2 \times 10^{20} cm^{-2}$. It is expected that $\approx$ 5500, $\approx$ 2200 and $\approx$ 1400 DA WDs will be detected in PSPC, C/Lexan/B and Be/Lexan bands (the survey bands) respectively, but large uncertainties are present in these estimates. However, resolving problems like these is an important reason for performing the survey. Approximately 1500 WDs are known to exist of which $\approx$ 30% (about 450) have temperatures > 20000K. Clearly most of those WDs detected by *ROSAT* will be unidentified and a considerable follow-up programme of optical observations will be needed. Realistic estimates of the numbers of detectable He-rich WDs cannot be made with current data. An all-sky survey will be of particular importance in population studies of these objects as *ROSAT* is very sensitive to those temperature ranges not easily studied by optical or UV observations.

Observations of a few WDs with *Einstein* and *EXOSAT* has shown what information can be obtained (eg. T_{eff}, N_H and H/He ratio) from soft X-ray photometry. The *ROSAT* sky survey will represent a huge increase in the statistical sample available for population studies, yielding an accurate luminosity function and the relationship between He abundances and T_{eff}.

5. ACKNOWLEDGEMENTS

ROSAT is a West German mission, led by MPE to which the UK has contributed the WFC. I would like to thank the project scientist Prof. J.Trümper for allowing me to discuss the XRT performance in this paper. The WFC is supported by the SERC, UK and is being constructed by a consortium comprising - Leicester University, Birmingham University, Rutherford-Appleton Laboratory, Mullard Space Science Laboratory and Imperial College, London.

6. REFERENCES

Barstow,M.A., 1988, these proceedings.

Barstow,M.A. and Pounds,K.A., 1988, proceedings of the NATO ASI, 'Hot Thin Plasmas in Astrophysics', ed. R.Pallavicini, 359.

Fleming,T., Liebert,J. and Green,R.F., 1986, *Astrophys.J.*, **308**, 176.

Paerels,F.B.S., Heise,J., Kahn,S.M. and Rodgers,R.D., 1986, *Astrophys.J.*, **322**, 315.

Paresce,F., 1984, *Astron.J.*, **89**, 1022.

Petre,R., Shipman,H.L. and Canizares,C.R., 1986, *Astrophys.J.*, **304**, 356.

Pfefferman,E.,et al., 1986, *Proc SPIE*, **733**, 519.

Sion,E.M., 1986, *Publ.astr.Soc.Pac.*, **98**, 821.

Trümper,J., 1984, *Physica Scripta*, T7, 209.

RESULTS OF A SPECTROPHOTOMETRIC SURVEY OF WHITE DWARF SUSPECTS IN THE SOLAR NEIGHBOURHOOD

I.Bues
Dr.Remeis-Sternwarte Bamberg,Astron.Institute
Universität Erlangen-Nürnberg,D-8600 Bamberg,FRG

OBSERVATION

320 blue stars of the Giclas and Luyten catalogues with positions $\pm 30^{\circ} \leq \delta \leq 15^{\circ}$ and magnitudes $12^{m} \leq m_{pg} \leq 15^{m}$ have been observed photometrically in UBVRI and Strömgren colours with the ESO 1m telescope at La Silla in order to increase the number of close-by white dwarfs. From their Strömgren colours more than 120 stars belong to the white dwarf region. But, as outlined by Rupprecht and Bues (1983), a combination of the photometric systems and the combined two-colour diagrams (R-I)/(U-V) and (R-I)/(u-b) provide additional information on binary components. Fig.1 shows a sample in the (R-I)/(u-b)diagram. For (u-b) < .2 and (R-I) > .2 a second component is present.

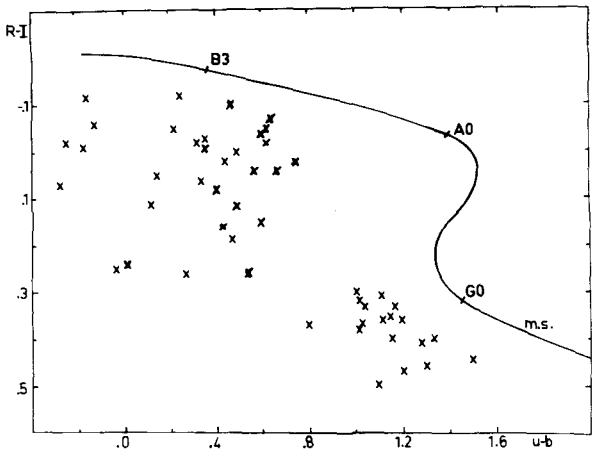

Fig.1 : combined two-colour diagram of observations

With these criteria in mind,we took 82 objects for further investigation. At the ESO 1.52m-telescope spectra (114 Å/mm,IDS+CCD) have been obtained for all white dwarfs and an analysis by model atmosphere technique has started to determine the distance of the objects. For three stars (GD (GD 1401,GD 1555,GD 1072) we did polarimetric measurements with the PISCO at the ESO 2.2m telescope,where GD 1072 yielded a positive result of 2% slightly variable linear polarization,the others did not show any polarization.

Here we would like to present our results for those stars of spectral type DA indicated by heavy colour in Fig.1 and with photometric data summarized in Table 1.

Table 1: WHITE DWARFS OF TYPE DA FROM COLOURS

NAME	V	B-V	U-B	U-V	R-I	y	b-y	m_1	u-b	d (pc)
L 550-52	14.20	.14	-.51	-.37	.04	14.33	.01	.47	.74	25
LP 611-52	15.24	.12	-.62	-.50	.08	15.53	.05	.31	.41	47
LP 906-28	15.05	.19	-.62	-.43	.11	15.03	.07	.33	.50	36
LP 734-74	15.53	.24	-.69	-.45	-.06	15.49	.11	.26	.59	39
LP 615-46	14.97	.23	-.60	-.37	.26	14.98	.14	.19	.56	30
LP 736-4	14.75	.27	-.96	-.69	.17	14.71	.22	.10	.41	49
LTT 4893	14.66	.12	-.59	-.47	-.13	14.54	.16	.20	.62	28
L 905-20	14.10	.04	-.89	-.85	.24	14.16	.03	.08	.01	34
LHS 2712	14.81	-.03	-.67	-.70	-.10	14.80	-.07	.30	.47	58
LTT 5410	14.61	.21	-.57	-.36	.06	-	-	-	-	25
LTT 5453	14.93	.32	-.61	-.29	.04	15.00	.16	.20	.54	25
LP 739-61	15.77	.15	-.66	-.51	-	15.77	-.06	.41	.53	54
LTT 6451	15.20	.20	-.59	-.39	-.07	15.16	.03	.30	.63	34
GD 1295	14.17	-.13	-.68	-.81	-.01	14.16	-.03	.15	.36	47
GD 1192	13.37	.10	-.61	-.51	-.04	13.37	.03	.41	.61	22
GD 1212	13.26	.18	-.57	-.39	.04	13.25	.08	.27	.67	16

ANALYSIS

Hydrogen line-blanketed LTE model atmospheres have been used to compute colours as well as fluxes in the range $16000^{\circ} \geq T_{eff} \geq 11000^{\circ}K$, log g=7 and 8. For a detailed comparison of the Balmer line region, we developed a new code of Stark profile calculation for H_{α} to H_{ϵ}. Fig.2 shows the region of H_{β} to H_{δ} for one of the cooler objects of our DA sample in direct comparison with flux and line profiles of a model atmosphere. The profile of each Stark component is computed in steps of .155Å and

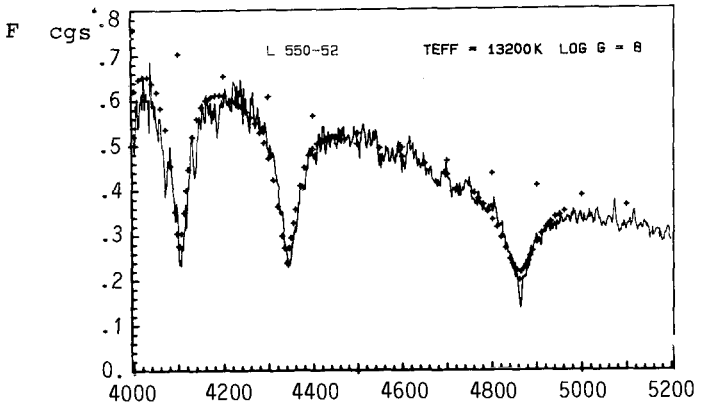

Fig.2: Direct comparison between the flux of a model atmosphere and an observed best fitting spectrum

then folded with other broadening mechanisms. The agreement with observed profiles is improved as compared to tabulated and interpolated values.

With T_{eff}, log g and the bolometric correction taken from a fit of a model atmosphere with white dwarfs of known distance we calculated photometric parallaxes of the stars in Table 1. The last column of the Table contains the results.The accuracy of the distance determination should be better than 15pc.

If compared to the total number of this most common type of white dwarfs in the intermediate range of temperature,our survey increases the number within 50 pc by 5 %. Our investigations of cooler objects,however,do not show a further increase of objects by number,as we had expected when we started the programme.

For 4 cool very blue subdwarfs (GD 806,GD 1439,G82-44,G152-67) with an abundance analysis by model atmospheres with $7000^{\circ} \gtrsim T_{eff} \gtrsim 5500^{\circ}K$, $5.5 \gtrsim \log g \leq 6.5$ and photometric parallaxes a distance of $\sim$100 pc for the G-stars and 500 pc for the GD stars has been determined.GD 806 is the most interesting object of this group with a reduction of heavy metals by a factor of at least 10^3 and C reduced by a factor of 10 only. Fig.3 shows an important part of the blue spectrum,where the Balmer lines are the strongest features by far and the weakness of CaII at $6500^{\circ}K$ is evident.

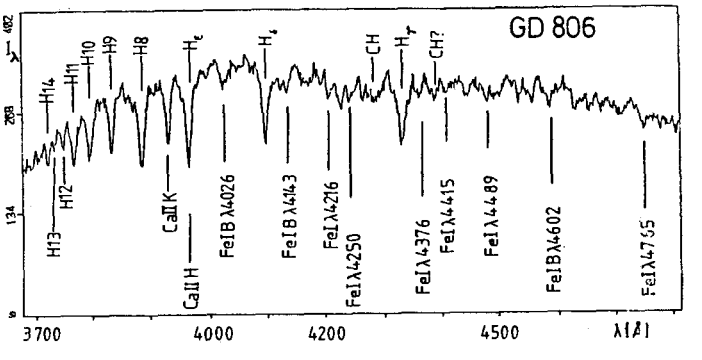

Fig.3: Blue spectrum of GD 806 (114 Å/mm)

The survey will be continued for another year to obtain a detailed analysis for white dwarfs and various kinds of subdwarfs.

REFERENCES

G.Rupprecht,I.Bues,1983, The Messenger 34,24

Three Double Degenerate Candidates

Diana Foss
Steward Observatory, University of Arizona
Tucson, AZ, 85721 USA

This poster reports the results of a search for variable radial velocities in 29 DA white dwarfs. The survey was sensitive to periods between 1^h and 66^d, although non-ideal sampling limited the longest practically detectable period to 2^d. Three stars were discovered to have radial velocity shifts at above the 3σ level. The discovery of these stars, along with that of Saffer, *et al.* (1988) can put only a lower limit on the space density of close binary white dwarfs, as this survey was less than 100% efficient in detecting radial velocity variations, and its efficiency depended strongly on period.

Introduction

Several authors (Paczynski 1985, Webbink 1984, Iben and Tutukov 1984) have proposed close pairs of degenerate stars as the progenitors of Type Ia supernovae (SNeIa), and subsequent calculations of the merger of such systems by Iben and Tutukov (1984, 1987), Arnett, Branch and Wheeler (1985), and Tornambé and Matteuchi (1987), among many others, have produced model spectra and light curves in good agreement with observations of real SNeIa. This theoretical framework has motivated workers to search for duplicity in supposedly single white dwarfs. Greenstein (1986) has found a handful of wide pairs of white dwarfs, but the only major systematic search until now, that of Robinson and Shafter (1987), failed to find any binaries. They concluded that the fraction of all supposedly single white dwarfs that are really double with periods between 30^s and 3^h is less than 1/20 with 90% probability. Nevertheless, Saffer, *et al.* (1988) have discovered that WD 0135-052 (EG 11, L 870-2), a popular spectrophotometric standard, is in fact a close, detached pair of DA white dwarfs. The present search was motivated by the lack of systematic observations sensitive to periods longer than three hours.

Observations

The observations were carried out using the 1.5 m telescope at Palomar Observatory on the nights of 19–21 June and 30 October–2 November 1985 and 23–27 February 1986. The instrument used was the 1.5 m's CCD spectrograph, using a 800 x 816 pixel TI CCD, and a 1200 line grating in first order. The observations covered a wavelength range between 4200 to 5100 Å and had a resolution of 240 km/sec. Forty-two bright white dwarfs were observed, 29 of which had spectra good enough to fit. All but 11 of these were subsequently observed by Robinson and Shafter, but the observations reported here were spaced such that much longer periods were sampled. The stars, listed in Table 1, were chosen, on the basis of their brightness, from the McCook and Sion (1984) catalog of spectroscopically identified white dwarfs. Each observation was bracketed by

Table 1

Star	$<\sigma_v>$ (km/sec)	Δt (hr)	Star	$<\sigma_v>$ (km/sec)	Δt (hr)
WD 0004+330	76.42	45.92	WD 1327-083	64.46	22.90
WD 0109-052	23.56	24.57			24.98
WD 0135-052	27.33	1.87	WD 1527+091	88.86	48.40
WD 0148+467	21.92	1.95	WD 1538+269	44.37	24.01
WD 0205+250	18.92	23.63			24.97
WD 0227+050	21.46	47.40	WD 1615-154	175.50	3.67
WD 0232+035	79.67	47.45			21.95
WD 0410+117	33.66	23.17			23.47
WD 0644+375	58.34	19.77			25.62
		3.46			45.42
		25.22			49.09
		22.33	WD 1647+591	71.24	3.77
WD 0612+177	70.47	20.59			46.48
		2.66			50.25
		22.95	WD 1919+145	134.98	2.25
		2.27	WD 2032+248	74.76	1.67
		19.93			47.20
WD 1105-048	62.71	23.75			48.87
WD 1134+300	76.47	23.14	WD 2039-202	140.60	47.22
		20.76			1.80
		3.79			49.02
		21.28	WD 2117+539	18.62	22.63
WD 1143+321	93.71	3.85	WD 2126+734	22.66	22.38
		22.53	WD 2149+021	25.79	2.70
		25.10			45.64
		21.40			48.34
WD 1254+223	81.93	3.55	WD 2256+249	39.27	21.03
		26.18			23.53
		22.63			44.56
		21.62	WD 2309+105	88.76	20.73
WD 1314+293	310.89	22.18	WD 2326+734	22.76	22.48
		23.12			23.07
		45.90			45.55

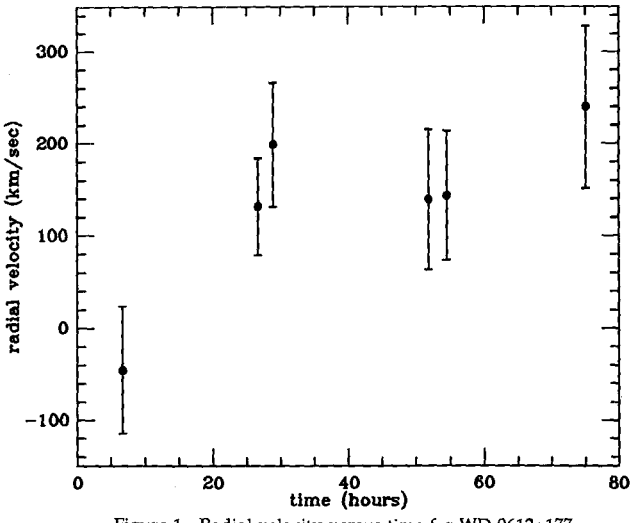

Figure 1. Radial velocity versus time for WD 0612+177.

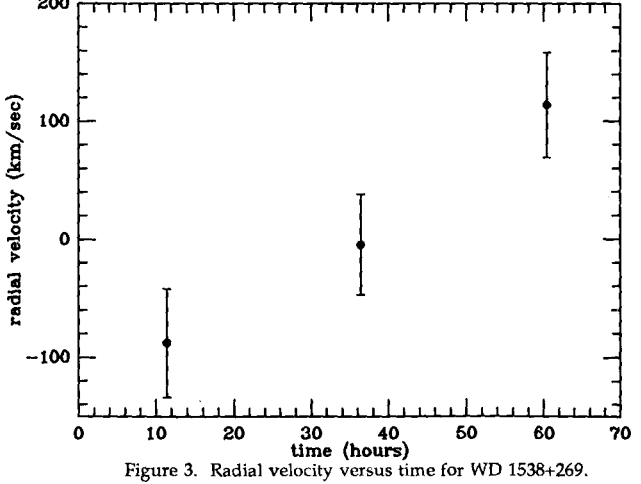

Figure 3. Radial velocity versus time for WD 1538+269.

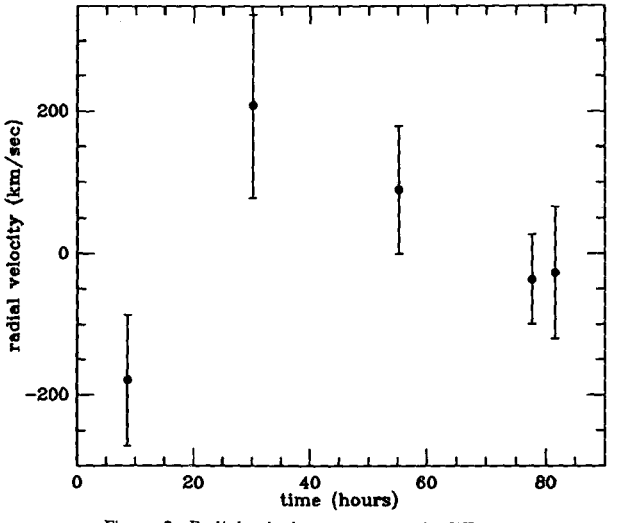

Figure 2. Radial velocity versus time for WD 1143+321.

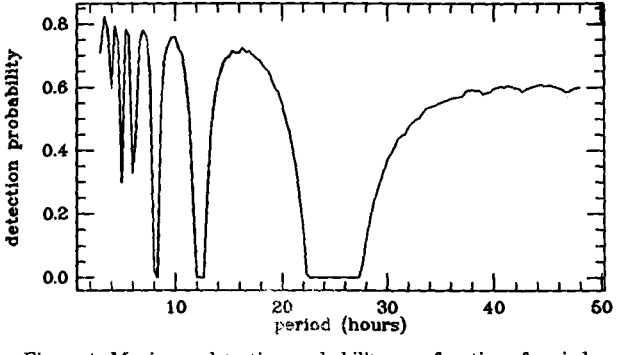

Figure 4. Maximum detection probability as a function of period for WD 0109-274, which was only observed twice, with an interval between observations of 24.57^{h}. Note the severe aliasing at periods corresponding to fractions of the observation interval.

spectra of a helium comparison arc lamp. Each star was observed at least twice, many three or four times, with observations separated by roughly either 3, 24, 48, or 72 hours.

The data were reduced using NOAO's Image Reduction and Analysis Facility (IRAF). The spectra were flat-fielded, sky-subtracted, summed down to one dimension and wavelength calibrated using the He arc spectra. They were not flux calibrated. The spectra were fit with a non-linear least-squares "pseudo" Lorentzian line profile, as described in Saffer, *et al.* (1988). A velocity shift of at least three times the 1σ errors from the fit and the wavelength calibration was considered the minimum believable difference. Three stars, WD 0612+177, WD 1143+321, and WD1538+239 met this criterion, as shown in Figures 1 through 3.

Discussion

Although three stars in the sample showed sufficient radial velocity variations to be counted as binaries in the analysis, one cannot therefore immediately calculate a space density of binary white dwarfs. Due to the non-ideal sampling of periods imposed by the intervals between observations, the probability of detecting a binary depends upon its period, dropping to zero when the period is equal to the observation interval. This is shown in Figure 4. Since radial velocity variations could not be detected with 100% efficiency, any space density calculated directly from these stars plus WD 0135-152 can only be a lower limit, as non-detections in this survey do not necessarily imply single stars. I plan to observe the three stars reported here as candidates, to confirm their radial velocity variability, and to determine their orbits.

References

Arnett, W.D., Branch, D. and Wheeler, J.C. 1985, *Nature*, **314**, 337.

Greenstein, J. E. 1986, *A. J.* **92**, 867.

Iben, I., Jr. and Tutukov, A. V. 1984, *Ap. J. Supp.* **54**, 335.

McCook, G. P. and Sion, E. M. 1984, *A Catalog of Spectroscopically Identified White Dwarfs*, (2nd edition, Villanova, Pa., Villanova Press).

Paczynski, B. 1985, in *Cataclysmic Variables and Low Mass X-Ray Binaries*, Eds. D. Q. Lamb and J. Patterson, (Dordrecht, Reidel), p. 1.

Robinson, E.L and Shafter, A.W. 1987 *Ap. J.* **322**, 296.

Saffer, R. A., Liebert, J. W. and Olszewski, E. W. 1988 *Ap. J.*, in press.

Tornambé, A. and Matteuchi, F. 1986, *M.N.R.A.S.*, **223**, 69.

Webbink, R. F. 1984, *Ap. J.*, **277**, 355.

THE CCD/TRANSIT INSTRUMENT (CTI) BLUE OBJECT SURVEY

J. Davy Kirkpatrick and John T. McGraw
Steward Observatory, University of Arizona
Tucson, Arizona 85721, U.S.A.

Introduction:

The CCD/Transit Instrument (CTI) is a 1.8 m, f/2.2 meridian-pointing telescope located on Kitt Peak. It has no moving parts, but utilizes two RCA charge-coupled devices (CCDs) aligned with columns in the east-west direction and operated in the "time-delay and integrate" (TDI) mode at the apparent sidereal rate to form an image of the sky as it transits (McGraw *et al.* 1986). The strip is 8.25 arcminutes wide north-south with length determined by the length of the night. Thus, each night the CTI surveys about 15 square degrees of the sky, or about 45 square degrees per year, to a nightly limiting magnitude of $m_V \geq 20$. One of the two CCDs in the focal plane always observes through a V filter while the other utilizes one of (U), B, R, or I, depending upon the sky brightness. These data are searched to find every detectable object and photometric parameters are calculated for each. These data become part of a Master List which contains the best estimate for each parameter and a History List which maintains a light curve for every detected object. The vital statistics of the project are listed in Table 1.

This paper describes our preliminary efforts at investigating the blue stellar component of these data bases. The CTI survey yields high-precision, homogeneous multi-color photometry to faint limiting magnitudes, thus allowing a statistically complete sample of objects which can be used for a wide variety of scientific programs. The photometric precision derives principally from utilization of the TDI technique which effectively averages all spatial instrumental corrections (bias and flat-field) into more stable linear functions.

In particular, we wish to spectroscopically identify white dwarf and subdwarf stars to faint limiting magnitude both in the galactic halo and in the disk. These stars can be used as probes of galactic structure in the solar vicinity. Thus far we have spectroscopically identified 110 objects which have been determined to be "very blue" on the basis of colors derived from B, V, R and I measurements. We use the spectroscopic identifications to refine the loci of white dwarfs, subdwarfs, etc. in our N-dimensional color space to fainter limiting magnitudes. Additionally, we begin an investigation of the motions and velocities of the white dwarfs we have discovered.

The Survey:

The blue candidates were selected from their outlying positions in color-magnitude or color-color diagrams. Each blue candidate is visually inspected in the CTI pixel data to ensure it is not contaminated by the halo of a nearby very bright star or merged with one or more stars. We also

reject candidates contaminated by CCD artifacts such as charge "bleeding" from bright stars. The objects which survive our visual test are promoted to our observing list.

TABLE 1: Survey Vital Statistics

1.8 m, f/2.2 Automated Telescope
Two RCA CCDs — 320 × 512 Pixels, 30 Microns in Size
Field Scale of 52 Arcsec mm^{-1} — Pixel Subtends 1.55 Arcsec
Declination of Strip — +28 Degrees
Width of Surveyed Strip — 8.26 Arcmin
Total Area Surveyed — 43.7 Square Degrees
Time History Recorded in V Bandpass
Time-averaged (U), B, V, R, I Colors Obtained

DETECTORS:
CCDs Have No Cosmetic Blemishes
"V" CCD — 40 Electron Readout Noise
— 10.78 Electrons/ADU
— Nightly Limiting Magnitude V = 21
"Color" CCD — 72 Electron Readout Noise
— 9.18 Electrons/ADU

CONTROL AND ACQUISITION COMPUTER SYSTEM:
— 16-bit Minicomputer
— Real-time Program "Herschel" Requires Minimal Human Response
— Data Stored on Disk During Acquisition
— Data Written to Magnetic Tape for Transport to Tucson

Thus far we have had 1.5 clear nights of spectroscopic observing time on the 4.5 m Multiple Mirror Telescope (MMT) and 6.5 nights on Steward Observatory's 2.3 m telescope on Kitt Peak. Preliminary statistical results are presented in Table 2. At the 2.3 m, we identify those objects with $m_V \leq 18.0$ in about 60 minutes; at the MMT we easily reach $m_V = 19.5$ in the same amount of time. Because the CTI photometric system must be "bootstrapped" internally to realize the full photometric precision of which the instrument is capable, the accuracy of our calibration has increased during the past year. Thus, Table 2 contains columns for objects observed during 1988 January – March and June – July. The photometry, though still preliminary, is much better for the latter observing period — this is reflected in the increased percentage of truly blue objects identified during this period. We anticipate calibration to about 0.01 mag at $m_V = 18$ as the ultimate goal towards which we are working. At this level, the percentage of correctly identified candidates will again increase dramatically. Additionally, because of uncharacteristically poor luck with weather, we have yet to observe the majority of our candidates with $m_V \geq 18$. Despite this, we have been able to identify brighter white dwarfs, subdwarfs, quasars, etc.

In Table 2 we have included subdwarfs in the basic stellar groups. Cataclysmic and related systems are included as "composite." No spatial information other than visual inspection was used to discriminate against galaxies, hence the inclusion of a few faint galaxies with bright nuclei. The two M stars were included from CTI colors which were very red; one of these is a dMe star.

TABLE 2: Preliminary Results

Type of Object	Total	January – March		June – July	
		$m_V < 17.0$	$m_V \geq 17.0$	$m_V < 17.0$	$m_V \geq 17.0$
DA's	8	1	4	0	3
Quasars	3	0	2	0	1
Seyferts	2	1	0	0	1
Other Galaxies	3	0	2	0	1
B stars	21	13	1	5	2
A stars	21	14	1	4	2
F stars	35	13	12	4	6
G stars	10	2	5	3	0
M stars	2	0	0	1	1
Composites	4	3	0	1	0
Planetary Nebulae	1	0	0	1	0
Totals	**110**	**47**	**27**	**19**	**17**

In the selection of candidates, we have utilized a technique for inspecting color N-space by making linear combinations of color, which correspond to arbitrary projections into a plane. Figure 1 shows such a diagram utilizing the B, V, R, I filter data in which blackbody colors are very nearly degenerate. This corresponds to a projection perpendicular to the main sequence. The objects we have observed thus far are marked. Now that we have confidence that our colors reliably indicate the types of objects we anticipate, we shall concentrate efforts on spectroscopically identifying the bluer objects in this diagram.

Spectroscopically Identified White Dwarfs:

Of the 110 objects thus far observed, eight are DA white dwarfs. Table 3 lists these stars along with preliminary V magnitude. The positions are encoded into the object name following the "CTI" designation. The positions are based on the J2000 equinox and are for epoch 1987.5. The number of characters per name is forced upon us in order to ensure uniqueness for each object in the CTI survey. CTI 104847.9+275823, also known as WD 1046+281, is the only white dwarf in the strip which has previously been spectroscopically identified (McCook and Sion 1987).

We have compared the positions of these eight white dwarfs with positions derived from the Palomar Sky Survey plates. The positions of the white dwarfs and a network of about 10 stars per object within a radius of four arcmin were measured using the two-axis Grant measuring engine at the National Optical Astronomy Observatory. Additional SAO stars across each POSS plate were also measured. Limits to the motion were derived from comparing positions on the POSS to positions derived from CTI data. POSS positions have estimated uncertainties of ± 0.1 arcsec

while CTI positional uncertainties are about ±0.2 arcsec. Within these limits, seven of the eight DA dwarfs showed no detectable motions, but the eighth, CTI 195027.4+275957, shows a motion of 0.20 arcsec yr^{-1}. Its galactic coordinates are $l = 64.^{\circ}64$ and $b = 0.^{\circ}48$, with a motion vector derived over the period 1951.5 to 1987.5 of $\Delta l = \Delta b = +0.14$ arcsec yr^{-1}. Another object with galactic coordinates $l = +51.^{\circ}92$ and $b = 45.^{\circ}36$ which is not yet spectroscopically identified, has a proper motion of 0.57 arcsec yr^{-1} moving principally north, perpendicular to the galactic plane. Clearly, comparing positions of CTI objects to those derived from the POSS will yield a number of interesting high motion objects. We plan to accomplish this comparison by simply digitizing the CTI strip on the POSS and utilizing the CTI software pipeline to accomplish the astrometry.

TABLE 3: Spectroscopically Identified White Dwarfs

Object	m_V	Date Observed	Telescope
CTI 035037.2+280044	18.0	15 Jan 1988	MMT
CTI 045934.1+280335	17.2	15 Jan 1988	MMT
CTI 054438.5+280224	17.9	15 Jan 1988	MMT
CTI 104847.9+275823	15.6	15 Jan 1988	MMT
CTI 135700.6+280448	17.1	13 Mar 1988	2.3 m
CTI 143808.4+275934	17.9	22 Jun 1988	2.3 m
CTI 163440.3+280306	17.1	11 Jul 1988	2.3 m
CTI 195027.4+275957	17.9	11 Jul 1988	2.3 m

Conclusions:

The CTI survey will be a valuable resource for discovering statistically complete samples of white dwarf (and other) stars utilizing an accurate, homogeneous photometric data set spanning colors from the ultraviolet to the red. The statistics of a complete sample grow in importance as we attempt to define the number of evolutionary "channels" capable of producing white dwarfs (*e.g.*, Shipman 1987, Fontaine and Wesemael 1987). We have thus far done spectroscopic observations intended to explore the validity of our colors, which are still undergoing calibration improvements. Our selection of white dwarf candidates will improve as this calibration progresses.

We have discovered seven new spectroscopically identified white dwarfs and this number will increase with available observing time. These objects will be made known to the community as they are discovered.

The positions derived from CTI data are of sufficient precision to discover high motion objects when compared to POSS-derived positions. The CTI pipeline is capable of directly discovering motion objects by comparing digitized POSS data to the CTI data bases.

Acknowledgements:

We gratefully acknowledge the contributions of Michael Cawson, Tom Hess, Charles Bridges and Brian Schmidt to this effort. We thank NOAO for access to the Grant machine. The CTI project is funded by NSF and NASA and is supported by the Data General Corporation.

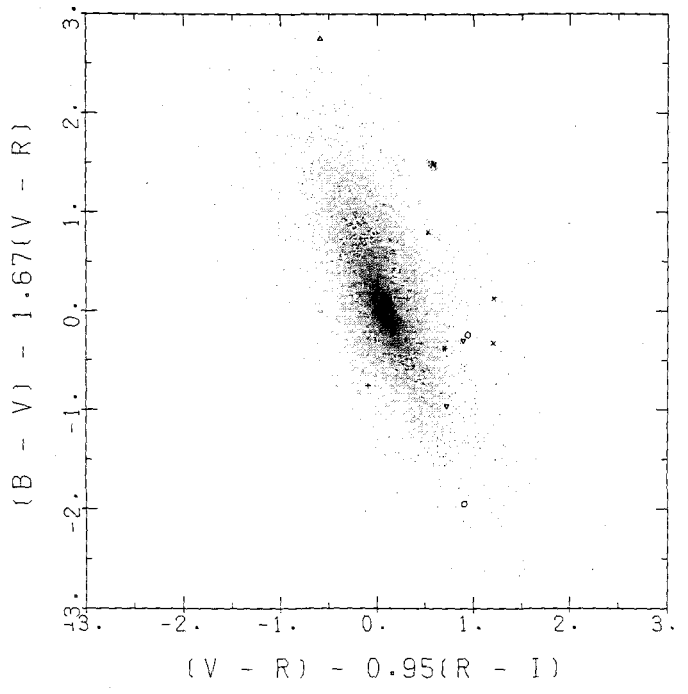

Type of Object	Symbol
DA's	★
Quasars	*
B stars	□
A stars	×
F stars	▽
G stars	o
M stars	+
Composites	·
Planetary Nebulae	△

Figure 1: A special plot whose axes are linear color combinations chosen because they are nearly blackbody degenerate; the main sequence stars occupy a minimal area of the plot. This figure shows some 33000 objects, 28 of which are objects spectroscopically identified. The symbols are given in the legend above. It should be noted that there are a fair number of obvious outliers which have not yet been spectroscopically identified. There are three possible reasons why any one of these has not yet been observed: (1) The object has colors which are unreliable because of a crowded field, charge "bleeding", etc. (*i.e.*, this plot contains *all* of the CTI images, not just the good ones). (2) The object is at some right ascension which has so far been unobservable. (3) The object has a magnitude which is fainter than about 18.00 — we just have not had sufficient time on the MMT to adequately observe many of the fainter candidates yet. This last reason is by far the most probable explanation for the number of unidentified outliers.

References:

Fontaine, G. and Wesemael, F. 1987, *The Second Conference on Faint Blue Stars, Proc. IAU Colloq. 95*, eds. A. G. D. Philip, D. S. Hayes and J. W. Liebert, 319.

McCook, George P. and Sion, Edward M. 1987, *Ap. J. Suppl.*, **65**, 603.

McGraw, J. T., Cawson, M. G. M. and Keane, M. J., *Instrumentation in Astronomy VI*, D. L. Crawford, Editor, Proc. SPIE 627, 60.

Shipman, H. L. 1987, *The Second Conference on Faint Blue Stars, Proc. IAU Colloq. 95*, eds. A. G. D. Philip, D. S. Hayes and J. W. Liebert, 273.

LOW MASS HYDROGEN ENVELOPES AND THE DB GAP

James MacDonald
Department of Physics and Astronomy,
University of Delaware, Newark, DE 19716

INTRODUCTION

The existence of a gap in the distribution of helium atmosphere white dwarfs at the effective temperature interval 30,000 K $\leq T_e \leq$ 45,000 K is well documented (Wesemael, Green and Liebert 1985; Liebert et al 1986; Green and Liebert 1987).

To explain the presence of this gap and other variations of the non-DA to DA ratio, it has been proposed (Fontaine and Wesemael 1987; Liebert, Fontaine and Wesemael 1987) that the helium-rich PG 1159 stars are the progenitors of essentially all white dwarfs. Some minute quantity of hydrogen of total mass, M_H, is assumed to be mixed in the outer helium envelope, and settle upward as the star cools from the PG 1159 stage. Eventually enough hydrogen is at the surface to make the star appear a DA. The star has to become DA before it cools down to $\approx$ 45,000 K and cools to $\approx$ 30,000 K as a DA. At this temperature, depending on M_H, the underlying helium convection zone may break into the hydrogen layer, diluting it and making the star a DB.

In order to test this hypothesis, envelope models for a 0.6 solar mass white dwarf have been computed for T_e's between 15,000 K and 80,000 K. The envelopes are mixtures of hydrogen and helium in diffusive equilibrium.

THE PHYSICAL MODEL

To calculate the envelope structure, the stellar radius and effective temperature are taken from the evolutionary models of Koester and Schönberner (1986) for a 0.6 solar

mass helium envelope white dwarf. The He/H ratio is specified at optical depth 10^{-3} and the stellar structure equations integrated inwards. The composition structure is determined by assuming that each species is in diffusive equilibrium due to balance between gravity, partial pressure gradients, radiative forces, and induced electric fields. Thermal diffusion has been not been included as it has been shown to be negligible in white dwarfs by Paquette et al (1987). Convective mixing is treated as a diffusive mixing process for which the diffusion coefficient is obtained from mixing length theory. Radiation forces on separate species are included by assuming a gray opacity law. The equation of state is based on Eggleton et al (1973) and Los Alamos radiative opacities for H/He mixtures are used. Full details of the calculations will be given elsewhere. However, because the results are sensitive to the treatment of convection, the mixing length theory employed is briefly discussed below.

In a convection zone, the structural gradient, ∇, is given in terms of the adiabatic gradient, ∇_a, and radiative gradient, ∇_r, by

$$\nabla = (\nabla_r + \sigma \nabla_a) / (1 + \sigma)$$

σ is a dimensionless quantity equal to the growth rate of small perturbations multiplied by t_{th}, the thermal time scale of a convective element of size equal to the mixing length, l, which is proportional to the pressure scale height. In radiative zones, $\sigma = 0$. The convective mixing diffusion coefficient is $\sigma\, l^2 / t_{th}$.

σ is the largest solution of

$$s^2 + s + A = 0$$

where

$$A = \frac{2}{3} (t_{th}/t_{dyn})^2 \left.\frac{\partial \ln \rho}{\partial \ln T}\right|_P (\nabla - \nabla_a)$$

and t_{dyn} is the dynamical time scale. This equation can be derived from equations in MacDonald (1983). Convection occurs if $A < 0$.

RESULTS AND CONCLUSIONS

The He/H ratio by mass at the photosphere (optical depth 2/3) is used to characterize whether a white dwarf is a non-DA or a DA. This quantity is plotted against T_e for three values of M_H in figures 1 and 2. The heading of each figure gives the mixing length ratio used. The lines are labelled by the logarithm of M_H in solar masses.

Figure 1

Mixing Length Ratio = 1

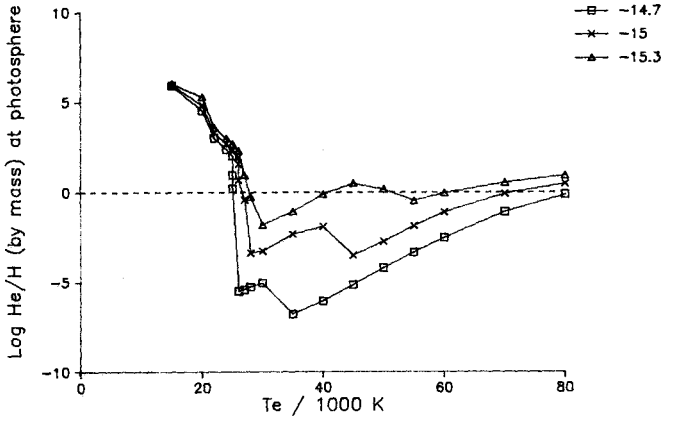

Figure 2

Mixing Length Ratio = 2

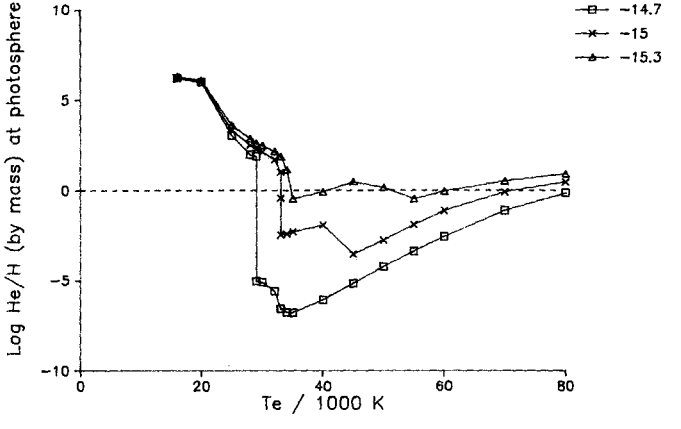

Figure 3

Mixing Length Ratio = 1

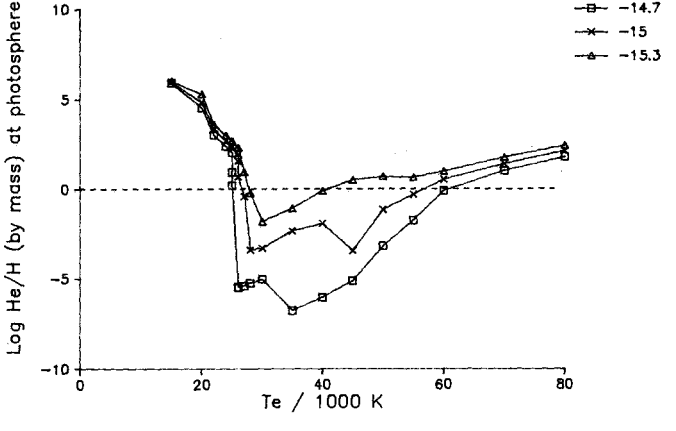

Figure 4

Mixing Length Ratio = 2

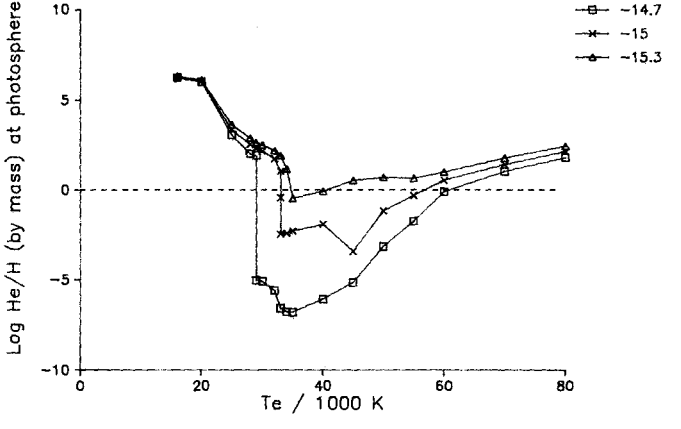

It is readily apparent that for $M_H \approx 10^{-15}$ solar masses, the photospheric He/H ratio undergoes significant changes as the star evolves. Levitation of helium by radiation forces, important at high effective temperatures, decreases as the star cools resulting in an increase in photospheric hydrogen. A small surface helium convection zone sets in at an effective temperature that is dependent on M_H. Since the presence of hydrogen tends to suppress the helium convection zone, the larger the amount of hydrogen, the cooler the star has to be before convection sets in. Convective mixing dredges up helium and the He/H ratio increases slightly before decreasing again. A deep helium convection zone develops when $T_e \approx 30{,}000$ K, rapidly transforming hydrogen-dominated atmospheres into helium-dominated atmospheres.

So far it has been assumed that the envelopes have had sufficient time to come into diffusive equilibrium as the star cools. To check this assumption, gravitational settling time scales for trace hydrogen have been computed as a function of depth for pure helium envelope models. By equating age with the gravitational settling time scale, the depth from which hydrogen will have floated to the surface can be found. If hydrogen is initially mixed no deeper than $\approx 10^{-6}$ solar masses from the surface, the envelope will be in diffusive equilibrium before the star has cooled to 80,000 K. Otherwise, not all the hydrogen has had time to float to the surface and the equilibrium models will underestimate the photospheric helium abundances. The results of an attempt to quantify this effect are shown in figures 3 and 4 for hydrogen initially mixed in the outer 10^{-5} solar masses of the envelope.

Given the uncertainties in convection theory, it can be seen from the figures that it is possible to construct evolutionary sequences that give the gap. The best model has mixing length ≈ 2, and a minimum allowed value of $M_H \approx 2\ 10^{-15}$ initially mixed in the outer 10^{-5} to 10^{-4} solar masses of the envelope.

REFERENCES

Eggleton,P.P., Faulkner,J. & Flannery,B.P. 1973 Astr. Ap. 23, 325.
Fontaine,G. & Wesemael,F. 1987 in IAU Colloquium No. 95, The Second Conference on Faint Blue Stars, ed. A.G.D. Philip, D.S. Hayes, and J. Liebert. (L. Davis Press, Schenectady) p319.
Green,R.F. and Liebert,J. 1987 in IAU Colloquium No. 95, The Second Conference on Faint Blue Stars, ed. A.G.D. Philip, D.S. Hayes, and J. Liebert. (L. Davis Press, Schenectady) p261.
Koester,D. & Schönberner,D. 1986 Astr. Ap. 154, 125
Liebert,J., et al. 1986 Ap. J. 309, 241.
Liebert,J., Fontaine,G. & Wesemael,F. 1987 Mem. Soc. Astr. It., 58, 17.
MacDonald,J. 1983. Ap. J. 273, 289.
Paquette et al 1987. Preprint.
Wesemael,F., Green,R.F. & Liebert,J. 1985 Ap. J. Suppl. 58, 379.

DIFFUSION AND METAL ABUNDANCES IN HOT WHITE DWARFS

Gérard Vauclair
Observatoire Midi-Pyrénées
14 av. E. Belin, 31400 TOULOUSE, France

1. Introduction

While the efficiency of gravitational settling to produce chemically pure atmospheres in white dwarf stars was outlined for the first time 30 years ago (Schatzman 1958), the competing role of the radiation flux in the hot white dwarfs was considered only 10 years ago (Fontaine and Michaud 1979; Vauclair, Vauclair and Greenstein 1979). At that time, there was more motivation to understand how metals could reappear in the long lived cool non DA white dwarfs, where diffusion time scales are shorter by orders of magnitude than evolutionary time scales. Various processes were invoked to help restore some metal content in the white dwarf atmospheres: convection mixing and dredge up, accretion of interstellar matter. In cool white dwarfs, the radiative acceleration is negligeable in the diffusion process; this is not the case at the hot end of the sequence where radiation may balance gravity. The short lived hot white dwarfs just started to become exciting with the contemporary discoveries that i) some show metallic lines in their spectra, both hydrogen rich and hydrogen poor; ii) some of these are pulsating. In the following years, the number of hot white dwarfs revealing trace abundance of metals has increased, mainly owing to IUE observations.

I do not intend here to make an exhaustive presentation of the observations. Such discussions may be found in recent reviews (Vauclair and Liebert 1987; Shipman 1987) and are also presented at this colloquium. In this paper, I prefer to stay on the theoretical side and present the results of the diffusion theory as they have been obtained, either to predict metal abundances to be expected in hot white dwarfs or to interpret observations of particular stars. Of course, the discovery of metallic lines in high dispersion IUE spectra of hot white dwarfs, as predicted by theory, was somewhat encouraging. However, now that so many hot white dwarfs show metallic lines, the theory has to be refined. Proper comparison of the observations with the theory should tell us about important mechanisms acting at this evolutionary phase. Important questions are still to be solved: i) what are the various channels conducting a dying star to the white dwarf final stage of evolution? ii) what is the link between the presence of metals in the atmosphere of the PG1159 stars and their instability? iii) what is the role of mass loss, selective or not, in that part of the HR diagram? The chemical composition observed in the atmosphere is affected by both the prior

evolution of the stars and the presently acting physical mechanisms. A detailed description of the physical mechanisms in action at this evolutionary phase should lead to a better understanding of the questions quoted above. IUE has opened a new and rich area of research but is limited in size. With the Hubble Space Telescope we hope to get of a statistically significant sample of hot white dwarf high resolution spectra. This is one of the strong motivations to pursue detailed diffusion computations.

In the presence of pressure, temperature, concentration gradients and radiation flux, an ion of a trace element is submitted to forces induced by the various gradients, and by the absorption of selective parts of the radiation flux through lines. It is well known (see for instance Vauclair 1983) that as long as the abundance of the diffusing particles is small, i.e. that the opacity due to these particles is much smaller than the total opacity of the gas, the radiative acceleration on the diffusing particles does not depend on their abundance. In the reverse case, when the absorption of radiation due to the diffusing particles cannot be neglected compared to the total opacity, the radiative acceleration is affected by saturation and becomes dependent upon the abundance. It is for this reason that equilibrium abundances may be reached. A large abundance of a given element will not be generally supported by the radiation flux as there are too many ions willing to absorb a limited number of photons at the ions absorption line wavelengths. As a consequence the upward radiative acceleration is not able to compensate the downward acceleration due to pressure and temperature gradients. The ions diffuse downwards. Doing so, their abundance decreases, their absorption lines progressively desaturate and the radiative acceleration increases. When the radiative acceleration may just balance the downward acceleration, the ions reach an equilibrium state where their diffusion velocity cancels exactly. This occurs for a value of the abundance that we call the equilibrium abundance. As a consequence of the dependence of the various forces with depth the equilibrium abundances must also vary with depth. In this paper, C, N, O and Si equilibrium abundances achieved by diffusion in two series of white dwarf models will be discussed and compared to observations. The two series cover a range in effective temperature of 50 000-150 000K for He rich envelopes, and of 30 000-100 000K for H rich envelopes. In one case the surface gravity is maintained constant ($\log g = 8.$) while in the other case, the surface gravity is allowed to change with effective temperature, according to realistic evolutionary sequence for a 0,6 $M_\odot$ white dwarfs (Koester and Schönberner 1986).

2. Metals in hot non-DA white dwarfs

In helium dominated envelopes, the low opacity is responsible for producing a high pressure in the atmosphere. This favors the radiative acceleration by increasing the collisional width of the absorption lines. On the other hand, the mass ratio of the diffusing particles in a helium dominated

environment is less than the equivalent mass ratio in a hydrogen dominated environment. Both effects act in the same direction in reducing the downward diffusion velocity, or, alternatively, in producing larger equilibrium abundances, in helium atmospheres.

Typical equilibrium abundances of C, N, O and Si in a hot He envelope white dwarf are shown in figure 1. In this $T_e = 100000K$, log g=8 model, carbon, nitrogen and oxygen are distributed with depth in two shells. The minima between the two shells correspond to the region in the star where the elements are in the noble gas state (CV, NVI, $OVII$). As is well known (Michaud et al. 1976; Vauclair, Vauclair and Greenstein 1979) resonance lines in the noble gas state are at much shorter wavelengths than the range where most of the continuum radiation flux is emitted. The resulting radiative acceleration experienced by the ions in this stage of ionization is too small to support the elements. The case of Si is somewhat more complicated due to the atomic structure. One generally finds an abundance distribution with two minima. The outermost minimum is due to the SiV noble gas.

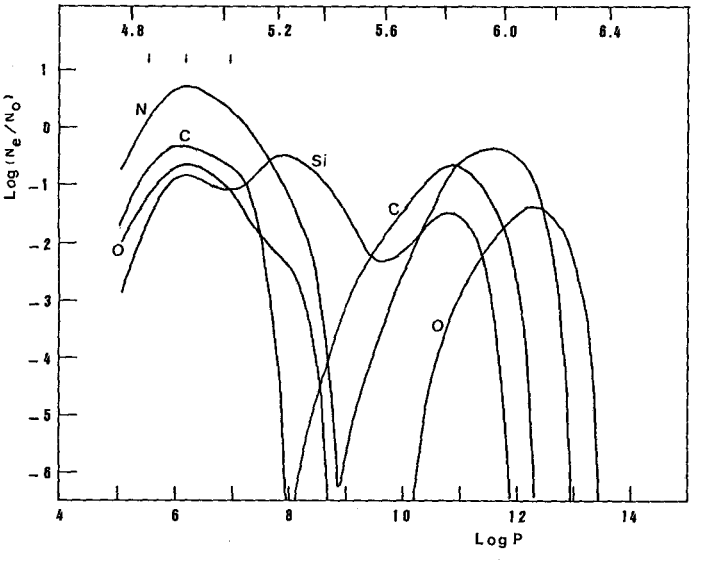

FIGURE 1. — C, N, O and Si diffusion equilibrium abundances in a 100 000K, log g = 8.0 He envelope. The abundances are given on logarithmic scale, in units of the solar abundance ratios. The lower scale is the gas pressure, while the upper scale is the temperature, both on logarithmic scale. The arrows show where the optical depth τ is 10^{-2}, 10^{-1} and 1 respectively. C, N and O are distributed in two clouds with the minimum of the equilibrium abundance correcponding to the region where they are predominantly in the noble gas (CV, NVI, $OVII$. Si distribution reflects the more complex atomic structure and show three maxima. In this model, the maxima of the upper metallic clouds occur at $\tau \simeq 10^{-1}$, well inside the line forming region.

How do the equilibrium atmospheric abundances vary with the effective temperature is illustrated in Figure 2. The Rosseland optical depth $\tau = 0.1$ has been choosen as a representative value of the line forming region. Figure 2 shows the equilibrium abundances of C, N, O and Si predicted by diffusion at that particular optical depth. The abundance supported in the atmosphere depends heavily on the temperature: on one hand, increasing T_e makes a larger radiation flux available for absorption; on the other hand, increasing T_e favors a larger fraction of the noble gas ion into the line forming region. The interplay of these two effects is responsible for the behavior of the equilibrium abundances in Figure 2. Carbon is mainly C*IV* (at 70%) at 50 000K with a small (2%) fraction of C*V*. C*V* increases to 20% at 60 000K. This is not enough to balance the increased radiation flux. At higher temperature however, the increasing flux cannot balance the effect of the increasing fraction of C*V* (81% at 80 000K, 100% at 150 000 K) in reducing the radiative acceleration. This explains the decrease of the carbon equilibrium abundance with increasing temperature. The situation is similar for nitrogen and oxygen except that it takes higher an effective temperature to get the noble gas in noticeable amount at $\tau = 0.1$. For silicon, the fraction of Si*V* in the 50 000K model is already of 75% and increases regularly up to 100 000K where it reaches almost 100%. This is responsible for the dramatic decrease of the equilibrium abundance with increasing T_e. At temperature higher than 120 000K, the fraction of Si*VI* starts to be large enough to make the radiative acceleration and the equilibrium abundance increasing with effective temperature. Negligeable at 50 000 and 60 000K, the effect on the equilibrium abundances of changing the surface gravity from the Hamada-Salpeter mass-radius relation to a more realistic evolutionary sequence (Koester and Schönberner 1986) cannot be neglected at higher effective temperature.

At this stage, how do the observations compare with the theory? At the very hot end of the white dwarf sequence, we even do not know the atmospheric chemical composition. The H and He poor object H 1504+65 (Nousek et al. 1986) is presently the hottest known degenerate star at $T_e \simeq 160$ 000K. While the absence of He lines at that temperature does not necessarily imply an helium poor atmosphere, ground based spectra definitely show O*VI* and C*IV* feature; O*VI* absorption at 1032 $\AA$ was also seen in a Voyager spectrum. If we believe for the time being, i.e. until we are able to modelize H 1504+65 atmosphere and derive relevant abundances, that this object could be a hot progenitor of the helium rich sequence, it is tempting to compare the predictions of diffusion theory with what is observed in that object. In the 150 000K model, carbon is almost entirely in the noble gas configuration, only a tiny fraction of $\simeq 10^{-3}$ still survives as C*IV*. C*V* would not be detectable: its resonance lines are too far in the EUV and the only line to fall in the long wavelength range of IUE ($\lambda 2273\AA$) originates from the first excited level which has negligeable population. With a total C/He = 2.5 -4.0 10^{-5}, the fraction C*IV*/He which could

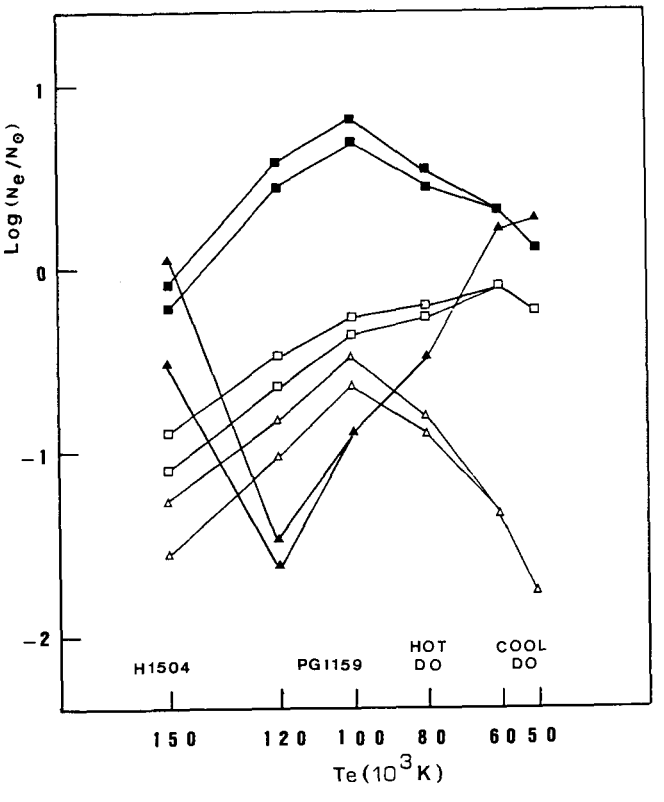

FIGURE 2. — Diffusion equilibrium abundances of C (□) N (■), O (△) and Si (▲) at optical depth $\tau = 10^{-1}$, as a function of T_e, in He atmosphere white dwarfs models. The approximate effective temperatures of the hot degenerate H 1504 + 65, of the PG 1159 stars, and of hot and cool DO stars are indicated. The equilibrium abundances predicted by diffusion are shown for two sequences of 0,6 M⊙ white dwarfs: the lower curves correspond to models with constant log g = 8.0, the upper curves correspond to the Koester and Schönberner (1986) evolutionary sequence. The two sequences cannot be distinguished for $T_e \leq 60000K$ for C, N, O and for $T_e \leq 100000K$ for Si.

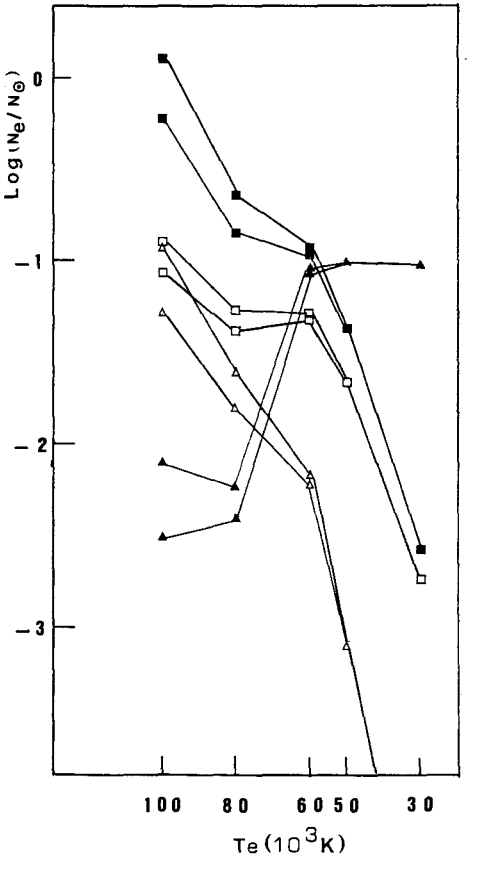

FIGURE 3. — The same as Figure 2 for H atmosphere white dwarf models. Sequences with gravity derived from the Hamada-Salpeter (lower curves) mass-radius relation and from the Koester-Schönberner evolutionary sequence (upper curves) cannot be distinguished for $T_e \leq 50000K$.

form the $\lambda 1550\mathring{A}$ resonance line is $\simeq 2. - 5. \times 10^{-8}$. Nitrogen is also mainly (at 98%) in the noble gas stage of ionization. The resonance lines are far in the EUV. The IUE long wavelength range could not detect the 1901.5 $\mathring{A}$ line which originates from the first excited level, not populated at that temperature. NV $\lambda 1240\mathring{A}$ should be present but only 2% of the total nitrogen is in the NV stage of ionization, mostly in excited states, a situation not favorable to the absorption from the ground state from which the line originate. Oxygen is approximately half OVI, half $OVII$ (46% and 53% respectively). This makes highly favorable the detection of OVI lines, as observed in H 1504+65, especially through the line at $\lambda 1033.8\mathring{A}$ which originates from the ground state. The OVI/He ratio in equilibrium at $\tau = 0.1$ is $\simeq 8 \times 10^{-6} - 3 \times 10^{-5}$. Silicon is mainly Si$V$ and SiVI none of which does have line in the IUE domain. Silicon, if it is there with the high abundance predicted by theory (from 3 times less than solar to solar) would remain undetected.

The range of effective temperatures 100 000K -120 000K is the domain of the PG 1159 stars. Inspection of figure 2 reveals that in this temperature range the equilibrium abundances of N and O reach their maximum value. Is that a pure coincidence? At 100 000K, carbon is still dominantly in the CV state but CIV accounts for almost 4%. Carbon is depleted by only a factor 2 compared to the sun. CIV resonance lines should be strong at these temperatures, which is observed in many PG 1159 stars (Bond et al. 1984; Sion, Liebert and Starrfield 1985; Wesemael, Green and Liebert 1985) and in the related pulsating central star of the planetary nebula K1-16 (Grauer and Bond 1984). It is more difficult to understand why NV $\lambda 1240\mathring{A}$ is not stronger in all stars of that temperature range. The predicted total nitrogen abundance at equilibrium is 5 to 7 times the solar value and 75% should be in the form of NV. NV is detected in some PG 1159 stars (Bond et al. 84; Sion, Liebert and Starrfield 1985; Wesemael, Green and Liebert 1985) but it is generally a weak line. The star KPD 0005+5106 also shows carbon lines but no nitrogen from low resolution IUE spectrum (Downes, Liebert and Margon 1985). Does this mean that nitrogen, which is always found more efficiently pushed upward by the radiative acceleration in our theoretical computations, has already been largely expulsed out of the star during the pre-PG 1159 phase, or depleted during previous nuclear burning episodes? Oxygen is only at 3% in the OVI stage but the dominant OIV and OV stages do not have strong lines in the IUE or visible wavelength range. With O/He $\simeq$ 1. -2. 10^{-4} (a deficiency of 6. -3. compared to the Sun) the oxygen equilibrium abundance reaches its maximum at that temperature. As a consequence, oxygen absorption lines (OVI) are expected at this temperature. They are effectively observed in a number of PG 1159 stars (Sion, Liebert and Starrfield 1985). As far as silicon is concerned, it is hardly detectable being in the SiV ionization stage. A tiny fraction of surviving SiIV (a few 10^{-3}) could be responsible for the weak SiIV barely seen in a few PG 1159. We still do not

have, at the time of writing, an abundance determination for PG 1159 stars. The present analysis, based on the assumption of an helium dominated envelope could become irrelevant to PG 1159 stars if the chemical composition is C/O dominated, as suggested by Starrfield et al. (1984) to trigger the instability. I have suggested elsewhere (Vauclair 1987) that the diffusion mechanism which naturally produces equilibrium clouds of C, N, O and Si in the supposedly helium rich outer layers of these stars could be responsible for both the presence of absorption lines of these species in the stellar spectra and of the instability observed in some of the PG 1159 stars.

At lower effective temperature (80 000K) our computations may be relevant to the hot DO. For these stars, whose prototype is PG1034+001, one **knowns** that they are helium dominated. In our 80 000K models, carbon is still dominantly in the CV configuration but CIV reaches almost 20%. Carbon is efficiently supported by the radiation field to approximately half the solar abundance (C/He $\simeq 2 \times 10^{-4}$). This equilibrium value at $\tau = 0.1$ is in good agreement with independent diffusion computation by Chayer et al. (1987) who find C/He $\simeq 4.10^{-4}$ at $\tau = 1$. But it is significantly in disagreement with the value derived from the observation (Sion, Liebert and Wesemael 1985) which is smaller by a factor 100. Nitrogen is found to be overabundant compared to the solar abundance (by a factor 3) which is in good agreement with the overabundance observed (Sion, Liebert and Wesemael 1985) and with the theoretical study of Chayer et al. (1987). Oxygen is found deficient by a factor 6 -8 compared to the Sun, which is a factor 10 smaller than the value predicted at $\tau = 1$ by Chayer et al. (1987). However the uncertainty on the observed abundance is large enough to accomodate the two independently derived theoretical values!

At the temperature of 60 000K -50 000K, the lower limit we have considered here for hot non -DA, in order to avoid helium convection zones, we are in the domain of the cool DO as HD 149199B (Bruhweiler and Kondo 1983; Sion and Guinan 1983). Unfortunately we do not have abundance determinations to compare with theory for that star. CIV dominates at $\tau = 0.1$ (74% at 60 000K, 70% at 50 000K). Carbon is supported by the radiation flux at a value close to the solar abundance (80% of the solar abundance at 60 000K, 60% at 50 000K). As a consequence strong CIV lines are expected and are observed. Nitrogen is predicted to be slightly overabundant compared to the Sun (by a factor 2 at 60 000K and 1.25 at 50 000K). However it is in the form of $NIII$ and NIV which do not have strong lines in the visible or in the IUE range. Weaker $NIII$ lines should be present but have not been detected. Oxygen is predicted to be deficient by larger factors (from 20 at 60 000K to 60 at 50 000K). The dominant ionization stages are $OIII$ and OIV which do not show lines neither in the visible nor in the UV accessible to IUE. While SiV is still dominant at this temperature, SiIV should be abundant enough (6% at 60 000K and 24% at 50 000K) to lead to absorption lines, especially at these temperatures where the theory predicts

detected in HD 149499B (Bruhweiler and Kondo 1983; Sion and Guinan 1983).

3. Metals in hot DA white dwarfs

For hot hydrogen envelope white dwarfs we consider the effective temperature range 30 000K -100 000K, as there is no DA hotter than 100 000K, or even hotter than 80 000K (Fleming, Liebert and Green 1986). The distribution of the equilibrium abundances are quite similar to the case discussed in figure1. The somewhat reduced radiative acceleration and enhanced downward acceleration make the amount of metals which may be supported smaller in hydrogen envelopes than in helium envelopes. Figure 3 shows the variations with effective temperature of the equilibrium abundances for C, N, O and Si computed at Rosseland optical depth $\tau = 0.1$ in pure hydrogen atmospheres, with log g = 8.0 and along the 0.6 M$\odot$ evolutionary sequence of Koester and Schönberner (1986). A comparison with the similar figure 2 for helium envelopes illustrates the differences. In the considered temperature range, radiative levitation cannot support more than the solar abundances, in contrast with the helium case with the only exception of N at the very hot end of the Koester and Schönberner sequence.

In many hot DA, IUE observations have revealed the presence of metallic absorption. In some cases, velocity differences between metallic lines and Balmer lines point to the existence of a wind, or of circumstellar material. In such cases, the predictions of the pure diffusion may be irrelevant and mass loss should be introduced in some way as one additional physical mechanism competing with diffusion (Michaud 1987). We are faced then to the difficulty that we do not know how to introduce mass-loss in a physically consistent way. The diffusion computations which are presented here may apply to those cases where the observed metallic lines form in the stellar photosphere. It is the case in the well discussed Feige 24 star, in which resonance lines of C*IV*, N*V* and Si*IV* have been discovered in high resolution IUE spectra (Dupree and Raymond 1982). Diffusion equilibrium abundances have been computed for that star (Morvan, Vauclair and Vauclair 1986; Chayer et al. 1987). Nitrogen and silicon abundances predicted by the diffusion theory are in good agreement with the value deduced from the observations (Wesemael, Henry and Shipman 1984). Carbon is predicted too strong, as in the case of the hot DO PG 1034+001 discussed earlier. It is also the case in cooler DA stars as W 1346 (Bruhweiler and Kondo, 1983) or CD -38° 10980 (Holberg et al., 1985) which do show only Si lines in their IUE spectra. Inspection of figure 3 shows that the radiatively supported abundances of C, N, O dramatically decrease with decreasing effective temperature. These elements are no more supported at the W 1346 and CD -38° 10980 effective temperatures, while Si remains radiatively supported to approximately 1/10 of the solar abundance. Diffusion predictions seem to be in qualitative agreement with the observations, but the Si abundance observed in W 1346, while uncertain by large a factor (Wesemael, Henry and a maximum for the Si abundance (at about twice the solar abundance). But Si*IV* has not been

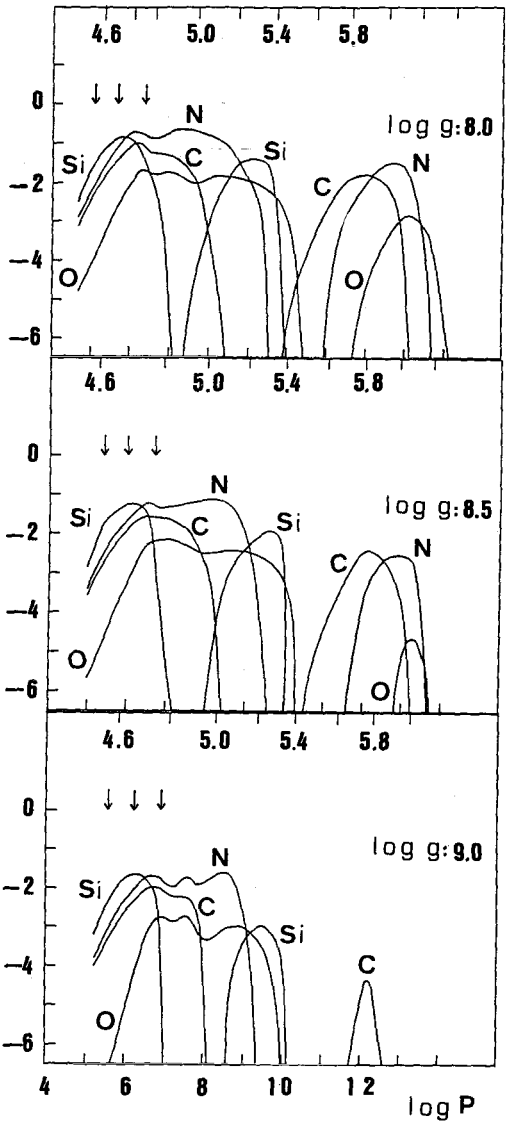

FIGURE 4. — Dependence of the metal clouds on changes in the surface gravity. The diffusion equilibrium abundances of C, N, O and Si in H white dwarf models supposed to represent PG 1210 + 533 at T_e = 56 000K, are shown for log g = 8.0, 8.5, 9.0. Each panel is similar to figure 1, with the lower scale of the bottom panel showing the common pressure scale while the upper scale in each panel indicates the run of the temperature in individual model. While the decrease of the equilibrium abundances with increasing gravity may be clearly seen, the C, N and Si abundances predicted in the line forming region are still large enough, even at log g = 9.0, to lead to absorption lines, which are not observed.

Shipman 1984), in still less than the one predicted by the diffusion theory (Morvan, Vauclair and Vauclair, 1986; Chayer et al. 1987).

There are at least two puzzling questions related to the hot DA white dwarfs: i) at the same effective temperature, some DAs with metallic lines show evidence of ongoing mass-loss, some other do not; for instance at about 62 000K, G 191-B2B shows evidence of mass loss (Bruhweiler and Kondo 1981) while Feige 24 does not; ii) at the same effective temperature, some DAs do show metallic lines, some other do not: while Feige 24 shows metallic lines, HZ 43 and PG 1210+533 at similar temperature do not. One may argue that the balance between the upward radiative acceleration and the downward acceleration due to pressure and thermal gradients strongly depends on the gravity (i.e. the mass) of the white dwarf. It has been found indeed that both HZ 43 (Holberg et al. 1986) and PG 1210+533 (Holberg et al. 1988) have higher than average log g. A test of the equilibrium abundances dependence on gravity as been performed in models of PG 1210+533 ($T_e \simeq$ 56 000K). Figure 4 shows C, N, O and Si clouds in equilibrium for three values of the surface gravity log g = 8.0; 8.5; 9.0. In spite of the decrease of the abundances with increasing gravity, there is still sufficient amount of C, N and Si in the line forming region to produce lines which have not been observed in a high resolution IUE spectrum. The sensitivity of diffusion equilibrium on gravity does not seem to be large enough to explain the absence of metals in high gravity hot hydrogen white dwarfs like HZ 43 or PG 1210+533. Consequently, interpreting the coexistence at the same effective temperature of DA stars with and without metals in their atmosphere remains a puzzle.

4. Conclusion

In the hot white dwarf stars, the radiative acceleration through absorption lines may be efficient enough to balance the gravitational field. An equilibrium state results where the elements are inhomogeneously distributed with depth. The theoretical computations have shown that C, N, O and Si may be supported in both hydrogen and helium rich white dwarf outer layers. A comparison with observations however is only qualitatively satisfactory at the present time. Some problems remain unsolved: i) nitrogen is observed to be weak in the PG 1159 stars while the theory predicts an overabundance of N/He compared to the solar N/H ratio, for helium rich envelopes in the relevant effective temperature range; ii) similarly, in the DO white dwarfs, carbon is predicted too strong compared to observations of hot DO, and Si, predicted also to be abundant in cool DO is not observed; iii) in hot hydrogen white dwarfs, we are faced to the unsolved problems of the coexistence, at the same temperature, of stars with ongoing mass flows, and of stars without observable mass flow where the absorption lines form in the photosphere; and the coexistence at the same temperature of white dwarfs with and without metallic absorption lines. The suspected

role of the surface gravity in solving this difference seems to have been overestimated.

In the theoretical computations summarized here, the assumption was implicitly made that there were enough diffusing particles in the stellar outer layers to fill in the cloud and reach the equilibrium abundance predicted by diffusion. However, one must keep in mind that one does not know the original metal abundances to start with the diffusion computation. What would happen if one of the considered species is missing or is present with such a low abundance that the corresponding equilibrium cloud could not be filled? One may expect that, because the equilibrium is not reached as a consequence of the abundance being too low the radiative acceleration should exceed the downward acceleration in that part of the atmosphere where the elements are not in the noble gas state. These elements could consequently be pushed out and leave the star in the form of a selective wind, as suggested by Vauclair, Vauclair and Greenstein (1979). In this case, the cloud predicted by the diffusion theory could not materialize.

The above mentionned difficulties point to the need for further theoretical progresses in the diffusion theory and in the stellar atmosphere modeling. Among other sources of uncertainty it should be outlined that the computations of the radiative acceleration at small optical depths should be improved, especially in the very hot white dwarfs where recent high dispersion IUE spectra reveal the importance of NLTE. Furthermore, if the observed elements are distributed inhomogeneously in the stellar outer layers, as predicted by diffusion, a number of other inconsistancies should be considered: i) the abundances derived from homogeneous model atmospheres cannot be directly compared to the diffusion predictions; synthetic spectra should include the inhomogeneous metal abundance distribution; ii) the flux distribution in model atmospheres itself may be affected by the presence of the metallic clouds; the differences with pure H or He atmosphere has to be evaluated. It should be larger in the atmospheres dominated by He, which has a low opacity compared to H. Would metal clouds in the atmosphere solve the difficulty of fitting the energy distribution in H 1504 + 65 with any existing model atmosphere? Last but not least, the question of the stability of such clouds should be addressed.

References

BOND, H. GRAUER, A.D., GREEN, R.F. and LIEBERT, J. 1984, Astrophys. J. **279**, 751

BRUHWEILER, F.C. and KONDO, Y. 1981, Astrophys. J. Letters **248**, L 123

BRUHWEILER, F.C. and KONDO, Y. 1983, Astrophys. J. **269**, 657

CHAYER, P., FONTAINE, G., WESEMAEL, F. and MICHAUD, G. 1987 in IAU Colloquium n° 95: The Second Conference on Faint Blue Stars, A.G.D. Philip, D.S. Hayes and J. Liebert, eds., L. Davis Press, Schenectady, p. 653

DOWNES, R.A., LIEBERT, J. and MARGON, B. 1985, Astrophys. J. **290**, 321

DUPREE, A.K. and RAYMOND, J.C. 1982, Astrophys. J. Letters **263**, L63

FLEMING, T., LIEBERT, J. and GREEN, R.F. 1986, Astrophys. J. **308**, 176

FONTAINE, G. and MICHAUD, G. 1979, Astrophys. J. **231**, 826

GRAUER, A.D. and BOND, H.E. 1984, Astrophys. J. **277**, 211

HOLBERG, J., WESEMAEL, F. and BASILE, J. 1986, Astrophys. J. **306**, 629

HOLBERG, J., SION, E.M., LIEBERT, J. and VAUCLAIR, G. 1988, in "A Decade of UV Astronomy with the IUE satellite", ESA SP-281, in press

HOLBERG, J., WESEMAEL, F., WEGNER, G. and BRUHWEILER, F.C. 1985, Astrophys. J. **293**, 294

KOESTER, D. and SCHÖNBERNER, D. 1986, Astron. Astrophys. **154**, 125

MICHAUD, G. 1987, in IAU Colloquium n° 95; The Second Conference on Faint Blue Stars, A.G.D. Philip, D.S. Hayes and J. Liebert, eds., L. David Press, Schenectady, p. 249

MICHAUD, G., CHARLAND, Y., VAUCLAIR, S. and VAUCLAIR, G. 1976, Astrophys. J. **210**, 447

MORVAN, E., VAUCLAIR, G. and VAUCLAIR, S. 1986, Astron. Astrophys. **163**, 145

NOUSEK, J.A., SHIPMAN, H.L., HOLBERG, J.B., LIEBERT, J., PRAVDO, S.H., WHITE, N.E. and GIOMMI, P. 1986, Astrophys. J. **309**, 230

SCHATZMAN, E. 1958, White dwarfs, North-Holland Publ. Comp., Amsterdam

SHIPMAN, H.L. 1987, in IAU Colloquium n° 95: The Second Conference on Faint Blue Stars, A.G.D. Philip, D.S. Hayes and J. Liebert, eds., L. David Press, Schenectady, p. 273

SION, E.M. and GUINAN, E.F. 1983, Astrophys. J. Letters **265**, L87

SION, E.M., LIEBERT, J. and STARRFIELD, S.G. 1985, Astrophys. J. **292**, 471

SION, E.M., LIEBERT, J. and WESEMAEL, F. 1985, Astrophys. J. **292**, 477

STARRFIELD, S.G., COX, A., KIDMAN, R.B. and PESNELL, W.D. 1984, Astrophys. J. **281**, 800

VAUCLAIR, G. 1987, in IAU Colloquium n° 95: The Second Conference on Faint Blue Stars, A.G.D. Philip, D.S. Hayes and J. Liebert, eds., L. David Press, Schenectady, p. 341

VAUCLAIR, G. and LIEBERT, J. 1987 in Exploring the Universe with the IUE Satellite, Y. Kondo ed., Reidel, Dordrecht, p. 344

VAUCLAIR, G., VAUCLAIR, S. and GREENSTEIN, J.L. 1979, Astron. Astrophys. **80**, 79

VAUCLAIR, S. 1983, in Astrophysical Processes in Upper Main Sequence Stars, 13th Advanced Course of the Swiss Society of Astronomy and Astrophysics, eds. B. Hauck and A. Maeder, Geneva Observatory

WESEMAEL, F., GREEN, R.F. and LIEBERT, J. 1985, Astrophys. J. Suppl. **58**, 379

WESEMAEL, F., HENRY, R.B.C. and SHIPMAN, H.L. 1984, Astrophys. J. **287**, 868

HELIUM ABUNDANCE IN THE PHOTOSPHERES OF HOT DA WHITE DWARFS

J. B. Holberg and K. Kidder
Lunar and Planetary Laboratory
J. Liebert
Steward Observatory
University of Arizona
Tucson, Arizona 85721
and
F. Wesemael
Département de Physique and Observatoire du Mont Mégantic
Université de Montréal

ABSTRACT

We have used optical and UV spectroscopy to determine He abundances and upper limits to He abundances in the photospheres of a selected sample of very hot hydrogen-rich white dwarfs. He abundances in the range log(He/H) -3 to -1.5 are observed in several of these DAs and upper limits of -3 determined for the remainder. In apparent contradiction to the relatively large He abundances inferred from soft X-ray observations for the hot DA G191 B2B, we find *no* evidence of He in the optical and UV.

INTRODUCTION

The issue of He abundance in the hottest H-rich degenerates is of interest for several reasons. First, in terms of the earliest stages of white dwarf evolution the observed pattern of H and He abundance with effective temperature is striking. The hottest degenerates all appear to be He-rich objects. Below 80,000 K, however, H-rich white dwarfs predominate with the white dwarf population becoming exclusively DA in the 45,000 K to 30,000 K region. He-rich stars reappear again as DBs below 30,000 K. This situation has prompted questions as to whether the composition of white dwarf photospheres change as these stars cool.

Second, soft X-ray observations of many DAs are currently interpreted as implying He abundances in the range log(He/H) -5 to -2. Is the observed opacity source due to He, or possibly other ions? If He is actually present, is it intrinsic to the photosphere of the DA, or is it the result of ongoing accretion from the interstellar medium? If it is intrinsic to the photosphere, how is He supported against the short gravitational settling times? Most of these questions lead directly to the issue of the thickness or the characteristic mass of the outer H envelope. Are DA envelopes predominantly thick ($M_H \sim 10^{-4}\ M_\odot$) as evolutionary calculations suggest? Or are they perhaps thin ($M_H < 10^{-8}\ M_\odot$) as implied by the existence of non-radial pulsations in the ZZ Ceti stars? These issues and questions have been the subject of numerous discussions in the literature (*e.g.* Fontaine and Wesemael, 1987; Koester, 1987; Liebert, Fontaine and Wesemael, 1986).

One approach to the question of He in the envelopes of DAs is to investigate the hottest such stars where He abundances are expected to be highest. A simple extrapolation of the empirical relation between soft X-ray inferred He abundance and effective temperature (Petre, Shipman and Canizares 1986) to temperatures above 60,000 K yields expected log(He/H) abundances of -3 to -2. At these levels He becomes spectroscopically detectible in the optical and UV (Wesemael, Liebert and Green 1984). In this

paper we present UV and optical spectroscopy of six very hot DAs, selected from the the sample of Palomar-Green (PG) DAs studied by Fleming, Liebert and Green (FLG, 1986). These stars were assigned to the highest luminosity bin ($8.75 < M_V < 7.25$) by FLG. All show blue colors and narrow H Balmer profiles. Initial results for these objects are presented in Holberg (1987). Here we present preliminary results from the determination of the He abundances of these objects. A more detailed discussion of these data will be provided elsewhere (Holberg *et al.* 1988, in preparation).

OBSERVATIONS AND ANALYSIS

We have obtained optical and UV spectra for all the stars in our sample of six hot DAs. The optical spectra, covering the 3850 to 4950 Å range are shown in Fig. 2 of Holberg (1987). Spectral resolution is approximately 2.5 Å , sufficient to provide both H Balmer profiles suitable for detailed modeling and to seek evidence for the presence of He features such as He II λ4686 and He I λ4471. The low dispersion UV spectra obtained with the IUE SWP camera are shown In Fig. 1. In addition to the six hot DAs from the PG sample we also obtained similar observations for PG1210+533, a hot DAO white dwarf, and G191 B2B, a well-studied hot DA (T_{eff} ~62,500 K).

We take the following approach to the determination of He abundances. First we estimate T_{eff} and log g from detailed fits to the H Balmer profiles using a two dimensional grid of pure H model atmospheres. These temperatures and gravities are in turn used to estimate He abundance from a related grid of models having fixed gravity (log g = 8.0) but covering a range of He abundance. Due to the weakness of the He lines, our He abundance estimates are obtained from equivalent widths rather than detailed line fits.

We employ two related sets of model atmospheres. For the H Balmer profiles, we use an extensive grid of pure H model atmospheres which are the optical counter parts of the UV grid employed by Holberg, Wesemael and Basile (1986). For the determination of He abundances we employ a grid of models having H-to-He ratios covering the range log(He/H) = -4.0(0.5)-1.5 and T_{eff} = 50,000(10,000)100,000 K; all of which assume a fixed log g of 8.0. For this grid, detailed profiles of He II λ1640 and λ4686 and He I λ4471 are computed. Both sets of models are line blanketed, assume local thermodynamic equilibrium (LTE), plane parallel geometry, and hydrostatic equilibrium. The He/H models assume an unstratified *homogeneous* mixture of He and H. For the H Balmer profiles the unified stark broadening theory of Vidal, Cooper and Smith (1973) is used, while for the He line profiles the calculations follow Wesemael (1981) and employ the results of Griem (1974).

The equivalent widths presented in Table 1 were all obtained in the same fashion using the wavelength windows indicated in the column heading of each line. In an effort to minimize bias, similar equivalent widths were measured for the He I and He II lines in the He/H model grid using the same wavelength windows and techniques. Where only an upper limit is given in Table 1, the measurement corresponds to a 2σ upper limit.

The equivalent width of the He II λ4686 line was used to estimate He abundances. At T_{eff} above 60,000 K the equivalent width of the line becomes relatively insensitive to the temperature. In contrast the He I λ4471 line rapidly disappears for temperatures in excess of 50,000 K or 60,000 K. The He II λ1640 line is also insensitive to temperature, however, the relatively low S/N of our IUE data makes this line a

poor primary indicator. The He II λ1640 and He I λ4471 lines serve mainly as consistency checks for the He abundances determined using He II λ4686.

The Paradox of G191 B2B

The relatively high S/N optical and UV spectra of G191 B2B can be used to place some rather restrictive upper limits on the He abundance in the photosphere of this star. The He II λ4686 (2σ) upper limit implies a corresponding upper limit of log(He/H) < -3.58. A similar but weaker upper limit of < -3.0 is obtained from the λ1640 line. Both results are in apparent conflict with the interpretation of the soft X-ray fluxes from G191 B2B obtained from *EXOSAT*. Assuming that the soft X-ray opacity of G191 B2B is due to He mixed homogeneously throughout the photosphere, Paerels *et al.* (1988) and Jordan *et al.* (1987), analyzing the same *EXOSAT* data, find consistent results, namely: log(He/H) > -2.49 and log(He/H) = -2.31 (+0.15 -0.27), respectively. These *lower limits* on He abundance are more than a factor of ten higher then our optical *upper limit*. In Fig. 2 we compare the observed G191 B2B optical and UV spectra in the vicinity of the He II λ4686 and λ1640 lines with synthetic profiles of these lines corresponding to a He abundance of log(He/H) = -2.5, the lowest value consistent with the soft X-ray data. It remains to be seen if model atmosphere calculations employing a chemically stratified photosphere are capable of explaining both the soft X-ray results and the optical and UV spectra.

DISCUSSION

In Table 2 we present results from the determination of He abundances for the stars in our sample of hot DAs. Three of these stars (PG0823+317, PG0846+249 and PG1305-017) exhibit detectible features due to He. For these stars we obtain He abundances in the range log(He/H) ~-2.5. The presence of He in the optical and the UV classifies these stars as DAOs (see Wesemael, Liebert and Green, 1985) and effectively doubles the number of known examples of stars in this class. In terms of effective temperature and He abundance, these stars would most closely resemble the central star of the low-surface brightness planetary nebula Abell 7. Wesemael, Liebert and Green (1985), in agreement with others, find T_{eff} = 65,000 ± 15,000 K and log(He/H) = -2.2 ± 0.15 for Abell 7. For the other stars which exhibit no detectible He features (PG1034+181, PG0950+139 and PG1108+325), we determine upper limits on He abundances of log(He/H) < -3.

This result can be contrasted with the results of Paerels *et al.* (1988), who find five out of the six stars observed in the soft X-ray with T_{eff} greater than 50,000 K exhibit inferred He abundances of a few times 10^{-3}. If our results are considered together with those for previously known DAOs and the soft X-ray results of Paerels *et al.*, a somewhat different more complex pattern of He abundance emerges. It would appear that hot (>50,000 K) H-rich degenerates exhibit a wide range of He abundance, extending from values below 10^{-5} for the well studied case of HZ 43 (Paerels *et al.* 1987) to values of ~$10^{-1.5}$ for obvious DAOs such as PG1210+533. The frequency with which high He abundance (>10^{-3}) is observed in such stars is clearly large, perhaps above 50%. Our results for G191 B2B, however, cast some doubt of the relevance of "He abundance" estimates obtained from homogeneously mixed He-H atmospheres. This would include optical/UV determinations as well as soft X-ray.

TABLE 1

EQUIVALENT WIDTHS (Å)

Name	He II λ1640	He II λ4686	He I λ4471	Hβ	Hγ	Hδ
EW Window	15Å	30Å	30 Å	100 Å	120 Å	100 Å
PG0134+181	2.1±0.4	<0.3	<0.3	2.8±0.2	4.2±0.3	3.2±0.3
PG0823+317	1.2±0.1	0.8±0.1	<0.2	3.6±0.1	4.8±0.2	2.9±0.2
PG0846+249	3.1±0.3	0.8±0.1	<0.2	2.7±0.2	4.8±0.2	2.5±0.2
PG0950+139	<0.5	0.8[a]	<0.2[a]	3.0±0.2[b]	3.2±0.2[b]	1.1±0.2[b]
PG1108+325	<0.7	<0.2	<0.3	2.8±0.2	5.1±0.2	2.7±0.2
PG1305-017	3.4±0.2	1.9±0.1	1.0±0.1	2.4±0.2	5.5±0.2	1.9±0.2
PG1210+533	2.4±0.1	1.9±0.1	0.9±0.1	4.8±0.1	9.0±0.2	5.0±0.1
G191 B2B	<0.8	<0.16	<0.16	3.4±0.1	6.4±0.2	2.7±0.2

a) Nebular contamination
b) Nebular emission components subtracted

Notes: all upper limits 2σ

TABLE 2

TEMPERATURES, GRAVITIES AND HELIUM ABUNDANCES

Name	T_{eff} (K)	log g	log (He/H)
PG0134+181	72,500 ± 5000	7.0 ± 0.5	< -3.3
PG0823+317	62,700 ± 4200	7.25 ± 0.25	-2.5 ± 0.25
PG0846+249	63,700 ± 5500	7.0 ± 0.35	-2.6 ± 0.25
PG0950+139	70,500 ± 5000	7.15 ± 0.5	< -2.2
PG1108+325	64,300 ± 5000	7.75 ± 0.35	< -3.5
PG1305-017	53,300 ± 3500	7.25 ± 0.35	~-1.0
PG1210+533	50,000[a]	8.0[a]	~-1.0
G191 B2B	62,250 ± 3520[b]	7.6 ± 0.4[b]	< -3.58

a) Wesemael, Liebert, and Green (1985)
b) Holberg, Wesemael, and Basile (1986)

Considerable theoretical doubt has already been cast on the validity of a stable homogeneous He/H photosphere with the elimination of radiative forces as a possible support mechanism for He in DA atmospheres. Vennes *et al.* (1988) have shown that radiative forces fail by several orders of magnitude to account for observed abundances of He. An alternative model suggested by these authors which may be capable of explaining both the observed pattern of He abundance as well as cases such as G191 B2B is a thinly stratified envelope. In this picture the observed He abundance is due to the equilibrium diffusion tail from an underlying He-rich layer which extends into the thin hydrogen photosphere at the surface. The apparent dependence of He on T_{eff} is primarily an optical depth effect, due to the dependence of the $\tau = 1$ level on T_{eff} and wavelength. One important aspect of this mechanism is the requirement of a very thin (10^{-14} $M_{\odot}$) hydrogen envelope.

REFERENCES

Fleming, T. A., Liebert, J., and Green, R.: 1986, *Astrophys. J.*, **308**, 176 (FLG).
Fontaine, G., and Wesemael, F.: 1987, in *IAU Coll. No. 95 The Second Conference on Faint Blue Stars*, A. G. D. Philip, D. S. Hayes and J. Liebert, eds., L. Davis Press, Schenectady, p. 319.
Griem, H.R.: 1974, *Spectral line Broadening by Plasmas* (New York Academic Press).
Holberg, J. B.: 1987, in *IAU Coll. No. 95 The Second Conference on Faint Blue Stars*, A. G. D. Philip, D. S. Hayes and J. Liebert, eds., L. Davis Press, Schenectady, p. 283.
Holberg, J. B., Wesemael, F., and Basile, J.: 1986, *Astrophys. J.*, **306**, 629.
Jordan, S., Koester, D., Wulf-Mathies, C. and Brunner, H.: 1987, *Astron. Astrophys.*, **185**, 253.
Kahn, S. M., Wesemael, F., Liebert, J., Raymond, J. C., Steiner, J. E., and Shipman, H.: 1984, *Astrophys. J.*, **278**, 255.
Koester, D.: 1987, in *IAU Coll. No. 95 The Second Conference on Faint Blue Stars*, A. G. D. Philip, D. S. Hayes and J. Liebert, eds., L. Davis Press, Schenectady, p. 329.
Liebert, J., Fontaine, G., and Wesemael, F.: 1987, *Mem. Soc. Ast. Ital.*, **58**, 17.
Liebert, J., *et al.*: 1988, in preparation.
Paerels, F. B. S., and Heise, J.: 1988, *Astrophys. J.* (in press).
Petre, R., Shipman, H. L., and Canizares, C. R.: 1986, *Astrophys. J.*, **304**, 356.
Vennes, S., Pelletier, C., Fontaine, G., and Wesemael, F.: 1988, *Astrophys. J.* (in press).
Videl, C. R., Cooper, J., and Smith, E.W.: 1973, *Astrophys. J. (Suppl.)*, 25,37.
Wesemael, F. 1981, *Astrophys.J. (Suppl.)*: **45**, 177.
Wesemael, F., Auer, L. H., Van Horn, H.M. and Savedoff, M. P.: 1980, *Astrophys. J. (Suppl.)*: **43**, 159.
Wesemael, F., Liebert, J., and Green, R. F.: 1984, *Publ. Astron. Soc. Pacific.*, **96**, 981.
Wesemael, F., Green, R. F., and Liebert, J.: 1985, *Astrophys. J. (Suppl.)*, **58**, 379.

FIGURE CAPTIONS

Fig. 1 A comparison of the *IUE* SWP spectra of the six hot DAs with those of PG1210+533 and G191 B2B. These spectra have been normalized to 1.0 at 1550 Å and off set vertically from each other. The flux scale is ergs cm^{-2} s^{-1} HZ^{-1}. Regions containing gross geocoronal Lyman α contamination and charged particle events have been deleted.

Fig. 2 UV (upper) and optical (lower) spectra of G191 B2B. These data indicate the lack of any features corresponding to He II λ1640 and λ4686. For comparison we show predicted He II features corresponding to log (He/H) = -3.6, our *upper limit* and -2.5, the *lower limit* found from soft X-ray observations.

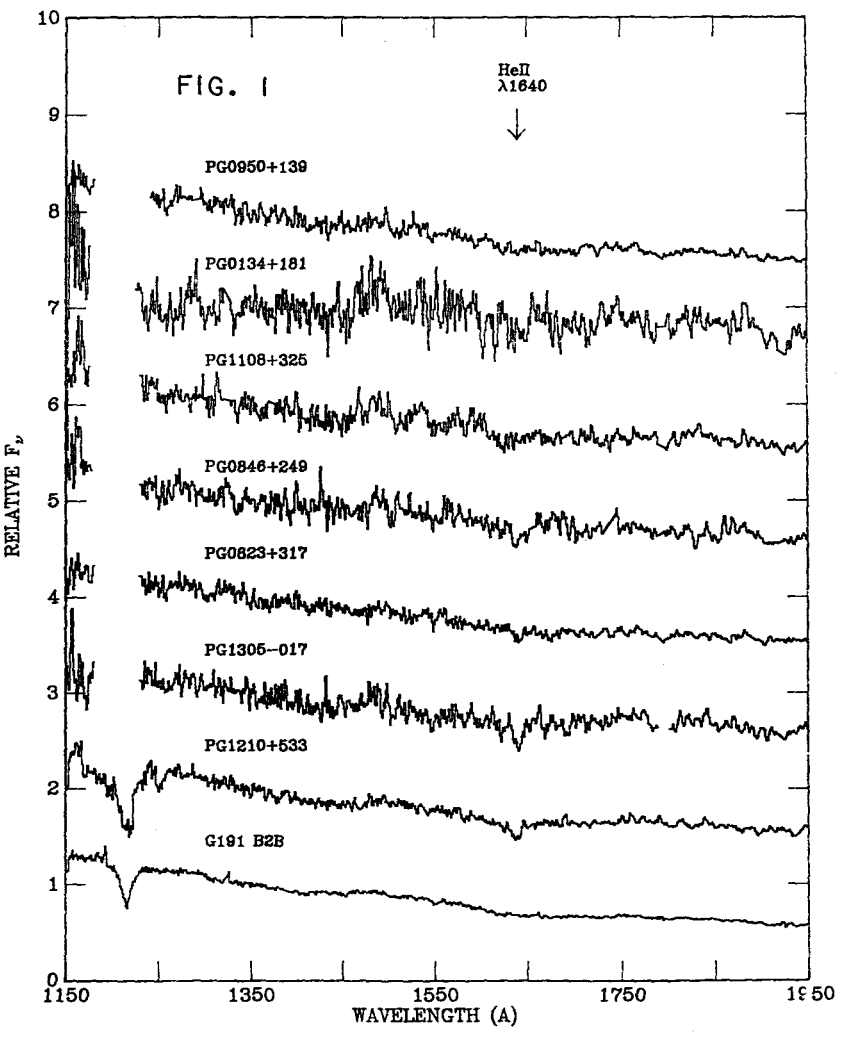
FIG. 1
HeII
λ1640
PG0950+139
PG0134+181
PG1108+325
PG0846+249
PG0823+317
PG1305−017
PG1210+533
G191 B2B
RELATIVE F_ν
WAVELENGTH (A)
1150
1350
1550
1750
1950

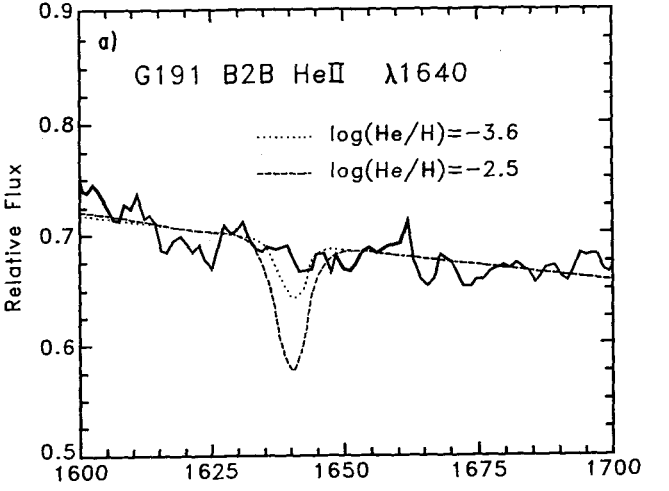
a)
G191 B2B HeII λ1640
log(He/H)=−3.6
log(He/H)=−2.5
Relative Flux
1600
1625
1650
1675
1700

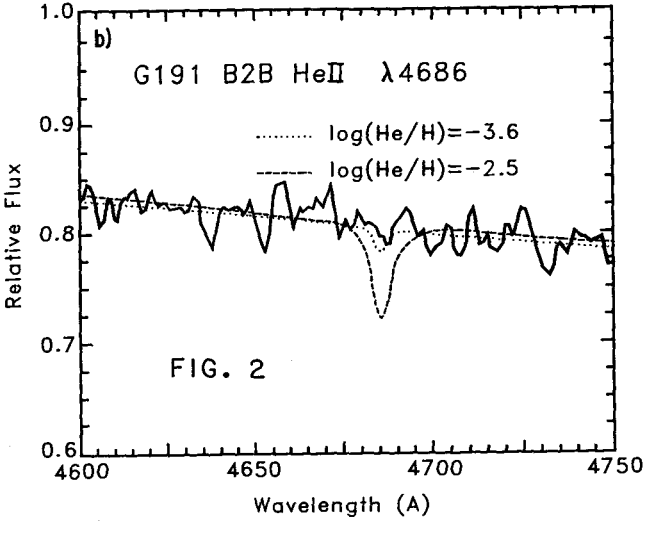
b)
G191 B2B HeII λ4686
log(He/H)=−3.6
log(He/H)=−2.5
Relative Flux
FIG. 2
4600
4650
4700
4750
Wavelength (A)

NON-LTE SPECTRAL ANALYSIS OF PG 1159-035

K. Werner, U. Heber, K. Hunger
Institut für Theoretische Physik und Sternwarte der Universität Kiel

Summary We present first preliminary results from an exploratory spectral analysis of PG1159-035. An effective temperature of 120000 K (±20000 K) and a surface gravity of about log g=7 are derived from optical and ultraviolet profiles of carbon and helium lines. NLTE model atmospheres are used which are composed of H (1%), He (19%), C (40%) and O (40%, mass fractions). The abundances adopted are in accordance with predictions of stellar pulsation theory. A direct spectroscopic determination is under way. The analysis of optical CIV lines is rendered difficult due to the lack of a reliable line broadening theory which would have to account for a gradual change to broadening by linear Stark effect. Due to the complexity of the spectral analysis, reliable abundance ratios can only be derived from a systematic investigation employing a large grid of models.

PG1159-035 is the prototype of a new class of extremely hot hydrogen-deficient pre white dwarfs. The spectra of these stars are characterized by a broad absorption trough at 4670Å, probably caused by HeII and CIV. Some members of this group (including PG1159-035) are known to be non-radial pulsators. The pulsation driving mechanism is probably cyclic ionisation of C and O. Theoretical calculations (Starrfield, 1987) predict that C (and O) must be more abundant than He (by mass), otherwise the stars were stable. In order to determine their atmospheric parameters and chemical composition, spectroscopic analyses are needed. However, due to the lack of adequate model atmospheres no reliable spectral analyses were available yet.

Since the spectral features are weak and broad, spectroscopic observations of high S/N ratios are required. We have obtained optical CCD-spectra of PG1159-035 using the EFOSC (transmission-echelle) spectrograph at the ESO 3.6m telescope, covering the wavelength range from 3900Å to 7600Å at about 3Å spectral resolution. PG1159-035 was also observed at the DSAZ (Calar Alto, Spain) using the B&C spectrograph attached to the 3.5m telescope. These spectra cover the wavelength range from 4000Å to 6000Å at a spectral resolution of 2.5Å. S/N ratios near 100 were achieved for the spectra from both sites. Ultraviolet spectra of low resolution (5Å) were obtained from the IUE data bank.

These spectra allow the detection of following lines: HeII (1640Å,5412Å,4859Å,4686Å), CIV (1550Å,5812Å,5802Å,5022Å,4789Å,4659Å,4646Å,4441Å) and OVI (5290Å). HeII (4686Å), CIV (4659Å) and OVI (5290Å) display central emission reversals, while CIV (5802Å,5812Å) are purely in emission. The spectra were analyzed using non-LTE model atmospheres adapted to the peculiar composition of the PG 1159 stars.

Non-LTE model atmospheres are indispensable for spectral analyses of PG 1159 stars, because large departures from LTE occur at the very high temperatures encountered. The effort to compute non-LTE models for the present analysis is far beyond the limits of the complete linearization technique (Auer and Mihalas, 1969). We therefore use a newly developed code, which is capable of handling many more non-LTE levels and opacities. It is based on operator perturbation techniques which gave way to a new generation of highly sophisticated non-LTE model atmospheres (Werner, 1987, 1988).

With this non-LTE code, a grid of plane parallel, static model atmospheres in the parameter range 75000 K $\leq T_{eff} \leq$ 140000 K and $5 \leq \log g \leq 8$ (cgs units) has been computed. Guided by the results of pulsation theory, we have chosen the following chemical composition for the initial models: H 1%, He 19%, C 40%, O 40% (by mass). We take into account line blanketing effects self-consistently. Altogether, the model atoms consist of 169 levels, 54 of which are explicitly treated in the statistical equilibrium equations. They all contribute to continuous opacities. 88 radiative bound-bound transitions are included into the model atmosphere computations as well. Table I shows in detail the number of non-LTE levels and lines in each ionization stage.

Table I

Non-LTE levels and line transitions in the adopted model atoms

ion		NLTE-levels	lines
hydrogen	I	5	6
	II	1	-
helium	I	1	-
	II	10	36
	III	1	-
carbon	III	1	-
	IV	21	46
	V	1	-
oxygen	IV	1	-
	V	6	-
	VI	5	-
	VII	1	-

A restricted model atom for hydrogen is sufficient, because this species is underabundant and does not determine the atmospheric structure significantly. On the other hand, the HeII atom has to include many levels, since it is known that the line transitions are responsible for considerable heating of the outer atmospheric layers. Like HeI, CIII is only weakly occupied. CIV is designed as the most detailed model atom, because our present analysis is essentially based on the lines of this ion. Oxygen (represented by 4 ionization stages) has been implemented into our model atmospheres. At the present state, no oxygen lines have been included. We

expect that the strong OV and OVI resonance lines influence only the outermost layers. The construction of a model atmosphere is as usual done with pure Doppler broadened line profiles. The emergent line profiles are calculated using fully broadened absorption coefficients. For HeII lines a reliable broadening theory exists (Griem, 1968). For CIV, however, considerable uncertainties in line broadening theory affect our analysis. The resonance doublet at 1550Å is the only observable CIV transition for which reliable line broadening data are available (Sahal-Bréchot and Segre, 1971). The optical transitions arise from highly excited energy levels (n=5-6) which are close to degeneracy, and for which a gradual transition from quadratic to linear Stark broadening occurs. An appropriate theory is still pending. We therefore assume as a first approximation broadening by linear Stark effect. The absorption coefficients are calculated after Unsöld (1968, p.320). The electrical microfield takes into account the mixture of the differently charged ions. As expected, the assumption of the linear Stark effect overestimates the broadening. This becomes evident when the line profiles are compared to those of the central star of NGC 246, whose carbon abundance is known (Husfeld, 1987). In order to reproduce the wings, the broadening parameter has to be reduced by a factor of 3. With this empirical reduction factor, our final CIV line profiles are calculated. The blue part of the characteristic absorption trough is calculated as a blend of 3 lines of CIV, namely 4646Å (transition 5d-6f), 4658Å(5f-6g), 4660Å(5g-6h). The red part is mainly due to HeII 4686Å. The calculations show, that if T_{eff} exceeds some critical value (e.g. 90000 K at log g=7), the line cores of CIV 4658Å and 4660Å develop central emission reversals. At an even higher T_{eff} (100000 K, log g=7) the core of the third CIV component (4647Å) also turns into emission. CIV 4441Å(5p-6d) appears in pure absorption, unless T_{eff} exceeds 120000 K (at log g=7). Varying the atmospheric parameters along a line parallel to the Eddington limit, the wings of these lines hardly change, which means that the cores are sensitive temperature indicators. The same applies to the CIV doublet 5802Å/5812Å (3s-3p), which turns into emission at T_{eff}=100000 K (log g=7). The CIV 1550Å resonance doublet may also be used to constrain T_{eff}, since its equivalent width rapidly decreases with increasing temperature.

From the computed spectra we derive for PG1159-035 as a preliminary result T_{eff}=120000 K and log g=7, but with considerable uncertainty. In Fig.1 we compare the observed absorption trough at 4670Å (EFOSC-spectrum, right panel) and the CIV doublet (5802, 5812Å, DSAZ-spectrum, left panel) to model predictions for T_{eff} = 100000 K, 120000 K and 140000 K at log g=7. As can be seen, the CIV lines in the trough fit best at about 110000 K. In contrary, the HeII 4686Å emission is strong enough only if T_{eff} is as high as 140000 K, in which case the CIV emissions appear too strong. Similarly, the CIV 5802Å,5812Å doublet is reproduced only if T_{eff} exceeds 120000 K. The best fit is obtained for 140000 K (at log g=7). In the UV, HeII 1640Å is reproduced well, but appears to be rather insensitive against variations of T_{eff}. From CIV 1550Å it follows that T_{eff} has to exceed 120000 K, otherwise this line would be too strong.

In order to check how the line profiles depend on the assumed abundances, we computed atmospheres with different compositions. All CIV lines turn out to vary only marginally from model to model, even if the abundance of any given species is decreased by one order of magnitude. It is found, that the atmospheric temperature structure changes the CIV/CV ionization balance in such a way, that the CIV population numbers are hardly changed, when the carbon abundance is varied. The discrepancy between the computed CIV and HeII lines in the absorption trough is milder when the He abundance is decreased, but at present we dare not to give any statement about abundance ratios. Also, on account of the uncertainty in T_{eff} it is premature to give an upper limit for the H abundance. Since we have 5 parameters that determine the structure of the atmosphere (T_{eff}, g, H/He, C/He, O/He), a much larger grid of models is required in order to reach a unique solution.

References

Auer,L.H.,Mihalas,D.: 1969, Astrophys. J. **158**, 641
Griem,H.R.: 1968, Phys. Rev. **165**, 258
Husfeld,D.: 1987, IAU coll. No. **95**, 237
Sahal-Bréchot,S.,Segre,E.R.A.: 1971, Astron. Astrophys. **13**, 161
Starrfield,S.: 1987, IAU coll. No. **95**, 309
Unsöld,A.: 1968, "Physik der Sternatmosphären", 2nd ed., Springer,Berlin
Werner,K.: 1987, in "Numerical Radiative Transfer",ed. W.Kalkofen,Cambridge Univ.Press
Werner,K.: 1988, Astron. Astrophys. (in press)

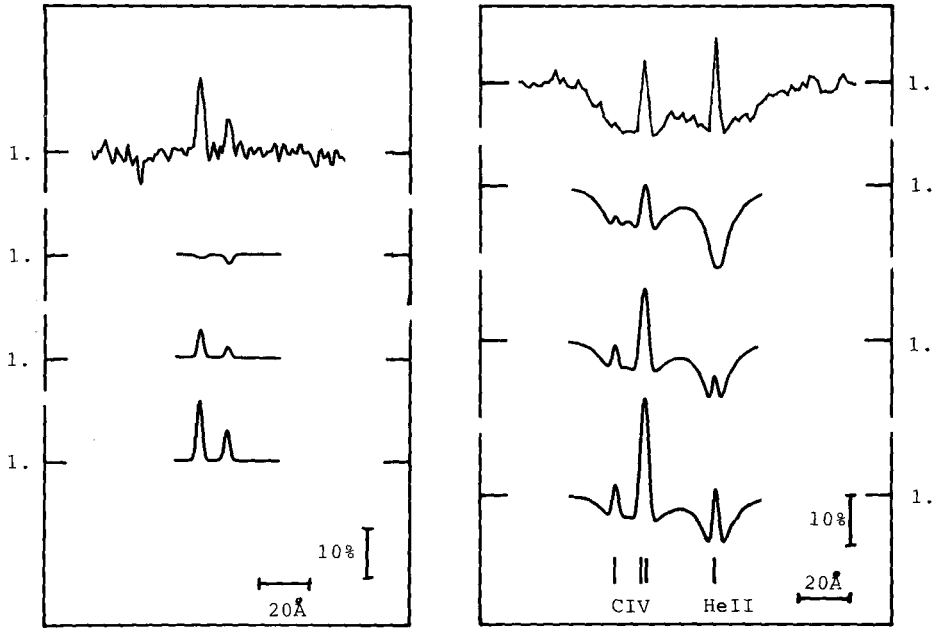

Fig.1 Comparison of the observed spectra of PG1159-035 (top) to model predictions for T_{eff} = 100000 K, 120000 K and 140000 K (bottom), see text.

X-ray Emission from Hot DA White Dwarfs; EXOSAT Results, and Implications for Atmospheric Models

Frits Paerels and John Heise
Laboratory for Space Research
Beneluxlaan 21, 3527 HS Utrecht, the Netherlands

Abstract

We present the observations of the photospheric X-ray spectra of hot DA white dwarfs, obtained with the 500 lines mm^{-1} Transmission Grating Spectrometer on EXOSAT. These spectra cover the full soft X-ray band, at high wavelength resolution and statistical quality. They allow us to do an accurate measurement of the photospheric parameters, particularly of effective temperature and chemical composition of the atmosphere.

We consider the case of HZ 43 in some detail. Model atmospheric spectra that satisfy all measured absolute optical, UV and X-ray fluxes turn out not to fit the *shape* of the measured X-ray spectrum. However, from a comparison of model spectra calculated with different model atmospheres codes we infer the existence of a 15% systematic uncertainty in the model fluxes at the shortest wavelengths ($\lambda < 100$ Å) in current model calculations. This can explain the fitting problem. Since the systematic uncertainty in the models is larger than the statistical uncertainty in the shape of the measured X-ray spectrum of HZ 43, we cannot at present use this measured shape to derive the effective temperature and gravity. We revert to broad band photometry, using the measured integrated soft X-ray flux and the optical flux, to determine $T_e = 45,000 - 54,000K, R/R_\odot = 0.0140 - 0.0165$. From the absence of the He II Ly edge at 227 Å in the measured spectrum, we set a upper limit on the photospheric helium abundance of He/H = 1.0×10^{-5}; this upper limit is independent of the uncertainties in the model calculations mentioned above.

1 X-rays from Hot DA White Dwarfs

The shape of the photospheric soft X-ray spectrum, and the total soft X-ray flux of hot DA white dwarfs are very sensitive to the photospheric parameters. The total X-ray flux is a steep function of effective temperature, and trace amounts of elements other than hydrogen will produce strong absorption edges in the X-ray/EUV spectrum (at high temperatures, these elements will be highly ionized, and the strong ground state absorption edges and the resonance lines will be in the extreme short-wavelength range). In contrast, the optical and UV spectrum becomes increasingly insensitive to the photospheric parameters with increasing effective temperature.

Soft X-ray observations are therefore obviously of great value to the observational investigation of a number of fundamental questions concerning the physics of hot white dwarfs. Improved estimates of T_e, stellar radius, and surface gravity from combined X-ray/UV/optical spectroscopy should provide the information to construct luminosity functions and evolutionary sequences. Mass estimates obtained from the measured gravity and radius can be used to experimentally verify theoretical mass-radius relations.

X-ray spectroscopy and photometry can reveal trace amounts of helium and metals in a hot, hydrogen dominated white dwarf atmosphere that are a factor 100 below the present optical spectroscopic detection limit, and so provide us with the means to study the chemical composition of the atmosphere in detail. In principle, the shape of the short-wavelength tail of the stellar spectrum is even sensitive to a possible stratification of elements in the outer envelope of the star. This is

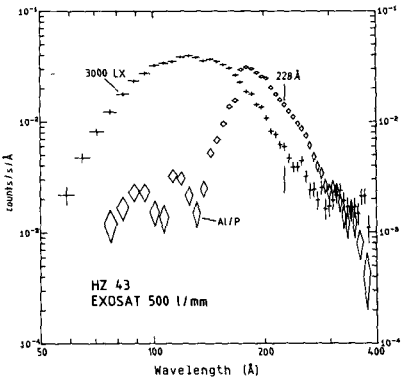

Figure 1. X-ray spectrum of HZ 43, measured with the 500 l mm^{-1} TGS, with the 3000LX and Al/P filters (background subtracted, positive and negative order spectra summed; error bars are 1σ photon counting errors). Location of the He II Ly edge has been indicated.

important information, because the atmosphere acts as a thermal blanket to the degenerate core, and hence influences the cooling rate of a white dwarf.

2 X-ray Observations of Hot White Dwarfs with EXOSAT

With the launch of the European X-ray Observatory EXOSAT, the Low Energy Imaging Telescopes and Transmission Grating Spectrometers (TGS) of which had a higher sensitivity and a larger dynamic range in the soft X-ray/EUV band than previous experiments (see Taylor [1985], de Korte *et al.* [1981]), it became possible to measure the X-ray spectrum with high sensitivity between 44 and 400 Å, with typical spectral resolution 6 Å. Comparison with model atmospheres spectra shows that we are thus able to observe the full X-ray spectrum of a hot white dwarf, between the intrinsic cutoff at short wavelengths, to the interstellar absorption cutoff in the EUV band.

We wanted to verify explicitly the conformity of the shape of the X-ray spectrum of hot DA white dwarfs to model atmospheres calculations, and to use the sensitivity of the X-ray spectrum to the stellar parameters to obtain improved estimates of these. We obtained X-ray spectroscopy of three hot DA's, HZ 43, Sirius B, and Feige 24. These are very bright X-ray/EUV sources, and they have been studied extensively in all wavelength bands. This made them the natural 'first choice' for observation with the EXOSAT Transmission Grating Spectrometers.

3 High Resolution Soft X-ray Spectroscopy of HZ 43

In the following, we will concentrate on the interpretation of the HZ 43 data. Apart from the fact that HZ 43 has an intrinsic interest as a typical hot DA and a bright X-ray/EUV source, its measured X-ray spectrum has an important implication for current model atmospheres calculations for hot, hydrogen-rich atmospheres. The reader interested in the Sirius B and Feige 24 data is directed to Paerels *et al.* (1988), and Paerels *et al.* (1986a), respectively.

HZ 43 was observed with the 500 lines mm^{-1} TGS on 28 june, 1983, for a total of 18,500 sec, with two different beam filters, the 3000LX and Al/P filters. The measured spectra are shown in Figure 1 as they appear in the spectrometer (counts s^{-1} $Å^{-1}$ vs. wavelength).

The position of the He II Ly edge at 227 Å has been indicated; no edge is detected in the Al/P spectrum (which has the highest statistical quality at the longer wavelengths). This absence can be converted into a sensitive upper limit on the fractional abundance of helium, He/H. We fitted model atmospheres spectra (which included the He II Ly series and edge) for varying He/H to the measured Al/P spectrum. T_e was fixed at 60,000 K, log g at 8.5; these values were chosen

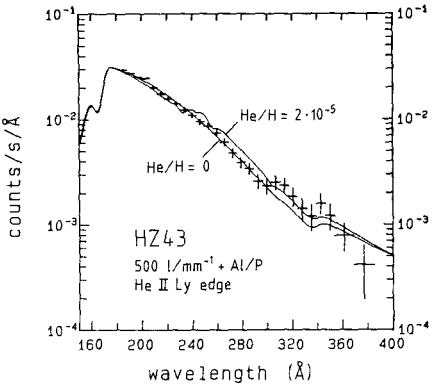

Figure 2. Al/P spectrum of HZ 43 between 170 and 380 Å, together with model atmospheres spectra at T_e = 60,000 K, log g = 8.5, $n_H = 1.4 \times 10^{18} cm^{-2}$, He/H = 0 and 2×10^{-5}, convolved with the spectrometer response. Best fit is for He/H = 0 ($\chi^2/26 = 1.25$), 99% confidence upper limit is at He/H = 1.0×10^{-5}.

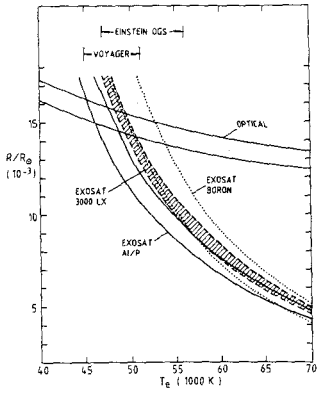

Figure 3. 99% Confidence constraints imposed on T_e and $R/R_\odot$ of HZ 43 by the measured total X-ray flux (in the 3000LX and Al/P spectra, and in photometric observation with the Boron filter), and by the visual magnitude. Intersection of X-ray and 'optical' constraint areas indicates parameter range for which consistent solution to all measured absolute fluxes is found, in terms of a single DA model spectrum. Horizontal bars at the top indicate 99% confidence estimates of T_e from EINSTEIN OGS and Voyager 2 spectra at $R/R_\odot = 0.015$.

to represent conservative upper limits on these parameters, yielding an equally conservative upper limit on He/H (the size of the He II edge decreases with increasing T_e and log g). The best fit is at He/H = 0 ($\chi^2/26 = 1.25$), the 99% confidence upper limit is at He/H = 1.0×10^{-5} (by number), as derived from standard χ^2 analysis. Figure 2 shows the Al/P spectrum in the region around the edge, together with a model spectrum at He/H = 0, and at He/H = 2×10^{-5}, both convolved with the spectrometer response. This last model was chosen to demonstrate that such a value for He/H is already emphatically excluded by the measured shape of the spectrum of HZ 43. The column density of absorbing neutral interstellar gas was determined likewise from the Al/P spectrum, and was found to be in the range $n_H = 6 - 16 \times 10^{17} cm^{-2}$, dependent on effective temperature, with a typical uncertainty of 0.4 in log n_H (99%).

Allowing for the ranges in He/H and n_H given above, and taking values of log g between 8 and 9, we determined the constraints imposed on T_e and stellar radius $R/R_\odot$ by the integrated X-ray flux as measured in the two spectra, and in a photometric exposure with the Boron filter on the Low Energy telescopes (through the ratio of measured X-ray flux to model flux at the stellar surface, using the distance, 63.3 pc, determined by Dahn *et al.* [1982]). Figure 3 shows these (99%) constraints, as well as the constraints imposed by the visual magnitude estimate $V = 12.99 \pm 0.03$, taken from Holberg *et al.* (1986). The intersection of the EXOSAT constraints and the 'optical' constraint gives the range of T_e and $R/R_\odot$ that yields models consistent with both the X-ray and optical absolute flux from HZ 43; we derive T_e = 45,000-54,000 K, $R/R_\odot$ = 0.0140-0.0165. At $R/R_\odot = 0.015$, the spectra measured with the EINSTEIN OGS and the Voyager 2 EUV spectrometer (Holberg *et al.* [1980]) yield effective temperatures that agree well with this solution (indicated at the top of Figure 3). Thus we determine the luminosity of HZ 43 to be $L/L_\odot = 1.0 - 1.5$.

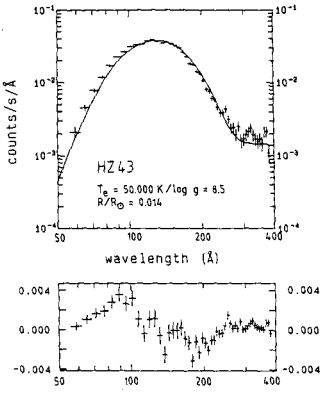

Figure 4. EXOSAT 500 l mm^{-1} TGS (3000LX) spectrum of HZ 43, fitted with a model spectrum at T_e = 50,000 K, $R/R_\odot = 0.014$, $\log g = 8.5$, He/H = 0, $n_H = 2 \times 10^{18} cm^{-2}$, that is consistent with measured optical/UV fluxes with respect to total X-ray flux. The spectral shape of the model is seen to exhibit a systematic difference with the measured shape of 15% in monochromatic flux shortward of 90 Å, indicative of a systematic uncertainty in the model spectra (see text).

When we fit model atmospheres spectra with parameters in the above ranges, however, we find that the shape of the model spectra does not match the shape of the measured spectrum at the shortest wavelengths ($\lambda < 90$ Å); χ^2 indicates that the models do not yield a statistically acceptable description of the shape of the 3000LX spectrum. At T_e = 50,000 K we have to assume a 15% systematic error in the model fluxes shortward of 90 Å. This is shown in detail in Figure 4 (3000LX data, and a model at T_e = 50,000 K, $\log g = 8.5$, He/H = 0, $n_H = 2 \times 10^{18} cm^{-2}$, $R/R_\odot = 0.014$; reduced $\chi^2 = 5.70$; the lower panel shows the post-fit residuals). This systematic error cannot be traced to a systematic error in the calibration of the spectrometer, and must be ascribed to the model atmospheres calculations. This conclusion is confirmed by the fact that corresponding model atmospheres spectra, calculated with different codes based on the same input physics show 15% differences in monochromatic flux at the shortest wavelengths (these are the models published by Petre *et al.* [1986] and Wesemael *et al.* [1980], and our own calculations). Having verified the numerical accuracy of our own code, we tentatively identify a different treatment of the ionization balance as the origin of the observed differences in output of the three codes, the short-wavelength tail of the spectrum being extemely sensitive to the ionization balance.

At present the exact source of the differences remains unresolved, nor can any of the three codes be identified a priori as the one being free of the systematic uncertainties mentioned. However, the three codes agree in monochromatic flux longward of 100 Å, so that the Al/P spectrum can be used to measure He/H and n_H independent of the specific code used to generate the models. In addition, the codes agree to within a few percent in integrated X-ray flux, so that our multicolor photometric determination of effective temperature and radius is valid, regardless of the systematic error diagnosed above. Improved accuracy in the estimate of T_e for HZ 43, and an estimate of $\log g$, using the shape of the measured X-ray spectrum has to wait until model atmospheres calculations appropriate to hot DA atmospheres are available, that are free of systematic uncertainties to the level of a few percent in monochromatic flux at the shortest wavelengths.

A full discussion of the HZ 43 data and their analysis can be found in Paerels *et al.* (1986b) and Heise *et al.* (1988).

references

Dahn, C. C., *et al.* (1982), *Astron. J.*, **87**, 419.

de Korte, P. A. J., *et al.* (1981), *Space Sci. Rev.*, **30**, 495.

Heise, J., *et al.* (1988), *Ap.J.* ,(*in press*).

Holberg, J. B., *et al.* (1980), *Ap.J.(Letters)*, **242**, L119.

Holberg, J. B., Wesemael, F., and Basile, J. (1986), *Ap.J.*, **306**, 629.

Paerels, F. B. S., *et al.* (1986a), *Ap.J.(Letters)*, **309**, L33.

Paerels, F. B. S., *et al.* (1986b), *Ap.J.*, **308**, 190.

Paerels, F. B. S., *et al.* (1988), *Ap.J.*, **329**, 849.

Petre, R., Shipman, H. L., and Canizares, C. (1986), *Ap.J.*, **304**, 356.

Taylor, B. (1985), *Adv. Space Res.*, **5**, 35.

Wesemael, F., *et al.* (1980), *Ap.J.Suppl.*, **43**, 159.

THE EFFECT OF CNO METAL ABUNDANCES ON THE SOFT X-RAY EMISSION FROM HE RICH WHITE DWARFS

M.A.Barstow

X-ray Astronomy Group, Physics Department, University of Leicester

University Road,Leicester, LE1 7RH, UK

ABSTRACT

Predicted soft X-ray fluxes for model atmospheres containing varying concentrations of CNO metals are compared with those observed by *EXOSAT* for the planetary nebula nucleus K1-16. An effective temperature in the range $\approx 125000 - 180000$K is determined for K1-16 and a limit on the concentration of CNO in the atmosphere (between 0.02 and 20×solar relative to He) obtained. Some comments on the application of the models to the apparently metal rich star H1504+65 are included.

1. INTRODUCTION

In recent years, soft X-ray emission has been detected from a number (≈ 30) of hot white dwarfs (WDs) by the *Einstein* and *EXOSAT* satellites. In general only photometric data from one or two bands are available. However, considerable success has been achieved in determining the interstellar HI columns and He abundances in DA WDs from such data with simple chemically homogeneous model atmospheres (eg. Petre et al, 1986; Paerels et al, 1987). Homogeneous atmospheres may not be physically realistic (see Vennes et al, 1988) but the indication of atmospheric composition obtained from the soft X-ray fluxes is not available from data in other wavebands. Modelling of hot He rich WDs has met with less success. Although the pure He models of Wesemael (1981) initially seemed to be able to explain observed *EXOSAT* count rates (Barstow, 1988), subsequent modelling (Holberg and Barstow, 1988) has revealed an unexpected enhancement in the flux distribution at wavelengths shortward of those covered by the Wesemael models and falling within the *EXOSAT* spectral range. Several He rich models with H:He abundances ranging from 0-1 were compared with the data but none were able to explain the relative intensities in thin lexan (3LX, $\approx 44 - 150$Å) and aluminium/parylene (Al/P, $\approx 44 - 240$Å) filters. For a given flux in the 3LX filter predicted Al/P fluxes were always higher than observed. Reduction of the Al/P flux relative to that in the 3LX band requires a steeper fall-off in the spectrum at energies above the HeII edge at 228Å. This can only be produced by the presence of additional opacity sources. Models containing CNO (Hummer & Mihalas, 1970) are available at appropriate temperatures and gravities ($\log g > 6$, $T > 5 \times 10^4$K) but have only been computed for solar abundances and do not consider OVI transitions, which have been observed in the very hottest DO WDs. A self-consistent model atmosphere code (Williams et al, 1987) has been modified to consider **all** ionisation states of CNO and determine the effect of these metals on the predicted soft X-ray fluxes. The results of comparing model predictions with observed soft X-ray fluxes for the stars K1-16, allowing limits to its effective temperature (T) and CNO abundances to be estimated, and H1504+65 are presented in this paper.

2. K1-16 SOFT X-RAY DATA AND MODELS

Eight hot DO WDs and related objects were observed by *EXOSAT* (Holberg and Barstow, 1988). The best photometric data were obtained for the planetary nebula nucleus K1-16 (in 4 filters). Observed count rates were 0.019 ± 0.0006, 0.0019 ± 0.0006, 0.0184 ± 0.0023 and 0.00084 ± 0.00050 count s^{-1} in 3LX, Al/P, 4LX (thick lexan, $\approx 44 - 140$Å) and B (boron, $\approx 67 - 120$Å) filters respectively. Furthermore, a firm upper limit on the line of sight interstellar absorbing column ($N_H = 2.36 \times 10^{20} cm^{-2}$) has been obtained from observations of a nearby QSO (Warwick et al, 1988) and its distance is known (1660pc; Kaler, 1983). K1-16 is chosen here to illustrate the results obtained with the model atmospheres. Temperatures for K1-16 are expected to be in excess of 80000K but it has not yet been possible to provide reliable estimates. The presence of CNO in He rich atmospheres is demonstrated by observations of CIV, CIII, NIII and OVI transitions in the optical and UV but their abundances remain undetermined.

The code used to compute the atmospheric models assumes LTE and a homgeneous composition. All ionisation species and excited states of CNO are included. Only continuum opacities are considered. Eddington fluxes have been calculated for models containing varying concentrations of H:He and He:CNO with the relative fractions of C:N:O held constant at solar values. The models cover frequencies from infra-red to soft X-ray, temperatures in the range 50000-200000K and log g values of 7 or 8 (Table I).

3. K1-16 RESULTS AND DISCUSSION

For a given T, N_H and model composition it is possible to calculate a predicted count rate for K1-16 in each *EXOSAT* filter by folding the model spectrum, normalised to the V magnitude (15.09), through the instrument response and an interstellar medium model. Count rates were predicted in each filter for each model temperature and a finely spaced grid of N_H values in the range $10^{18} - 10^{22} cm^{-2}$. The resulting tables were interpolated to determine the values of T and N_H corresponding to the observed K1-16 count rates. A family of constant count rate curves can then be displayed in the (T,N_H) plane as depicted in figure 1 for the model HHECNO111. The 3 curves shown for each filter correspond to the observed count rate and $\pm 1\sigma$ statistical errors. A model can be said to be consistent with the data if there is at least one region on the plot where all four sets of contours overlap. Table I summarises the results of these analyses on each model atmosphere, indicating the allowed ranges of temperature.

There is a band of models that are consistent with the observed K1-16 data. This implies that the concentration of CNO in the atmosphere of K1-16 lies between $0.02 \times$ solar and $20 \times$ solar (relative to He). However, constant relative proportions of C:N:O and a homogeneous distribution have been assumed. Adjusting the C:N:O ratios may alter this limit. If the atmosphere is non-homogeneous or layered the 'measured' CNO abundance reflects the opacity of the overlying material (probably nearly fully ionised H and He, cf. Vennes et al, 1988). The results are not very sensitive to either the concentration of H or the value of log g and altering these just modifies the allowed range of T. Imposing the known upper limit to N_H ($2.36 \times 10^{20} cm^{-2}$) allows the maximum values of T to be reduced but does not further constrain the acceptable range of models.

TABLE I. Details of the atmospheric models studied and the temperature ranges allowed by each model for the observed K1-16 filter count rates.

Model	Abundances[1]		log g	T range (K)	T limits for K1-16 (K)	T upper limit for
	H:He	CNO:He		of model		$N_H = 2.36 \times 10^{20} cm^{-2}$
HHECNO100	S	S	7.0	50000-200000	145000-181000	155000
HECNO100	0	S	7.0	50000-200000	160000-181000	168000
HHECNO101	1	S	7.0 (8.0)	50000-200000	157000(150000)-185000(177000)	164000(167000)
HHECNO111	1	0.1S	7.0	50000-200000	138000-169000	147000
HHECNO121	1	0.01S	7.0	50000-200000	NONE	NONE
HHECNO131	1	0.02S	7.0	50000-200000	NONE	NONE
HHECNO141	1	0.05S	7.0	50000-200000	125000-164000	144000
HHECNO151	1	10.0S	7.0	50000-177000[2]	158000-177000	NONE[3]
HHECNO161	1	20.0S	7.0	50000-168000[2]	NONE	NONE
HHECNO161	1	20.0S	8.0	50000-200000	NONE	NONE

[1] S=Solar abundance; He:H=0.063, He:C=4.17×10^{-4}, He:N=8.71×10^{-5}, He:O=6.92×10^{-4}.
[2] Static model unstable above this temp. [3] No consistent model with this N_H

Figure 1. Curves of constant count rate, calculated for model HHECNO111, corresponding to the observed K1-16 fluxes and $\pm 1\sigma$ errors. The filter designations are as noted in the text.

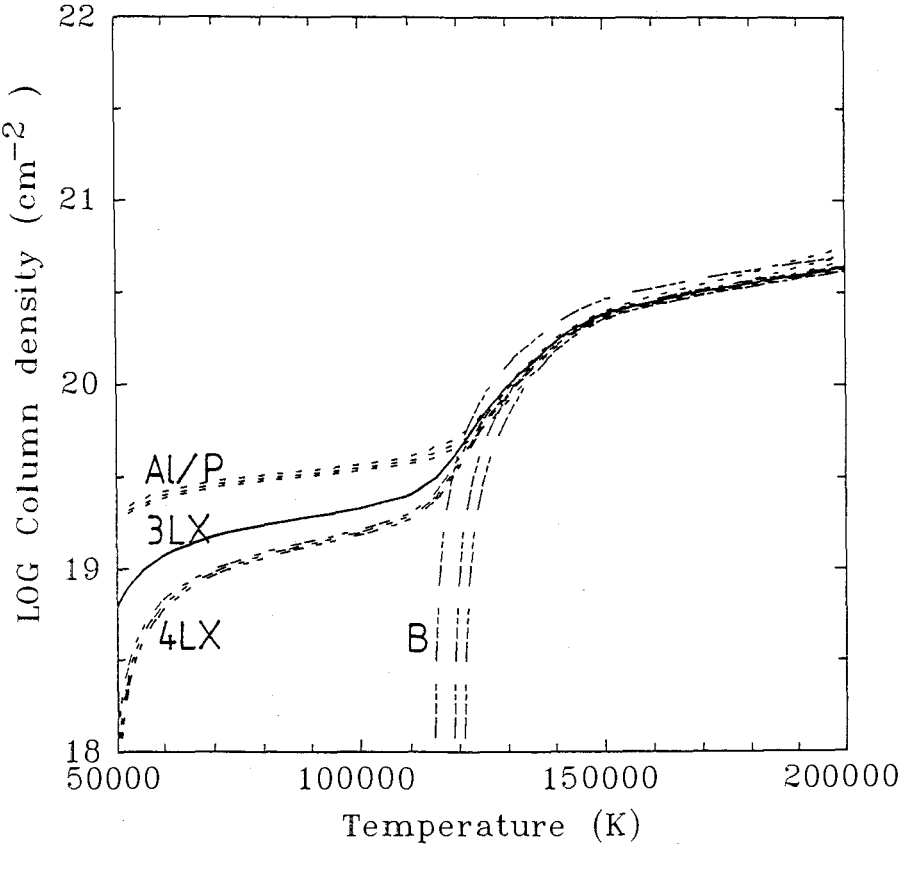

4. H1504+65

H1504+65 has been found to be an extraordinarily hot compact star that is apparently devoid of H and He (Nousek et al, 1986). Such estimates as can be made indicate that T is $\approx$ 160000K and $7 < \log g < 8$. Nousek et al were unable to match the observed *EXOSAT* count rates (6.97 ± 0.04-3LX, 0.47 ± 0.02-Al/P, 0.017 ± 0.002-B) to existing model atmospheres. The 3LX and Al/P count rates of H1504+65 can be predicted by the HHECNO101 (solar CNO) model, yielding $172000 < T < 200000$K and $4.4 \times 10^{19} < N_H < 10^{20}$. This is consistent with the estimates of Nousek et al, including their determination of N_H ($6.0 \pm 2.0 \times 10^{19}$cm^{-2}) from HI lyman alpha absorption. However, the corresponding B rate is a factor 2-3 lower than observed. Increasing the abundance of CNO appears to reduce this discrepancy but a high gravity ($\log g \approx 8$) is needed if a static atmosphere is to exist at the correspondingly higher temperatures required to generate the observed soft X-ray fluxes. Given the similarity between filter pass bands, it is difficult to see how any model might be modified to lower the B count rate sufficiently relative to the rates in the 3LX and Al/P filters.

Analysis of the structure of the HHECNO101 model indicates that for T$\approx$ 200000K He is almost completely ionised throughout the atmosphere. Consequently, the apparent lack of He may merely be due to the absence of observable transitions, as is the case for H in PG1159-035 and similar objects. Although further study of H1504+65 with these model atmospheres is necessary, these initial results suggest that it is not perhaps as anomalous as first supposed. It seems likely that it is closely related to the PG1159 group of objects (which includes K1-16) and that its observed peculiarities are a consequence of its high temperature.

6. ACKNOWLEDGEMENTS

I would like to thank Dr A.R.King for giving me access to the original model atmosphere programme and both Dr King & Dr J.B.Holberg for advice and encouragement during this work. I also acknowledge the support of the SERC through a Research Associateship.

7. REFERENCES

Barstow,M.A., 1988, Proceedings of the NATO ASI, Hot Thin Plasmas in Astrophysics, in press.

Holberg,J.B. and Barstow,M.A., 1988, in preparation.

Hummer,D.G. and Mihalas,D., 1970, *Mon.Not.R.astr.Soc.*, **147**, 339.

Kaler,J.B., 1983, *Astrophys.J.*, **271**, 188.

Nousek,J.A., Shipman,H.L., Holberg,J.B., Liebert,J., Pravdo,S.H., White,N.E. and Giommi,P., 1986, *Astrophys.J.*, **309**, 230.

Paerels,F.B.S., Heise,J., Kahn,S.M. and Rodgers,R.D., 1987, *Astrophys.J.*, **322**, 315.

Petre,R., Shipman,H.L. and Canizares,C.R., 1986, *Astrophys.J.*, **304**, 356.

Vennes,S., Pelletier,C., Fontaine,G. and Wesemael,F., 1988, preprint.

Warwick,R.S., Barstow,M.A. and Yaqoub,T.Y., 1988, in preparation.

Wesemael,F., 1981, *Astrophys,J.Suppl.*, **45**, 177.

Williams,G.A., King,A.R. and Brooker,J.R.E., 1987, *Mon.Not.R.astr.Soc.*, **266**, 725.

CHEMICAL STRATIFICATION IN WHITE DWARF ATMOSPHERES AND ENVELOPES

D.Koester
Department of Physics and Astronomy
Louisiana State University

I. Introduction

The theory of gravitational separation of elements under the combined influence of gravity and electric fields (Schatzman 1958) has been very successful in explaining the general mono-elemental composition observed in most hot white dwarf atmospheres. Today the exceptions to the rule - DO and DAO with mixed compositions (Wesemael et al.1985), DA with traces of helium (Kahn et al. 1984, Petre et al. 1986, Jordan et al.1987, Paerels 1987), DAB (Liebert et al. 1984), and DBA (Shipman et al. 1987) - pose a problem, because they seem to demand a mechanism that counteracts gravitational separation. Such a mechanism that satisfies the observational constraints is very hard to find, and this has led in recent years to the growing conviction that we indeed observe the equilibrium state of diffusion, but in white dwarfs with extremely thin hydrogen layers that remain transparent (at least in the EUV) in many objects (Jordan and Koester 1986, Liebert et al.1987, Vennes et al. 1987, Fontaine et al.1988, Vennes et al.1988).

In this paper I will briefly review the mechanism that might compete with diffusion and maintain a homogenously mixed composition in the atmosphere - with an overall negative result that has been found by others before. Theoretically we clearly expect layered envelopes, with hydrogen on top of helium and an abundance profile in the transition layer determined by diffusion equilibrium (including in general the effects of radiation pressure). In cases with observed He and H in the atmospheres this automatically means that the total H mass must be very small.

In section III I will then discuss the empirical evidence for such atmospheres, using a new grid of model atmospheres with stratified element abundances and applying it to typical mixed abundance cases at the hot end of the white dwarf temperature sequence.

II. Theoretical arguments

II.1. Diffusion time scales

It has been known for a long time that the time scales for diffusion are extremely short in the atmospheres of hot white dwarfs. However, they increase strongly with depth in the envelope,

and if we are interested in the time it takes to reach the complete equilibrium distribution for a given total hydrogen mass, the time scales evaluated at the final transition layer between H and He are more appropriate. As long as we consider only thin hydrogen layers, they remain small compared to the cooling age (see Table 1).

Table 1: H/He diffusion time scales (years) evaluated at the transition layer of the equilibrium distribution

	T_{eff}				
log $M_H/M_\odot$	60000	50000	40000	30000	20000
-10	1387	1457	1538	1635	1798
-11	298	316	336	362	393
-12	63	68	73	79	87
-13	13	14	15	17	19
-14	2.8	3.0	3.3	3.6	4.1
-15	0.6	0.6	0.7	0.8	0.9
-16	0.1	0.1	0.1	0.2	0.2
-17	0.02	0.03	0.03	0.03	0.04
cooling age	$1.6\ 10^6$	$2.7\ 10^6$	$5.3\ 10^6$	$1.5\ 10^7$	$7.9\ 10^7$

The numbers in Table 1 have been calculated with the most recent diffusion coefficients of Paquette et al.(1986). Detailed time dependent calculations for a H layer mass of approximately 10^{-10} $M_\odot$(Vennes et al.1988) have confirmed the values in the first row.
Which physical mechanisms might prevent this rapid separation of H and He?

II.2 Meridional circulation

The effect of rotation on large scale internal motions (Eddington- Vogt meridional circulation) seems still not to be completely understood. Tassoul and Tassoul (1983) found a stationary solution for a cooling white dwarf with the assumption that viscous stresses exactly balance the transport of angular momentum in the surface boundary layer. They discuss a 0.8 $M_\odot$white dwarf with L = 10^{-2} $L_\odot$and find the result that the flow velocities are negligible everywhere ($v_r \approx 10^{-13}$, $v_t \approx 10^{-9}$ cm/s near the surface). In his discussion of mechanisms competing with diffusion Michaud(1987) used estimates derived from this solution to arrive at the same conclusion. It is not clear to me, whether this result can really be generalized. Besides the basic assumption about the viscosity there are additional problems

i. Tassoul and Tassoul(1983) show in their paper that the time scale for the development of the stationary solution is larger than 10^{10} years, much longer than the ages of hot white dwarfs.

ii. Their solution was obtained for L = 10^{-2} $L_\odot$and M = 0.8 $M_\odot$. Circulation velocities increase with luminosity and decrease with mass, they could therefore be substantially larger for a 60000 K ($\approx L_\odot$) white dwarf of 0.6 $M_\odot$

In order to get another estimate for the expected magnitude I have therefore used an expression for the mass flow derived from a paper by Kippenhahn and Möllenhoff(1974)

$$\rho v = \frac{L\omega^2}{4\pi GMg\delta}$$

where ω is the angular velocity,g the local gravitational acceleration, and $\delta = -(\partial ln\rho/\partial lnT)_p$. This expression is strictly valid only for the interior. One might argue, however, that conservation of mass demands that $\rho v r^2$ must be of the same order of magnitude near the surface. Pavlov and Yakovlev (1978) derive a very similar expression for the outer layers of a white dwarf; the values derived from their formula are about a factor of 2 larger. The velocities obtained in this way are compared to the diffusion velocities in Table 2. As is evident from the formula, the effect depends on the square of the angular velocity (or rotational velocity at the equator). White dwarfs are generally found to be extremely slow rotators (Greenstein and Peterson 1973, Pilachowski and Milkey 1984,1987, Koester and Herrero 1988); I have therefore conservatively assumed a rotational velocity of 50 km/s.

Table 2: Comparison of diffusion velocities (upper line) with velocity of meridional circulation at the transition layer for a rotational velocity of 50 km/s. Velocities are in cm/s; numbers in brackets are powers of 10.

	T_{eff}				
log $M_H/M_\odot$	60000	50000	40000	30000	20000
-10	1.6 (-5)	1.4 (-5)	1.2 (-5)	9.8 (-6)	7.3 (-6)
	3.2 (-7)	1.4 (-7)	5.2 (-8)	1.4 (-8)	2.4 (-9)
-11	4.9 (-5)	4.2 (-5)	3.6 (-5)	2.9 (-5)	2.2 (-5)
	2.1 (-6)	9.3 (-7)	3.4 (-7)	9.5 (-8)	1.5 (-8)
-12	1.5 (-4)	1.3 (-4)	1.1 (-4)	8.7 (-5)	6.5 (-5)
	1.5 (-5)	6.1 (-6)	2.3 (-6)	6.2 (-7)	1.0 (-7)
-13	4.7 (-4)	4.0 (-4)	3.4 (-4)	2.7 (-4)	2.0 (-4)
	9.1 (-5)	4.0 (-5)	1.5 (-5)	4.1 (-6)	6.7 (-7)
-14	1.5 (-3)	1.3 (-3)	1.0 (-3)	8.2 (-4)	5.9 (-4)
	6.0 (-4)	2.6 (-4)	9.8 (-5)	2.7 (-5)	4.4 (-6)
-15	4.7 (-3)	4.0 (-3)	3.3 (-3)	2.6 (-3)	1.8 (-3)
	3.9 (-3)	1.7 (-3)	6.4 (-4)	1.8 (-4)	2.9 (-5)

-16	1.5 (-2)	1.3 (-2)	1.0 (-2)	8.1 (-3)	5.7 (-3)
	2.6 (-2)	1.1 (-2)	4.2 (-3)	1.2 (-3)	1.9 (-4)

-17	4.9 (-2)	4.1 (-2)	3.3 (-2)	2.6 (-2)	1.8 (-2)
	1.7 (-1)	7.5 (-2)	2.8 (-2)	7.6 (-3)	1.2 (-3)

For the deeper layers in cool models the results are about the same as the velocity (along the surface) in the solution of Tassoul and Tassoul(1983) and circulation is indeed negligible.

This is, however, not true for more luminous white dwarfs with very thin H layers: in the models below the dashed lines in the table circulation velocities are larger than diffusion velocities! The numbers are of course very approximate estimates. They ignore completely the stabilizing influence of the composition gradient near the surface, and are very probably overestimates in view of the work of Tassoul and Tassoul (1983). Nevertheless, the fact that circulation could be much more important in the hot objects is intriguing in view of the observed pattern of He abundances vs. effective temperature.

II.3 Mass loss

The possibility of mass loss in hot DA has been inferred from the presence of shortward-shifted absorption components of highly ionized species (Bruhweiler and Kondo 1983) and mass loss rates of up to 10^{-8} $M_\odot$/year (Hamann et al. 1984) are known to occur in central starsof planetary nebulae (at much higher luminosities). The interaction of diffusion with mass loss has been discussed in detail by Michaud (1987). For continuity reasons of the flow, mass loss leads to a systematic velocity in the transition region which is superposed on the diffusion velocity. It is easy to estimate with the numbers in Table 2 that these velocities are comparable if the mass loss is of the order of 10^{-15} $M_\odot$/year. With somewhat different assumptions about the original abundance distribution Michaud(1987) derived 10^{-14} as the critical rate at which diffusion becomes ineffective.

While this seems at first sight a relatively small number any mass loss of this size must certainly be excluded in the present context. As is obvious from the range covered by the tables and for reasons than will become clear below, I am especially interested in the range of total hydrogen masses below 10^{-13} $M_\odot$. Such a thin layer would be lost almost immediately if mass loss of the critical size existed. It might well be, however, that mass loss in previous evolutionary phases has led to these thin H layers and stopped when it came close to the H/He transition zone, although at the moment this is pure speculation. For the remainder therefore let us simply assume that mass loss, if present, is small enough not to interfere with diffusion.

II.4 Accretion of interstellar matter

Accretion has been studied and dismissed as possible explanation for the He seen in hot DA and DAO most recently by Fontaine et al. (1988). The main arguments are

i. there is evidence in favor of a weak wind or static halo in hot DA (see above)

ii. the accretion rate necessary to compete with diffusion ($\approx 10^{-16}$ $M_\odot$/year) is much higher than expected for an isolated hot white dwarf in the tenuous interstellar medium. The typical time between cloud encounters, where accretion rates could be higher, is $\approx 5\ 10^7$ years, larger than the lifetime of the hottest DA.

II.5 Radiative levitation

Selective radiation pressure on helium has been invoked for some time (Petre et al. 1986, Shipman 1987,1988) as an explanation for the helium seen in DAO and in the EINSTEIN and EXOSAT observations of a number of DA.

However, Vennes et al. (1988) have recently calculated the time dependence of the element stratification for two sequences of models, with approximately 10^{-7} and 10^{-10} $M_\odot$ total hydrogen content, including radiative forces on helium. Radiation pressure indeed increases the equilibrium surface abundance of He, but these abundances fail by at least two orders of magnitude to explain the observations. They conclude that the H layers must be even thinner than they had assumed in their calculations. Estimating the He abundance at an (EUV) optical depth of one from an equilibrium abundance profile and comparing with observations they arrive at H layer masses in the range 10^{-13} to 10^{-15} $M_\odot$.

While this should give the right order of magnitude to be expected, there are some obvious problems associated with this procedure. The emerging stellar flux, especially in the EUV, originates from a wide range in geometrical depth with greatly varying He abundance. On the other hand, the observational abundances they use for comparison have been determined assuming homogenous model atmospheres.

Whether thin stratified atmospheres can really explain e.g. the accurate EXOSAT broad band fluxes can only be demonstrated using theoretical models that take this stratification into account. In section III I will report the results of such an attempt.

II.6 Convection

The main conclusion of the discussion above is that there are strong theoretical reasons to expect simple gravitational separation of He and H to work in hot white dwarfs. If this is to explain the observed He abundance in DA/DAO the transition zone of the equilibrium profile must reach into the photosphere - if we interpret this in a broader sense, including the "EUV photosphere". The hydrogen layer must then obviously be very thin, of the order of 10^{-14} $M_\odot$ or less, and the depth dependence of the H/He ratio has to be taken into account consistently in atmospheric models and synthetic spectra calculations.

Inhomogenous atmosphere models - assuming a pure H layer on top of a pure He envelope with an infinitely thin transition zone - have been considered previously by Heise and Huizenga (1980), Muchmore(1982, 1984), and Price and Shipman(1985). The first systematic study using realistic transition zones was performed by Jordan and Koester(1986). I have since then extended the available model grid and will report in section III some preliminary applications.

Before doing so, we must, however, consider another effect that might compete with diffusion, that is convection. Because the presence of an abundance gradient in the atmosphere can considerably change the temperature gradient, this can only be done by studying convective instability in consistent flux constant atmospheres. The results of this study are given in Table 3.

Table 3: Convective instability in stratified H/He atmospheres
- stable
+ convectively unstable in transition zone
(+) unstable outside transition zone
— models above this line would optically appear as a "pure" DA

	T_{eff}/1000 K						
log $M_H/M_\odot$	60	50	40	35	30	25	20
-13.3	-	-	-		-		-
-14.3	-	-	-		-		-
-15.3	-	-	-		-		+
-16.3	-	-	+	+	+		(+)
-16.9				(+)	(+)	(+)	
-17.1				(+)	(+)	(+)	
-17.3	-	-	(+)		(+)		+
-18.3	-	-	(+)		(+)		(+)

The first point to note in this table is the dashed line, which separates models showing only H lines (above) from those showing in addition HeI or HeII line. The effect of increasing H opacity with decreasing temperature as mentioned by Vennes et al.(1988) does not play a major role. Only for a total H mass very close to 10^{-16} $M_\odot$could a star show H and He above 40000 K and turn into a pure DA somewhere between 40000 and 30000 K. But even this would never happen in reality, because it would be masked by the effects of convection. The plus signs in the table mark models with convectively unstable regions within the transition layer. The He mass in this unstable region is always at least an order of magnitude larger than the total hydrogen mass - these models are certainly not realistic. This is not that clear with the models with (+), which stands for convectively unstable regions outside the direct transition zone ("contamination" less than 1%). Whether the thin hydrogen layer could remain stable in such a case is not clear (Arcoragi and Fontaine 1980). The above table casts some doubt on Liebert et al.'s(1987) explanation for the missing DB between 40000 and 30000 K. I have found no models that would look like a DA and turn into a DB at 30000 K. The grid is coarse, and there might be a H mass for which this happens. But this H layer would have to be extremely fine tuned on some value near 10^{-16} $M_\odot$and it seems to me quite unlike that that can be true for all DB.

III. Application of stratified atmospheres to observations

III.1. Cool DO and DAO stars

The cool DO stars - with the prototype HZ21 - are defined by Wesemael et al.(1985) as showing HeI features together with HeII + H blends, whereas the DAO show broad H and sharp

HeII 4686 (Prototype HZ34). The He/H abundance ratios - as determined from homogenous atmospheres - are typically 1 (DO) resp. 10^{-2}.
A detailed analysis using stratified atmospheres has not been done yet. Figure 1 shows that at least qualitatively the observed optical characteristics can be reproduced, although the He lines (especially HeI) tend to be quite broad because they originate in higher pressure regions than in a homogenous atmosphere. For a final decision of course the wealth of UV data has to be used as well.

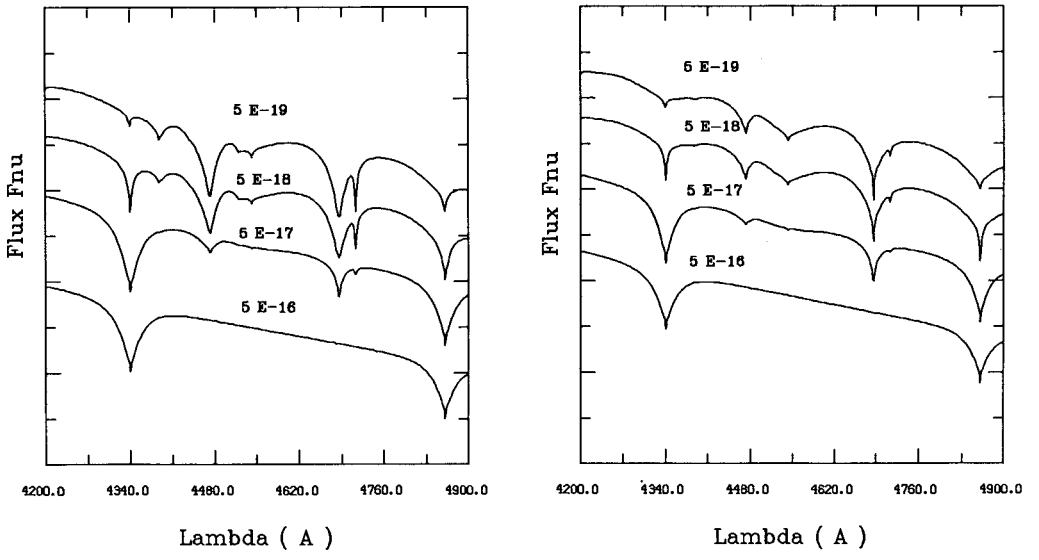

Fig 1: Optical spectra for stratified atmospheres of 50000 K (left) and 60000 K (right), showing H, HeI, and HeII lines.

III.2 EUV observations of DA

Observations in the soft X-ray and EUV regions, covering the 228 Å absorption edge of HeII, have so far provided the only opportunity to study the He/H abundance ratio in hot DA white dwarfs that show no trace of helium at optical wavelengths. After the pioneering discoveries of EUV radiation from Sirius B, HZ43, Feige24, and G191-B2B (Mewe et al. 1975a,b; Hearn et al. 1976; Margon et al. 1976a,b; Lampton et al. 1976; Holberg et al. 1980) a more systematic study has been made possible in recent years with the EINSTEIN and EXOSAT satellites. A surprising result of these studies was that a small but finite ($\geq 10^{-5}$) amount of helium was necessary in almost all cases to explain the observations (Kahn et al. 1984, Petre et al. 1986, Jordan et al. 1987, Paerels et al. 1987, Paerels 1987, Paerels and Heise 1988). Even less expected was a trend of increasing He abundance with increasing effective temperature of the white dwarf found originally by Petre et al.(1986) from their analysis of EINSTEIN data and confirmed by Jordan et al.(1987) from EXOSAT observations of 9 DA.

The only clear exception to that trend in both samples was HZ43, which seems to have a low He abundance compared to other objects in the same temperature range.
Kahn et al. 1984 proposed two possible mechanisms as explanation for the finite observed He abundances: accretion from interstellar matter and selective radiative acceleration on He ions, supporting them against gravity in the atmospheres. In view of the observed relation between He/H and T_{eff}, Petre et al.(1986) favored the second process, because only this can naturally lead to such a correlation. However, Vennes et al.(1988) demonstrated that the the amount of helium that can be supported by radiative forces is too small by at least two orders of magnitude to account for the observations. All abundance determinations in the above mentioned studies were based on the assumption of a homogeneous, mixed He/H atmosphere, although as discussed in section II one would theoretically expect an abundance stratification.
Can such atmospheres provide an alternative, satisfactory explanation?
I have studied this question using the sample of 9 DA white dwarfs from our first paper (Jordan et al. 1987), which have been observed in at least two filters of the LE experiment (Al/P and Lexan 3000). In addition the observations of CD-38°10980 and PG1658+440 as given by Paerels and Heise (1988) were included. The analysis was very similar to that of Jordan et al.(1987) with the exception that the parameter He/H abundance is now replaced by the total hydrogen layer mass (in $M_\odot$). It is indeed possible to find solutions for M_H and the interstellar column density (the only free parameters) that reproduce the observations, and a sample of the results for M_H is given in Table 4.

Table 4: Hydrogen layer thickness determined from EXOSAT broad band EUV observations

object	T_{eff}	M_H
G191-B2B	60000	$4.74\ 10^{-16}$
HZ43	57000	$1.21\ 10^{-14}$
GD246	55000	$5.75\ 10^{-15}$
GD257	55000	$5.11\ 10^{-15}$
GD153	42000	$1.21\ 10^{-14}$
LB1663	37000	$8.80\ 10^{-15}$
GD659	37000	$2.29\ 10^{-14}$*
GD394	36000	$3.25\ 10^{-14}$*
PG1658+440	31000	$2.63\ 10^{-14}$*
GD391	27500	$1.08\ 10^{-14}$*
CD-38°10980	24950	$3.80\ 10^{-14}$*

In all cool objects marked with an asterisk there is a well defined solution corresponding to the temperature value given in the table, which is the assumed temperature for that object. However, if I use the lowest temperature allowed by optical and UV observations, a solution with a much thicker H layer (corresponding to a pure hydrogen atmosphere) is also possible,

consistent with the results of Paerels and Heise (1988). The values for M_H nicely fall into the range estimated by Vennes et al.(1988). Although there is no single-valued relation to T_{eff}, a tendency for thinner H layers at the hot and thicker at the cool end of the sequence is apparent, again with the notable exception of HZ43. This is very reminiscent of the relation between He abundances and effective temperature obtained from homogenous atmospheres. If both explanations - homogeneous vs. layered atmospheres - are possible, we are left with the difficult question, which is the correct one. I cannot answer that question at the moment, but want to mention two arguments, one slightly in favor of stratified atmospheres, one against them:

i. A major problem with the EXOSAT observations has been the discrepancy between the EUV spectrum and the broad band filter observations of HZ43. In their table of the results from EUV photometry Paerels and Heise(1988) give for HZ43 the He abundance derived from the non-visibility of the HeII λ228 edge without mentioning the very accurate observations for 5 different filters. These are in fact completely incompatible with the low He abundance they obtain as long as the temperature is confined to the interval obtained from optical and UV observations, as was demonstrated by Jordan et al.(1987). If the temperature is lowered to 50000 K, the value favored by Heise et al.(1988) in their second paper on the EUV spectrum of HZ43, we obtain a He abundance of 3 10^{-6} from Fig. 1 in Jordan et al.(1987) and the discrepancy between spectra and broad band filters disappears.

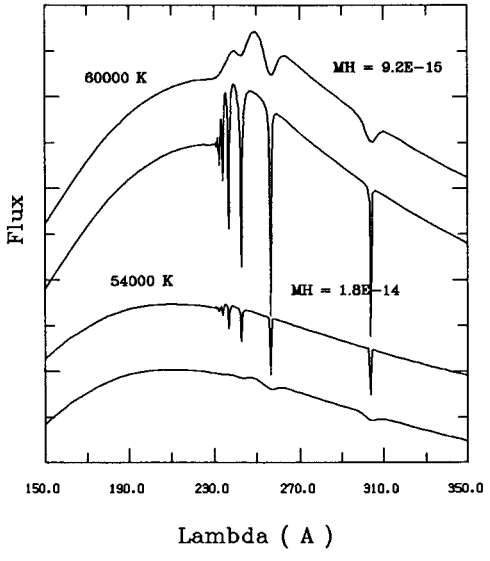

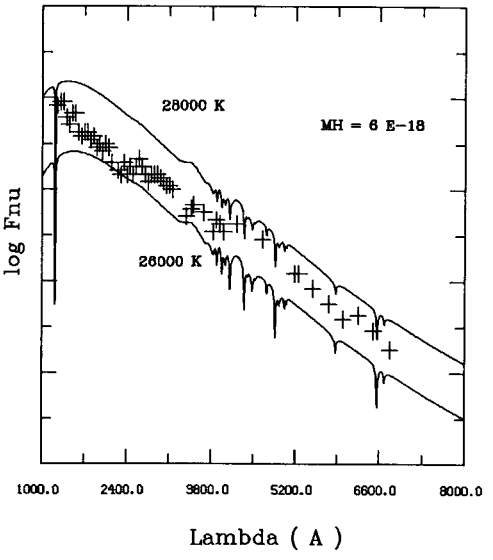

Fig. 2 (left): Theoretical EUV spectra of two models for HZ43 that reproduce the EUV filter data.
Fig. 3 (right): Energy distribution in GD323 compared with two theoretical models, shifted vertically to avoid confusion.

There is a chance that an interpretation in terms of stratified atmospheres can remove this discrepancy at somewhat higher temperatures, more in accord with the other observations. Fig. 2 shows two theoretical EUV spectra at the high and low end of the temperature range for HZ43 I assumed(57000± 3000 K), which both reproduce the observed EUV filter fluxes. They have been smoothed to the resolution of the grating spectrum of 6 Å . In the hot model the absorption edge remains clearly visible, whereas in the cool one, which has a slightly higher H mass, it has disappeared, in part due to the strong overlapping of the high series members of the HeII Lyman series. The lines are broader than in a homogeneous model because He is present only in regions of the atmosphere with higher pressures. At this resolution only the absorption lines near 250 and 300 Å remain visible and an indication for such features can indeed be seen in the LEXAN3000 spectrum in Fig. 2 in Heise et al. 1988.

ii. Another problem with the EXOSAT data has been that the derived interstellar column densities for some objects (e.g. HZ43 and G191B2B) contradict the results from Voyager observations of the range shortward of the Lyman edge (Jordan et al. 1987, Heise et al. 1988, Holberg 1987). The required column densities are even larger for the solutions obtained with stratified atmospheres. Heise et al. (1988) propose the solution that the interstellar hydrogen along these lines of sight is strongly ionized, leading to low HI densities, whereas the opacity observed in the EUV is due to neutral He.

III.3 The DAB star GD323

This unique object, which has an energy distribution from the UV to the red characteristic of a helium-dominated atmosphere around 30000 K, but lines of H and He much too weak for this temperature has been analyzed in great detail by Liebert et al.(1984) using homogenous model atmospheres. They were not able to find a consistent fit, and after a discussion of all alternatives the only hypothesis that survives - as they put it - is the assumption of a stratified atmosphere, which could not be tested at that time due to the lack of detailed models. In our paper (Jordan and Koester 1986) we did not attempt an analysis but suggested that the spectrum looks more like a homogenous, He-rich atmosphere around 40000 K. As was pointed out by Liebert et al.(1987), however, the He lines in such a model would be too strong. I have therefore calculated an additional model grid with much finer parameter spacing and tried to fit all observed data.

Although it is not possible to find a single model that perfectly matches all observations, the remaining discrepancies are indeed much smaller than for homogeneous atmospheres and the range of parameters necessary to fit all data is confined to $T_{eff} = 27000 \pm 1000$ K, $M_H = (7.5 \pm 2.5)\ 10^{-18}\ M_\odot$. Fig.3 shows the overall energy distributions, Fig.4 three representative optical spectra, while Table 5 gives a detailed comparison of observed and theoretical colors and equivalent widths. The observed data are from Liebert et al.(1984). From colors and He lines the 26000 K model is favored, whereas the weakness of the H lines demands a slightly higher temperature. As can be seen from Fig. 3, models in this range also reproduce the overall energy distribution fairly well, though not perfectly.

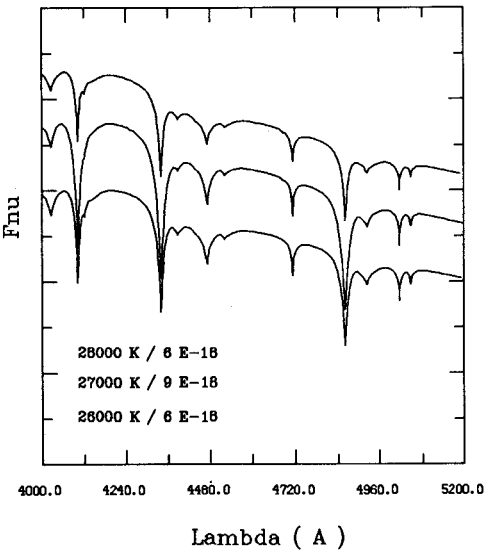

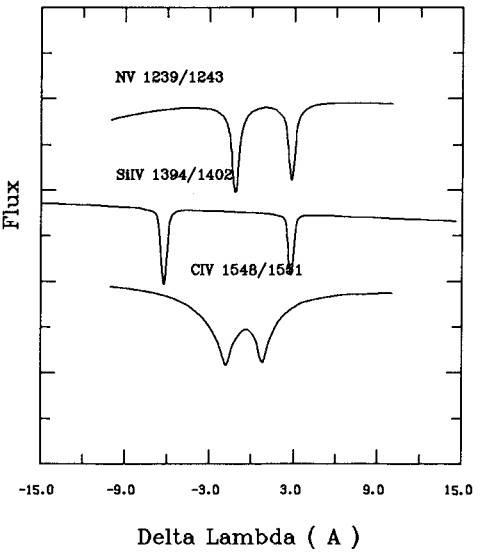

Fig. 4 (left): 3 theoretical optical spectra for GD323 with parameters near the optimum solution.
Fig. 5 (right): Theoretical calculation for lines produced in "metallic clouds" in Feige 24.

Table 5: Observed and theoretical colors and equivalent widths for GD323

		T_{eff}[K] / M_H[$M_\odot$]		
	observed	28000	27000	26000
		$6\ 10^{-18}$	$8\ 10^{-18}$	$1\ 10^{-17}$
Johnson B-V	-0.13	-0.17	-0.15	-0.13
Johnson U-B	-1.08	-1.13	-1.12	-1.08
Stroemgren b-y	-0.10	-0.07	-0.08	-0.09
Stroemgren u-b	-0.24	-0.28	-0.25	-0.18
MC u-v	-0.47	-0.58	-0.55	-0.49
MC g-r	-0.56	-0.64	-0.65	-0.69
H beta	7.0-10.0	3.9	7.3	12.9
H gamma	5.6-10.0	4.6	7.1	11.3
H delta	3.0-4.0	2.4	5.1	10.5
He 4471	1.7-2.5	1.0	1.6	2.1
He 4713	1.0-1.7	0.8	1.0	1.0

Very shallow convection zones appear in all models in the underlying helium, but do not reach into the transition zone (defined by "impurities" larger than 1%). The mass in these

convective regions is typically 10^{-15} to 10^{-16} $M_{\odot}$; even a small contamination with H of the order of 1 % should be mixed homogenously and could significantly change the abundance profile. Such a calculation might provide the final answer to the GD323 puzzle. GD323 is thus the only clear case, where homogenous models fail and stratified models provide a much more consistent fit as was originally suggested by Liebert et al.(1984).

III.4 Highly ionized metals in Feige 24

Although this is not related to the problem of He/H ratios it is nevertheless an interesting test case for the action of diffusion in hot DA. The two models proposed so far to explain the presence of metals are accretion from the close binary companion and radiative levitation (see Vauclair(1987) and Shipman(1987) for recent reviews).

Morvan et al.(1986) and Vauclair(1987) have calculated the radiation pressure on the observed elements and found that in equilibrium they are accumulated in the form of clouds in the photosphere. I have taken the abundance distribution with optical depth from Vauclair (1987) and calculated a theoretical spectrum for a 60000 K model, which is shown in Fig. 5. The equivalent widths for these lines are given in Table 6 and compared to the observed values, taken from Wesemael et al.(1984), who analysed the observations with homogeneous model atmospheres.

Table 6: Observed equivalent widths (in mÅ) in Feige 24 and comparison with theoretical "cloud" models

	observed	theoretical
SiIV 1394	97.7	170
1402	75.6	126
NV 1238	63.6	187
1242	60.9	136
CIV 1548	104.0	1920
1551	108.0	

In view of the preliminary nature of these calculations and the large uncertainties involved in the computation of radiative acceleration the results for Si and N are encouraging. On the other hand, the result for C is far outside the acceptable range. In regard to the main question of this paper, whether diffusion (including radiative levitation) alone can explain the trace elements in hot DA, the Feige 24 data remain inconclusive at this time.

IV. Conclusions

For theoretical reasons as well as from the observation that in almost all white dwarfs one element is dominating we expect diffusion to be the most important mechanism. In this picture, however, it is very difficult to explain the traces of He found in many hot DA, because diffusion time scales are too short and radiation pressure too small. A possible solution could be to assume that the total amount of hydrogen is very small ($< 10^{-14}$ $M_{\odot}$, much smaller than predicted by evolutionary calculations) and that the He or metals are part

of an equilibrium abundance profile reaching into the visible or EUV photosphere. For the DAO a detailed analysis of the feasibility of such models has still to be performed, but it seems possible. The EUV observations of He can at least as well be explained by stratified models as by homogenous, but neither of the possibilities can be excluded.

The DAB GD323 provides the strongest evidence that homogenous models are insufficient to explain the observations, and the calculations discussed above favor stratified models. The hydrogen layers necessary to explain the observations have masses around 10^{-17} $M_{\odot}$, about the same as would be necessary for the DAO. GD323 could then be regarded as descending from that hotter class, but what happens in the intermediate range (30000 to 40000 K), where no objects with He lines are known?

The preliminary results for the metals in Feige 24 are inconclusive. The visibility of these lines is predicted by theory, but at least the carbon lines are much stronger than observed. It is possible that an improved understanding of the effects of radiation pressure might remove the remaining discrepancies.

In summary: No clear contradictions to the assumptions of very thin stratified H/He layers have been found, but convincing evidence for it is also scarce. The strongest argument remains the lack of any other acceptable theory for the He traces in DA.

Acknowledgement: This work was supported in part under NASA grant NAG5-990.

REFERENCES

Arcoragi,J.-P., Fontaine,G. 1980, *Astrophys.J.***242**,1208

Bruhweiler,F.C., Kondo,Y. 1983, *Astrophys.J.***269**,657

Fontaine,G., Wesemael,F., Vennes,S., Pelletier,C. 1988, *paper presented at the 171st. meeting of the American Astronomical Society*, Austin, January 1988

Greenstein,J.L., Peterson,D.M. 1973,*Astron.Astrophys.***25**,29

Hamann,W.R., Kudritzki,R.-P., Mendez,R.H., Pottasch,S.R. 1984, *Astron.Astrophys.***139**,459

Hearn,D.R., Richardson,J.A., Bradt,H.V.D., Clark,G.W., Lewin,W.H.G., Mayer,W.F., McClintock,J.E., Primini,F.A., Rappaport,S.A. 1976,*Astrophys.J. (Letters)***203**,L21

Heise,J., Huizenga,H. 1980, *Astron. Astrophys.* **84**,280

Heise,J., Paerels,F.B.S., Bleeker,J.A.M., Brinkman,A.C. 1988, *Astrophys.J.* in press

Holberg,J.B., Sandel,B.R., Forrester,W.T., Broadfoot,A.L., Shipman,H.L., Barry,J.L. 1980, *Astrophys.J. (Letters)* **242**, L119

Holberg,J.B. 1987, in IAU Coll.**95**, *The second conference on faint blue stars*, ed. A.G.Davis Philipp, D.S.Hayes, J.Liebert, L.Davis Press, Schenectady,p.285

Jordan,S., Koester,D. 1986, *Astron. Astrophys. Suppl.* **65**,367

Jordan,S., Koester,D., Wulf-Mathies,C., Brunner,H. 1987, *Astron. Astrophys.* **185**,253

Kahn,S., Wesemael,F., Liebert,J., Raymond,J., Steiner,J., Shipman,H.L. 1984, *Astrophys.J.* **278**,255

Kippenhahn,R., Möllenhoff,C. 1974, *Ap.SpaceSci.* **31**,117

Koester,D., Herrero,A. 1988, *Astrophys.J.* in press

Lampton,M., Margon,B., Paresce,F., Stern,R., Bowyer,S. 1976, *Astrophys.J. (Letters)* **203**,L71

Liebert,J., Wesemael,F., Sion,E.M., Wegner,G. 1984, *Astrophys.J.* **277**,692

Liebert,J., Fontaine,G., Wesemael,F. 1987, *Mem. Soc. Astron. Italiana* **58**,17

Margon,B., Malina,R., Bowyer,S., Stern,R., Paresce,F. 1976a, *Astrophys.J. (Letters)* **203**,L25

Margon,B., Lampton,M., Bowyer,S., Stern,R., Paresce,F. 1976b, *Astrophys.J. (Letters)* **210**,L79

Mewe,R., Heise,J., Gronenschild,E.H.B.M., Brinkman,A.C., Shriver,J., den Boggende,A.J.F. 1975a, *Nature* **256**,711

Mewe,R., Heise,J., Gronenschild,E.H.B.M., Brinkman,A.C., Shriver,J., den Boggende,A.J.F. 1975b, *Astrophys.J. (Letters)* **202**,L67

Michaud,G. 1987, in IAU Coll.**95**, *The second conference on faint blue stars*, ed. A.G.Davis Philipp, D.S.Hayes, J.Liebert, L.Davis Press, Schenectady,p.249

Muchmore,D. 1982, *Astrophys.J.* **259**,749

Muchmore,D. 1984, *Astrophys.J.* **278**,769

Paerels,F.B.S., Heise,J. 1988, *Astrophys.J.* in press

Paerels,F.B.S., Heise,J., Kahn,S.M., Rogers,R.D. 1987, *Astrophys.J.* **322**,315

Paerels,F.B.S. 1987, *Thesis*, University of Utrecht

Paquette,C., Pelletier,C., Fontaine,G., Michaud,G. 1986, *Astrophys.J. Suppl.* **61**,197

Pavlov,G.G., Yakovlev,D.G. 1978, *Sov. Astron.***22**,595

Petre,R., Shipman,H.L., Canizares,C.R. 1986, *Astrophys.J.* **304**,356

Pilachowski,C.A., Milkey,R.W. 1984, *PASP***96**,821

Pilachowski,C.A., Milkey,R.W. 1987, *PASP***99**,836

Price,C.W., Shipman,H.L. 1985, *Astrophys.J.* **295**,561

Schatzman,E. 1958, *White Dwarfs* ,Amsterdam, North Holland

Shipman,H.L. 1988, to appear in IAU Symposium No.**131**, *Planetary Nebulae*, D.Reidel, Dordrecht

Shipman,H.L. 1987, in IAU Coll.**95**, *The second conference on faint blue stars*, ed. A.G.Davis Philipp, D.S.Hayes, J.Liebert, L.Davis Press, Schenectady, p.273

Shipman,H.L., Liebert,J, Green,R.F. 1987, *Astrophys.J.* **315**,239

Tassoul,M., Tassoul,J.-L. 1983, *Astrophys.J.* **267**,334

Vauclair,G. 1987, in IAU Coll.**95**, *The second conference on faint blue stars*, ed. A.G.Davis Philipp, D.S.Hayes, J.Liebert, L.Davis Press, Schenectady, p.341

Vennes,S., Pelletier,C., Fontaine,G., Wesemael,F. 1987, in IAU Coll.**95**, *The second conference on faint blue stars*, ed. A.G.Davis Philipp, D.S.Hayes, J.Liebert, L.Davis Press, Schenectady, p.665

Vennes,S., Pelletier,C., Fontaine,G., Wesemael,F. 1988, *preprint*

Wesemael,F., Green,R.F., Liebert,J. 1985, *Astrophys.J. Suppl.* **58**,379

ORIGIN OF THE DA AND NON-DA WHITE DWARF STARS

Harry L. Shipman
Physics and Astronomy Department, University of Delaware
Newark, DE 19716 USA

I. INTRODUCTION

Understanding the origin of DA and non-DA stars -- the bifurcation of the white dwarf cooling sequence -- is one of oldest and perniciously difficult problems in the white dwarf research field. Processes which could play a role have been discussed for years. For example, the idea of diffusive element separation was suggested by Schatzman (1958). The suggestion of convective mixing goes back at least as far as Strittmatter and Wickramasinghe (1971) and Shipman (1972), and this process was actively discussed by a number of authors in the 1970s (see the excellent resume by D'Antona and Mazzitelli 1979).

Recently, two developments have sharpened the debate and brought this question back to center stage. First has been the appearance of two reasonably detailed theoretical proposals for the origins of the bifurcation of white dwarfs into DA and non-DA stars. A second development has been a considerable improvement in our understanding of the composition of the central stars of planetary nebulae, of the nebulae themselves, and of the conditions under which they are formed. An excellent review of the planetary nebula evidence will soon be available (Torres-Peimbert 1988).

My purpose in this paper is to review various proposals for the bifurcation of the white dwarf cooling sequence. There is only a small overlap with two reviews on the chemical composition of white dwarfs presented in the past year (Shipman 1987, 1988). This review complements Sion (1986), in that I focus more on particular mechanisms and scenarios while Sion focuses primarily on the phenomenology. I begin (section II) with a discussion of the evidence in favor of "primordial" theories, theories in which the basic bifurcation of the white dwarf sequence is rooted in events which predate the white dwarf stage of stellar evolution. Section III discusses a competing type of theory, the "mixing" theories in which processes occurring during the white dwarf stage are responsible for the existence of DA or non-DA stars, and the evidence in favor of them. In section IV, the difficulties faced by each class of theory are discussed. Section VI presents a "modest proposal" -- a scenario which seems to me to be most consistent with the current evidence.

II. PRIMORDIAL THEORIES

General Description: This class of theory is one where the distinction between DA and non-DA is hypothesized to lie in the pre-white dwarf stage of stellar evolution (see Figure 1 on the next page). Most recently, the recognition of the thermal pulse phenomenon in the evolution of AGB stars (see, e.g., Renzini 1983, Iben and Renzini 1983, Iben 1984, Iben and MacDonald 1985, 1986, Renzini 1988) has led to a specific proposal that the phase of the onset of the superwind phase determines whether or not the superwind will carry off all of the H envelope. If the H envelope is carried off, a bare He core remains which will turn into a non-DA; if some of the H envelope remains, the remnant will be a DA star with a H shell of order 10^{-4} solar masses.

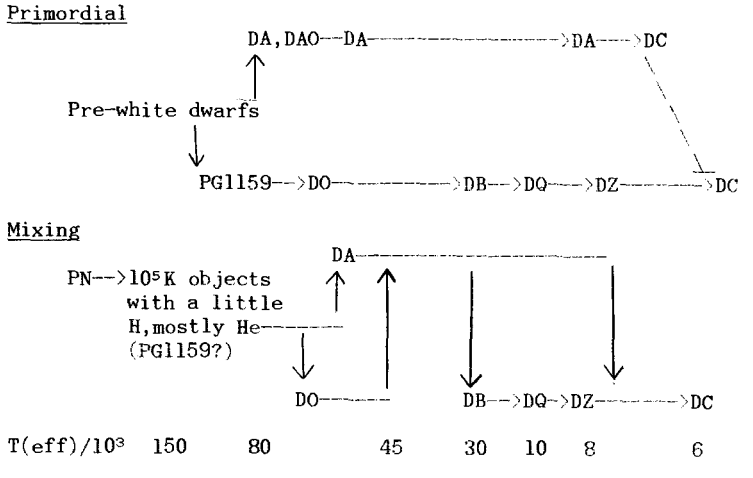

Figure 1: Two extreme explanations for the chemical evolution of white dwarf stars.

Several authors have composed variations on this theoretical theme. For example, Schonberner suggested some years ago (Schonberner 1977) an evolutionary connection between the well-known set of H-deficient red giants (e.g., R Cor Bor stars) and the non-DA stars. Most discussion about H-deficient stars seems to presume that they contribute only a few percent of the remnants of low-mass stars; Schonberner pointed out that, at the time, the deathrate of H-deficient stars was quite uncertain and could be considerably higher. A more modern estimate would be useful.

The Nature of Central Stars of Planetary Nebulae: One strong reason for believing in primordial scenarios for the origin of the white dwarf bifurcation, is that signs of this bifurcation are seen in the central stars of planetary nebulae (CSPN). In the standard classification system for CSPN, two of five

classes of central star spectra are ostensibly hydrogen-poor. The O VI stars are defined by the presence of the O VI doublet at 3811-3834 A, and the WC stars are analogous to the main sequence Wolf-Rayet stars. Sion, Liebert, and Starrfield (1986) mentioned the possibility of a connection between the O VI stars and the PG1159 group of white dwarf stars.

Because of the difficulties in determining whether a spectrum with weak H lines in fact indicates a deficiency of H, a most important recent development has been the analysis of the spectra of a number of CSPN by Kudritzki and collaborators (see Mendez et al. 1986, 1988; Mendez 1987, Kudritzki 1988). A significant number of CSPN show a H deficiency, with an extreme being NGC 246's central star with T(eff) = 130,000 K, H/total < 0.1, He/total = 0.5-0.9, and C/total = 0.1-0.5. 6 of the 22 CSPN with He abundances in Mendez et al. (1988) have y (= N(He/[N(H)/N(He)]) > 0.15; this is 27% of the total. At the other end of the distribution are some CSPN which are distinctly He-poor such as the central star of NGC 7293 with y = 0.009.

Were all of the CSPN as extreme as the two stars described above, the connection between these objects and the two compositional classes of white dwarf stars would be quite clear, especially considering that the proportion of H-deficient objects among the CSPN and among the white dwarf stars are quite similar. In fact, the situation is somewhat more complicated. Most H-deficient CSPN show much more modest enhancements, and among the others a "normal" (i.e., solar) He/H ratio seems more common than a genuine He deficiency. Nevertheless, the idea of a connection between the H-deficient central stars and at least the hottest non-DA white dwarf stars has been discussed rather extensively within the planetary nebula community, if not within the white dwarf community.

There has been considerable debate in the planetary nebula literature as to whether the H-deficient CSPN have any other distinguishing features. Renzini (1988) argues on theoretical grounds that Pop II stars and massive white dwarfs (descended from massive progenitors) should have a greater propensity to produce more massive remnants. There is some observational support for this hypothesis, in that there is some evidence that higher mass CSPN tend to have higher He/H ratios. However, the data (and the theory) are sufficiently uncertain to make all authors rather tentative. The existence of Sirius B as a massive (1.06 solar masses) DA white dwarf is a conspicuous counterexample to any putative trend, if a trend exists.

Nature of the Ejecta from the Superwind Phase: The simple existence of planetary nebulae requires that an evolutionary phase characterized by fast mass loss rates (> roughly 10^{-6} solar masses/yr) must exist (e.g., Renzini 1983). Observations of OH/IR stars confirm that a "superwind" phase exists, with slow velocities (15 km/sec) and with mass loss rates of 10^{-5} to 10^{-4} solar masses/yr. Following this phase, CSPN continue to lose mass, with higher velocities (2000 km/s) but lower mass loss rates (10^{-10} to 10^{-7} solar masses per year; see, e.g.,

Habing 1988). We can see the nature of the matter which is pushed off the star in these evolutionary phases by observing and analyzing the most spectacular manifestation of the planetary nebula phenomenon, namely the nebula itself. Two important objects which may be telling us something important about the origins of the DA and non-DA white dwarfs are the planetary nebulae Abell 30 and Abell 78, objects sufficiently unusual that Mendez has put them in a class by themselves in classifying CSPN (Mendez et al. 1986). The nebulae in these objects contain regions which are almost pure He (Hazard et al. 1980, Jacoby and Ford 1983). I find that this is clear evidence that in some cases at least the superwind phase has reached down below the hydrogen envelope and laid bare the He layer, surrounding a degenerate C/O core.

As is the case with photospheric compositions, the extreme cases of Abell 30 and Abell 78 represent the bitter end of a distribution of nebular chemical compositions which shows, in many cases, evidence that the mass loss process has reached down into stellar layers which have been affected by nucleosynthetic processes. Peimbert and Torres-Peimbert (1983) review work in which they have identified a class of nebulae enriched in He and N. C enrichments are also observed in many objects. Correlations between these enrichments and various stellar evolutionary hypotheses tend to fit general trends in both theory and observation, though details remain to be worked out (Kaler 1985). While the we are a long way away from a clear model which can be tested definitively, there is a clear indication that in many cases the mass loss process which leads to the formation of planetary nebulae digs down to the He layer of the AGB star and exposes processed material.

Generalities and Suggestions for Future Work: Whether or not there is a direct connection between the H-deficient CSPN and/or the H-deficient planetary nebulae and the non-DA white dwarfs, clearly stars which are about to become white dwarfs can scarcely be regarded as a homogeneous class of objects which are then divided into DA's and non-DA's by processes occuring within the white dwarf phase of stellar evolution. The phenomenology strongly suggests a causal connection. A number of future lines of research are suggested on the basis of the above discussion:

Continued study of the composition of the central stars: Many of the conclusions cited above depend on the analysis of the spectra of CSPN by Mendez et al. (1988). The numbers are small, and it's not clear that the sample is not contaminated by selection effects which lead to the preferential discovery of nebulae of, for example, high surface brightness -- which may be related in some unknown way to various properties of the central star. Unfortunately the planetary nebula field has no equivalent of the PG survey, and selection effects may enter in unknown ways. Perhaps the only hope is to continue to study abundances of progressively fainter stars and to hope that selection effects, should they exist, will either become obvious, or that the sample will become

sufficiently well-characterized that they become reduced to an acceptable level.

Particular open questions that suggest themselves are the following:

* What is the range of He/H in the central stars?

* Is there any correlation between He/H and other elemental abundances (particularly the abundance of the CNO elements)?

* How do central star abundance anomalies correlate with nebular abundance anomalies?

* What is the frequency of H-defecient central stars?

* Is there any correlation between H-deficiency and and T(eff) or the mass of the central star?

* What is the deathrate of the classical H-deficient stars?

Winds in Central Stars of Planetary Nebulae: IUE observations in particular have demonstrated that the very high luminosity planetary nebulae, stars with luminosities exceeding 500-1000 solar luminosities, are losing matter continuously as shown by the existence of P Cygni line profiles. For reviews see Heap (1983) and Perinotto (1983). While the wind velocities are high (up to 4000 km s^{-1} in the case of Abell 30 and 78; Kaler, Mo, and Pottasch 1985) the inferred mass loss rates are not too high and rather uncertain. Adopted rates range from 10^{-10} to 10^{-7} solar masses per year, though estimates exist for only a handful of stars.

Over a planetary nebula lifetime of order 10^3 yr, the most rapid mass loss rates could have a significant effect on the structure of the central stars. The H layers left over from AGB evolution contain about 10^{-4} solar masses of material; central stars losing mass at the highest rates which were quoted could completely deplete such a layer during the planetary nebula phase and greatly change the photospheric composition of the central star. It is an open question as to whether this occurs in any star, not to mention whether the phenomenon is sufficiently widespread as to be interesting in an overall evolutionary context. Winds in CSPN are a sufficiently new phenomenon that there are many obvious questions which still need answers. Mass loss rates need to be placed on a firmer footing; the types of stars which do have winds need to be delineated more precisely; and the duration of the wind phase needs to be estimated.

The PG1159 Stars: An additional puzzle regarding the nature of pre-white dwarfs is suggested by the existence of the PG1159 stars, which, considered together with the unusual object H1504+65, occupy the same region of the HR diagram which contains the CSPN. The space density of the PG1159 stars derived by Green and Liebert (1987) of 3 X 10^{-8} pc^{-3}, combined with a lifetime of 10^5 yr suggested by empirical determinations of dP/dt (Winget et al. 1985), suggests a birthrate of 3 X 10^{-14} pc^{-3} yr^{-1}, about 0.1 times the birthrate of single white dwarf stars according to the statistics of Fleming, Liebert, and Green (1986). A more precise delineation of the duration of the "PG1159" phase will be required to

determine whether 10^6 yr is really the correct time to use in this calculation, since it refers to the e-folding time for a structural change in a PG1159 star rather than the time it takes for the star to cool through the PG1159 phase. Considering that this birthrate could be a factor of 3 or even 10 too low, it's possible that the PG1159 stars represent a significant feeder channel into the white dwarf part of the HR diagram. A more precise determination of the space density and birthrate of PG1159 stars, which is in principle possible with better interpretation of their spectra and with discovery of additional objects from the southern hemisphere surveys, is another important open question.

My principal point in calling attention to the existence of the PG 1159 stars is that, considering them and the CSPN together (which one certainly should since they occupy the same part of the HR diagram), there are a number of different types of stars feeding into the upper end of the white dwarf cooling sequence. We don't know the He/H ratios of the PG stars precisely but suspect they are certainly > 1 (Wesemael, Green, and Liebert 1985), corresponding to $y > 0.5$. This strengthens the conclusion that white dwarf precursors have a wide range of He/H ratios. The analysis of O subdwarfs by Kudritzki and collaborators (see Kudritzki 1988; see also Thejll, Charache, and Shipman, in this volume) indicate a similar range of He abundances.

Additional Evidence for Particular Primordial Scenarios: The evidence discussed above regarding the nature of the CSPN tends to support primordial models in general, entirely apart from the particular mechanism which is invoked to explain the origin of DA's and non-DA's. The particular scenario proposed most recently is the idea developed by Iben, Renzini, and co-workers that the phasing of the onset of the superwind, relative to the cycle of He shell flashes, determines whether a star will evolve into a DA or a non-DA. This particular scenario has the advantage of predicting roughly the right relative abundance of DA's and non-DA's (the predicted ratio is about 4:1, which broadly speaking reflects the actual distribution). In addition, the differences between the parent masses and total ages (not just cooling times) of the two types of white dwarfs are expected to be subtle at most. (Subtle differences might be important in explaining the changing ratio of DA:non-DA as a function of T(eff); see section IV below). While we can't observe parent masses and ages of white dwarfs directly, we can observe remnant masses and kinematic properties, which are correlated with total ages and parent masses. The differences between DA's and non-DA's are, at the present time, undetectable.

III. MIXING SCENARIOS

One reason that debate about the origin of DA's and non-DA's has become refreshingly active has been a proposal, articulated in increasing detail in

recent years, that during the white dwarf cooling sequence DA's change into non-DA's and vice versa. The initial presentation of this idea was at the 6th European Workshop on White Dwarf Stars (Liebert, Fontaine, and Wesemael 1987); for subsequent articulations of it see Liebert 1986; Fontaine and Wesemael 1987: Vennes, Pelletier, Fontaine, and Wesemael 1988). Because of these recent reviews of the "case for thin layers," my discussion will be brief and will tend to distinguish from evidence which argues for mixing and accretion in general as opposed to evidence for this proposal that essentially all white dwarf stars have hydrogen layers of 10^{-13} solar masses.

In general, I define "mixing" scenarios as ones in which processes which transform non-DA stars into DA stars, or vice versa, account for the simultaneous existence of both classes of objects. I refer to these as mixing scenarios since convective mixing, in contrast to accretion, seems to be the predominant process , especially so in the thin layer scenario. There are reasons (section V below) to suspect that the role of accretion in the DA/non-DA bifurcation is minimal.

Number Statistics of DA and Non-DA Stars: The single most powerful argument in favor of the role of mixing processes in the chemical evolution of white dwarf stars is that the number ratio of DA's to non-DA's changes dramatically with effective temperature (Liebert 1986 and references therein). Figure 2 below, similar to a diagram in Liebert's review, summarizes the situation:

$T(eff)/10^3$-->	150	75	50	30	15	10	8	6
Type:								
H	//////////	DA	V471		ZZ Ceti			DC
Hybrid H/He	DAO			DBA		DZA		
He	PG1159	DO	///DB		DQ		DZ	
DA/non-DA ratio:	0(!)	7:1	infinite(!)		4:1			1:1

Figure 2: The major spectroscopic classes of white dwarf stars, and the ratio of the two major types, as a function of T(eff). Diagonal slashes (///) represent regions of T(eff) where examples of that particular compositional class don't exist.

Several major transitions are indicated in Figure 2. Starting at the high temperature end of the white dwarf sequence, it is now well established (see, e.g., Fleming, Liebert, and Green 1986, Holberg 1987) that the hottest DA stars have temperatures of 80,000 K and that the hottest non-DA stars have considerably higher temperatures, with the extreme being H1504+65 with T(eff) = 160,000 K. At about T(eff) = 45,000 K, the non-DA stars disappear from sight (or at least from the PG survey), to reappear at T(eff) = 30,000 K. From 30,000 K to 12,000 K, the DA/non-DA number ratio assumes its "canonical" value of 4:1. At very cool temperatures, the ratio increases to 1:1.

Proponents of the mixing scenario interpret these changing number ratios as evidence that DA's are changing into non-DA's and vice versa. The specific

mechanism, as outlined by Fontaine and Wesemael (1987), is based on the proposition that the hydrogen layers in the DA stars are quite thin, 10^{-13} solar masses according to the latest numbers of Vennes et al. (1988). The scenario then works something like the following, as sketched by Fontaine and Wesemael (1987): At very high temperatures, all white dwarf stars appear as PG 1159 stars. The hydrogen is uniformly mixed through their outer layers and so these objects have He-dominated atmospheres, as observed. By the time a star cools to a temperature of 80,000 K, hydrogen diffusing upward through the atmosphere makes some white dwarfs begin to appear as DA stars. By the time white dwarfs cool to a temperature of 45,000 K, diffusion will have separated the mixtures in all white dwarfs, so that all white dwarfs appear as DA stars (explaining the "gap" in the DB sequence). At the lower end of the gap, at T(eff) = 30,000 K, the helium convection zone will break through the thin H surface layer, and transform those stars with thin H surface layers into DB stars again. Several billion years later, when temperatures between 5,000 and 10,000 K are reached, a deep convection zone in the DA's will turn most of the stars into non-DA stars, as was suggested many years ago (Strittmatter and Wickramasinghe 1971, Koester 1976, Vauclair and Reisse 1977, D'Antona and Mazzitelli 1979).

The Montreal group has pointed out that this scenario has the advantage of explaining the observed pattern of photospheric X-ray emission in DA white dwarf stars. Observations of white dwarfs in the x-ray spectral region with the EINSTEIN satellite (Petre, Shipman, and Canizares 1986) have suggested that some opacity source, widely interpreted as helium, increases in its relative abundance with increasing T(eff) in the DA stars. Subsequent observations with EXOSAT (Jordan et al. 1987, Paerels and Heise 1988, ApJ submitted) have clouded the picture somewhat; my own reading of the data is that the correlation is still there, though there are stars which do not appear to follow the abundance pattern (as the original white dwarf X-ray source, HZ 43, stands out as a conspicuous exception to the correlation). Vennes et al. (1988) contend that interpreting the X-ray absorber as He, and interpreting the correlation as due to radiation pressure, requires the existence of very thin H layers on the surfaces of hot DA white dwarfs. It is this analysis which produces the figure of 10^{-13} solar masses which is referred to so frequently in this paper. Another suggestion that the H layer mass is thinner than 10^{-4} solar masses comes from the interpretation of ZZ Ceti pulsations, discussed extensively in other papers at this conference (Brassard, Wesemael, and Fontaine, this volume).

Since the Montreal group is actively exploring this particular scenario, I won't suggest any open questions here. It is true that, at the moment, the only aspect of it where published papers explore it in quantitative detail is the use of thin layers and stratified atmospheres to explain the behavior of X-ray emission from DA white dwarfs. The major problem, as will be discussed in some detail below, is to find whether a consistent definition of what constitutes a

"thin layer" can account for each of the major transitions outlined above, in a way that is consistent with the observations.

IV. DIFFICULTIES WITH EACH SCENARIO

Each of the scenarios sketched above faces some solid pieces of evidence which must be reconciled with it. The changing number statistics illustrated in Fig. 2 present a serious challenge to someone who finds the simplicity of the primordial scenarios to be quite appealing. How can one explain the changing abundances of DA's and non-DA's if this fundamental characteristic is, like sex in human beings, set at the birth of a star as a white dwarf? Advocates of the mixing scenario must face, in general terms, the fact that the separation between He-rich and He-poor stars seems to be established prior to the entry of stars onto the white dwarf cooling sequence. In addition, the thickness of the H layer left after AGB evolution is sufficiently large that general evolutionary considerations would suggest "DA or non-DA forever:" Either the entire H layer is stripped off and the star remains as a non-DA, or that most of it remains ($\sim 10^{-4}$ solar masses) and it is forever a DA.

Primordial Scenarios: Here the principal problem appears to be the changing number ratios illustrated in Figure 2; some changes can be explained readily, and some cannot. The absence of DA's at T(eff) > 80,000 K seems to be one of the more tractable problems. The extension of H shell burning just prior to entry into the white dwarf cooling track can prevent a pre-white dwarf with a significant layer of H from contracting too much and becoming too hot. If there were more hot DA stars discovered (as their will be when the southern hemisphere surveys for faint blue stars, and the necessary follow-up spectroscopy, have been completed), the high temperature boundary of the DA stars can be established more precisely. It also may be possible that additional calculations of the evolution of hot pre-white dwarfs with hydrogen layers of various thicknesses would enlighten matters.

Can the primordial scenario explain the DA X-ray data? The Montreal group has shown that the naive interpretation of the data — that radiation pressure pushes He up to the surface -- won't work. An interesting question for the future, which EUV spectroscopy can illuminate, is whether the X-ray opacity source is indeed He. The few spectra which do exist don't show any promise (so far) of resolving this question unambiguously. When the Extreme Ultraviolet Explorer provides additional spectra in the early 1990s, we may be able to make significant progress.

The existence of the DB gap between 30,000 and 45,000 K may prove to be one of the most difficult problems to solve, in the context of the primordial scenario. While there are some uncertainties in the DB temperature scale, a sufficient number of different models were used by Liebert et al. (1986) that it

would seem difficult to change the temperature of the hottest DB (or the coolest DO) by ~ 30%, especially considering that model uncertainties generally affect lines more than continua, and the continua were used to establish the existence of the gap. Is it possible that DB's cool much faster than DA's in this temperature range? Differential cooling rates which were sufficiently large could solve the problem.

At the cool end, it seems reasonably clear that mixing does occur, as has been known for some time (see D'Antona and Mazzitelli 1979). As D'Antona (1986) emphasized, one can directly use the thicknesses of H convection zones established by various modelers in the 1970s to determine the range of H convective zone thicknesses. Greenstein's (1986) data show that the relative abundance of DA stars seems to start dropping by 9,000 K (though the numbers are small) and is definitely established by 7,000 K. The models published in D'Antona and Mazzitelli indicate that for at least some DA stars the H shell has thinned out to 10^{-9} solar masses. The persistence of DA compositions at very low temperatures (around 5,000 K) indicate that some DA stars have H layers as thick as roughly 10^{-6} solar masses.

Because most expectations are that the hydrogen shells left on red giant stars will have masses of 10^{-4} solar masses, Greenstein's data, interpreted at face value, may present a real problem to the primordial scenario. While there are difficulties in observing the very coolest stars, and even more serious difficulties around the interpretation of the observations, the diminution of the DA/non-DA value from its canonical value of 4:1 is clearly established at temperatures (>7,000 K) where the interpretation of the spectra is reasonably secure. One way around this problem is diffusion induced hydrogen burning (Michaud, Fontaine, and Charland 1984), though Iben and MacDonald (1985, 1986) suggest that only a factor of 2 reduction in envelope thickness can be obtained. Other possibilities are that winds in CSPN, or possible in the white dwarf phase itself (such as the shortward-shifted features detected by Bruhweiler in IUE observations) may play a role. Still another possibility is that there is some physics missing (convective overshoot? rotation? convection in partially degenerate layers?) in the models of the envelopes of cool DA stars which produces mixing with layers of 10^{-4} solar masses, though D'Antona (1986) believes that the stability of such thick layers seems well determined. Another possibility (Iben and MacDonald 1985, 1986) is that the very coolest white dwarfs are the descendants of a different stellar population than the hotter ones, and that characteristics of this population are more favorable for the formation of non-DA stars.

Outstanding problems suggested by the foregoing discussion are:

* What is the temperature of the hottest DA star?
* Is He opacity the real interpretation of the X-ray observations of hot DA

white dwarfs?

* Is there any way of explaining the "DB gap"?

* Just when does the DA/non-DA ratio change from 4:1 to 1:1? (This will require better model atmospheres as well as additional observations.)

* Can diffusion induced hydrogen burning work?

* Do CSPN winds affect the thickness of the H layer in DA stars?

* Is there any way to mix 10^{-4} solar masses of hydrogen into the interiors of cool DA stars?

Mixing Scenarios: These scenarios also face a number of difficulties. Some of the difficulties are particular to the thin-layer proposal recently discussed by the Montreal group, but some seem endemic to any scenario which appeals mainly to processes occurring within the white dwarf evolutionary stage to account for the existence of DA's and non-DA's. The two most fundamental difficulties in the latter category have been recognized for some time:

How does 10^{-4} solar masses of H thin out to 10^{-13} solar masses during the planetary nebula ejection stage? It is true that even in the primordial scenarios also, apparently, require a reduction in the thickness of the hydrogen layer in order to produce mixing at cool temperatures. However, in the primordial scenario, there is 10^{9} years of white dwarf evolution to do the job. In addition, diffusion will tend to concentrate H layers at the surface of the star, so if whatever is destroying the H operates at the interior of the star, there is a natural mechanism which can thin out the H layer and still leave a little remaining at the surface.

The mixing scenario requires a much shorter time scale for thinning out the H layer. If one interprets the scenario in its simple form, where the ancestors of all white dwarf stars are "PG1159" stars, then only 10^{2} to 10^{4} years separates a DA star's departure from the AGB from its entry onto the white dwarf cooling sequence where, apparently, all stars have H layer masses very close to 10^{-13} solar masses. To be fair, however, the observations only require that the thin layer be estabilshed by temperatures of order 45,000 K, giving one a (little) more time. There is the difficulty that to account for the absence of DB stars, the X-ray observations, and the presence of DB stars with T(eff) just below 30,000 K, virtually all white dwarfs have a thin H layer on the top of precisely the same thickness. This thickness is of order 1 part of 10^{9} of the original H layer. It is hard to imagine a mechanism for thinning the H layer which is this finely tuned, which will always remove all but 10^{-9} of the H (and not leave more or remove it completely).

How can the mixing scenario be reconciled with the range of He/H ratios found in white dwarf precursors? Characteristics of white dwarf precursors suggest strongly, though do not compel, that the distinction between DA and non-DA stars has been established among the central stars of planetary nebulae (see above). As

the mixing scenario has been presented so far, the PG 1159 stars have been seen as the ancestors of all white dwarfs. This is incorrect. The temperatures and the birthrates of PG1159 stars indicate that they evolve in parallel with the planetary nebula central stars, not as their evolutionary descendants. The deathrates of PG1159 stars are only 1/10 of the birthrate of white dwarfs, but could be as high as the birthrate of non-DA white dwarfs (which is 1/4 the birthrate of DA white dwarfs in the primordial scenario, and agrees within uncertainties with the deathrates of PG1159 stars). Within the uncertainties, it is easily possible that all non-DA white dwarfs are made from PG1159's. The role of the sdO stars is yet to be determined.

In any case, if the mixing scenario is to remain viable, it has to account for a variety of compositions among white dwarf precursors.

The next indication of compositional change is at the red end of the DB gap, where stars are purported to change from all DA's to a mixture of DA's and DB's. Some of the hottest DB stars are the DB variables, just below this gap, with only PG 0112+104 being a nonvariable DB hotter than the DB instability strip. Small aperture IUE observations currently under way can demonstrate or contradict the presence of H in the hottest DB's just below the gap (Shipman and Liebert, in preparation). D'Antona and Mazzitelli's (1979) graphs indicate that the thickness of the He convective layer is rather small at T(eff) = 30,000 K, suggesting that the residual H might still be visible. Further theoretical exploration of the expected H abundance in the hottest DB stars would be desirable.

While the thin-layer scenario explains the differing ratios of DA's to non DA's illustrated in Figure 2, much work remains to be done until (and if) it is to be accepted as an explanation for the chemical evolution of white dwarf stars. Part of the job, which the Montreal group is actively working on, is a theoretical investigation of envelope evolution in an effort to determine whether the scenario sketched out in the previous paragraph does indeed work. In particular, are the envelope thicknesses envisaged for particular types of white dwarfs consistent with the whole picture? For example, if you postulate that hot DA white dwarfs have a hydrogen layer of 10^{-13} solar masses, can you still explain, on a quantitative basis, why the next mixing phenomenon starts at 10,000 K and is not complete until 6,000 K? D'Antona (1986, referring to earlier work by D'Antona and Mazzitelli 1979) suggests that such a thin layer would mix at hotter temperatures. The following questions occur to me as ones which may be particularly ripe for observational or theoretical investigation at the present time:

* When convective mixing turns DA stars into non-DA stars at 30,000 K is the transition complete and abrupt, or is there a temperature range at which we expect to find a substantial number of stars with mixed composition? Is this where stars like GD 323 (Liebert et al. 1984) fit in? Would one expect all DB stars just below the 30,000 K transition to have at least some residual H?

* How can this scenario account for the existence of at least some DA stars at temperatures considerably cooler than 10,000 K (Greenstein 1986)?

* Is it really He that is providing the X-ray opacity in the hot DA stars?

* Green and Liebert (1987) argue that the number densities of PG 1159 and DO stars are inconsistent with these objects serving as the only feeder channel into the white dwarf cooling sequence. Is it possible to incorporate the CSPN as a separate feeder channel into this scenario?

VI. A MODEST PROPOSAL

With all of the difficulties presented by each scenario, let me close by suggesting a modest proposal, largely unoriginal, which seems to be least inconsistent with the observational data. While it is largely similar to the primordial scenario proposed above, there is an important variation on the theme which is subject to experimental test. The proposed scenario is presented below in Figure 3.

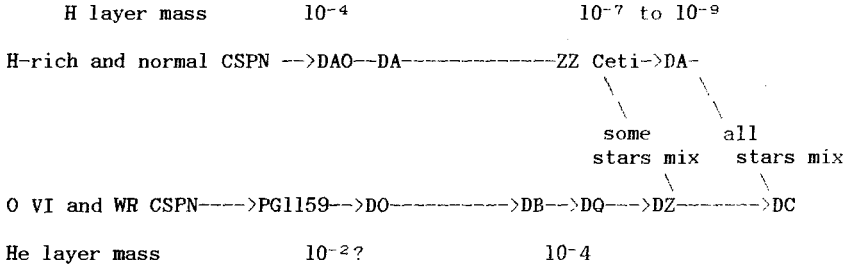

Figure 3. A modest proposal for the chemical evolution of white dwarf stars.

This proposal is basically a two-channel scenario with some additional provisos. In the DA channel, some process -- mass loss and diffusion induced nuclear burning are two possibilities -- reduces the H layer mass from its initial value of 10^{-4} solar masses, the most plausible value from the late stages of red giant evolution, to the value of $<10^{-7}$ which seems to be now required by our interpretation of the ZZ Ceti stars. A range of H layer masses is most consistent with the statistics of very cool DA stars, allowing some DA stars to turn into non-DA stars by convective mixing at temperatures like 9,000 K, with others persisting as DA's down to around 5,000 K.

The non-DA channel is basically similar to that outlined in the primordial scenario, but I mention one additional circumstance. The explanation of the DQ stars as resulting from convective dredge-up of the carbon by Fontaine et al. (1984) suggests, on the basis of rather preliminary calculations, that the thickness of the He layer required to mix the DQ stars should be about 10^{-4} solar masses. While the calculations are rather rough and the agreement with the

functional form of the (C/He) versus T(eff) relation is a bit approximate, the conclusion that the He layer must be thinner than the canonical 10^{-2} solar masses left at the end of the red giant stage seems reasonably firm.

These considerations suggest that some mechanism operates in both channels to reduce the thickness of the outermost layer of white dwarf stars. It does not have to be as finely tuned as in the mixing scenarios, and it can operate over the 10^9 years which separate a newly born white dwarf from the 10,000 K range where we empirically determine white dwarf envelope thicknesses. A modest stellar wind is one possibility; the required mass loss rates are 10^{-11} solar masses/yr for the non-DA's and 10^{-13} solar masses/yr for the DA's. Detection of such a wind is remotely possible for the DA's, depending on its temperature and velocity structure. If diffusion induced nuclear burning can be made to work, this is another way of thinning down the H layer. For this proposal to be viable, of course, we must find a way around the phenomena which it can't explain: the X-ray emission from DA stars and the DB gap are the most serious (see section IV above).

Little has been said about accretion in this paper. Two recently discovered pieces of evidence suggest that accretion from the ISM has little to do with whether a particular white dwarf becomes a DA or a non-DA star. Oswalt et al. (1988) discovered a binary system containing a DA star and a DB star. Since these stars have shared a common trajectory through the interstellar medium (and thus a common accretion history), accretion has had nothing to do with the DA/DB bifurcation in this case. In addition, recent investigations of several DBAZ stars (Kenyon, Shipman, Sion, and Aannestad 1988, Kenyon, Sion, and Aannestad 1988) suggest that the H in these stars comes from accretion, in other words that non-DA stars can successfully resist H pollution.

I thank Alvio Renzini for his cogent and well-deserved criticism of my talk at Mexico City which led to a better understanding on my part of how important the diversity among planetary nebula central stars is in the context of the problem discussed here, and I thank my colleague Jim MacDonald for discussions. I also thank the National Science Foundation (grant AST 87-20530) and NASA (NAG 5-972 and NAG 5-348) for financial support.

REFERENCES

D'Antona, F., and Mazzitelli, I. 1979, Astr. and Ap., 74, 161.

D'Antona, 1986, Memorie della Societa Astronomica Italiana 58, 123.

Fleming, T.A., Liebert, J., and Green, R.F. 1986, Ap.J. 308, 176.

Fontaine, G., Villeneuve, B., Wesemael, F., and Wegner, G. 1984, Astrophys.J. (Letters) 277, L61.

Fontaine, G., and Wesemael, F, 1987 Proceedings of IAU Colloquium 95: the Second

Conference on Faint Blue Stars, D.S. Hayes, J. Liebert, and A.G.D. Philip, eds., (Schenectady: L. Davis Press), 319.

Green, R.F. and Liebert, J. 1987, IAU Colloquium 95, 261.

Greenstein, J.L. 1986, Astrophys. J., 304, 334.

Habing, H., 1988, in Torres-Peimbert 1988, in press.

Hazard, C. et al. 1980, Nature 285, 463.

Heap, S.R. 1983, in IAU Symposium 103: Planetary Nebulae, ed. D.R. Flower, (Dordrecht: Reidel), 375.

Holberg, J. 1987, IAU Colloquium 95, (see Fontaine and Wesemael above),285.

Iben, I., jr. 1984, Ap.J. 277, 333.

Iben, I., jr, and MacDonald, J. 1985, Ap. J., 296, 540.

Iben, I., jr, and MacDonald, J. 1986, Ap. J., 301, 164.

Iben, I., jr., and Renzini, A. 1983, Ann. Rev. Astr. Ap. 21, 271.

Jacoby, G. H., and Ford, H.C. 1983, Astrophys.J. 266, 298.

Jordan, S., Koester, D., Wulf-Mathies, C., and Brunner, H. 1987, Astron. Astrophys., in press.

Kaler, J.B., Mo,J.H., and Pottasch, S.R. 1985. Astrophys.J. 288, 305.

Kaler, J.B. 1985, Ann. Rev. Astron. Astrophys. 23, 89.

Kenyon, S., Shipman, H., Sion, E., and Aannestad, P. 1988, Astrophys. J. Letters, (in press).

Kenyon, S., Sion, E., and Aannestad, P. 1988, Astrophys. J. Letters, in press.

Koester, D. 1976, Astron.Astrophys. 52, 415.

Kudritzki 1988, in Torres-Peimbert 1988.

Liebert, J. 1986, in Proceedings of IAU Colloquium No. 87: Hydrogen-Deficient Stars and Related Objects, eds. K. Hunger, D. Schonberner, and N. K. Rao, (Dordrecht: Reidel), p. 367.

Liebert, J., Wesemael, F., Sion, E.M., and Wegner, G. 1984, Ap.J., 277, 692.

Liebert, J., F. Wesemael, C. Hansen, G. Fontaine, H. Shipman, E. Sion, D. Winget, and R. Green, Ap.J. 309,241.

Liebert, J., Fontaine, G., and Wesemael, F. 1987, in Memoria della Societa Astronomica Italiana: 58, 17.

Mendez, R.H., Miguel, C.H., Heber, U., and Kudritzki, R.P. 1986, in Proceedings of IAU Colloquium No. 87: Hydrogen-Deficient Stars and Related Objects, eds. K. Hunger, D. Schonberner, and N. K. Rao, (Dordrecht: Reidel), p. 323.

Mendez, R.H. 1987, IAU Colloquium 95 (see Fontaine and Wesemael above), 191.

Mendez, R.H., Kudritzki, R.P., Herrero, A., Husfeld, D., and Groth, H.G. 1988, Astron. Astrophys. 190, 113.

Mendez 1988, in Torres-Peimbert 1988, in press.

Michaud, G., Fontaine, G., and Charland, Y. 1984, Ap.J., 280, 247.

Oswalt, T., Sion, E., and Hintzen, P. 1988, Astrophys.J. Letters, in press.

Paerels, F., and Heise, J. 1988, Astrophys. J., submitted.

Peimbert, M., and Torres-Peimbert, S. 1983, in IAU Symposium 103:Planetary

Nebulae, ed. D.R. Flower, (Dordrecht: Reidel), 375.

Perinotto, M. 1983, IAU Sumposium 103.

Petre, R., Shipman, H.L., and Canizares, C.L. 1986, Ap.J. 304, 356.

Renzini, A. 1988, in Torres-Peimbert 1988.

Renzini, A. 1983, in Planetary Nebulae, ed. D. R. Flower, p. 267.

Schatzman, E. 1958, White Dwarfs.

Schonberner, D. 1977, Astr. Ap. 57, 437.

Shipman, H. 1988, in Torres-Peimbert 1988.

Shipman, H. 1987, IAU Colloquium 95, (see Fontaine and Wesemael above), 273.

Shipman, H.L. 1972, Ap. J.,177, 723.

Sion, E.M. 1986, Publ. Astron.Soc.Pac. 98, 821, 1986.

Sion, E. M., Liebert, J., and Starrfield, S.G. 1985, Astrophys.J. 292, 471.

Strittmatter, P.A., and Wickramasinghe, D.T. 1971, Mon. Not. Roy. Astron. Soc., 152, 47.

Torres-Peimbert, S., ed. 1988 Proceedings of IAU Symposium 131: Planetary Nebulae, in press.

Vauclair, G., and Reisse, C. 1977, Astron.Astrophys. 61, 415.

Vennes,S., Pelletier, C., Fontaine, G., and Wesemael, F. 1988, Astrophys.J. (in press).

Wesemael, F., Green, R.F., and Liebert, J. 1985, Ap. J. Suppl., 58, 379.

Winget, D., Kepler, S., Robinson, E.L., Nather, R.E., and O'Donoghue, D. 1985, Ap.J. 292, 606.

MODEL ATMOSPHERES FOR VERY COOL HYDROGEN-RICH WHITE DWARFS

France C. Allard
Rainer Wehrse
Institut f. Theoret. Astrophysik der Universität
Im Neuenheimer Feld 561, D 6900 Heidelberg

I. Introduction

In recent years cool white dwarfs have been studied for various aspects (see e.g. Winget et al.,1987 Winget and van Horn, 1987, Koester, 1987, Liebert, 1980) and much effort has been invested in attempts to interpret the energy distributions of these stars (Greenstein, 1984, Zeidler-K.T. et al, 1986, Liebert et al., 1987, and others). However, it seems that in spite of these efforts the spectra in particular of the very cool objects with effective temperatures below about 6000 K are not yet fully understood, since they are extremely diverse and each objects needs special consideration. In addition, the analyses are extremely difficult because the principal constiuents of the atmospheres (H, He) and elements , which may donate the majority of electrons, are essentially invisible. Since usually only one ionisation stage of an element is present, this implies that the gas pressure P_g is high (compared e.g. to the solar photosphere), the accurate value of P_g , however, cannot be determined reliably.

Similarly, the red dwarfs and subdwarfs exhibit spectra with very different line blanketing, e.g. the Na D lines of G 5-22 and Gl 388 differ in their equivalent widths by more than than a factor of ten (Allard et al., in preparation). It should be noted that the gas pressures in these stars and the white dwarfs may be roughly similar since increases in temperature and gravity change P_g in opposite directions.

Since for M (sub-) dwarfs the spectral differences must due to changes in gravities, effective temperatures, and metal abundances, but not in the hydrogen to helium ratio, we have started a large project to investigate the possible spectral appearances of hydrogen-rich atmospheres with low temperatures and high gravities . It is a special aim to find out to what extent the spectra of the very cool white dwarfs can be understood by means of hydrogen-rich atmospheres only. For this purpose we have calculated a grid of hydrogen-rich atmospheres for both very cool white dwarfs and red dwarfs. In this paper we report first results of this investigation.

In the next section we describe the construction of the atmospheric models. Their basic properties and the resulting energy distributions are briefly discussed in the final chapter III.

II. Model Construction

We have calculated models with the following ranges of parameters: T_{eff} = 3500, 4000, 5000, 6000 K, log g = 5, 7, 8, [Fe/H] = -2, -4, -6. The relative abundances of the metals and the He/H ratio are assumed to be solar. In addition, a few models with T_{eff} = 3000 and 2800 K, with log g = 9 and with solar abundances have been computed.

They are calculated with a revised and updated version of the program previously used for white dwarf atmospheres (Wehrse, 1975, Liebert et al., 1987). The basic assumptions (hydrostatic and local thermodynamic equilibrium, energy transport by radiation and convection) are kept. Major modifications refer to
(i) a new equation of state. The routines are now able to handle flexibly a very large number of species (the number is effectively limited only by the availability of the nessary spectroscopic data and by the computer time the user is willing to spend for the solution of the non-linear system of equilibrium and balance equations);
(ii) checks for the applicability of the impact approximation in all calls for metal line profiles. If a test is negative, the Voigt function is replaced by the quasi-static profile function (Traving, 1960);
(iii) the use of continuum absorption cross-sections from the compilation by Mathisen (1984) replacing some older approximations;
(iv) the consideration of various molecular bands (cf. Wehrse, 1981).

Since we are considering metal poor models mainly and since due to the high pressures hardly show up in the spectra we have taken into account only 50 lines which are presumably the strongest. Evidently, the absorption of the large number of smaller lines is not lost, it will be considered in a separate paper.

III. Results and Discussion

As expected, the pressures in these are considerably lower than in helium-rich configurations (Kapranides and Böhm, 1982), but with $P_g > 10^6$ dyn/cm^2 at $\tau = 1$ for all models they are always much higher than e.g. in the corresponding layer of hotter main sequence stars and lead to very strong line broadening and molecule formation.

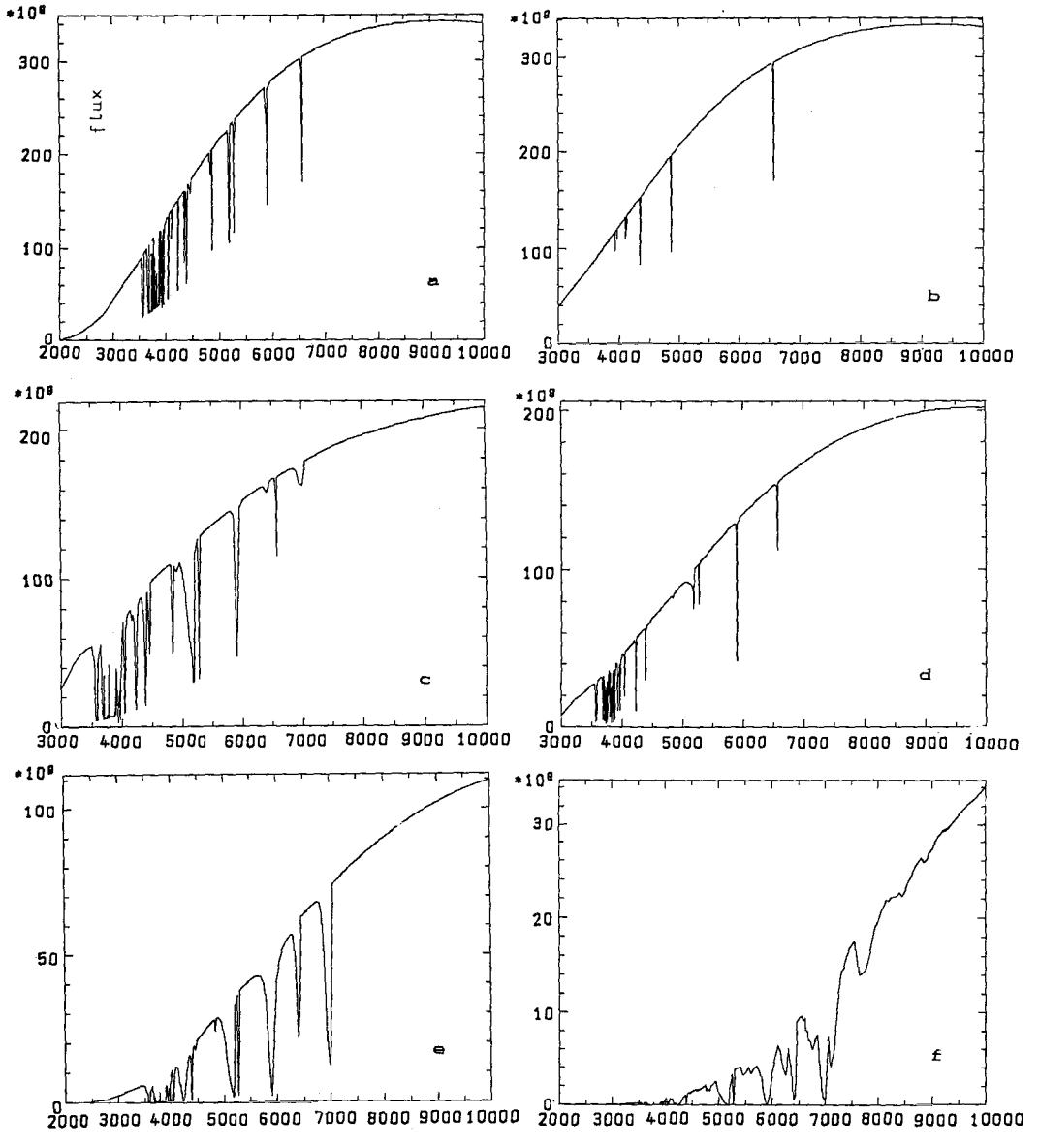

Fig. 1. Examples for calculated spectra: a) T_{eff}= 6000K, [Fe/H] =-2, log g =8; b) T_{eff}= 6000K, [Fe/H] =-6, log g =8; c) T_{eff}= 5000K, [Fe/H] =-2, log g =8 ; d) T_{eff}= 5000K, [Fe/H] =-4, log g =8; e) T_{eff}= 4000K, [Fe/H] =-2, log g =8; f) T_{eff}= 2800K, [Fe/H] =-2, log g =5.

For some models with intermediate parameters we encounter severe difficulties to converge the temperature stratification. We suspect that in the coolest parts of these atmospheres the sudden appearance of water vapor causes an ambiguity in the solution for $T(\tau)$ similar to that found for CO in the outer solar photosphere (cf. Muchmore et al. 1988), but that it is our case much harder to control because the convection is strong and reaches to rather low depths. However, several tests are still needed to confirm this hypothesis.

The calculated spectra (for a few examples see Fig. 1) have the following characteristics:
(i) For effective temperatures 5000-6000 K and [Fe/H] > -5 metal lines dominate; the Hα line is the only Balmer line still visible at T_{eff}= 5000 K.
(ii) Even for [Fe/H] = -6 a few strong metal lines are still visible.
(iii) For effective temperatures of 4000 K and below molecular bands prevail. They make the spectra of white dwarfs and red subdwarfs of some lower temperatures to appear qualitatively rather similar.
(iv) Quasi-static van der Waals broadening is not important for most lines for these parameters, however a moderate increase in the damping constants and/or gravities suffices to change this conclusion.

References:

Greenstein, J.L. 1984, Astrophys. J. **276**,602

Kapranides,S., Böhm, K.H. 1982, Astrophys. J. **256**, 227

Koester,D. 1987, Proc. IAU Coll. 95, Davis Philip,A.G., Hayes ,D.S., Liebert, J.W., eds. 1987, p.329

Liebert, J. 1980, Ann. Rev. Astron. Astrophys. **18**, 363

Liebert,J., Wehrse,R., Green,R.F. 1987, Astron. Astrophys. **175**, 173

Mathisen,R. 1984, Inst. of Theoret. Astrophys. Univ. Oslo, Pub. 1

Muchmore,D., Kurucz, R.L., Ulmschneider,P. 1988, Astron. Astrophys. **201**, 138

Traving,G. 1960, Über die Theorie der Druckverbreiterung, Verlag Braun, Karlsruhe.

Wehrse,R. 1975, Astron. Astrophys. **39**, 169

Wehrse, R. 1981, Mon. Not. Roy. Astron. Soc. **195**, 553

Winget,D.E., Hansen,C.J., Liebert,J., van Horn,H.M.,Fontaine,G., Nather, R.E., Kepler,S.O., Lamb,D.Q. 1987, Astrophys. J. **315**,L77

Winget,D.E., van Horn, H.M. 1987, Proc. IAU Coll. 95, Davis Philip,A.G., Hayes ,D.S., Liebert, J.W., eds. 1987, p.363

Zeidler-K.T.,E.-M., Weidemann,V., Koester,D. 1986, Astron. Astrophys. **155**,356

AN ULTRAVIOLET LOOK AT THE BLUE EDGE OF THE ZZ CETI INSTABILITY STRIP

R. Lamontagne, F. Wesemael, and G. Fontaine
Département de Physique, Université de Montréal
and
G. Wegner
Department of Physics and Astronomy, Dartmouth College
and
E. P. Nelan
University of Texas / S.T.Sc.I.

It has already been shown that most, and probably all, of the DA white dwarfs become variable in a narrow temperature range as they cool down (Fontaine *et al.* 1982). Optical photometry and spectrophotometry has led to several determinations of the boundaries of this instability strip. The strip has been found to cover the range 10300 - 13600 K (McGraw 1979), 10400 - 12100 K (Greenstein 1982), 10000 - 13000 K (Weidemann and Koester 1984) and 11000 - 13000 K (Fontaine *et al.* 1985). Theoretical calculations show that the location of the blue edge is very sensitive to the efficiency of convection used in the unpertubed models (Winget *et al.* 1982; Winget and Fontaine 1982; Fontaine, Tassoul, and Wesemael 1984). Also, the sharpness of this boundary depends on the range of stellar mass and thickness of the hydrogen envelope found in ZZ Ceti stars. Recently, Wesemael, Lamontagne, and Fontaine (1986) and Lamontagne, Wesemael, and Fontaine (1987) have obtained and compared ultraviolet observations of several DA white dwarfs, in or near the instability strip, with published model calculations from Nelan and Wegner (1985), hereafter NW, and Koester *et al.* (1985), hereafter KWZV. They determined the boundaries of the variability region at 11400 - 12500 K or 11700 - 13000 K depending on which grid was used. We present here a reanalysis of these *IUE* observations with an improved grid of model atmospheres in order to define more precisely the location of the blue edge.

The main change to our earlier analyses is the use of a new grid of model atmospheres for DA stars, calculated by two of us (GW and EPN), which removes minor inconsistencies present in earlier calculations of the emergent fluxes. Our data base includes ten ZZ Ceti stars (half of the known sample) and several other DA white dwarfs near the blue edge of the instability strip. The program stars were either observed by us in November and December 1984 and December 1986, or obtained from the *IUE* archives through the Astronomical Data Center. The standard *IUE* calibration for the SWP camera was used in the reduction (Bohlin and Holm 1980). We included the correction derived by Hackney, Hackney, and Kondo (1982) to account for wavelength- and exposure-dependent continuum distortions near 1600Å, and the absolute recalibration of the *IUE* cameras from Bohlin (1986). We also took into account the sensitivity degradation of the SWP camera over time, as described by Bohlin and Grillmair (1988). All these corrections tend to increase the observed flux at longer wavelengths. This results in a slightly lower estimate for the effective temperature of a star in that temperature domain (typically less than $\sim$ 50 K). Before fitting the observations to the model fluxes, each spectrum was smoothed with a five point box-filter. The spectrum was then averaged in bins of 20Å shortward of 1650Å and 30Å longward of that limit. This procedure provides a sufficient spectral resolution at short wavelengths, while ensuring a less noisy continuum near the end of the spectral region. Each bin was weighted equally in the fitting procedure. Finally, the calculated fluxes were forced to match the observations longward of 1650Å. We performed several numerical experiments in which we either fit unsmoothed observations, assigned different weights to each bin (e.g. proportional to its standard deviation), or matched the continuum at a longer wavelength (e.g. 1800Å). The resulting temperatures derived for each star were similar within $\sim$ 100 K.

Effective temperatures were determined using the three different grids of models discussed above. As expected, the temperature ordering of our sample remains the same within each grid. The average temperature difference between fits with our new models and the earlier NW grid is 370 K. The agreement is now much improved with the KWZV grid; our new fits yield a temperature higher than that of the KWZV fits by less than 100 K. This is illustrated in Figure 1 where we display the three fits for the hottest ZZ Ceti star in our sample, G117-B15A. Note that the fits obtained with the earlier NW grid and the KWZV grid differ slightly (ΔT_e < 200 K) from those presented in Wesemael, Lamontagne, and Fontaine (1986) because of small changes

in the fitting procedure and the inclusion of new calibration and sensitivity degradation information. It is particularly instructive to note that the main uncertainty in the determination of the effective temperature may now well reside not with the *IUE* calibration, but with the model calculations.

Also, despite noticeable differences between the KWZV models and our improved grid (see Figure 1), the effective temperatures we derive for all our stars are consistent. We are led to conclude that the temperature of the blue edge, defined by G117-B15A, the hottest ZZ Ceti star in our sample, is near 12900 K with an uncertainty of about 200 K. This result is in very good agreement with previous determinations based on optical observations. For example, Weidemann and Koester (1984) assign a temperature of 13010 K for G117-B15A; Fontaine *et al.* (1985) locate the blue edge at 13000 K. We note that the Strömgren colors of McGraw (1979) would yield $T_e \simeq 13200$ K for G117-B15A when compared to the predicted colors of more modern model atmospheres than he used. A somewhat discrepant determination is that of Greenstein (1982); he assigns a lower temperature of 12100 K to G117-B15A, based on MCSP data and the AB79 absolute-flux calibration. On the Hayes-Latham scale, his temperature would be $\sim$ 500 K higher. Purely spectroscopic determinations (as opposed to photometric means) may help resolve the remaining discrepancies. Such analysis of spectroscopic data on selected ZZ Ceti stars is now underway (Daou *et al.* 1988).

This work was supported in part by the NSERC Canada, by the NSF Grant AST 85-15219 and by a E.W.R. Steacie Fellowship to one of us (GF).

Bohlin, R. C. 1986, *Astrophys. J.*, **308**, 1001.

Bohlin, R. C. and Grillmair, C. J. 1988, *Astrophys. J. Suppl.*, **66**, 209.

Bohlin, R. C. and Holm, A. V. 1980, *NASA IUE Newsl.*, **10**, 37.

Daou, D., Wesemael, F., Bergeron, P., Fontaine, G., and Holberg, J. B. 1988, these Proceedings.

Fontaine, G., Bergeron, P., Lacombe, P., Lamontagne, R., and Talon, A. 1985, *Astron. J.*, **90**, 1094.

Fontaine, G., McGraw, J. T., Dearborn, D. S. P., Gustafson, J., and Lacombe, P. 1982, *Astrophys. J.*, **258**, 651.

Fontaine, G., Tassoul, M., and Wesemael, F. 1984, in *Proceedings of the 25th Liège Astrophysical Colloquium : Theoretical Problems in Stellar Stability and*

Oscillations, A. Noels and M. Gabriel, eds., Université de Liège, p.328.

Greenstein, J. L. 1982, *Astrophys. J.*, **258**, 661.

Hackney, R. L., Hackney, K. R. H., and Kondo, Y. 1982, in *Advances in Ultraviolet Astronomy: Four Years of IUE Research*, NASA CP-2238 (NASA, Washington, DC), p.335.

Koester, D., Weidemann, V., Zeidler K.-T., E. M., and Vauclair, G. 1985, *Astron. Astrophys.*, **142**, L5.

Lamontagne, R., Wesemael, F., and Fontaine, G. 1987, IAU Colloq. No. 95, *The Second Conference on Faint Blue Stars*, A. G. Davis Philip, D. S. Hayes, and J. W. Liebert, eds., L. Davis Press, p.677.

McGraw, J. T. 1979, *Astrophys. J.*, **229**, 203.

Nelan, E. P. and Wegner, G. 1985, *Astrophys. J.*, **289**, L31.

Weidemann, V. and Koester, D. 1984, *Astron. Astrophys.*, **132**, 195.

Wesemael, F., Lamontagne, R., and Fontaine, G. 1986, *Astron. J.*, **91**, 1376.

Winget, D. E. and Fontaine, G. 1982, in *Pulsations in Classical and Cataclysmic Variable Stars*, J. P. Cox and C. J. Hansen, eds., Joint Institute fo Laboratory Astrophysics, Boulder, p.46.

Winget, D. E., Van Horn, H. M., Tassoul, M., Hansen, C. J., Fontaine, G., and Carroll, B. W. 1982, *Astrophys. J.*, **252**, L65.

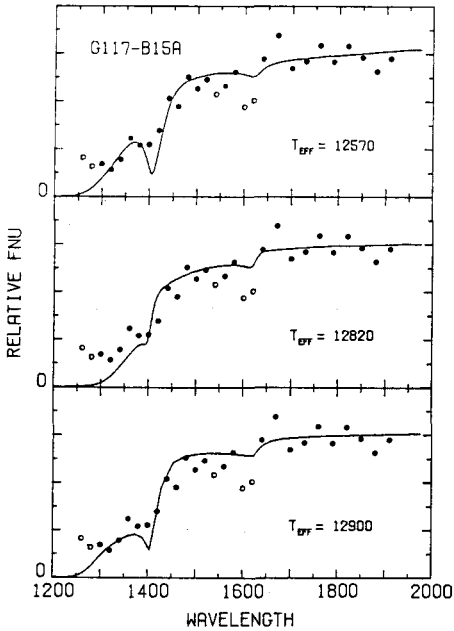

Figure 1. Optimal fits to the spectra of G117-B15A obtained with the Nelan and Wegner (1985) grid (top panel), the Koester *et al.* (1985) grid (middle panel), and our improved grid (bottom panel). Open circles correspond to bins excluded from the fitting procedure.

SPECTROSCOPIC STUDIES AND ATMOSPHERIC PARAMETERS OF ZZ CETI STARS

D. Daou, F. Wesemael, P. Bergeron, and G. Fontaine
Département de Physique, Université de Montréal
and
J. B. Holberg
Lunar and Planetary Laboratory, University of Arizona

The pulsating ZZ Ceti stars cover a narrow range of effective temperatures along the cooling sequence of DA white dwarfs (see, eg., Winget and Fontaine 1982). Fast-photometric searches for pulsating stars in that class have provided strong evidence that the ZZ Ceti phase is an evolutionary phase through which all cooling DA stars will eventually go through (Fontaine *et al.* 1982). Recent investigations, based on optical or ultraviolet photometry and spectrophotometry, have set the boundaries of the instability strip at temperatures near 10,000-11,000 K and 12,000-13,000 K, respectively (McGraw 1979; Greenstein 1982; Weidemann and Koester 1984; Fontaine *et al.* 1985; Wesemael, Lamontagne, and Fontaine 1986; Lamontagne, Wesemael, and Fontaine 1987, 1988).

Our recent endeavours in the study of these variable stars have focused on two specific goals: 1) To investigate theoretically ways to determine, or at the very least constrain, the pulsation properties of ZZ Ceti stars, in particular the ℓ value of the pulsation modes (Brassard, Wesemael, and Fontaine 1987); 2) To improve our knowledge of the time-averaged atmospheric properties of ZZ Ceti stars in order to test specific predictions of the current linear, non-adiabatic g-mode pulsation calculations. Up to now, we have concentrated our efforts in the latter area on narrow-band photometry and ultraviolet spectrophotometry from *IUE* to study, in a consistent manner, reasonably large subsamples of the ZZ Ceti stars.

Relatively high signal-to-noise (S/N$\gtrsim$20) optical spectrophotometry at intermediate resolution ($\sim$3Å) provides another, independent, means of determining basic atmospheric parameters for the variable DA white dwarfs. Indeed, Schulz and Wegner (1981) have demonstrated that simultaneous spectrophotometry of the lower

(Hβ or Hγ) and higher (Hδ or Hε) Balmer lines permits reasonably accurate determination of both T_e and log g in the ZZ Ceti range (with typical uncertainties of ±500 K and 0.25 dex in effective temperature and surface gravity, respectively). This technique seems to have been largely overlooked and, indeed, there has not yet been any systematic study of the optical spectrophotometric properties of ZZ Ceti stars at resolution sufficient to render a comparison with detailed synthetic spectra useful. We have thus embarked on a study of the spectroscopic properties of ZZ Ceti stars with the following aims: Firstly, to provide an independent estimate of the temperature of the boundaries of the instability strip, and the ordering of pulsating stars within it. Secondly, to provide the first spectroscopic estimates of the surface gravity in a large sample of ZZ Ceti stars (spectroscopic fits to two ZZ Ceti stars can be found in Weidemann and Koester 1980). Such estimates will permit a better interpretation of the observed variation in strength of the quasi-molecular λ1400 and λ1600 features in ZZ Ceti stars, since current modelling of these features predicts a significant dependence of their strength on log g (Nelan and Wegner 1985). Furthermore, attention has already been drawn to candidates with possible peculiar gravities in the ZZ Ceti sample. Ross 548, for example, is a suspected low-gravity object (log g$\leq$7.5; Fontaine *et al.* 1985 and references therein) on the basis of its Strömgren colors, while current interpretation of the very short period (109 s) of G226-29 requires a large gravity instead (log g $\geq$8.5; Kepler, Robinson, and Nather 1983).

To this end, we have secured optical spectra at 2.5Å resolution of half a dozen ZZ Ceti stars with the Steward 2.3m reflector, Cassegrain spectrograph and intensified, photon-counting Reticon. The spectra span the range 3900-5000Å, and thus provide good coverage of Hγ, Hδ, and Hε, with partial coverage of Hβ or H8 as well. On the theoretical side, we use a grid of recently-developed LTE model atmospheres for DA stars (e.g. Bergeron, Wesemael, and Fontaine 1988) in our analysis of these data.

Our data analysis technique relies on the sensitivity of various Balmer lines to T_e and log g discussed by Schulz and Wegner (1981). We first fit the Hγ and Hδ profiles of each star at various surface gravities [log g= 7.5 (0.25) 8.5] in order to get a gravity-dependent estimate of the effective temperature. This locus of acceptable T_e-log g combinations is then explored in fits to the gravity-sensitive Hε line. We find the latter to be an effective gravity discriminant as its strength

varies quite dramatically with gravity in the 7.5-8.5 interval. The surface gravity is then fixed by that fit; any other available line (Hβ or H8, depending on the grating tilt for that particular observation) is then checked for consistency.

As an illustrative example, a sample fit to the variable star G226-29 is shown in Figure 1. This is by no means our final fit to this star, as our analysis has been largely exploratory up to this point. And indeed, the indicated temperature, near 11,000 K, is significantly lower than those determined from multichannel spectrophotometry (11,700 K, Greenstein 1982; or 12,470 K, Weidemann and Koester 1984) and ultraviolet spectrophotometry (~12,080 K, an average of estimates given in Wesemael, Lamontagne, and Fontaine 1986).

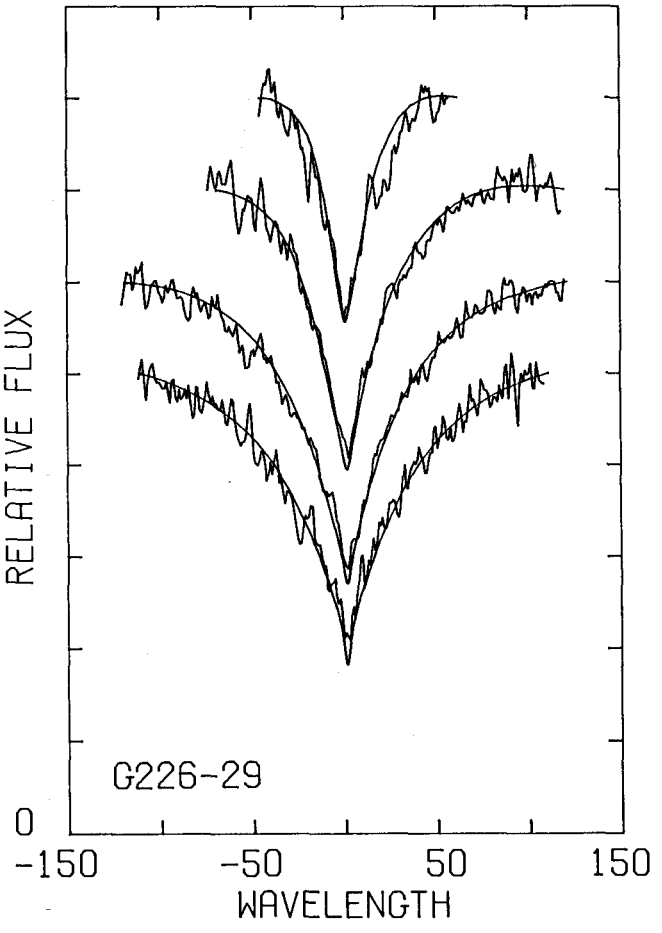

Fig. 1. Sample fits to the spectrum of G226-29. The lines are, from bottom to top, Hβ, Hγ, Hδ, and Hε. The model shown has T_e = 11,000 K, log g = 8.30.

While spectroscopic analysis are essentially free from the calibration problems inherent to optical photometry and ultraviolet spectrophotometry, studies of the high Balmer lines (Hδ and above) seem particularly sensitive to the adopted description of the perturbation of the higher levels of the hydrogen atom. Our current synthetic spectra treat that pressure ionization in terms of a classical Debye model for the last bound level, coupled with an Inglis-Teller cutoff for the last visible level. Some exploratory calculations suggest that the computation of the monochromatic opacity within the framework of the occupation probability formalism developed by Hummer and Mihalas (1988, see also Däppen, Anderson and Mihalas 1987), might lead to noticeable changes in the spectral region under study (see Bergeron, Wesemael, and Fontaine 1988). We note, however, that in contrast to cooler DA stars, where the level perturbation is dominated by interactions with neutral atoms (Bergeron, Wesemael, and Fontaine 1987, 1988), charged particles are here the dominant level perturbers. Clearly these uncertainties, none of which have been explored previously, need to be evaluated in great detail before spectroscopic determinations of effective temperatures and surface gravities of ZZ Ceti stars become trustworthy.

We are grateful to R. Lamontagne for his help in this analysis. This work was supported in part by the NSERC Canada, and by a E.W.R. Steacie Fellowship to one of us (GF).

Bergeron, P., Wesemael, F., and Fontaine, G. 1987, IAU Colloq. No. 95, *The Second Conference on Faint Blue Stars*, A. G. Davis Philip, D. S. Hayes, and J. W. Liebert, eds., L. Davis Press, p.661.

Bergeron, P., Wesemael, F., and Fontaine, G. 1988, these Proceedings.

Brassard, P., Wesemael, F., and Fontaine, G. 1987, IAU Colloq. No. 95, *The Second Conference on Faint Blue Stars*, A. G. Davis Philip, D. S. Hayes, and J. W. Liebert, eds., L. Davis Press, p.669.

Däppen, W., Anderson, L., and Mihalas, D. 1987, *Astrophys. J.*, **319**, 195.

Fontaine, G., Bergeron, P., Lacombe, P., Lamontagne, R., and Talon, A. 1985, *Astron. J.*, **90**, 1094.

Fontaine, G., McGraw, J. T., Dearborn, D. S. P., Gustafson, J., and Lacombe, P. 1982, *Astrophys. J.*, **258**, 651.

Greenstein, J. L. 1982, *Astrophys. J.*, **258**, 661.

Hummer, D. G. and Mihalas, D. 1988, *Astrophys. J.*, in press.

Kepler, S. O., Robinson, E. L., and Nather, R. E. 1983, *Astrophys. J.*, **271**, 744.

Lamontagne, R., Wesemael, F., and Fontaine, G. 1987, IAU Colloq. No. 95, *The Second Conference on Faint Blue Stars*, A. G. Davis Philip, D. S. Hayes, and J. W. Liebert, eds., L. Davis Press, p.677.

Lamontagne, R., Wesemael, F., and Fontaine, G. 1988, these Proceedings.

McGraw, J. T. 1979, *Astrophys. J.*, **229**, 203.

Nelan, E. P. and Wegner, G. 1985, *Astrophys. J.*, **289**, L31.

Schulz, H. and Wegner, G. 1981, *Astron. Astrophys.*, **94**, 272.

Weidemann, V. and Koester, D. 1980, *Astron. Astrophys.*, **85**, 208.

Weidemann, V. and Koester, D. 1984, *Astron. Astrophys.*, **132**, 195.

Wesemael, F., Lamontagne, R., and Fontaine, G. 1986, *Astron. J.*, **91**, 1376.

Winget, D. E. and Fontaine, G. 1982, in *Pulsations in Classical and Cataclysmic Variable Stars*, J. P. Cox and C. J. Hansen, eds., Joint Institute for Laboratory Astrophysics, Boulder, p.46.

FINITE ELEMENT ANALYSIS OF DIFFUSION PROCESSES IN WHITE DWARFS

C. Pelletier, G. Fontaine, and F. Wesemael

Département de Physique, Université de Montréal

The spectral evolution of white dwarfs is governed by diffusion processes which enter into competition with mechanisms such as mass loss, convective mixing, and accretion from the interstellar medium in various phases of the evolution. Until recently, our theoretical understanding of the chemical evolution of these stars has been limited by the very severe numerical difficulties which plague a time-dependent description of the problem. Indeed, diffusion problems in white dwarf interiors and envelopes are particularly demanding from a computational standpoint: they involve relative chemical abundances spanning many orders of magnitude, time integration length of a few billion years, and many physical processes operating with greatly different time constants. We have already introduced in the field a robust numerical technique based on an implicit finite difference scheme designed for nonlinear two-point boundary value problems (Pelletier 1986). This method has been used to investigate a number of problems related to the spectral evolution of white dwarfs (Pelletier 1986; Pelletier *et al.* 1986; Dupuis *et al.* 1987). As requirements for further progress in the field become more exacting and in the interest of improving the efficiency, we have sought to develop even more powerful numerical techniques. We briefly introduce here an efficient computational approach to diffusion problems in white dwarfs based on a *Galerkin finite element method* to solve the convective-diffusion equation in an evolving white dwarf model. As an illustrative example, we discuss some sample results of a detailed investigation of the problem of chemical sedimentation (H, He, and C) in the envelopes of hot white dwarfs and the formation of DA stars.

The convective-diffusion problems encountered in simulating white dwarf evolution are governed by a general nonlinear parabolic equation of the form

$$\frac{\partial u}{\partial t} = \frac{\partial}{\partial r}\left(D(r,u)\frac{\partial u}{\partial r}\right) + F(r,u,\frac{\partial u}{\partial r}) \tag{1}$$

where u is a normalized relative abundance, D and F are general nonlinear functions containing information about the diffusion properties, the model's physical parameters, geometry and external forces, and (r,t) are the radius and time. The fundamental concept of a finite element algorithm is the assumption of known functional dependence for $u(r,t)$ on disjoint, contiguous subdomains of the integration interval; these subdomains are termed finite elements. The first task is to expand the dependent variable u in terms of a set of basis functions $\{\phi_j^{(e)}(r)\}$, each of which is a low-order polynomial (usually a Lagrange interpolating polynomial) of compact support (*i.e.* $\phi_j^{(e)}$ is non-zero over only one element). We assume that u is adequately interpolated on each element by a truncated power series of the form

$$\tilde{u}(r,t) = \sum_{j=1}^{l} c_j(t)\phi_j^{(e)}(r) \tag{2}$$

where $\{c_j(t)\}$ is the set of unknown coefficients of the basis functions and $l-1$ is the degree of the polynomial basis; the interest is thus shifted toward the coefficients $c_j(t)$ which completely specify the solution. We next

insert these expansions into (1) and form what is called a residual:

$$R(r;c) = \frac{\partial \tilde{u}}{\partial t} - \frac{\partial}{\partial r}\left(D(r,\tilde{u})\frac{\partial \tilde{u}}{\partial r}\right) - F(r,\tilde{u},\frac{\partial \tilde{u}}{\partial r}) \tag{3}$$

The residual is a representation of the numerical error introduced on each element by the power series (2); the Galerkin formulation aims at minimizing (3) by orthogonalizing the error to the basis functions. We thus impose for each element:

$$\int_e R(r;c)\phi_j^{(e)}(r)\,dr = 0 \qquad j = 1,\ldots,N \tag{4}$$

(N = number of elements). This process yields for the $c_j(t)$ a system of first-order ordinary differential equations (ODE) of the form:

$$[K]\{C\}' + [L]\{C\} + \{M\} = \{0\} \tag{5}$$

where the coefficients of matrix $[K]$ are given by the orthogonalization properties of the polynomial basis, the coefficients of $[L]$ are related to integrals of function D and the vector $\{M\}$ contains integrals of F and information about the boundary conditions (the superscript prime denotes differentiation with respect to time). Using the finite element procedure transforms an initial-boundary-value problem in a pure initial-value problem. With finite difference theory, the K matrix in equation (5) would be defined as the identity matrix. Finite element theory predicts that $[K]$ be non-diagonal with bandwidth a function of discretization and the degree of the polynomial basis.

If P denotes the degree of the polynomial basis ($P = 3$ in our simulations), then equation (5) is made of $NP + 1$ highly non-linear stiff ODE (an ODE system is called stiff if it has both very rapidly/slowly changing components; a white dwarf is prone to this situation since the diffusion time scales widely differ from one end of the integration domain to the other). The primary difficulty with a stiff system is that most conventional methods for solving it require unrealistic small values of the time step and the solution either blows up or cannot be computed in an affordable CPU time. Even if one can bear the expense, classical methods of solution require so many steps that roundoff errors invalidate the solution. To perform the complete computation, we must use specially designed techniques for stiff systems; we adopted the famous Gear backward differentiation formulas modified to take into account the special structure of (5) induced by the finite element formulation (*c.f.* Gear 1971 and Hindmarsh 1977).

We are currently using this finite element technique in an ungoing detailed investigation of the problem of element sedimentation in the envelopes of hot white dwarfs. The basic premise is the idea that PG 1159-type stars could be the progenitors of the majority of the white dwarfs (Fontaine and Wesemael 1987). In this scenario, it is envisioned that very small traces of H (the tail of the original distribution) are left in the envelope of a pre-white dwarf after the final phase of significant mass loss has terminated. The expected structure of such an object is that of a C/O core surrounded by a He-rich mantle and a He-dominated atmosphere. With time, hydrogen diffuses to the surface and, when an atmosphere worth of this element has accumulated, a newborn DA star can be observed.

In our time-dependent simulations of such events, we have idealized the situation by considering an initial discontinuous distribution made of an almost pure C core surrounded by an almost pure He layer; this mimics very roughly the sharp front due to past He-burning reactions.

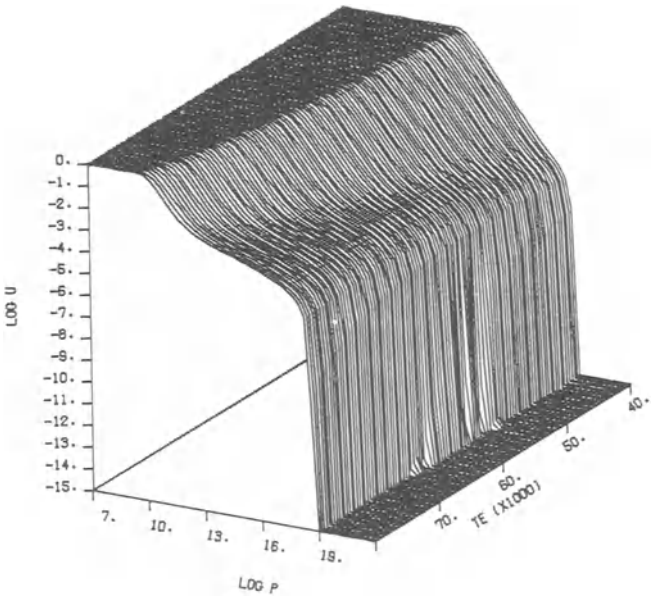

Figure 1. Evolution of the hydrogen distribution in a 0.6 $M_\odot$ model. The star almost instantly becomes a DA, having at 80,000 K a hydrogen layer of $\log q(H) \approx -11.7$; at 40,000 K, $\log q(H) \approx -8.7$.

For simplicity, the small traces of H in the envelope are assumed to be initially uniform. Diffusion alters very quickly these initial configurations. Thus, the evolution of the H distribution is followed in presence of residual H burning and in presence of a changing background due to the diffusion of He and C in the model. Fig. 1 illustrates a sample result for the evolution of a 0.6 $M_\odot$ model with a relatively large quantity of H. The figure shows how the H profile ($\log u \equiv \log\{n(H)/[n(H)+n(He)+n(C)]\}$) given in terms of the pressure ($\log P$) evolves with decreasing effective temperature. In this particular sequence, the assumed quantity of H is so large ($\log u = -4.0$ uniformly distributed in the initial phases), that H accumulates very quickly at the surface and the model turns into a DA white dwarf in about 225 years. These rapid phases are not shown in the figure, and the first profile illustrated corresponds to an age of a 80,000 K star; already a significant layer of H (much more than the thickness of an atmosphere) has built up. The presence of residual nuclear burning is quite obvious as it creates a sharp quasi-stationary front. The hydrogen located above that front is submitted to the concentration gradient's downward pull and the upward push of the pressure gradient. As can be seen, the natural tendency of hydrogen to "float" clearly wins and the top layer simply thickens with time. Nuclear burning slows down the general migration but cannot prevent the transformation of the star into a DA object. The separation is completed when the profile reaches a quasi-equilibrium configuration around $T_e \simeq 40,000$ K. This particular computation required some 6664 time steps with a moving grid made of 120 elements.

Convective-diffusion simulations in white dwarfs are large numerical problems, so efficiency is important. The Galerkin finite element formulation presented here performed very satisfactorily, with increased efficiency when

compared to finite difference codes. For instance, the new code has on the average completed a typical run 5 times faster then the old one used by Pelletier *et al.* (1986) with no significant differences in the results. The overall performance of the finite element method has been quite impressive for all the simulations that we attempted (for further applications, see the paper by Dupuis *et al.* 1988). The resulting algorithm is accurate, fast and stable even for numerically "explosive" problems involving hydrogen.

This research has been supported by the NSERC Canada and a E.W.R. Steacie Fellowship to one of us (GF).

References

Dupuis, J., Pelletier, C., Fontaine, G., and Wesemael, F. 1988, these proceedings.

Dupuis, J., Pelletier, C., Fontaine, G., and Wesemael, F. 1987, in *IAU Colloquium 95, The Second Conference on Faint Blue Stars*, eds. A.G.D. Philip, D.S. Hayes, and J. Liebert (Schenectady: L. Davis Press), p. 657.

Fontaine, G., and Wesemael, F. 1987, in *IAU Colloquium 95, The Second Conference on Faint Blue Stars*, eds. A.G.D Philip, D.S. Hayes, and J. Liebert (Schenectady: L. Davis Press), p. 319.

Gear, C. W. 1971, *Numerical Initial Value Problems in Ordinary Differential Equations* (Prentice-Hall).

Hindmarsh, A. C. 1977, *GEARB: Solution of Ordinary Differential Equations Having Banded Jacobian*, Lawrence Livermore Lab. Rep. UCID-30059.

Pelletier, C. 1986, Ph.D. thesis, Université de Montréal.

Pelletier, C., Fontaine, G., Wesemael, F., Michaud, G., and Wegner, G. 1986, *Astrophys. J.*, **307**, 242.

HEAVY ELEMENT ABUNDANCES PREDICTED BY RADIATIVE SUPPORT THEORY IN THE ATMOSPHERES OF HOT WHITE DWARFS

P. Chayer, G. Fontaine, and F. Wesemael
Département de Physique, Université de Montréal

The surface composition of a white dwarf evolves as a result of the interaction of several mechanisms, the most important of which being gravitational settling. In the early phases of the evolution, theory shows that selective radiative levitation can occasionally defeat settling and, thus, prevent the formation of a pristine pure hydrogen (helium) atmospheric layer in a hot DA (non-DA) white dwarf (Fontaine and Michaud 1979; Vauclair, Vauclair, and Greenstein 1979). The exciting discovery of sharp metallic features in the ultraviolet spectra of several hot DA and non-DA stars alike resulting from the work of several investigators has provided the essential motivation for further theoretical investigations of radiative levitation in the atmospheres of white dwarfs. Additionnal impetus comes from the continuing investigations of hot DA white dwarfs carried out by Bruhweiler and Kondo which have already revealed a most interesting observational pattern of heavy elements in these stars (Bruhweiler 1985). Moreover the recent availability of theoretical equivalent widths of selected astrophysically important ultraviolet metal lines in hot DA white dwarfs (Henry, Shipman, and Wesemael 1985) makes a comparison between theory and observations -in at least this type of stars- a timely and useful exercise.

We have recently completed a detailed investigation of the effects of selective radiative support on C, N, O, and Si in model atmospheres and envelopes of both DA and non-DA white dwarfs. For each of these elements, and for a large number of models, we have derived the abundance profiles as a function of depth which are obtained by assuming an equilibrium between gravitational settling and radiative levitation. The bulk of our calculations are formally valid in optically thick layers only, i.e. in regions below the Rosseland photosphere. This is the same level of approximation which has been used so far in the few investigations devoted to radiative forces in white dwarfs (Vauclair, Vauclair, and Greenstein 1979; Morvan, Vauclair, and Vauclair 1986). Radiative accelerations have also been computed for a small subset of models taking into account the effects of radiative transfer in optically thin layers and the non-uniform abundance profile on the synthetic spectra. As in the case of hot B subdwarfs discussed by Bergeron *et al.* (1988), we find that the non-uniformity of the equilibrium abundance distribution of an element sup-

ported by radiative levitation does not generally lead to line profiles and strengths which are markedly different from the line profiles and strengths obtained under the assumption of a uniform distribution with a value of the abundance equal to that of the non-uniform model at the Rosseland photosphere. The full results of our investigation will be presented elsewhere (Chayer *et al.* 1988). In this short communication, we restrict ourselves to some sample results.

Fig.1 (Fig.2) shows the equilibrium abundance profiles for DA (non-DA) models with $M/M_{\odot}=0.6$. Note that the envelope parameters have been taken from the evolutionary tracks of Winget, Lamb, and Van Horn (1988); the gravity therefore decreases (as it should) with increasing effective temperature. As compared to cosmic abundance ratios, only underabundances of C, N, O, and Si can be supported by radiative levitation in the outermost layers of DA white dwarfs with $M/M_{\odot}=0.6$. The qualitative behavior of the equilibrium abundance profile is the same for C, N, and O. In particular, note that the surface abundance decreases monotonically with decreasing effective temperature for these elements. At high effective temperatures, there are two reservoirs supported by radiative forces. These two reservoirs are separated by a layer in which the dominant ionization state is that of the noble gas configuration which implies that radiative support is considerably reduced there. For $T_e<40{,}000$K, only the outer reservoir can be supported. The behavior of the surface abundance of Si is qualitatively different because that element goes through its noble gas configuration in the surface layers for the effective temperatures illustrated here. Thus, small traces of silicon can be supported at the photosphere of 0.6 $M_{\odot}$ DA white dwarf models with $T_e\geq 75{,}000$K, no support is possible in the range $75{,}000\text{K}>T_e\geq 50{,}000$K, and silicon can again reappear at the surfaces of cooler white dwarfs.

The surface abundances of the four elements considered all decrease monotonically with decreasing effective temperature in models of non-DA white dwarfs (Fig.2). At high effective temperatures ($T_e\geq 75{,}000$K), slight overabundances of N can pollute the atmospheres of these stars, but, otherwise, underabundances are predicted. These are generally smaller than in the case of hot DA stars. However, the appearance of a superficial helium convective zone around $T_e\approx 65{,}000$K plays against radiative support in the cooler objects because radiative levitation can only be effective at the base of the convection zone where ionization is more complete and bound-bound absorption becomes less important. Below $T_e\approx 35{,}000$K, radiative support becomes totally negligible in the atmospheric layers of He-rich white dwarfs. The formation of a helium convection zone also prevents Si from reappearing at lower effective temperatures; no Si is predicted in the atmospheres of 0.6 $M_{\odot}$ non-DA white dwarfs with $T_e<85{,}000$K.

The results of our extensive calculations should be eventually used in a detailed comparison of the predictions of radiative support theory with the observations. Currently, such a comparison remains quite limited because detailed abundance analyses have been carried out for only three hot white dwarfs: the DA stars Wolf

1346 and Feige 24 and the DO object PG 1034+001. Chayer *et al.* (1987) have demonstrated that there are large discrepencies between the predicted and observed C abundances for both Feige 24 and PG 1034+001. They suggest that another mechanism (such as a weak wind) possibly interferes with settling and radiative levitation in these hot objects. At the very least, it appears that the idea of a simple equilibrium between gravitationel settling and radiative support does not pass the test in these stars.

Further evidence in that direction is gained by using the sample of some 20 bright, hot DA white dwarfs currently being investigated by Bruhweiler and Kondo. Pending the final results of their detailed studies, Bruhweiler (1985) has nevertheless announced a most interesting observational pattern of heavy elements in hot DA stars: while no features are detected (at the 15 mÅ level) in high-resolution *IUE* spectra of a minority of objects, only Si features are observed for stars with $T_e \leq 40{,}000K$ in the rest of the sample, and features of Si, C, and N are observed in the hotter stars. This qualitative pattern can be contrasted to the predictions of radiative support theory. As an illustrative example, we have used the predicted abundances at the Rosseland photosphere of our 0.6 $M_\odot$ DA models to derive the strenghts of several spectral features which are accessible in the *IUE* window. In this process, we have used the equivalent widths computed in the spectrum synthesis study of Henry, Shipman, and Wesemael (1985). The results are shown in Fig.3 which puts in evidence the predicted equivalent width of a given spectral line as a function of effective temperature. Oxygen features have not been considered by Henry, Shipman, and Wesemael (1985) because they are only of relevance to effective temperatures higher than that of the hottest known DA white dwarf in the *IUE* spectral range. Even adopting a very conservative detection limit of 100 mÅ, we find that the observed abundance pattern is not reproduced as carbon features for example would still be easily detectable in DA white dwarfs with $T_e \leq 40{,}000K$. Coupled to the fact that no features are observed in some of the DA objects in the Bruhweiler and Kondo sample, this suggests very strongly that the predictions of simple radiative support theory are inadequate. We note that the absence of metallic spectral features in some of the hot DA stars observed with the *IUE* in the high resolution mode is usually blamed on known (or expected) higher gravities in these stars. Preliminary inspection of our detailed results indicates that, while the expected photospheric abundances are indeed reduced in higher gravity objects, spectral features should still be detectable.

The main conclusion of this paper is that simple radiative support theory fails to explain the observed abundance pattern of heavy elements in hot white dwarfs. At least one other mechanism must interfere with gravitational settling and radiative levitation in such objects. We note that the studies of Bruhweiler and Kondo (1981, 1983) already point to a very natural candidate: the presence of weak winds. The work of these investigators strongly suggests that the outermost layers of very hot white dwarfs are permeated with a wind which eventually dies out with cooling. It is important to point out that such winds do not need to, and indeed cannot, be

very large. This is because abundance anomalies (the large underabundances usually observed in white dwarfs) cannot be built if the wind velocity is much larger than the diffusion velocities of various species. Michaud (1987) finds somewhat weak constraints of $3X10^{-11}$ - $3X10^{-16}$ $M_{\odot}yr^{-1}$ for the maximun mass loss rate allowing chemical sedimentation and settling in white dwarfs. We note that a mass loss rate as small as 10^{-21} $M_{\odot}yr^{-1}$ can still play havoc with the predicted surface abundances in presence of radiative support. For example, we cannot help but notice that the outer reservoirs of C and N are opened at the surface of a DA white dwarf and could easily be emptied by such a wind in the hot phases of the evolution (Fig.1). At the same time the reservoir of Si is not opened at the surface in a significant effective temperature range. Hence, it is strongly tempting to speculate that first C and then N are totally expelled from the photosphere of DA white dwarfs in the very hot phases of the evolution, while Si "hides" below the surface until it is caught by the effects of wind and becomes eventually visible in the later phases of the evolution. A dependance on gravity for the effects of winds is also easily envisioned. Whether or not this speculative scenario is at all correct rests with a detailed investigation of the interaction between settling, radiative levitation, and mass loss in hot white dwarfs. We have embarked on such a project and will report our results in due time.

This work was supported by NSERC Canada, and by a E.W.R. Steacie Fellowship to one of us (GF).

Bergeron, P., Wesemael, F., Michaud, G., and Fontaine, G. 1988, *Ap. J.*, in press.
Bruhweiler, F.C. 1985, *Bull. Amer. Astron. Soc.*, **17**, 559.
Bruhweiler, F.C., and Kondo, Y. 1981, *Ap. J. (Letters)*, **248**, L123.
Bruhweiler, F.C., and Kondo, Y. 1983, *Ap. J.*, **269**, 657.
Chayer, P., Fontaine, G., Wesemael, F. and Michaud, G. 1987, in *IAU Colloquium No. 95, The Second Conference on Faint Blue Stars*, A. G. D. Philip, D. S. Hayes and J. Liebert, eds., L. Davis Press, Schenectady, p. 653.
Chayer, P., Fontaine, G., Wesemael, F. and Michaud, G. 1988, in preparation.
Fontaine, G., and Michaud, G. 1979, *Ap. J.*, **231**, 826.
Henry, R.B.C., Shipman, H.L., and Wesemael, F. 1985, *Ap. J. Suppl.*, **57**, 145.
Michaud, G. 1987, in *IAU Colloquium No. 95, The Second Conference on Faint Blue Stars*, A. G. D. Philip, D. S. Hayes and J. Liebert, eds., L. Davis Press, Schenectady, p. 249.
Morvan, E., Vauclair, G., and Vauclair, S. 1986, *Astr. Ap.*, **163**, 145.
Vauclair, G., Vauclair, S., and Greenstein, J.L. 1979, *Astr. Ap.*, **80**, 79.
Winget, D.E., Lamb, D.Q., and Van Horn, H.M. 1988, in preparation.

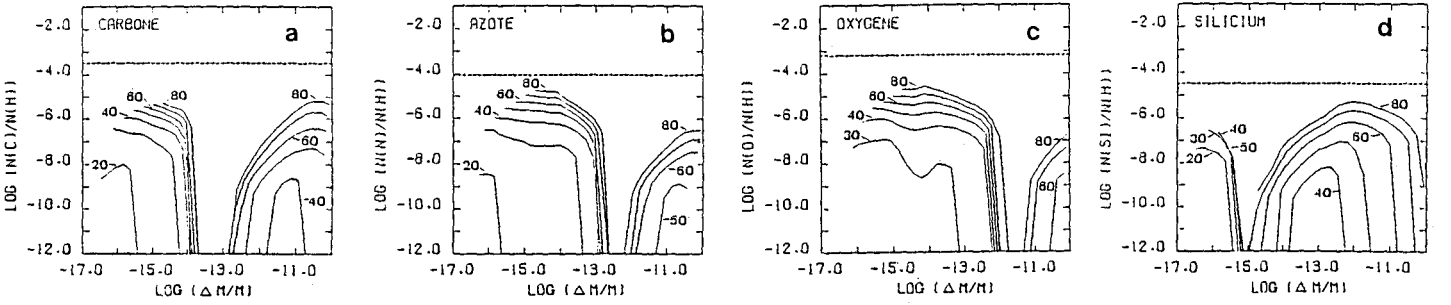

Fig. 1

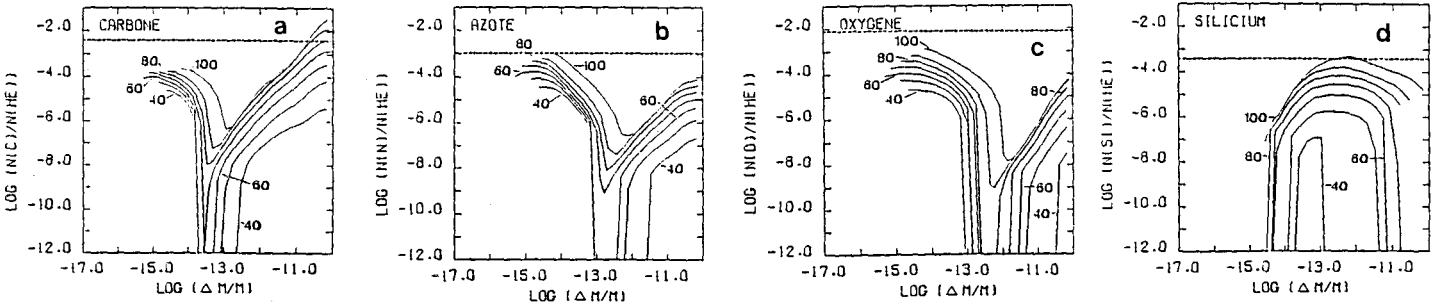

Fig. 2

Fig. 1 a),b),c),d). Equilibrium abundance profiles for DA models with $M/M_{\odot}$=0.6. The effective temperatures of each model are indicated by a number ($X10^{3}K$).

Fig. 2 a),b),c),d). Same as fig. 1, but for non-DA models.

Fig. 3. Predicted equivalent widths of a few spectral lines as a function of effective temperature. The wavelengths of each spectral line are: C II (1335 Å), C III (1176 Å), C IV (1250 Å), N V (1240 Å), Si II (1263 Å), and Si IV (1395 Å).

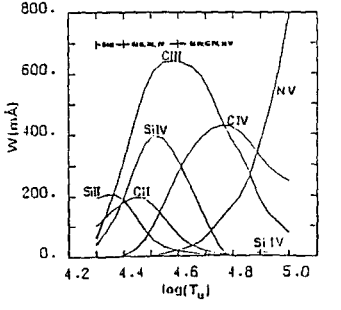

Fig. 3

SECOND-ORDER EFFECTS DUE TO ROTATION IN PULSATING DA WHITE DWARFS

P. Brassard, F. Wesemael, and G. Fontaine.
Département de Physique, Université de Montréal

The ZZ Ceti star L 19-2 is a stable pulsator whose light curve has now been deciphered with the help of over 300 hours of white light, high-speed photometry (O'Donoghue and Warner 1982, 1987, hereafter ODW). The analysis indeed reveals the presence in the light curve of five coherent oscillations, with periods ranging from 113s to 350s. Among those, the 192s oscillation possesses three components, almost equally separated in frequency. Most importantly, the slight, but statistically significant, inequality in the frequency spacing of the triplet has been interpreted by these authors as second-order splitting of rotationally-perturbed g-mode oscillations. And indeed, the measured splitting appears consistent with the theoretical predictions of Chlebowski (1978), which are based on somewhat archaic white dwarf models. As pointed out by ODW, it is clearly of great interest to investigate 1) to what extent theoretical predictions based on more realistic, current-generation white dwarf models agree with ODW's identification, and 2) to what extent such second order effects can, eventually, be used to identify individual pulsation modes or constrain the structural parameters of variable white dwarf stars. Motivated by these questions, we have initiated a study of second-order effects due to rotation in ZZ Ceti stars, and we report here the first results of this program.

The perturbed state of a star undergoing non-radial oscillations can be written as a superposition of eigenmodes, each characterized by one eigenfrequency and three quantum numbers: k, the radial wavenumber, and l and m the spherical harmonics indices which describe the angular geometry. For a non-rotating star, the eigenfrequencies are degenerate in m, and depend only on k and l. In the presence of slow rotation ($\Omega \ll \sigma_{kl}$) we can write, for an external observer

$$\sigma_{klm}=\sigma_{kl}+m(1-C_{kl})\Omega+O(\Omega^2) \ , \qquad (1)$$

where C_{kl} is a function of the structure of the star and of the particular eigenmode. The pulsation mode is now split in 2l+1 equally-spaced frequencies. A nice example of this splitting is the 109.2s triplet in G226-29, with observed frequencies of 9.134721, 9.150865, and 9.167009 mHz separated by 0.016144 mHz (Kepler, Robinson, and Nather 1983).

It is also possible to expand equation (1) to include second-order terms (Chlebowski 1978; Saio 1981; Smeyers and Martens 1983). We write, following Chlebowski's notation

$$\sigma_{klm}=\sigma_{kl}+m(1-C_{kl})\Omega+\frac{1}{2\sigma_{kl}}(P_{kl}-m^2Q_{kl})\Omega^2+O(\Omega^3) \ . \qquad (2)$$

For large-k modes in white dwarfs, the *asymptotic* values of P and Q are given by

$$P=\frac{4[2l(l+1)-3]}{(2l-1)(2l+3)} \quad \text{and} \quad Q=\frac{4l(l+1)(2l^2+2l-3)-9}{l^2(l+1)^2(2l-1)(2l+3)} \ . \qquad (3)$$

The approach of Saio (1981) is used to calculate P and Q.

Equations (1) and (2) are valid only if solid body rotation is assumed for the star. If differential rotation is included, equation (1) should be rewritten (Hansen, Cox, and Van Horn 1977)

$$\sigma_{klm}=\sigma_{kl}+m(1-C_{kl}-C'_{kl|m|})\Omega \ . \qquad (4)$$

We ignore departures from solid body rotation here, as Tassoul and Tassoul (1983) have shown that such departures are likely to be small in white dwarfs. In addition, we leave out as well the perturbations to the eigenfrequencies that could be caused by a magnetic field, as recently shown by Jones *et al.* (1988).

We have thus adapted Saio's (1981) formalism, developed for a polytropic star, to the case of more realistic stellar configurations. Furthermore, to evaluate the second order terms, the distorted geometry of the star caused by rotation is first required. To this end, we used a Clairaut-Legendre expansion (see, for example, Tassoul 1979), although more elaborate methods are possible. Sample calculations of the first- and second-order splitting terms (C,P and Q, respectively) are presented in Table 1 for a model at 0.8 $M_{\odot}$, with a hydrogen (helium) fractional layer mass of 10^{-12} (10^{-2}) and an effective temperature of 11,519K, taken from the extensive evolutionary sequences of Tassoul, Fontaine, and Winget (1988).

TABLE 1

First- and Second-order Splitting Terms
$M/M_{\odot}$=0.8 , T_e=11,519K

l	k	Period(s)	C_{kl}	P_{kl}	Q_{kl}
1	1	222.4	0.457	0.868	-0.039
1	2	270.4	0.270	1.174	0.063
1	3	291.0	0.458	0.873	0.185
1	4	371.0	0.444	0.895	-0.073
1	5	394.9	0.436	0.909	0.126
1	6	455.8	0.484	0.828	-0.035
1	∞	-----	0.500	0.800	-0.050
2	1	129.2	0.134	1.751	0.270
2	2	165.8	0.144	1.741	0.249
2	3	191.9	0.004	1.901	0.293
2	4	219.7	0.151	1.734	0.279
2	∞	-----	0.166	1.714	0.274

Similar calculations were performed for a number of models culled from several evolutionary sequences of varying stellar mass, and hydrogen and helium layer masses in order to compare the predicted second-order splitting with that measured by ODW. We summarize, below, the observed structure of the 192s mode in L 19-2.

TABLE 2

Observed Structure of the 192s oscillation in L19-2			
Period (s)	Frequency (mHz)	$\Delta\nu$ (mHz)	ε (mHz)
192.128824	5.2048411	0.0129912	$-(1.9\pm0.4)\times10^{-5}$
192.609575	5.19184989	0.0129931	
193.092808	5.1788568		

On the basis of equation (2), the measured second-order splitting ε can be related to the Q coefficient by

$$Q=-\varepsilon\nu_0\left[\frac{\Delta m(1-C_{kl})}{\Delta\nu}\right]^2 . \qquad (5)$$

For a l=1 mode, the value of C is of the order of C=0.4±0.1 (see Table 1) and thus the ODW measurement yields Q=0.02±0.01. A comparison with the Q-values displayed in Table 1 suggests that small, positive values are possible only for some low-k modes. Furthermore, a period as short as 192s for l=1 can only be reproduced for low-k values (k=1 or 2) if the stellar mass is 0.8 $M_\odot$ and both the helium and hydrogen layer masses are small. These constraints are summarized in Table 3. For a given model, the range of values of k corresponding to Q>0 is indicated, as well as the minimal period (minimal k). The results suggest that the range of allowed values of k decreases with decreasing H and He outer layer masses, and that the minimal period decreases as well. If the 192s oscillation of L 19-2 is to be associated with a l=1 mode, the star must have a higher than average gravity for a white dwarf. This is amenable to observational verification. At the same time, however, this solution is by no means unique; indeed our analysis suggests that both the Q-measurement and the observed period might also be consistent with a l=3 mode in a DA star at M$\geq$0.6$M_\odot$ with thick ($M_{He}\geq10^{-2}$) helium layers. This would require that only the components with m=0,±1 of the 192s mode and m=0,±3 of the 113s mode be

observable. Clearly, we have only scratched the surface, and the potential of this new tool for the study of L 19-2, and ZZ Ceti stars in general, has barely been tapped.

TABLE 3

Modes with Q>0 (l=1), in Various Stellar Models				
Mass	$\log(M_{He})$	$\log(M_H)$	k=123456789	Minimal Period (s)
0.6	-2	-6		315
0.6	-2	-10		330
0.6	-2	-12		300
0.6	-6	-10		280
0.6	-6	-12		280
0.8	-2	-6	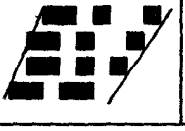	250
0.8	-2	-10		265
0.8	-2	-12		255
0.8	-6	-12		235

We are grateful to B. Warner for drawing our attention to and triggering our interest in this remarkable observational result, and to S.D. Kawaler, M. Tassoul and P. Smeyers for useful discussions. This work was supported in part by the NSERC Canada, by the Fund FCAR (Québec), and by a E.W.R. Steacie Memorial Fellowship to one of us (GF).

REFERENCES

Chlebowski, T. 1978, *Acta Astr.*, **28**, 441.

Hansen, C.J., Cox, J.P., and Van Horn, H.M. 1977, *Ap. J.*, **217**, 151.

Jones, P.W, Pesnell, W.D., Hansen, C.J., and Kawaler, S.D. 1988, Preprint.

Kepler, S.O., Robinson, E.L., and Nather, R.E. 1983, *Ap. J.*, **271**, 744.

O'Donoghue, D., and Warner, B. 1982, *M.N.R.A.S.*, **198**, 293.

O'Donoghue, D., and Warner, B. 1987, *M.N.R.A.S.*, **228**, 949.

Saio, H. 1981, *Ap. J.*, **244**, 299.

Smeyers, P., and Martens, L. 1983, *Astr. Ap.*, **128**, 133.

Tassoul, J.L. 1979, *The Theory of Rotating Stars*, (Princeton : Princeton University Press), p. 96.

Tassoul, M., Fontaine, G., and Winget, D.E. 1988, in preparation.

Tassoul, M., and Tassoul, J.L. 1983, *Ap. J.*, **267**, 334.

ARE PULSATIONS A USEFUL PROBE OF THE STRUCTURE OF THE OUTER LAYERS OF WHITE DWARFS ?

P. Brassard, G. Fontaine, and F. Wesemael
Département de Physique, Université de Montréal
S.D. Kawaler
Center for Solar and Space Research, Yale University

The most fundamental aspect of white dwarf seismology is the determination of the gravity-mode (g-mode) period structures of models of isolated pulsating white dwarfs. These stars show multiperiodic luminosity variations which result from the superposition of excited pulsation modes. Among the many oscillation modes available in the very rich nonradial g-mode spectra of white dwarfs, the observed modes are selectively chosen by a filtering mechanism. Although the period evolution is strongly tied to the core temperature evolution in a white dwarf, the period structure remains largely specified by the mechanical properties of the star. The most basic structural feature of a white dwarf is its highly degenerate interior, which leads to nearly isothermal and nearly isentropic stratifications in the core region containing more than 99% of the mass of the star. In particular, because the density gradient is almost adiabatic throughout the interior of a white dwarf, the Brünt-Väisälä frequency (see below) is very small there and low-order g-modes cannot propagate. As a result, g-modes are essentially envelope modes in white dwarfs, with large amplitudes occuring only in the non-degenerate outer layers. One can thus expect that g-modes in white dwarfs are extremely sensitive to envelope properties such as compositional stratification and partial ionization mechanisms. Compositional stratification is, in fact, the second structural feature of a white dwarf model which has strong effects on the period structure. Indeed, trapped modes result when a resonance or near-resonance occurs between the local g-mode radial wavelength and the thickness of one of the composition layers. This results in a period structure which strongly bears the signature of compositional stratification in the outer layers. Thus, it has been widely accepted that white dwarf pulsations probe primarily the outer layers of these stars. This point of view has been borne out by detailed pulsation calculations carried out by several independant groups (see Winget 1987 and references therein).

A surprisingly different stance has been taken recently by Pesnell (1987; see also Cox *et al.* 1987) who claims that g-modes of white dwarfs probe much deeper than previously thought. Although such modes have generally very small core amplitudes, the point is made that the only appropriate method to describe where the period of a mode is determined is to consult the weight function of the pulsation mode. As an illustrative example, Pesnell (1987) shows the weight function of a particular g-mode (noted g_1^2 here, l=2,k=1) for a DA white dwarf model computed by Tassoul, Fontaine, and Winget (1988). The model has a total mass of 0.6 $M_\odot$. It has a C-rich core surrounded by a He-rich layer itself surrounded by a H-rich layer. The composition transition layers are treated under the assumption of diffusive equilibrium, which, for the particular model of interest, implies that there are some traces of helium extending down to the center of the star. The effective temperature of the model is T_e=13,969K, and the hydrogen (helium) layer has a mass equal to 10^{-10} (10^{-2}) times the total mass of the star. The results of Pesnell (1987) indicate, surprisingly, that the period of the g_1^2 mode (which is found to be 59.0s) is determined in the central regions of the model; the weight function showing a maximum at about the half-way point in radius. The results are the same for both the Lagrangian pulsation code developed by Pesnell and for an Eulerian version provided that, in the latter case, the square of the Brünt-Väisälä frequency is evaluated numerically to take into account the varying chemical composition due to the presence of helium traces in the deep core. Alarmingly, the period of the g_1^2 mode and, more generally, the complete spectrum of the model are found by Pesnell (1987) to be *quite different* from that of earlier calculations carried out by Winget (1981) using the same model. Pesnell suggests that his taking into account the changing chemical composition in the deep core (ignored in the Winget calculations) makes the difference. If correct, this would mean that the basic period structure cannot be computed with any amount of confidence because it seems so sensitive to the presence of small traces of helium in the core. For simplicity, the model has been computed under the assumption of diffusive equilibrium, but actual time-dependent diffusion calculations carried out by Pelletier (1988) show that this assumption breaks down in the very deep core of a white dwarf with an age characteristic of pulsating DA stars. Thus, the helium distribution in the core of a DA model can only be specified by time-dependent calculations and, until detailed results of such calculations exploring a large volume of parameter space become available, white dwarf seismology would remain next to useless if the interpretation given by Pesnell (1987) is correct.

Motivated by the past successes of white dwarf seismology based on Eulerian calculations (in particular the prediction and subsequent discovery of DB variable stars; see Winget and Fontaine 1982), we have felt that this new concept of period formation in the core of a white dwarf should be carefully examined. We have therefore embarked, with a fresh look, on a detailed investigation of the period structure of the DA model analyzed by Pesnell. In the process, we have discovered a basic shortcoming of the methods used by that author which (1) explains the discrepant results, and (2) has far-reaching implications for the results of his Lagrangian calculations in degenerate stars in general.

The period structure of a stellar model is largely specified by the spatial distribution of the square of the Brünt-Väisälä frequency which is defined by

$$N^2=-g\left[\frac{1}{\rho}\frac{d\rho}{dr}-\frac{1}{\Gamma_1 P}\frac{dP}{dr}\right] , \qquad (1)$$

where g is the local gravity, r is the radial coordinate, ρ is the density, P is the pressure, and Γ_1 is the first adiabatic exponent. In degenerate stars, it is useful (indeed essential in the deep core; see below) to transform equation (1). It can be shown (cf. Brassard *et al.* 1988) that N^2 can be rewritten as

$$N^2=\frac{\rho g^2}{P}\frac{\chi_T}{\chi_\rho}\left(\nabla_{ad}-\nabla+\left[-\frac{1}{\chi_T}\frac{\partial \ln P}{\partial \ln X}\bigg|_{\rho,T}\frac{d\ln X}{d\ln P}\right]\right) , \qquad (2)$$

where χ_T and χ_ρ are the usual logarithmic pressure derivatives, ∇_{ad} is the adiabatic temperature gradient, ∇ is the actual temperature gradient, and X is the mass fraction of one element at a two-ion composition interface. Written in this form, the contribution of the composition transition zones are explicitly included in the term in brackets. This term is always positive and has non-negligible values only in regions where the abundances of two ionic species are comparable, i.e. in the transition zones themselves. These typically cover relatively narrow regions, some two pressure scale heights wide. In particular, the presence of small traces of helium in the deep core of our model *cannot* affect the values of N^2 there. The dominant physical effect is the fact that $\partial \ln P/\partial \ln X|_{\rho,T}\rightarrow 0$ in the central regions because the pressure of highly degenerate matter for material with $\mu_e=2$ is the *same* for a given set (ρ,T), whatever the proportions of the He/C mixture.

We have used the Eulerian code developed by Hansen (see Kawaler, Hansen, and Winget 1985) to analyze the adiabatic period structure of the DA model discussed by Pesnell (1987). The continuous curve in Fig. 1 shows the distribution of N^2 in terms of the radius. The small localized structure aroud $r/R \approx 0.93$ is associated with the He/C transition zone. A sharp feature, barely visible around $r/R \approx 0.995$, is associated with H/He transition zone located in the outermost layers ($\log \Delta M/M \approx -10$). The N^2 profile is generally quite smooth and any discontinuities or quasi-discontinuities (such as the structures associated with the composition transition zones) are potential features for resonance effects. Our calculations indicate that the period of the g_1^2 mode is 122.8s in reasonable agreement with the older calculations of Winget (1981) which give 142.3s, but a far cry from the 59.0s obtained by Pesnell (1987). Note that we recover *exactly* the results of Winget (1981) by ignoring the effects of the composition transition layers on the Brünt-Väsäilä frequency as was done in that study. Interestingly, however, we can reproduce the results of Pesnell (1987) performing the following experiment: we now calculate N^2, not with equation (2), but rather with the numerical derivatives occuring in equation (1). This procedure is implicit in the Lagrangian formulation of Pesnell and was *required* by him in his Eulerian code in order to recover the results of the Lagrangian calculations.

The dashed curve in Fig. 1 shows the resulting N^2 profile for our reference model. As compared to the continuous curve, additional structure and two spurious "convection" zones (negative values of N^2) have appeared. It is obvious that the N^2 profile presented by Pesnell (1987) in his Fig. 1 is quite similar to our dashed curve; apparently, the spurious "convection" zones were suppressed by Pesnell. All other features of Pesnell's figure are accurately reproduced, however. As noted before, the quasi-discontinuities that are present in our dashed curve and in the N^2 profile shown by Pesnell (1987) can isolate and trap certain modes if resonance conditions are met. These modes are trapped in the *deep interior*, however, implying very large kinetic energies and very low growth rates. More importantly, it is the large systematic differences observed between the dashed and continuous curves in our Fig. 1 that are directly responsible for the large differences found in the period of the same mode. We find, in our altered calculation, a period of 58.7s for the g_1^2 mode, very close to the value of Pesnell (1987) but quite different from our original estimate. The fundamental reason for this discrepancy is that a numerical evaluation of the derivatives appearing in equation (1) encounters serious difficulties

in degenerate matter. Indeed, with a slight rearrangement of terms, we can write

$$N^2 = -\frac{g}{P}\frac{dP}{dr}\left[\frac{d\ln\rho}{d\ln P} - \frac{\partial \ln\rho}{\partial \ln P}\bigg|_s\right] , \qquad (3)$$

where s is the specific entropy per gram. In the nearly adiabatic interior of a degenerate star, the numerical evaluation of derivatives boils down to computing N^2 by *taking the difference* of two nearly equal quantities. By contrast, our formulation of N^2 given by equation (2) is reliable everywhere. In the deep core, the term in bracket does not contribute, ∇ is also negligibly small because of the nearly isothermal conditions, ∇_{ad} remains a number with typical values slightly under 0.4, and N^2 is evaluated by *multiplying* various quantities. Of course, the two formulations are equivalent in principle, and we indeed observe that the two curves shown in Fig. 1 merge together for large values of r/R, i.e. in the outer layers where the degree of degeneracy decreases substantially. Thus, numerical evaluations of derivatives implicit in the Lagrangian formalism of Pesnell lead to unreliably noisy N^2 profiles in white dwarf models with concomitant dramatic consequences on the period structure. Not surprisingly, the region of period formation is also affected by these problems. For example, Fig. 2 constrasts the two weight functions which we have computed for the g_1^2 mode of interest. The continuous curve refers to the weight function for the eigenmode computed with our equation (2) for N^2 and leading to a period of 122.8s. Quite clearly, the mode is an envelope mode. By contrast, the dashed curve, based on the use of equation (1), leads to the conclusion that the period is formed in the deep interior as in Pesnell (1987). We have thus clearly identified the origin of the discrepant period and weight function of the eigenmode discussed by Pesnell (1987). We feel that this numerical experiment should put to rest the idea that white dwarf pulsations probe the deep core.

In summary, we have found evidence that the implicit numerical differencing used in the Lagrangian pulsation code of Pesnell leads to very serious difficulties when used with models of degenerate stars. These difficulties are at the origin of his suggestion (Pesnell 1987) that white dwarf periods are formed in the deep interior. We reaffirm the prior results of other investigations; g-mode pulsations in white dwarfs are truly envelope modes. The implications of our findings on the work of Cox *et al.* (1987) need to be carefully evaluated. In particular, the *basic period structure* of their models (i.e. the most fundamental aspect of asteroseismology) is

clearly open to question. Because of this, their *nonadiabatic* results concerning primarily driving and damping must be considered premature; thus, their conclusions about the complete insensitivity of the ZZ Ceti theoretical blue edge temperature to the hydrogen layer mass remain clearly questionable.

We are grateful to D.E. Winget for useful discussions. This work was supported in part by the NSERC Canada, by the fund FCAR (Québec), and by a E.W.R. Steacie Fellowship to one of us (GF).

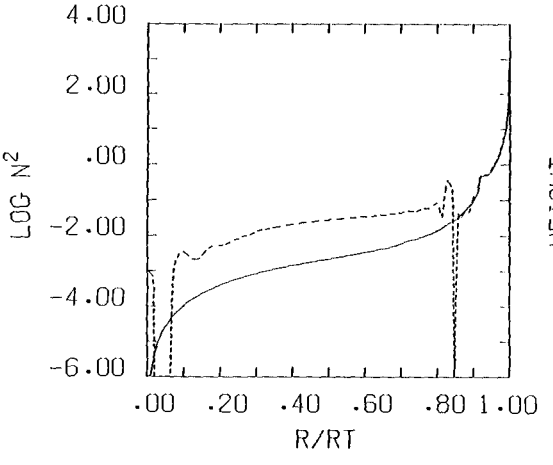

Fig. 1 - The square of the Brünt-Väisälä frequency as a function of radius for our DA white dwarf model. The continuous curve corresponds to the computations based on equation (2); the dashed curve to those based on equation (1) with numerical derivatives.

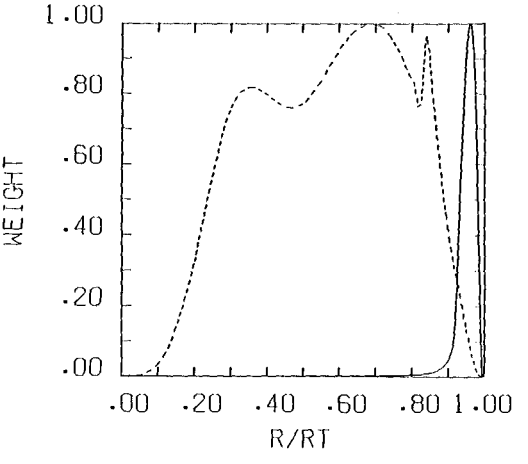

Fig. 2 - The weight function of the g_1^2 mode in terms of the radius. The continuous and dashed curves correspond to the two sets of calculations referred to in the previous caption

REFERENCES

Brassard, P., Fontaine, G., Wesemael, F., Tassoul, M., and Kawaler, S.D. 1988, in preparation.
Cox, A.N., Starrfield, S.G., Kidman, R.B., and Pesnell, W.D. 1987, *Astrophys. J.*, **317**, 303.
Kawaler, S.D., Hansen, C.J., and Winget, D.E. 1985, *Astrophys. J*, **295**, 547.
Pelletier, C. 1988, private communication.
Pesnell, W.D. 1987, in *Stellar Pulsation : A Memorial to John P. Cox*, A.N. Cox, W.M. Sparks, and S.G. Starrfield eds., Springer-Verlag, Berlin, p. 363.
Tassoul, M., Fontaine, G., and Winget, D.E. 1988, in preparation.
Winget, D.E. 1981, Ph. D. thesis, University of Rochester.
Winget, D.E. 1987, in *Highlights of Astronomy*, J.P. Swings ed., p. 221.
Winget, D.E., and Fontaine, G. 1982, in *Pulsations in Classical and Cataclysmic Variable Stars*, J.P. Cox and C.J. Hansen eds., University of Colorado, Boulder, p. 46.

COOLING OF WHITE DWARFS WITH ACCOUNT OF NON-EQUILIBRIUM BETA-PROCESSES

G.S.Bisnovatyi-Kogan
Space Research Institute, Academy of Sciences, USSR
Profosyuznaya 84/32, Moscow 117810, USSR

Non-equilibrium heating of white dwarfs during two-step neutronization and formation of small but finite core of the new phase is a main source of energy in these stars when the temperature is sufficiently small and Coulomb crystal becomes degenerate.

I. Introduction

Existence of Chandrasekhar mass limit of white dwarfs $M_{ch} = 5.83/\mu_z^2$, $\mu_z = A/z$, is connected with the prevalence of the relativistic degenerate electrons in pressure. When neutronization is taken into account, the maximal value of mass is smaller and is reached at finite density (Schatzman, 1958). The central density of the white dwarf with limiting mass is larger than threshold density of neutronization. Such star has a small, but finite core of new phase (Seidov, 1967). The neutronization threshold for the iron is equal to $\rho_{co} = 1.15\ 10^9$ g/cm³. The neutronization goes through two steps

$$Fe^{56} + e^- \rightarrow Mn^{56} + \nu\ , \quad Mn^{56} + e^- \rightarrow Cr^{56} + \nu \qquad (1)$$

The density on the boundary of the core of new phase is equal to $\rho_{c_1} = 1.25\ 10^9$ g/cm³ and make the jump in 26/24 times. The threshold Fermi energy of the electrons for the first reaction from (1) is equal to $\mathcal{E}_{Fe}^{(1)} = 3{,}70$ MeV, and for the second one is much smaller $\mathcal{E}_{Fe}^{(2)} = 1.61$ MeV. The second reaction goes in non-equilibrium conditions and leads to heating (Bisnovatyi-Kogan and Seidov, 1970). The amount of produced heat is equal to 476 keV on one reaction (1) taking into account the formation of excited state of Mn^{56} at $\rho > 1.24\ 10^9$ g/cm³. The models of cold iron white dwarfs with finite core of Cr^{56} are calculated by Bisnovatyi-Kogan and Seidov (1970). The parameters of the limiting mass model are:

$$M_C/M_o \approx 1.4\ 10^{-3}\ , \quad \Delta\rho_c/\rho_{c_1} \approx 0.022\ , \quad \Delta M/M_o \approx 2.1\ 10^{-4} \qquad (2)$$

Here M_C is the mass of the chromium core in the star of limiting mass; $M_o = 1.18\ M_\odot$ is the mass of the cold iron star at $\rho_c = \rho_{co}$ or $\rho_c = \rho_{c_1}$;

$\rho_{c_1} + \Delta\rho_c$ and $M_o + \Delta M$ are the central density and the mass of the limiting configuration. The non-equilibrium heating during the formation of new phase core leads to essential prolongation of the late stages of cooling, when the heat capacity of degenerate crystal at low temperatures is small (Mestel and Ruderman, 1967). Rough estimations of this prolongation have been done by Bisnovatyi-Kogan and Seidov (1970). Quantitative results have been obtained by Bisnovatyi-Kogan (1987).

2. White dwarf with final chromium core at nonzero temperature

When the mass of the white dwarf is equal to $M = M_o + \Delta M$, then its temperature T_f at central density ρ_{co} is determined by relation (Bisnovatyi-Kogan, 1966; Bisnovatyi-Kogan and Seidov, 1969, 1970):

$$T_f = \frac{A}{\mu_z^{4/3}} \frac{\rho_{co}^{1/3}}{1.710^{-7}} \frac{\delta M}{M} = 1.24\ 10^{11} \frac{\delta M}{M} = \beta \frac{\delta M}{M} \qquad (3)$$

Here $M_o = M(\rho_{co}, T=0)$, $A = 56$. Cooling of the white dwarf with $M = M_o + \delta M$ leads to the formation of chromium core. The curve $M_T(\rho_c)$ has a maximum, and the curve $T_M(\rho_c)$ has a minimum, where quadratic relations are valid

$$M_T(\rho_c) = M_{max}(T) - \alpha(\rho_c - \rho_{cm})^2 \qquad (4)$$

$$T_M(\rho_c) = T_{min}(M) + \gamma(\rho_c - \rho_{cm})^2 \qquad (5)$$

Here α, γ, $\rho_{cm} = \rho_{c_1} + \Delta\rho_c$ are approximately constants and formally $T_{min} < 0$ for $M < M_o + \Delta M$ from (2). Taking into account that $T = T_f$ from (3) when $\rho = \rho_{c_1}$, we find T_{min} from (5) and obtain

$$T = T_f + \gamma[(\rho_c - \rho_{cm})^2 - (\rho_{c_1} - \rho_{cm})^2] = \beta\frac{\delta M}{M} + \gamma[(\Delta\rho_c - \delta\rho_c)^2 - \Delta\rho_c^2] \qquad (6)$$

Using relations $\delta M = \Delta M$ when $T = 0$ and $\delta\rho_c = \Delta\rho_c$ from (2) we find γ and finally obtain the relation between $\delta\rho_c$ and T for given δM in the form:

$$\delta\rho_c = \Delta\rho_c\left[1 - \left(1 + \frac{T}{\beta}\frac{M_o}{\Delta M} - \frac{\delta M}{\Delta M}\right)^{1/2}\right] \qquad (7)$$

Using (2) and quadratic dependence of $\rho(r)$ near the center (Chandrasekhar, 1957) we find the connection between the mass of chromium core

m_c and central density $\rho_c = \rho_{c_1} + \delta\rho_c$ of the star:

$$\frac{m_c}{M_\odot} = \frac{M_c}{M_\odot}\left(\frac{\delta\rho_c}{\Delta\rho_c}\right)^{3/2} \approx 1.1\,10^{-14}(\delta\rho_c)^{3/2} \qquad (8)$$

The white dwarf with $\delta M < \Delta M$ is stable at T = 0 and has chromium core with the mass $m_c < M_c$. When $\delta M > \Delta M$ the loss of stability occurs at the finite temperature $T_c > T_{min}$.

3. Evolution with account of non-equilibrium heating

The approximate theory of white dwarf cooling leads to relation between luminosity L and the temperature of isothermal core T (Schwarzschild, 1958)

$$L \approx 5.75\,10^5 \frac{\mu T^{3.5}}{\mu_z^2} \frac{M/M_\odot}{x_z(1+x_H)} \approx 2.0\,10^6 \frac{M}{M_\odot} T^{3.5} \quad \frac{ergs}{sec} \qquad (9)$$

Here in the envelope we take $x_z = 0.1$, $x_H = 0$, $\mu = 1.38$, $\mu_z = 2$ and Krammers opacity have been used. The energy losses due to heat capacity source of nondegenerate nuclei $\dot{Q}_T$ and degenerate crystal $\dot{Q}_D$ are (Shapiro and Teukolsky, 1983)

$$\dot{Q}_T = \frac{3}{2}\frac{kM}{Am_p}\dot{T}, \quad \dot{Q}_D = \frac{16\pi^4}{5}\frac{kM}{Am_p}\left(\frac{T}{\theta_{DC}}\right)^3\dot{T} \qquad (10)$$

The losses due to nonequilibrium neutronization source are

$$\dot{Q}_\nu = -(476\,keV)\frac{\dot{m}_c}{Am_p} \qquad (11)$$

The equation

$$\dot{Q} = -L \qquad (12)$$

determines the evolution of the white dwarf where $\dot{Q} = \dot{Q}_T + \dot{Q}_\nu$ for $T > 0.1\,\theta_{DC}$ and $\dot{Q} = \dot{Q}_D + \dot{Q}_\nu$ for $T < 0.1\,\theta_{DC}$. Here θ_{DC} is the central value of $\theta_D = \hbar\omega_i/k \approx 1.6\,10^3\sqrt{\rho}$ = Debye temperature for the iron. Solving equation (12) with account of (7)-(11) for $M = M_0 + \Delta M$ we obtain the following solutions (Bisnovatyi-Kogan, 1987):

$$\tau \approx 2.8\cdot 10^{15}\left[T_7^{-2.5} - T_{7,0}^{-2.5} + 0.2\left(T_7^{-3} - T_{7,0}^{-3}\right)\right] sec \qquad (13)$$

for nondegenerate case with $\dot{Q}_T$ and

$$\tau \approx 2.8\,10^{15}\left[\left(\frac{T_0}{0.1\theta_{DC}}\right)^3 T_{7,0}^{-2.5} - \left(\frac{T}{0.1\theta_{DC}}\right)^3 T_7^{-2.5} + \right. \qquad (14)$$

$$+ 0.2\,(T_7^{-3} - T_{7,0}^{-3})\Big] \quad sec$$

for degenerate case with $\dot{Q}_D$. Here τ is the cooling time from initial temperature T_o up to temperature T, $T_7 = T/10^7$K, $0.1\ Q_{DC} \approx 5.5\ 10^6$K. Cooling to the temperature $T_7 = 0.55$ is $\sim$27% longer with account of nonequilibrium heating according to (13). Cooling up to almost zero temperature from $T_{7,0} = 0.55$ without $\dot{Q}_\nu$ last $\sim 4\ 10^8$ years and with account of $\dot{Q}_\nu$ after cosmological time $t_c = 2\ 10^{10}$ years the temperature reaches $T = T_* \approx 10^6$ K. Stars with $M > M_o + \Delta M$ collapse after cooling and because of $\dot{Q}_\nu$ the temperature at the beginning of collapse is always greater than T_*.

References

Bisnovatyi-Kogan G.S., 1966, Astron. Zh., 43, 89.

Bisnovatyi-Kogan G.S., 1987, Pisma Astron. Zh., 13, 1014.

Bisnovatyi-Kogan G.S., Seidov Z.F., 1969, Astrofizika, 5, 243.

Bisnovatyi-Kogan G.S., Seidov Z.F., 1970, Astron. Zh., 47, 139.

Chandrashekhar S., 1957, An Introduction to the Study of Stellar Structure, Dover edition.

Mestel L., Ruderman M., 1967, Month. Not. R.A.S., 136, 27.

Schatzman E., 1958, White Dwarfs, North. Holl. Pub. Comp.

Schwarzschild M., 1958, Structure and evolution of the stars, Princeton Univ. Press.

Seidov Z.F., 1967, Astrofizika, 3, 189.

Shapiro S.L. and Teukolsky S.A., 1983, Black holes, white dwarfs and neutron stars, John Wiley Interscience Publ.

THERMONUCLEAR EXPLOSION IN BINARIES: WHITE DWARF HELIUM STAR

E.Ergma, A.V.Fedorova, A.M.Khohlov
Astronomical Council AS USSR
Pjatniskaja 48, 107019 Moscow, USSR

Abstract

Evolutionary sequences of a binary system consisting of a helium star in the stage of core helium burning and a white dwarf are presented. Different ways of He burning in the envelope of a dwarf are discussed. Incomplete helium burning is discussed with relation to occurence of possible observational features.

1. Introduction.

In a close binary system with a white dwarf component mass exchange is apparantly the unique mechanism leading to thermal instability and to the explosion of the white dwarf. Spherical-symmetric calculations of accretion on the white dwarf of matter with various chemical composition show that thermal instability occurs only for certain accretion rates and initial parameters of the binary (Iben and Tutukov, 1984).

In the case of hydrogen-helium accretion occurence of unstable hydrogen burning is highly probable. The most powerful hydrogen flashes may be connected with nova phenomeon (Gallegher and Starrfield 1984).

By carbon accretion conditions for Supernova explosions are realized in a wide range of mass accretion rates ($\dot{M} < 2 \cdot 10^{-6}$ $M_\odot$/yr, Nomoto and Iben,1985, Khohlov, 1985).But for stationary mass accretion during long time intervals it is necessary that the initial parameters of the binary satisfy the following conditions: 1) $M_1 + M_2 > 1.4\ M_\odot$, 2) $M_2 < 0.6\ M_\odot$ (Cameron and Iben, 1986). Although the scenario including systems with two degenerated CO dwarfs is very promising it is doubtful if the required number of such systems is enough (but see Iben and Tutukov, 1984)

Analysis of observational data for SN I shows that they are not a homogenous class. At present one can state that there exsist SN Ia, SN Ib and besides a part of SNI spectra is impossible to classify (Branch, 1986, Filipenko and Porter, 1986). The possibility of other types of SN I although not so numerous can not be excluded.

In this paper we discussed the possibility of thermonuclear explosion in binaries with a helium star and a CO white dwarf. The observational behaviour of such a flash should be different from an explosive carbon burning case (for two degenerate CO dwarfs).

II. Necessary conditions for the realization of explosive helium burning in accreting CO dwarfs.

The investigation of He accretion on CO dwarfs has shown that almost indepently of the dwarf mass, if the mass accretion rate is less $(2\text{-}3)\cdot 10^{-8}$ $M_\odot$/yr helium burning starts at densities $> 10^6$ $g\cdot cm^{-3}$ (Taam, 1980a,b, Nomoto, 1986, Khohlov and Ergma,1989).

As was shown by Nomoto and Sugimoto (1977) for these densities helium burning is explosive (see also Mazurek, 1973).

It is necessary to determine which binaries have the required accretion rate $(2 - 3)\cdot 10^{-8}$ $M_\odot$/yr?

First there is the possibility of formation of double degenerate binaries with helium and CO dwarfs (Iben and Tutukov, 1984, 1986). But the required mass accretion rate is reached only when mass of the secondary is less than 0.1 $M_\odot$.

Second the evolution of a non-degenerate helium star with central helium burning filling its Roche lobe may provide the required accretion rate as it was shown by Savonije et.al (1986), Iben et al. (1987), and Fedorova and Ergma (1989).

Fedorova and Ergma have found that the accretion rate in the binary with a helium star and a CO dwarf is determined by two factors: 1) the mass relation $q= M_{He,2} / M_{co}$, 2) the central helium abundance during the filling of Roche lobe by the secondary. On Fig.1 a plot of the mass transfer rate as a function of the mass of the secondary for a fixed mass of the system $M_1 + M_2 = 1.532$ $M_\odot$ is presented. As calculations show in the case $q= 1$ the accretion rate remains $2\cdot 10^{-8}$ $M_\odot$/yr during several ten millions of years. Therefore it is possible to accumulate on the surface of a CO dwarfs a thick helium layer. For $q > 1$ mass accretion occurs from time to time with very high mass transfer rates.

3. Possible burning ways.

In the case of $\dot{M} < 4\cdot 10^{-8}$ $M_\odot$/yr the condition for explosive helium burning can be realized when the density in the envelope is $(10^6 - 10^8)$ g cm^{-3} depending on the initial mass of the white dwarf.

The mass of the white dwarf at that time must not necessary equal the Chandrasekar limit but may be much less. It is clear that for a mass transfer rate less than 10^{-8} $M_\odot$/yr and a larger initial mass of the CO dwarf unstable carbon burning may start in the center (Arnett, 1969 We are investigating the noncentral helium burning case.

He burning kinetics differ from the kinetics of carbon burning. The 3α reaction that provides C^{12} nuclei for the succeding - capture reactions ($C^{12} + \alpha$, $O^{16} + \alpha$, ... , Ni^{56}) depens weakly on the temperature if $T \gtrsim (0.5 - 1) \cdot 10^9$ K (Fowler et.al., 1975). For This Temperature range the helium burning time depens mainly on the density and may be approximated as (Khohlov, 1989)

$$\tau_{He} = \frac{12}{A^* \rho^2 \lambda_{3\alpha} Y^2_{He,0}} \left[\left(Y_{He,0} / Y_{He,1} \right)^2 - 1 \right] \qquad (1)$$

where A^* is the mass number of α - capture products (see Khohlov and Ergma,1985) $\lambda_{3\alpha}$ is the 3α reaction rate (Fowler et.al. 1975), $Y_{he,0} = 0.25$ is the initial and $Y_{he,1}$ the final helium abundance (we assume that helium will be exhausted if $Y_{he,1} = 0.1\ Y_{he,0}$.)

$$\lambda_{3\alpha} = 2.79 \cdot 10^{-8} / T_9^3 \exp(-4.4027/T_9) \qquad (2)$$

the width of the steady detonation wave in the helium is

$$\xi_{He,d} = D \rho_0 / \rho_s \tau_{He} (T_s, \rho_s) \qquad (3)$$

where T_s, ρ_s are the temperature and density behind the front of shock wave, D - the velocity of detonation wave, ρ_0 - initial density of matter. For the Chapman-Joughe Detonation the dependence ρ_s, T_s and D with ρ_0 is (Khohlov, 1989).

$$\xi_{He,c-J} \simeq 4 \cdot 10^9 / \rho_0^{1.87} \text{ cm} \qquad (4)$$

By comparision of $\xi_{He,c-J}$ with the characteristic scale of the density change $L \sim \rho (dp/dr)^{-1} \sim 10^7$ cm it follows that for $\rho < 5 \cdot 10^6$ $g \cdot cm^{-3}$ $\xi_{He,c-J} / L > 1$. That means that for such values of densities the steady detonation wave although initiated will be destroyed On Fig.2 the distribution of density with Lagranian masses for various initial mass of the white dwarfs is presented. From this Fig. follows that for $M \lesssim 1\ M_\odot$ most of the white dwarf mass is below $\rho \sim 5 \cdot 10^6$ $g \cdot cm^{-3}$. For These dwarfs the incomplete helium burning may take place in the regime of deflagration or due to weak shock waves.

The incomplete helium burning (as compared with burning in the detonation wave) may lead to a less energy production and hence smaller expansionvelocity. In more massive dwarfs ($M > 1M_{\odot}$) detonation is inevitable. Of course more Hydro-dynamic calculation with careful examination of the burning front in the thermal instability region is needed.

4. Possible observational consequences.

A. The expansion velocity may be estimated as

$$v = \sqrt{2 q M_b / M} \qquad (5)$$

where q -caloricity of the nuclear matter, M_b - the mass in which nuclear burning takes place. For $q = q_{He} = 1.5 \cdot 10^{18}$ erg/g and $M_b/M \sim$ $\sim$ (0.1-0.3) $M_{\odot}$ we obtain $v \simeq 10^4$ km/s that is observed in SN I.

B. The chemical composition in the case of explosive helium burning completly differs from that of explosive carbon burning. The explosive helium burning is determined by the characteristic time of (α, p), (α, γ) and (α,n) reactions on α-multiple nuclei (for example $C^{12}, O^{16}, \ldots Ni^{56}$) and the rate of the 3α reaction (Khohlov, 1984, Khohlov and Ergma, 1986). On Fig.3 A^* is presented in dependence of ρ and T . During the whole burning the abundances of nuclei with $A < A^*$ and $A > A^*$ are very small. From Fig. 3 it is evident that the smaller the atomic weight of A nuclei between C and Fe (Si,S, Ca et.al) the larger densities and smaller temperatures are required for their synthesis. The dotted line on the figure presents ρ and T for explosive helium burning. It is clear that the formation of Si and S is practically impossible and the formation of Ca also meets with difficulties.

D. Incomplete burning means that the chemical composition of the expanding envelope may be helium and carbon+oxygen.

References.

Arnett W.D. 1969,Astrophys.Space Sci. 5,180
Branch D. 1986, Ap.J. 300, L51
Cameron A.G.W., Iben I.Jr. 1986, Ap.J. 305, 228
Gallagher J.S., Starrfield S. 1978, Ann. Rev. Astron. Astrophys,16,171
Fedorova A.V., Ergma E. 1989 Pisma Astron. Zh. (in press)
Filipenko A.V., Porter A.C. 1986 Palomar Observatory , Caltech Astrophysics preprint
Fowler W.D., Caughlan G.R., Zimmerman B.A. 1975 Ann. Rev. Astrophys. 13, 69
Iben I.Jr. Tutukov A.V. 1984 Ap.J.Suppl. 54, 535
Iben I.Jr., Tutukov A.V., 1986, Ap.J. 311, 742
Iben I.Jr., Nomoto K., Tornambe A., Tutukov A.V. 1987, Ap.J. 317,717
Khohlov A.M. 1984, Pisma Astron. Zh. 10, 297

Khohlov A.M. 1985, Pisma Astron. Zh. 11,755
Khohlov A.M. 1989 Naycnye Inform. Asron. Council (in press)
Khohlov A.M/, Ergma E.V. 1985 , Astrophysika 23, 605
Khohlov A.M., Ergma E.V. 1989, Astrophysika (in press)
Mazurek T.J. 1973, Astrophys.Space Sci. 23, 365
Nomoto K. 1986, Ann. N.Y. Acad. Sci. 470, 294
Nomoto K., Iben I.Jr., 1985, Ap.J. 297, 531
Nomoto K., Sugimoto D. 1977, PASJ 29, 765
Savonije E.J., de Kool M., van den Heuvel E.P.J. 1986, Astron. Astrophys. 155, 51

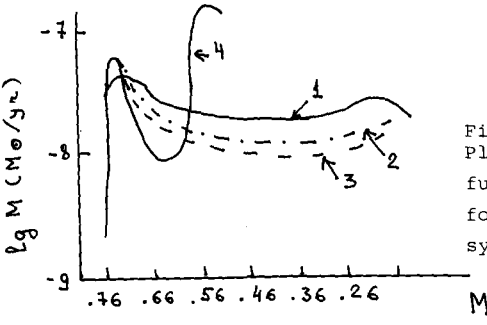

Fig.1
Plot of mass transfer rate as function of the secondary mass for an assumed fixed mass of the system 1.532 $M_\odot$ and Y_c = 0.97 (1), = 0.658(2), =0.413 (3), = 0.097(4)

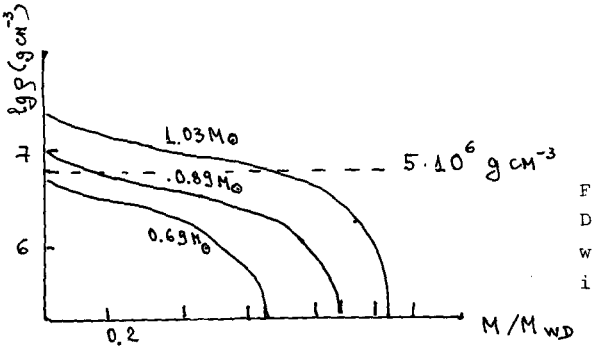

Fig. 2
Density distribution with lagrangian mass in the white dwarfs

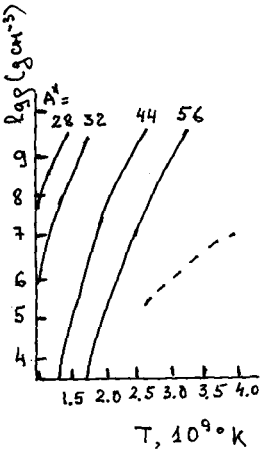

Fig.3
A^* = const lines in the (ρ,T) plane for more abundant nuclei which are synthesized in explosive helium burning The dotted line presents ρ and T for explosive helium burning

THE PHASE DIAGRAM OF HIGH DENSITY BINARY MIXTURES AND THE LUMINOSITY FUNCTION OF SINGLE WHITE DWARFS

Isern, J.[1], Garcia-Berro[2,5], E., Hernanz[3], M., Mochkovitch, R[4].

[1]Centre d Estudis Avançats de Blanes, CSIC
17300 Blanes (Girona), Spain
[2]Departament de Física Aplicada ETUETOPB-UPC
[3]Departament de Física i Enginyeria Nuclear ETSEIB-UPC
[4]Institut d Astrophysique de Paris
[5]Departament de Física de l Atmosfera, Astronomía i Astrofísica UB

For the last two decades, plasma physics developments have led to a better understanding of physical conditions in white dwarfs interiors. Following the pioneering work of Mestel (1952), the problem of white dwarf cooling has been a subject of continuous interest until the present time. In the early sixties, Kirzhnits (1960), Abrikosov (1960), and Salpeter (1961) recognized the importance of Coulomb interactions in the dense plasma which forms the white dwarf interior. A first-order transition from liquid to solid phase was predicted and the resultant release of latent heat was shown to somewhat affect the cooling rate (Mestel and Ruderman, 1967). Subsequently, improved theoretical luminosity functions (number of white dwarfs per pc^3 and per magnitude interval as a function of luminosity) taking into account not only Coulomb interactions but also neutrino losses, and using detailed atmosphere models (Van Horn, 1968; Koester, 1972; Lamb and Van Horn, 1975; Shaviv and Kovetz, 1976; Sweeney, 1976). Recently, Iben and Tutukov (1984) have discussed the evolution of a 0.6 $M_\odot$ carbon-oxygen white dwarf from its nuclear burning stages to complete crystallization. Their luminosity function agrees reasonably well with observations in the range $-4 \leq \log(L/L_\odot) \leq 4$ but it predicts an excess of white dwarfs at low luminosities. Indeed, the luminosity function derived from observations grows monotonically until $\log(L/L_\odot) \simeq -4.5$ ($M_v \simeq 16$) and then makes an abrupt shortfall (Liebert, Dahn and Monet, 1988). The agreement between theory and observations is so good in the aforementioned range luminosity that we can wonder as to whether it is possible not only to test the theory of white dwarf cooling but also to obtain information on the galactic structure and evolution. One example of that is the use of the cutoff in the white distribution to determine the age of the galactic disk (Schmidt, 1959). Using this method, Winget et al. (1987) have found that the galactic disk age

could be of the order of 9 Gyr old, in agreement with some predictions from nucleocosmochronology (Fowler et al. 1987).

Nevertheless before using the white dwarf luminosity function as a diagnostic tool of galactic evolution, it is necessary to ensure that we understand the properties of white dwarfs. Three are the main sources of uncertainty: 1) The difficulty of discovering very faint white dwarfs, i.e. is the luminosity function complete? (Liebert, Dahn and Monet, 1988). 2) The equation of state and opacity of the outer layers which control the characteristic cooling time during the late epochs (Iben and Tutukov, 1984). 3) The existence of additional sources of energy due to a chemical differetitation of white dwarf induced by the crystallization process (Mochkovitch, 1983; Garcia-Berro et al., 1988a, b), and the distribution of the chemical elements and its influence on the thermal contents of the star (Mazzitelli and D'Antona, 1986)

The confirmation of either carbon miscibility of inmiscibility in solid phase requires the knowledge of the free energy of the completly ionized carbon-oxygen plasma in both liquid and solid phases. The free energy of the liquid can be well approximated by assuming ion-sphere charge averaging and ideal entropy of mixing (Hansen et al., 1977). To determine the free energy of the solid phase is a more complicated task, as it has been illustrated by the pioneering work of Stevenson (1980). This author obtained either miscibility if the Madelung energy of the alloy was computed assuming ion-sphere averaging or inmisicibility, with a pronounced eutectic in the fluid-solid coexistence diagram, if the adopted electrostatic energy was that of a random alloy. Very recently, Barrat et al. (1988), using a density functional approach, have shown that the phase diagram for a completely ionized carbon-oxygen mixture is of the "spindle" form, with a change of concentration upon freezing but carbon and oxygen remaining completely miscible in the solid phase. This phase diagram is the most physically self consistent calculation up to date. It is necessary, however, that the simplifications that have been introduced, that are valid for a one component plasma, are also valid for a binary or more complicated mixture. So, in view of the uncertainties, it seems useful to compute and compare the effects of the different phase diagrams on the luminosity function of white dwarfs.

We have computed the cooling process of a 0.6 $M_{\odot}$ white dwarf (see details in Garcia-Berro et al., 1988) made of an homogeneous mixture composed by half carbon and half oxygen by mass. Probably this is not a very realistic case, as it has been shown by Mazzitelli and D'Antona

(1986), but the actual distribution and abundances of both elements are very uncertain as they depend on the adopted treatement of convection and on the rate of the ^{12}C (α , γ) ^{16}O reaction the later being still poorly determined (Filipone, 1988). Table I shows the time at which the white dwarf reaches different values of the luminosity for the cases of: a) Total miscibility in the solid phase without any change at the phase transition. b) Total miscibility in the solid phase but with the chemical separation introduced by the diagram of Barrat, Hansen and Mochkovitch (1988). c) Partial separation of carbon and oxygen due to an eutectic diagram, and d) Total separation (see Garcia-Berro et al. 1988a for a discussion of the last two cases).

Table 1: Ages of the models (Gyr)

$-\log(L/L_\odot)$	Model a	Model b	Model c	Model d
2.00	0.11	0.11	0.11	0.11
2.50	0.31	0.31	0.31	0.31
3.00	0.76	0.76	0.76	0.76
3.50	1.73	1.76	1.73	1.73
3.75	2.96	3.21	2.58	2.58
4.00	4.43	5.03	4.41	4.41
4.25	6.11	6.98	7.58	9.81
4.50	8.06	9.06	10.33	22.71

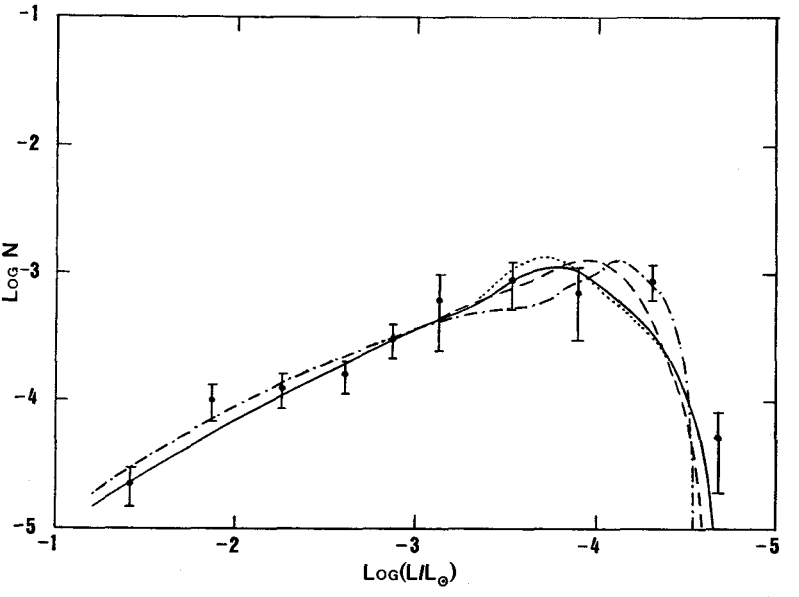

Figure 1. White dwarf luminosity functions in cases a) solid line, b) dotted line, c) dashed line, and d) dashed-dotted line, asuming Salpeter's IMF and a constant SFR. They have been normalized to give the observed value at $\log(L/L_\odot) = -3$. Observational data are from Liebert. et al. (1988).

The release of gravitational energy not only slows down the cooling process, but also produces a bump in the luminosity function. These bumps can be reduced assuming that white dwarfs have a scale height similar to that of Mira variables. Figure 1 shows that the luminosity functions constructed in this way roughly fit the observations if the age of the galactic disk is chosen to be: 8, 9, 9.5 and 15 Gyr for cases a, b, c and d respectively.

We conclude that if the phase diagram of Barrat et al. (1988) is correct, the age of the galactic disk should be of the order of 9 Gyr in agreement with Winget et al. (1987). Furthermore, as the shape of the luminosity function strongly depends on the adopted dilution factor, improved observational luminosity functions together with a better understanding of the cooling process could provide useful constraints to the studies of galactic evolution.

REFERENCES

Abrikosov, D.A., 1960, Soviet Phys. JETP 12, 1254
Barrat, J.L., Hansen, J.P., Mochkovitch, R., 1988, Astron. Astrophys. 199, L15
Fowler, W.A., 1987, Q.J. R. Astron. Soc. 28, 87
Garcia-Berro, E., Hernanz, M., Isern, J., Mochkovitch, R., 1988a, Astron. Astrophys. 193, 141
Garcia-Berro, E., Hernanz, M., Isern, J., Mochkovitch, R., 1988b, Nature 333, 644
Hansen, J.P., Torrie, G.M., Viellefoisse, J.P., 1977, *Phys Rev* A16, 2153
Iben, I., Tutukov, A.V., 1984, Astrophys. J. 238, 685
Kirzhnits, D.A., 1960, Soviet Phys JETP 11, 365
Koester, D., 1972, Astron. Astrophys. 16, 459
Lamb, D.Q., Van Horn, H.M., 1975, Astrophys. J. 200, 306
Liebert, J., Dahn, C.C., Monet, D.G.,1988, Astrophys. J., in press
Mazzitelli, I., D'Antona, F., 1986, Astrophys. J. 311, 762
Mestel, L., 1952, Monthly Notices Roy. Astron Soc. 112, 583
Mestel, L., Ruderman, M.A., 1967, Monthly Notices Roy. Astron Soc. 136, 27
Mochkovitch, R., 1983, Astron. Astrophys. 122, 212
Salpeter, E.E., 1961, Astrophys. J. 309, 210
Schmidt, M., 1959, Astrophys. J. 129, 243
Shaviv, G., Kovetz, A., 1976, Astron Astrophys. 51, 383
Stevenson, D.J., 1980, J. Phys. Suppl. No 3, 41, C2/61
Sweeney, M.A., 1976, Astron. Astrophys. 49, 375
Van Horn, H.M., 1968, Astrophys. J.151, 227
Winget, D.E., Hansen, C.J., Liebert, J., Van Horn, H.M., Fontaine, G., Nather, R..E., Kepler, S.O., Lamb, D.Q., 1987, Astrophys. J. (Letters) 315, L77

A Variational Approach to Understanding White Dwarf Evolution

M. A. Wood and D. E. Winget*
The University of Texas at Austin

I. Background

The observed falloff in the white dwarf luminosity function at $\log(L/L_\odot) \approx -4.5$ (Liebert, Dahn, and Monet 1988) is most easily explained as a result of the finite age of the Galactic disk. Using a simple perturbation approach as our method and a white dwarf evolution code as our tool, we have mapped the sensitivity of the ages of the model sequences in this low-luminosity regime to the uncertainties in the input physics and model parameters. We present here a preliminary overview of what we've learned.

II. The Code

We have updated the White Dwarf Evolution Code of Lamb and Van Horn (1975) to include both carbon and oxygen in the core. We interpolate to the mixture composition using our pure-C and pure-O tables and the additive-volume technique (Fontaine, Graboske, and Van Horn 1977). The envelope subroutines calculate stratified H/He/C envelopes of essentially arbitrary layer masses within the range 0 to $\sim 10^{-2}M_\star$, and treat the composition transition zones as discontinuities. Because the equation of state tables referenced by the envelope routines do not include crystallization, a given sequence ends when the crystallization front reaches the core/envelope boundary.

III. Two Representative Sequences

In Figure 1 we plot $\log(L/L_\odot)$ *vs.* $\log(Age)$ and in Figure 2 we plot $\log(T_c)$ *vs.* $\log(Age)$ for two representative model sequences. The first simulates a $0.6M_\odot$ WD with a 50/50 C/O mixture in the core and an outer helium layer with mass $10^{-4}M_\star$ (sequence CO60400**). The second simulates a $0.7M_\odot$ WD with the C/O convective overshooting profile found by Mazzitelli and D'Antona (1986, hereafter MD) as shown in their Figure 4, and a helium layer with mass $10^{-2}M_\star$ (sequence MD70200). Roughly speaking, the MD composition profile has $X_{12} \sim .25$ from the center to $q(\equiv M_r/M_\star) = 0.5$, and $X_{12} \approx 0.4 \cdot q + 0.3$ for $0.5 < q < (1 - M_{env})$. Tables 1 and 2 contain the summary listings for the two sequences.

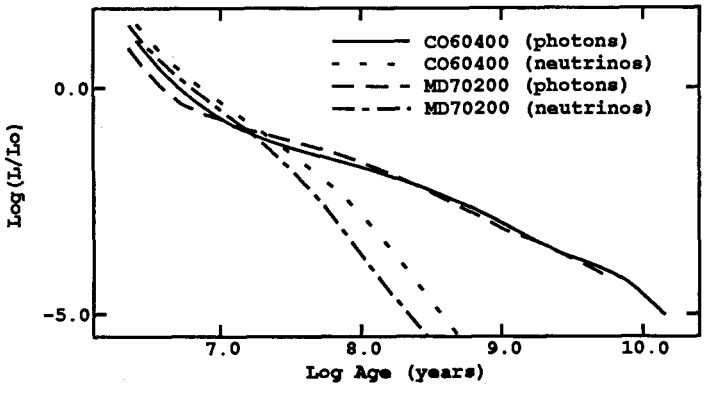

Figure 1: $\text{Log}(L/L_\odot)$ *vs.* $\text{Log}(Age)$. The MD70200 sequence is younger than the CO60400 sequence at the lowest luminosities. As expected, the plateau caused by the onset of crystallization (near $\log(L/L_\odot) = -3.6$) is larger in the sequence which crystallizes at a lower luminosity. Note that above $\log(L/L_\odot) \sim -1.0$, neutrino cooling dominates photon energy losses.

* Alfred P. Sloan Fellow

** For all sequences, "CO" implies a 50/50 mix throughout the interior, "C" implies pure carbon, "O" implies pure oxygen, and "MD" implies the profile shown in MD's Figure 4.

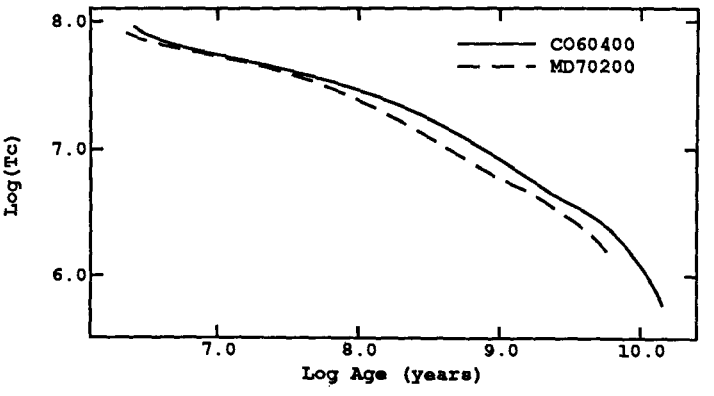

Figure 2: Log(T_c) *vs.* Log(Age). The MD70200 sequence has a lower core temperature than the CO60400 sequence as a result of the neutrino cooling in the core. Note also the sharp drop in the core temperature as Debye cooling sets in at the lowest luminosities.

TABLE 1

CO60400: Sequence Summary

$\log(L/L_\odot)$	Age	$\log(T_c)$	$\log(P_c)$	$\log(\rho_c)$	$\log(R_\star)$	$\log(L_\nu/L_\odot)$	$M_x/M_\star$	T_{eff}
−0.6	$9.097e+06$	7.747	23.231	6.533	8.969	−0.22	0.	35496
−0.8	$1.173e+07$	7.722	23.238	6.537	8.963	−0.48	0.	31803
−1.0	$1.596e+07$	7.690	23.244	6.541	8.958	−0.77	0.	28525
−1.2	$2.350e+07$	7.650	23.249	6.545	8.954	−1.14	0.	25534
−1.4	$3.807e+07$	7.594	23.254	6.549	8.950	−1.63	0.	22902
−1.6	$6.584e+07$	7.523	23.260	6.553	8.946	−2.25	0.	20518
−1.8	$1.106e+08$	7.445	23.264	6.556	8.942	−2.96	0.	18335
−2.0	$1.750e+08$	7.364	23.268	6.559	8.939	−3.71	0.	16413
−2.2	$2.645e+08$	7.278	23.271	6.562	8.936	−4.43	0.	14663
−2.4	$3.822e+08$	7.191	23.274	6.563	8.933	−5.06	0.	13137
−2.6	$5.426e+08$	7.099	23.276	6.565	8.931	−5.65	0.	11715
−2.8	$7.432e+08$	7.009	23.278	6.566	8.929	−6.19	0.	10474
−3.0	$1.001e+09$	6.921	23.280	6.567	8.928	−6.71	0.	9345
−3.2	$1.337e+09$	6.832	23.281	6.568	8.927	−7.22	0.	8330
−3.4	$1.781e+09$	6.742	23.282	6.569	8.926	−9.96	0.	7437
−3.6	$2.385e+09$	6.646	23.283	6.569	8.925	< -10.00	0.	6634
−3.8	$3.511e+09$	6.549	23.284	6.570	8.924	< -10.00	0.27	5922
−4.0	$5.165e+09$	6.434	23.284	6.571	8.924	< -10.00	0.63	5280
−4.2	$7.017e+09$	6.298	23.285	6.571	8.923	< -10.00	0.87	4704
−4.4	$8.677e+09$	6.177	23.285	6.571	8.923	< -10.00	0.96	4204
−4.6	$1.026e+10$	6.065	23.286	6.572	8.923	< -10.00	0.99	3745

TABLE 2

MD70200: Sequence Summary

$\log(L/L_\odot)$	*Age*	$\log(T_c)$	$\log(P_c)$	$\log(\rho_c)$	$\log(R_\star)$	$\log(L_\nu/L_\odot)$	$M_x/M_\star$	T_{eff}
−0.6	7.926e + 06	7.747	23.573	6.763	8.924	−0.24	0.	37389
−0.8	1.237e + 07	7.704	23.586	6.772	8.918	−0.71	0.	33560
−1.0	1.925e + 07	7.656	23.596	6.779	8.910	−1.17	0.	30171
−1.2	3.437e + 07	7.578	23.601	6.783	8.906	−1.90	0.	27016
−1.4	5.845e + 07	7.491	23.606	6.786	8.904	−2.72	0.	24176
−1.6	9.121e + 07	7.404	23.610	6.789	8.900	−3.53	0.	21581
−1.8	1.327e + 08	7.318	23.612	6.790	8.897	−4.20	0.	19288
−2.0	1.868e + 08	7.233	23.615	6.792	8.896	−4.77	0.	17235
−2.2	2.566e + 08	7.149	23.617	6.794	8.894	−5.28	0.	15417
−2.4	3.486e + 08	7.065	23.619	6.795	8.892	−5.77	0.	13757
−2.6	4.684e + 08	6.982	23.620	6.796	8.891	−6.26	0.	12260
−2.8	6.310e + 08	6.898	23.621	6.797	8.890	−6.75	0.	10945
−3.0	8.426e + 08	6.816	23.622	6.797	8.888	−7.22	0.	9779
−3.2	1.148e + 09	6.743	23.622	6.797	8.891	< −10.00	0.	8696
−3.4	1.730e + 09	6.646	23.623	6.798	8.890	< −10.00	0.06	7754
−3.6	2.362e + 09	6.548	23.624	6.799	8.887	< −10.00	0.38	6927
−3.8	3.250e + 09	6.450	23.623	6.798	8.893	< −10.00	0.66	6133
−4.0	4.381e + 09	6.336	23.624	6.799	8.888	< −10.00	0.86	5505
−4.2	5.773e + 09	6.192	23.623	6.798	8.895	< −10.00	0.96	4859

IV. Variation of Selected Parameters

For the remainder of this paper we focus on the ages of the low-luminosity white dwarfs. Although Liebert, Dahn and Monet (1988) give $\log(L/L_\odot) = -4.5$ as the nominal luminosity of the falloff, they make the point that there is some uncertainty in this result. With this in mind, we will report the differential effects (in Gyr) that the variation of selected model input quantities has on the ages at the luminosities $\log(L/L_\odot) = -4.4$ and -4.6, as compared with some standard model. We denote these age differences as $\Delta\tau_{-4.4}$ and $\Delta\tau_{-4.6}$.

- The phase diagram of the dense C–O plasma has only recently been computed using a density functional approach by Barrat, Hansen, and Mochkovitch (1988, hereafter BHM). They found that the two nuclear species are miscible in the solid phase, but that the solid phase should be slightly more oxygen-rich than the fluid phase. They further suggest that convection will redistribute the carbon and oxygen, allowing the buildup of an oxygen-rich core. BHM estimate that the gravitational potential energy released by this redistribution will extend the WD lifetime by roughly +0.5 Gyr at the luminosity of the falloff. At present, our code does not include convection in the core, and so we cannot directly incorporate the BHM results; however, we were interested in the sensitivity of the WD ages to the uncertainty in the freezing temperature. We considered the two cases, $T_{xtal} = T_{xtal}(C)$, and $T_{xtal} = T_{xtal}(O)$. Between the sequences CO60300 and CO60400 these two different prescriptions gave $\Delta\tau_{-4.4} \approx 0.30$ Gyr and $\Delta\tau_{-4.6} \approx 0.45$ Gyr, where the $T_{xtal}(C)$ model was the older in each case. These results suggest that we will not be too far wrong if we use $T_{xtal} = X_{12} \cdot T_{xtal}(C) + X_{16} \cdot T_{xtal}(C)$, and this is what we use for the remainder of the C–O core models.
- As mentioned above, we have considered two different C/O profiles in our C–O models, a 50/50 mix and the MD profile. Comparing the two, we find $\Delta\tau$(CO70400 → MD70400) ≈ +0.4 Gyr.
- We have varied the helium layer mass in several DB sequences, and find that $\Delta\tau$ is remarkably linear as a function of $\log(M_{He}/M_\star)$ at a given luminosity in our $0.6M_\odot$ sequences. The best fit to the results at $\log(L/L_\odot) = -4.4$ over the range $10^{-2} > M_{He}/M_\star > 10^{-5}$ is

$$\tau_{-4.4} = 5.92 - 0.86 \cdot \log(M_{He}/M_\star) \text{ Gyr},$$

and the best fit at $\log(L/L_\odot) = -4.6$ over the range $10^{-3} > M_{He}/M_\star > 10^{-5}$ is

$$\tau_{-4.6} = 6.01 - 1.29 \cdot \log(M_{He}/M_\star) \text{ Gyr.}$$

The conductive opacities for carbon are higher than those for helium, and so the thinner the helium layer, the longer the evolutionary timescale. Pelletier *et al.* (1986) used accretion-diffusion theory to understand the abundances of C found in cool DB white dwarfs, and found that their models which had $10^{-3.5} > M_{He}/M_\star > 10^{-4}$ most closely matched the observations. This implies an uncertainty in $\tau_{-4.5}$ of order ± 0.5 Gyr.

- Finally, we need to worry about uncertainties in the the radiative opacities. As an extreme test of the sensitivity of the WD ages to the radiative opacities we arbitrarily divided the $Z = 10^{-3}$ radiative opacities by a factor of 10. The resulting effect on the ages is small: $\Delta\tau_{-4.4} = -0.5$ Gyr and $\Delta\tau_{-4.6} = -0.6$ Gyr.

V. Summary and Conclusions

We have used a variational approach to map out the effects that uncertainties in the theoretical model parameters have upon the derived ages near the observed cutoff in the white dwarf luminosity function. We find that although there are a number of parameters whose uncertainties imply uncertainties in $\Delta\tau_{-4.5}$ of order ± 0.5 Gyr, none of the parameters we explored causes a shift in the age so large as to bring into question the value of the technique. On the contrary, because our internal theoretical uncertainties are fairly small and getting smaller with time, we feel that our results underscore the power of using the observed white dwarf luminosity function for studying the history of star formation in our galaxy.

This work was supported in part by NASA Training Grant NGT–50210 and by NSF grants AST 85–52457, and AST 86–00507.

References

Barrat, J.L., Hansen, J.P., and Mochkovitch, R. 1988, *Astron. Astrophys. (Letters)*, **199**, L15.

Fontaine, G., Graboske H.C. Jr., and Van Horn, H.M. 1977, *Ap. J. (Suppl.)*, **35**, 293.

Lamb, D.Q., and Van Horn, H.M. 1975, *Ap. J.*, **200**, 306.

Liebert, J., Dahn, C.C., and Monet, D.G. 1988, *The Luminosity Function of White Dwarfs*, *Ap. J.*, Sept. 1, Part 1 (in press)..

Mazzitelli, I., and D'Antona, F. 1986, *Ap. J.*, **308**, 706.

Pelletier, C., Fontaine, G., Wesemael, F., Michaud, G., and Wegner, G. 1986, *Ap. J.*, **307**, 242.

The Effect of Varying Helium and Hydrogen Layer Masses on the Pulsation Properties of White Dwarf Models

by
P.A. Bradley, D.E. Winget[1], and M.A. Wood

1 Introduction

Currently, there are disagreements on the theoretical pulsation properties of DA white dwarf models. Winget and his group (cf Winget 1981, Winget and Fontaine 1982, Winget *et al.* 1981, 1982) use $0.6M\odot$ evolutionary white dwarf models, to find that $(T_{eff})_{blue}$ is sensitive to the mass of the hydrogen layer and very sensitive to the treatment of convective efficiency. However, $(T_{eff})_{blue}$ is relatively insensitive to the helium layer mass. Winget and collaborators also find that the hydrogen layer must be restricted to $10^{-8} > M_H/M_\star > 10^{-12}$ for $(T_{eff})_{blue}$ to occur at $\sim 10,500$K in models with ML1 convection (see below). More efficient (ML2) convection pushes the blue edge up to $\sim 12,200$K, which is still short of the observed blue edge of $\sim 13,000$K.

These conclusions are not in agreement with the results of Cox *et al.* (1987) use white dwarf models that have a mass of $0.6M\odot$, with hydrogen and helium layer masses of $10^{-4}M_\star$ each. These models violate the requirement that the helium layer mass must be at least 100 times greater than the hydrogen layer mass in order to avoid overlapping transition zones (cf. Acouragi and Fontaine 1980). In spite of the unphysical nature of the models, Cox et al. find a blue edge temperature for pulsational instability ($(T_{eff})_{blue}$) at $\sim 11,500$K for models with hydrogen layer masses of $10^{-4}M_\star$ and $10^{-8}M_\star$. Neither group considered the red edge of the instability strip, other than to note that convection-pulsation interactions would be important at lower temperatures.

The aim of this paper is to clarify the discrepancies in the theoretical results and refute some earlier erroneous conclusions made about ZZ Ceti stars. In this study, we use *evolutionary* models of static DA white dwarfs described by Winget (1981) and Winget and Fontaine (1982). These $0.6M\odot$ models have pure carbon cores with an overlying helium layer and an outer layer of pure hydrogen. For this study, we use a treatment of the Brunt-Väisälä frequency that is self-consistent in all regions of the model, including the composition transition zones. We neglect convection-pulsation interactions throughout. In this preliminary study, we examine the pulsation properties of $0.6M\odot$ white dwarf models in response to changes in the mass of the hydrogen layer and convective efficiency for a fixed helium layer mass of $10^{-2}M_\star$. In addition, we examined a model with a helium layer mass of $10^{-5}M_\star$ to see if $(T_{eff})_{blue}$ is sensitive to the helium layer mass.

We use two different numerical methods for the adiabatic analysis; one is the Newton-Raphson relaxation method described in Winget (1981), and the other is a Runge-Kutta integrator developed by Carl Hansen with a subroutine for interpolating extra shells if the resolution is insufficient. Kawaler (1986) describes this program and its advantages for computing adiabatic quantities. Only the Newton-Raphson method is available for computing the nonadiabatic results.

For future convenience, the quantities $M_\star$, M_H, and M_{He} are hereafter specified by the notation of the following example: 60208 refers to a $0.6M\odot$ sequence, with $M_{He}= 10^{-2}M_\star$, and $M_H= 10^{-8}M_\star$. The convective efficiency is specified in the following manner. ML1 convective efficiency refers to the mixing-length theory of Böhm-Vitense (1958), with the mixing length equal to one pressure scale height. ML2 convective efficiency refers to the mixing length theory of Böhm and Cassinelli (1971) with the mixing length equal to one pressure scale height. Finally, ML3 convective efficiency uses the same mixing-length theory of ML2, but the mixing length is twice the pressure scale height.

2 Determination of $(T_{eff})_{blue}$ and $(T_{eff})_{red}$

To determine $(T_{eff})_{blue}$ and $(T_{eff})_{red}$, we use linear interpolation to find the zero point of the growth rates for several modes (where possible). The resultant average value for $(T_{eff})_{blue}$ and $(T_{eff})_{red}$ along with the temperature of the nearest stable and unstable model are plotted versus the hydrogen layer mass in figure 1.

Our results confirm and supplement those of Winget (1981). We find $(T_{eff})_{blue}$ to be $\sim 10,500$K with ML1 convection for hydrogen layer masses between $10^{-12}M_\star < M_H < 10^{-8}M_\star$. We also find that for M_H greater than $10^{-8}M_\star$, the value of $(T_{eff})_{blue}$ drops to ~ 8000K and is insensitive to the treatment of convection. When M_H is $10^{-14}M_\star$, we find that the models are unstable between 16,400K and 12,400K, much hotter than the observed instability strip. The change in helium layer mass does not have any effect of the value of $(T_{eff})_{blue}$.

Our most significant finding is that with ML3 convection, $(T_{eff})_{blue}$ is $\sim 13,000$K for the 60210 and 60209 sequences, in excellent agreement with the observed blue edge and the results of Fontaine *et al.* (1984). This is in contrast with the result of Cox *et al.* (1987) who were unable to get $(T_{eff})_{blue}$ above $\sim 11,500$K. The red edge of these two sequences,

[1]Alfred P. Sloan Research Fellow.

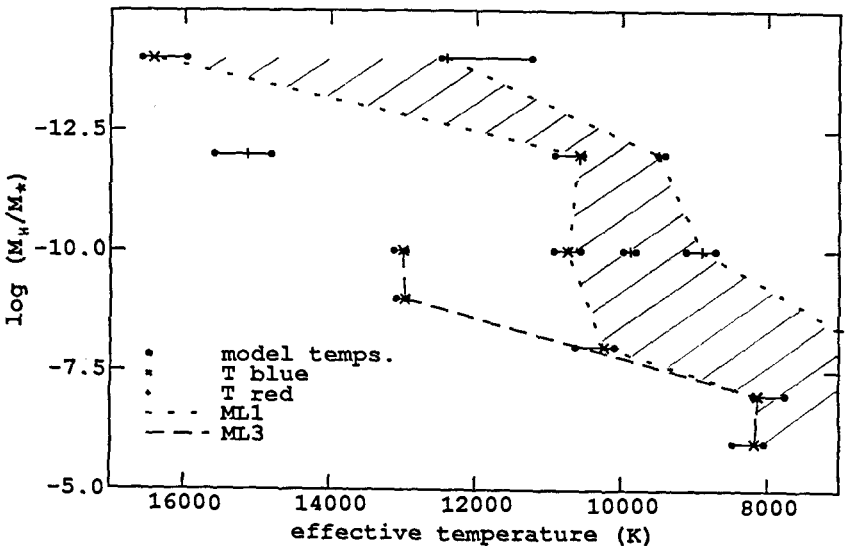

Figure 1: The value of $(T_{eff})_{blue}$ is plotted versus the hydrogen layer mass fraction, $\log(M_H/M_*)$. The hatched region shows the location of the g-mode instability strip.

$\sim 10,000$K, is about 1000K cooler than the observed red edge again suggesting that convection-pulsation interactions are important.

3 Mode Trapping

The rich spectrum of g-modes that are excited in theoretical models suggests that a filter mechanism is at work. Winget et al. (1981) proposed that mode trapping, which arises from a resonance between the wavelength of a g-mode oscillation and the thickness of the hydrogen layer could provide the answer. We find mode trapping in our models and prove that the presence of the H/He interface is vital for mode trapping to exist. In figure 2, we show the kinetic energies for $\ell = 2$ g-modes versus the period for various treatments of the Brunt-Väisälä frequency.

Notice that when the H/He transition zone is neglected or the Schwarzchild A criterion is used, the presence of mode trapping all but disappears. In contrast, using the self-consistent treatment of the Brunt-Väisälä frequency or neglecting the He/C transition zone produces a sharp minimum in the kinetic energy for $k = 6$. Since the kinetic energy of a g-mode is inversely proportional to the growth rate of that mode, the presence of mode trapping suggests that the trapped mode will be easier to excite, and will be preferentially driven at the expense of other modes.

4 Theoretical $\dot{\Pi}$ Values

We also computed theoretical values of rates of period change ($dP/dt \equiv \dot{\Pi}$) for representative g-modes of each sequence at various temperatures and find that the values range from $\sim 10^{-14}$ s/s to $\sim 10^{-16}$ s/s. In general, $\dot{\Pi}$ decreases with decreasing T_{eff} and $\dot{\Pi}$ increases with increasing radial order k for a given T_{eff}. Figure 3 shows the behavior of $\dot{\Pi}$ versus T_{eff} for representative values of k for the 60210 ML1 sequence, the 60210 ML3 sequence, and a 60410 ML1 sequence with a carbon core and discontinuous transition zones.

Where the two sequences overlap, there is good agreement between their values of $\dot{\Pi}$ at low values of k and gets worse with increasing k. Our values of $\dot{\Pi}/\Pi$ range from $\sim 5 \times 10^{-17}$ 1/s to $\sim 10^{-18}$ 1/s. These values are nearly independent of k for a given T_{eff} and decrease slightly with decreasing T_{eff}.

The best available observational values of $\dot{\Pi}$ are for R548 with an upper limit of $\dot{\Pi} < 9.6 \times 10^{-15}$ s/s (Tomaney 1987) and for G117-B15A with an upper limit of $\dot{\Pi} < 1.25 \times 10^{-14}$ s/s (Kepler et al. these proceedings). Due to the short pulsation periods, the g-modes of these stars have low values of k suggesting that the theoretical $\dot{\Pi}$ values are most likely a few times 10^{-15} s/s. This implies that observational detection of $\dot{\Pi}$ for these stars is still a few years away.

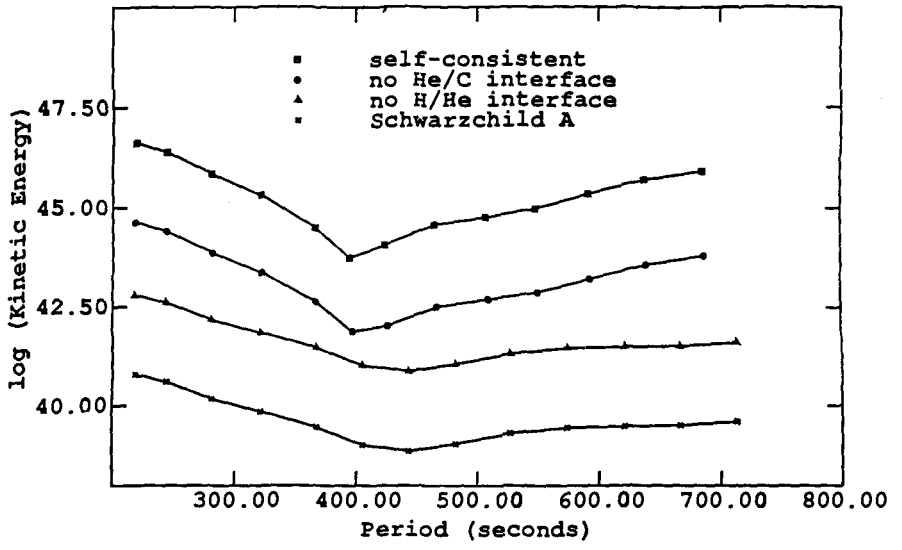

Figure 2: A plot of log(kinetic energy) versus the period of $\ell = 2$ g-modes for a 60510 model ($T_{eff} = 9141$K).

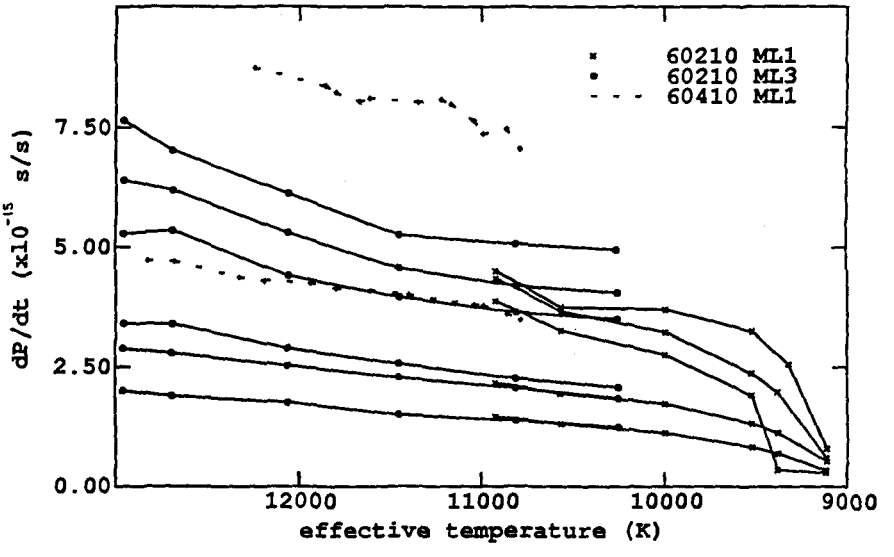

Figure 3: $\dot{\Pi}$ versus T_{eff} for $\ell = 2$ g-modes of the 60210 ML1 sequence (x), the 60210 ML3 sequence (•), and the 60410 ML1 (C/O) sequence (+).

5 Conclusions

We present results of a linear adiabatic and nonadiabatic analysis of several sequences of evolutionary white dwarf models. These preliminary results allow us to conclude the following:

1. Efficient (ML3) convection is required for the theoretical blue edge to match the observed blue edge. Contrary to the results of Cox et al. (1987), we find pulsational instabilities exist for models up to 13,000K, but only for hydrogen layer masses of $10^{-9}M_{\star}$ and $10^{-10}M_{\star}$. However, if M_H is $10^{-7}M_{\star}$ or greater, the blue edge drops to $\sim$ 8,000K, independent of convective efficiency.

Therefore, this detailed reinvestigation contradicts the conclusions of Cox *et al.* (1987) of white dwarf models with thick hydrogen layers being able to pulsate with temperatures appropriate for the ZZ Ceti instability strip.

2. Matching the observed value of $(T_{eff})_{red}$ must wait until convection-pulsation interactions are included.

3. We find that mode trapping occurs when the Brunt-Väisälä frequency is computed in a self-consistent manner and demonstrate the H/He transition zone is responsible for this phenomena. We agree with Winget et al. (1981) that this a likely filtering mechanism for selecting which unstable g-modes will be excited to detectable amplitudes, although nonlinear calculations are required to verify this.

4. Our theoretical calculations of $\dot{\Pi}$ range from $\sim 10^{-14}$ s/s to $\sim 10^{-16}$ s/s. In addition, our $\dot{\Pi}/\Pi$ values range from $\sim 5 \times 10^{-17}$ 1/s to $\sim 10^{-18}$ 1/s. The theoretical values are still lower than the observed upper limits for R548 and G117-B15A. This should change with a few more observing seasons worth of data.

This work was supported by the National Science Foundation under grants AST 85-52457 and AST 86-00507 through the University of Texas and Mc Donald Observatory.

References

[1] Acouragi, J.P. and Fontaine, G., 1980, Ap. J., **242**, 1208.

[2] Böhm, K.-H. and Cassinelli, J. 1971, Astr. Ap., **12**, 21.

[3] Böhm-Vitense, E. 1958, Zs. f. Ap., **46**, 108.

[4] Cox, A.N., Starrfield, S.G., Kidman, R.B., and Pesnell, W.D. 1987, Ap. J., **317**, 303.

[5] Fontaine, G., Tassoul, M., and Wesemael, F. 1984, in *Theoretical Problems in Stellar Stability and Oscillations: Proc. of the 25th Int. Ap. Colloq.* , ed. A. Noels and M. Gabriel, (Coint-Ougree, Belgium: Universite de Liege), 328.

[6] Kawaler, S.D., 1986, Ph. D. Thesis, University of Texas.

[7] Kepler, S.O., Vauclair, G., Nather, R.E., Winget, D.E., and Robinson, E.L. 1988, these proceedings.

[8] Tomaney, A.B. 1987, in *IAU Colloquium No. 95: The Second Conference on Faint Blue Stars*, ed. A.G.D. Philip, D.S. Hayes, and J.W. Liebert, (Schenectady; Davis Press), P. 673.

[9] Winget, D.E., 1981, Ph. D. Thesis, University of Rochester.

[10] Winget, D.E., Van Horn, H.M., and Hansen, C.J. 1981, Ap. J., **245**, L33.

[11] Winget, D.E., and Fontaine, G. 1982, in *Pulsations of Classical and Cataclysimic Variable Stars*, ed. J.P. Cox and C.J. Hansen, (Boulder;University of Colorado Press), P. 46.

[12] Winget, D.E., Van Horn, H.M., Tassoul, M., Hansen, C.J., Fontaine, G., and Carroll, B.W. 1982, Ap. J., **252**, L 65.

DISCOVERY OF THE SIXTH DBV STAR: CBS 114

D. E. Winget* and C. F. Claver

McDonald Observatory and Department of Astronomy,
The University of Texas at Austin

Though widely spread across the H-R diagram the compact pulsators have much in common. All are multi-periodic, and most have extremely complex light curves. All appear to be pulsating in nonradial g-modes, with temperature variations responsible for the bulk of the light modulations. The g-modes are global in nature and, typically, many are excited in each pulsator, so they are a rich source of seismological information about the interior regions of the white dwarf stars.

The pulsating DB white dwarf stars (DBV's) form one of the three distinct classes of pulsating compact objects currently known. We find these classes nearly uniformly distributed in $log\ T_e$ spanning virtually the whole range of the white dwarf cooling sequence, from the hot DOV stars at $log\ T_e \sim 5$ to the DAV (ZZ Ceti) stars at $log\ T_e \sim 4$; the DBV stars, with $logT_e \sim 4.5$, fall in the middle.

In this paper we present the discovery of pulsations in the DB white dwarf $CBS114$ (Wagner, *et al.* 1988, Pesch and Sanduleak 1986), thereby making this object the 6th known DBV.

The light curves of our two runs on this object are shown in Figure 1. These data were obtained with the 2.1 m telescope at McDonald Observatory using unfiltered light and a blue-sensitive (RCA 8850) phototube. The effects of extinction, as well as long time-scale transparency variations, have been removed by dividing the data by a best fit 3rd order polynomial after sky- subtraction.

The peak-to-peak amplitude of the pulsations in this object are about 0.3 mag and have a quasi-period of about 650 s. The Fourier transforms of the light curves are shown in Figure 2. These transforms readily demonstrate the complex nature of the light curve: more than 20 statistically significant peaks occur in each of the runs. The power appears in a series of frequency bands, with the largest amplitude band centered on a period of about 650 s – the quasiperiod evident in the light curve. These results are typical of 5 of the 6 known DBV stars—the exception is $PG1351+489$ (cf. Winget 1988) with its nearly monoperiodic structure.

The power is distributed in bands of power evenly spaced in frequency, as is also typical of the DBV stars. Thus the bands are not simple harmonics of the large amplitude groups – a pattern one might expect from such a high amplitude, presumably nonlinear, pulsator. The large number of frequencies present in most of the DBV stars indicates that the band-pass of the mode selection mechanism is rather broad, particularly as compared to the bulk of the ZZ Ceti stars. This is consistent with the mode-trapping theory (cf. Bradley *et al.* these proceedings). Unfortunately this kind of loose correlation is as far as we can go with the current observational data.

Since the light curves of none of the complex DBV stars has been completely resolved, the relations between the frequencies of the pulsations are unknown, so a comparison (beyond the simple search for harmonics) with even the simplest nonlinear theories is not currently possible. Therefore, until extended

* Alfred P. Sloan Fellow

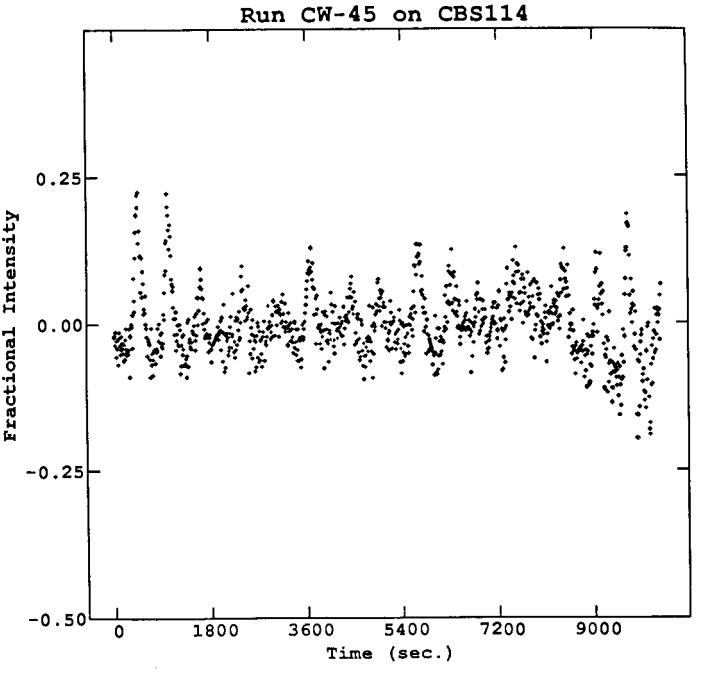
Run CW-45 on CBS114
Fractional Intensity
0.25
0.00
-0.25
-0.50
0
1800
3600
5400
7200
9000
Time (sec.)

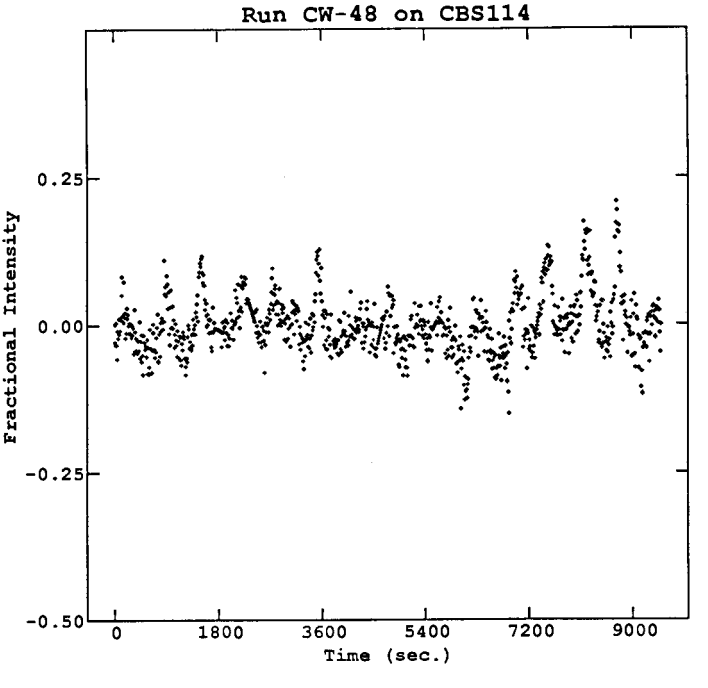
Run CW-48 on CBS114
Fractional Intensity
0.25
0.00
-0.25
-0.50
0
1800
3600
5400
7200
9000
Time (sec.)

Figure 1

time-base data is obtained for these objects the seismological information contained in the rich structure of their pulsations will remain hidden.

This work was supported in part by grants, AST 85–52457 and AST 86–00507, from the National Science Foundation.

References

Pesch, P., and Sanduleak, N. 1986, *Ap. J. Suppl*, **60**, 543.

Wagner, R. M., Sion, E. M., Liebert, J., Starrfield, S. G. 1988, *Ap. J.*, **328**, 213.

Winget, D. E., *Seismological Investigations of Compact Stars*, in *Advances in Helio- and Asteroseismology*, eds. J. Christensen and S. Frandsen (Copywrite 1988 by the IAU.).

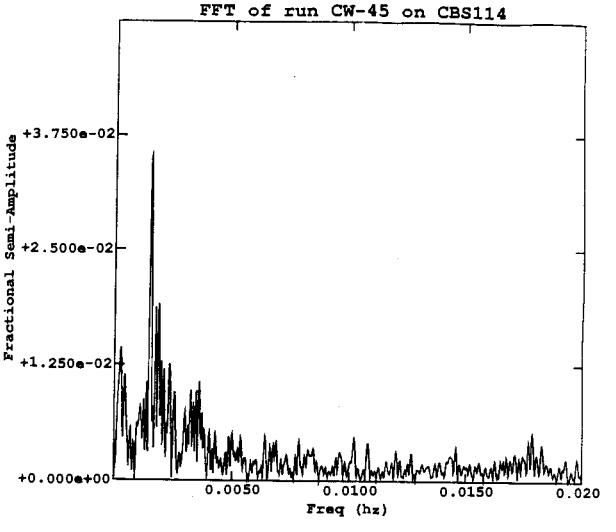

Figure 2

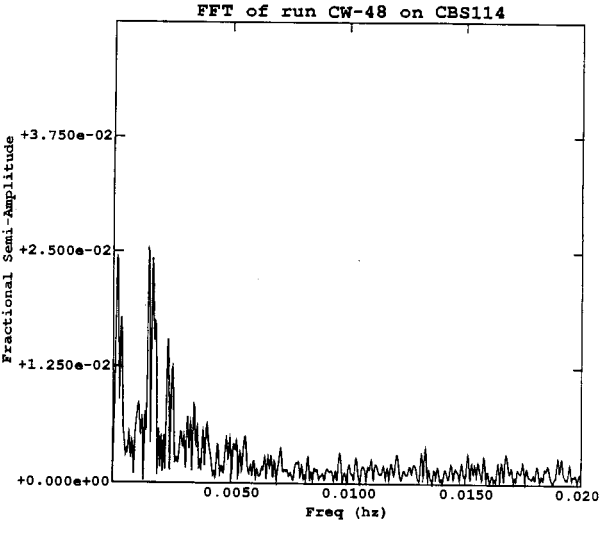

OPTICAL FREQUENCIES IN *V471 TAU*

D. E. Winget* and C. F. Claver

McDonald Observatory and Department of Astronomy,
The University of Texas at Austin

V471 Tau is a spectroscopic and eclipsing binary system located in the Hyades cluster. The binary consists of a *K2V* and a hot DA white dwarf star (Nelson and Young 1970). Soft x-ray observations reveal strong modulation at periods of $554.7 \pm 0.3s$ and $277.5 \pm 0.1s$ (Jensen 1985, Jensnen et al. 1986).

Robinson et al. (1988) reported the detection of the 555 s period in the optical. This period was about a factor of 20 reduced in mean amplitude in their data relative to the soft x-ray amplitude. They also found that it varied in amplitude from run to run by more than a factor of 2.5, dropping below detectability on several runs. They found some evidence for the 277.5 s period in several runs, but never at high enough amplitude to measure reliably. In addition, they noted that several of their runs had statistically significant power at other frequencies, but noted that in their six runs none of the additional frequencies repeated themselves. Robinson et al. also used observations near the eclipse of the white dwarf to demonstrate that most of the pulsed light is coming from the white dwarf.

We report on optical high speed-photometric observations of the system (Table 1). Our observations were made in the Strömgren u band in order to minimize the contribution of the K2V star. All of our data were taken on the 2.1 m telescope at the University of Texas' McDonald Observatory on Mt. Locke, using the Nather 2-star photometer system. The data were reduced as described in Hine (1988).

Journal of Observations: High-Speed Photometry [1]

Run Number	Date (UT)	Run Start (UT)	Length (sec)	Telescope (m)
DEW25	17 Feb. 1988	01:50:43	15450	2.1
DEW28	18 Feb. 1988	02:11:40	12100	2.1
DEW38	22 Feb. 1988	02:09:50	11510	2.1

Table 1

We have detected both frequencies found in the x-ray: the 554 s period (first detected in the optical by Robinson et al. 1988) and the 277 s period. Both periods vary significantly in amplitude from night to night; during our runs the 277 s harmonic had the largest amplitude. Its fractional semi-amplitude varies from 6×10^{-4} to 1.2×10^{-3}. We have found evidence for a number of additional frequencies with statistically significant amplitudes in individual runs and at least one frequency ($P = 410s$) which is present in all three runs at constant—albeit low—fractional semi-amplitude of 4.5×10^{-4}.

* Alfred P. Sloan Fellow

[1] Data taken with Nather 2-star photometer (cf. Nather, R. E., 1973, *Vistas in Astronomy*, 15, 91).

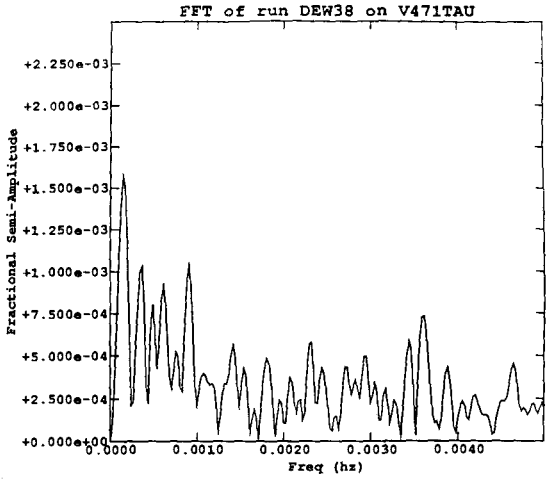
FFT of run DEW38 on V471TAU
Fractional Semi-Amplitude
+2.250e-03
+2.000e-03
+1.750e-03
+1.500e-03
+1.250e-03
+1.000e-03
+7.500e-04
+5.000e-04
+2.500e-04
+0.000e+00
0.0000
0.0010
0.0020
0.0030
0.0040
Freq (hz)

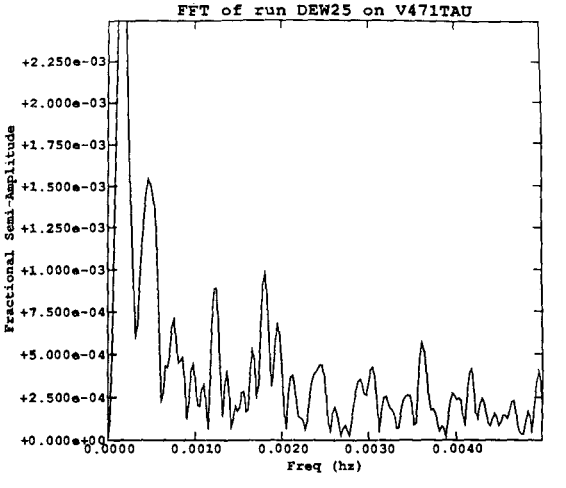
FFT of run DEW25 on V471TAU
Fractional Semi-Amplitude
+2.250e-03
+2.000e-03
+1.750e-03
+1.500e-03
+1.250e-03
+1.000e-03
+7.500e-04
+5.000e-04
+2.500e-04
+0.000e+00
0.0000
0.0010
0.0020
0.0030
0.0040
Freq (hz)

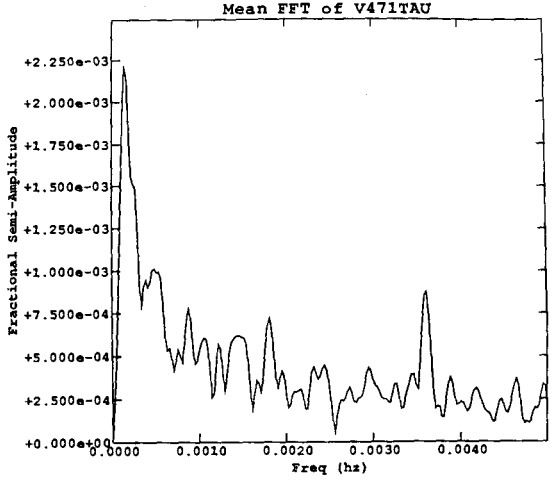
Mean FFT of V471TAU
Fractional Semi-Amplitude
+2.250e-03
+2.000e-03
+1.750e-03
+1.500e-03
+1.250e-03
+1.000e-03
+7.500e-04
+5.000e-04
+2.500e-04
+0.000e+00
0.0000
0.0010
0.0020
0.0030
0.0040
Freq (hz)

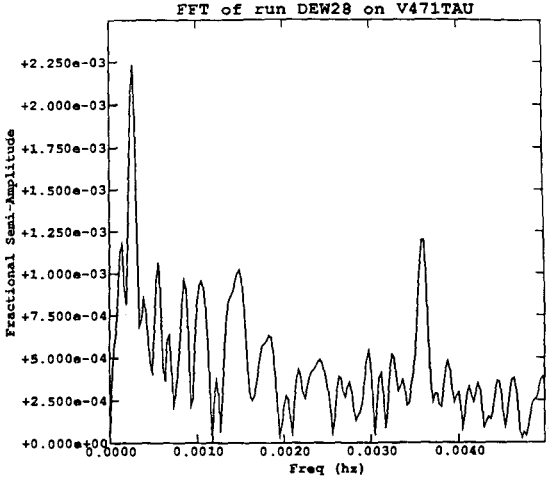
FFT of run DEW28 on V471TAU
Fractional Semi-Amplitude
+2.250e-03
+2.000e-03
+1.750e-03
+1.500e-03
+1.250e-03
+1.000e-03
+7.500e-04
+5.000e-04
+2.500e-04
+0.000e+00
0.0000
0.0010
0.0020
0.0030
0.0040
Freq (hz)

As pointed out by Robinson et al., the presence of peaks in the power spectra in addition to the 555 s, and the 277.5 s peaks, implies nonradial pulsations of the white dwarf. Our observations provide strong evidence that at least some of the frequencies observed in the white dwarf component are due to nonradial pulsations. However, these observations do not exclude the possibility that the 554 s or the 277 s modulations are due to dark/bright spots resulting from wind accretion on a rotating magnetic white dwarf.

We introduce the possibility that the nonradial pulsations may be Rossby modes instead of, or in addition to, the g-modes suggested by Robinson et al. Also, we point out that the excitation mechanism for the modes may be external—the result of the wind in the K2 star, or due to a theoretically expected hot DA instability strip.

In principle it is possible, with long uninterrupted data sets, to determine which, if any, frequencies are r-modes, which are g-modes, and which come from possible dark/bright spots on the white dwarf. For example, recall that we observe the amplitude of each of the optical periods to be variable over timescales less than or of order a day. If the period disappears and then reappears with a different phase, it cannot be due to rotation—it must be due to pulsation. Whether the pulsation is an r-mode or g-mode can be determined by the spacing between it and the other periods: r-modes have integer period ratios, while g-modes in general do not. If a period maintains its phase as its amplitude changes, it could be due to pulsation or rotation; however, if it is a g-mode pulsation the phase coherence implies that the amplitude modulation is due to the presence of closely spaced frequencies corresponding to different m-values. Finally, if the excitation is external and the amplitude modulation is caused by fluctuations in the wind from the K2V star, then the periods will not maintain phase.

In order to resolve these questions we are currently planning extended time- base observations using the Whole Earth Telescope (cf. Nather 1988, these proceedings) during November 1988.

This work was supported in part by grants, AST 85–52457 and AST 86–00507, from the National Science Foundation.

References

Hine, B. P. A., III, 1988, *A Search for Pulsations in Planetary Nebulae Nuclei*, (Ph D. Thesis: University of Texas at Austin).

Jensen, K. A., 1985, *IAU Circ.*, **No. 4102.**

Jensen, K. A., Swank, J. H., Guinan, E. F., Sion, E. M., and Shipman, H. L. 1986, *Ap. J. (Letters)*, **309**, L27.

Nelson, B., and Young, A. 1970, *P.A.S.P.*, **82**, 699.

Robinson, E. L., Clemens, J. C., and Hine, B. P. 1988, *Ap. J. (Letters)*, **331**, L29.

The Time Dependence of the Phases of the Harmonics Relative to the 1490 sec Fundamental in PG1346+082

J. L. Provencal, J. C. Clemens, G. Henry, B. P. Hine,
R. E. Nather, D. E. Winget*, M. A. Wood
McDonald Observatory and Department of Astronomy
The University of Texas at Austin
U.S.A.

S. O. Kepler
Instituto de Fisica
Universidade Federal do Rio Grande do Sul
Brazil

G. Vauclair, M. Chevreton
Observatoire Midi-Pyrenees et Observatoire de Meudon
France

D. O'Donoghue, B. Warner
Department of Astronomy
University of Cape Town
South Africa

A. D. Grauer
University of Arkansas at Little Rock
U.S.A.

Lilia Ferrario
Australian National University
Australia

INTRODUCTION

White dwarf stars provide important boundary conditions for the understanding of stellar evolution. An adequate understanding of even these simple stars is impossible without detailed knowledge of their interiors. PG1346+082, an interacting binary white dwarf system, provides a unique opportunity to view the interior of one degenerate as it is brought to light in the accretion disk of the second star as the primary strips material from its less massive companion (see Wood *et al.* 1987).

PG1346+082 is a photometric variable with a four magnitude variation over a four to five day quasi-period. A fast Fourier transform (FFT) of the light curve shows a complex, time-dependent structure of harmonics. PG1346+082 exhibits flickering – the signature of mass transfer. The optical spectra of the system contain weak emission features during minimum and broad absorption at all other times. This could be attributed to pressure broadening in the atmosphere of a compact object, or to a combination of pressure broadening and doppler broadening in a disk surrounding the compact accretor. No hydrogen lines are observed and the spectra are dominated by neutral helium. The spectra also display variable asymmetric line profiles.

OBSERVATIONS

Extended coverage photometry (Nather, these proceedings) of the variable star PG1346+082 in March 1988 (coverage given in Table 1) reveals at least 13 distinct periodicities distributed in a narrow band around 1500 s and in a second band around 1300 s. There are two dominant peaks at 1471 s and 1493 s. The fourier transform (FT) of the entire data set demonstrates that both main frequencies are coherent over the run length. Fourier transform analysis of the individual runs shows many cases where the harmonics of both the 1493 s period and the 1471 s period are simultaneously present.

Although we have not yet constructed detailed models of the system, the presence of so many identifiable periodicities suggests that we are observing pulsations at the surface of the accreting white dwarf. This is plausible: the system remained at or near minimum for most of the eighteen days of the run, so the competition from disk

* Alfred P. Sloan Fellow

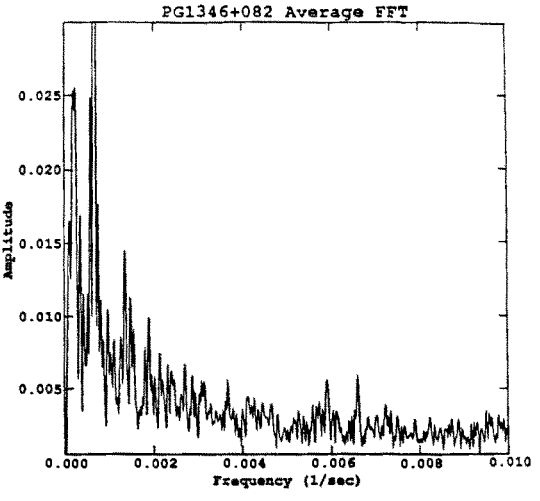

Figure 1 *Average FFT of PG1346+082. This FFT was obtained by averaging the FFTs of runs bph72, s4238 and s4246.*

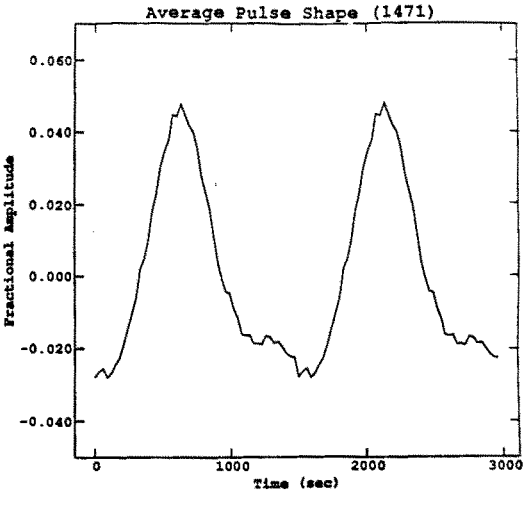

Figure 2 *Average pulse shape of the 1471 second fundamental over the entire data set.*

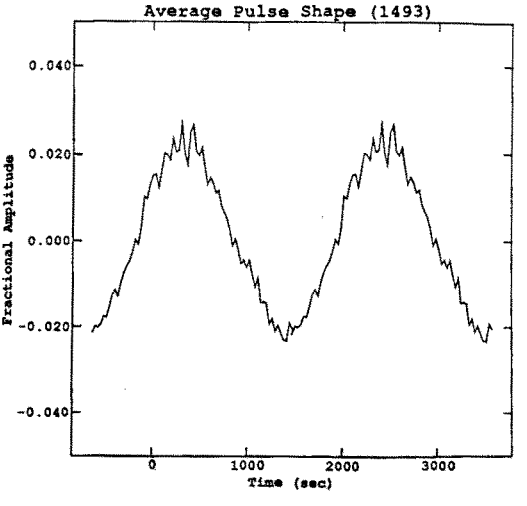

Figure 3 *Average pulse shape of the 1493 second fundamental over the entire data set.*

Table 1
Journal of Observations

Run	Location	Date	Time of Run Start (UT)	Length of Observation (hr)	Integration Time (sec)
ren18	Texas	9 March	6:28:20	1.772	10
ren19	Texas	9 March	8:39:20	1.867	10
ren20	Texas	9 March	11:24:50	0.478	10
a3	Australia	9 March	14:30:00	4.064	10
ren22	Texas	10 March	6:13:20	5.603	10
pg13a	France	10 March	22:57:06	5.173	6
ren24	Texas	11 March	5:47:00	6.067	10
pg13b	France	11 March	24:03:06	4.395	6
tol-0005	Chile	12 March	3:56:00	4.933	10
ren26	Texas	12 March	5:36:10	4.283	10
bph67	Hawaii	12 March	10:57:00	4.333	10
a10	Australia	12 March	13:41:01	4.972	10
s4227	South Africa	12 March	23:08:20	4.067	10
pg13c	France	12 March	23:20:06	5.233	6
tol-0011	Chile	13 March	3:23:00	5.625	10
ren28	Texas	13 March	5:54:08	5.931	10
bph68	Hawaii	13 March	9:18:00	5.967	10
a11	Australia	13 March	13:49:00	4.772	10
pg13d	France	13 March	23:21:06	5.052	6
tol-0017	Chile	14 March	4:10:00	2.658	10
ren29	Texas	14 March	5:24:10	5.514	10
bph69	Hawaii	14 March	8:57:00	0.639	10
a14	Australia	14 March	14:43:01	3.614	10
tol-0022	Chile	15 March	3:16:00	2.375	10
ren31	Texas	15 March	5:23:30	6.289	10
bph70	Hawaii	15 March	8:54:00	6.367	10
a19	Australia	15 March	14:46:00	3.817	10
ren33	Texas	16 March	5:23:30	6.339	10
s4238	South Africa	17 March	22:21:40	4.917	10
ren35	Texas	18 March	5:18:30	6.361	10
bph71	Hawaii	18 March	8:42:00	6.567	10
a23	Australia	18 March	13:24:00	1.211	10
ren37	Texas	19 March	5:19:00	5.502	10
bph72	Hawaii	19 March	8:45:00	6.547	10
maw3	Texas	20 March	4:29:00	7.150	10
bph73	Hawaii	20 March	8:38:00	6.677	10
a26	Australia	20 March	13:15:02	0.689	10
s4246	South Africa	20 March	22:27:20	4.800	10
maw5	Texas	21 March	4:33:52	7.086	10
bph74	Hawaii	21 March	8:41:00	6.483	10
a28	Australia	21 March	14:32:01	3.503	10
s4250	South Africa	21 March	22:54:20	4.550	10
maw7	Texas	22 March	4:17:00	6.558	10
bph75	Hawaii	22 March	8:40:00	6.425	10
maw10	Texas	23 March	4:16:00	7.333	10
bph76	Hawaii	23 March	8:28:00	2.347	10
s4253	South Africa	23 March	0:28:10	2.683	10
maw12	Texas	24 March	4:05:50	7.453	10
maw14	Texas	25 March	4:11:30	7.325	10
s4256	South Africa	25 March	23:40:50	3.367	10
maw16	Texas	26 March	7:37:20	3.892	10

luminosity was small, and the surface temperature of the accretor lies within the instability strip for DB (helium atmosphere) white dwarfs. Other explanations are possible, however, and we will explore them.

FFTs of the individual data sets, see Figure 1, show a remarkable harmonic structure associated with the two dominant frequencies. Significant power is detected out to the 13th harmonic for both of the main peaks. However, the character of the harmonic structure associated with each frequency is different. Although harmonics of both frequencies are present in the FFTs of the individual runs, only the low order harmonics of the 1471 s peak appear in the FT of the entire data set. Thus, the higher order harmonics of the 1471 s period and the entire harmonic structure of the 1493 s peak are not coherent over the 18 day run.

There are three traditional sources for these coherent modulations in a binary system. Assuming the twin degenerate, interacting binary model of Wood *et al.* (1987): the orbit of the pair, the rotation of the accreting white dwarf, and non-radial pulsations in the accreting white dwarf. Obviously, at most only one of the 13 periodiocities can be the orbital period, and its character could well be distinctly different from the others. We determined the average pulse shape of the two dominant frequencies in an attempt to identify the orbital period. The average pulse shape of the 1471s periodicity over the entire run, presented in Figure 2, is definitely not a sine wave. Taken together with the presence of coherent harmonics, this points to the nonlinearity of the pulsation. The combination of a coherent fundamental and coherent lower order harmonics mimics the structure seen in all other DB variables, strongly suggesting g-mode pulsation as its origin. The average pulse shape of the 1493 s period, presented in Figure 3, matches a sine function to within measurement error, and its harmonics are not coherent. The 1493 s period is of comparable amplitude to the 1471 s oscillation, so if the driving mechanisms are similar, the 1493 s pulsation should be nonlinear as well. It is not. In view of these differences, we identify the 1471 s period as an oscillation of the white dwarf and the 1493 s peak as either the orbital period of the system or the rotation period of the accreting white dwarf.

Evidence (discussed in detail in Wood *et al.*) indicates that PG1346+082 is an interacting binary white dwarf system of extreme mass ratio: the mass-losing object is estimated to have only $0.03 M\odot$, comparable to the planetary mass assumed in simplified models of the early solar system. Steady state calculations of the tidal interactions of a planet with a disk indicate that the disk would become strongly perturbed in a multi-armed spiral pattern of shocks (Lin and Papaloizou, 1986). These shocks are most evident in the outer regions of the disk. A complex, variable structure of harmonics of the orbital period, such as is seen in PG1346+082, might be envisioned as the natural outcome of such a model. If these assumptions, similar to those proposed by O'Donoghue et al., are correct, the time-evolution of the harmonics of the orbital period could be a valuable probe of the disk structure. It may be possible to map out the density distribution and track mass transfer, as it flows through the disk, through variations in amplitude of one harmonic with respect to the others.

CONCLUSIONS

On the basis of our preliminary analysis of the harmonic structure, we suggest that the 1493 s oscillation is either the orbital period of the system or the rotation period of a magnetized, accreting white dwarf. The 1471 s is most probably a nonradial oscillation of the primary white dwarf since its character mimics that of oscillations seen in single DB variables.

We suggest that the harmonics of the 1493 s period arise in the disk of PG1346+082. Each of the harmonics arise in a different physical location where resonant density enhancements reprocess the radiation from the central object, but whose precise location can vary on the accretion flow.

If this suggestion is correct, PG1346+082 provides us with a unique opportunity to examine the time-dependent changes in the harmonics and thus probe the structure of the disk. Variations in amplitude of one harmonic relative to others could be a valuable probe of density distribution and the flow of mass in the disk. In particular we should be able to follow the large changes in brightness (from magnitude 17.2 to magnitude 13) and in this way and determine its physical origin.

This work was supported by the National Geographic Society, the Able Hanger Foundation, and the National Science Foundation through grants AST 85-52457 and AST 86-00507.

REFERENCES

Lin D. N., and Papaloizou, J. 1986, *Ap. J* **307** 395.

O'Donoghue, D., and Kilkenny, D., *High Speed Spectroscopy and Photometry of the Interaction Binary White Dwarf V803 Cen (AE-1)*, preprint, 1988

Wood, M.A., Winget, D. E., Nather, R. E., Hessman, F. V., Liebert, J., Kurtz, D. W., Wesemael, F., Wegner G., 1987,*Ap. J.* **313**, 757.

A NEW HYDROGEN EQUATION OF STATE FOR LOW MASS STARS

D. Saumon and G. Chabrier
Department of Physics and Astronomy
University of Rochester
Rochester, NY 14627-0011
USA

1) INTRODUCTION

Studies of the structure and evolution of low mass stars, brown dwarfs and giant planets require an equation of state (EOS) that includes a detailed, accurate model of the strongly non-ideal behavior of matter in these cool, compact objects [Fig. (1)]. Physical processes in the outer layers of white dwarfs, especially the analysis of the pulsation properties of ZZ Ceti stars, depend sometimes critically on the thermal properties of partially ionized hydrogen. In view of the substantial developments in the statistical physics of dense fluids and plasmas over the past decade, the computation of a new, independent EOS for astrophysical applications is justified. The statistical mechanical models which we present for hydrogen can be adapted to treat both pure helium and hydrogen-helium mixtures.

2) DESCRIPTION OF THE MODEL FREE ENERGY

We have developed two different models to compute the EOS of pure hydrogen. At low density ($\log \rho < 0$), low temperature ($\log T < 4$), we consider a mixture of hydrogen atoms and molecules. At high densities ($\log \rho > 0$) and at high temperatures ($\log T > 5$), we use a model of protons interacting with a responsive, neutralizing electron background. In the intermediate region of partial ionization, the two models are combined as described below.

a) The Neutral Model

Assuming factorization of the partition function of the system, the free energy of the H/H_2 mixture becomes:

$$F_I = F_{trans} + F_{conf} + F_{int} + F_{qm}. \quad (1)$$

The translational free energy, F_{trans} is the ideal gas contribution of all particles. The configuration term, F_{conf}, represents the interactions between the different particles in their ground states. It is evaluated in the framework of the WCA fluid perturbation theory (Weeks, Chandler and Andersen 1971) In this theory, the interaction potential $\phi(r)$ is split into a repulsive reference potential $\phi^{ref}(r)$, and a weak, attractive, perturbation potential $\phi^{pert}(r)$. We approximate the free energy of the reference system by that of a hard sphere fluid, which is known analytically (Mansoori *et al.* 1971), whereas the contribution of the perturbation potential is given by the first term of the

free energy expansion:

$$F_{conf}(N,V,T,x_1,x_2) = F_{hs}(\sigma_{\rm H},\sigma_{\rm H_2}) + \frac{1}{2}\frac{N^2}{V}\sum_{i,j=1}^{2} x_i x_j \int \phi_{ij}^{pert}(r) g_{ij}^{0}(r)\, d^3r. \qquad (2)$$

In Eq. (2), N is the total number of particles, V is the volume of the system and $g_{ij}^0(r)$ represents the pair correlation functions of the reference system. The concentrations x_H and x_{H_2} in the H/H_2 fluid are determined by the condition of chemical equilibrium, with the temperature- and density-dependent hard sphere diameters $\sigma_{\rm H}$ and $\sigma_{\rm H_2}$ *calculated through a thermodynamic criterion* (Weeks, Chandler and Andersen 1971). The internal energy and pressure obtained by numerically differentiating Eq. (2) are in excellent agreement with the results of Monte Carlo simulations of the H/H_2 mixture (Saumon, Chabrier and Weis 1988). The potential functions $\phi_{ij}(r)$ are fitted to realistic potentials obtained from *ab initio* calculations (Kolos and Wolniewicz 1965, Porter and Karplus 1964) and from experiments (Ross, Ree and Young 1983).

The internal free energy, F_{int}, includes all known levels for H_2 (Huber and Herzberg 1979). The effects of interparticle interactions upon the internal levels are treated with the formalism of Hummer and Mihalas (1988). In their approach, the energy of the bound states is unperturbed, but each level is assigned an occupation probability which ensures self-consistency between the interaction terms [Eq. (2)] and their effect on the internal partition function. The occupation probability provides a smooth cutoff of the otherwise diverging H partition function.

Quantum diffraction effects are included in F_{qm}, the first term of the Wigner-Kirkwood $\hbar^2$ expansion.

Figure 2 shows the concentration of atoms in the H/H_2 mixture as given by the condition of chemical equilibrium, using Eq. (1) for the free energy. We find that pressure-dissociation of molecules is significant in regimes characteristic of giant planets and brown dwarfs.

b) The Fully Ionized Model

In this regime, the ions are classical particles, while the electrons – which constitute a polarizable, inhomogeneous medium – range from a fully degenerate to a nearly classical state. The hamiltonian of this system is:

$$H = H_i + H_e + V_{ie}, \qquad (3)$$

where H_i is the hamiltonian of the ions in a uniform neutralizing background, H_e is the jellium hamiltonian for the electrons (Pines and Nozières 1966) and V_{ie} describes the ion-electron interaction. Assuming this last term to be small and thereby retaining only the linear contribution, Eq. (3) can be rewritten (Ashcroft and Shroud 1978):

$$H = H^{eff} + H_e, \qquad (4)$$

where

$$H^{eff} = \sum_i \frac{p_i^2}{2m_i} + \frac{Z^2}{2V}\sum_{k\neq 0}\frac{4\pi e^2}{k^2}\left[\frac{\rho_{\vec{k}}\rho_{\vec{k}}^*}{\epsilon(k,\omega=0)} - N_i\right] \qquad (5)$$

is the hamiltonian of the screened ionic fluid. In Eq. (5), N_i is the number of ions, $\rho_{\vec{k}}$ is the Fourier component of the ion density and $\epsilon(k,0)$ is the temperature- and density-dependent Lindhard

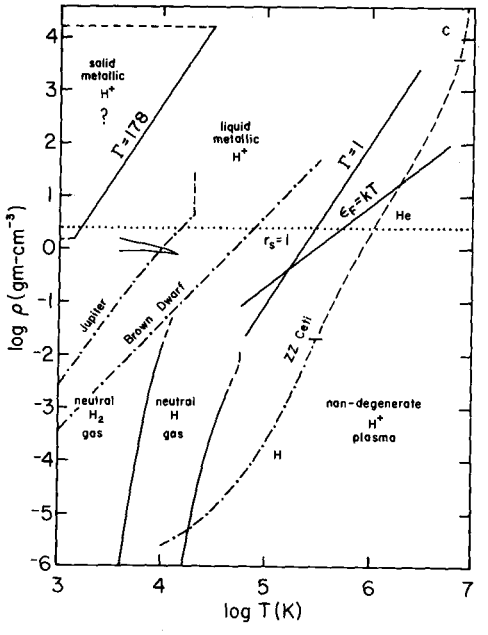

Figure 1. $(\rho - T)$ phase diagram of hydrogen. A few physical regimes are identified. Above the $\Gamma = 1$ line, the plasma is strongly coupled. Electrons are degenerate above the line $\epsilon_F = kT$. The narrow wedge near $\log T = 4$ and $\log \rho = 0$ indicates the location of the possible first-order phase transition. Adiabats of Jupiter and a brown dwarf are shown along with a ZZ Ceti model. Adapted from Fig. 2 of Van Horn (1986).

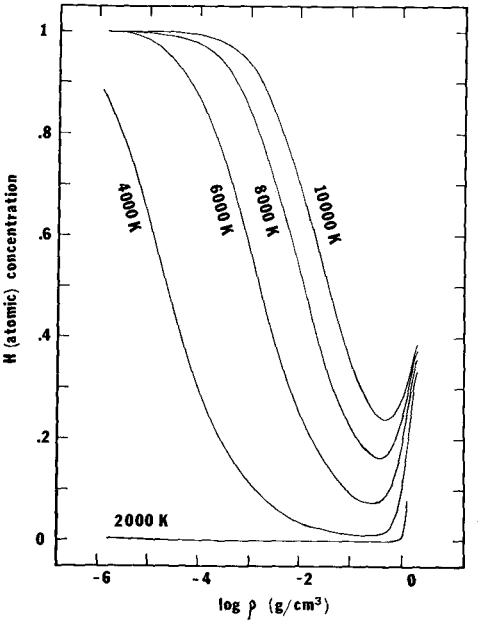

Figure 2. Atomic hydrogen concentration as a function of density and temperature, computed with the neutral model F_I . Note the effect of pressure dissociation near $\log \rho = 0$.

screening function of the electron fluid in the adiabatic approximation (Lindhard 1954). As long as the dielectric function $\epsilon(k,0)$ includes a local field correction (LFC) to describe the exchange and short-range correlation effects in the quantum electron fluid, this model gives excellent results for the thermodynamics of a fully ionized hydrogen plasma, even in the low degeneracy, nearly classical regime for the electrons (Chabrier 1988). This LFC is an important contribution at intermediate densities ($\log \rho < 0.5$).

The free energy corresponding to the hamiltonian of Eqns (4) and (5) reads:

$$F_{II} = -kT \ln[Tr \exp^{-\beta H}] = F_i^0 + F_e^0 - kT \ln \int e^{-\beta U^{eff}} d^3 r_N + F_{xc} + F_{qm}, \qquad (6)$$

where the trace is taken over the states of the coupled ion-electron system, $\beta = 1/kT$, and U^{eff} represents the last term on the r.h.s. of Eq. (5). The superscript ^{0} denotes the perfect gas contribution (classical or degenerate). F_{xc} is the exchange and correlation free energy of the electron gas. We adopted the excellent analytical fit of Ichimaru, Iyetomi and Tanaka (1987) which is valid for any degree of degeneracy. Finally, F_{qm} represents the Wigner-Kirkwood quantum correction calculated for a screened ionic fluid.

At densities lower than $\log \rho = -0.5$, the linear approximation used in Eq. (5) is no longer valid. In this region, we use an interpolation between the free energy given by Eq. (6) and the low density ($\log \rho < 2$) limit given by the two-component Debye-Hückel free energy, corrected for the quantum nature of the electrons (DeWitt 1969, the reader should be aware of a misprint in the expression for βF_{ring}).

At high densities ($\log \rho > 0.5$), our model free energy recovers the results obtained by DeWitt and Hubbard (1976) with a zero temperature dielectric function in the RPA approximation. It also emcompasses the Thomas-Fermi model. In the region of intermediate density ($\log \rho \approx 0$) or intermediate degeneracy ($\epsilon_F \approx kT$), it represents a significant improvement over these models.

c) Partial ionization

The problem of temperature ionization, where the departures from the ideal gas behavior are small, is well understood. We recover the known limits by combining F_I and F_{II} with appropriate concentration factors and imposing the conditions of chemical equilibrium.

The pressure ionization problem, however, is more delicate. The simplest way to treat it is to interpolate smoothly between the two model free energies along isotherms. Another possibility, suggested by different authors (Robnik and Kundt 1983, Ebeling and Richert 1985, Marley and Hubbard 1988), is that pressure ionization is a first-order phase transition between a mostly neutral fluid and a fully ionized plasma.

Following standard procedure (Landau and Lifshitz 1959), we explored this possibility, using a superposition of F_I and F_{II} together with the condition of chemical equilibrium, and found a phase transition, with a critical point defined by $P_c = 0.40$ MBar, $T_c = 16500$K, $\rho_c = 0.30$ g cm^{-3}. The Jupiter adiabat goes through the phase transition line(*cf.* Fig. 1), but substellar objects may be too hot for this plasma phase transition to occur.

3) CONCLUSION

We have developed a new EOS for hydrogen in a temperature and density domain relevant to low mass stars, giant planets, and the outer layers of DA white dwarfs, using the most sophisticated tools presently available in statistical physics. We believe that this EOS incorporates significant improvements over existing equations of state, especially in the intermediate density regime ($-3 < \log\rho < 0$) and the partial ionization zone (Saumon, Chabrier and Van Horn 1988). Using two sophisticated free energy models, we calculated a critical transition line and a critical point and found that a plasma phase transition might occur in the interior of giant planets (Saumon and Chabrier 1988).

We wish to thank Professor H. M. Van Horn for his continuous interest in this work and a careful reading of this manuscript. This work was supported in part by NSF gran AST87-06711, a NATO fellowship to G.C. and a NSERC of Canada scholarship to D.S.

REFERENCES

Ashcroft, N. W., and Stroud, D., 1978 in *Solid State Physics*, **33**, H. Ehrenreich, F. Seitz and D. Turnbull, eds., Academic Press, New York, p. 2.

Chabrier, G., 1988 submitted to *Phys. Lett. A.*

DeWitt, H. E., 1969 in *Low Luminosity Stars*, S. S. Kumar, ed., Gordon and Breach Science Publishers, New York, p. 211.

DeWitt, H. E., and Hubbard, W. B., 1976 *Astrophys. J.*, **205**, 295.

Ebeling, W. and Richert, W., 1985 *Phys. Status. Solidi.*, **128**, 467.

Huber, K. P., and Herzberg, G., 1979 *Molecular Spectra and Molecular Structure. IV. Constants of Diatomic Molecules*, Van Nostrand Reinhold Co., New York, p. 240ff.

Hummer, D. G., and Mihalas, D., 1988 *Astrophys. J.*, in press.

Ichimaru, S., Iyetomi, H., and Tanaka, S., 1987 *Phys. Rep.* **149**.

Kolos, W., and Wolniewicz, L., 1965 *J. Chem. Phys.*, **43**, 2429.

Landau, L. D., and Lifshitz, E. M., 1959 *Statistical Physics*, Pergamon, Oxford, p. 251ff.

Lindhard, J., 1954, *K. Dan. Videnskab. Selskab. Mat. Phys. Medd.*, **28**, 8.

Mansoori, G. A., Carnahan, N. F., Starling, K. E., and Leland, T. W., Jr., 1971 *J. Chem. Phys.*, **54**, 1523.

Marley, M. S., and Hubbard, W. B., 1988 *Icarus*, **73**, 536.

Pines, D., and Nozières, P., 1966 *The Theory of Quantum Liquids*, Benjamin, New York.

Porter, R. N., and Karplus, M., 1964 *J. Chem. Phys.*, **40**, 1105.

Robnik, M., and Kundt, W., 1983 *Astron. Astrophys.*, **120**, 227.

Ross, M., Ree, F. H., and Young, D. A., 1983 *J. Chem. Phys*, **79**, 1487.

Saumon, D., and Chabrier, G., 1988 in preparation.

Saumon, D., Chabrier, G., and Van Horn, H. M., 1988 in preparation.

Saumon, D., Chabrier, G., and Weis, J. J., 1988 submitted to *J. Chem. Phys.*

Van Horn, H. M., 1986 *Mitt. Astron. Ges.*, **67**, 63.

Weeks, J. D., Chandler, D., and Anderson, H. C., 1971 *J. Chem. Phys.*, **54**, 5237.

MAGNETIC FIELDS IN WHITE DWARFS

Gary D. Schmidt
Steward Observatory, University of Arizona
Tucson, Arizona 85721, USA

1. Introduction

Just one year ago at the 2nd Conference on Faint Blue Stars, two review papers were presented summarizing the observational characteristics and attempts at spectral modeling of isolated magnetic white dwarfs (see Schmidt 1987 and Wickramasinghe 1987, respectively). Because much of that information is still relevant, this paper will concentrate on some of the progress which has occurred since the time of that meeting, and on highlighting current problems in the area of research. Using specific examples for illustration, the discussion concentrates on the single stars. Magnetic binary systems are considered from the point of view of the white dwarfs themselves.

2. Recent Identifications and the Current Magnetic Sample

During the past year, two new white dwarfs were added to the list of known magnetic stars: a DA with a polar field of ~ 24 MG (1 MG = 10^6 G), found in the course of a QSO survey (Foltz and Latter 1988), and a unique DC + magnetic DQ wide binary (Ruiz and Maza 1988, also reported at this meeting). As summarized in Table 1, this brings the current sample to a total of 26 stars spanning the range in field strength ~ 1-1000 MG.

Magnetic candidates are drawn from a variety of sources. Prior to the advent of electronic array detectors, spectroscopy was generally not adept at distinguishing diffuse, shallow features, so many of the early magnetic stars were identified through the continuum circular polarization which is induced by the field (e.g. Kemp 1970; Angel 1977). The polarization arises because of circular dichroism, which at low and intermediate fields, resembles a splitting of the continuum opacity functions for opposite handed modes of propagation of the electric vector. As shown in Fig. 1, this effect results in a fractional optical polarization of V ≈1% at a field of 50 MG (dependent also on opacity source and field orientation). Above ~100 MG, however, the simple Zeeman analogy breaks down as the opacity sources depart substantially from their zero-field functional form and propagation modes become elliptical. Linear polarization then begins to appear, again dependent on geometry, but amounting to P ≈1% at a strength of 200 MG and

climbing rapidly thereafter (Fig 1.). Clearly, the sensitivity of polarimetric surveys is limited to strong magnetic fields.

Fortunately, magnetic sensitivities of the low members of the hydrogen Balmer series fall in the range 5-15Å/MG, so surface strengths as weak as 10 MG are easily recognized in most modern survey-quality spectroscopy. This is the origin of many of the recent discoveries, esp. the PG sample. Of course, for DC spectral types or in field strength regimes where features are severely smeared, spectroscopy loses its effectiveness (see, however, the discrete features of H in PG1031+234 [Latter, Schmidt, and Green 1987], at nearly 10^9 MG).

Comparatively weak fields, 10^{5-6} G, should be detectable in principle through wavelength shifts of the high-order Balmer lines resulting from the quadratic Zeeman effect (e.g., Preston 1970). Values another factor of 10 smaller might be recognized as subtle broadening of the non-LTE cores of Hα in the cooler DAs, assuming the profile could be distinguished from rotational smearing. The idea of recognizing comparatively weak magnetic fields through "magnetoseismology" has also been recently suggested by Jones et al. (1988, and summarized by Kawaler at this meeting), but considering the paucity of pulsating white dwarfs, this technique is not likely to be of assistance in discovering significant numbers of low-field stars.

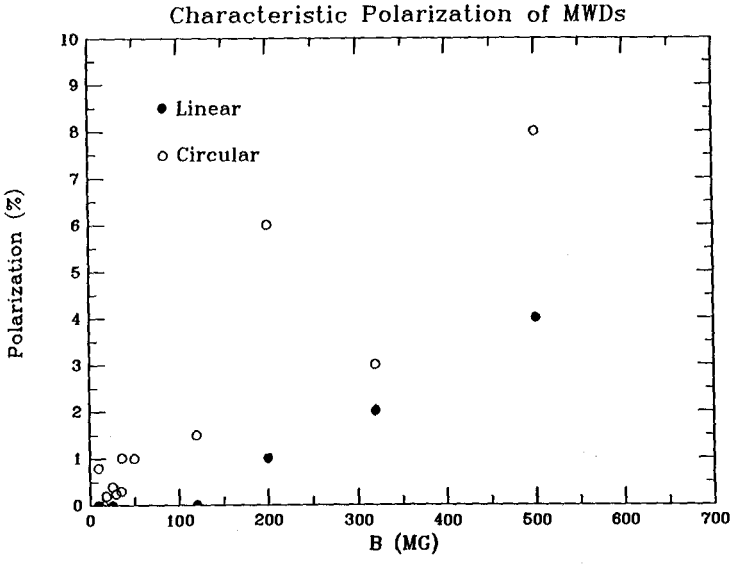

Fig. 1. The observed characteristic levels of continuum circular and linear polarization in the optical for the stars listed in Table 1. Although temperature, opacity source, viewing angle and field structure cause a wide dispersion in the degree of polarization at any given field value, the general trends are useful for estimating field strengths on stars with featureless or unidentified spectra.

TABLE 1

ISOLATED MAGNETIC WHITE DWARFS

Object	T (K)	Spectral features	Period	<P> (%)	<V> (%)	Bp (MG)
PG 0136+251	45000	H				2
PG 1658+441	30000	H				3.5
G141-2	5600	H				5
GD90	12000	H			<.15	9
G 99-37	6200	C2,CH		<.1	.8	10
KUV 03292+0035	15000	H				12
GD 356	7500	H(em)			<.05	15
HS 1254+3430	15000	H				15
KPD 0253+5052	20000	H	4.1h		.2	18
1136-014		H				24
G 99-47	5700	H		<.1	.4	25
KUV 813-14	10400	H			.25	29
PG 1533-057	20000	H				31
Feige 7	22000	H,He	2.2h		.3	35
BPM 25114	20000	H	2.8d		1	36
PG 1313+095	15000	H	5.4h		1	~50
GD 116	15000	H				65
ESO 439-162	6300	C2				~100
G 195-19	8000	none	1.3d	<.13	.8	~100
PG 1015+015	10000	H	1.6h		1	120
G 227-35	7000	?		.25	2	~150
LP 790-29	8600	C2		1	6	200
G 240-72	6000	?		1	.5	~200
GD 229	16000	?		4	<.2	>200
GrW +70 8247	14000	H		2	3	320
PG 1031+234	15000	H	3.4h	4	8	500

Taking together the early searches for magnetic fields (see the historical perspective in Liebert 1988), line profile studies, surveys for rotation (e.g. Pilachowski and Milkey 1987), and the now-popular quest for short-period double-degenerate binaries, a reasonable estimate might be that the line spectra of ~1/3 of known white dwarfs have been observed with sufficient dispersion and signal-to-noise ratio that fields in the range ~10^{5-6} G would have been discovered. Yet, none have. The current definite detection limit is represented by PG 1658+441 at a polar value of ~3.5 MG, and PG 0136+251 is a probable magnetic star with a strength about a factor of two weaker (Liebert et al. 1983). Thus, it would appear that the distribution of degenerates with surface field strength as presented by Schmidt (1987) is a reasonable approximation to reality: overall, the magnetic sample (1-1000 MG) comprises no more than ~2-3% of the total number of known white dwarfs, and the broad distribution shows a moderate but probably significant preference for the range ~10-100 MG. We conclude that by far the majority of white dwarfs possess fields below a surface strength of 10^5 G.

The distribution of white dwarf primary stars with magnetic field strength is an important topic of discussion among Cataclysmic Variable (CV) enthusiasts, since

a strong field can dictate such basic features as the dynamics of accretion, the emitted energy distribution, spin/orbit synchronization, and probably even the long-term evolution of the system. For the purposes of this conference, the situation can be summarized as follows: field strengths on about half of the AM Her systems have been directly measured to fall in the range 20-55 MG, and the remainder of these 15 synchronized binaries are probably very similar. Another dozen or so systems, called the DQ Her binaries or Intermediate Polars, show coherent optical and X-ray brightness modulations which are associated with a magnetic field on the rotating primary star, but the field is too weak (or the system too large) to disrupt the accretion disk and synchronize the spin and orbital motions. The spectrum of near-infrared circular polarization detected from one such binary confirms its magnetic nature and suggests a surface field value of ~5-10 MG (West et al. 1987).

Not only are very strong-field (B>100 MG) primaries conspicuous in their absence among known CVs, but weak and intermediate-field systems are far more numerous than their counterparts in the field. More than 20% of all known CVs are magnetic, and the AM Her and DQ Her binaries mentioned above comprise more than 1/3 of all systems with orbital periods shorter than two hours. Although some of the discrepancy vis-a-vis field degenerates can be attributed to the enhanced X-ray luminosity (therefore enhanced detectability) resulting from magnetically channeled accretion, it is unlikely that this is an order-of-magnitude effect. One avenue for consideration is the effect that a strong magnetic field might have on the production of a short-period binary during the common-envelope phase of evolution.

3. Field Morphology

Wickramasinghe (1987) provides an excellent recent review of the relevant physics and attempts at spectral modeling of fields on the known magnetic white dwarfs. In general, the distribution of field strength over the photosphere is best deduced from the profiles of Zeeman-displaced absorption lines, while the run of circular and linear polarization through a line and/or the rotational modulation of continuum polarization can be used to infer field direction. Since hydrogen is the only element for which reasonably complete and accurate Zeeman calculations exist (e.g., Henry and O'Connell 1985; Wunner et al. 1987), such work has thus far been confined to the magnetic DAs.

The recent study of Grw +70°8247 by Wickramasinghe and Ferrario (1988) is a particularly credible exercise if only because of the wealth of high quality data on this bright, well-observed star. Modeling of both the rich line spectrum as well as

circular and linear spectropolarimetry were attempted, with the result that a pole-on dipole of 320 MG polar strength yielded reasonably good fits to the data. However, particular problems were noted in matching features longward of ~6000Å and the polarimetric profiles of the lines. S. Jordan, in a paper presented at this meeting, applies a similar approach to Grw +70°, and obtains somewhat better agreement with the red transitions but even poorer polarimetric profiles. No doubt a portion of this difficulty results from the fact that, although the Zeeman pattern of hydrogen is reasonably well in hand, the atmospheric physics and opacity functions in fields as strong as those on Grw +70°8247 are not currently tractable (Wickramasinghe 1987). Until those problems are resolved, it is difficult to contemplate substantial improvements to the models for very high-field objects.

Perhaps most informative are the results for the rotating magnetic stars (see Fig. 2). As an example, Wickramasinghe and Cropper (1988) have recently studied phase-resolved spectroscopy and spectropolarimetry of the ~100 MG star PG 1015+015, which rotates with a period of 99^m. At this field strength the use of shifted zero-field opacity curves is more secure, and the opportunity to study a full range of viewing angles greatly reduces ambiguities in the possible geometries. Unfortunately, the star is sufficiently faint that the polarimetry was of little use aside from defining the continuum behavior with rotational phase. The authors conclude that the field morphology approximates that of a centered dipole with polar strength of ~120 MG which is oriented roughly orthogonal to the spin axis of the star.

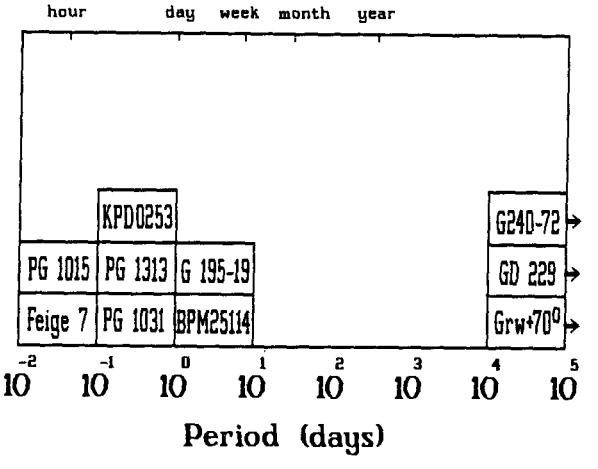

Fig. 2. Distribution of rotation periods deduced from periodic variations in the circular polarization of magnetic white dwarfs. The very long periods shown for a few stars are based on the assumption of an oblique rotator and the absence of detectable variations in polarization over more than a decade of monitoring.

It should not be inferred from the above examples that the field patterns on all white dwarfs are dipolar in nature. The most strongly magnetized white dwarf identified to date, PG 1031+234, exhibits a hydrogen Zeeman pattern which depicts fields between 200 and nearly 1000 MG through its 3^h24^m rotation period (Schmidt et al. 1986). Although the overall structure on the surface of this star suggests a dipole with a polar strength in the vicinity of 500 MG (Latter et al. 1987), the most intense fields are found in a single magnetic "spot". In attempting to model PG 1031+234, Schmidt et al. (1986) found the distortions to the phase-resolved continuum polarization curve caused by this spot so severe that the ignorance of high-field atomic physics was deemed a second-order effect.

Although the rather simple field morphologies deduced for the majority of magnetic stars studied to date would seem to indicate the presence of well-organized underlying global structures, white dwarfs are sufficiently dense that even hundred-MG fields can be anchored in a relatively thin skin. Such an explanation has been proffered for the magnetic "spot" on PG 1031+234, and chromospheric activity has been proposed to account for the apparently rather tangled field on surface of the unique magnetic emissionline degenerate GD 356 (Greenstein and McCarthy 1985).

4. The Magnetic Nova V1500 Cygni

The recent discovery that Nova Cygni 1975 occurred in a magnetic binary system (now designated V1500 Cyg) provides a unique opportunity to study the effects which a strong magnetic field has on the nova event (and, perhaps ultimately vice versa). Among known novae, the 1975 event was an exceedingly fast eruption: rising at least 19 magnitudes above the POSS plate limit to an apparent visual magnitude of V = 1.8 and declining by 3 mags in just 4 days. At maximum light, the absolute visual magnitude of Mv = -10.2 marked Nova Cygni as one of the brightest of such events. These facts, in part, have led to the conclusion that the mass of the white dwarf primary in this binary is nearly at the Chandrasekhar limit (see the recent review by Lance, McCall, and Uomoto 1988).

The post-nova decline was marked by peculiar brightness oscillations on a timescale somewhat longer than 3 hours. Well-observed by Patterson (1979) and others, the period of these variations decreased by more than 4 minutes in the year following outburst; when observations resumed following the winter of 1976, the period had stabilized at an intermediate value of $3^h\ 21^m$. The fluctuations have continued at that period with a fixed ephemeris to the current mean brightness of V = 17.1 and amplitude ~0.5-1 mag. Although the oscillations were generally thought to reflect rotational or orbital motion, the aperiodicity was not readily explained at the time.

In 1987, V1500 Cyg was found to exhibit optical circular polarization modulated on a period some 3.5 minutes shorter than the post-1977 photometric period (Stockman, Schmidt, and Lamb 1988). Like the AM Her systems, this was interpreted by the authors to indicate the emission of optical cyclotron radiation in a magnetic field >10 MG from the vicinity of the accreting post-nova primary. The polarimetric period then reflects the rotation period of the magnetic white dwarf; the only reasonable explanation for the post-1977 stable photometric oscillation is the cyclical appearance of the inner heated hemisphere of the tidally-locked corotating secondary star.

A binary period of 3^h21^m places V1500 Cyg near the long-period extreme of the phase-locked systems, but among other AM Her binaries. Moreover, the presence of a magnetic field sufficient to give rise to optical cyclotron emission and the near-synchronism of V1500 Cyg even after the nova outburst suggested to Stockman et al. that the binary was indeed a synchronized AM Her system prior to eruption. The proposed process by which it became uncoupled involves frictional angular momentum transfer (e.g. MacDonald 1980) from the orbiting secondary to the primary while the white dwarf was bloated beyond the size of binary system (see Stockman et al.). The authors show that the concept of a magnetic pole-accretor provides a ready explanation for the entire post-eruption photometric history of the system (Fig. 3).

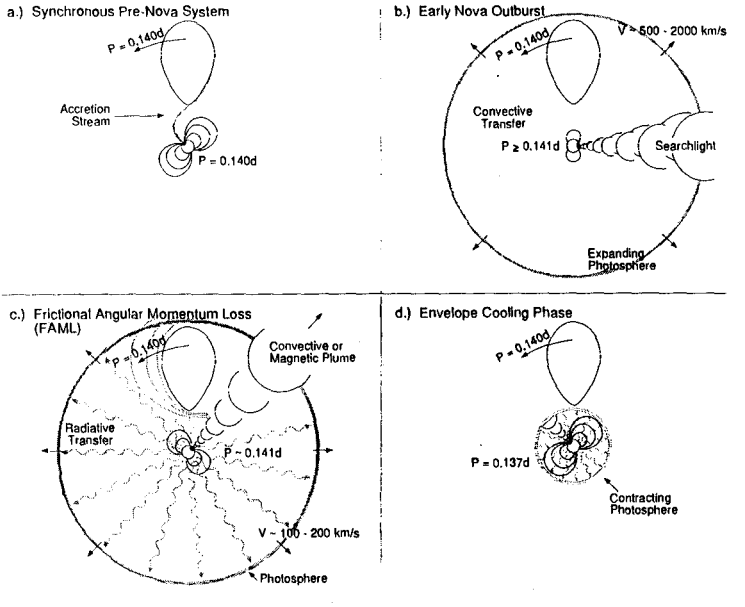

Fig. 3. An explanation of the remarkable photometric variations observed during the first few years following the eruption of Nova Cygni 1975. The system begins the process as a phase-locked magnetic AM Her system, accreting primarily onto one magnetic pole. Decoupling of the spin and orbital periods occurs due to frictional angular momentum transfer between the secondary and primary star when the atmosphere is distended beyond the extent of the binary system.

The mechanism by which spin/orbit synchronization occurs in a magnetic CV is a topic of popular concern, since the phenomenon is also linked to the orbital period evolution of the binary. For fields typical of AM Her variables, estimates of the timescale for phase-locking generally fall in the range 10^3 - 10^5 years; indeed, V1500 Cyg must resynchronize during that period if it is to avoid a period runaway due to future nova events. For these timescales, the required time derivative of the rotational period falls in the range

$$7 \times 10^{-9} > \dot{P} > 7 \times 10^{-11},$$

respectively. The past year of polarimetric study of V1500 Cyg by the author and collaborators has yielded a rotational ephemeris accurate to better than 0.1 sec, and the timing residuals from strict periodicity provide a limit of $\dot{P} < 4 \times 10^{-9}$ (Fig. 4). Thus, the data already exclude phase-locking on a timescale of 10^3 years. With the sensitivity scaling as (time)^2, there is good reason to believe that continued monitoring over the next few years will directly test synchronizing theories.

The magnetic field strength on V1500 Cyg has not yet been measured. Due to its distance and intervening absorption, the system is rather faint, and with the current light output dominated by the heated secondary, searches for Zeeman features due to the white dwarf's photosphere are unpractical. An attempt is currently underway to obtain a crude estimate of the field strength through measurement of the spectrum of polarized cyclotron flux. With this in hand, many aspects of the eruption and postnova behavior of V1500 Cyg will be placed on a more quantitative footing.

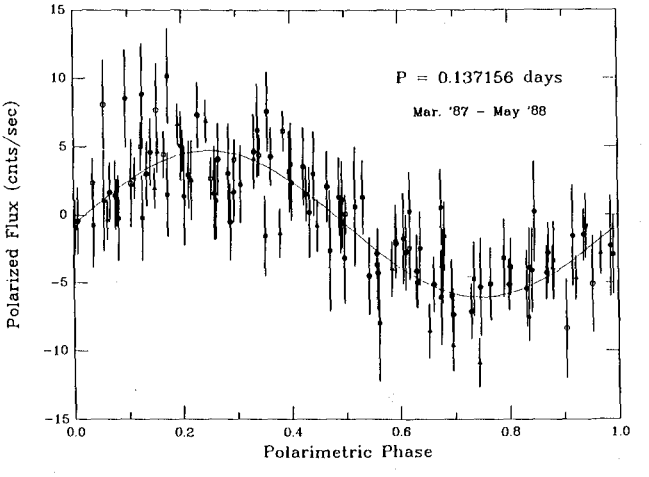

Fig. 4. One year of polarimetric monitoring of V1500 Cyg phased on a single period. Different symbols represent various epochs of observation. The uncertainty in period is less than 0.1 sec; timing residuals from strict periodicity imply $\dot{P} < 4 \times 10^{-9}$.

The author is especially grateful to C. Foltz, M. Ruiz, and J. Maza for ensuring the timeliness of this review by providing information on recent magnetic discoveries prior to their publication. The recent developments on the unique magnetic nova system V1500 Cyg presented here are to be included in a future publication (Schmidt and Stockman 1988). Research by the author on magnetic white dwarfs and magnetic binary systems is supported, in part, by the National Science Foundation through grant AST 86-19296.

References

Angel, J. R. P. 1977, Ap. J., 216, 1.

Foltz, C. B., and Latter W. B. 1988, private communication.

Greenstein, J. L. and McCarthy, J. K 1985, Ap. J., 289, 732.

Henry, R. J. W., and O'Connell, R. F. 1985, Pub. A. S. P., 97, 333.

Jones, P. W., Pesnell, W. D., Kawaler, S. D., and Hansen, C. J. 1988, preprint.

Kemp, J. C. 1970, Ap. J., 162, 169.

Lance, C. M., McCall, M. L., and Uomoto, A. K. 1988, Ap. J. Suppl., in press.

Latter, W. B., Schmidt, G. D., and Green, R. F. 1987, Ap. J., 320, 308.

Liebert, J., Schmidt, G. D., Green, R. F., Stockman, H. S., and McGraw, J. T. 1983, Ap. J., 264, 262.

Liebert, J. 1988, Pub. A. S. P., in press.

MacDonald, J. 1980, M. N. R. A. S., 191, 933.

Patterson, J. 1979, Ap. J., 231, 789.

Pilachowski, C., and Milkey, R. W. 1987, Pub. A. S. P., 99, 836.

Preston, G. W. 1970, Ap. J. Lett., 160, L143.

Ruiz, M. T. and Maza, J. 1988, preprint.

Schmidt, G. D. 1987, in The Second Conference on Faint Blue Stars, proc. IAU Colloquium No. 95, ed. A.G.D. Philip, D. S. Hayes, and J. W. Liebert (Schenectady: L. Davis Press), pp. 377-388.

Schmidt, G. D., and Stockman, H. S. 1988, in preparation.

Schmidt, G. D., West, S. C., Liebert, J., Green, R. F., and Stockman, H. S. 1986, Ap. J., 309, 218.

Stockman, H. S., Schmidt, G. D., and Lamb, D. Q. 1988, Ap. J., in press.

West, S. C., Berriman, G., and Schmidt, G. D. 1987, Ap. J. (Letters), 322, L35.

Wickramasinghe, D. T. 1987, in The Second Conference on Faint Blue Stars, proc. IAU Colloquium No. 95, ed. A.G.D. Philip, D. S. Hayes, and J. W. Liebert (Schenectady: L. Davis Press), pp. 389-400.

Wickramasinghe, D. T., and Cropper, M. 1988, preprint.

Wickramasinghe, D. T., and Ferrario, L. 1988, Ap. J., 327, 22.

Wunner, G., Geyer, F., and Ruder, H. 1987, Astrophys. and Sp. Sci., 131, 595.

The Magnetic white dwarfs in AM Her variables

D.T. Wickramasinghe
Department of Mathematics
Australian National University
CANBERRA A.C.T.

§1. Introduction

There are now some 15 cataclysmic variables that have been recognised as being of the AM Her type. They are characterised by the presence of variable circular and linear polarisation in the optical and IR spectral regions, approaching 40% in some systems. The polarized radiation has been attributed to high harmonic cyclotron emission from hot (~ 5 – 30 Kev) plasma located at accretion shocks near the poles of a highly magnetised (~ 20 – 60 MG) white dwarf primary. There is hope that the study of the rich variety of phenomena exhibited by these systems will eventually enable us to probe the magnetic field structure of the underlying white dwarfs, perhaps even in more detail than has been possible with the isolated magnetic white dwarfs (Wickramasinghe (1987), Schmidt (1987)).

In this paper we review the theory of AM Her variables concentrating on recent developments concerning the interpretation of intensity and polarisation observations. More general reviews covering other aspects can be found in a series of articles that have recently been published in the proceedings of the Vatican Observatory conference on circumstellar polarisation.

§2. The basic model and system characteristics

The basic model that has been developed to explain these systems is shown schematically in Figure 1. The systems have the following characteristics :

- material leaving the inner Lagrangian point L_1 is chanelled via field lines directly onto the surface of the magnetic white dwarf without the formation of an accretion disc.
- the material impacts onto two extended regions EA and EB on the white dwarf surface where stand off shocks are formed.
- the shocks have temperature and density structure and have a variable height above the stellar surface which depends, in a complicated manner, on the specific accretion rate (Stockman (1988)). The hard X-rays are produced in a high density core covering a fractional area $f \sim 10^{-5}$ of the white dwarf surface. (Buermann (1988)). The polarized optical-IR emission arises from a more extended ($f \sim 10^{-3} - 10^{-4}$) and lower density region surrounding the X-ray core. (Bailey (1988), Schmidt (1988)).

- The cyclotron and X-ray regions are surrounded by a low density accretion halo. The material in this region impacts directly on the white dwarf surface, evidently without the formation of a shock. The halo gives rise to non photospheric Zeeman split Balmer lines which are seen in absorption against the background cyclotron flux. (Wickramasinghe, Visvanathan and Tuohy (1987), Schmidt (1988)).
- Resolvable cyclotron emission features are sometimes seen from the accretion shocks. The spacing of the cyclotron harmonics gives a direct and accurate determination of the magnetic field strength at the shock. (Wickramasinghe and Meggitt (1982), Ferrario et al (1988), Ferrario and Wickramasinghe (1988)).
- the systems are observed in both high and low states. During a low state photospheric Zeeman lines are detected from the underlying magnetic white dwarf and phase dependent observations can be used to study the field structure. (Wickramasinghe and Martin (1985)).

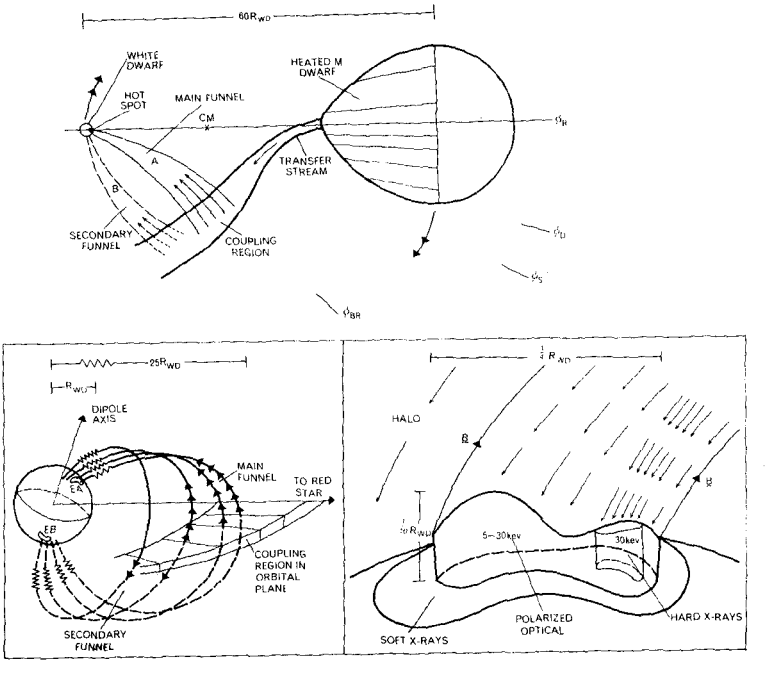

Figure 1 Top panel : View from above the orbital plane.
Bottom left panel : The two accretion funnels leading to extended shocks EA and EB on the white dwarft surface.
Bottom right panel : Structure of a shock.

We proceed to discuss some of these characteristics in more detail concentrating in particular on the recent evidence for two pole emission and for extended shock structures.

§2.1 Accretion along closed field lines

There is now overwhelming evidence in support of the view that there are two well separated cyclotron emission regions on the white dwarf surface. In systems such as AM Herculis and VV Puppis, the two regions are simultaneously visible for a part of the rotational cycle indicating that they are displaced by a significant amount from the magnetic poles (Wickramasinghe (1988), Meggitt and Wickramasinghe (1988), §2.3). The presence of such regions can be explained in one of three ways.

(i) If the coupling region has a small radial and azimuthal extent in the orbital plane, accretion may occur onto the foot points of a closed field line that lies entirely within the Roche equipotential. Otherwise accretion can only occur onto the closer foot point (Ferrario, Wickramasinghe and Tuohy (1988)). The situation is ilustrated in Figure 2.

(ii) If the coupling region has a small radial but large (~ 90°) azimuthal extent in the orbital plane (as depicted in Figure 1), accretion may occur onto a second region from material that is coupled to field lines further downstream, even if the coupling radius is large and accretion cannot occur onto two spots along closed field lines. The two spots are expected to be centered on different magnetic longitudes and to exhibit linear extension mainly in the magnetic longitudinal direction.

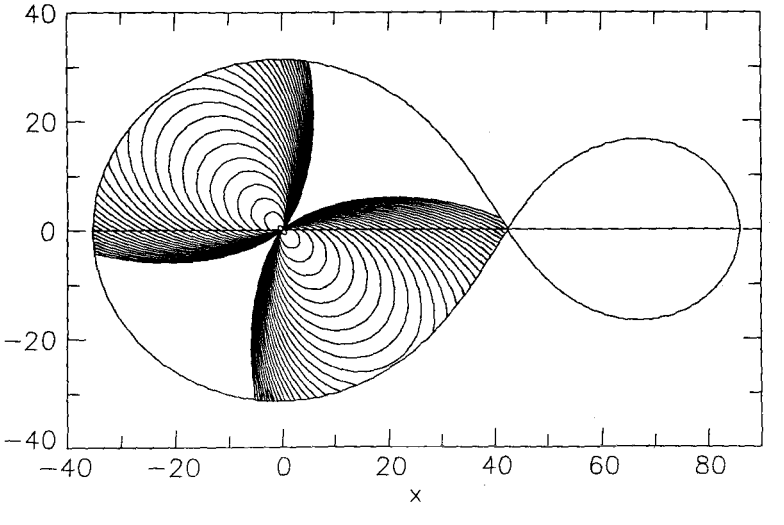

Figure 2 Closed field lines contained within the critical Roche lobe for a mass ratio q = 0.25 . The Z axis is perpendicular to the orbital plane.

(iii) If the coupling region has a large radial and small azimuthal extent, perhaps as a result of a clumpy accretion flow (Buermann (1988)), accretion may occur onto two spots which are on the same magnetic longitude. The spots are then expected to exhibit significant linear extension in the magnetic latitudinal direction and not be centered near the foot points of a single closed field line (Figure 2).

Clearly for a given dipole inclination θ_d , a larger orbital period P_{orb} , or a smaller polar field strength B_p will favour two pole accretion. Likewise, for a given P_{orb} and B_p , two pole accretion is more likely in systems with smaller θ_d .

The accretion pattern on the surface will also depend on θ_d . The curves of constant magnetic pressure in the orbital plane will be nearly circular and will map onto the surface in a ribbon that follows curves of constant magnetic latitude. For an inclined dipole the curves of constant magnetic pressure will be oval and will map onto the surface in ribbons that cross curves of constant magnetic latitude. These would be the patterns expected in case (ii). However the actual shapes will depend on whether cases (i), (ii) or (iii) are more appropriate.

Meggitt and Wickramasinghe (1988) recently analysed the linear polarisation pulse and angle observations of VV Puppis and AM Herculis for spot positions assuming that they are located at the foot points of closed field lines. The resulting geometrical model gave results in good agreement with the circular polarisation observations and eclipse constraints supporting the idea of accretion along closed field lines. The small discrepancies between the model and observations could be resolved by assuming that the emission regions were slightly displaced in magnetic longitude as is expected for a coupling region of finite azimuthal extent in the orbital plane or if the dipole is offset from the centre as discussed by Wickramasinghe and Martin (1985). The model fits indicate that the shocks are displaced by $\sim 10°$ from the magnetic poles (§2.3).

A different picture emerged from an attempt to carry out a similar analysis of the linear polarisation observations of EF Eri. Meggitt and Wickramasinghe (1988) noted that the pulses and polarisation angles, if interpreted straightforwardly, suggested the presence of four spots on the white dwarf surface. They argued in favour of a geometrical model in which two of the spots were located near the magnetic poles and the other two roughly 90° degrees away near the magnetic equator. Since the regions could not be connected by closed field lines in a dipole field distribution, they discussed the possibility of a predominantly quadrupolar field distribution. However, it has recently become apparent that it may also be possible to interpret these observations by assuming two extended ribbon like emission regions in an underlying dipolar field structure. We show in §2.2 that a single ribbon, could under certain circumstances, mimic two spots in its polarisation properties. For this interpretation to be viable for EF

Eri it is necessary for the emission regions to be extended mainly in magnetic latitude as is expected if the coupling region has a significant radial extension as in (iii) above or for the dipole to be strongly offset. We conclude that while the general idea of accretion along closed field lines appears to be correct for systems such as VV Puppis and AM Herculis, there are other systems where the situation may be more complicated.

§2.2 Properties of accretion ribbons

The theory of cyclotron emission has been recently reviewed by Wickramasinghe (1988). We note that the total opacity τ_κ due to cyclotron absorption, in the collisionless approximation, is given by $\tau_k = \Lambda_s \kappa_f(T_e, \theta, \omega/\omega_c)$ where

$$\Lambda_s = 2.01\ 10^6(s/10^6\ \mathrm{cm})(N_e/10^{16}\ \mathrm{cm}^{-3})(B/3.10^7\mathrm{G})^{-1}$$

N_e and T_e are the electron number density and temperature respectively, $\mathbf{B}$ is the magnetic field strength, $\omega_c = eB/m_ec$ is the cyclotron frequency, s is the path length and θ is the angle between the direction of propagation and $\mathbf{B}$. κ_f is a strong function of T_e, θ and harmonic number n $(= \omega/\omega_c)$ and has a value ~ 1–10 near the cyclotron fundamental. Since $\Lambda_s \sim 10^5 - 10^8$ in the accretion shocks it follows that cyclotron opacity plays a dominant role in determining their radiation properties.

Early attempts at analysing observations were based on the assumption that the shocks were structureless and could be characterised by a point source with the same value of Λ_s at all angles θ to the field. The properties of these models can be summarised as follows :

- The slope of the energy distribution defined by the harmonic peaks is a strong function of frequency in the optically thin (high harmonic) regime. At $\theta = 90°$, $I_\omega \propto \omega^p$ where $p = -8, -5, -3$ and -1.4 for $T_e = 10, 20, 50$ and 100 Kev respectively. The radiation is strongly polarised ranging from being circular along the field to linear perpendicular to the field.
- For $\Lambda_s \sim 10^5$–10^8 the lower harmonics are self absorbed. As a consequence the spectrum at low harmonics is of the black body Rayleigh-Jeans type $(I_\omega \propto \omega^2)$ and is unpolarised (Figure 3).
- The radiation is strongly angle dependent being beamed perpendicular to the magnetic field. The beaming effect is strongest at high harmonics.

The point source models were successful in explaining the general characteristics of the observations, such as the presence of linear pulses near $\theta \sim 90°$ and the strong angular dependence of intensity and circular polarisation. They failed in three major respects. Firstly, they were unable to explain the flat $(I_\omega \propto \omega^{-1-0})$ polarized energy distributions seen over an extended wavelength region in some systems, such as AM Herculis itself. Secondly, the values of Λ deduced from the

optical cyclotron spectra were typically a factor of ~ 100 smaller than the values that were required to explain the X-ray luminosities. Finally, the models predicted symmetrical light and polarisation curves which were contrary to observations.

Recently cylindrically symmetric models have been constructed which allow for density and temperature variations across the shock in response to a decrease in the specific accretion rate away from the axis of the cylinder (Wickramasinghe and Ferrario (1988a), Stockman (1988), Wu and Chanmugam (1988)). In the central regions the shock in bremsstrahlung dominated and the electron temperature approaches the adiabatic shock value. If the accretion rate drops sufficiently rapidly away from the center, the shock becomes dominated by cyclotron cooling in the outer regions and the electron temperature falls below the adiabatic shock value. Wickramasinghe and Ferrario (1988a) have modelled the density variations by assuming a central core ($r \leq r_0$) with constant Λ_h and an outer region ($r > r_0$) with a "Λ profile" specified by $\Lambda_h(r) \propto r^{-\delta}$, where r is the distance away from the axis of the cylinder. Here, h is the shock height perpendicular to the surface and δ is an index determined by the accretion profile and the physics of the shock. The temperature variations have been modelled by assuming a constant T_e (= T_e (0)) for $r \leq r_0$ and a linear drop in temperature from $T_e(0)$ to $T_e(1)$ for $r > r_0$. For a bremsstrahlung dominated shock $h \propto N_e^{-1}$ and $\delta = 0$ irrespective of accretion profile. Large values of δ are only possible in a cyclotron dominated shock, and then only if the accretion rate drops rapidly across the shock. The models (Figure 4) show that flat polarized energy distributions are predicted over an extended frequency range, for large values of δ (~ 4–6).

Wickramasingle and Ferrario (1988a) also showed that by offsetting the cylindrical emission region from the magnetic pole, asymmetric light and polarisation curves can be produced. However, the asymmetries were not large enough to explain observations of systems such as VV Puppis and V834 Cen .

From our discussion in §2.1 it is evident that the emission region is more likely to have linear structure than cylindrical structure. Wickramasinghe and Ferrario (1986) have recently carried out calculations of ribbon like emission regions on the surface of a white dwarf with a dipolar field structure. The emission region is approximated by a strip in the magnetic colatitude (θ) - magnetic longitude (ψ) plane defined by $\theta_1, \theta_2, \theta_2^*$ and ψ_1, ψ_2. $\psi = 0, \pm\pi$ on the plane through the dipole axis perpendicular to the orbital plane. The strip has an angular thickness $\Delta\theta = (\theta_1 - \theta_2)$ and follows lines of constant magnetic colatitude if $\theta_2 = \theta_2^*$. Models have been constructed for a range of parameters assuming a constant value of T_e (= 10 Kev) and Λ_h (= 10^5) across the shock. The results (Figure 5) show that ribbons produce larger asymmetries in the polarisation and intensity curves than offset cylindrical emission regions. We note the following

- the projected area effect results in a double humped light curve even for regions that are not extended. However, strongly asymmetric double humped light curves are calculated only for strips with a significant angular extent in ψ.
- for extended strips, the pulses need not coincide with the intensity maxima.
- for strips that are significantly elongated in magnetic latitude, partial eclipses produce triangular type intensity profiles.

The above characteristics have been noted in V834 Cen by Cropper (1988) who discussed the possibility of an accretion ribbon. However it should not be concluded that significant linear extension is a common property of the shocks in all AM Her type systems. The amount of extension is likely to depend critically on the dipole inclination (§2).

§2.4 Two pole emission

Several AM Her variables show a reversal in the sign of circular polarisation for part of the rotational phase (Bailey (1987)). The circular polarisation will change sign if the projection of the field along the line of sight changes sign. The reversals could be due to (a) a significant shock height above the stellar surface (b) an inclined (non radial) field direction at the location of the shock or (c) the presence of a second cyclotron emission region on the white dwarf surface of opposite field polarity. The recent detection of 3 linear pulses in EF Eri, AM Herculis and VV Puppis (Piirolla (1988) has shown beyond any doubt that there are some systems in which a second emission region makes an important contribution to the polarized radiation. It seems likely that the observed reversals in most systems are mainly due to (b) and (c), the shock height ($h/R_{wd} \lesssim 0.1$) being generally small in comparison to its extension across the surface (Wickramasinghe (1988), Stockman (1988)).

We illustrate the characteristics of two pole emission by presenting in Figure 6 the predictions of the model for AM Herculis based on linear polarisation angle data and the assumption that accretion occurs onto the foot points of closed field lines (§2.2). The contributions from the two poles are presented separately without eclipses in the top right panel, and with eclipses in the bottom left panel. The pole which is eclipsed between $\phi = 0.0$–0.2 is the main (hard X-ray) pole and is responsible for circular polarisation of negative sign during the bright phase. The second pole (the soft X-ray pole) is visible between phases $\phi \approx 0.0$–0.4 and contributes circular polarisation of opposite sign. The second zero crossing of circular polarisation is determined by a balance between the two poles and is expected to vary with epoch, precisely as observed. An intriguing feature of the model is that *both* poles contribute a linear pulse at phase $\phi = 0.0$. In fact, it is likely that the pulse at $\phi = 0.0$, which has traditionally been attributed to the main pole, may in fact originate mainly from the second pole.

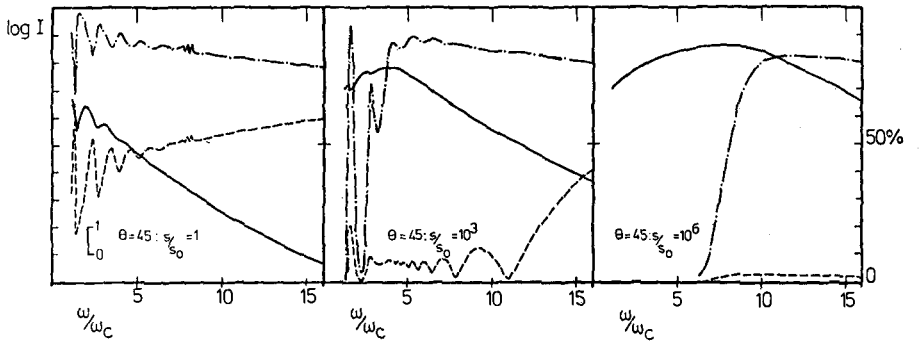

Figure 3 Radiative transfer effects on the intensity and polarisation spectra for $T_e = 20$ Kev for various $\Lambda = s/s_0$. The dashed curves and dash-dotted curves are percentage linear and circular polarisation respectively.

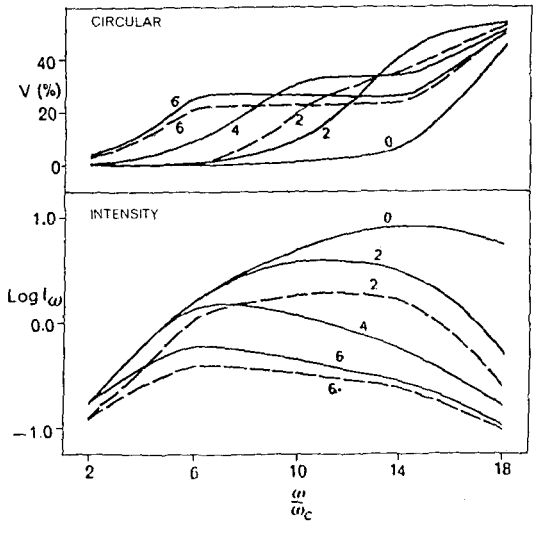

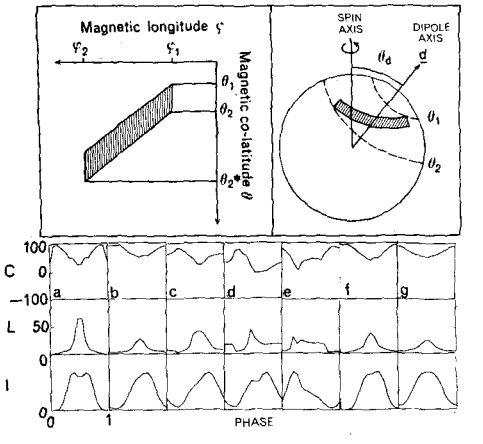

Figure 4 Left panel :Intensity and circular polarisation for cylindrically symmetric shocks. The curves are labelled by δ. The models have $T_e(0) = 10$ Kev, $\Lambda_h(0) = 2\,10^8$ and are viewed at $i = 60°$ to the axis of symmetry. The dashed curve correspond to models with a declining temperature with $T_e(1) = 10$ Kev.

Figure 5 Right panel : Intensity (I) linear (L) and circular (C) polarisation for ring type geometries. The models have $T_e = 10$ Kev, $\Lambda_h = 10^5$, $i_{orb} = 50°$, $\delta_d = 20°$ and $\omega/\omega_c = 9$. The models are labelled by $\theta_1, \theta_2, \theta_2^*, \Psi_1, \Psi_2$ (a) 10,15,15,–2,+2 (b) 10,15,15,0,180 (c) 10,15,35,0,180 (d) 10,15,55,0,180 (e) 10,15,45,–180,0 (f) 10,15,15,0,90 (g) 10,15,15,0,360.

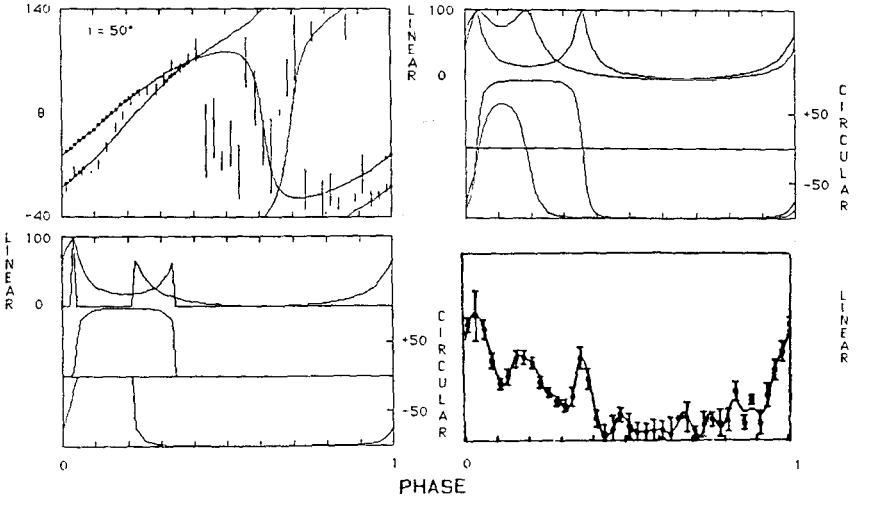

Figure 6 Fits to the linear polarisation angle data on AM Herculis from Piirola (1988) illustrating the two spot model. The spot positions are deduced on the assumption of accretion along closed field lines in a dipole field distribution.

§3. Conclusions

We have presented a brief review of some of the new developments that have occurred in the theory of the AM Her variables during the past two years. The main results are as follows :

- The specific accretion rate and hence the temperature and density are likely to vary across the shock. It is possible to construct structured shock models in which the hard X-rays originate from a compact high density core (with $\Lambda_h \sim 10^8$) and the optical and near IR radiation from a surrounding lower density region (with $\Lambda_h \sim 10^5$–10^7). These models yield energy distributions that are in closer agreement with observations than previous point source models.
- The shocks may exhibit linear ribbon like extension across the surface. Thus geometrical effects could be important in interpreting polarisation and intensity light curves.
- Most systems have two active cyclotron emission regions displaced by $\sim 10°$ from the magnetic poles. Both regions are simulateneously visible for part of the rotational cycle.

We have shown that by combining these effects, many of the previously unexplained phenomena can be interpreted, at least in a semi quantitative manner.

References

Bailey, J., 1988 in "Polarized radiation of circumstellar origin", G. Coyne, A. Magalhaes, A.F.J. Moffat, R.E. Schulte-Ladbeck, S. Tapia and D.T. Wickramasinghe, eds; Vatican press.

Cropper, M., 1988, Mon. Not. Roy. Ast. Soc. (in press).

Ferrario, L., and Wickramasinghe, D.T., 1988 (these proceedings).

Ferrario, L., Wickramasinghe, D.T. and Tuohy, I.R., 1988, Ap.J. (submitted)

Meggitt, S.M.A. and Wickramasinghe, D.T., 1988, Mon. Not. Roy. Ast. Soc. (in press).

Piirola, V., 1988 in "Polarized radiation of circumstellar origin" G. Coyne, et al. eds; Vatican press.

Schmidt, G., 1987, I.A.U. Coll. No.95 on Faint Blue Stars, A.G. Davis Philip, D.S. Hayes and J. W. Liebert, eds, L. Davis Press.

Schmidt, G., 1988 in "Polarized radiation of circumstellar origin" G. Coyne et al. eds, Vatican press.

Stockman, H.S., 1988 in "Polarized radiation of circumstellar origin" G. Coyne et al. eds, Vatican press.

Wickramasinghe, D.T., 1988 in "Polarized radiation of circumstellar origin" G. Coyne et al. eds, Vatican press.

Wickramasinghe, D.T., 1987, I.A.U. Coll. No 95 on Faint blue stars, A.G. Davis Philip, D.S. Hayes and J.W. Liebert, eds, L. Davis Press.

Wickramasinghe, D.T. and Martin, B., 1985, Mon. Not. Roy. Ast. Soc. **212**, 353.

Wickramasinghe, D.T. and Ferrario, L., 1988a, Ap. J. (in press)

Wickramasinghe, D.T. and Ferrario, L., 1988b, Ap. J. (in preparation)

Wickramasinghe, D.T., Visvanathan, N.V. and Tuohy, I.R., 1987, Ap. J. **318**, 326.

Wu, K. and Chanmugam, G., 1988, Ap. J. (in press.)

EVIDENCE OF COMPLEX FIELD STRUCTURE IN THE MAGNETIC WHITE DWARF IN EXO 033319–2554.2

Lilia Ferrario and D. T. Wickramasinghe

The Australian National University, Canberra, Australia

ABSTRACT

We present detailed theoretical models for polarisation and spectroscopic data from EXO 033319–2554.2 that suggest the presence of two cyclotron emission regions of field strengths $B \sim 5.6 \times 10^7$ G and $B \sim 2.8 \times 10^7$ G, and which are separated by about 90° on the surface of the white dwarf. The large difference in magnetic field strength and the proximity of the two regions imply a more complex field structure than that of a centred dipole field distribution if it is assumed that the regions are connected by closed field lines.

I. INTRODUCTION

EXO 033319–2554.2 was recently reported to be an eclipsing soft X-ray source with a period of 127.7 minutes (Osborne *et al.* 1988). Bailey *et al.* (1987) confirmed its magnetic nature through the detection of circularly polarised light. More interestingly, the spectroscopic data show that EXO 033319–2554.2 is the second AM Her system to exhibit cyclotron harmonics in its optical spectrum similar to those first discovered in VV Puppis.

II. THE CYCLOTRON SPECTRUM

Spectroscopy of EXO 033319 – 2554.2 was obtained by Ferrario *et al.* (1988). The data corresponding to $\phi = 0.9$ and $\phi = 0.1$ are shown in Figures 1 and 2 respectively.

Since $\phi = 0.9$ corresponds to the centre of the bright phase, we assume that the angle θ between the line of sight and the field direction for the main emission region is at a minimum at this phase. The absence of large ($\geq$ 200 Å) shifts in

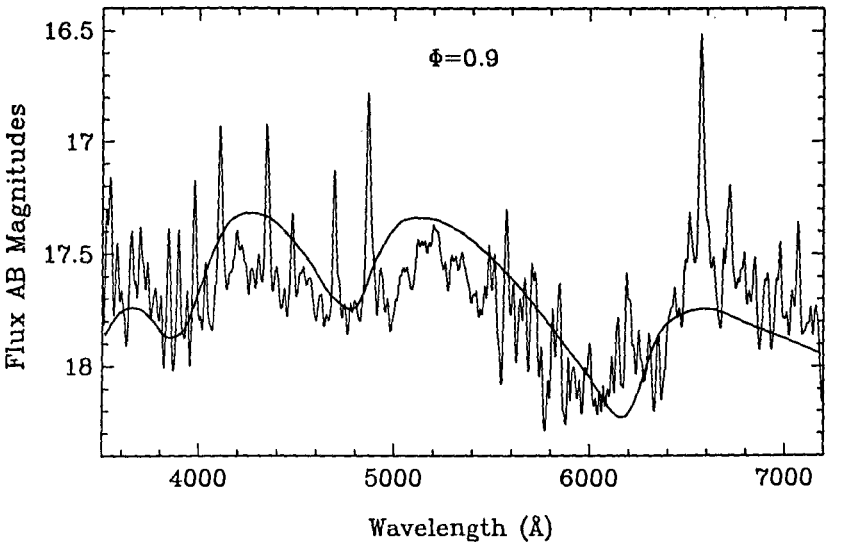

Figure 1. A broad band spectrum of EXO 033319 − 2554.2 acquired by Ferrario *et al.* (1988). The solid line represents our best fit for a magnetic field $B = 5.6 \times 10^7$ G and viewing angle $\theta = 75°$.

the positions of the harmonics with phase indicates that $\theta \geq 75°$ during the bright phase. We have constructed models following Wickramasinghe and Meggitt (1985) assuming point source cyclotron emission regions. We include in Figure 1 the best fit spectrum calculated for the data at $\phi = 0.9$ assuming $\theta = 75°$. The model has $B = 5.6 \times 10^7$ G and an optical depth parameter $\Lambda = 1.1 \times 10^3$ for an electron temperature $T_e = 20$ keV. The features at 4200Å, 5200Å and 6550Å are identified with harmonic numbers 5, 4 and 3. This result is in close agreement with that reported by Beuermann, Thomas and Schwope (1988) who also detected the presence of cyclotron harmonics.

The spectrum at $\phi = 0.1$ exhibits a further emission peak at 4720Å and a broad depression centred near 5650Å. We have interpreted these features to be also of cyclotron origin arising from a second emission region. The best fit model is included in Figure 2. This region has $B = 2.8 \times 10^7$ G, $\Lambda = 3.2 \times 10^5$, $T_e = 10$ keV, and is assumed to be viewed at $\theta = 90°$. The peaks at 4720Å and 5400Å correspond to harmonic numbers 9 and 8 while the dip at 5650Å occurs at the blue edge of harmonic number 7 which is optically thick and almost completely undetectable. The peak at 6650Å is attributed to the main emission region which

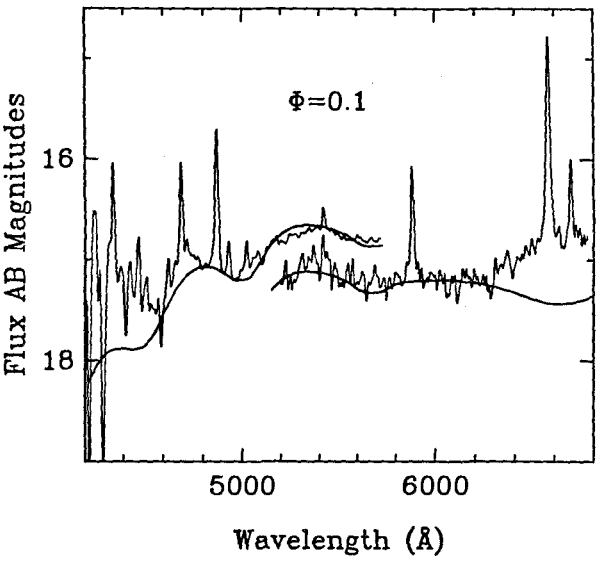

Figure 2. Spectra of EXO 033319−2554.2 at $\phi = 0.1$ obtained by Ferrario *et al.* (1988). The solid line represents our best fit for a magnetic field $B = 2.8 \times 10^7$ G and viewing angle $\theta = 90°$.

is assumed to be also visible at $\phi = 0.1$. We note that there is some evidence that the feature at 4720Å is also seen at $\phi = 0.3$ (Figure 4 of Ferrario *et al.* 1988), indicating that the second cyclotron emission region may still be making some contribution to the total light at this phase. This is in agreement with the length of the bright phase in the circular polarisation data obtained by Berriman and Smith (1988, see their Figure 1a) only one night after our AAT spectroscopy.

It has recently been argued by Ferrario, Wickramasinghe and Tuohy (1988) that, except for special orientations of the magnetic axis, the emission regions on the white dwarf surface are likely to occur near the foot points of closed field lines. If this hypothesis is correct, the observed ratio of field strengths for the emission regions in EXO 033319–2554.2 rules out a centred dipole field distribution. However, the observed ratio of 2:1 is consistent with that expected for the field strengths at the foot points of closed field lines which connect the polar and equatorial regions in a centred quadrupole field distribution. Such a field distribution has recently been proposed by Meggitt and Wickramasinghe (1988) for the AM Herculis variable 2A0311–227. However, it should be emphasised that the physics of the coupling region is not yet fully understood so that other possibilities cannot be excluded.

II. POLARISATION BEHAVIOUR

Circular polarimetry of EXO 033319–2554.2 was obtained by Ferrario *et al.* (1988) (Figure 3). The data show circular polarisation reaching $\sim 10\%$ in the blue and lasting from about $\phi = 0.65$ to $\phi = 0.2$. Furthermore, a reversal in the sign of the circular polarisation is evident from $\phi = 0.1$ to $\phi = 0.2$.

We have constructed theoretical polarisation curves by adding the contributions from two point source cyclotron emission regions contributing polarisation of opposite sign and characterised by the same parameters used to interpret the cyclotron spectra. The emission regions are 90° apart on the white dwarf surface at colatitudes of 15° (5.6×10^7 G region) and 105° (2.8×10^7 G region). The orbital inclination is 88°. The location of the higher field cyclotron emission re-

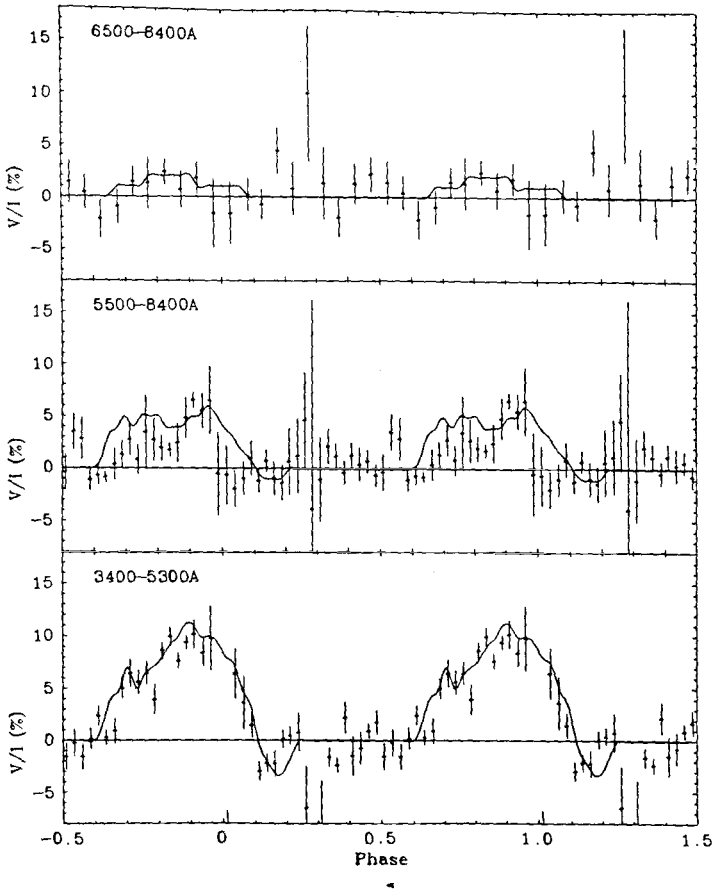

Figure 3. Circular polarisation data for EXO 033319 − 2554.2 obtained by Ferrario *et al.* (1988) and theoretical polarisation curves obtained by adding the contributions of two cyclotron emission regions (see text).

gion and the orbital inclination are chosen to be consistent with the values determined by Ferrario *et al.* (1988). We assume that the contribution to the circularly polarised light from the lower field region is half of the contribution from the higher field region and that the unpolarised background is about four times less important for the bluest of the presented bands. The latter assumption may be justified by noting that the red star is only likely to make an important contribution to the total light for $\lambda \geq 7000$ Å.

In our model the main emission region ($B = 5.6 \times 10^7$ G) is visible from $\phi = 0.65$ to $\phi = 0.1$ and the secondary emission region from $\phi = 0.65$ to $\phi = 0.25$, and they are viewed most directly at $\phi = 0.85$ and $\phi = 0.95$ respectively. We point out that the lengths of the bright phases corresponding to the two regions are in complete agreement with our spectroscopic observations. Namely, the main emission region is eclipsed by the body of the white dwarf at $\phi = 0.1$ which coincides with the phase of last detection of cyclotron harmonics originating from the 5.6×10^7 G region. The eclipse of the secondary region is also in excellent agreement with the spectroscopic data, which show the presence of cyclotron harmonics from the 2.8×10^7 G region until $\phi = 0.3$. Berriman and Smith (1988) also suggest the presence of two cyclotron emission regions by comparing the circular polarisation data that they obtained on two consecutive nights. In one night they detected a reversal in the sign of the circular polarisation data, similar to that detected by us, but this reversal was not present in the next night. A temporal variation in the zero crossing of the circular polarisation curve and a change in the percentage of the polarised light can be explained as a change in the balance between the two poles in response to a change in the accretion rate.

REFERENCES

Bailey, J. A., Ferrario, L., Tuohy, I. R., Wickramasinghe, D. T., and Hough, J. H. 1987, *IAU Circ*, # 4517.

Berriman, G., and Smith, P. S. 1988, *Ap. J.*, **329**, L97.

Beuermann, K., Thomas, H. C., and Schwope, A. 1988, *Astr. Ap.*, **195**, L15.

Ferrario, L., Wickramasinghe, D. T., and Tuohy, I. R. 1988, *Ap. J.*, submitted.

Ferrario, L., Wickramasinghe, D. T., Bailey, J. A., Tuohy, I. R., and Hough, J. H. 1988, *Ap. J.*, in press.

Meggitt, S.M.A., and Wickramasinghe, D.T. 1988, *M. N. R. A. S.*, in press.

Osborne, J. P., Giommi, P., Angelini, L., Tagliaferri, G., and Stella, L. 1988, *Ap. J.*, **328**, L45.

Wickramasinghe, D. T., and Meggitt, S. M. A. 1985, *M. N. R. A. S.*, **216**, 857.

PHASE CORRELATED SPECTRA OF MAGNETIC WHITE DWARFS

I.Bues and M.Pragal
Dr.Remeis-Sternwarte Bamberg,Astron.Institute
Universität Erlangen-Nürnberg,D-8600 Bamberg,FRG

ABSTRACT. New photometric and polarimetric observations of the magnetic white dwarfs G 99-37 and G 99-47 are in accordance with a period of 4.117h and 0.97h respectively.Spectra taken at various phases could be correlated and analyzed by model atmosphere technique.

INTRODUCTION

G99-37 and G99-47 belong to the group of white dwarfs with moderate magnetic field strengths.G99-37 shows strong spectral features of carbon (CH,C_2,CI),which can be understood with a helium-rich composition(He/C =1000)at $T_{eff} \approx 6000^{\circ}K$ and $B \gtrsim 10^3$Tesla (Liebert,1977,Bues,1986a,Bues et al.1986b).G99-47 is slightly cooler and the spectrum is nearly continuous with a Zeeman split H_α line,which proposes a pure hydrogen atmosphere (Angel at al.1981) at $B \approx 1.5 \times 10^3$ Tesla.
In our spectra,taken in 1983 and 1985,slight changes and shifts of the spectral features could be observed.But it was not possible to derive a period which would be expected for a centred dipole model and could reproduce the variation with different model atmospheres.
That is why we decided to take new photometric,spectroscopic and polarimetric data in order to analyze them by improved model atmosphere technique.

OBSERVATIONS

During Nov.1987 we used the ESO 1m-telescope at La Silla for photometric measurements in the UBVRI and Strömgren system and obtained 51 and 22 observations within 3 nights and the ESO 2.2m-telescope for polarimetry with 29 observations within 3 nights and 13 in one night,respectively.
The Bamberg period analysis program,normally used for binary stars,calculated periods of 4.117h for G99-37 and .97h for G99-47.
If we take the strongest linear polarization for phase 1.00,the IDS spectra of 1986 and the CCD spectra of 1987 (ESO 1.52m,114 Å/mm) can be correlated to phases as shown in Table 1 for G99-37.

TABLE 1:Spectra and their phases of G 99-37

JD	phase	
2446712.8667	.01	IDS
2446713.8493	.74	IDS
2446714.8507	.57	IDS
2447112.8451	.16	CCD
2447113.8181	.83	CCD
2447113.8389	.95	CCD
2447114.8007	.55	CCD
2447114.8229	.68	CCD
2447266.5073	.73	CCD

The two spectra of Fig.1 demonstrate well the shift of the band heads and the variation in strengths for the C_2 (0,0),(2,2),(1,0) and (3,2)-transition.CH is less involved in phase changes.

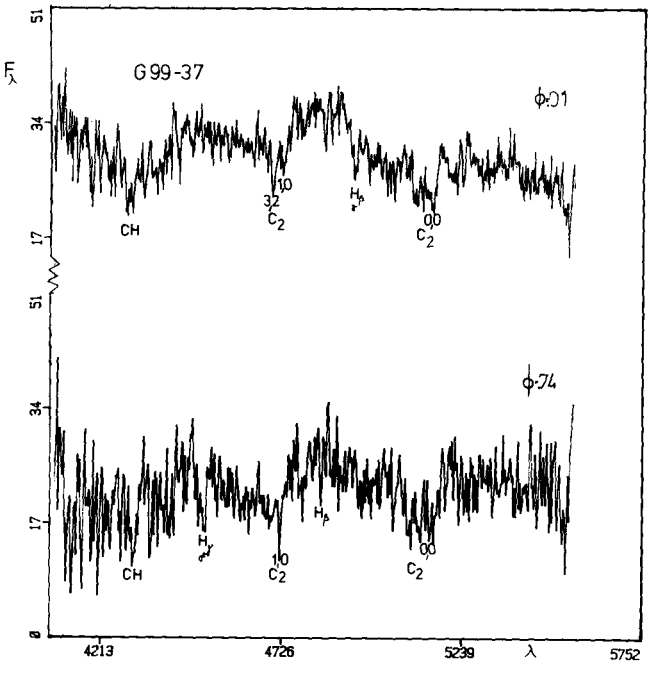

Fig.1: Two blue IDS-spectra of G99-37 with phases .01 and .74
C_2 (1,0) and H_δ show the strongest displacements.

For G 99-47,Fig.2 shows the strongest H_γ feature with the π-component shifted by only 20Å in the lower part,which corresponds to the smallest field,the upper Zeeman triplet is correlated to the H_γ field determined by Liebert et al.(1975) to be 5.6×10^2 Tesla.Due to the very short period and the necessary exposure times of at least 10 min,the phase

correlation for less noisy spectra (30 min exp.time) is not of much use for a reproduction of the spectrum by model atmospheres.

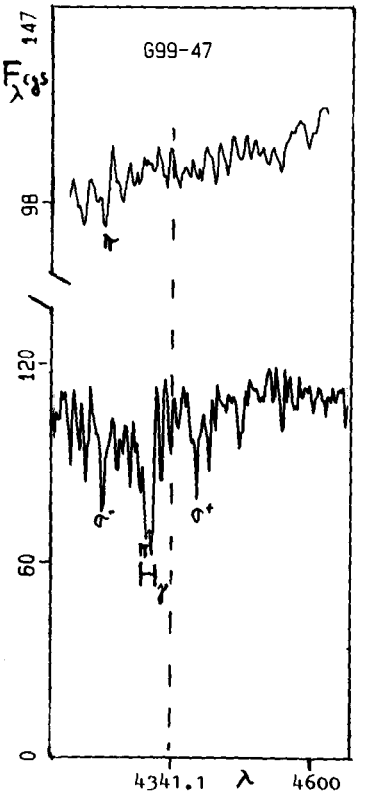

Fig.2:2 spectra of the H_γ region of G99-47 with short exposure times.The unshifted position of H_γ is indicated.

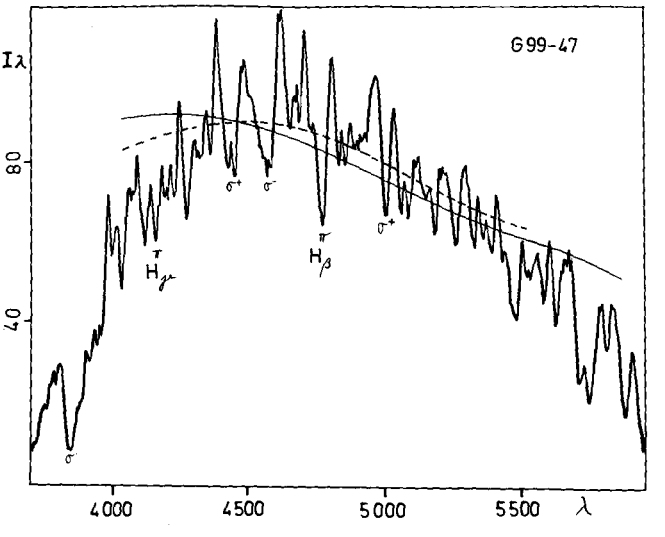

Fig.3 :Flux of a model atmosphere of 6000 K, $B=10^3$ Tesla compared to a transformed IT spectrum(10min exposure time)

ANALYSIS

For white dwarfs with $T_{eff} \leq 7000^oK$ and observed polarization of more than 2% line and band shifts due to the quadratic Zeeman effect are important for the Rosseland mean of the opacity since the major part of the flux is radiated in the visible region of the spectrum.A certain amount of carbon has to be taken into account already for the initial parameters like $\varkappa$ and P_g. We calculated tables for gas pressures of 10^5 to 10^{10} and temperatures of 11000^0 to 5000^oK for several magnetic fields. Model atmospheres have been computed for T_{eff}= 6000 K and 7000 K,log g

=8 for H/He=1000 and 10^{-3}. Special emphasis is taken for the absorption of the Balmer lines,single rotational transitions of C_2 and CH,where the semiempirical parameters,derived by Pragal (1986) from our earlier spectra of G 99-37 were used.

For the combined solution of radiation and polarization in the model atmosphere a modified Unno scheme was solved by numerical integration. Fig.3 shows the result for a high field strength of G99-47,the spectrum appears to be continuous due to the high pressure.The outer structure of the hydrogen atmosphere should be calculated in more detail to obtain line profiles.

For G 99-37,Fig.4 demonstrates the behaviour of the C_2 band heads for $i=90^{o}$,where a detailed structure of (0,0),(1,1) and (2,2) is obtained for $B>10^{3}$Tesla.So we are optimistic aboutour theoretical treatment of C_2 with magnetic field strength for various phases of G 99-37 and the other stars with carbon and stronger fields to get information on field strength and composition.

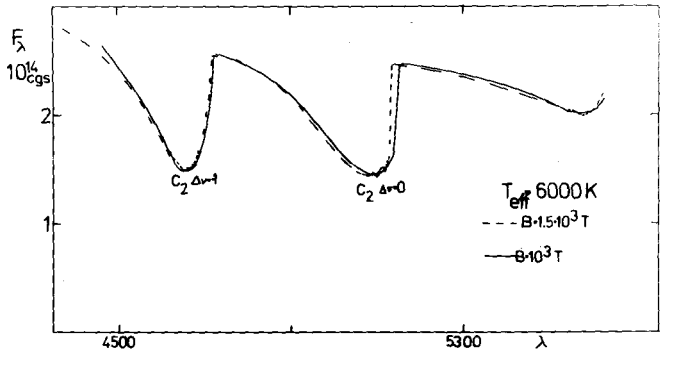

Fig.4 The flux of a model atmosphere relevant for phase .45 of G99-37 with B= 10^{3}Tesla, phase .01 with B= 1.5×10^{3}Tesla.(H/He=10^{-3},H/C=10)

REFERENCES

Angel,J.R.P.,Borra,E.F.,Landstree,J.D.1981,Ap.J.Suppl.,45,457

Bues,I.1986a,IAU Coll.87,391

Bues,I.,Pragal,M. 1986b,Mem.S.A.It.58,97

Liebert,J.1977,PASP 89,78

Pragal,M.,1986,Diploma Thesis Universität Erlangen-Nürnberg

Synthetic Spectra of Magnetic White Dwarfs

Stefan Jordan
Institut für Theoretische Physik und Sternwarte der Universität Kiel
Olshausenstraße 40, D-2300 Kiel 1, Federal Republic of Germany

Abstract

A new program for the calculation of theoretical spectra and wavelength dependend degrees of the linear and circular polarization for magnetic white dwarfs with hydrogen atmospheres has been developed. The main improvement compared to previous models is a more realistic treatment of the bound-free absorption and of the magnetooptical parameters arising from free electrons in the continuum. For the newly discovered magnetic white dwarf HS 1254+3430 a polar field strength of 18 MG was found. Calculations for the high field object Grw +70°8247 confirms the results of Wickramasinghe and Ferrario (320 MG) but gave a better fit to the spectrum at wavelengths larger than 6200 Å.

Introduction

From the position of the Zeeman components in the spectrum of magnetic white dwarfs approximate field strenths can be determined. To get more infomation about the field structure detailed computer models are necessary. Martin and Wickramasinghe (see Wickramasinghe and Ferrario, 1988 for references) analyzed four DA white dwarfs between 5 and 36 MG by solving the equations of radiative transport in a magnetized atmosphere and using the Zeeman calculations of Kemic (1974). Since 1984 line data for $B \gtrsim 10^8$G are available (Rösner et al., 1984 and Forster et al., 1984, Tübingen; Henry and O'Connell, 1984) and made the interpretation of objects with very strong fields possible. Assuming a dipol with a polar field strength of $B_p = 320$ MG Wickramasinghe and Ferrario (1988, referred to as WF) were able to get a good fit to the spectrum of the famous object Grw +70°8247 between 3500 and 6200 Å. The calculated flux at longer wavelengths and the prediction for the linear and circular polarization showed major discrepancies with the observations made by Angel et al. (1985).

New synthetic spectra have been computed with the program described in this paper. They confirm the field configuration of Grw +70°8247 found by WF but give a better agreement with the observed flux between 6200 and 9200 Å. Since polarization is more sensitive to changes in the continuum opacities than the flux, the calculated polarization still differs seriously from the observed values.

Model Description

Special attention was given to the physics at fields higher than 100 MG. The details of the model will be described in a forthcoming paper. Here only a short synopsis can be given:

- Zero field pure hydrogen model atmospheres (Koester et al, 1979) for $\log g = 8$ have been used to determine the temperature and pressure stratification. This can only be justified if Lorentz forces do not dominate the hydrostatic structure at optical depths $\gtrsim 10^{-2}$. Provided that the decay of the global magnetic field of the star is responsible for the electric current distribution in the outer layers - only slow rotation is allowed in this case rotating - a procedure of Landstreet (1987) can be applied to estimate the strength of the Lorentz forces. With the new data of Wendell et

al. (1987) for the decay time of the field, which differ by up to a factor of eight from the values of Fontaine et al. (1973) used by Landstreet, it can be shown that Lorentz forces are negligible even at fields higher than 100 MG.

Since the measured degree of polarization normally amounts only to a few percent (<7% in Grw +70°8247) the normal equation of radiative transport is sufficient for the model atmosphere.

A test calculation indicates that cyclotron absorption can become important at $B > 100$ MG and lead to somewhat smaller temperatures at small optical depths compared to the models that are the basis for the spectra of Grw +70°8247 presented in this paper.

- The stellar surface is devided into a grid of small elements by circles of constant latitude and longitude (the magnetic pole defines the orientation of the spherical coordinate system). After a field configuration (e.g. a centered dipol) is specified the average vector and the variation of the magnetic field is determined for each element.
- On each surface element the coupled equations of radiative transport in a magnetized plasma (Hardorp et al., 1976) is solved for the Stokes parameters I, Q, U and V by a method similar to that of Martin und Wickramasinghe (1979). The results must be integrated in order to get the emergent flux and polarization for the whole stellar disc.
- New tables from the Tübingen group (by courtesy of Wunner, 1986) - containing a narrower grid of line positions and opacities than the published data - make it possible to take quick oscillations of the line strengths with varying magnetic field (Wunner et al, 1986) into account.
- While exact data for the lines are available the situation concerning the continuum opacities is very unsatisfactory. The first order approximation of Lamb and Sutherland (1974) is still the only existing method to calculate hydrogen bound-free absorption for different changes of the magnetic quantum number Δm. The procedure calculates the oscillator strengths from zero field values at a frequency shifted by the Larmor value $(eB/4\pi m_e c)\Delta m$. As one can see from the asymptotic behaviour of the line components the position of the absorption edges can not be described by this simple Zeeman splitting even at arbitrarily small fields. To get correct wavelengths for the bound-free threshold the energy difference between the exactly known bound states and the minimum energy of the lowest Landau level that can be reached by a specific Δm transitions is used here. At the Balmer edge 12 transitions (4 for each Δm) with 8 different wavelenths are found (see figure 1). The Lamb and Sutherland opacities are distributed to the different Δm components by applying the Wigner Eckart theorem.

While thus the begin of the bound-free absorption is known, problems have to be expected if the Lamb and Sutherland approximation is used for the calculation of the absorption strengths at $B \gtrsim 5 \cdot 10^7$G .

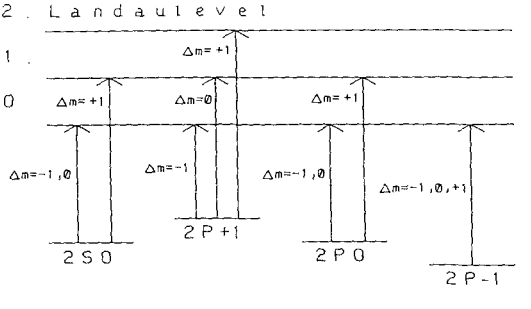

Figure 1: bound-free transitions at the Balmer edge with minimum energy difference.

- Cyclotron absorption is included allowing for simultaneous broadening of the absorption profile by the Doppler effect and collisions of electrons.
- The magnetooptical parameters of the lines are calculated following a method of Wittmann (1974). The formulae of Pacholczyk (1976) have been used by Martin und Wickramasinghe (1982) to calculate the Faraday and Voigt effect arising from free electrons in the continuum. The singularity at the cyclotron frequency in this formulae is avoided here by using a consistent approach (Jordan and O'Connell, 1987) that takes electron collisions into account.

• The profiles of the opacities and the magnetooptical parameters are broadened by the magnetic field variation over a single surface element. This minimizes numerical bumps resulting from the discretization of the stellar disc and the number of surface elements neccessary for the computation.

Results

The program was tested by calculating synthetic spectra for the 36 MG object BPM 25114 which has already been analyzed by Martin und Wickramasinghe (1978). The agreement with the observation is somewhat better in detail mainly because of the new line opacities used here.

The observed spectrum of HS 1254+3430 was compared to theoretical spectra for models with different field configurations and effective temperatures. A good agreement was found for $B_p = 18 \pm 2$ MG, a viewing angle with respect to the dipol axis of $i = 70° \pm 20°$ and $T_{eff} = 14000 \pm 2000$ K (see figure 2).

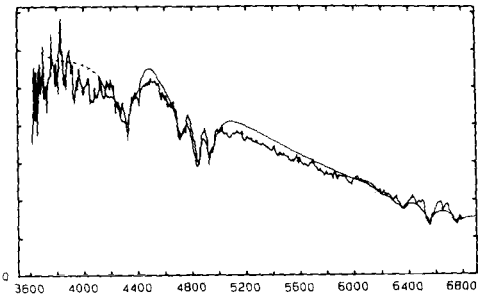

Figure 2:
Synthetic spectrum for $T_{eff} = 15000K$, $B_p = 18$ MG and $i = 70°$ compared to the observation of HS 1254+3430 (Hagen et al., 1987).

Grw +70°8247 has a much stronger field strength. Figure 3 (top) compares a synthetic spectrum for $T_{eff} = 16000$ K with the observations of Angel et al. (1985, the two center curves) and confirms the result of WF (bottom, $T_{eff} = 14000$ K) who found a dipol field with $B_p = 320$ MG and $i = 30°$.

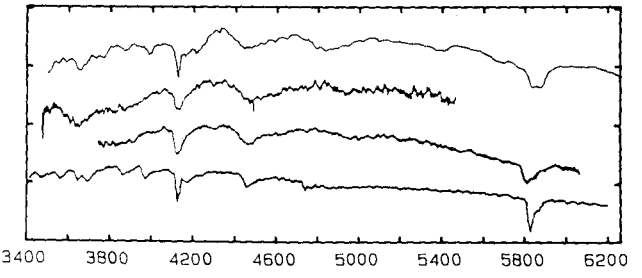

Figure 3:
Spectra of Grw +70°8247 (see text for explanations)

While WF were not able to obtain a good fit in the red and infrared region (figure 4a) figure 4b gives a reasonable agreement with the observed flux distribution.

The absolute strength and the wavelength dependence of the linear and circular polarization predicted by the model used here still differs seriously from the observations and shows no improvement compared to the results of WF.

While the flux calculations suggest that the total continuum opacity is fairly good reproduced by the new method, the contributions of the different Δm transitions are not correctly described by the Lamb and Sutherland approximation at strong fields. Further progress can therefore only be expected when consistend multichannel calculations for the continuum absorption become available.

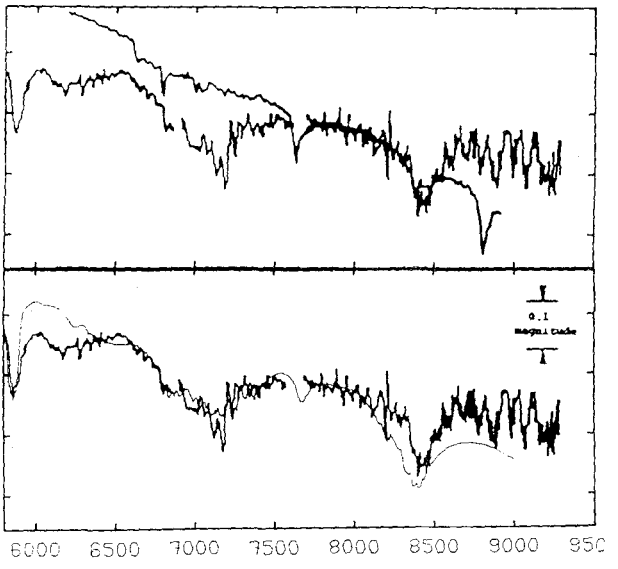

Figure 4a:
Synthetical spectrum of Grw +70°8247 at long wavelengths (Wickramasinghe and Ferrario, 1988)

Figure 4b:
New fit

References

Angel, J.R.P., Liebert, J. & Stockman, H.S., 1985: *Astrophys. J.* **292**, 260

Fontaine, G., Thomas, J.H. & Van Horn, H.M. ,1973: *Astrophys. J.* **184**, 911

Forster, H., Strupat, W., Rösner, W., Wunner, G., Ruder, H. & Herold, H., 1984: J. Phys. B: *AT. Mol. Phys.* **17**, 1301

Hagen, H.-J., Groote, D., Engels, D., Haug, U., Toussaint, F. & Reimers, D., 1987: *Astron. Astrophys.* **183**, L7

Hardorp, J., Shore, S.N. & Wittmann, A., 1976: *Physics of A_p stars*, IAU-Colloquium No. 32, 41

Kemic, S.B., 1974: *Joint Inst. Lab. Astrophys.* Rep. No. 113

Jordan, S.H. & O'Connell, R.F., 1987: unpublished

Koester, D., Schulz, H. & Weidemann, V., 1979: *Astron. Astrophys.* **76**, 262

Landstreet, J.D., 1986: *Mon. Not. R. astr. Soc.*, **225**, 437

Martin, B. & Wickramasinghe, D.T., 1978: *Mon. Not. R. astr. Soc.* **189**, 883

Martin, B. & Wickramasinghe, D.T., 1979: *Mon. Not. R. astr. Soc.* **183**, 533

Martin, B. & Wickramasinghe, D.T., 1982: *Mon. Not. R. astr. Soc.* **200**, 993

Pacholczyk, A.G., 1976: *Radio Galaxies*, Pergamon Press, London

Rösner, W., Wunner, G., Herold, H. & Ruder, H., 1984: J. Phys. B: *At. Mol. Phys.* **17**, 29

Wendell, C.E. & Van Horn, H.M., 1987: *Astrophys. J.* **313**, 284

Wickramasinghe, D.T. & Martin, B. , 1986: *Mon. Not. R. astr. Soc.* **223**, 323

Wickramasinghe, D.T. & Ferrario, L., 1988: *Astrophys. J.* **327**, 222

Wittmann, A., 1974: *Sol. Phys.* **35**, 11

Wunner, G., Rösner, W., Herold, H. & Ruder, H., 1985: *Astr. Astrophys.* **149**, 102

Masses and Magnetic Fields of White Dwarfs in Cataclysmic Variables

J.P. LASOTA[1], J.M. HAMEURY[2], A.R. KING[1,2,3]

[1]DARC, Observatoire de Paris, Section de Meudon, F-92195 Meudon Principal cédex, France
[2]DAEC, Observatoire de Paris, Section de Meudon, F-92195 Meudon Principal cédex, and Université Paris 7, France
[3]Astronomy Department, University of Leicester, Leicester LE17RH, UK

Summary

We show that the existence of the AM Her period spike implies (i) a unique white dwarf mass $\simeq 0.6-0.7M_\odot$ for most magnetic CV's (ii) nova explosions remove exactly the accreted mass from magnetic white dwarfs, and (iii) the maximum magnetic field for most CV's is $\leq 4 \times 10^7$ G. The existence of the spike is very strong support for the idea that the period gap results from a drastic reduction of angular momentum losses when the secondary star becomes fully convective.

1. Introduction

The period distribution of AM Herculis magnetic cataclysmic binaries is well known to be highly non-uniform. In particular, there is a large, highly significant[1] accumulation (6 out of 15) of systems in the interval 113.5 – 114.8 minutes. Recently we (Hameury et al.[2], hereafter HKLR) proposed an explanation for this in terms of the resumption of mass transfer after these systems have crossed the period gap. When accretion resumes at a period of about 2 hr, the fully convective secondary star undergoes a short (Kelvin-Helmholtz time) episode of adiabatic expansion, until it is sufficiently far out of thermal equilibrium that it can contract under the influence of mass loss. Therefore, the orbital period first increases by 2 to 3 min, reaches a maximum, and decreases. This produces two effects which combine to enhance the discovery probability at this point: (i) the mass transfer rate $-\dot{M}_2$ is about twice the value for a star close to the main sequence contracting in response to mass loss, and (ii) the expansion and subsequent contraction of the secondary lengthens the time spent near the initial period. To give the observed period "spike" requires most systems to have similar parameters when mass transfer resumes at the lower edge of the period gap: otherwise the initial value of P_0 would not be the same and the spike would be smeared out. The secondary stars are naturally rather similar if, as suggested by Rappaport et al.[3] and Spruit & Ritter[4], the gap is *caused* by them becoming fully convective. Thus at the spike, $M_2 \simeq 0.2$ M$_\odot$. Further, the period spike implies constraints on the primary masses which have been examined by Hameury et al.[5](hereafter HKL). Higher masses cause a narrower period gap and hence a higher value P_0 of the initial period below the gap. The discovery of EXO 033319–2554.2 at a period of 127 min implies a significantly larger white dwarf mass (unless it is one

of the rare systems which *form* in the period gap). This prediction was subsequently supported by radial-velocity measurements[6]. Thus, contrary to the suggestion of Berriman & Smith[7], the existence of an AM Her system at 127 min does not necessitate a modification of our model, but actually provides strong confirmation of its validity. In two recent papers[8,9] we have examined the implications of the values of M_1 predicted for the spike and EXO 033319-2554.2 for the underlying mass distribution, nova efficiency and magnetic fields.

2. Mass loss, secular evolution and nova efficiency.

HKL calculate the secular evolution of CV's in which a fraction β of the transferred mass is ultimately retained by the white dwarf, i.e. the primary and secondary masses vary with time according to:

$$\frac{dM_1}{dt} = -\beta \frac{dM_2}{dt} \tag{1}$$

Thus $\beta < 0$ implies that nova explosions gradually reduce the mass of the white dwarf despite the accretion. The evolution is assumed to be driven by angular momentum losses via gravitational radiation and magnetic braking. The secondary is modelled as two polytropes (convective envelope and radiative core) after the prescription of Rappaport et al[3]. (see HKLR for full details). HKL consider the cases $\beta = 0, \pm 0.5$ and $\beta = 2e^{-M_1^4} - 1$, the latter describing situations in which mass ejection is much stronger in high mass systems. In each case it was required that the period P_0 at which the systems resume mass transfer after crossing the gap be 115 min. The resulting values of M_1 for systems in the spike and EXO 033319-2554.2 are shown in table 1:

β	M_1 (spike)/$M_\odot$	M_1 (EXO)/$M_\odot$	P_{max} (hr)	$P_{in,min}$(hr)
0	0.70 ± 0.10	1.27 ± 0.12	7.2	4.0
-0.5	0.48 ± 0.13	1.0 ± 0.2	10	–
0.5	0.80 ± 0.01	1.43 ± 0.01	5	–
$2e^{-M_1^4} - 1$	0.80 ± 0.01	1.09 ± 0.01	4.5	–

Table 1: required masses of the primary and secondary for different values of β. It has been assumed (i) that the initial secondary mass is 0.6 $M_\odot$ and (ii) that the spike in the period distribution is at 115 min exactly; the range in M_1 does not take into account the width of the spike. This adds ~ 0.05 $M_\odot$ to the uncertainties in M_1. P_{max} is the maximum period for stable mass transfer of a system which would resume mass transfer at a period of 114 min, assuming that the secondary is on the initial main sequence when it first enters into contact (in this case, the secondary mass is not fixed at 0.6 $M_\odot$). $P_{in,min}$ is the shortest period at which a system can form if the existence of the spike is not to require a relation between M_1 and M_2.

Systems with initial primary masses $M_{1,in}$ can in principle form at any period P_{in} less than P_{max}, defined as the maximum period for which mass transfer is stable, assuming that the secondary is on the main sequence. At periods ≥ 4 hr, the systems would be intermediate polars[10,11]. P_{in} and the initial secondary mass are related by the usual Roche lobe condition:[12]

$$P_{in} \simeq 9\ M_{2,in}/\mathrm{M}_\odot\ \mathrm{hr} \qquad (2)$$

In all cases except $\beta = 0$ however, $M_{1,in}$ must be tightly specified as a function of $M_{2,in}$ if the subsequent evolution is to pass through the spike (i.e. resume mass transfer) at the correct period $P_0 \simeq 114$ min. This is a direct consequence of the fact that if $\beta \neq 0$, the value of M_1 at a given period depends not only on $M_{1,in}$, but also on how much mass the white dwarf has lost or gained during the subsequent evolution, and hence for how long mass transfer has been running. The actual value of P_0 is *very* sensitive to the value of the mass ratio M_2/M_1 at the upper edge of the gap. This can be understood by realizing that the gap occurs because during the mass transer phase the secondary is out of equilibrium and therefore oversized with respect to its main sequence radius. When the braking mechanism is suddenly interrupted (or severely reduced) the secondary star contracts towards its main sequence configuration. The length of the gap will depend on how far its radius was from the main sequence value. For a given braking mechanism, this in turn depends on the mass ratio M_1/M_2. Unless $\beta \neq 0$ there must therefore be an unexplained relation between the initial $M_{1,in}$ and $M_{2,in}$. We deduce that β has to be very close to zero. Even for $\beta = 0$ a system may miss the spike if it was born too close to the upper edge of the gap, and consequently the secondary did not have enough time to build up the required deviation from thermal equilibrium. One has then a minimum initial period $P_{in,min} = 4$ hr and a minimum initial secondary mass $M_{2,in} = 0.45\ \mathrm{M}_\odot$.

The conclusion that $\beta \simeq 0$ is supported by nova models[9]: in magnetic systems the field prevents mixing and therefore does not allow for the ejection of more mass than the amount accreted, but the white dwarf loses almost all the accreted material during the optically thick wind phase of the outburst.

The analysis of initial mass distribution and selection effects[8] shows that strongly magnetic CV's can be divided into two groups:

1. the low ($\simeq 0.7\ \mathrm{M}_\odot$) mass group which accounts for $\sim 90\%$ of observed magnetic CV's and 90–99% of all magnetic CV's, and 2. high mass, with white dwarf masses in the range 1–1.4 $\mathrm{M}_\odot$;EXO 033319-2554.2 and V 1500 Cyg are the two known members of this class.

3. Magnetic field strengths

Most AM Her binaries have white dwarfs magnetic fields[13] $B_1 \leq 3 \times 10^7$ G[13], whereas isolated white dwarfs can have fields up to at least[14] 5×10^8 G. Since most properties of magnetic binaries depend on the magnetic *moment*, the upper limit on magnetic *field* was difficult to understand. However, if one neglects the high mass group we may regard AM Her systems as having effectively a unique white dwarf mass. With R_1 essentially fixed at $\simeq 8 \times 10^8$ cm, the limit on B becomes a limit on μ_1 through $\mu_1 = 5 \times 10^{33} B_7$ G cm^3 where B_7 is B_1 in units of 10^7 G. We have shown[9] that, $\mu_1 \geq 2 \times 10^{34}$ G cm^3, (thus, fields stronger than $B_7 \simeq 4$) implies catastrophic angular momentum losses $\dot{J}$ as a result of coupling of the secondary stellar wind with the *white dwarf* magnetic field[13]. These drive the secular evolution so rapidly that the systems enter a prolonged period gap at $P \sim 5$ hr, remaining as detached systems for a time of order the Hubble time. Some of these systems may in fact be observed as apparently isolated, rapidly rotating and highly magnetic white dwarfs[14], or as *non*–magnetic white dwarfs with brown dwarf companions.

4. Conclusions

The AM Her period spike implies that:

(i) the period of 114 min is special: all secondaries are identical at the lower edge of the gap, (ii) $M_1 \simeq 0.6 - 0.7 M_\odot$ for most systems, (iii) M_1 stays constant during the evolution; nova outbursts on magnetic CV's eject just the accreted matter, (iv) the mass of EXO 033319-2554.2, with a period of 127 min is $\simeq 1.3\ M_\odot$, (v) for most systems $B_{max} \leq 4 \times 10^7$ G.

References

1. Morris, S.L., Schmidt, G.D., Liebert, J., Stocke, J., Gioia, I. & Maccacaro, T., 1987. *Astrophys. J.*, **314**, 641.
2. Hameury, J.M., King, A.R., Lasota, J.P. & Ritter, H., 1988a. *Mon. Not. R. astr. Soc.*, **231**, 535.
3. Rappaport, S., Verbunt, F. & Joss, P.C., 1983. *Astrophys. J.*, **275**, 713.
4. Spruit, H.C. & Ritter, H., 1983. *Astr. Astrophys.*, **124**, 267.
5. Hameury, J.M., King, A.R. & Lasota, J.P., 1988b. *Astr. Astrophys.*, **195**, L12.
6. Beuermann, K., Thomas, H.C. & Schwope, A., 1988. *Astr. Astrophys.*, **195**, L15.
7. Berriman, G. & Smith, P.S., 1988. *Astrophys. J.*, **329**, L97.
8. Hameury, J .M., King, A.R., Lasota, J.P. & Livio, M., 1988c. *Mon. Not. R. astr. Soc.*, , .submitted
9. Hameury, J .M., King, A.R. & Lasota, J.P., 1988d. *Mon. Not. R. astr. Soc.*, , .submitted
10. King, A.R., Frank, J. & Ritter, H., 1985. *Mon. Not. R. astr. Soc.*, **213**, 185.
11. Hameury, J .M., King, A.R. & Lasota, J.P., 1986. *Mon. Not. R. astr. Soc.*, **218**, 695.
12. Warner, B., 1976. in *Structure and evolution of close binary systems*, IAU symposium No 73, eds. P. Eggleton, S. Mitton and J. Whelan, Reidel, Dordrecht, Holland, p. 85.
13. Schmidt, G., Stockman, H.S. & Grandi, S.A., 1986. *Astrophys. J.*, **300**, 804.
14. Schmidt, G., 1987. *Mem. Soc. Astron. It.* **209**, 227.

G117-B15A: HOW IS IT EVOLVING?

S.O.Kepler
Instituto de Fisica
Universidade Federal do Rio Grande do Sul
Brazil,

G.Vauclair
Observatoire Midi-Pyrenees
France,

and
R.E.Nather, D.E.Winget, and E.L.Robinson
McDonald Observatory and Department of Astronomy
The University of Texas at Austin
U.S.A.

ABSTRACT. The measurement of the rate of change of period with time for the g-mode pulsations in ZZ Ceti stars is a direct measurement of the cooling timescale for a DA white dwarf, which in turn can give a totally independent measurement of the age of the galactic disk. Using asteroseismology, we have obtained a rate of change of the period of the dominant pulsation in the light curve of the ZZ Ceti star G117-B15A of $dP/dt = (12.5 \pm 5.5) \times 10^{-15}$ s/s, equivalent to a timescale for period change of $P/\dot{P} = (5.5 \pm 2.4) \times 10^8$ yr, which is consistent with the theoretical value for the cooling timescale of a DA white dwarf around 11,000 K.

1. INTRODUCTION

The ZZ Ceti stars are the single normal DA white dwarfs which show luminosity variations. Fontaine *et. al.* (1982) and Greenstein (1982), using a homogeneous set of colors, found that *all* observed DA white dwarfs in the color range corresponding to effective temperatures in a narrow strip ($\sim$ 1400 K wide) around 11000 K were ZZ Ceti stars. Similar results were obtained from IUE spectra (Wesemael, Lamontagne and Fontaine 1986). There are 20 known ZZ Cetis, all multiperiodic, with periods ranging from 109 to 1186 sec and peak-to- peak light variations from 2 to 34 %. The observed variations are due to nonradial g-mode pulsations (Kepler 1984) and, since each periodicity constrain independently the properties and structure of the star, the observed pulsations can *ideally* be used to infer the whole structure of the white dwarf, as demonstrated by the mode trapping calculations of Winget *et. al.* (1982). For a review of the properties of the ZZ Ceti stars, see Winget (1988). The timescale for period change for the pulsations observed in the ZZ Ceti stars is directly proportional to the cooling timescale of the white dwarf, which can be transformed to the white dwarf birth rate through the measurement of their space densities. The rate of period change also gives directly the core composition, since the cooling timescale is directly related to the equation of state of the white dwarf core and can be used to distinguish among different core-composition white dwarfs (Robinson and Kepler 1980, Winget and Van Horn 1987). Most importantly, the white dwarf cooling timescale gives a totally independent measurement of the age of the galactic disk (Winget *et al.* 1987).

Continuing our work reported in Kepler *et. al.* (1982), we have observed one the simplest ZZ Ceti stars, G117-B15A, with high speed photometry to measure its rate of period change.

Table 1
Journal of Observations since 1982

Run	Length of Observation (hr)	Integration Time (sec)	Fractional Semi-Amplitude	BJDD at Maximum (244 0000.0+)	Error (sec)
2593	0.9	10	0.024	4637.776174	1.6
2597	7.0	10	0.023	4641.624287	0.5
2629	2.1	10	0.022	4992.789531	1.2
2633	6.6	10	0.021	4994.689956	0.7
2637	3.4	10	0.024	4996.744801	0.8
2640	3.7	10	0.024	4997.723649	0.7
JES1	2.9	10	0.021	5021.716661	1.0
2869	3.2	10	0.022	5703.860004	1.4
2870	5.6	10	0.028	5734.642701	0.7
2872	2.4	10	0.025	5735.643972	0.8
ER60	3.8	5	0.023	6113.763716	0.7
ER110	1.8	5	0.021	6443.775386	1.0
3096	5.9	5	0.023	6468.630178	0.5
3106	1.2	10	0.024	6473.718679	0.9
3141	1.0	10	0.022	6523.620086	1.3
3143	1.0	10	0.020	6524.613917	1.3
AT13*	3.8	5	0.018	6768.855451	2.3
9004	2.0	10	0.022	6794.935676	1.0
9009	1.2	10	0.018	6796.928219	1.9
9012	1.9	10	0.022	6797.924535	1.3
9014	2.8	10	0.024	6798.903378	0.9
DEW1	1.7	10	0.018	6823.663537	1.5
DEW2	4.5	10	0.020	6825.651132	1.6
GV1	2.4	6	0.022	7231.328096	1.1
REN23	3.0	10	0.022	7231.612054	0.7
GV2	1.5	6	0.017	7232.396626	3.4
REN25	2.4	10	0.020	7232.623291	2.7
GV3	2.9	6	0.019	7233.343090	2.1
REN27	2.2	10	0.022	7233.634506	1.9
GV4	3.4	6	0.022	7234.319475	1.3
GV5	3.2	6	0.020	7235.313250	1.6
REN30	2.7	10	0.021	7235.607168	1.2
REN32	2.5	10	0.022	7236.610922	0.9

* data taken on the 91 cm telescope, with companion inside aperture

2. OBSERVATIONS

In 1982 we used our 85 hours of high speed photometry on the star to show that the light curve of G117-B15A has at least six pulsation modes simultaneously excited with periods of 107.6 s, 119.8 s, 126.2 s, 215.2 s, 271.0 s, and 304.4 s. The 215.2 s pulsation has a fractional semiamplitude of 0.022, nearly 3 times greater than that of any other pulsation and dominates completely the light curve. We could then derive an upper limit for the rate of change of period with time of $|\dot{P}| \leq 7.8 \times 10^{-14}$ s/s for this pulsation.

We have since then obtained additional 80 hours of high speed photometry using a two-star photometer (Nather 1973) on the 2.1m Struve telescope, plus 4 hours on the 91 cm telescope, at

McDonald Observatory, plus another 13 hours on the 1.9 m telescope at Haute Provence Observatory to improve our estimate of the rate of period change for this pulsation. The data now spans 13 years. The observations were obtained with a blue-sensitive bialkali phototube, and as G117-B15A is rather faint, V=15.52 (Eggen and Greenstein 1965), all measurements were obtained in unfiltered light in order to improve the photon detection rate. The amplitudes observed should be used with caution, since they are wavelength dependent (Robinson, Kepler, and Nather 1982, Brassard, Wesemael and Fontaine 1987), and the effective wavelength of our white-light photometry is not well determined. Table 1 gives a journal of the observations since 1982. The quoted errors throughout this paper are one standard deviation.

3. DATA ANALYSIS

The method for data reduction and conversion of the time base from UTC to the more uniform Barycentric Julian Dynamical Date (prior Barycentric Julian Ephemeris Date) was described in Kepler *et. al.* (1982).

The first step of our analysis was to take Fourier transforms of each night's data to verify which pulsations were present. We had to take in account that only on the runs longer than about 4 hours we could see the three largest amplitude pulsations separetely, and that the three smallest amplitude pulsations could only be seen in power spectra taken with all the seasonal data at once. Our conclusion is that the pulsational power spectrum of G117-B15A has remained the same during the 13 years we have observed the star; all the 6 pulsations detected in 1982 are still present in the data, with the 215.2 s pulsation dominating the light curve.

4. THE UPPER LIMIT TO $\dot{P}$

Our method of measuring the rate of period change is as follows: first, we fit a sinusoidal with a period of 215.2 s to the data by least squares to obtain the time of maximum of the pulsation for each night's data. After converting the obtained time of maxima to the barycenter of the solar system, we calculate the difference between the observed (O) times of maxima and the times of maxima calculated (C) using a linear ephemeris starting on our first observation, obtaining therefore an (O-C) diagram (Figure 1). Unique cycle counts E were obtained for each night since the period derived in 1982 was extremely accurate, permitting us to bridge the whole data base without any possibility of cycle count error. The fairly large apparent scatter in the diagram is an artifact of the varying quality of the different runs; no data point lies more than 3 σ away from zero.

The rate of period change for the pulsation, as well as a correction to the period and phase, can then be obtained by fitting a parabola to the (O-C), since:

$$(O-C) = E_0 + P \cdot E + \frac{1}{2} P \cdot \dot{P} \cdot E^2$$

where E_0 is the epoch of observation, P is the period, E is the number of cycles elapsed since E_0, and $\dot{P}$ is the rate of change of period with time, dP/dt.

Using this formulae to fit a parabola by weighted least-squares to the 69 times of maxima obtained since 1975, one for each run of data, we obtain:

$$E_0 = \text{BJDD } 2442397.917521 \pm 0.000007 \text{ days}$$

$$P = 215.1973870 \pm 0.0000013 \text{ sec}$$

$$dP/dt = (12.5 \pm 5.5) \times 10^{-15} \text{ s/s}$$

or

$$P/\dot{P} = (5.5 \pm 2.4) \times 10^8 \text{ yr.}$$

The observed $\dot{P}$ should be considered only as an upper limit, since our measurement of it is still not converging to any value, as can be seen from Table 2, which gives the result of the parabola fit to the (O-C) including data obtained from 1975 up to that year.

Table 2
Evolution of the P Measurement

Year	dP/dt
1980	$(5.5 \pm 4.7) \times 10^{-14}$
1981	$(5.3 \pm 2.3) \times 10^{-14}$
1982	$(0.4 \pm 2.2) \times 10^{-14}$
1984	$(0.5 \pm 1.3) \times 10^{-14}$
1985	$(0.4 \pm 1.1) \times 10^{-14}$
1986	$-(0.6 \pm 0.8) \times 10^{-14}$
1987	$-(0.4 \pm 0.7) \times 10^{-14}$
1988	$(1.2 \pm 0.6) \times 10^{-14}$

5. DISCUSSION

The observational upper limit on the rate of period change can be compared with the theoretical rate of period change of nonradial g- mode pulsations calculated by Winget (1981), Wood and Winget (1988), and Bradley, Winget and Wood (1988 - these Proceedings), caused by the cooling of the white dwarf. The calculations were made with linear, nonadiabatic pulsation code, and used evolutionary models for carbon core white dwarfs incorporating stratified H/He envelopes consistent with diffusion equilibrium. For models corresponding to the ZZ Ceti stars, they found $\dot{P} \approx 3 \times 10^{-15}$ s/s ($P/\dot{P} \approx 2 \times 10^9$ yr) for a pure carbon core white dwarf and modes with low k and ℓ values, at a temperature of $T_{eff} \approx 13000$ like G117-B15A. As demonstrated by Dziembowski (1977), simple geometrical considerations imply that the observed modes are low ℓ values. Since the heat leakage is proportional to the mean atomic weight of the core composition, the rate of change of period with time for a white dwarf with Fe core can be as large as $\dot{P} \approx 1.4 \times 10^{-14}$ s/s ($P/\dot{P} \approx 5 \times 10^8$ yr), for low k and ℓ g-modes. Our results are therefore still consistent with the theoretical expectations for g-modes, even for models with an Fe-core.

Since our limit on $P/\dot{P}$ will continue to improve quadratically with the time baseline the star is observed, or about 17 % per year nowadays, we expect to reach the precision predicted time scale for a C/O core in 10 years. If, on the other hand, the value for $\dot{P}$ we obtained is real, in 2 years it will be a 3 σ measurement. We can therefore measure the evolutionary timescale for a cool white dwarf, equivalent to that measured by Winget *et al.* (1985) for the hot white dwarf PG1159-035. These measurements are crucial to an independent way of directly measuring the age of the galactic disk, which in turn can be used to measure the age of the Universe.

In order to measure a rate of change of period with time of the order of 10^{-14} s/s, like the one observed in G117-B15A, there is a very stringent restriction on the dynamical environment of the white dwarf, since even a planet of the mass of Jupiter, and at the same distance from the white dwarf that Jupiter is from the Sun, would give an apparent rate of change of the pulsation period, i.e., of the arrival time of the pulses of the order of 10^{-12} s/s, with the times of maxima varying periodically as the pulsating star moves around the barycenter of the system. That means that to give a $\dot{P}$ of the order of 10^{-14} s/s, the white dwarf cannot have any body of even a large planet mass orbiting it. The technique of measuring rates of change of periods with time may therefore prove itself ultimately capable of detecting planets outside the solar system, in addition to producing information on the stellar structure and evolution.

This work was partially supported by grants from CNPq-Brazil, NSF-USA, and CNRS-France.

REFERENCES

Brassard, P., Wesemael, F., and Fontaine, G. 1987, *in Proceedings of the IAU Colloquium 95, The Second Conference on Faint Blue Stars*, ed. A.G.D.Philip, D.S.Hayes, and J.W.Liebert, (L.Davis Press, Schenectady), p. 669.

Dziembowski, W. 1977, *Acta Astron.*, **27**, 203.

Eggen, O.J., and Greenstein, J.L. 1965, *Ap. J.*, **141**, 183.
Fontaine, G., McGraw, J.T., Dearborn, D.S.P., Gustafson, J., and Lacombe, P. 1982, *Ap. J.*, **258**, 651.
Greenstein, J.L. 1982, *Ap. J.*, **258**, 661.
Kepler, S.O. 1984, *Ap. J.*, **286**, 314.
Kepler, S.O., Robinson, E.L., Nather, R.E., and McGraw, J.T. 1982, *Ap. J.*, **254**, 676.
Nather, R.E. 1973, *Vistas in Astronomy*, **15**, 91.
Robinson, E.L., and Kepler, S.O. 1980, *Spa. Sci. Rev.*, **27**, 613.
Robinson, E.L., Kepler, S.O., and Nather, R.E. 1982, *Ap. J.*, **259**, 219.
Wesemael, F., Lamontagne, R., and Fontaine, G. 1986, *Astron. J.*, **91**, 1376.
Winget, D.E. 1981, Ph.D. Thesis, University of Rochester.
Winget, D.E. 1988, *in Proceedings of IAU Symposium 123, Advances in Helio- and Asteroseismology*, ed. J.Cristensen-Dalsgaard and S. Frandsen, (D.Reidel, Dordrecht), p. 305.
Winget, D.E., Hansen, C.J., Liebert, J., Van Horn, H.M., Fontaine, G., Nather, R.E.,Kepler, S.O., and Lamb, D.Q. 1987, *Ap. J.*, **315**, L77.
Winget, D.E., Kepler, S.O., Robinson, E.L., Nather. R.E., and O'Donoghue, D. 1985, *Ap. J.*, **292**, 606
Winget, D.E., and Van Horn, H.M. 1987, *in Proceedings of the IAU Colloquium 95, The Second Conference on Faint Blue Stars*, ed. A.G.D.Philip, D.S.Hayes, and J.W.Liebert, (L.Davis Press, Schenectady), p. 363.
Winget, D.E., Van Horn, H.M., Tassoul, M., Hansen, C.J., Fontaine, G., and Carrol, B.W. 1982, *Ap. J.*, **252**, L65.

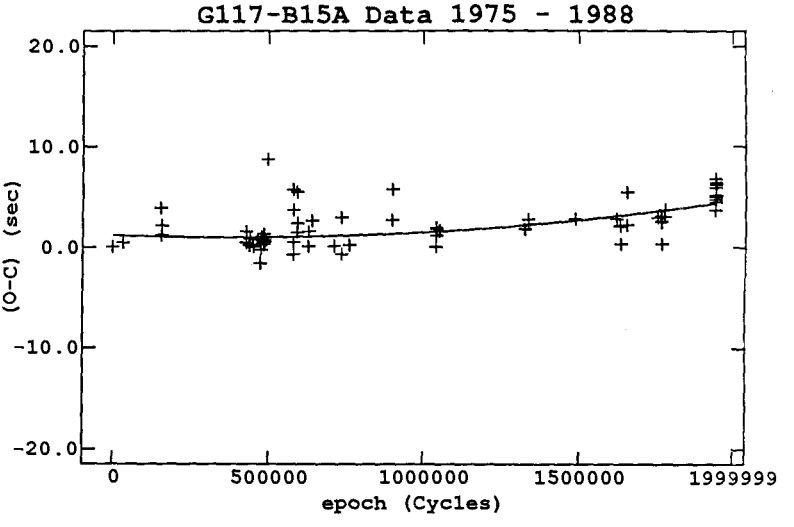

Figure 1. *The (O-C) diagram for the 215.2 s pulsation of G117-B15A. The observed times of maxima are listed in Table 1, and the calculated times of maxima were derived using a linear ephemeris starting on BJED 244 2397.917507.*

PRESSURE SHIFTS OF METAL LINES IN COOL WHITE DWARFS

Gordon L. Hammond
Astronomy Program, Department of Mathematics
University of South Florida, Tampa, FL 33620

Abstract

Model atmosphere techniques and an experimentally confirmed theory of collision broadening of CaII H and K by helium have been combined to show that the difference in velocity shifts for the two lines is a sensitive diagnostic for the H/He abundance ratio in cool, metallic line white dwarfs.

I. Introduction

Greenstein (1972) discussed the role of pressure shifts in his analysis of the radial velocity of the DZ8 van Maanen 2. He measured a discrepancy of 29 km/s in velocity of the two fine structure components, H and K, of CaII. Now that high resolution spectra of DZ stars are becoming available (see, for example, Wagner, Sion, Liebert and Starrfield 1988; Liebert, Wehrse and Green 1987), and the theoretical approach to neutral collision broadening has recently improved beyond the classical treatments of van der Waals and Lennard-Jones interaction potentials, a more precise study of pressure shifts in these high density atmospheres seems warranted.

The goals of this work are to provide corrections to observed radial velocities for more accurate gravitational redshift determinations, and to determine if the fine structure shift behavior might provide evidence of the H/He ratios. This evidence can be crucial in studies of accretion hypotheses (e.g., Aannestad and Sion 1985; Zeidler, Weidemann and Koester 1986).

II. Collision Broadening and Shifts

Laboratory measurements of both broadening and shifts of CaII H and K by helium under white dwarf atmospheric conditions were made by Hammond (1975). Those damping constants were used in a white dwarf model atmosphere program (Hammond 1974), but the experimental shifts were small and the temperature range was too small for accurate determination of the temperature dependences.

A recent theoretical study of the perturbation of both H and K lines of CaII by helium collisions was made by Monteiro, Cooper, Dickinson and Lewis (1986) using model potential methods. That work predicts broadening and shift parameters under impact approximation conditions, and the temperature dependence of these quantities.

The excellent agreement between experiment and theory for the damping constants has already been described (Hammond 1987). The agreement for shifts is shown in Figure 1, where least squares fits to both theory plus experiment (a), and to theory alone (b), are shown. Aside from some numerical noise in

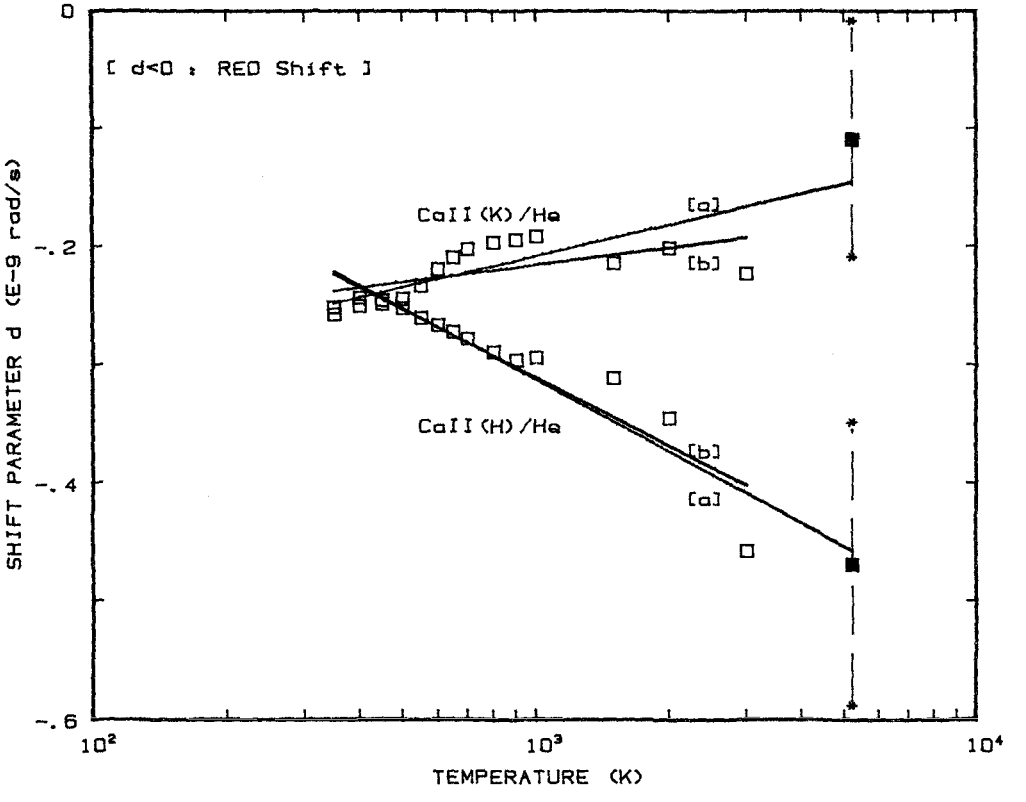

Fig. 1-- Temperature dependence of the CaII H & K line shift parameters. The experimental points (filled squares) show the probable errors from nine measurements at an average temperature of 5200 K.

the theoretical points (open squares), there is good agreement in magnitude, temperature dependence, and shift direction. The fits for theoretical plus experimental points, (a), have been added to the model atmosphere code.

III. Model Atmosphere Program

The early form of the code was written by Bell (1970) for work on G and K giants. Hammond (1974) modified it to treat high gravity stars, paying close attention to obtaining flux constancy in the presence of strong convection. The program yields flux-constant, non-grey, LTE models, and calculates UBVRI and uvby colors and several MCSP colors (Greenstein 1984). The H and K line

profiles are calculated at 2 Å intervals from 3888 to 4012 Å. The line fluxes are convolved with an instrumental slit function of 4 Å half-width. The wavelength shifts are measured by fitting a trigonometric series expansion to the line cores. The wavelength of the bisector of the core can thus be determined to 0.05 Å (4 km/s). This technique simulates the Greenstein Grant machine method used on photographic spectra, and is applicable to electronic spectra where noise at the minima also reduces precision. The fitting function also can fit the asymmetric profiles exhibited by the cool, helium rich models.

IV. Results and Discussion

Inspection of Fig. 1 indicates the H line shifts much more than the K line at temperatures greater then 1000 K, and the difference in shift, V(H)-V(K), will then be a function of atmospheric pressure. That pressure, in turn, will be a function of the H/He ratio due to the differing opacities of H^- and He^-. It only remains to determine the magnitude of the differential shift.

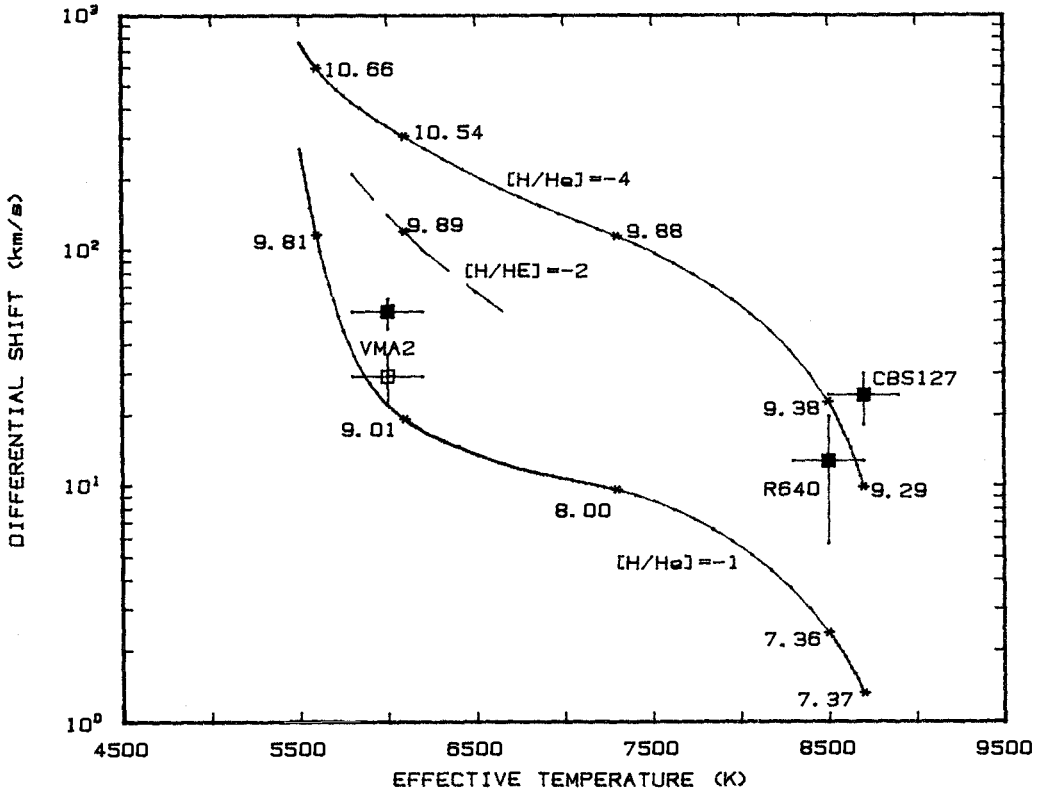

Fig. 2-- Differential shifts from the model grid and observational data. Points (*) on the curves are labeled with log Pg at tau=0.10. The filled squares are from data supplied by Sion (1988); the open square is from Greenstein (1972).

The results from a grid of models with effective temperatures from 5600 K to 8700 K and H/He abundance ratios from 10% to 0.01% are shown in Figure 2. All models were calculated with log g = 8.0, and the metal abundances were adjusted to yield equivalent widths of H plus K of about 35 Å, a value typical of cool DZ stars. The upper limit of 10% hydrogen was dictated by the lack of data on the shifts of H and K by hydrogen collisions. The grid models are labeled with log Pg at tau = 0.10; the curves are empirical cubic spline fits.

There is a clear separation of the helium rich models from the hydrogen contaminated models; the differential shift increases by about 1 dex for the helium rich models at any effective temperature. At differential shifts greater than about 50 km/s, the core of the H line becomes noticeably red asymmetric due to the high gas pressures and large shift parameters. This is also the regime where the impact approximation becomes invalid for the line wings (helium number densities greater than 5.E+21/cc), and the regime where departures from the ideal gas equation of state may become important. It remains to be seen whether any real DZ stars exhibit such large differential shifts and asymmetry.

The differential shift for vMa2 (open square, Greenstein 1972) and for several DZ stars with high resolution electronic spectra (filled squares, Sion 1988) are shown in Fig. 2; the effective temperatures are from matching model and observed colors and continuum fluxes. The agreement between the old photographic measurements and the new data for vMa2 is good and indicates a H/He ratio between 1% and 10%, a result that agrees with a determination from infrared colors (Hammond 1974). The result for Ross 640, log(H/He) = -4, agrees with the hydrogen abundance found by Liebert (1977) from very weak Balmer lines. Several other cool DZ stars with strong H and K lines have been observed at high resolution by Sion (1988) and are now being analyzed in the above fashion. The present results show that the differential shift, coupled with accurate effective temperatures, can reveal the H/He abundance ratio in cool DZ stars within quite narrow limits.

References

Aannestad, P. A., and Sion, E. M. 1985, A. J.,90,1832.
Bell, R. A. 1970, M.N.R.A.S.,148,25.
Greenstein, J. L. 1972, Ap. J.,173,377.
Greenstein, J. L. 1984, Ap. J.,276,602.
Hammond, G. L. 1974, Ph.D. Dissertation, University Maryland, College Park, MD
Hammond, G. L. 1975, Ap. J.,196,291.
Hammond, G. L. 1987, Bull. AAS,19,755.
Liebert, J. 1977, Astr. Ap.,60,101.
Liebert, J., Wehrse, R., and Green, R. F. 1987, Astr. Ap.,175,173.
Monteiro, T., Cooper, I.,Dickinson, A., and Lewis, E. 1986, J. Phys. B,19,4087
Sion, E. M. 1988, private communication.
Wagner, R., Sion, E. M., Liebert, J., and Starrfield, S. 1988, Ap. J.,328,213.
Zeidler-K.T., E.-M., Weidemann, V., and Koester, D. 1986, Astr. Ap.,155,356.

A NEW TEMPERATURE DETERMINATION FOR SIRIUS B FROM IUE: IMPLICATIONS FOR THE OBSERVED SOFT X-RAY FLUXES

K. Kidder and J.B. Holberg
Lunar and Planetary Laboratory, University of Arizona
Tucson, Arizona 85721
and
F. Wesemael
Département de Physique and Observatoire du Mont Mégantic
Université de Montréal

ABSTRACT

We have used IUE archive observations to obtain a new and independent estimate of the effective temperature of Sirius B. In this effort we have modeled the observed Lyman alpha profile of Sirius B as a function of effective temperature and find; T_{eff} = 24,500 ± 500 K. This temperature is in good agreement with a recent result obtained from analysis of EXOSAT soft X-ray spectra of Sirius B. In addition to providing confirmation of the soft X-ray result, this temperature implies that Sirius B is significantly cooler and larger in radius than most previous estimates. The radius, R = 0.090 ± 0.005 $R_{\odot}$, implied by the lower temperature is well in excess of the radius of fully degenerate star having the mass of Sirius B. This investigation employed a unique set of SWP archive spectra, acquired with Sirius B in the small aperture, which have proved to be free of scattered light contamination from Sirius A.

INTRODUCTION

Sirius B has long been an object of particular interest and the subject of numerous detailed studies. Among the many reasons for the continued attention received by this star are its well determined astrometric mass and parallax, the nature of its soft X-ray emission, and its association with Sirius A. The latter circumstance has been the motivation for a wide range of suggestions regarding its evolutionary history. A major source continuing uncertainty regarding Sirius B has been its effective temperature. Achieving a reliable estimate for T_{eff} would help reduce uncertainties in the radius of Sirius B, allowing critical comparisions with mass-radius relationships, and also provide an important verification of the interpretations of various soft X-ray observations of this star.

Strong renewed interest in Sirius B developed in 1975 with the detection of soft X-ray emission (Mewe *et al.* 1975) from the Sirius system. Initially this was interpreted as coronal emission from either Sirius A or B; however, it was subsequently realized that the observations could be explained on the basis of photospheric emission from the pure hydrogen atmosphere of Sirius B (Shipman 1976), provided the temperature was high enough. Since 1975 Sirius B has been intensively observed by a large number of spacecraft including in the X-ray: ANS, HEAO 1, Einstein, and EXOSAT; and in the Ultraviolet: Copernicus, IUE, and Voyager. In spite of the well known problems posed by the proximity to Sirius A these efforts have succeeded in reducing many of the uncertainties associated with Sirius B, most notably its effective temperature. Current estimates have converged on temperatures in the range 26,000 K ± 2000 K. A recent thorough discussion of the observational constraints on the temperature and radius of this star is

contained in Holberg, Wesemael, and Hubeny (1984) and Thejll and Shipman (1987). Interest now focuses on modeling the soft X-ray flux in terms of the effective temperature and photospheric helium content. Whether or not the temperature of Sirius B is closer to 25,000 K or 27,000 K has important implications for the interpretation of the soft X-ray emission, the helium content of its atmosphere, as well as models of its internal structure. Recently, Paerels *et al.* (1980) have determined that T_{eff} = 25,500 ± 500 Å, R = 0.0079 to 0.0085 $R_{\odot}$ and He/H = < $2x10^{-5}$, best describe the overall energy distribution of Sirius B from the soft X-ray to the optical.

OBSERVATIONS AND ANALYSIS

In 1980 a series of five IUE SWP spectra (SWP 10073, 10074, 10076, 100122, and 10023) of Sirius B were acquired by M. Savedoff. Each consisted of a doubly exposed large and small aperture spectrum of Sirius. At the time Sirius B was located a distance of 10.14" and a position angle of 47.09° from Sirius A. A visual inspection of these spectra in the IUE archives revealed little apparent contamination from Sirius A, particularly in the important region of the broad Ly α profile. Subsequent analysis confirmed that three small aperture spectra (SWPs 10076, 10122 and 10123) were indeed free from any detectible contamination. This was verified in two ways. First, these spectra were found to be of identical shape, in spite of various exposure levels, and could be compared directly with similar IUE spectra of an analogous DA, CoD -38° 10980 (T_{eff} = 24,500 K and log g = 8.05). Except for the 1175-1250 Å region, where the Ly α profiles of the two stars are expected to differ due to different gravities, the spectral ratio was flat. Second, we successfully performed preliminary fits to the Ly α profile over the range 1150 to 1350 Å using a set of model atmospheres having gravities of log g = 8.5 to 8.65. A comparison of one such model, covering the entire SWP wavelength range, is shown in Fig. 1. In this comparison and that with CoD -38° 10980 *no* evidence of wavelength dependent contamination from Sirius A was found, in particular none which increased toward longer wavelengths. The expected wavelength dependence of any *spectrally neutral* scattered component from Sirius A is illustrated in Fig. 1 by a scaled template SWP observation of a typical A1 V star (δ UMi).

We analyzed the Ly α profile of Sirius B using techniques and model atmosphere grids similar to those used in the study of Ly α profiles in other DA white dwarfs (Holberg, Wesemael and Basile 1986). In this study it was demonstrated that the detailed analysis of DA Ly α profiles provide a reliable means of temperature estimation over the range 20,000 K to in excess of 60,000 K. Briefly, our procedure was to use the unnormalized small aperture fluxes for Sirius B and to fit for T_{eff} . This differs from previous Ly α profile analysis which was done on an absolute flux scale. Previous results have shown that the primary penalty paid for normalizing at 1300 Å is an approximate factor of two increase in uncertainty in the resulting T_{eff}.

We find that the Ly α profile of Sirius B indicates an effective temperature of T_{eff} = 24,500 ± 500 K. This result is significantly lower but still compatible with an earlier Sirius B Ly α result by Böhm-Vitense, Dettmann, and Karprandis (1979), who obtained 26,000 ± 1000 K. These authors employed an early epoch large aperture SWP observation of Sirius B in which an effort was made to exclude Sirius A from the large aperture. Their results were primarily based on comparisons of the data with theoretical Ly α profiles and depended on two alternate calibrations of the short wavelength end of the SWP camera.

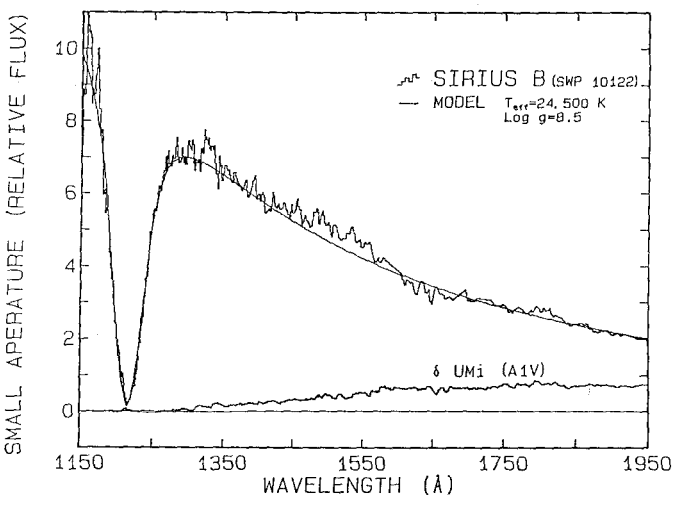

Figure 1 A comparison of the small aperture energy distribution of Sirius B from SWP 10122 with that of a model atmosphere specified by T_{eff} = 24,500 K and log g = 8.5. The ability of the model to generally match the observations throughout the SWP wavelength range is compelling evidence for the lack of any significant spectral contamination from Sirius A. An indication of the expected spectral shape of such contamination is illustrated by the arbitrarily scaled SWP energy distribution of the A1 star δ UMi.

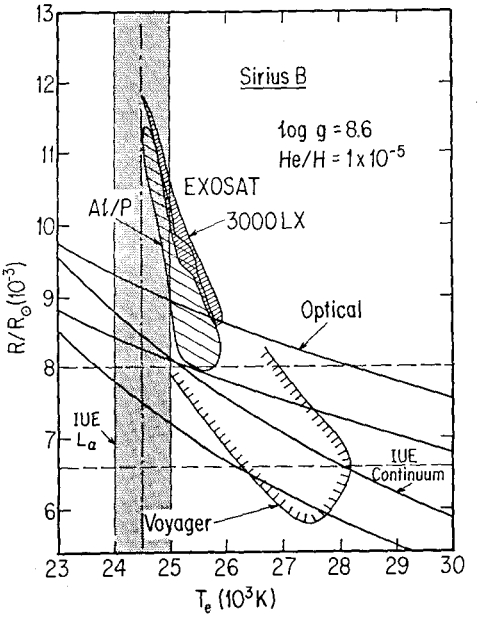

Figure 2 A comparison of existing constraints on the temperature and radius of Sirius B. The IUE Ly α results described here are shown as the vertical stippled region between 24,000 K and 25,000 K. The EXOSAT soft X-ray results of Paerels *et al.* (1988) are indicated by the two irregular hatched regions labeled "Al/P" and "3000 LX." The remaining regions correspond to ground-based photometry ("Optical"), the SWP spectrophotometry of Böhm-Vitense *et al.* ("IUE"), and Voyager far UV spectrophotometry ("Voyager"). These are all taken from Holberg *et al.* (1985). The horizontal dashed lines represent a 99% confidence range of radii corresponding to a 1.053 ± 0.005 $M_{\odot}$, ^{12}C white dwarf satisfying the Hamada-Salpeter mass-radius relationship.

DISCUSSION

In Fig. 2 we compare our new IUE results with previous constraints on the temperature and radius of Sirius B, including the recent EXOSAT results of Paerels et al. (1988). As can be seen, the Ly α and EXOSAT results are reasonably consistent for $T_{eff} \sim 25{,}000 \pm 500$ K and $R > 0.008\ R_{\odot}$. Additionally, if the analysis of the Voyager data were extended into this range of lower temperature and larger radii, it would also pass through this region. Considering all of the constraints the most consistent range of radii for Sirius B lies in the range $R = 0.0090 \pm 0.0005\ R_{\odot}$. Such radii are significantly larger than the range $R = 0.0072 \pm 0.0003\ R_{\odot}$ which are predicted for a fully degenerate star with a ^{12}C core using the Hamada and Salpeter (1961) relationship for an astrometric mass of $M = 1.053 \pm 0.0028\ M_{\odot}$ (Gatewood and Gatewood, 1978). Recently, Thejll and Shipman (1987) in reviewing the available observational constraints concluded that for T_{eff} between 26,000 to 28,000 K Sirius B lay 1 to 2 σ above the Hamada-Salpeter mass-radius relation. The larger radius implied by our cooler T_{eff} confirms this result and further increases the degree of the discrepancy.

The IUE Ly α results we present here are preliminary in that several of the SWP images have yet to be re-reduced to current IUE processing standards. Existing reprocessed images indicate that the additional data will serve to improve the S/N of the Ly α profiles and will not materially influence any of our results. A complete analysis and discussion of these data will be presented elsewhere.

The authors wish to acknowledge their debt to the IUE Guest Observer, M. P. Savedoff, who obtained these unique observations of Sirius B at a time when its separation from Sirius A was still great enough to avoid contamination. This work has been supported in part by NASA Training Grant NGT-50305 and NASA Grant NAGW-147. F. Wesemael wishes to acknowledge support from the NSERC, Canada.

REFERENCES

Böhm-Vitense, E., Dettmann, T., and Kaprandis, S.: 1979, *Astrophys. J. (Letters)*, **232**, L189.
Gatewood, G. D., and Gatewood, C. V: 1978, *Astrophys. J.*, **225**, 191.
Hamada, T., and Saltpeter, E. E.: 1961, *Astrophys. J.*, **134**, 683.
Holberg, J. B., Wesemael, F., and Hubeny, I.: 1984, *Astrophys. J.*, **280**, 679.
Holberg, J. B., Wesemael, F., and Basile, J.: 1986, *Astrophys. J.*, **306**, 329.
Mewe, R., Heise, J., Groneschild, E. H. B. M., Brinkman, A. C., Schrijver, J. and Den Boggende, A. J. F.: 1975, *Nature Phys. Sci.*, **256**, 711.
Paerels, F. B. S, *et al.*: 1988, *Astrophys. J.*, **329**, 849.
Shipman, H. L.: 1976, *Astrophys. J. (Letters)*, **206**, L67.
Thejll, P., and Shipman, H. L.: 1987, *Pub. Astron. Soc. Pacific*, **98**, 922.

THE DETECTION OF IONIZED HELIUM AND CARBON IN THE PULSATING DB DEGENERATE GD358

Edward M. Sion
Department of Astronomy and Astrophysics
Villanova University

James Liebert
Steward Observatory
University of Arizona

Gerard Vauclair
Observatoire de Toulouse
France

Gary Wegner
Department of Physics and Astronomy
Dartmouth College

I. Introduction

Spectroscopic observations of hot white dwarfs utilizing the Explorer (IUE) high resolution spectrograph have led to the important discovery of ion absorption features (undetectable at low resolution) which have been ascribed to wind outflow in some cases (cf. Bruhweiler and Kondo 1983) and formation at the photosphere (cf. Sion and Guinan 1983; Bruhweiler and Kondo 1983; Dupree and Raymond 1982) in others. These line features, often weak and sharp, have presented a fundamental challenge to current understanding of the complex interplay of physical processes which control observed surface abundances in white dwarfs: gravitational/thermal diffusion, selective radiative support of ions, mass loss, convective dilution and mixing, and accretion (cf. the review by Vauclair, this volume and references therein).

Unfortunately IUE echelle observations have been possible only for the brightest dozen or so hot white dwarfs of spectral types DA, DAO, and DO, due to the exceedingly long exposure times required. Until the observations reported in this paper, IUE echelle data for non-DA stars was restricted to objects with Teff > 47000K. Moreover, since no high resolution IUE observation had ever been attempted for a DB, one of us (E.M.S.) proposed that at least one IUE echelle spectrum of a DB should be part of the IUE archives and might reveal some surprises, following the precedence set by other unexpected detections in the IUE echelle spectra of hot white dwarfs. Arrangements for a joint US-European exposure and choice of targets were made by one of us (J.L.). As a result we have therefore extended our IUE echelle observations downward

in temperature to the essentially pure helium composition DB white dwarfs by combining back to back US and European low background IUE observing shifts. We have selected as the most optimum target, GD358, prototype of the class of six known pulsating DB stars and one of the hottest DB stars. Our objectives were: (1) to search for any evidence of metals in the photosphere (2) search for possible mass outflow; (3) place stringent constraints on the carbon abundance in a hot DB; and (4) look for evidence of absorption wings at Lyman alpha + He II (1215A). The results of this search are presented below.

II. Observations

Two separate high resolution IUE spectra of GD358 were obtained during the 10 th and 11 th observing episodes. The first image SWP31432, was obtained on day 211, 1987 with an exposure time of 1054 minutes. The exposure was begun and terminated during contiguous half US2 shifts with approximately 16 hours of intervening ESA and US1 time. The second image SWP33681 was obtained on day 152, 1988 with an exposure time of 755 minutes. This observation was accomplished without contiguous half US2 time. Before each exposure, a low resolution SWP image of GD358 was taken to verify centering.

The spectroscopic data was analyzed with the NASA Goddard Regional Data Analysis Facility (RDAF) software via a phone link between the Vax 8350 and the Department of Astronomy and Astrophysics at Villanova University where a Tektronix 4014-1 terminal and Tektronix 4611 copier were utilized for the measurements and display.

III. Results and Summary

The first image SWP31432 was examined in the echelle orders containing the strongest ion transitions of C, N, O, Si and in the wavelength region of He II. This spectrum revealed the presence of numerous interstellar absorption lines identified in table 1. The velocity of the local interstellar medium (LISM)in the direction to GD358 was found to be -27 km/s. In addition absorption features identified as C II (1335.7077) and He II (1640.474) with an equivalent widths of 150 mA and 250 mA respectively, were found to be redshifted with respect to the LISM by 34 km/s. Close examination of the photowrites revealed no obvious artifacts which could account for the line. The identification of a similar feature at C II (1334.5323) was complicated by a reseaux redward of the interstellar line. Since the detection of redshifted C II and He II was unexpected and provides important data points at high DB

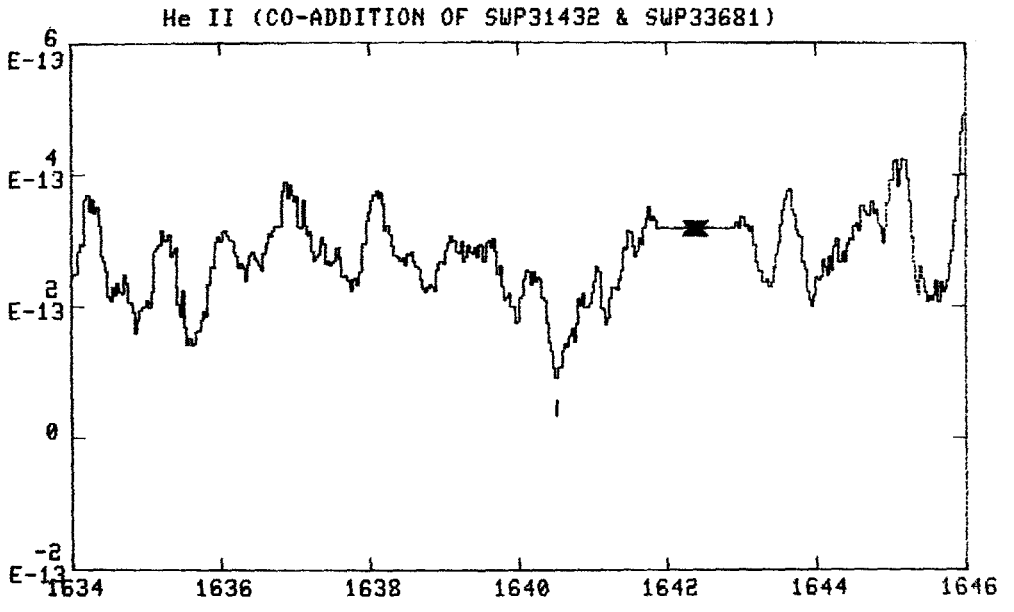

Figure 1----Flux (ordinate, cgs) versus wavelength (abscissa) in Angstroms for the co-added images (SWP31432+SWP33681).

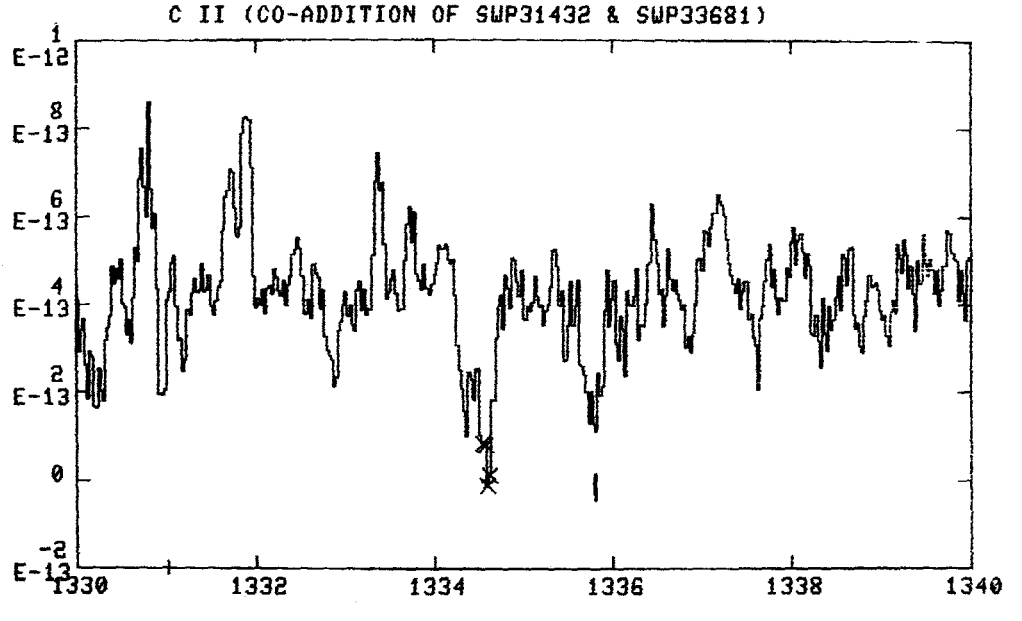

Figure 2.---Same as figure 1 except in the wavelength region of C II. The velocity at the vertical tick mark is 6 km/s.

temperatures for tests of convective dredgeup mechanisms (Fontaine et al 1984) and the hot DB temperature scale, a second image was obtained (SWP33681) 10.2 months later in order to confirm the features.

A close examination of the backup image (SWP33681) and comparison with SWP31432 revealed He II and C II at the same redshift (6-7 km/s) as in SWP31432, thus confirming the reality of both features. In both spectra, the equivalent width of He II was measured to be approximately 250 mA.

The two images were coadded in the wavelength regions of He II and C II and the results of the coaddition are shown in figures 1 and 2. Figure 1 is a flux versus wavelength plot of the He II (1640) coaddition with 10 point smoothing. The feature appears fairly symmetric but with the possible suggestion of multiple components slightly redward and blueward of the central core. These weaker components appear in both individual images. The width of the He II line can be used to place limits on the rotational velocity and magnetic field of GD358 pending a successful model fit to the line profile data in figure 1.

The coaddition of the C II wavelength region is displayed in figure 2 where a flux versus wavelength plot reveals the possible redshifted C II (1335.7077) absorption line with an equivalent width of 134 mA. The central velocity of the line is 6 km/s, which agrees with the velocity of the He II feature. This velocity coincidence with He II strengthens somewhat, the reality of the C II feature.

The Lyman alpha + He II (1215) region reveals no clear evidence of absorption wings flanking the geocoronal emission. The other echelle orders appear devoid of possible stellar features except for a possible doubled emission feature at Si II with the red side of the emission having a redshift in agreement with He II.

Pending a full model atmosphere analysis now in progress by one of us (G.W.), we can only speculate on the implications of the He II detection. The hot DB temperature scale is presently controversial (cf. Oke, Weidemann and Koester 1984; Liebert et al 1986) with IUE temperature determinations, excluding optical data, yielding significantly higher temperatures for the hottest DB stars and thus a hotter pulsational instability blue edge. The atmospheric parameters of GD358 in particular, were explicitly derived by Koester et al. (1985) from high signal to noise spectrophotometry. It is possible that the hot DB temperature scale may now have to be revised upward in

view of our He II detection. If so, this would favor the higher hot DB temperature scale of Liebert et al. (1986) and could place GD358 in the so-called DO-DB gap (30000K-45000K) where to date, no helium-rich degenerates have been found.

If the C II feature is real, the presence of carbon at the effective temperature of GD358 (Teff = 25-28000K), may not be inconsistent with the convective dredgeup theory (Fontaine et al 1984) for the origin of photospheric carbon in cooler helium-rich degenerates. The dredgeup, by helium convection, of carbon from its equilibrium diffusion tail extending upward from the carbon-oxygen core, predicts a low abundance of carbon in the hottest DB stars. It is even possible that alternative explanations for carbon in GD358 may have to be sought perhaps in connection with the non-radial g-mode pulsations of GD358. These possibilities are currently being explored with new diffusion calculations by one of us (G.V.). Encouraged by the unexpected detections reported here for GD358 we plan to obtain one or two additional IUE echelle images of hot DB stars accessible with back to back US-European exposures. Our model atmosphere analysis will be reported in a subsequent paper.

This work was supported by NASA grant NAG5-343 and in part by NSF grant AST88-02689, both to Villanova University and in part by NSF grants AST88-40482 (J.L.) and AST85-15219 (G.W.).

References

Bruhweiler, F., and Kondo, Y.1983, Ap.J., 269, 657.

Dupree, A., and Raymond, J. Ap.J. (Letters), 263, L63.

Fontaine,G., Villenueve,B., Wesemael, F., and Wegner, G. 1984, Ap.J. (Letters), 277, L51.

Koester, D., Vauclair, G., Dolez, N., Oke, J.B., Greenstein, J.L., and Weidemann, V.1985, Astr. Ap. 149, 423.

Liebert, J., Wesemael, F., Hansen, C.J., Fontaine, G., Shipman, H.L., Sion, E.M., Winget,D., and Green, R.F.1986, Ap.J., 309, 612.

Oke, J.B., Weidemann, V., and Koester, D.1984, Ap.J., 281, 276.

Sion, E.M., and Guinan, E.F.1983, Ap.J.(Letters), 265, L87.

TIME-DEPENDENT STUDIES OF THE SETTLING OF HEAVY ELEMENTS IN THE ENVELOPES OF COOL WHITE DWARFS

J. Dupuis, C. Pelletier, G. Fontaine, and F. Wesemael

Département de Physique, Université de Montréal

Gravitational settling is widely accepted as being a fundamental physical process acting upon superficial layers of white dwarfs and resulting in an important alteration of their atmospheric composition. Several investigators have been interested by the problem of gravitational settling in white dwarfs (Fontaine and Michaud 1979; Vauclair, Vauclair, and Greenstein 1979; Alcock and Illarianov 1980; Muchmore 1984; Paquette *et al.* 1986). As pointed out in Paquette *et al.* 1986, they all reached the same qualitative conclusion: the gravitational settling time scales of metals in cool white dwarfs are small compared to their evolutionary time scales. These stars should therefore have their photospheres depleted of metals if there is no extrinsic source such as accretion for example. This is consistent with the observational fact that most of the cool white dwarfs spectra just show hydrogen and helium lines while the absence of metallic lines indicates a strong depletion of metals. Although the qualitative agreement between theory and observations is satisfactory, only time-dependent calculations can lead to a thorough understanding of the heavy element abundance patterns in cool white dwarfs. In particular, the predicted abundance of an element within the framework of the accretion-diffusion model does depend explicitly on the results of such calculations. We have already presented some preliminary results of numerical simulation of accretion episodes of heavy elements into white dwarfs (Dupuis *et al.* 1987). As part of an ongoing detailed investigation of these processes, we focus here exclusively on the mechanism of gravitational settling in white dwarfs in order to clear some confusion which has appeared in the literature.

The usual notion of an e-folding diffusion time scale strictly applies at the base of the convection zone of a stellar model after having made a number of approximations. If an element can be considered as trace and if ordinary diffusion can be neglected (*i.e.* the concentration gradient is much smaller than its equilibrium value; see Fontaine and Michaud 1979), then it is a simple matter to show that, *at the base of a convection zone*, the abundance of a given element is given by,

$$u = u_0 \exp(-t/\theta) \tag{1}$$

where θ, the diffusion or settling time scale, is given by,

$$\theta = \frac{g}{4\pi G} \frac{q}{\rho \mid \omega \mid} \tag{2}$$

where G is the gravitational constant, g is the local gravity, q is the fractional mass, ρ is the density, and ω is the diffusion velocity of the trace element with respect to the background ($\omega < 0$). The exponential behavior shown in equation (1) is *not* valid in regions below the convection zone and the notion of an e-folding diffusion time scale loses its significance there. The time-dependence of the abundance at a given shell can only be obtained from a solution of the continuity equation and, generally, the behavior is *very* different from an exponential

behavior. We illustrate the point here with a few sample results. The diffusion equation for gravitational settling is solved with a new technique based on a Galerkin-type finite element formulation briefly described in Pelletier *et al.* (1988). We consider the settling of a typical heavy element, namely calcium, in the envelopes of *He*-rich white dwarf models with $T_e \leq 25,000$ K. For a given model, we have set the initial calcium abundance equal to its solar value ($u(Ca) = 5.96 \times 10^{-6}$) throughout the envelope. We have then followed the evolution of the abundance profile during an interval of time equal to the age of the model. In Figure 1, the result of such a simulation is shown for calcium diffusing in a 10,000 K, 0.6 $M_\odot$ *He*-rich white dwarf having a *He* layer mass $\log \Delta M(He)/M = -3.5$ and computed with the standard treatment of convection. Each curve gives the logarithmic abundance of calcium as a function of the logarithmic mass fraction for increasing integration time from top to bottom. First, one should notice that the calcium abundance profile evolution is followed during more than 9×10^8 years and that the surface abundance (the value at $\log q \approx -6.2$) varies almost over 25 orders of magnitude without significant loss of precision. Such a simulation required 170 cubic elements and took 331 time steps, which means about 160 CPU seconds of execution time on the Université de Montréal's CYBER 855. A noteworthy feature is that the overall mass of calcium contained in the envelope is conserved to better than 1 %. In Figure 2, we show the logarithmic abundance of calcium as a function of logarithmic time in unit of years for 8 different layers in the envelope. The curve labelled 1 is the solution at the surface of the envelope which is delimited by the bottom of the superficial *He* convection zone, and the 7 remaining curves labelled 2 to 8 are the solution at increasingly deeper layers separated by approximately half a dex in mass. The continuous curves are the numerical solutions while the dotted curves are the exponential solutions defined by the local diffusion time scales as discussed above. The surface abundance (curve 1) is falling as expected almost exponentially with time, the increasing difference with the exponential solution is due to the sligth buildup of the concentration gradient which slows down the settling of calcium. From a practical and observational point of view, this result is not different from those of previous studies: calcium falls under its detection level in an interval of time small compared to the age of the model (at $T_e = 10^4$ K, age $= 9 \times 10^8$ years). This can also be understood with the help of figure 1, the calcium profile near the surface relaxes rapidly during the first 10^7 years where the concentration gradient is negligibly small. After 10^7 years, settling tends to be opposed by the concentration gradient which causes the deviation from the exponential solution to become even more important on curve 1 of figure 2.

The behavior of the solution in deeper layers is quite different from the exponential solution and is understood in the following way: before a time about equal to the local settling time scale, the local abundance exceeds the exponential solution values because calcium coming from overlying layers is causing a temporary enrichment. Thereafter, the depletion in calcium in the overlying layers starts being felt and the local calcium abundance is getting smaller than the predicted exponential abundance. Finally, when the concentration gradient sets in, the settling is slowed down and the calcium abundance becomes greater than the exponential solution. These results show that the exponential solution associated to the local settling time scale is a good approximation of the surface behavior but that it is not even a good order of magnitude estimate of the solution in deeper layers. This illustrates the need for complete time-dependent studies of gravitational settling since simple *e*-folding time scale estimates are not good approximations of the real solution.

In Figure 3, the logarithmic surface abundance of calcium is shown as a function of logarithmic time (years) for models with effective temperatures ranging from 2.5×10^4 K to 8×10^3 K. For the five models shown, the surface

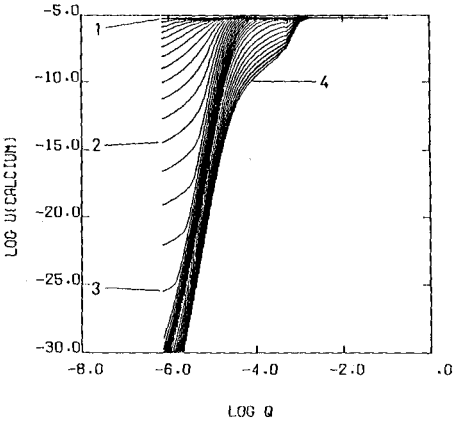

Fig. 1. Evolution of the Ca abundance profile in a 10,000 K, 0.6 $M_\odot$, He-rich white dwarf ($\log q(He) = -3.5$) with $ML1$ convection. The curves labelled 1 to 4 are respectively the profiles after 1.67×10^4, 4.1×10^6, 1.01×10^7, and 9.01×10^8 years of settling.

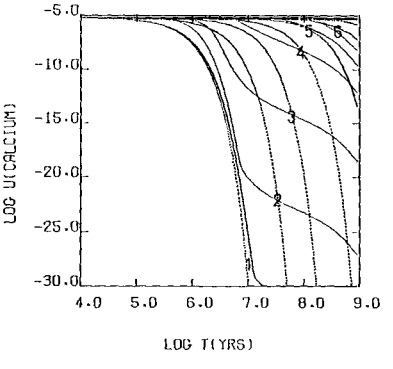

Fig. 2. Evolution of the Ca abundance at 6 depths in the envelope of the model of fig. 1. The continuous and dotted curves are respectively the numerical and exponential solutions. Curves 1 to 6 are associated to layers of $\log \Delta M/M = -6.14, -5.5, -5., -4.5, -4., -3.5$.

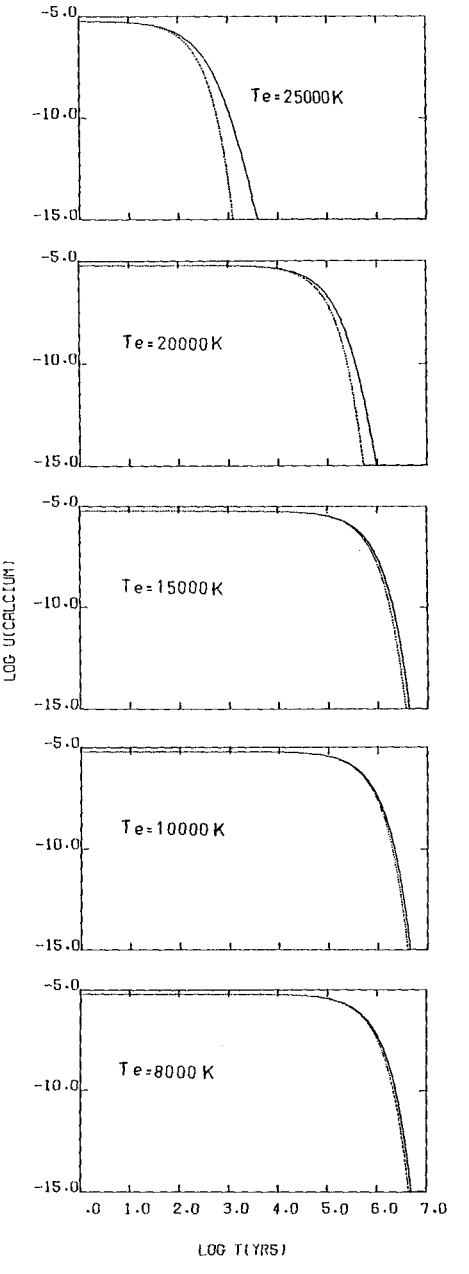

Fig. 3. Surface abundance as a function of time in He-rich white dwarfs with T_e ranging from 25,000 to 8,000 K. The continuous and dotted curves represent similar solutions as in fig. 2.

solution behaves almost exponentially as expected but with a departure from the pure exponential solution which is clearly increasing with effective temperature. This temperature-dependent departure is first explained by the fact that the diffusion time scales are smaller for the hotter models implying that local equilibrium could be reached faster. Also, the equilibrium gradient are smaller for hotter models which makes the equilibrium easier to reach. At equilibrium, the tail of the distribution goes as $u \propto q^{\beta}$ where $\beta = (1+Z_1)A_2/A_1 - Z_2 - 1$ (Pelletier *et al.* 1986). The quantity β gets smaller in hotter models since the base of the convection zone is upper in the envelope thus implying smaller ionization of both the main species (Z_1) and the trace element (Z_2) and therefore smaller equilibrium gradients.

Another unexpected result of time-dependent studies of gravitational settling is that heavy elements do not sink into the deep core of a white dwarf as could be naively expected. Instead, the heavy elements accumulate at the base of the envelope. This behavior is clearly seen in figure 1 where calcium has not been depleted for $\log q \geq -3$. This can be explained as follows: the diffusion equation can be written (Pelletier *et al.* 1986),

$$\omega_{12} = D_{12}(1+\gamma)\left[-\frac{\partial \ln C_2}{\partial r} + \left(\frac{A_1 Z_2 - A_2 Z_1}{Z_1 + \gamma Z_2}\right)\frac{m_p g}{kT} + \left(\frac{Z_2 - Z_1}{Z_1 + \gamma Z_2}\right)\frac{\partial \ln P_i}{\partial r}\right] \tag{3}$$

where the first term corresponds to ordinary diffusion and the second and third terms are responsible for gravitational settling. Deep in the envelope, the trace element can be almost completly pressure ionized and that makes the factor $(A_1 Z_2 - A_2 Z_1)$ very small. In addition, when the plasma is degenerate, the third term also becomes small since the temperature and density distribution are close to being uniform thus making the ionic pressure gradient $(\partial \ln P_i/\partial r)$ also small. The interesting consequence is to slow down and then stop settling in these layers which creates a significant accumulation of heavy elements. Such an accumulation zone could affect the conductive opacity by an increase in the number of highly ionized electron scatterers, thus slowing down the rate at which heat is flowing toward the outer layers. It remains to be seen whether or not this effect is sufficiently large to slow down significantly the cooling rates of white dwarfs. We are exploring more carefully this interesting possibility.

This research has been supported by the NSERC Canada, the fund FCAR (Québec) and a E.W.R. Steacie Fellowship to one of us (GF).

References

Alcock, C. and Illarionov, A. 1980, *Astrophys. J.*, **235**, 534.

Dupuis, J., Pelletier, C., Fontaine, G., and Wesemael, F. 1987, in *IAU Colloquium 95, The Second Conference on Faint Blue Stars*, eds. A.G.D. Philip, D.S. Hayes, and J. Liebert (Schenectady: L. Davis Press), p. 657.

Fontaine, G., and Michaud, G. 1979, *Astrophys. J.*, **231**, 826.

Paquette, C., Pelletier, C., Fontaine, G., and Michaud, G. 1986, *Astrophys. J. Suppl.*, **61**, 197.

Pelletier, C., Fontaine, G., Wesemael, F., Michaud, G., and Wegner, G. 1986, *Astrophys. J.*, **307**, 242.

Pelletier, C., Fontaine, G., and Wesemael, F. 1988, these proceedings.

Vauclair, G., Vauclair, S., and Greenstein, J. L., 1979, *Astron. Astrophys.*, **155**, 356.

THE ATMOSPHERIC COMPOSITION OF THE HOT PRE-DEGENERATE STAR H1504+65 REVISITED

S. Vennes, G. Fontaine, and F. Wesemael
Département de Physique, Université de Montréal

Nousek *et al.* (1986) have recently announced the discovery of a remarkable hot compact star, H1504+65, which *appears* to have an atmosphere devoid of hydrogen and helium. Although the object seems significantly hotter than the related PG1159 stars, its suggested atmospheric composition remains at variance with the He-rich composition inferred for the latter stars (Wesemael, Green, and Liebert 1985). Nousek *et al.* (1986) have brought forward convincing arguments against a H-dominated atmosphere in H1504+65; it seems that the object is definitely not an extremely hot DA star. On the other hand, the case against a He-rich atmosphere is much weaker and is based on the following circumstantial arguments: (1) no helium lines are detected in the spectrum of H1504+65 (the detection limit is $\approx$0.5 Å), (2) the ultraviolet continuum slope is steeper than that predicted from pure helium models *extrapolated* to effective temperatures larger than the upper limits of available grids (T_e = 200 000 K for log g=7), and (3) the *EXOSAT* observations appear to conflict with the He interpretation, although suitable models (with high effective temperatures) are not readily available in this case also. Because of the lack of appropriate models, Nousek *et al.* (1986) have been careful not to rule out completely the possibility of a He-rich atmosphere for H1504+65. In particular, they admit that He II lines could probably be undetectable if H1504+65 had an effective temperature substantially larger than T_e = 150 000 K. Nevertheless, they have found it tempting to hypothesize an atmosphere devoid of both hydrogen and helium. Coupled with the presence of weak C IV and O VI features in the spectrum of H1504+65, this has led to the suggestion that H1504+65 is actually a bare C/O nucleus (cf. Shipman 1987). Although this suggestion is interesting, it has undeservedly remained unchallenged and we have felt it appropriate to reexamine the case against a He-rich atmosphere with the help of further modelling efforts.

A detailed spectral synthesis study of a hot star such as H1504+65 presumably requires the inclusion of NLTE effects. Modelling of such objects is indeed proving to be quite a challenging task, as demonstrated by Werner, Heber, and Hunger (1988) for the case of PG1159-035. In addition, it is quite possible that the atmosphere of H1504+65 is expanding through the action of a residual wind and such an effect may have to be included as well (e.g., Kudritzki 1987). Short of these complications, one can nevertheless hope to constrain the atmospheric parameters of

H1504+65 with the help of simpler, plane-parallel, static, LTE models covering the appropriate region of parameter space. To supplement the published models used by Nousek *et al.* (1986) -specifically the pure H models of Wesemael *et al.* (1980) extending to 200 000 K, the pure He models of Wesemael (1981) extending to 200 000 K, and the solar composition models of Hummer and Mihalas (1970) for nuclei of planetary nebulae-, we have computed a small grid of unblanketed uniform models with log g=7.0 and $T_e(10^3K)$= 120,140,160, and 180. The chemical compositions which have been considered are (1) pure He, (2) He-dominated with the addition of C, N, O, and Ne in solar proportions, (3) a similar mixture with the "metal" abundances reduced by a factor of 10, and (4) a half-and-half C/O composition by number. We report here on some partial results of an ongoing analysis of H1504+65 based on these models.

Our first clue is the energy distribution slope observed in H1504+65. Nousek *et al.* (1986) report a relationship $H_\lambda \propto \lambda^{-4.1 \pm 0.1}$ in the 1250-1800 Å range and extending into the optical region. We find that *none* of our models can account for such a steep spectral index. For example, the ultraviolet spectral index of our pure He models varies between 3.72 and 3.80 in the range $120 \leq T_e(10^3K) \leq 180$. It varies between 3.72 and 3.82 in the same temperature range for the two He-rich compositions with C, N, O, and Ne absorbers. The C/O models do not fare any better than the He-dominated atmospheres and, if anything, are slightly more discrepant with a predicted spectral index varying between 3.83 and 3.76 in the same temperature interval. It is thus clear that the chemical composition does not affect strongly the ultraviolet continuum slope in the range of temperature considered. In particular, invoking an atmosphere devoid of H and He does *not* help in explaining the observed ultraviolet spectral index. Inclusion of NLTE effects may well not affect significantly the present results, as the relevant opacities in the spectral range of interest are dominated by free-free transitions. It may be necessary to consider an expanding atmosphere around H1504+65 to account for the large spectral index observed.

Another result comes from an analysis of the *EXOSAT* data with our grid of model atmospheres. H1504+65 was observed with the LE1 detector through three different filters. The observed count rates were: 6.97 ± 0.04 counts s^{-1} (thin Lexan; LX), 0.47 ± 0.02 counts s^{-1} (Al/Parylene; Al/P), and 0.017 ± 0.002 counts s^{-1} (Boron; B) (Nousek *et al.* 1986). Taking into account the known instrumental response, the predicted count rate in a given filter can be computed as a function of the interstellar neutral hydrogen column density (n_H) for a model which is normalized to the observed visual magnitude (V=16.24). For a known observed count rate, this procedure gives a unique value of n_H for a given effective temperature and, thus, leads to a curve in the $\log(n_H)$-T_e plane. More generally, the procedure gives rise to a family of curves (or band) by taking into account the measurement uncertainties. Acceptable models correspond to regions of the log n_H-T_e plane where the bands for the three different filters overlap. An additional constraint comes from the independent estimate of n_H ($0.6 \pm 0.2 \times 10^{20}$ cm^{-2}) given in Nousek *et al.* (1986)

and based on the detection of an interstellar Lyα feature in the small-aperture SWP *IUE* spectrum of H1504+65.

Figure 1 summarizes our results for the pure He models. It is seen that a consistent solution is not possible so that we can exclude these models. One of the reasons is that our high-temperature, pure He models are too bright in the EUV bandpass and, consequently, require an interstellar absorption which is too large as compared to the Lyα limit. Some atmospheric EUV absorbers are clearly needed. As shown by figure 2 (which illustrates the results for the models with the He-rich composition with C, N, O, Ne abundances at 1/10 of their solar values), the situation indeed improves significantly if such absorbers are included. We now find a marginal solution in the range $150 \leq T_e\,(10^3\mathrm{K}) \leq 160$ for the LX and Al/P filter data although the B band does not fit. A better solution is obtained if the abundances of the C, N, O, Ne absorbers are raised to their solar values. Figure 3 indeed shows that He-dominated models with $155 \leq T_e(10^3\mathrm{K}) \leq 180$ can account for the *EXOSAT* LX and Al/P filter data as well as the Lyα constraint on n_H. A virtually identical solution, suggesting a temperature range $160 \leq T_e(10^3\mathrm{K}) \leq 180$, is obtained for the C/O atmospheres. Thus, the *EXOSAT* data *cannot* discriminate between C/O atmospheres and He-rich atmospheres with solar traces of heavy elements. It should be noted that the lack of success experienced by Nousek *et al.* (1986) in their attempt at explaining the *EXOSAT* data in terms of the model atmospheres of Hummer and Mihalas (1970) is caused by the limitations of these exploratory models. Indeed, not all appropriate ionic species are included in these models (notably O VI), and expected photoionization edges are not included at wavelengths shorter than 100 Å.

We note that the B count rate appears too small for all of our model atmospheres. As an illustrative example, we find mutually consistent solutions for all data if we arbitrarily multiply the observed B count rate by a factor of 5 (see Fig. 3 and Fig. 4, in particular). It is not entirely clear at this stage why the B filter count rate remains inconsistent with the rest of the data but at least two possibilities exist. Because the B filter does not map out the same spectral range as the other filters, it is possible that other absorbers than He, C, N, O, and Ne affect significantly (and in a relative sense) the flux in this bandpass. This will have to be checked with models including a large number of absorbers. Moreover, it is possible that the B count rate has been underestimated because its point spread function has turned out to be much wider than initially estimated according to the discussion of Chiappetti and Davelaar (1984).

It is also of interest to point out that this analysis is entirely consistent (and this includes the problem with the B filter) with the independent study presented by Barstow (1988). Using his own grid of models with input physics quite similar to ours, Barstow finds that the LX and Al/P data of H1504+65 can be understood in terms of model atmospheres with log g = 7.0 and $172 \leq T_e(10^3\mathrm{K}) \leq 200$. His preferred atmospheric composition is far from extreme with H and He in a one-to-one

ratio (by number) and solar abundances of C, N, and O. This is quite similar to our own results for the He-rich models with solar abundances of C, N, O, and Ne, as H is not expected to play a major role at the temperatures of interest.

We can summarize the fundamental results of this paper in the following way: we find that we cannot discriminate between He-rich atmospheres with solar traces of heavy elements and exotic C/O atmospheres for H1504+65 on the basis of the observed ultraviolet slope and *EXOSAT* data. This weakens considerably the case against the He interpretation. Under those circumstances, we favor the simplest interpretation, i.e. that of a He-rich atmosphere for H1504+65. It remains to be shown that *He II lines indeed fade below the detection level of* ≈ 0.5 Å in the range $155 \leq T_e(10^3 K) \leq 180$, our best estimate of the effective temperature of H1504+65. In addition, the observed line strengths of the few C IV and O VI features in the spectrum of H1504+65 must remain consistent with the predictions of He-rich model atmospheres with traces of C and O. We are currently considering these particular questions. Ultimately, a full NLTE calculation, possibly coupled to an expanding atmosphere, may be required to understand completely this extraordinary object.

This research has been supported in part by the NSERC Canada, by the fund FCAR (Québec), and by a E.W.R Steacie Fellowship to one of us (GF).

Barstow, M.A. 1988, these Proceedings.
Chiappetti, L., Davelaar, J. 1984, *EXOSAT EXPRESS* no. 8.
Hummer, D.G., and Mihalas, D. 1970, *Mon.Not.Roy.Astron.Soc.*, **147**, 339.
Kudritzski, R. 1987, in *IAU Colloquium 95, The Second Conference on Faint Blue Stars*, eds. A.G.D. Philip, D.S. Hayes, and J. Liebert (Schenectady: L.Davis Press), p.177.
Nousek, J.A., Shipman, H.L., Holberg, J.B., Liebert, J., Pravdo, S.H., White, N.E., and Giommi, P. 1986, *Astrophys.J.*, **309**, 230.
Shipman, H.L. 1987, in *IAU Colloquium 95, The Second Conference on Faint Blue Stars*, eds. A.G.D. Philip, D.S. Hayes, and J. Liebert (Schenectady: L.Davis Press), p.273.
Werner, K., Heber, U., and Hunger, K. 1988, these Proceedings.
Wesemael, F. 1981, *Astrophys.J.Suppl.*, **45**, 177.
Wesemael, F., Auer, L.H., Van Horn, H.M., Savedoff, M.P. 1980, *Astrophys.J.Suppl.*, **43**, 159.
Wesemael, F., Green, R.F., and Liebert, J. 1985, *Astrophys.J.Suppl.*, **58**, 379.

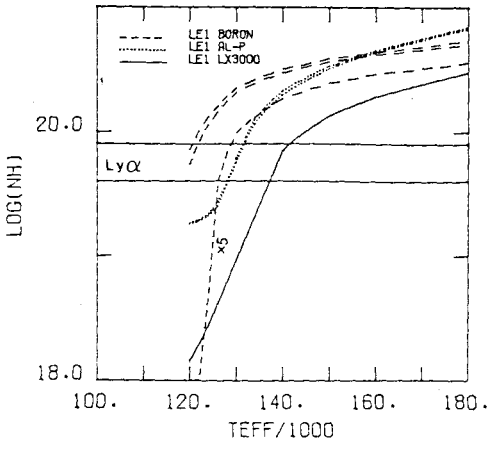

Figure 1. Relationship between the interstellar neutral hydrogen column density and effective temperature for pure He models of H1504+65 with log g=7.0. The continuous, dotted, and dashed lines correspond to family of curves consistent with the observed EXOSAT count rates in the LX, AI/P, and B filters, respectively. The lower dashed curve labeled "X 5" corresponds to a B count rate arbitrarily multiplied by a factor of 5. The two horizontal lines define the region where n_H is constrained through Lya observations.

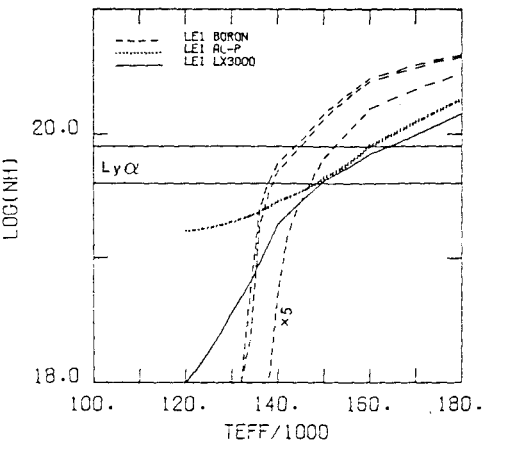

Figure 2. Same as Fig. 1, but for He-rich atmospheres with traces of C, N, O, and Ne at 1/10 solar values.

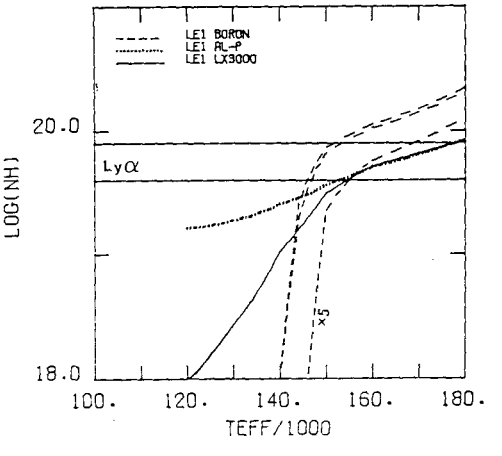

Figure 3. Same as Fig. 1, but for He-rich atmospheres with solar abundances of C, N, O, and Ne.

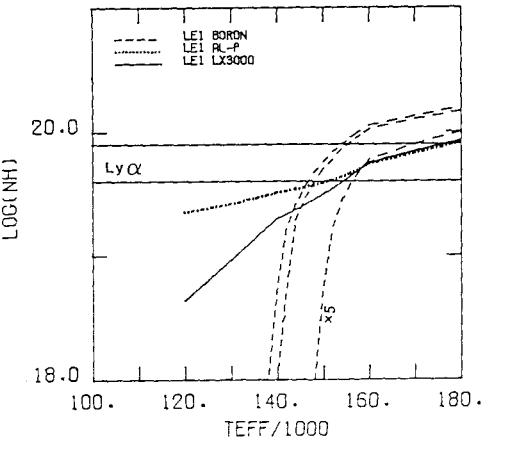

Figure 4. Same as Fig. 1, but for C/O atmospheres. C and O are in equal proportions by number.

STRATIFIED MODEL ATMOSPHERES FOR HOT DA WHITE DWARFS

S. Vennes, G. Fontaine, and F. Wesemael
Département de Physique, Université de Montréal

Observations of hot DA white dwarfs in the EUV/soft X-ray range have revealed that, in a majority of cases, the detected flux is less than that expected from pure hydrogen atmospheres. This implies an extra opacity source which must be due to the presence of small traces of heavier elements. These elements are generally not spectroscopically detected in hot DA white dwarfs, but the large sensitivity of the EUV/soft X-ray broad-band flux to the presence of extra absorbers can be used with profit to *infer* their abundances. For simplicity, it has been assumed that *only* helium provides the required opacity source in the majority of the analyses carried out so far. In this context, Vennes *et al.* (1988a) have recently reviewed in details the mechanisms that could be responsible for the presence of small traces of helium in the atmospheres of hot DA white dwarfs. They favor a model in which these stars are interpreted as stratified objects with an outer layer of hydrogen which is sufficiently thick that radiation in the visible escapes only from H-rich regions, and yet sufficiently thin that the EUV/soft X-ray radiation escapes from deeper layers, polluted by the tail of the helium distribution which extends upwards. This model accounts naturally for the positive correlation observed between the inferred helium abundance and the effective temperature in hot DA stars studied at short wavelengths. If the model is correct, hot DA white dwarfs as a class must have very thin outer hydrogen layers with estimated masses in the range $-13 \geq \log q(H) \equiv \log (M(H)/M) \geq -15$.

In order to follow up on the work of Vennes *et al.* (1988a), it is necessary to compute stratified model atmospheres for detailed analyses of individual stars. Our aim is to take advantage of the homogeneous *EXOSAT* photometric measurements of several hot DA white dwarfs (Paerels 1987), and ultimately derive the values of log q(H) for these stars. Our model atmospheres consist of a pure H layer on top of a pure He layer in diffusive equilibrium. These models are similar to those of Jordan and Koester (1986) in the treatment of the

composition transition layer, but extend to larger values of log q(H) as suggested by the work of Vennes *et al.* (1988a). Cruder stratified models based on discontinuous composition interfaces have already been discussed by Heise and Huizenga (1980) and Muchmore (1982). The present models assume LTE and are hydrogen line-blanketed. The current grid is for log g=8.0 and effective temperatures $T_e(10^3$ K)=25, 30, 40, 50, and 60. For each effective temperature, models are computed with hydrogen layer masses log q(H) = -15.5, -15.0, -14.5, -14.0, -13.5, and -13.0. Models with $T_e(10^3$ K)=25 and 30 and log q(H)< -14.5 were found to be convectively unstable in the composition transition zone and were therefore rejected as the presence of convection is inconsistent with the assumption of diffusive equilibrium. For comparison purposes, we have also computed another grid of models using the same physics but, this time, for homogeneous chemical compositions with He/H ratios in the range 10^{-10} to 10^{-2}. Details on these uniform models as well as the stratified models can be found in Vennes (1988).

We have used our grid of stratified model atmospheres to derive preliminary values of log q(H) for the sample of 15 hot DA white dwarfs observed with the *EXOSAT LE* filters (Paerels 1987). If an extra EUV opacity source is required, the procedure implicitly assumes that it is due to helium alone. The method is currently limited by the availability of models with only one value of the gravity (log g=8.0). According to Vennes *et al.* (1988a), scatter in gravity is likely to play an important role in the interpretation of short wavelength observations of hot DA stars. In the present experiment, we have used the best estimate of the effective temperature of a given object as available in the literature, and have sought a consistent solution for all filter measurements in the q(H)-n(H) plane (where n(H) is the interstellar neutral hydrogen column density). Self-consistent solutions were obtained for the vast majority of our sample stars. The most outstanding exception is HZ 43 for which no acceptable solution has been found. This is likely to be caused by its significantly larger than average gravity. Our results are summarized in Figure 1 which shows a plot of the inferred hydrogen layer mass log q(H) as a function of the effective temperature. Our procedure has led to the inference of two upper limits, four lower limits, and eight values of log q(H) in the *EXOSAT* sample of hot DA stars. The inferred values are in the range $-13 \geq \log q(H) \geq -15$ in agreement with the estimates of Vennes *et al.* (1988a), and show that hot DA white dwarfs must indeed have very thin outer hydrogen layers if helium absorption is responsible for the extra EUV opacity required by most of the observations. We note that our estimates of log q(H) are consistent with those of Koester (1988) who has recently performed an analysis similar to ours for 11 of the 15 objects in the *EXOSAT* sample (we express the hydrogen layer mass in terms of a

fraction of the stellar mass of a 0.6 $M_\odot$ object, whereas Koester expresses log q(H) in terms of a fraction of the solar mass). In agreement with Koester (1988), we point out to a possible weak trend between log q(H) and T_e; the hotter stars appear to have smaller values of q(H).

Before further conclusions can be drawn as to the properties of layered models of hot DA stars, it is appropriate to recall that the short wavelength *photometric* measurements do not permit to discriminate between helium and other potential absorbers. Fortunately, however, H/He layered model atmospheres leave spectral signatures which are quite characteristic. This is particularly true in the EUV range where the flux is very sensitive to the presence of small traces of helium as indicated previously. As an illustrative example, Figure 2a shows synthetic EUV spectra for uniform models with various He/H ratios, and log(g) = 8.0 and T_e = 60 000 K. Profiles for the He II Lyman series are computed following Auer and Mihalas (1972) and the spectrum is convolved with a gaussian of FWHM=6 Å, representative of the *EXOSAT* resolution. Note that the curves are displaced vertically for clarity. By contrast, Figure 2b shows the synthetic EUV spectra of stratified models with log q(H) = -15.0, -14.5, -14.0, and -13.5, respectively. The gravity and the effective temperature are the same as for the uniform models. A comparison of the two figures clearly shows that the continuum shortward of the 228 Å edge behaves quite differently in the two cases. Likewise, the line profiles are different; they are obviously broader in the layered models because the lines are formed deeper into the photosphere. Our own experience with theoretical count rate spectra of *EXOSAT* indicates that EUV spectroscopy can distinguish between layered and uniform atmospheres in DA white dwarfs. Currently, such data exist for only three DA white dwarfs: Sirius B (Paerels *et al.* 1988) and HZ 43 (Heise *et al.* 1988) which appear to have pure hydrogen atmospheres (corresponding to lower limits on log q(H)), and Feige 24 (Vennes *et al.* 1988b) which is better explained in terms of a H-rich atmosphere polluted by a host of heavier elements presumably supported by radiative levitation. Thus, the jury is still out on the existence of layered DA atmospheres with very thin hydrogen layers. The DAO stars, particularly the interesting object PG 1210+533 discussed by Holberg *et al.* (1987) could well represent the most promising tests of the stratified model. Future experiments, such as *EUVE* and *ROSAT* may provide definitive answers to these questions.

This research has been supported in part by the NSERC Canada, by the fund FCAR (Québec), and by a E.W.R Steacie Memorial Fellowship to one of us (GF).

Auer, L.H., and Mihalas, D. 1972, *Astrophys. J. (Suppl.)*, **24**, 193.
Heise, J., and Huizenga, H. 1980, *Astron. Astrophys.*, **84**, 280.

Heise, J., Paerels, F.B.S., Bleeker, J.A.M., and Brikman, A.C. 1988, *Astrophys. J.*

Holberg, J.B., Sion, E.M., Liebert, J., and Vauclair, G. 1987, *Bull. Amer. Astron. Soc.*, **19**, 1041.

Jordan, S., and Koester, D. 1986, *Astron. Astrophys.(Suppl.)*, **65**, 367.

Koester, D. 1988, these Proceedings.

Muchmore, D. 1982, *Astrophys.J.*, **259**, 749.

Paerels, F.B.S. 1987, Ph.D. thesis, University of Utrecht.

Paerels, F.B.S., Bleeker, J.A.M., Brinkman, A.C., and Heise, J. 1988, *Astrophys.J.*, **329**, 849.

Vennes, S. 1988, Ph.D. thesis, Université de Montréal.

Vennes, S., Pelletier, C., Fontaine, G., and Wesemael, F. 1988a, *Astrophy.J.*, **331**, 876.

Vennes, S., Chayer, P., Fontaine, G., and Wesemael, F. 1988b, these Proceedings.

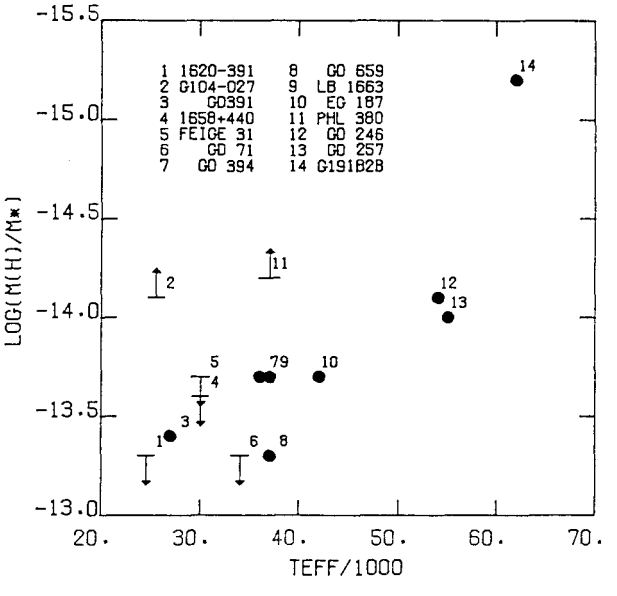

Figure 1. Relationship between the inferred hydrogen layer mass log q(H) and the effective temperature for 14 hot DA stars observed photometrically with *EXOSAT*.

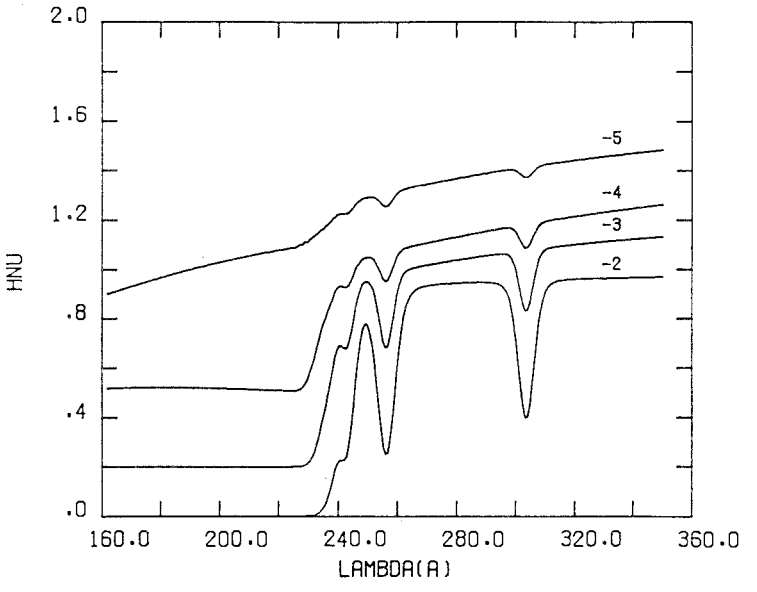

Figure 2a. Synthetic EUV spectrum of homogeneous model atmospheres with log He/H = -5, -4, -3, and -2 from top to bottom, respectively. The models have log g = 8.0 and T_e = 60 000 K.

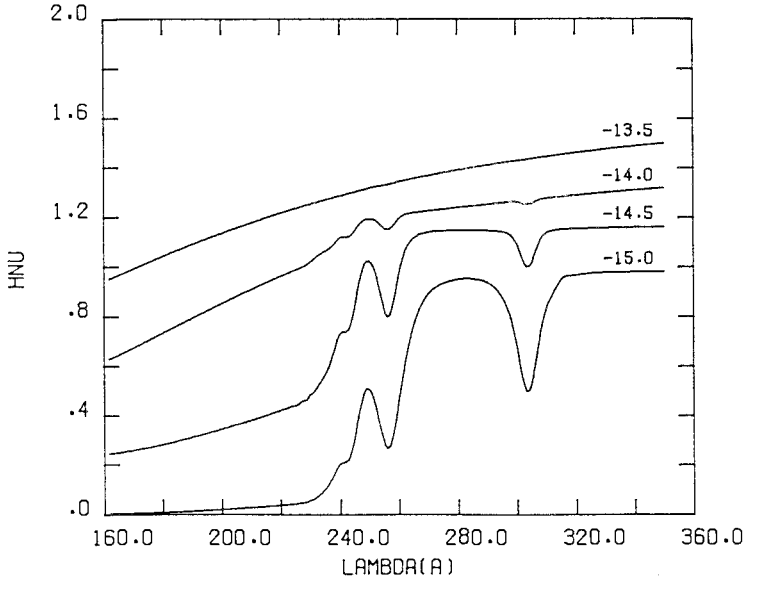

Figure 2b. Similar to Fig. 2a, but for stratified models with log q(H) = -13.5, -14.0, -14.5, and -15.0, from top to bottom, respectively.

AN EXPLANATION FOR THE EUV SPECTRUM OF FEIGE 24

S. Vennes, P. Chayer, G. Fontaine, and F. Wesemael
Département de Physique, Université de Montréal

Feige 24 is a bright DA white dwarf which has been studied extensively both from ground-based and space-borne observatories. The best determination of its fundamental atmospheric parameters are that of Holberg, Wesemael, and Basile (1986) who have used detailed model atmosphere analyses in conjunction with optical, *IUE*, and *Voyager* data. They give log g = 7.23±0.35 and $T_e(10^3K)$=55±5. The question of the atmospheric composition is more involved as small traces of heavy elements would not be observable in the optical spectrum of such a hot, hydrogen-dominated atmosphere. If it were isolated, Feige 24 would presumably only show the usual bland optical spectrum of a typical DA white dwarf, i.e. the hydrogen Balmer line series, but the presence of a M dwarf companion complicates its spectrum. On the other hand, Feige 24 belongs to a handful of hot DA white dwarfs sufficiently bright that ultraviolet spectroscopy in the high resolution mode of the *IUE* has been possible. Following the theoretical expectation of Vauclair, Vauclair, and Greenstein (1979), it was discovered that the photosphere of Feige 24 contains small amounts of C, N, and Si (Dupree and Raymond 1982). Spectral synthesis techniques used by Wesemael, Henry, and Shipman (1984) indicate the following abundances: log(C/H)=-6.4±0.6, log(N/H)=-5.3±1.0, and log(Si/H)=-6.3±0.9. The most plausible explanation to account for these small abundances is the influence of selective radiative forces possibly coupled to a weak wind (Chayer *et al.* 1987).

Further interest in Feige 24 was generated by the publication of the exciting *EXOSAT* observations of that star (Paerels *et al.* 1986). Feige 24 was already known to be a strong EUV source (Margon *et al.* 1976), but *EXOSAT* revealed for the first time an unexpected spectrum in that wavelength range. Indeed, the observed EUV spectrum of Feige 24 has, until now, defied any explanation. It consists of an essentially featureless continuum which shows a maximun around 250 Å and which can be nominally fitted with a black body energy distribution with T=31,000K, assuming an interstellar neutral hydrogen column density of n_H=1.2X10^{19}cm2 (Paerels *et al.* 1986). These authors have ruled out (1) a pure hydrogen spectrum, (2) a spectrum for a hydrogen atmosphere containing uniform traces of helium, and (3) a spectrum for a hydrogen atmosphere containing the small traces of C, N, and Si at the levels determined by Wesemael, Henry, and Shipman (1984). Paerels *et al.* (1986) concluded by pointing out to the need for more sophisticated model atmospheres including, in particular, chemical stratification.

As a natural follow-up to our recent detailed investigation of mechanisms that could account for the purported presence of helium in the photospheres of hot DA stars (Vennes *et al.* 1988), we have computed a grid of stratified model atmospheres consisting of a layer of pure H sitting on top of a layer of pure He in diffusive equilibrium (Vennes, Fontaine, and Wesemael 1988). The question that arises is whether or not such a stratification could account for the EUV spectrum of Feige 24. The basic idea here is that the hydrogen layer must be sufficiently thick that a pure hydrogen spectrum is formed in the optical region, and, yet, sufficiently thin that the EUV flux escaping from deeper layers is regulated by the opacity of helium in these regions. Our calculations show that the EUV spectrum of Feige 24 cannot be explained in terms of a H/He stratified atmosphere.

Fig. 1 shows the count rate spectrum of Feige 24 as observed with *EXOSAT* (crosses). In a manner very similar to Fig. 2a of Paerels *et al.* (1986), we show the predictions of hydrogen model atmospheres with uniform traces of helium (He/H = 10^{-4} and 10^{-5}, respectively). These illustrative models have log g=8.0, T_e=50,000K, and a value of n_H=3.5X10^{18} is assumed. The continuum lines correspond to theoretical convolved spectra taking into account the response of the spectrometer and its effective area, and degraded by a typical FWHM resolution of 6 Å. Fig. 1 shows clearly why Paerels *et al.* (1986) rejected hydrogen models with uniform traces of helium for Feige 24.

By comparison, Fig. 2 illustrates the predictions of layered model atmospheres having the same basic parameters as those shown in Fig. 1. Two models are shown, one with a hydrogen layer so thick (log $\Delta M(H)/M$ = −14) that the EUV spectrum is practically the same as that of a pure H model, and one with a thinner hydrogen layer (log $\Delta M(H)/M$ = −15) which allows helium to pollute the EUV photosphere and reduce considerably the flux at short wavelengths. Note that spectroscopy can easily distinguish between a layered and a uniform H/He atmosphere. However, the layered atmosphere hypothesis must be rejected for Feige 24 for fundamentally the same reason as for uniform models: if helium is to be sufficiently abundant to quench the short-wavelength flux, it also leaves an obvious signature, namely an absorption edge at 228 Å which is not observed in this particular star.

This result has prompted us to consider an alternate possibility which we have alluded to in Vennes *et al.* (1988). It has been recognized at the outset by the various workers in the field that the required soft X-ray/EUV opacity source needed to explain the observations of hot DA stars may not be totally provided by helium but also, in large part, by heavier elements. It was for reasons of simplicity that helium became the favorite absorber. In the case of Feige 24, the known presence of C, N, and Si has remained suggestive even though Paerels *et al.* (1986) concluded that models with traces of these elements could not explain the observations. This is because the *IUE* window can only reveal a relatively small number a metallic resonance lines, and the detection of only C, N, and Si in the *IUE* spectrum of Feige 24 cannot be interpreted as a lack of other elements. Quite the contrary, if

small abundances of C, N, and Si are (presumably) supported by radiative levitation, we expect that a host of other elements can be supported too. Thus, we envision a situation in which many different metals with low abundances are present in the atmosphere of Feige 24. These metals would lead to a large number of small absorption edges which are smoothed over because of the finite resolution of *EXOSAT* (~6 Å), and whose cumulative effect is to quench the short-wavelength flux.

As an illustrative example, we have computed the synthetic EUV spectrum of a model of Feige 24 with log g = 7.23 and T_e = 55,000K. The model is H-dominated with small uniform traces of 10 elements: He, C, N, O, Ne, Na, Si, S, Ar, and Ca. These particular elements were chosen for the presence of photoionization edges in the 190-350 Å *EXOSAT* range and for the absence of resonance lines (except for C, N, and Si) in the 1200-3000 Å *IUE* range at the effective temperature of interest. It is important to note that the abundances that were chosen are entirely consistent with the abundances which we have computed for each element from radiative support theory. Some adjustments of individual abundances have been made, but this does not change the central result of our experiment.

Fig. 3 contrasts the predicted spectrum (continuous line) with the observed EUV count rate spectrum of Feige 24. Our synthetic spectrum is normalized to the visual magnitude of the object (V=12.56), so that the result presented in Fig. 3 is an absolute fit, not a simple fit to the shape of the EUV spectrum. The agreement is gratifying. Of course, we cannot pretend that there exists a unique fit; our choice of absorbers is somewhat arbitrary and other possibilities exist. We have left out a potentially great number of absorbers, and a detailed comparison at the level of small residual features in the theoretical curve cannot realistically be made. In fact, the prospect for such a comparison remains unlikely until we understand in details what governs the relative and absolute abundances of trace species in the atmospheres of hot white dwarfs. We know that the predictions of simple radiative support theory -which assumes a perfect equilibrium between gravitational settling and radiative levitation- are not consistent with the observations. It is thought that weak winds play havoc with the abundances of metals supported by radiation in hot white dwarfs (Chayer, Fontaine, Wesemael 1988). Until we have a decent theory of these phenomena, we must remain satisfied with the qualitative picture described here. We strongly believe, however, that the basic idea is correct: the EUV spectrum of Feige 24 can simply be explained by the cumulative effects of a host of trace absorbers in a hydrogen atmosphere.

If this idea is indeed correct, then it raises a number of interesting questions concerning the interpretation of EUV/soft X-ray data in terms of layered atmospheres. In particular, is Feige 24 an exception or a typical DA white dwarf? A qualitative comparison between the DA stars observed in the EUV range as discussed by Vennes *et al.* (1988) and the sample of DA objects in the high resolution *IUE* mode by Bruhweiler and Kondo (Bruhweiler 1985) is of interest here. We find, from the limited information available, that seven objects out of seven which require a

EUV opacity source also show some metallic features in their *IUE* spectra. Are these all similar to Feige 24 in the sense that their EUV fluxes are regulated by a cumulative metallic opacity? In that case, there would no need to invoke thin hydrogen layers for those stars. We find this possibility rather suggestive, but we cannot be certain because, except for Feige 24, we do not know the abundances of the elements detected with the *IUE*. This is underscored by the puzzling fact that we also find three objects in the EUV sample which do not require a EUV opacity source (i.e. they emit like pure hydrogen models), and, yet, also show metallic features in their *IUE* spectra. At the very least, this suggests that the abundances of the metals detected must be very small in order not to quench significantly the EUV flux. Thus, the presence of metals in the *IUE* spectra of a DA star does not necessarily eliminate the need for H/He layered atmospheres.

In that context, it should be remembered that the case for layered atmospheres is very strong for the DAO stars which are hot progenitors of ordinary DA stars. Vennes *et al.* (1988) find that this model is the only viable one for that type of objects. As evolution proceeds, DAO stars cool to become ordinary DA stars and, therefore, must retain their layered configurations. The observations of the DAO object PG 1210+533 by Holberg *et al.* (1988) reinforce strongly the conclusion of Vennes *et al.* (1988). Thus, it may very well be the case that the effects of both H/He stratification and metallic absorption regulate the EUV flux of hot DA white dwarfs. The opacity could be dominated in some stars (such as Feige 24) by metallic absorption, in other stars by H/He stratification (in cases where a wind has expelled the heavy elements from the star for example), and in other cases by both mechanisms. Before the question is definitely settled, we will have to await the results of future experiments which should provide the definitive test. The available *Einstein* and *EXOSAT* photometric observations can currently be understood either within the framework of H/He layered atmospheres or within the framework of metallic absorbers. The answer lies with EUV spectroscopy, since uniform models, stratified models, and models with metals have quite different spectral signatures.

This research has been supported in part by the NSERC Canada, by the fund FCAR (Québec), and a E.W.R. Steacie Memorial Fellowship to one of us (GF).

Bruhweiler, F.C. 1985, *Bull. Amer. Astron. Soc.*, **17**, 559.
Chayer, P., Fontaine, G., Wesemael, F. and Michaud, G. 1987, in *IAU Colloquium No. 95, The Second Conference on Faint Blue Stars*, A. G. D. Philip, D. S. Hayes and J. Liebert, eds., L. Davis Press, Schenectady, p. 653.
Chayer, P., Fontaine, G., and Wesemael, F. 1988, these proceedings.
Dupree, A.K., and Raymond, J.C. 1982, *Astrophys. J. Letters*, **263**, L63.
Holberg, J.B., Wesemael, F., and Basile, J. 1986, *Astrophys. J.*, **306**, 629.
Holberg, J.B., Sion, E.M., Liebert, J., and Vauclair, G. 1987 *Bull. Amer. Astron. Soc.*, **19**, 1041.
Margon, B., Lampton, M., Bowyer, S., Stern, R., and Paresce, J. 1986 *Astrophys. J.*

Letters, **210**, L79.
Paerels, F.B.S., Bleeker, J.A.M., Brinkman, A.C., and Heise, J. 1986 *Astrophys. J. Letters*, **309**, L33.
Vauclair, G., Vauclair, S., and Greenstein, J.L. 1979, *Astron. Astrophys.*, **80**, 79.
Vennes, S., Pelletier, C., Fontaine, G., and Wesemael, F. 1988, *Astrophys. J.*, in press.
Vennes, S., Fontaine, G., and Wesemael, F. 1988, these proceedings.
Wesemael, F., Henry, R.B.C., and Shipman, H.L., 1984, *Astrophys. J.*, **287**, 868.

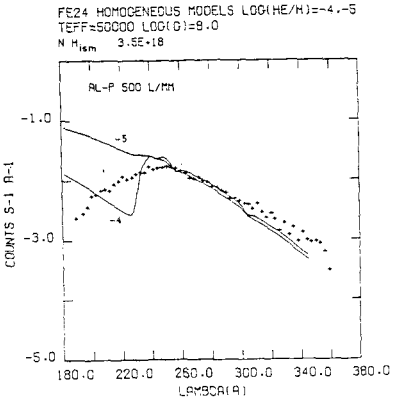

Figure 1. Synthetic spectra of homogeneously mixed H-He atmospheres convolved with the spectrometer response and compared with the measured spectrum (crosses).

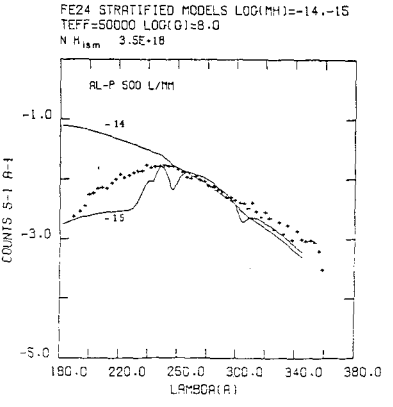

Figure 2. Same as figure 1 but for stratified H-He atmospheres.

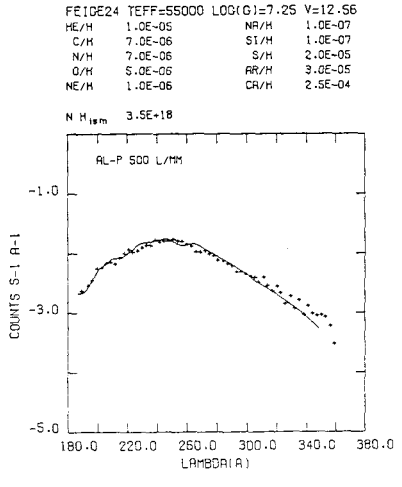

Figure 3. Synthetic spectrum in the EUV range with uniform light metal traces. The listed abundances are relative to hydrogen by number.

GRAVITATIONAL REDSHIFTS FOR HYADES WHITE DWARFS*

G. Wegner
Department of Physics & Astronomy, Dartmouth College

I. N. Reid
California Institute of Technology

R. K. McMahan
Harvard-Smithsonian Center for Astrophysics

I. INTRODUCTION

Precise white dwarf gravitational redshifts can only be obtained utilizing systems of known distance and space velocity. Binaries with known orbits such as 40 Eri B are rare, and although common proper motion pairs have proven highly useful(Wegner 1973; Koester 1987; Wegner & Reid 1987), there are some problems in their interpretation. Another approach is to employ white dwarfs in open clusters; they not only have known systemic velocities, but also provide information on the progenitors of the white dwarfs. Of the nearby galactic clusters, the Hyades currently give the best information for achieving accurate gravitational redshifts; the members are relatively bright and nearby and their kinematics are well known.

Nevertheless until now, the velocities of the Hyades white dwarfs have never been systematically studied at high enough resolution using modern instruments. Earlier photographic data have been reported by Greenstein & Trimble (1967), Trimble & Greenstein (1972) in their pioneering work on gravitational redshifts and Greenstein *et al.* (1977) have published a few high resolution measures but as their investigation was never intended to specifically study the Hyades, it does not contain many observations.

Several studies of the Hyades provide white dwarf suspects (Luyten 1971, van Altena 1969). Here, we limit our list to six objects given by van Altena (1969) as high probability DA Hyades and add the DBA star which is also a likely Hyad (Greenstein 1974).

*Some of the spectroscopic observations were obtained at the Multiple Mirror Telescope Observatory, a joint facility of the University of Arizona and the Smithsonian Institution.

II. OBSERVATIONS

It is well known (Greenstein & Peterson 1974, Greenstein *et al.* 1977; Wegner 1980) that the Balmer lines, particularly Hα and to somewhat less extent Hβ, have sharp cores at high resolution suitable for obtaining accurate velocities and rotations for the white dwarfs. Grabowski, Madej & Halenka (1987) have also shown how pressure shifts are unimportant in these cores. For this purpose, observations of the Hyades white dwarfs were secured during 1987-1988 using the Hale 200-inch telescope at Mount Palomar and the Multiple Mirror Telescope (MMT) on Mount Hopkins. In addition some data taken with the McGraw-Hill 1.3 m telescope in 1984-1986 were also included with lower weight.

The observations with the 200-inch telescope were made using the double spectrograph employing a dichroic beam splitter and two Texas Instruments CCD detectors. The slit width was 2" and with 600 lines/mm gratings, this yielded simultaneous acquisition of Hα and Hβ at resolutions of 1.1 Å. The Palomar spectra were reduced independantly by GW and INR using the IRAF and FIGARO reduction programs respectively, the core positions estimated by eye, and the resulting velocities averaged.

The MMT spectra were secured using the 'Big Blue' spectrograph with an echellette grating in the 8th order, yielding resolution of about 0.7 Å at Hα. Data reductions were made at the CfA and velocities again measured by eye.

The spectra at Hβ obtained with the Mark II spectrograph and a Reticon detector on the 1.3 m telescope at Kitt Peak had about 2 Å resolution. This instrument is described further in Wegner & McMahan (1985).

Nightly velocity standards were observed from which instrumental zero point corrections were obtained and comparison spectra were taken before and after each stellar spectrum. Usually Hyades stars with accurately measured radial velocities in Table I of Hanson & Vasilevskis (1983) were employed as the standards.

TABLE I

Measurements of Heliocentric Velocities for Hyades White

Name	EG	V(km/sec)	Weight
HZ 4	26	+70.1 ± 3.8	6.3
LB 227	29	+86.8 ± 4.5	6.0
VR 7	36	+76.0 ± 3.4	8.2
VR 16	37	+71.2 ± 2.5	8.1
HZ 7	39	+78.0 ± 7.3	7.3
HZ 14	42	+63.9 ± 6.4	7.3
LP475-242	316	+95.3 ± 4.0	2.0

In combining spectra from different instruments, a weighting scheme was used. The MMT and Palomar Hα measures were weighted equally, for it appears that the greater dispersion of the former compensates the higher signal-to-noise ratio of the latter. Consequently, for a given night, the Palomar velocities have twice the weight of the MMT data as both Hα and Hβ were usually observed with the double spectrograph. The McGraw-Hill 1.3 m data were weighted 0.1 for each night's observation.

The resulting heliocentric velocities measured for high probability Hyades are given in Table I. For the DBA, the velocity was obtained from the well defined Hα line and is unaffected by the pressure shift problems of helium.

III. COMPARISON WITH THE MASS-RADIUS RELATION

In order to obtain gravitational redshifts for the stars in Table I, three quantities are needed: (1) the convergent point, (2) the Hyades distance modulus, (3) knowledge of the three dimensional structure of the Hyades and where the white dwarfs happen to fall in it. For the present discussion, we have used the convergent point of Gunn *et al.* (1988) *viz.*, $A = 98.2 \pm 1.1$ deg., $D = +6.1 \pm 1.0$ deg., and velocity $S = 48.0 \pm 0.27$ km/sec. The much debated Hyades distance modulus was taken to be 3.25 mag. from Hanson's (1980) discussion of trigonometric values and keeping in mind recent results *e.g.* of Stefanik and Latham (1985), Cameron (1985) and Peterson & Solensky (1987).

TABLE II

Radii and Gravitational Redshifts for Hyades White Dwarfs

Name	$T_{eff}(^{o}K)$	$\log R/R_{\odot}$	$S\cos\lambda$	V_{RS}	$M/M_{\odot}(^{12}C)$
HZ 4	14362	-1.85	36.8	33.3	0.62
LB 227	15467	-2.06	38.1	48.7	0.78
VR 7	19435	-1.92	39.9	36.1	0.66
VR 16	23436	-1.94	40.3	30.9	0.60
HZ 7	21239	-1.93	41.3	35.6	0.65
HZ 14	27824	-1.96	42.1	21.8	0.47
LP475242	16545	-2.03	41.8	53.5	0.81

Effective temperatures, T_{eff}, for the Hyades DAs can be found in McMahan (1986) and Koester, Schulz & Weidemann (1979); the radii were computed using the average of these T_{eff} and photometric data tabulated in McCook & Sion (1987). For the DB, T_{eff} was taken to be the average of Wegner & Nelan (1987) and Oke, Weidemann & Koester (1984). Table II gives the adopted T_{eff} and radii

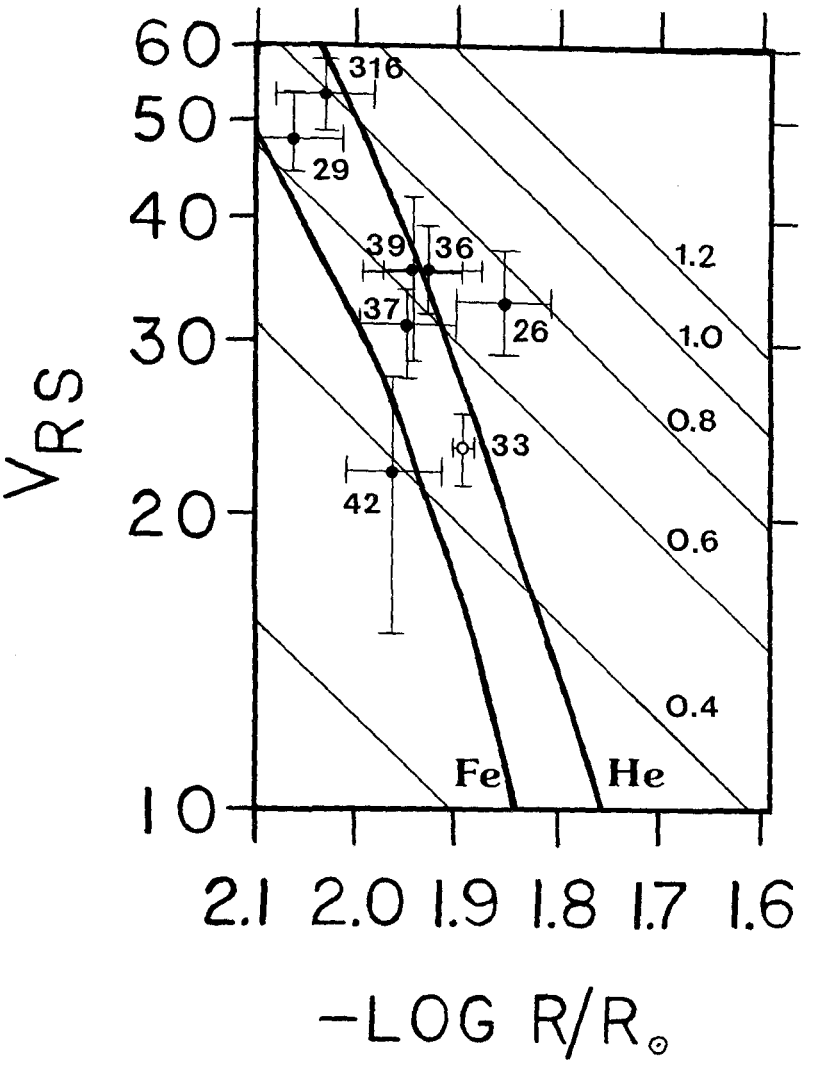

FIG. 1. *Comparison between the observed redshifts and radii of the Hyades white dwarfs in Tables I and II and the theoretical predictions of the Hamada & Salpeter (1961) Fe^{56} and He^4 mass-radius relations. The expected C and O compositions lie between these two. The the thin lines running down from left to right are loci of the constant mass labled in solar units. The open circle denotes the position of 40 Eri B from Wegner (1980).*

along with predicted radial components of cluster motion and the final gravitational redshifts. See the above references for a discussion of the errors.

The V_{RS} are shown as a function of $\log R/R_\odot$ in Figure 1. Also plotted are lines of constant mass and loci corresponding to the helium and iron Hamada & Salpeter (1961) mass-radius relations which bracket the expected values for CO. The measured Hyades redshifts appear to confirm the mass-radius relation's shape well but in detail HZ4 appears to be either higher than expected or the radius observed is too large. Possible ways to fix this include correcting the star's distance modulus or modifications to the mass-radius relation, but as Koester & Schönberner (1986) have shown, a non-zero temperature with a small addition of hydrogen should not appreciably modify the radius at this Teff. Another possibility is that HZ 4 is a binary like L870-2.

The mean mass of the Hyades white dwarfs from our redshifts appears to be $0.66 \pm 0.05\ M_\odot$ on the assumption of a carbon mass-radius relation. This is significantly above the $0.58\ M_\odot$ found for the DAs in field common proper motion pairs (Koester 1987; Wegner & Reid 1987) and elsewhere. As shown, *e.g.*, by Weidemann & Koester (1983), this gives information on the relation between the initial and final mass for a star evolving to the white dwarfs state and the associated mass-loss mechanisms.

IV. CONCLUSIONS

The new gravitational redshifts for the Hyades white dwarfs appear to confirm the shape of the mass-radius relation. They also show that the mean mass for the Hyades white dwarfs is measureably higher than for the field white dwarfs. In future work we plan to use our data to refine the temperature scale and distances and to determine the rotation rates for the these stars.

This work was partially supported by the National Science Foundation through Grant AST85-15219.

REFERENCES

Cameron, L. M. 1985, *Astron. & Astrophys.*, **152**, 250.
Grabowski, B., Madej, J. & Halenka, J. 1987, *Astrophys. J.*, **313**, 750.
Greenstein, J. L. 1974, *Astrophys. J. (Letters)*, **189**, L131.
Greenstein, J. L., Boksenberg, A. Carswell, R., & Shortridge, K. 1977, *Astrophys. J.*, **212**, 186.
Greenstein, J. L. and Peterson, D. M. 1973, *Astron. & Astrophys.*, **25**, 29.
Greenstein, J. L. and Trimble, V. L. 1967, *Astrophys. J.*, **149**, 283.
Hamada, T. & Salpeter, E. E. 1961, *Astrophys. J.*, **134**, 683.

Hanson, R. 1980, in *Star Clusters*, IAU Colloq. No. 85, J. E. Hesser, ed., (Dordrecht: Reidel), p.71.
Hanson, R. & Vasilevskis, S. 1983, *Astron. J.*, **88**, 844.
Luyten, W. J. 1971, *The Hyades*, (Minneapolis: Univ. Minnesota).
Koester, D. 1987, *Astrophys. J.*, **322**, 852.
Koester, D. & Schönberner, D. 1986, *Astron. & Astrophys.*, **154**, 125.
McCook, G. P. & Sion, E. P. 1987, *Astrophys. J. Suppl.*, **65**, 603.
McMahan, R. K. 1986, Ph.D. Thesis, Dartmouth College.
Oke, J. B., Weidemann, V. & Koester, D. 1984, *Astrophys. J.*, **281**, 276.
Peterson, D. M. & Smolensky, R. 1987, *Astrophys. J.*, **315**, 286.
Stefanik, R. P. and Latham, D. W. 1985, in *Stellar Radial Velocities*, Proc. IAU Colloq. No. 88, A. G. D. Philip and D. W. Latham, eds., (Schenectady: L. Davis Press), p.213.
Trimble V. & Greenstein, J. L. 1972, *Astrophys. J.*, **177**, 441.
van Altena, W. F. 1969, *Astron J.*, **74**, 2.
Wegner, G. 1973, *Mon. Not. R. astr. Soc.*, **165**, 271.
Wegner, G. 1980, *Astron. J.*, **85**, 1255
Wegner, G. & McMahan, R. K. 1985, *Astron. J.*, **90**, 1511.
Wegner, G. and Nelan, E. P. 1987, *Astropys. J.*, **319**, 916.
Wegner, G. and Reid, I. N. 1987, in *The Second Conference on Faint Blue Stars*, Proc. IAU Coloq. No. 95, A. G. D. Philip, D. S. Hayes, and J. W. Liebert, eds., (Schenectady: L. Davis Press), p. 649.
Weidemann, V. & Koester, D. 1983, *Astron. & Astrophys.*, **121**, 77.

THE HIGH RESOLUTION SPECTRUM OF THE PULSATING, PRE-WHITE DWARF STAR PG 1159-035 (GW VIR) (1)

James Liebert (2)
Steward Observatory, University of Arizona
AZ 85721

F. Wesemael (2)
Département de Physique and Observatoire du Mont Megantic,
Université de Montréal, C.P. 6128, Succ. A,
Montréal, PQ, H3C 3J7, Canada

D. Husfeld
Institut für Astronomie und Astrophysik
der Universität München, Scheinerstrasse 1
D-8000 München 80

R. Wehrse (2)
Institut für Theoretische Astrophysik der
Universität Heidelberg, D-6900 Heidelberg, F.R. Germany

S. G. Starrfield
Department of Physics, Arizona State University
Tempe, AZ 85287

and

E. M. Sion
Department of Astronomy, Villanova University
Villanova, PA 19085

I. INTRODUCTION

First reported at the IAU Colloquium No. 53 on White Dwarfs (McGraw *et al.* 1979), PG 1159-035 (GW Vir) is the prototype of a new class of very hot, pulsating, pre-white dwarf stars. It shows complicated, nonradial pulsation modes which have been studied exhaustively, both observationally and theoretically. The effective temperature has been crudely estimated as 100,000 K with $\log g \sim 7$ (Wesemael, Green and Liebert 1985, hereafter WGL).

(1) Optical data reported here were obtained at the Multiple Mirror Telescope (MMT) Observatory, a facility operated jointly by the Harvard-Smithsonian Center for Astrophysics and the University of Arizona.

(2) Guest Observers with the International Ultraviolet Explorer (IUE) Observatory, which is sponsored and operated by the National Aeronautics and Space Administration, the European Space Agency and the Science Research Council of the United Kingdom.

The optical spectrum shows broad absorption features attributable primarily to He II, C IV and O VI, often with central emission reversals; no hydrogen lines are seen. The abundances in the atmosphere are of great interest with respect to the pulsational driving mechanism. The preliminary analysis of WGL assumed that the star had a composition similar to the hot DO white dwarfs, with helium the dominant constituent. However, Starrfield *et al.* (1984) predicted that the pulsational driving required very high abundances of oxygen and/or carbon near the surface; too much helium would quench the pulsations. This prediction led directly to the discovery of the O VI features at optical wavelengths (Sion, Liebert and Starrfield 1985). However, the ultraviolet wavelengths accessible to the International Ultraviolet Explorer (IUE) Observatory are of greater importance in the identification and analysis of spectroscopic features due to CNO ions and potentially those of any heavier elements. In this paper we report results from a long IUE echelle observation covering the short wavelength (SWP) bandpass. Additional low resolution IUE data and a high resolution observation of the optical 4686A region were also obtained.

II. THE OBSERVATIONS

Contiguous European and US1 shifts, were used to obtain a 17 hour SWP echelle exposure on 1984 May 16-17. The spectrum showed a rich spectrum of absorption lines. Identified transitions, velocities and estimated equivalent widths are listed in a forthcoming paper by the same authors. We summarize the principal findings below.

Lines showing cores distinct enough for velocity estimates included N V 1238, 1242A (Fig. 1), N IV 1270A, O V 1371A, and C IV 1548, 1551A (Fig. 2). The Si IV 1394, 1402A doublet is not seen. There is little evidence for fast or slow wind components in any resonance lines. C IV shows strong, broad absorption at both doublet reversals, with possible evidence for central emission reversals. The C IV values (+13, +24 km/sec) are marginally consistent with each other, but significantly lower than the average found from the other lines (+35 km/sec). Since the C IV cores are poorly defined, we accept the latter as the most likely photospheric velocity. A consistent set of low excitation lines at a velocity of -28 km/sec is attributed to an interstellar cloud.

One very broad feature, with an equivalent width of nearly 2A and spanning 1341-55A (Fig. 3), is shallow and complicated compared with the other strong lines. This feature had been noted in low dispersion IUE spectra of PG 1159-035 and similar stars (WGL, Bond *et al.* 1984), but its wavelength remained ambiguous. The new spectrum shows that our earlier suggested identifications with C III and N III are incorrect. We have found that this and other broad features noted in the high dispersion image may be identified with transitions of highly-excited levels of C IV, calculated by one of us (D.H.) in analyzing the spectrum of the central star of the planetary nebula NGC 246 (Husfeld 1987).

An optical spectrum was obtained with the Multiple Mirror Telescope on 1988 January 2 showing the emission reversal at the center of the broad 4686A absorption (see WGL). The stellar radial velocity, as measured by cross-correlation of the central feature with a Gaussian emission

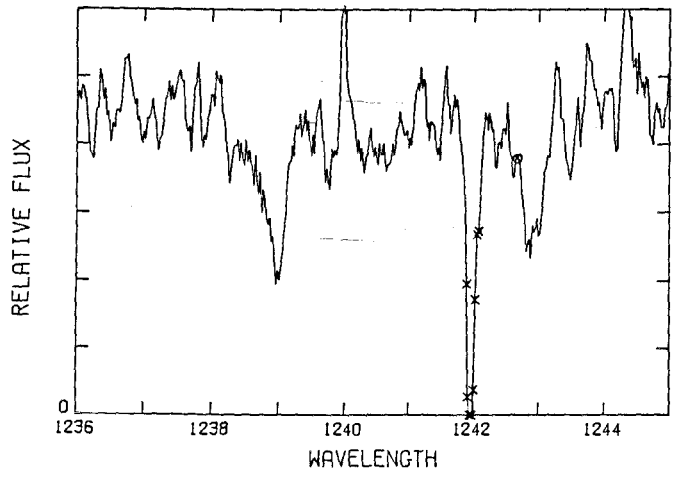

Figure 1. A detailed plot of the region of the N V 1238.82, 1242.80A doublet in the high dispersion spectrum.

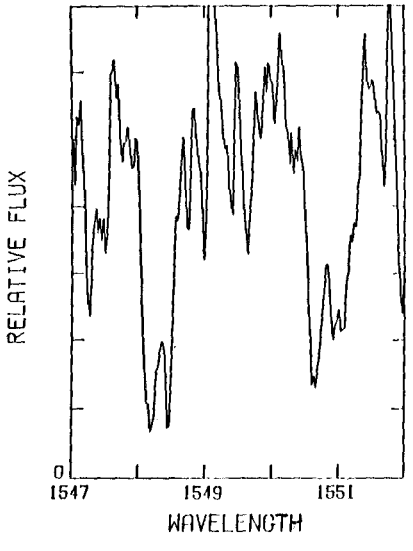

Figure 2. A similar plot showing the C IV 1548.18,1550.77 A doublet.

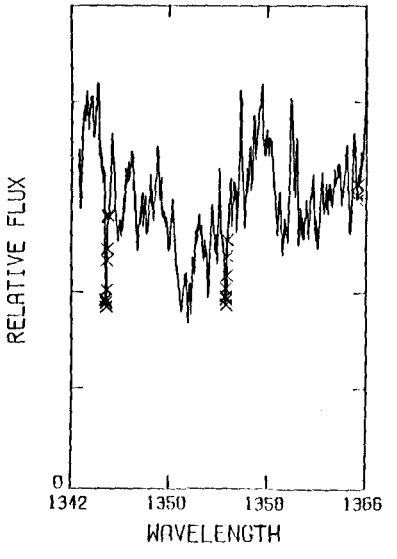

Figure 3. A plot of the likely C IV absorption (and possibly other) features in the 1346-54A region of the high dispersion spectrum which has a total measured EW of nearly 2A. Identified transitions include lines at 1351.2A, 1352.9 and 1358.6A.

line profile is +48.4±2.9 km/sec assuming identification with He II, and +80 km/sec assuming C IV. However, recent calculations of Kudritzki (1987) applicable to helium-rich planetary nebula nuclei and hot subdwarfs predict such a feature will be caused by ongoing mass loss, and may show a velocity shift with respect to the photosphere.

III. IMPLICATIONS

We have found that the ultraviolet spectrum of PG 1159-035 is dominated by features due to highly-ionized carbon, nitrogen and oxygen. While the identified ions are consistent with the diffusion calculations reported by Vauclair (1989) assuming a helium-rich atmosphere, the result underscores the possibility that the atmosphere may be dominated by a combination of CNO elements. This would be consistent with the pulsational driving mechanism of Starrfield *et al.* (1984). A detailed analysis employing non-LTE atmospheres treating the CNO ions will clarify this question, and the paper of Werner, Heber and Hunger (1989) represents the first such exploratory calculations.

This work was supported in part by NASA IUE grant NAG 5-38, by NSF grant AST 88-40482 and by the NSERC Canada.

REFERENCES

Bond, H.E., Grauer, A.D., Green, R.F. and Liebert, J. (1984). Astrophys. J. **279**, 751.

Husfeld, D. (1987). In *The Second Conference on Faint Blue Stars, IAU Coll. 95*, edited by A.G.D. Philip, D.S. Hayes and J. Liebert (Davis, Schenectady NY) p. 237.

Kudritzki, R. (1987). In *The Second Conference on Faint Blue Stars, IAU Coll. 95*, edited by A. G. Davis Philip, D. S. Hayes and J. W. Liebert (Davis, Schenectady NY), p. 177.

McGraw, J.T., Starrfield, S.G., Liebert, J. and Green, R.F. (1979). In *White Dwarfs and Variable Degenerate Stars, Proc. IAU Coll. 53*, edited by H.M. Van Horn and V. Weidemann, (Univ. of Rochester Press, Rochester NY), p. 377.

Sion, E.M., Liebert, J. and Starrfield, S.G. (1985). Astrophys. J. **292**, 471.

Starrfield, S.G., Cox, A.N., Kidman, R.B. and Pesnell, W.D. (1984). Astrophys. J. **281**, 800.

Vauclair, G. 1989, this conference.

Werner, K., Heber, U. and Hunger, K. 1989, this conference.

Wesemael, F., Green, R.F. and Liebert, J. (1985). Astrophys. J. Suppl. Ser. **58**, 379 (WGL).

POLARIZED RADIATION FROM INHOMOGENEOUS ACCRETION COLUMNS IN AM HERCULIS BINARIES

Kinwah Wu and G. Chanmugam
Department of Physics and Astronomy, Louisiana State University
Baton Rouge, LA 70803, USA

Abstract

The polarization of radiation emitted by inhomogeneous accretion columns is found to be significantly different from homogeneous columns. A good fit to the V-band circular polarization light curve of EF Eri is obtained using the two-core model with temperature kT=15keV, magnetic field B=26MG, and dimensionless plasma parameter $\Lambda \approx 10^6$.

I. Introduction

The AM Herculis binaries, a subclass of cataclysmic variables, consist of a magnetic white dwarf rotating synchronously and accreting matter from a lower main-sequence secondary through an accretion column. A distinguishing characteristic of these systems is the strong circular polarization ($\sim$ 10%) observed in the optical and infrared bands (e.g. Liebert and Stockman 1985, Lamb 1985). Such polarized radiation is believed to be due to cyclotron emission arising from the post-shock region in the accretion column, or its vicinity.

In most calculations, the emitting region was considered to be a homogeneous plasma slab (Chanmugam and Dulk 1981, Barrett and Chanmugam 1984) or a hemisphere (Wickramasinghe and Meggitt 1985) with a temperature $kT \approx 10$ keV, a magnetic field $B \approx 30$ MG, and a dimensionless plasma parameter $\Lambda \equiv 4\pi Nel/B \sim 10^6$ (e.g. Chanmugam and Wu 1987), where N is the electron number density and l the characteristic size of the plasma. However, the predicted optical spectra of these homogeneous models have a very steep slope in the optically thin part and a sharp peak in the transition between the optically thick and optically thin regions, which is in contrast to the flat spectra observed. The predicted polarization is also much higher in the optical band but much lower in the infrared band when compared with the observations.

Recently, inhomogeneous accretion columns have been studied (e.g. Schmidt, Stockman and Grandi 1986; Wu and Chanmugam 1988; Wickramasinghe and Ferrario 1988), and these columns have been found to produce flatter spectra; thus providing better fits to

the spectra of ST LMi, V834 Cen, and EF Eri (Wu and Chanmugam 1988). In addition, the inhomogeneous models can also explain the different sizes of the optical and X-ray emitting regions observed by Beuermann (1987). The effects of inhomogeneities on the polarization, which have not been discussed previously, are examined in this paper. The V-band polarization curve of the system EF Eri is fitted using one of the inhomogeneous models, the two-core model.

II. Polarization

Consider an infinite plasma cylinder with a uniform temperature and a uniform magnetic field parallel the the symmetry axis, but an electron density varying across the cylinder. Three types of electron density profiles, homogeneous, Gaussian, and two-core, are studied here. The Robinson and Melrose (1984) analytic formulae for the cyclotron absorption coefficients are used in solving the radiative transfer equations.

In figure 1 the polarization is plotted against the viewing angle θ, with the magnetic field, for the harmonic number $s = 7$. In all cases the electron density profiles are normalised to have an accretion luminosity equivalent to that due to a homogeneous cylinder with $N = 10^{16} cm^{-3}$. The temperature is kT=10keV, the magnetic field 25MG, and the radius of the cylinder $10^7 cm$. Negligible circular polarization is produced by the homogeneous cylinder for $90° \geq \theta \geq 60°$, compared to a few % for the the two inhomogeneous cylinders (Figure 1a). When θ decreases, the circular polarization due to both the homogeneous cylinder and the cylinder with the Gaussian density profile increases rapidly. The former reaches 80%, the latter 70%, while for the two-core profile it increases slowly up to about 30%. All cylinders produce about 1% linear polarization at $\theta \sim 30° - 60°$, but at $\theta \approx 90°$ only the inhomogeneous cylinders produce significant linear polarization ($\approx 15\%$) (Figure 1b). In Figure 2 the circular polarization is plotted against $\log(1/\lambda)$, where λ is the wavelength of the radiation in μm, for the same parameters as in figure 1. Compared to the homogeneous models, the inhomogeneous models generally produce larger circular polarization in the infrared band but smaller circular polarization in the optical band.

III. EF Eri

The optical spectrum of EF Eri, unlike that of ST LMi, is very flat and hence cannot be explained by homogeneous models. However, Wu and Chanmugam (1988) obtained a good fit to the optical spectra using the two-core model with the parameters: kT=15keV, $R = 10^7 cm$, $N_{core} = 10^{17} cm^{-3}$, $N_{shell} = 10^{14} cm^{-3}$, and $(R_{core}/R_{shell})^2 = 0.05$. These values are adopted here to fit the observed V-band polarization light curve obtained by Piirola, Reiz, and Coyne (1987). Polarization light curves for homogenous models with

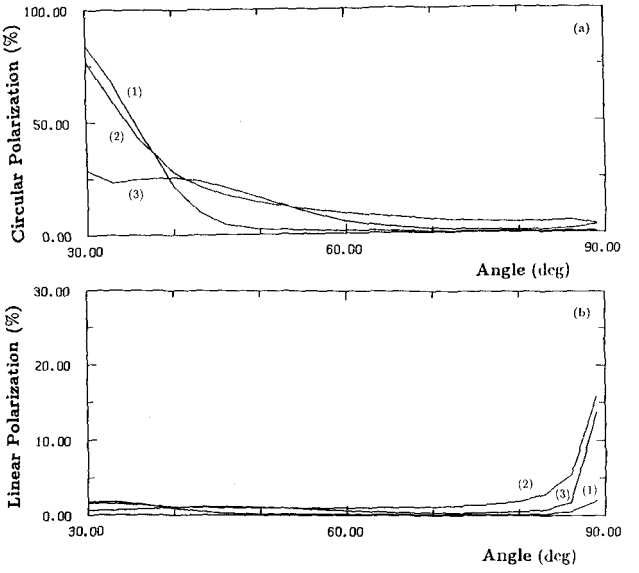

Figure 1: (a) The circular polarization is plotted against θ for $s = 7$ for cylinders with $R = 10^7 cm$, kT=10keV, B=25MG and $\bar{N} = 10^{16} cm^{-3}$. Curve 1 corresponds to a homogeneous cylinder, curve 2 a Gaussian cylinder, and curve 3 a two-core cylinder. (b) The linear polarization is plotted against θ for cylinders with the same parameters as (a).

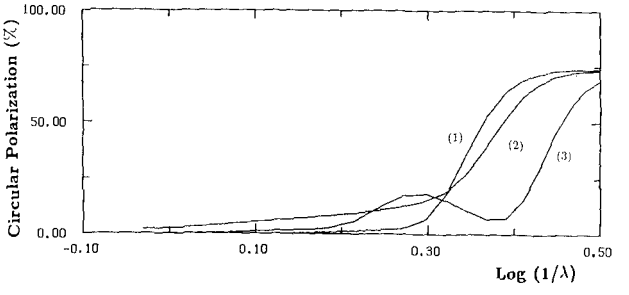

Figure 2: The circular polarization is plotted against $\log(1/\lambda)$ for $\theta = 60°$, where λ is given in μm. Curve 1 corresponds to a homogeneous cylinder, curve 2 a Gaussian cylinder, and curve 3 a two-core cylinder. The parameters are the same as those in figure 1.

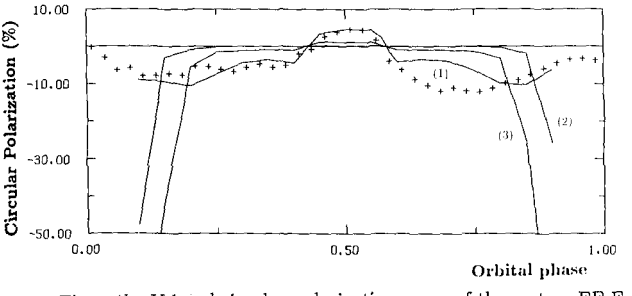

Figure 3: Fit to the V-band circular polarization curve of the system EF Eri: curve 1 corresponds to a two-core cylinder with kT=15keV, $N_{core} = 10^{17} cm^{-3}$, $N_{shell} = 10^{14} cm^{-3}$, $(R_{core}/R_{shell})^2 = 0.05$ and $R = 10^7 cm$, curve 2 a homogeneous cylinder with $N = 10^{16} cm^{-3}$ and $R = 10^7 cm$, and curve 3 a homogeneous cylinder with $N = 10^{16} cm^{-3}$ and $R = 10^6 cm$.

$N = 10^{16} cm^{-3}$ and $R = 10^6 cm, 10^7 cm$ are also generated for comparison (Figure 3). The two-core model clearly provides better fits to both the optical spectrum and the circular polarization.

IV. Conclusions

Our calculations shows that inhomogeneous cylinders generally produce larger circular and linear polarization at angles close to 90° compared with homogeneous cylinders, but smaller polarization at $\theta \approx 30°$ for a given harmonic number. The inhomogeneous cylinders also produce larger circular polarization in the infrared band. A good fit to the V-band circular polarization curve of EF Eri is obtained, showing that the parameters of the emitting region are kT= 15keV, B=26MG, and $\Lambda \approx 10^6$. Such values are identical to those used to fit the optical continuum in Wu and Chanmugam (1988), thus implying the self-consistency of our model and the significance of inhomogeneities on the spectrum and polarization.

This research was supported by NSF grant AST-8700742.

References

Barrett, P. E., and Chanmugam, G. 1984, *Ap. J.*, **278**, 298.
Beuermann, K. 1987, *Ap. Space Sci.*, **131**, 625.
Chanmugam, G., and Dulk, G. A. 1981, *Ap. J.*, **244**, 569.
Chanmugam, G., and Wu, K. 1987, *Ap. Space Sci.*, **131**, 657.
Lamb, D. Q. 1985, in *Cataclysmic Variables and Low-Mass X-Ray Binaries*, ed. D. Q. Lamb and J. Patterson (Dordrecht: Reidel), p. 179.
Liebert, J., and Stockman, H. S. 1985, in *Cataclysmic Variables and Low-Mass X-Ray Binaries*, ed. J. Patterson and D. Q. Lamb (Dordrecht: Reidel), p.151.
Piirola, V., Reiz, A., and Coyne, G. V. 1987, *Astr. Ap.*, **186**, 120.
Robinson, P. A., and Melrose, D. B. 1984, *Australian J. Phys.*, **37**, 675.
Schmidt, G. D., Stockman, H. S., and Grandi, S. A. 1986, *Ap. J.*, **300**, 804.
Wickramasinghe, D. T., and Meggitt, S. M. A. 1985, *M.N.R.A.S.*, **216**, 857.
Wickramasinghe, D. T., and Ferrario, L. 1988, *Ap. J.*, in press.
Wu, K., and Chanmugam, G. 1988, *Ap. J.*, *15 Aug.*, in press.

THOMSON SCATTERING IN MAGNETIC FIELDS

Barbara Whitney
Department of Astronomy
University of Wisconsin—Madison

ABSTRACT

The equation of transfer in Thomson scattering atmospheres with magnetic fields is solved using Monte Carlo methods. Two cases, a plane parallel atmosphere with a magnetic field perpendicular to the atmosphere, and a dipole star, are investigated. The wavelength dependence of polarization from a plane-parallel atmosphere is qualitatively similar to that observed in the magnetic white dwarf Grw+70°8247, and the field strength determined by the calculation, 3.2×10^8 G, is quantitatively similar to that determined from the line spectrum. The dipole model does not resemble the data as well as the single plane-parallel atmosphere.

INTRODUCTION

The most strongly magnetic white dwarfs have surface field strengths in the range of 10^8-10^9 G. In order to explain the strong linear and circular polarization of these objects, one needs to know the polarization and angular dependence of the important absorption processes in a magnetic white dwarf. Several people (e.g., Martin and Wickramasinghe 1978, Wickramasinghe and Martin 1979, Wickramasinghe and Ferrario 1988, Nagendra and Peraiah 1984) have modelled the continuum polarization spectra of magnetic white dwarfs using the dichroic opacities of Kemp (1977) for free-free absorption, and Lamb and Sutherland (1974) for bound-free. Both of these opacities were derived in the weak field limit, $\omega_c/\omega \ll 1$ ($\omega_c = eB/mc$, the cyclotron frequency). For large field strength, that is, $\omega_c/\omega \gg 1$, the motion of electrons is confined along the field lines, and the opacity expressions of Lodenquai *et al.* (1974) can be used, though they do not provide a complete description of the angular dependence of the cross sections. Lauer *et al.* (1983) present polarization and angular dependence of bremsstrahlung for the case of $h\omega \ll kT \ll h\omega_c$ in fields so strong that electron motion perpendicular to the field is confined to the first Landau level. For weaker fields ($\omega < \omega_c$) and $h\omega < kT$, Stokes parameters for free-free absorption are given by Wickramasinghe and Meggitt (1985).

For $kT \sim h\omega \sim h\omega_c$, as is the case for the atmospheres of the strongest magnetic white dwarfs, a continuum opacity for which the polarization and angular dependence of the cross sections is known exactly is Thomson scattering. Since the behavior of other opacities may be similar to that of Thomson scattering, it is instructive to examine the polarization properties of a Thomson scattering atmosphere.

MODEL ATMOSPHERES

Stokes parameters for electron scattering in a constant magnetic field along z were derived classically using the method of Chou (1986), and then integrated to give cross sections which depend on direction and polarization of the incident radiation. These cross sections agree with Herold (1979) in the non-relativistic limit. Radiative transfer in a plane parallel atmosphere with magnetic field along z was solved using a Monte Carlo method. For arbitrary field orientations, the radiative transfer was solved in an atmosphere that was tilted with respect to the z-axis, and the results transformed into the coordinate frame of the atmosphere.

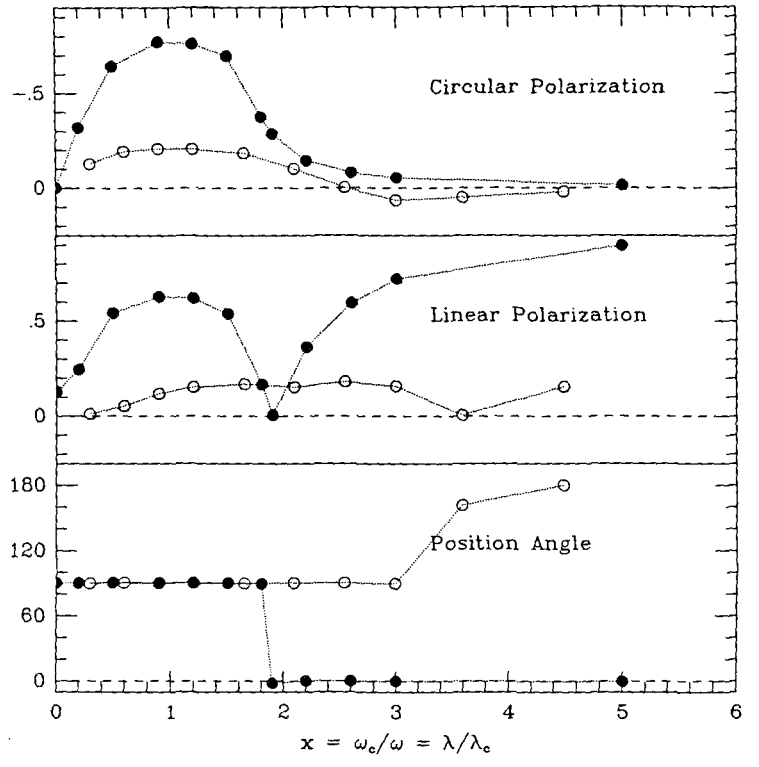

Figure 1 — Fractional polarization (1=100%) is plotted as a function of $x = \omega_c/\omega = \lambda/\lambda_c$. The filled circles show polarization from a plane-parallel atmosphere with magnetic field along the -z axis, perpendicular to the atmosphere. The viewing angle is 60° from the z-axis. Open circles are from a dipole model viewed 60° from the south pole.

The filled circles of Figure 1 show the results of a model atmosphere with the magnetic field along the negative z axis, and an optical depth of three. Unpolarized grey light is incident normal to the bottom of the atmosphere. The polarization of scattered light emerging from the top at an angle of 60°

from the normal is shown here for several different values of $x = \omega_c/\omega = \lambda/\lambda_c$. At this angle the linear polarization is comparable to the circular, as it is in Grw+70°8247. As expected, the circular polarization is largest at the cyclotron frequency, that is, $\omega = \omega_c$. An interesting feature of the linear polarization is the change in position angle at $\omega_c/\omega = 1.9$. This jump occurs at all exit angles. It can be understood as follows: When no field is present, radiation emerging from a plane parallel semi-infinite Thomson scattering atmosphere is linearly polarized with a position angle of 90° with respect to the zenith (Chandrasekhar, 1960). In weak magnetic fields, the cross section for scattering is large when the electric vector of the incoming photon is perpendicular to the field, which in this case is also perpendicular to the atmosphere. This gives rise to linear polarization with a position angle of 90°. When the cyclotron frequency becomes much greater than that of the incident radiation, the electron can only be excited at the frequency ω when the electric vector of the incident radiation is parallel to the field. The scattered radiation is linearly polarized at a position angle of 0°. With this behavior in mind, we can interpret the results of a dipole model.

A DIPOLE MODEL

A grid of plane-parallel atmospheres was solved, each atmosphere having a magnetic field orientation and strength appropriate for its latitude on the surface of a dipole sphere. The outgoing radiation was integrated over the surface of the sphere. The optical depth of each atmosphere is $\tau = 3$, because it takes less computing time than larger depths and it gives similar answers. The difference in polarization between an atmosphere of $\tau = 3$ and $\tau = 6$ depends on field strength, but is never more than 20% for ω_c/ω greater than 0.1.

Since Monte Carlo solutions provide outgoing radiation at all angles, the dipole star can be rotated and viewed at any angle. The open circles in Figure 1 show the results for a viewing angle of 60° from the south pole. Again, 60° was chosen because the linear polarization is comparable to circular at this angle. The results are different than those in the plane-parallel case. The circular polarization changes sign at $\omega_c/\omega \approx 3$ even though we are looking down the south pole and so expect only negative polarization. The reason for this is that the negative polarization from the south pole is small at $\omega_c/\omega = 3$ but the positive polarization from the equator, where the field lines are pointing away from us, is large because there $\omega_c/\omega \approx 1.5$. Another difference from the plane-parallel atmosphere is that the position angle of the linear polarization does not rotate until $\omega_c/\omega \approx 3.5$. Both the linear and circular polarization are not as large as in the single atmosphere.

COMPARISON WITH OBSERVATIONS

Continuum polarization data of Grw+70°8247 have been obtained by Landstreet and Angel (1975). The magnitude of the circular polarization has a narrow absorption feature at 3400A, increases to -5% at 4500 A, and then decreases with increasing wavelength. The linear polarization peaks at 4% at about 3900 A, then decreases to less than 1% by 5000 A. Its position angle rotates by 90° at about 5700 A. The polarization then starts to increase at about 7500 A and reaches 6% at 10000 A.

If we match the wavelength of the position angle rotation of the single atmosphere model shown in Figure 1 (solid dots) to the rotation of the data at 5700 A, then the cyclotron wavelength of the atmosphere is $\lambda_c = \lambda/x = 5700/1.9 = 3353$ A, which corresponds to a field strength of 3.2×10^8 G. Angel, Liebert, and Stockman (1985) estimated the field strength of Grw+70°8247 to be $(1.6\text{-}3.5)\times10^8$ G from identification of hydrogen lines. Henry and O'Connell (1984) estimated the field to be $(4.0\text{-}7.6)\times10^8$ G from the shifted wavelength of Ly-α. The similarity of the polarization and field strength of the plane parallel atmosphere to Grw+70°8247 is intriguing. However, the plane parallel model does not exactly fit the data: The dip in linear polarization at 5700 A is much wider in the data than in the model, and the circular polarization of the data decreases more slowly with wavelength than the model.

The dipole model does not fit the data very well. The field strength required to match the rotation of the position angle is 6.7×10^8 G at the pole (half that at the equator). This would put the peak of the circular polarization at 1600 A. The circular polarization would change sign at 4100 A, which is not at all like the data. If we match the circular polarization peak to the data, then of course the problem is that the position angle rotation occurs at about twice the wavelength of the data.

The dipole model can be modified so that more radiation is incident on the atmospheres at the poles than at the equator. This brings the wavelength of the position angle rotation down with respect to the circular polarization peak, and in fact widens out the linear polarization dip to look more like the data. But to get this fit requires 25 times more radiation at the poles than at the equator, which may be unreasonable.

This work is supported by contract NAS5-26777 for the Wisconsin Ultraviolet Photo-Polarimeter Experiment.

REFERENCES

Angel, J. R. P., Liebert, J., and Stockman, H. S. 1985, *Ap. J.*, **292**, 260.

Chandrasekhar, S. 1960, *Radiative Transfer* (New York: Dover).

Chou, C. K. 1986, *Astrophys. and Space Sci.*, **121**, 333.

Henry, R. J. W., and O'Connell, R. F. 1984, *Ap. J.*, **282**, L97.

Herold, H. 1979, *Phys. Rev. D*, **19**, 2868.

Kemp. J. C. 1977, *Ap. J.*, **213**, 794.

Lamb, F. K., and Sutherland, P. G. 1974, in *IAU Symposium 53, Physics of Dense Matter*, ed. C. J. Hansen (Dordrecht: Reidel), p. 265.

Landstreet, J. D., and Angel, J. R. P. 1975, *Ap. J.*, **196**, 819.

Lauer, J., Herold, H., Ruder, H. and Wunner, G. 1983, *J. Phys.B: At. Mol Phys.*, **16**, 3673.

Lodenquai, J., Canuto, V., Ruderman, M., Tsuruta, S. 1974, *Ap. J.*, **190**, 141.

Martin, B., and Wickramasinghe, D. T. 1978, *Mon. Not. R. astr. Soc.*, **183**, 533.

Nagendra, K. N., and Peraiah, A. 1984, *Astrophys. and Space Sci.*, **104**, 61.

Wickramasinghe, D. T., and Ferrario, L. 1988, *Ap. J.*, **327**, 222.

Wickramasinghe, D. T., and Martin, B. 1979, *Mon. Not. R. astr. Soc.*, **188**, 165.

Wickramasinghe, D. T., and Meggitt, S. M. A. 1985, *Mon. Not. R. astr. Soc.*, **214**, 605.

H-ALPHA EMISSION IN HOT DEGENERATES AND OB SUBDWARFS

Neill Reid
105-24, California Institute of Technology, Pasadena, CA 91125

Gary Wegner
Dept. Physics & Astronomy, Dartmouth College, Hanover, NH 03755

Based on observations obtained using the 60-inch telescope at Palomar Observatory which is jointly owned by the California Institute of Technology and the Carnegie Institution of Washington and on observations obtained with the 200-inch Hale telescope which is owned by the California Institute of Technology.

1. Introduction

The intial observations of white dwarf stars and their immediate precursors, the hot subdwarfs, suggested that these stars possess the simplest (and, aesthetically, the most pleasing) spectra of any astronomical object. The high gravity leads to the spectrum being dominated, in the most stars, by broad lines of either hydrogen or helium, depending on the composition of the photospheric layers, with a few stars exhibiting lines from both species. However, the more detailed observations of recent years have revealed a higher degree of complexity. In particular, absorption lines of high excitation species (N V, C IV, etc.) have been detected in the ultraviolet spectra of several hot white dwarfs (Bruhweiler & Kondo, 1982) and, most recently, high resolution optical spectra have shown that one of the latter stars, the hottest known DA, G191-B2B, exhibits significant emission in the core of the H-alpha absorption line (Reid & Wegner, 1988). Following up the latter observation, we have obtained high resolution spectra of a number of hot subdwarfs, with temperatures ranging from $\sim 20,000K$ to more than 60,000 K. Most of these stars also exhibit Balmer emission, at $H\beta$ as well as $H\alpha$ in at least one case. We suggest the temperature reversal in the stellar atmosphere may be a function of the He/H ratio at the level of the photosphere.

2. G 191-B2B

Before describing our observations of hot subdwarfs, we briefly summarise the conclusions drawn from our spectroscopy of the DA white dwarf G191-B2B (see Reid & Wegner, 1988, for further details). Figure 1 shows the H-alpha profile, with the emission clearly evident. This star is the common proper motion companion of a main sequence K-dwarf. The trigonometric parallax measurement of the white dwarf leads to a distance of 45 parsecs, implying a separation of 2200 astronomical units between the two stars. Thus there is no question of an interaction between the two stars. Infrared photometry rules out an optically undetected close M-dwarf companion, while time-resolved spectroscopy argues against G191-B2B being a white-dwarf - white-dwarf binary, such as L870-2 (Saffer, Liebert & Olszewski, 1988). Finally, there is no evidence for spatially extended emission (or forbidden

O [III] emission), as one might expect if the the white dwarf were ionising the surrounding remnants of a planetary nebula.

Since G191-B2B is in a wide binary, the main sequence companion can be used to estimate the space velocity. Our observations show that the $H\alpha$ emission is centrally situated within the absorption core, and the observed wavelength corresponds to a redshift of about 18 km/sec. The same redshift is observed for the ultraviolet lines of C IV, N V and Si IV that are observed in this star. On this basis we have suggested that both sets of lines have their origin close to the photospheric surface and that the velocity difference we observe is the Einstein or gravitational redshift. As a corollary of this hypothesis, we require a temperature inversion in the white dwarf atmosphere to permit these lines to exist.

3. Observations

We have obtained intermediate dispersion spectroscopy of a further sample of OB subdwarfs, mainly selected from the preliminary catalogue produced by Kilkenny, Heber & Drilling (1988). The stars cover a range in effective temperatures from $\sim 24,000K$ to $\sim 65,000K$ (Table 1). Most of these observations were obtained with the echelle spectrograph on the 60-inch telescope at Palomar Observatory (McCarthy, 1987). This spectrograph uses a TI 800 × 800 format CCD as the detector, gives a spectral coverage from $\sim 4000\mathring{A}$ to $\sim 8000\mathring{A}$ and a velocity resolution (2 pixels) of $\sim 15km/sec$ at $H\alpha$. The spectra were reduced using the same techniques employed in our analysis of the spectroscopic observations of G 191-B2B (Reid & Wegner, 1988).

In addition to these observations, we also obtained spectra of two stars, Feige 67 and BD +28 4211, using the double spectrograph on the 200-inch Hale telescope. These spectra have a resolution of $1.6\mathring{A}$ (2 pixels) at $H\alpha$ and $1.0\mathring{A}$ at $H\beta$ and are therefore less sensitive to the presence of weak emission. Nonetheless, emission is detected at $H\alpha$ in both stars, while BD +28 4211 is the only star in our sample with convincing emission at $H\beta$. Figure 2 presents examples of our spectroscopic observations. The large-scale undulations in the spectra reflect residual effects of the echelle blaze function - these data have not been flux calibrated - while the narrow absorption lines are terrestial atmospheric features.

4. Discussion

Table 1 summarises the results of our observations so far. All save one of the subdwarfs with photospheric effective temperatures of 38,000 K or more have detectable emission in the core of the $H\alpha$ line, although only BD +28 4211, as we noted above, has convincing emission at $H\beta$. Unfortunately this last star has not been analysed using models atmospheres, but the He I and Balmer line strengths are very similar to those observed in Feige 67, and we have adopted an effective temperature of 40,000 K. in both this star and the (perhaps) slightly hotter BD +25 4655 the peak of the $H\alpha$ emission reaches close to the level of the neighbouring continuum. The hotter subdwarf LS IV-12, with a temperature comparable to that of G191-B2B, has a broad core to the absorption at $H\beta$, which may arise from emission filling in the central part of the absorption. We suggested that there is marginal evidence for similar low-level emission in G191-B2B.

The full-width half-maximum estimates made for the several stars with emission cores are all comparable, particularly allowing for the uncertainties involved in the measurement. None show evidence for extended emission and, as we noted in

Table 1

star	$H\alpha$	EW mÅ	FWHM Å	$H\beta$	EW mÅ	FWHM Å	T_{eff}	type
HD 4539	no	-	-	no	-	-	24,500	sdB
Feige 108	no	-	-	no	-	-	31,600	sdB
Feige 67	yes	120	1.5	no	-	-	38,900	sdO
Feige 110	yes	100	1.1	no	-	-	40,000	sdO
BD +28 4211	yes	400	1.5	yes	25	0.9	40,000	sdO
BD +25 4655	yes	145	1.2	no	-	-	42,200	sdO
Feige 34	yes	-	-	no	-	-	>50,000	sdO
LS IV-12	yes	140	1.2	?	-	-	60,200	sdO
G191-B2B	yes	90	1.5	?	-	-	62,250	DA

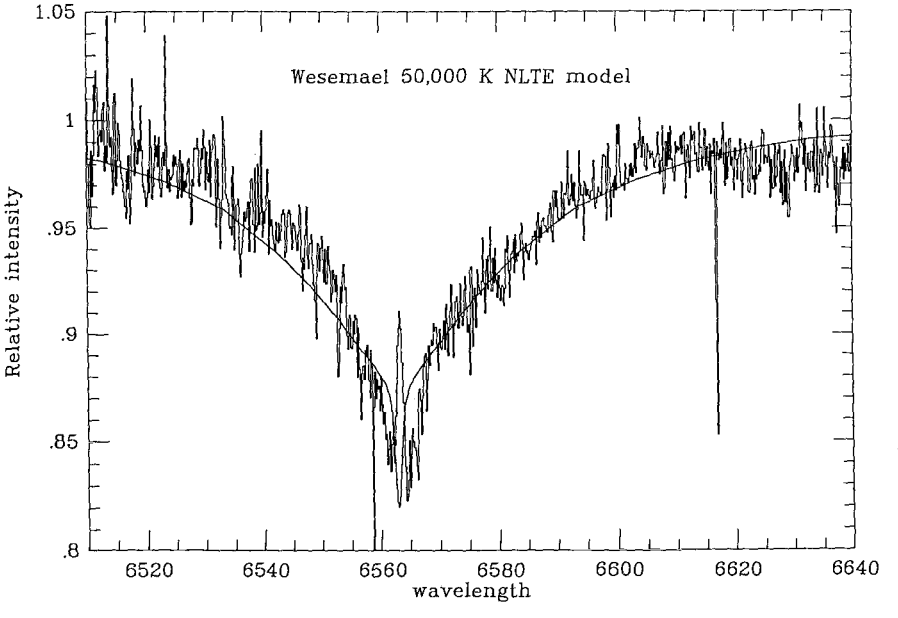

Figure 1. The $H\alpha$ profile of the hot white dwarf G191-B2B

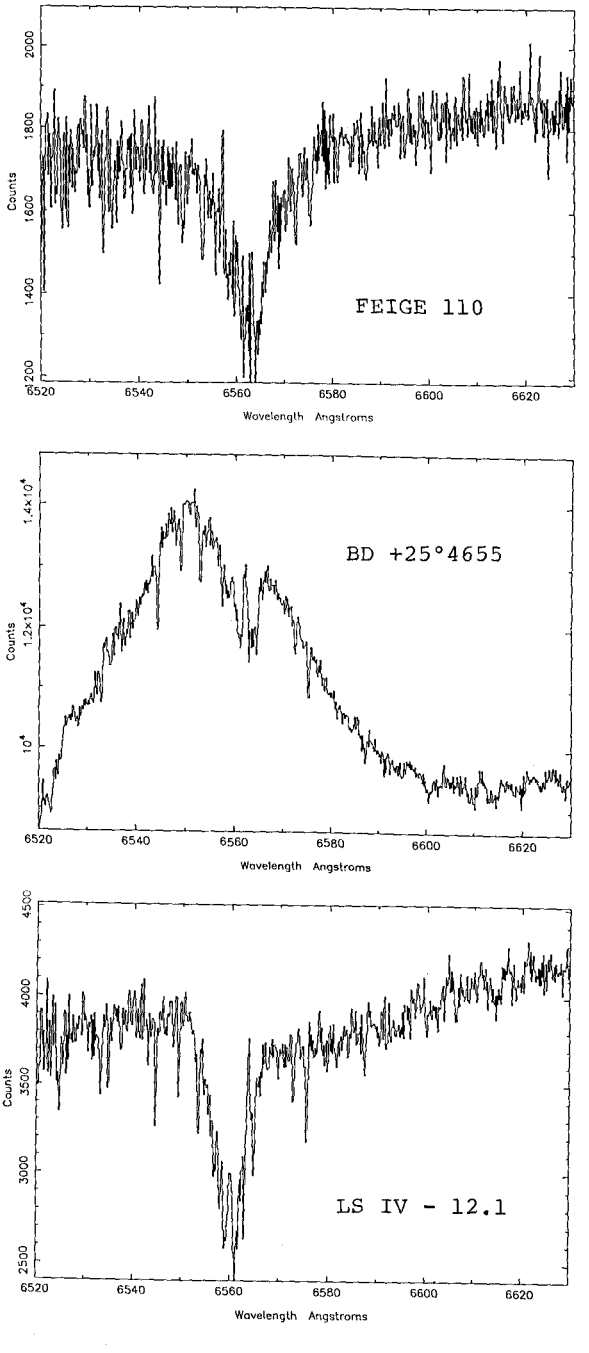

Figure 2. Balmer line profiles for a selection of the hot subdwarfs listed in Table 1.

the case of G191-B2B, the observed line widths are consistent with the Stark broadening expected near the top of the stellar photosphere. The only hot subdwarf in which there is no clear evidence of emission is Feige 34, where we have obtained only a relatively low signal-to-noise spectrum (figure 2).

The presence of Balmer emission requires the existence of a temperature inversion in the stellar atmosphere. We are currently investigating the stability of chromospheres and coronae in white dwarfs (Reid & Collier Cameron, in prep.), but such temperature inversions have already been predicted in some atmosphere models. Wesemael's (1981) calculation of the temperature distribution in an NLTE, pure-He white dwarf model with effective temperature 70,000 K predicts a temperature minimum at the point where He II becomes transparent, with the overpopulation of the He II ground state leading to heating of the upper layers. Jordan & Koester (1986) find that a similar temperature structure can occur in stratified H/He white dwarf models which possess a thin outer shell of hydrogen. Vennes et al. (1988) have shown that optical and soft X-ray observations imply a trend of decreasing He/H ratio with decreasing photospheric temperature amongst white dwarf stars. This they interpret as partly due to cooling effects and partly due to an increase in the mass and thickness of the outer layer of hydrogen. While only one of the stars in our sample is a white dwarf, it may be significant that, as the hottest known DA, it has a high He/H ratio. Similarly, the hotter sdO stars are generally regarded as He-rich, while the sdB and sdOB stars have He-poor atmospheres, and the lower He/H abundances in the latter stars may account for the absence of Balmer emission.

Further observations and more detailed models are required to determine the range of effective temperature, surface gravity and photospheric abundances of those stars exhibiting Balmer emission, and we are currently embarking on such a project. However, it seems likely that the characteristics of these emission cores can furnish information on the atmosphere structure in hot white dwarfs and subluminous OB stars.

This work was partially supported by the National Science Foundation through Grant AST85-15219.

References

Bruhweiler, F.C, & Kondo, Y., 1982, *Astrophys. J.*, **259**, 232
Jordan, S., & Koester, D., 1986, *Astr. Astrophys. Suppl.* , **65**, 367
Kilkenny, D., Heber, U. & Drilling, J.S., 1988, 2nd *Faint Blue Stars Conference*, ed. Liebert, Davis Philip, p. 731
Reid, I.N. & Wegner, G., 1988, *Astrophys. J.*,**in press**
Saffer, R.A., Liebert, J., & Olszewski, E.W., 1988, *Astrophys. J.*, **in press**
Vennes, S., Pelletier, C., Fontaine, G. & Wesemael, F., 1988, *Astrophys. J.*, submitted
Wesemael, F., 1981, *Astrophys. J. Suppl.*, **45**, 177

GRAVITATIONAL REDSHIFTS AND THE MASS-RADIUS RELATION

Gary Wegner
Department of Physics & Astronomy, Dartmouth College

I. INTRODUCTION

The gravitational redshift is one of Einstein's three original tests of General Relativity and derives from time's slowing near a massive body. For velocities well below c, this is represented with sufficient accuracy by:

$$V_{RS} \approx GM/cR \approx 0.635\ M/M_{\odot}/R/R_{\odot}\ \text{km/ sec.}$$

As detailed by Will (1981), Schiff's conjecture argues that the gravitational redshift actually tests the principle of equivalence rather than the gravitational field equations. For low redshifts, solar system tests give highest accuracy. LoPresto & Pierce (1986) have shown that the redshift at the Sun's limb is good to about $\pm 3\%$. Rocket experiments produce an accuracy of $\pm 0.02\%$ (Vessot *et al.* 1980), while for 40 Eri B the best white dwarf, the observed and predicted V_{RS} agree to only about $\pm 5\%$ (Wegner 1980).

While using white dwarfs is not the most stringent test of general relativity, one can assume its validity and employ it as a tool to probe the white dwarfs. Here, the mass-radius relation is examined and then used to constrain non-Newtonian gravitational force laws.

II. PRESSURE SHIFTS IN THE LINES

The role of pressure shifts is important for interpretating white dwarfs' radial velocities. These appear to be manageable for pure hydrogen atmospheres, but many difficulties remain for the helium dominated atmospheres.

For hydrogen, it has long been known that in high density plasmas, the Balmer lines show assymetries. (Shipman & Meehan 1976). Recent work of Grabowski *et al.* (1987), however shows that the velocities measured depend on resolution. The narrow cores of the Balmer lines are relatively unaffected, while in the line wings, there are asymetries that could lead to redshifts of the size found in the early work described in § 2.2. Consequently, if measurements are made in the line cores at sufficiently high resolution, pressure shifts can be ignored.

For He I, there is much uncertainty. Greenstein & Trimble (1967), Wegner (1973), and Koester (1987) all point out that each individual line gives its own redshift in the spectra of the DBs. Additional laboratory and theoretical work are needed to clarify this problem before the He I lines of DB stars can be reliably used. A possible project would be to use the Hα line in DBA stars to calibrate them. Hammond's recent work for Ca II reported in these proceedings suggest that this problem is tractable for the DZ stars.

III. WHITE DWARF GRAVITATIONAL REDSHIFT MEASUREMENTS

2.1 Individual Stars with well-known Orbits.

The earliest attempt to observe any gravitational redshift was for Sirius B by Adams (1925). However, this value is questionable due to problems with scattered light from A. Greenstein, Oke, & Shipman (1971) derived $V_{RS} = 89 \pm 16$ km/sec. Indeed, Sirius B has proven difficult in the visual due to the proximity of Sirius A and several investigators including the author have attempted measurements and failed. The mass is well established as 1.053 ± 0.028 $M_\odot$ (Gatewood & Gatewood 1978), but there are still questions about the radius (cf. Kidder, Holberg, & Wesemael these proceedings).

The white dwarf most amenable to direct comparison of M, R, and the redshift is 40 Eri B. Popper's (1954) classical study of the star yielded the often quoted value of $+21 \pm 4$ km/sec. Greenstein & Trimble (1972) found a redshift of $+23 \pm 5$ km/sec for this object. More recent work by Wegner (1979, 1980) suggests a slightly higher value, *viz.* $+23.9 \pm 1.3$ km/sec, which may be inconsistent with the astrometric mass of 0.44 $M_\odot$.

Other binaries may be usable for determining gravitational redshifts, but present additional problems. Procyon B has never been measeured, while Stein 2051 (Strand & Kallarkal these proceedings) and G107-70 (Harrington *et al.* 1981) have orbits, but they are of spectral class DC and require examination at higher signal-to-noise and resolution.

2.2 Statistical Methods

The determination of the K-term for the white dwarfs yields a mean gravitational redshift through the relation:

$$RV_{Obs} = K - Scos\lambda + Vp_{ec}$$

This approach was pioneered by Greenstein & Trimble (1967) and Trimble & Greenstein (1972) who obtained $K = +65 \pm 5$ km/sec, which is discrepant with the mean mass near 0.6 $M_\odot$ found from using log g which should yield a mean redshift near +31 km/sec for a carbon composition.

More recent studies suggest a lower K. Wegner (1974) observed southern white dwarfs and derived $+43 \pm 14$ km/sec and even more recently, Greenstein *et al.* (1977) obtained $+44.6 \pm 5.7$ km/sec from high resolution data of 13 stars.

2.3 Common Proper Motion Systems

Common proper motion (CPM) binaries containing a white dwarf are numerous and using them to study redshifts seems most promising. If such a system is really gravitationally bound, the orbital contribution to the observed radial velocity is typically of order ± 1 km/sec, below the usual precision of measurement. Often, however, these systems are more distant and have more uncertain distances.

Nevertheless, large numbers of CPM objects exist and the first lists were compiled by Luyten (1969) and used by Eggen & Greenstein (1965) to study white dwarfs. A few individual redshifts were obtained by Greenstein & Trimble (1967) and Trimble & Greenstein (1972). More recently there has been a renewed interest in these systems and the article by Sion &

Oswalt in these proceedings contains further references to Oswalt's and other work cataloging CPM systems containing white dwarfs,

The first systematic attempt to utilize the brighter systems was Wegner (1973) who obtained image-tube spectra of the white dwarf members and high resolution photographic spectra of the bright non-degenerate components of 5 systems in the southern hemisphere. These data were used to further obtain evolutionary parameters for the white dwarfs. Sion & Guinan (1985) have applied this technique to the DO white dwarf HD149499 using *IUE* Wegner's (1978a) radial velocity for A to derive $V_{RS} = \pm 17 + 5$ km/sec.

The star CoD-38°10980 is an example of how things can go wrong (Holberg *et al.* 1985). Here, the distance is not well known despite several parallax measures and the redshift, near +40 km/sec (Wegner 1978b; Koester 1987) disagrees with that predicted from log*g*.

Nevertheless, recent application of modern digital detectors has yielded greatly improved accuracy for the measurements of redshifts. The values derived in Koester (1987), Wegner & Reid (1987) and elsewhere give both much improved internal and external accuracy.

2.4 White Dwarfs in the Hyades and Other Galactic Clusters

White dwarfs in galactic clusters represent another method of obtaining gravitational redshifts with the added advantage of a known cluster age. However, there can be kinematical complications and most galactic clusters are too distant for high resolution studies of the white dwarf members.

The Hyades is the nearest with a number of white dwarf members at about the 14th magnitude. These stars are discussed elsewhere in these proceedings (Wegner, Reid, & McMahan 1988).

The next nearest clusters include the Pleiades and Praesape. The one Pleiad with V = 16.5 is correspondingly more difficult, so far has defying recent efforts at determining a redshift. Praesape (Luyten 1962) should be reachable with 5-m class instruments. A number of even fainter white dwarfs have been located in other clusters, notably through the efforts of Koester & Reimers (1985 and refs. therein), Anthony-Twarog (1982), and Romanishin & Angel (1980) but these are currently unreachable at sufficiently high resolution and signal-to-noise for redshifts.

IV. THE MASS-RADIUS RELATION AND THE MASS DISTRIBUTION

The theoretical mass-radius relation (Chandrasekahr 1934) has stood the test of time well, despite many subsequent elaborations on the equation of state, but it has never been closely verified empirically as discussed by Weidemann in these proceedings. The richness of details that can be learned is obvious and deserves study.

Except for the few visual binary white dwarfs, the mass-radius relation must be tested by working with combinations of observed quantities, *e.g.* gravity $g = GM/R^2$ or redshift, $V_{RS} = 0.635(M/M_\odot)/(R/R_\odot)$ km/sec. Using g suffers from large errors. McMahan (1988) has reduced the uncertainties, but for studying individual stars in the mass-radius relation,

errors of order ±0.05 dex are needed in both log g and log R. However, as an error of ±3 km/sec translates to about ±0.03 $M_\odot$, it appears possible to make some meaningful conclusions utilizing gravitational redshifts.

Table I presents data derived from the presently best available V_{RS}, taken from Wegner & Reid (1987), Koester (1987)in addition to the stars in Wegner, Reid & McMahan (1988), and references in § 2.1. Sirius B is plotted using Gatewood & Gatewood (1978) for the mass. The radii have been taken from sources in Wegner, Reid, & McMahan (1988), except Sirius B where Thejll & Shipman (1986) was used. Masses correspond to the redshifts if the stars lie on the carbon Hamada & Salpeter (1961) mass-radius relation. Weights are assigned as in the Hyades paper.

TABLE I

Data on White Dwarfs in Binaries with Reliable Redshifts

Name	V_{RS}	$\log R/R_\odot$	$M/M_\odot$	Weight	Name	V_{RS}	$\log R/R_\odot$	$M/M_\odot$	Weight
Sirius B	+89.0	-2.12	1.04	4	G154-B5A/B	+24.5	-1.91	0.51	2
40 Eri B	+23.9	-1.87	0.50	19	G200-39/40	+32.5	-1.98	0.61	2
L970-27/30	+19.9	-1.88	0.44	4	L587-77A	+36.1	-1.87	0.66	2
W485A/B	+24.9	-1.83	0.52	4	LDS455	+51.2	-2.07	0.80	2
W672A/B	+21.2	-1.84	0.46	4	L481-60	+27.9	-1.84	0.56	2
G142-B2A/B	+27.4	-1.94	0.55	2	CD-38:10980	+40.0	-1.93	0.69	4
G148-6/7	+27.0	-1.91	0.54	2	L268-92	+30.2	-1.88	0.59	2

Figure 1 presents a histogram of the masses from Table I and the Hyades in Wegner, McMahan, & Reid (these proceedings). The masses have been derived from V_{RS} on the assumption that each star lies on the Hamada & Salpeter (1961) carbon mass-radius relation. Although the number of objects is still small, the field stars reproduce the relation discussed in Prof. Weidemann's lecture. The difference in unwieghted mean mass for the Hyades (0.66 ± 0.05 $M_\odot$) and the field objects (0.57 ± 0.03 $M_\odot$ excluding Sirius B) seems to be significant and could show real differences in the parent star masses.

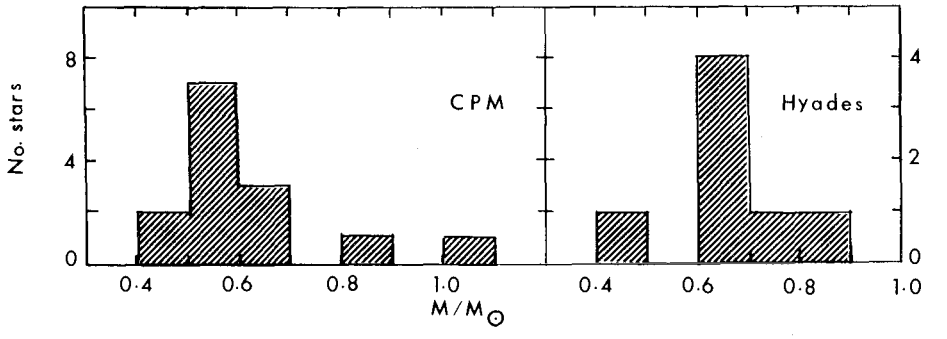

FIG. 1. The distribution of masses for white dwarfs from the gravitational redshifts published in Koester (1987), Wegner & Reid (1987), and Wegner, Reid, & McMahan (1988), derived on the assumption that all stars lie on the Hamada-Salpeter carbon mass-radius relation.

The center panel of Figure 2 shows all stars in Figure 1 compared with the Hamada & Salpeter (1961) C mass-radius relation. The data points are fit reasonably well and this is clearly better than that given by n = 1.5 polytropes. The scatter is larger than expected from errors in V_{RS} and this could reflect imprecision in logR arising through the distance determinations.

Future work must include an assessment of the role of spectroscopic binary white dwarfs like L870-2 (Cf. Bragaglia *et al.* and Saffer & Liebert, these proceedings) on enhancing the scatter in the mass determinations.

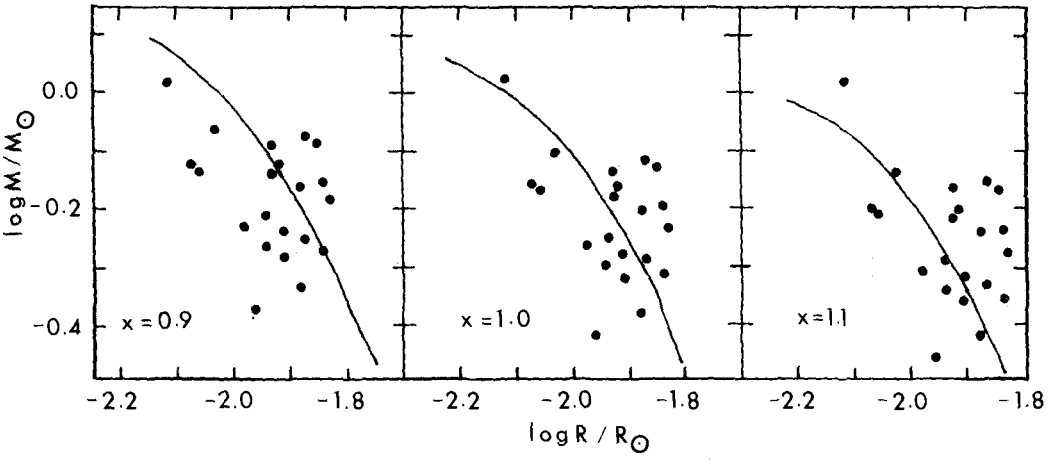

FIG. 2. Positions of the white dwarfs with the best observed gravitational redshifts compared with the Hamada-Salpeter pure carbon mass-radius relation, scaled for different values of the gravitational constant as given by the parameter $x = G_O/G_\infty$.

V. CONSTRAINTS ON THE DISTANCE DEPENDANCE OF GRAVITY

Although white dwarfs cannot compete with other measurements of the gravitational redshift as tests of general relativity, they can still be used to study certain aspects of the gravitational force law. Extended supergravity theories predict the addition of a Yukawa term to the usual Newtonian gravitational potential, so that

$$U(r) = -G_\infty M/r(1 + \alpha e^{-r/\lambda}),$$

with the resulting modified gravitational attraction, $F = G(r)M/R$, with $G(r) = G_\infty\{1 + \alpha(1 + R/\lambda)e^{-r/\lambda}\}$.

For values of λ between a few m to km, empirically determining α has proven difficult and the results are presently controversial. Long (1976) described experimental measures of α and more recently, the work of Echardt *et al.* (1988), Thielberger (1987) and Stubbs *et al.* (1987) using terrestrial experiments have found differing results at about the few per cent level.

For white dwarfs the equation of state is well known and stellar evolution establishes that they should mostly have CO cores. Sugimoto (1972) and Blinnikov (1978) made use of the fact that for the Chandrasekhar (1934) mass-radius relation, the mass and radius have the

following scaling with gravity :

$$M_\infty = M_0 x^{-1.5} \text{ and } R_\infty = R_0 x^{-0.5}, \text{ where } x = (G_\infty/G_0).$$

Hut (1981) argued that the corresponding variation in the Hamada & Salpeter (1961) mass-radius relation also scales with G to about 0.2% and found from Sirius B that $x = 0.98 \pm 0.08$. As well, 40 Eri B gives a similar result (Wegner 1980).

The limits on x can be diminished using the radii and masses of white dwarfs from their gravitational redshifts. Both V_{RS} and $\log R/R_\odot$ are observed quantities and do not scale with x. The derived mass will be:

$$M/M_\odot = V_{RS}(R/R_\odot)/0.635/x.$$

Consequently, for each value of x, there is a mass-radius relation and a corresponding point for each of the white dwarfs.

Using the data in Figure 2 from § IV and scaling the Hamada & Salpeter (1961) carbon mass-radius relation with x as above, a least squares best fit yields $x = 0.994 \pm 0.012$(s.d). For Sirius B, the position was fixed using the Gatewood & Gatewood (1978) mass and Thejll & Shipman's (1986) radius. The possible complications of assuming the zero-temperature C mass-radius relation must be emphasized at this point. Nevertheless, this derived value of x is compatable with terrestrial experiments that find x differing little from unity and has an accuracy comparable to those investigations.

VI. CONCLUSIONS

While the results described in this article are preliminary due to the small numbers of stars available, the use of gravitational redshifts as a probe of the properties of white dwarfs seems most promising. Recent advances in digital detectors has made this possible and detailed data on mass distributions can be expected as measurements for more systems become available. White dwarfs can also probe the gravitational force and do not seem to support large deviations from the Newtonian law.

This work was partially supported by the National Science Foundation through Grant AST85-15219.

REFERENCES

Adams, W. S. 1925 *Proc. Nat. Acad. Sci.*, **11**, 382.
Anthony-Twarog, B. J. 1982, *Ap. J.*, **255**, 245.
Blinnikov, S. I. 1978, *Astrophys. Space Sci.*, **59**, 13.
Chandrasekhar, S. 1934, *M. N. R. A. S.*, **95**, 207.
Echardt, D., Jekeli, C., Lazarewicz, A., Romaides, A. & Sands, R. 1987, *Phys. Rev. Lett.*, **56**, 3.
Eggen, O. J. & Greenstein, J. L. 1965, *Ap. J.*, **141**, 83.
Gatewood, G. D. & Gatewood, C. V. 1978, *Ap. J.*, **225**, 191.
Grabowski, B., Madej, J., & Halenka, J. 1987, *Ap. J.*, **313**, 750.
Greenstein, J. L., Boksenberg, A. L., Carswell, R., & Shortridge, K. 1977, *Ap. J.*, **212**, 186.
Greenstein, J. L., Oke, J. B., & Shipman, H. L. 1971, *Ap. J.*, **169**, 563.
Greenstein, J. L. & Trimble, V. L. 1967, *Ap. J.*, **149**, 283.

Hamada, T. & Salpeter, E. E. 1961, *Ap. J.*, **134**, 683.
Harrington, R. S., Christy, J. W., & Strand, K. Aa. 1981, *A. J.*, **86**, 909.
Holberg, J. B., Wesemael, F., Wegner, G., & Bruhweiler, F. C. 1985, *Ap. J.*, **293**, 294.
Hut, P. 1981, *Phys. Lett. B*, **99B**, 174.
Koester, D. 1987, *Ap. J.*, **322**, 852.
Koester, D. & Reimers, D. 1985, *Astr. Ap.*, **153**, 260.
Long, D. R. 1976, *Nature*, **260**, 417.
LoPresto, J. C. & Pierce, K. 1986, *Bull. Am. Astr. Soc.*, **18**, 989.
Luyten, W. J. 1962, *A Search for Faint Blue Stars XXXI. One Thousand Blue Stars in the Region of Praesepe*, (Univ. of Minnesota: Minneapolis).
Luyten, W. J. 1969, *Proper Motion Survey with the Forty-eight Inch Schmidt Telescope, XVII, Binaries with White Dwarf Components*, (Univ. Minnesota: Minneapolis).
McMahan, R. K. 1988, *Ap. J.*, in press.
Popper, D. M. 1954, *Ap. J.*, **120**, 316.
Romanishin, W. & Angel, J. R. P. 1980, *Ap. J.*, **235**, 992.
Sion, E. M. & Guinan, E. F. 1985, *Ap. J. (Letters)*, **265**, L87.
Stubbs, C., Adelberger, E., Raab, F., Gundlach, J., Heckel, B., McMurray, K., Swanson, H., & Watanabe, R. 1987, *Phys. Rev. Lett.*, **58**, 1070.
Sugimoto, D. 1972, *Prog. Theor. Phys.*, **48**, 699.
Thieberger. P. 1987, *Phys. Rev. Lett.*, **58**, 1066.
Thejll, P. & Shipman, H. L. 1986, *P. A. S. P.*, **98**, 922.
Trimble, V. L. & Greenstein, J. L. 1972, *Ap. J.*, **177**, 441.
Vessot, R. F. C. et al. 1980, *Phys Rev. Lett.*, **45**, 2081.
Wegner, G. 1973, *M. N. R. A. S.*, **165**, 271.
Wegner, G. 1974, *M. N. R. A. S.*, **166**, 271.
Wegner, G. 1978a, *M. N. R. A. S.*, **182**, 111.
Wegner, G. 1978b, *M. N. R. A. S.*, **187**, 17.
Wegner, G., 1979, *A. J.*, **84**, 650.
Wegner, G., 1980, *A. J.*, **85**, 1255.
Wegner, G. & Reid, I. N. 1987, in *Proc. IAU Colloq. 95, The Second Conference on Faint Blue Stars*, ed. A. G. D. Philip, D. S. Hayes, & J. W. Liebert, (L. Davis Press: Schenectady), p. 649.
Wegner, G., Reid, I. N., & McMahan, R. K. 1988, These proceedings.
Will, C. M. 1981, *Theory and Experimentation in Gravitational Physics*, (Cambridge University Press: Cambridge), p. 38ff.

THE SEARCH FOR CLOSE BINARY EVOLVED STARS

Rex A. Saffer and James Liebert
Steward Observatory, University of Arizona

ABSTRACT: We report on a search for short-period binary systems composed of pairs of evolved stars. The search is being carried out concurrently with a program to characterize the kinematical properties of two different samples of stars. Each sample has produced one close binary candidate for which further spectroscopic observations are planned. We also recapitulate the discovery of a close detached binary system composed of two cool DA white dwarfs, and we discuss the null results of Hα observations of the suspected white dwarf/brown dwarf system G 29-38.

I. INTRODUCTION

Evolved close binary systems have long been predicted to exist as the survivors of common envelope evolution in binary systems with much larger initial separations (cf. Iben and Tutukov 1979, 1984). Driven by gravitational wave radiation, their merger has been proposed to explain the origins of Type Ia Supernovae (SN Ia), the cataclysmic variables, some hot subdwarfs, and the helium-rich R CrB giants (Webbink 1979, 1984; Tutukov and Yungelson 1979, 1987; Iben and Tutukov 1984, 1987; Paczyński 1967, 1981, 1985; Tournambé and Matteucci 1986; Webbink and Iben 1987).

Although theoretical work in this area has proceeded apace, until recently the only observational results of the search for very short-period pairs of evolved stars have been negative. Robinson and Shafter (1987) reported null results from a comprehensive spectrophotometric radial velocity search for the very close white dwarf pairs of most interest for the merger hypothesis of SN Ia formation. They found no pairs with orbital periods between 30 seconds and 3 hours among their sample of 44 white dwarfs and concluded that close binaries in this period range cannot constitute more than 1/20 of the local population of white dwarfs. The discovery by Saffer, Liebert, and Olszewski (1988) of a close double DA white dwarf system with a period of 1.56 days (further described in §IV) confirms the existence of products of common envelope evolution, but it does little to explain the apparent lack of very short-period pairs. It is important to continue the search for both short-period and longer-period pairs in order to improve understanding of the late stages of stellar evolution.

II. OBSERVATIONS AND RADIAL VELOCITY MEASUREMENTS

All observations (save one described in §V) were obtained at the Multiple Mirror Telescope (MMT) Observatory. The echelle spectrograph and photon-counting Reticon were centered at either Hα or at He II λ4686. The first sample for which these observations have been obtained comprises a subset of the hot, helium-rich subdwarf O (SdO) stars drawn from the ultraviolet-excess surveys of Green, Schmidt, and Liebert (1986) and Downes (1986). Results from a second sample composed of white dwarf/M dwarf common proper motion pairs drawn from the Luyten catalogues will be discussed separately in detail (Oswalt, Hintzen, Sion,

and Liebert, in preparation). Multiple radial velocity measurements have been made only for the first sample. However, each sample has produced one evolved binary candidate for which spectroscopic follow-up is planned.

Figure 1 shows a) a typical spectrum of an sdO star showing absorption at He II λ4686 and b) a much higher quality spectrum showing an emission reversal in the line core. High resolution observations of sdO stars often show a sharp core in the He II λ4686 absorption line, making it possible to measure relatively precise radial velocities in spite of the Stark-broadened profiles and poor signal-to-noise ratios of most of the spectra. Radial velocities were measured by fitting modified Lorentzian profiles to the spectral features using the algorithm of Levenberg and Marquardt. Standard uncertainties were computed from the covariance matrices of the fits.

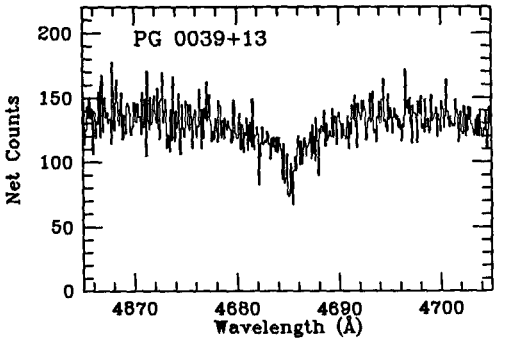

Figure 1a.

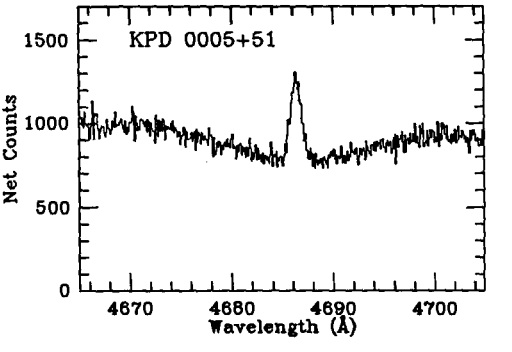

Figure 1b.

III. RESULTS FROM THE HOT SUBDWARF SAMPLE

We have measured radial velocities for 53 sdO stars drawn from the Palomar Green (PG) and Kitt Peak Downes (KPD) surveys (Green, Liebert, and Saffer, GLS, in preparation), of which 39 have two or more independent observations. Standard errors range from 10 km s^{-1} for stars with spectra having very sharp absorption cores or emission reversals to more than 100 km s^{-1} for stars with weak features or with spectra having very poor signal-to-noise ratios. Most measurements have standard errors of 30–50 km s^{-1}. Within the errors, only one star, PG 1102+499, shows radial velocity variations. Two spectra obtained in 1988 January and March show variation of the line profile shape (Figure 2). The velocity separation of the absorption cores in the March spectrum is $\Delta V = 124 \pm 42$ km s^{-1}. Further observations are scheduled to confirm the binary nature of the object and determine its orbital and stellar parameters. Of the remaining 39 objects with two or more independent observations, only 14 have weighted radial velocities which differ statistically from zero, and of these, only 3 have radial velocities exceeding ± 100 km s^{-1}. One object, PG 1047-066, has a single measured velocity of $+293.0 \pm 34.2$ km s^{-1} (Figure 3).

More observations are planned for those stars with only one radial velocity measurement. Even so, the 39 stars with 2 or more measurements constitute a statistically significant sample for characterizing the kinematic properties of the sdO stars in the solar neighborhood. The relative dearth of high-velocity stars indicates that 1) the stars in the sample are predominately young and old disk objects, and 2) the percentage of sdO stars with a close binary companion of comparable mass is small. The discovery of only one binary candidate does not strongly support the hypothesis that the blue and extended blue horizontal branch stars are the core helium-burning products of close binary evolution. However, the sample is composed of the very hottest subdwarfs ($T_{eff} \gtrsim 30{,}000$ K), and it well could include

stars hot and/or luminous enough to be normal products of post-asymptotic giant branch evolution. A better test of the binary hypothesis of hot subdwarf formation might be made using the subdwarf B (sdB) stars, since their range of temperatures better separates them from the post-AGB tracks of single stars.

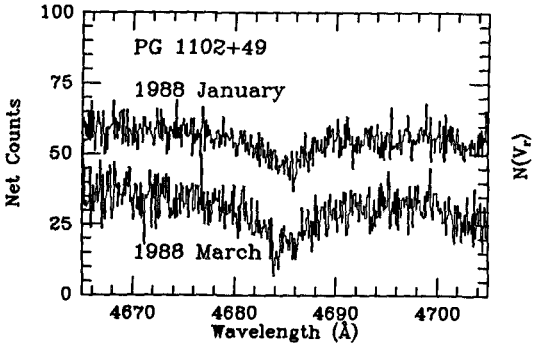

Figure 2.

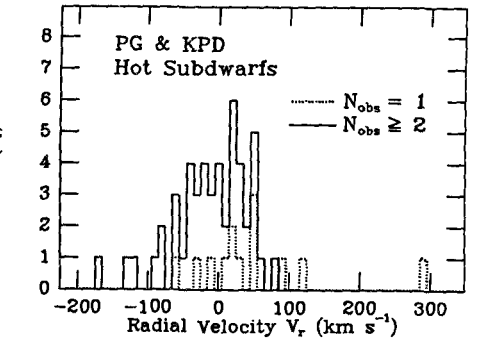

Figure 3.

IV. L 870-2: A CLOSE DOUBLE DA WHITE DWARF BINARY SYSTEM

In the 1988 November 15 issue of the Astrophysical Journal, Saffer, Liebert, and Olszewski (SLO, 1988) report the discovery that the well-studied cool white dwarf L 870-2 (EG 11, WD0135-052) is a double-lined spectroscopic binary composed of two DA white dwarfs. The orbital and stellar parameters of the system were determined from observations obtained at the MMT in 1987 September and November. Figure 4 shows representative spectra of the system at conjunction and quadrature, and Figure 5 shows the best-fit sine curves to all phased velocities measured when the two components were clearly resolved. The estimated orbital period is 1.56 days and the maximum velocity separation of the components is 147 km s^{-1}.

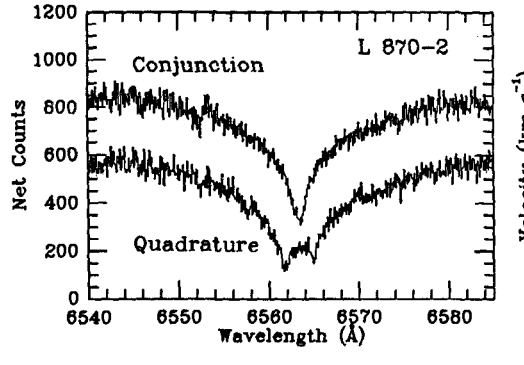

Figure 4.

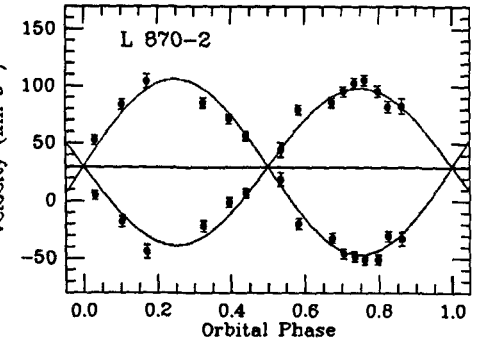

Figure 5.

Previous atmospheric and astrometric analyses indicate that the surface gravities and masses of the stars are significantly smaller than those of field white dwarfs (Koester, Schulz, and Weidemann 1979; Shipman 1979; Schulz and Wegner 1981; Greenstein 1985; Bergeron *et al.* 1988). Combined with the 1.56 day orbital period, the small masses imply that, if gravitational wave radiation is the only angular momentum loss mechanism, a merger will not occur for many Hubble times and will not produce a SN Ia. Even so, the existence of this system demonstrates that close detached pairs of degenerate stars *do* emerge from phases of common envelope evolution.

The circumstances surrounding the discovery of the binary nature of the system deserve further discussion. Greenstein (1985) showed that L 870–2 is 1.1 magnitudes overluminous in an H–R diagram plotting M_V versus the multichannel (g–r) color. In Figure 6, we show a similar diagram using the color (v–i)+(g–r) favored by Greenstein (1986) as the independent variable. In this diagram, L 870–2 lies some 1.5 magnitudes above the quadratic fit to the data. If the two components of an unresolved binary system contribute equally to the combined light, as SLO argue for L 870–2, the total luminosity should exceed that of a single star by 0.75 magnitude. The excess of 1.5 magnitudes can be explained by the smaller than average mass (and larger than average radius) of both components of the system. Another example is G 107–70, which was noted to be overluminous in the same diagram before it was discovered to be a barely-resolved binary (Strand, Dahn, and Liebert 1976). Thus, it may be possible to discover other close binary white dwarfs from spectroscopic or photometric observations of stars which appear overluminous in H–R diagrams, provided that accurate parallaxes can be measured. In fact, our own interest in the L 870-2 system in this regard has been driven strongly by its extremely accurate parallax measurement. We applaud and encourage the practitioners of this most venerable profession.

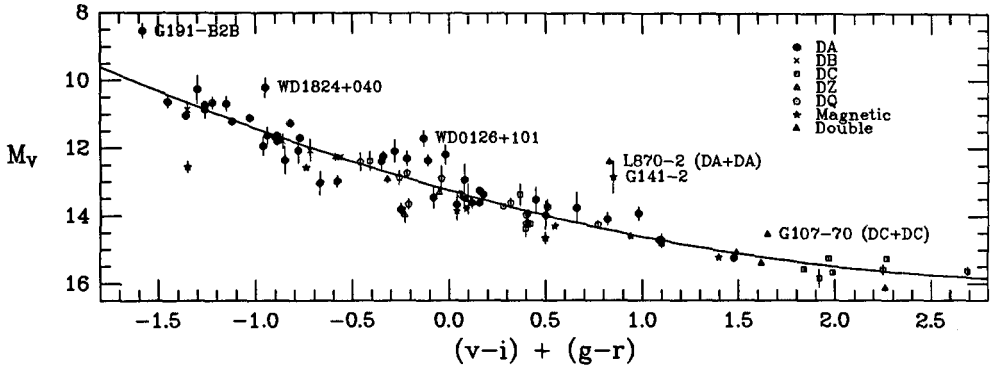

Figure 6.

V. Hα OBSERVATIONS OF THE SUSPECTED WHITE DWARF/BROWN DWARF BINARY SYSTEM G 29–38

We have obtained high dispersion spectroscopy of the Hα absorption line of the cool DA white dwarf G 29–38 (Liebert, Saffer, and Pilachowski, submitted). This is the star for which a recently detected infrared excess has been suggested to be due to a possible brown dwarf companion by Zuckerman and Becklin (1986, 1987). Echelle spectra obtained at the MMT and at the Mayall 4m telescope in 1987 December show no evidence for radial velocity variations larger than $\sim 1.1 \pm 8.7$ km s^{-1} and are used to derive a weighted heliocentric radial velocity $V_r = 33.7 \pm 4.3$ km s^{-1} for the white dwarf. Precise radial velocity measurements are possible in spite of the highly Stark-broadened Hα wings thanks to the presence of a sharp, non-LTE core. No emission component from the hypothesized secondary star is detected.

These negative results do not constitute strong evidence against the companion hypothesis, since the expected orbital velocity of the white dwarf component could be quite small (Shipman, MacDonald, and Sion, 1988), and the companion's line emission could be too faint to be detected. However, the observation of the sharp absorption core restricts the possible rotation of the white dwarf to $\leq$ 40 km s^{-1} and ensures that any surface magnetic field has a strength $\leq 10^5$ gauss. These results make it unlikely that the DA white dwarf has previously been spun up in a cataclysmic variable accretion phase.

VI. SUMMARY

In the past year, we have witnessed a veritable explosion of interest in and results from the search for close binary evolved stars. The discovery by SLO that L 870–2 is binary conclusively demonstrates that close detached pairs of evolved stars can and do emerge from post-main sequence evolution in binary star systems. The discovery of a binary hot subdwarf by GLS implies that the cores of the component stars need not have evolved to the degenerate configuration, and it raises questions which recommend the re-examination of the standard theories of post-main sequence evolution, especially as they apply to the formation of the hot subdwarfs.

VII. REFERENCES

Bergeron, P., Wesemael, F., Liebert, J., Fontaine, G., and Lacombe, P. 1988, these proceedings.

Downes, R. A., 1986, *Astrophys. J. Suppl.*, **61**, 569.

Green, R. F., Schmidt, M., and Liebert, J. 1986, *Astrophys. J. Suppl.*, **61**, 305.

Greenstein, J. L. 1985, *Publ. Astron. Soc. Pac.*, **97**, 827.

Greenstein, J. L. 1986, *Astron. J.*, **92**, 867.

Iben, I. and Tutukov, A. V. 1984, *Astrophys. J. Suppl.*, **54**, 335.

Iben, I. and Tutukov, A. V. 1987, *Astrophys. J.*, **313**, 727.

Koester, D., Schulz, H. and Weidemann, V. 1979, *Astron. Astrophys.*, **76**, 262.

Paczynski, B. 1967, *Acta Astron.*, **17**, 287.

Paczynski, B. 1981, *Acta Astron.*, **31**, 1.

Paczynski, B. 1985, Cataclysmic Variables and Low Mass X-Ray Binaries, Eds. D. Q. Lamb and J. Patterson, (Dordrecht: Reidel), p. 1.

Robinson, E. L. and Shafter, A. W. 1987, *Astrophys. J.*, **322**, 296.

Saffer, R.A., Liebert, J., and Olszewski, E. 1988, *Astrophys. J.*, **334**,, in press.

Schulz, H. and Wegner, G. 1981, *Astron. Astrophys.*, **94**, 272.

Shipman, H. L. 1979, *Astrophys. J.*, **228**, 240.

Shipman, H. L., MacDonald, J., and Sion, E. M. 1988, preprint.

Strand, K. Aa., Dahn, C. C., and Liebert, J. 1976, *Bull. A. A. S.*, **213**, 468.

Tournambè, A. and Matteucci, F. 1986, *M. N. R. A. S.*, **223**, 69.

Tutukov, A. V. and Yungelson, L. R. 1979, *Acta Astron.*, **29**, 665.

Tutukov, A. V. and Yungelson, L. R. 1987, Second Conference on Faint Blue Stars, (IAU Colloquium 95), Eds. A. G. D. Philip, D. S. Hayes and J. Liebert, (Schenectady: L. Davis Press), p. 435.

Webbink, R. F. 1979, White Dwarfs and Variable Degenerate Stars, (IAU Colloquium 53), Eds. H. M. Van Horn and V. Weidemann (Rochester: University of Rochester), p. 426.

Webbink, R. F. 1984, *Astrophys. J.*, **277**, 355.

Webbink, R. F. and Iben, I. 1987, Second Conference on Faint Blue Stars, (IAU Colloquium 95), Eds. A. G. D. Philip, D. S. Hayes and J. Liebert, (Schenectady: L. Davis Press), p. 445.

Zuckerman, B. and Becklin, E. E. 1986, *Astrophys. J. (Letters)*, **319**, L99.

Zuckerman, B. and Becklin, E. E. 1987, *Nature*, **330**, 138.

THE NEARBY BINARY, STEIN 2051 (G175-34AB)

K. Aa. Strand
3200 Rowland Place, NW
Washington, D.C. 20008

V. V. Kallarkal
U.S. Naval Observatory
Washington, D.C. 20392

ABSTRACT

Photographic observations of the large proper motion binary, Stein 2051, extended over the period 1966-87, do not support that it is a triple system as previously reported (Strand, 1977). The orbital motion is nearly linear over this interval; however, when results of plates from the Vatican Astrographic Zone from 1908-11 are included, a mass ratio is obtained, leading to a mass of $0.50\odot$ for the white dwarf component, given the calculated mass of $0.24\odot$ for the red dwarf component.

ASTROMETRIC RESULTS

Stein 2051 (04:31.2, +58°59' (2000)) is listed in the catalog of double stars from the Vatican Zone of the Astrographic Catalog (Stein, 1930). This binary has the largest proper motion discovered in the Lowell survey (Giclas et al., 1965), where it is designated G175-34AB and identified as Stein 2051, a white dwarf/main sequence dwarf binary.

A total of 251 plates was obtained with the U.S. Naval Observatory 61-inch astrometric reflector over the interval 1965-87. Both components on these plates were measured (by V.K.) on the semi-automatic measuring machine, using the same reference frame of seven stars for the epoch 1965.7 described in the previous paper (Strand, 1977). The combined solution gives a relative parallax of 0".178+".001 (m.e.), leading to an absolute parallax of 0".180, given the mean parallax of 0".002 for the reference stars (Vyssotsky and Williams, 1948).

The annual proper motions of the two components are 2".4217+".0001 (m.e.) towards 146°.9 and 2".3614+".0003 (m.e.) towards 144°.8 for the equinox 2000. These motions include the effects of the orbital motions

of the components, and since these must display equiform curves with the one shown by the relative motions of the two components, they can be derived by successive approximations by varying the proper motion of the system. This was accomplished by the determination of the equiform triangles displayed by an early, a midpoint, and a late epoch normal place (the Vatican 1910, USNO 1966, and the USNO 1985 places, respectively).

Comparing the dimensions of the triangle displayed by the relative motion of the two components with those of each of the two components, we find relative values of 0.674+.004 (m.e.) for A and 0.325+.005 for B yielding a mass ratio M_B/M_A of 2.07. The proper motion of the system is 2.3832 towards 145°.4, giving a tangential velocity of 60 km/sec, which is quite normal for an old disk population system.

MASSES OF THE COMPONENTS

The average of the Hardie and Heiser(1966) and the Eggen and Greenstein (1967) photometric results yield apparent magnitudes for the components of m_v(A)=11.09 and m_v(B)=12.44. With the above parallax the absolute magnitudes are M_v(A)=12.37 and M_v(B)=13.62. That for A is normal for a dM4 star, as classified by Eggen and Greenstein(1967).

Based upon a mass-visual magnitude relation established for late M-dwarf main sequence stars (Strand 1977), the mass of the A component is 0.24$\odot$. Using the mass ratio herin derived, the white dwarf has a mass of 0.50$\odot$. Eggen and Greenstein (1967), and Liebert (1976) have classified the spectrum as a CD white dwarf. Spectrophotometric scans and Stromgreen photometry were fit to model atmospheres with hydrogen/metal deficient composition by Liebert, who derived a temperature of 7050±400K, a radius of 0.011±.002R$\odot$, and a surface gravity of 8.03±.12.

Although the position angle of the relative orbit has changed 70 over the interval 1909-1987, the orbit is still indeterminate and is estimated to remain so for several centuries, because of the linear motion so far observed. The mass of the white dwarf depends, therefore, entirely upon the assumed mass of its red companion, and its uncertainty is therefore twice the uncertainty of that of the companion. estimated at 0.03. However, in view of the paucity of known masses of white dwarfs, Stein 2051B represents an important data-point on this subject. While it is slightly more massive than 40 Eri B (0.43), it is nearly equal in mass to each of the two white-dwarf components of the binary G107-70 (Harrington et al., 1981).

ACKNOWLEDGEMENTS

We are indebted to the staff of the U.S. Naval Observatory, Flagstaff Station, for the plates taken during the course of the general parallax program, and to R. S. Harrington for his assistance in the reduction of the data.

REFERENCES

Eggen, O.J. , Greenstein, J.L.: 1967, Astrophys.J.150,927
Giclas, H.L., Bunham, R.Jr., Thomas, N.G.: 1965, Lowell Obs.Bull.No.129
Hardie, R.H., Heiser, A.M.: 1966, Publ. Astron. Soc. Pacific 78, 171
Harrington, R.S., Christy, J.W., Strand, K.Aa.: 1981, Astron.J.86,909
Liebert, J.: 1976, Astrophys.J.210, 215
Strand, K.Aa.: 1977, Astron.J.82, 745

White Dwarfs in Globular Clusters

G.G. Fahlman and H.B. Richer
Department of Geophysics and Astronomy
University of British Columbia

I. Introduction

Surrounding the galaxy, with an aloofness appropriate to their great age, the globular clusters have played a starry role in the development of much of modern astronomy. In particular, they continue to be vital laboratories for testing our ideas of stellar evolution (Renzini and Fusi Pecci 1988). Through the study of cluster color-magnitude diagrams (CMD's), all the major phases in the life of a common low mass star can be traced, save one. The final sequence, the locus of cooling white dwarfs, remains unexplored. We are forced to glean our knowledge of this evolutionary phase from the study of a heterogeneous sample of relatively nearby stars. Although remarkable progress has been made, the prospect of observing white dwarfs in globular clusters offers the potential for new insights into old problems; e.g., the DA/DB dichotomy, and perhaps a resolution of some of the outstanding issues connected with the clusters themselves.

The advantages of using globular clusters for the study of white dwarfs include the following. (i) White dwarfs are the only known endpoint for the current population of stars in globular clusters. Indeed, this has been true for many billions of years and hence globulars should be <u>full</u> of white dwarfs. Estimates of their numbers will be given shortly. (ii) The clusters are rich and compact stellar systems so that a limited search area can be effective in discovering large numbers of white dwarfs. (iii) The white dwarfs in any one cluster are derived from a chemically homogeneous (with the known exception of ω Cen) and coeval parent population whose distance and age are reasonably well known. (iv) Given the apparently low incidence of duplicity in globular clusters, the evolutionary path of most stars should be unaffected by the complications of binary star evolution.

On the other hand, there are two serious obstacles to be faced. (i) The clusters are distant: the nearest has an apparent distance modulus of 12.3 mag. and a typical value is perhaps 15.0 mag. Even the brightest cluster white dwarfs appear as very faint objects. Direct observation of the vast majority of the white dwarf population is simply not feasible now or in the forseeable future. (ii) The stellar density within the cluster is high. Deep photometric fields are invariably crowded and therefore our ability to see the faint white dwarfs is severely compromised.

To the above, we might add that the globular clusters exhibit a metal deficiency compared to the disk stars and that there is a range of about 2 dex in metallicity among them. We should remain alert to the possibility that there could be systematic differences between the cluster white dwarfs and those commonly observed in the solar neighbourhood and further, that similar differences might exist from cluster to cluster.

II The Expected Number of White Dwarfs

There are two issues to be discussed: (i) the number of observable white dwarfs and (ii) the total number of white dwarfs in a cluster. The technique of estimating the number of bright and hence observable white dwarfs has been thoroughly discussed by Renzini (1985) following an earlier presentation by Fusi Pecci and Renzini (1979). Briefly, the method is based on the assumption that stars are conserved during their relatively rapid post main sequence (pms) evolution. Consequently the number of stars in any given pms phase is simply proportional to the time spent in that phase. The 'constant' of proportionality can be written as the product of the specific evolutionary flux and the visual luminosity of the cluster (Renzini and Buzzoni 1986, Renzini 1988).

We can take a more direct tact starting with the expression

$$N_{wd}(<M_v) = N_{hb}\ t_c(<M_v)\ /\ t_{hb} \tag{1}$$

where $N_{wd}(<M_v)$ is the number of white dwarfs brighter than absolute magnitude M_v; N_{hb}, the total number of stars now on the horizontal branch; $t_c(<M_v)$, the cooling time to reach M_v and t_{hb}, the horizontal branch lifetime. This expression is valid as long as the present value of N_{hb} does not differ sensibly from the past values, an assumption which is quite reasonable for any observable extent of the cooling sequence. Convenient expressions for the cooling times can be obtained from Green (1980):

$$\begin{aligned} \log t_c &= 4.85 + 0.32\ M_v \qquad & M_v > 11.3 \\ \log t_c &= -1.01 + 0.84\ M_v \qquad & M_v < 11.3 \end{aligned} \tag{2}$$

and for t_{hb} a value of 10^8 yrs may be used (Renzini 1977).

In principle N_{hb} can be obtained by simply counting the number of horizontal branch stars but this is generally practical only in a limited area of any given cluster. A summary of available data can be found in Buzzoni et al (1985).

We note that N_{hb} should be equal to the number of stars which evolve off the main sequence over the time t_{hb}. Turning to the isochrones of VandenBerg and Bell (1985), (for definiteness, we use the metal rich isochrone with Z=0.003, appropriate to M71; there will be some metallicity dependence in the following results), we find that the stellar mass at the turnoff (defined as the bluest point in the isochrone) changes by only $\Delta m_{hb} \approx 1.6 \times 10^{-3}\ M_\odot$ over the time t_{hb} at an age of 16 Gyr. While continuity of the mass spectrum of the cluster is debatable over such a small range, we nevertheless will assume that $N_{hb} = A\ f(m)\ \Delta m_{hb}$ where A is a normalization constant and f(m) is the functional form of the mass distribution. The constant A can be obtained by counting stars over some convenient interval. With CCD detectors, it is possible to reach well below the main sequence in many clusters and a suitable range to determine A would be from the turnoff to 3 magnitudes below. Designating this number by N_{-3}, we have

$$N_{hb} = N_{-3}\ \Delta m_{hb}\ /\ \Delta m_{-3} \approx 7.4 \times 10^{-3}\ N_{-3} \tag{3}$$

where $\Delta m_{-3} = 0.22$ from the isochrones. Substituting into equation (1), we find

$$N_{wd}(<M_v) = 6.8 \times 10^{-11}\ N_{-3} t_c\ (<M_v) \tag{4}$$

That this estimate of N_{wd} is consistent with Renzini's prescription can be shown as follows. A detailed study of the stellar population in M71 by Richer and Fahlman (1988b) demonstrates that essentially all the visible stellar luminosity comes from stars more massive than 0.33 $M_\odot$. Moreover, in that cluster the visible mass to light ratio is 0.57 and the mean mass of the stars involved is 0.63 $M_\odot$ so that $N(>0.33\ M_\odot) = 0.9\ L_v$. We find that $N(>0.33\ M_\odot) = 2.5\ N_{-3}$ and therefore

$$N_{wd}(<M_v) = 3.0\times10^{-11}\ L_v\ t_c\ (<M_v). \qquad (5)$$

This agrees completely with Renzini's (1988) result for M3. Although it must be admitted that exact agreement is fortuitous, our result certainly supports the basic correctness of Renzini's approach based on the concept of specific evolutionary flux.

Using the star counts of Lee (1977a,b,c), we have calculated the expected numbers of white dwarfs in three clusters with more or less complete data using equation (1). These are listed in Table 1. Taking the necessary data from the compilation of Webbink (1985), we have used equation (5) to estimate the number of bright white dwarfs in some nearby clusters. These are in Table 2. Since M4 (NGC 6121) appears in both tables, the difference in the estimates probably reflects the inherent uncertainty in these formulae.

Table 1

Predicted Number of White Dwarfs

Cluster	$(m-M)_v$	N_{HB}	$N_{WD}(M_v<)$		$N_{WD}(V<26)$
			10	12	
NGC 3201	14.15	175	43	857	767
NGC 6121	12.75	148	34	676	1699
NGC 6809	13.80	209	51	1024	1186

Table 2

White Dwarfs in Nearby Clusters

Cluster	$(m-M)_v$	$\log L_c/L_0$	$N_{WD}(M_v<10)$	$N_{WD}(V<26)$
47 Tuc	13.46	5.79	453	13400
ω Cen.	13.98	6.10	925	18929
NGC 6121	12.75	4.73	39	1982
NGC 6397	12.30	4.56	27	1850
NGC 6752	13.20	5.02	77	2800

In order to estimate the total population of white dwarfs, two important parameters are needed: (i) m_c, the upper mass limit for white dwarf progenitors and (ii) x, the mass spectral index, defined by a power law parameterization of the mass function, $dN/dm = A\ m^{-(1+x)}$. Neither of these parameters is without controversy and

the assumption of a power law may be particularly egregious. The total number of white dwarfs is then obtained from

$$N_d = A\int_{m_o}^{m_c} m^{-(1+x)} dm \qquad (6)$$

where m_o is the present day turnoff mass.

An upper limit to m_c of about 8-9 $M_\odot$ is set by the ability of a star to form a degenerate CO core after the exhaustion of central helium (Iben and Renzini 1983). Observationally, the existence of massive white dwarfs in the open cluster NGC 2516 shows convincingly that progenitor masses of up to 8 $M_\odot$ are possible at least in population I stars (Weidemann and Koester 1983). A value of $m_c = 5\ M_\odot$ is sometimes used as in Meylan (1988). This limit is based on the linear relationship between the initial, m_i, and final mass, m_{wd} proposed by Iben and Renzini (1983)

$$m_{wd} = 0.53\eta^{-0.082} + 0.15\eta^{-0.35}(m_i - 1) \qquad (7)$$

where η is a parameter scaling the mass loss rate. A value of $\eta = 1/3$ is generally consistent with the distribution of white dwarf masses (Weidemann and Koester 1983) and also with the masses of the nuclei of population II planetary nebulae (Heap and Augensen 1987). With $\eta = 1/3$, the above formula yields an upper limit of $m_i = m_c \approx 5M_\odot$. While equation (7) is certainly a convenient parameterization of a complex relationship, it is becoming evident that the mass lost is a function of the initial mass; i.e., $\eta = \eta(m_i)$ (Weidemann 1984, 1987). For this reason, the 5 $M_\odot$ limit is somewhat artificial. In practise the estimated numbers are not strongly dependent on m_c for values of $x \geq 1$.

One of the most remarkable results to emerge from the CCD studies of globular cluster luminosity functions is the apparent relationship between x and the cluster metallicity (McClure et al 1986). Metal rich clusters tend to have flat luminosity functions ($x \approx 0$) whereas the metal poorest have the steepest functions ($x \geq 1$). The initial result has been softened somewhat because of the question of mass segregation corrections (Pryor, Smith and McClure 1986) and some of the recent results on metal poor clusters are ambiguous (at best): see Richer, Fahlman and VandenBerg (1988) for a discussion of M30 and the results of Stetson and Harris (1988) for M92. It may well turn out that a single power law representation of the mass function is generally inappropriate as indicated for M13 by Drukier et al (1988). What does seem to be clear is that the metal rich clusters 47 Tuc (Hesser et al 1987) and M71 (Richer and Fahlman 1988b) have essentially flat luminosity functions to <u>well</u> below the turnoff.

We have calculated the expected number and total mass of white dwarfs in a strawman cluster with a luminosity of 10^5 $L_\odot$ where the light is assumed to come from stars between 0.8 and 0.4 $M_\odot$ with a mean mass of 0.6 $M_\odot$. The white dwarfs are assumed to have a mean mass of 0.6 $M_\odot$ and $m_c = 8\ M_\odot$. The results are shown in Table 3 where we have also listed the total mass of the progenitor stars, M_{pg}, and the mass lost by the cluster in forming the remnants, ΔM. It can be seen that the extrapolation of the flat mass functions, as seen in the metal rich clusters, implies an uncomfortably large mass lost during the early evolution of the cluster. A continuation of the mass function to even more massive stars, which presumably produce heavy remnants, exacerbates the problem.

Table 3

Total Number of White Dwarfs

X	N_{WD}	$M_{WD}/M_\odot$	$M_{pg}/M_\odot$	$\Delta M/M_\odot$
0	3.4×10^5	2.1×10^5	1.1×10^6	8.7×10^5
1	9.7×10^4	5.8×10^4	2.0×10^5	1.4×10^5
2	3.7×10^4	2.2×10^4	5.4×10^4	3.2×10^4

III Expected Properties of the White Dwarfs

Fusi Pecci and Renzini (1979) pointed out that the cosmic scatter in the masses of the observable white dwarfs is expected to be very small. They estimated $m_{wd} = 0.515 \pm 0.015\ M_\odot$, where the uncertainty reflects primarily the metallicity variation among the clusters.

Such a small spread is not an obvious result. The isochrones of VandenBerg and Bell (1985) show that a coeval population of clusters with a metallicity range $-0.49 > [Fe/H] > -2.27$ will have a systematic variation of about $0.08\ M_\odot$ in their turnoff masses at 16 Gyr. A strictly linear relationship between initial and final masses would give a corresponding systematic variation in the white dwarf masses.

Such a naive interpretation is unlikely to be correct. Before reaching the white dwarf state, the star must lose approximately $0.3\ M_\odot$ and even a slight differential mass loss with metallicity could well narrow (or broaden!) the original mass difference. Evidence that the initial mass range is ultimately narrowed comes from two observations discussed in Renzini and Fusi Pecci (1988): (i) the maximum luminosity on the AGB can be used to infer the mass of the CO degenerate core destined to become the white dwarf, and (ii) the eight post-AGB stars observed by de Boer (1985) appear to span a very small mass range, $\Delta m \approx 0.02\ M_\odot$ when compared to the corresponding Schönberner (1983) models. With regard to the former, the small number of identified AGB stars mitigates against finding the absolutely brightest possible star. For the latter, an additional point is the determination of the stellar luminosity contribution below the Lyman limit; de Boer assumed that this was the same as that for population I stars at the same effective temperature. In spite of these caveats, the observations do currently support the hypothesis of a small mass range among the white dwarfs in different clusters. The higher luminosities of the AGB stars in metal rich clusters suggests that they will have slightly more massive white dwarfs than their metal poorer cousins (see also Schönberner 1987).

A related question is the mass spread among the stars in a given cluster. For guidance here, we appeal to the recent models of synthetic horizontal branches reported by Lee, Demarque and Zinn (1988). These calculations are based on the assumption that the HB stars have a (truncated) Gaussian distribution in mass. The mass dispersion required for most clusters leads to a full width at half maximum in the distribution of $0.14\ M_\odot$. According to Renzini (1977), the mass spread in the resulting white dwarfs should be reduced by a factor of $\approx 1/6$ due to mass loss during the final AGB phases. Therefore, within the cluster, the typical mass spread should be $\Delta m \approx 0.02\ M_\odot$.

We conclude from this discussion that one can anticipate cluster cooling sequences to be very tightly delineated and to define almost identical loci irrespective of cluster metallicity. Of course, if observations should indicate otherwise, two possible culprits can be readily identified: (i) the mass loss mechanism, and (ii) non standard evolution.

The existence of a mass spread on the HB is direct evidence that the mass loss process must involve an unaccounted for stochastic component which allows rather substantial variations in the total mass lost. If similar stochastic factors apply along the AGB, it is not completely clear that the mass spread introduced along the HB will be decreased by the full factor of 1/6. Given that the termination of the AGB phase is controlled by the mass remaining in the envelope, it does seem reasonable to expect some reduction to occur.

The question of non standard evolution includes a number of issues. For example, a cluster like M15 has an extended blue HB which cannot be modelled with the parameters appropriate to other clusters (Lee, Demarque and Zinn 1988). Indeed, the whole issue of why differences exist in the HB morphology of clusters with similar metallicity (cf Buonanno, Corsi and Fusi Peci 1985) remains unresolved and points to a deficiency in our understanding of the parameters which control the late stages of stellar evolution (Fusi Pecci 1986). Whether such unknowns might manifest themselves in the white dwarf sequence is a moot point.

The possibility that stars may bypass the AGB or even the HB on their route to the white dwarf stage must be entertained. This can occur in the course of binary star evolution (Iben and Tutukov 1986) and is possibly the explanation for the two anomalous planetary nebula central stars described by Mendez et al (1988) which surely will become white dwarfs. We have already noted that binaries seem to be rare in globulars but there are two situations to be wary of: (i) the very open globulars tend to contain blue straggler stars whose masses appear to be about twice that of the subgiants (Nemec and Harris 1987), and (ii) those clusters in an advanced state of dynamical evolution, like M15, in which a large number of binaries may form in the core (see Elson, Hut and Inagaki 1987). A second possibilty is that HB stars with very small envelopes may evolve to the blue, through the sdB and sdO regions, and then to the white dwarf region (Schönberner and Drilling 1984, Heber et al 1987). This consideration is relevant to those clusters with extended blue horizontal branches, like M15 or NGC 6752.

An imaginative suggestion made by Bailyn et al (1988) is that the extended blue horizontal branch stars are the result of a collision between a main sequence star and a white dwarf. This leaves the latter with a small envelope and appearing as a blue drooper off the horizontal branch. It is interesting to note that the merger of two helium dwarfs considered by Iben and Tutukov (1986) would also result in an object appearing as an sdB which, as Caloi et al (1986) show, is just what a blue drooper looks like. These ideas raise the intriguing possibility that the blue droopers of horizontal branch are generically (if not filially) related to the blue stragglers of the main sequence.

Finally we note that Renzini (1985) has suggested that perhaps 20% of the post AGB stars might experience a final helium shell flash which could turn the star onto the path leading to a non-DA white dwarf. Given the observed difference between the high luminosity end of the DA and DB/DO sequences (Greenstein 1988), it appears that a

significant fraction of non-DA white dwarfs could confuse an intrinsically narrow cooling sequence.

The mass estimates for the bulk of the cooler white dwarfs depend on the initial-final mass relationship discussed in the last section. The practical issue is the number of white dwarfs whose masses exceed the mass of the visible stars. Such high mass remnants will be segregated in the central region of the cluster and, if sufficiently numerous, can have a significant influence on the dynamical evolution of the cluster. The linear relationship of Iben and Renzini (1983) predicts a rather larger number of higher mass remnants than the non-linear relationship favoured by Weidemann (1984). In any case, the mean mass of the white dwarfs is not expected to be very different from that of the luminous main sequence stars and so they should be distributed throughout the cluster, more or less following the surface brightness profile.

IV Observational Evidence for White Dwarfs in Globular Clusters

There are basically three approaches for studying the white dwarf population in globular clusters: (i) indirect, based on dynamical models of the cluster, (ii) semi-direct, based on observations of individual objects related to white dwarfs including immediate precursors and binary systems, and (iii) direct observation of individual white dwarfs. Each of these is discussed in turn below.

(1) Indirect Studies based on Globular Cluster Dynamics.

The basic mechanism forcing the evolution of a globular cluster is thought to be long range, gravitational two body encounters. This process, known as dynamical relaxation, drives the cluster toward a state of energy equipartition; a state which it can never achieve. The cluster developes a core-halo structure. The cores are collapsing toward, or have already reached, an almost singular state while the halo suffers a truncation from the tidal field of the Galaxy (see Elson, Hut and Inagaki 1987 for a recent review of this field).

In general, the structure of any cluster can be reasonably well represented by the well known King (1966) models. One important point to realize is that most of the available observational data pertains only to the luminous stars, chiefly those at the turnoff and the evolved stars above. These span an extremely narrow mass range. For this reason, the apparent agreement between the data and the single mass King models is somewhat illusionary. Dynamical relaxation leads to mass segregation in the cluster; the heavier stars are more centrally concentrated than the lighter stars. The bulk of the cluster mass may well be distributed quite differently from the relatively bright stars. However the internal motions of the stars depend on the total mass in the cluster and therefore information about the unseen mass, including the white dwarfs, can be obtained through kinematical studies.

Illingworth (1976), Pryor et al (1988) and Peterson and Latham (1987), among others, have measured the central velocity dispersion in a number of clusters. The results, interpreted with King models, show that the central values of the cluster mass to light ratio are in the range 1 - 3. Given that the visible stars typically have $M/L \leq 0.6$, this is clear evidence that about 2/3 of the cluster mass is

unaccounted for by the brighter stars. Of course the dim stars on the lower main sequence contribute to the mass. In principle, given a mass spectrum and a plausible low mass cutoff, it is possible to calculate their contribution and hence determine at least the total mass of dark remnants in the cluster. In practise, this is not likely to be a very meaningful exercise for two reasons. (i) The low mass stellar population is very poorly constrained by current data and may not be simply related (i.e., with a power law) to the more visible stars (Drukier et al 1988). (ii) Mass segregation must be taken into account. To model this, one needs to assume a global mass function and thus the problem becomes circular. Evidently more constraints are needed.

One approach is indicated by Richer and Fahlman (1988b) who were able to derive surface density profiles for stars in separate mass bins. Mass segregation is clearly seen but, within the framework of multimass King models, the data appears most consistent with a large population of low mass ($<0.3\ M_{\odot}$) stars. We were unable to place meaningful constraints on a dark remnant population.

A complementary technique is to observe the velocity dispersion profile. A few studies of this type have been done and are conveniently collected in Meylan (1987). Both the kinematical and surface brightness profiles (of the brighter stars) are simultaneously fit with a series of multimass King models. This exercise involves varying a number of parameters describing the mass spectrum, including dark remnants. A recent example is Meylan's (1988) discussion of 47 Tuc. He used equation (7) with $\eta = 1/3$ to specify the white dwarf population. From a grid of some 400 models, his best 15 all have about 1/3 of the present cluster mass in the form of white dwarfs. Unfortunately, what is not clear from this work (or other similar studies) is whether one is compelled by the data to include such a large white dwarf component.

In contrast to the above work, which is all based on King models, Murphy and Cohn (1988) have used the Fokker-Planck equation to model the evolution of a multimass component cluster through to the core collapsed phase, where the cluster exhibits a power law surface brightness profile near the center. Observations of the power law in two well observed clusters (M15 and NGC 6624) are shallower than the predicted slope for a single component cluster. Murphy and Cohn attribute this to the fact that dark heavy remnants can dominate the potential in the central power law region whereas the lighter, luminous stars are more dispersed. Both the apparent slope and the radial extent of the power law depend fairly sensitively on the fraction and maximum mass of the dark remnants. This result, upon development of the model to more closely match the evolution in real clusters, holds considerable promise for quantifying at least part of the remnant population.

(2) Semi-Direct Observations.

We have already mentioned the eight cluster post-AGB stars studied by de Boer (1985) and shown by Renzini (1985) to place very tight constraints on the mass range of cluster white dwarfs. This is a list which surely can be added to.

Another interesting group of stars worth further exploration in this context are the extremely blue horizontal branch stars of the kind found, for example, in NGC 6752. These have been studied recently by Caloi et al (1986), Crocker, Rood and O'Connell (1986), and Heber et al (1987). These stars appear to be 'ordinary' horizontal branch stars with extremely small envelope masses and may be related

(cluster analogues) to the field sdB stars. For sufficiently small envelope masses ($\leq 0.01\ M_{\odot}$), such stars are expected to evolve to the blue, passing through a hot sdO phase on their way to becoming white dwarfs (Heber et al 1987, see also Schönberner and Drilling 1984).

There is only one planetary nebula known to be in a globular cluster, K648 in M15, recently discussed in some detail by Adams et al (1984). The central star is one of the post-AGB objects studied by de Boer (1985) and is also discussed by Schönberner (1987) and Clegg (1987).

There are two known; i.e., spectroscopically confirmed, cataclysmic variables which are probably members of globular clusters, M5 V101 (Margon, Downes and Gunn 1981) and V4 in M30 (Margon and Downes 1983). Both appear to be examples of dwarf novae. They are very faint objects and apart from their existence little else can be said. However it might be noted that these two dim stars are the most tangible evidence currently available that there are indeed white dwarfs in globular clusters. Shara et al (1986) have identified a candidate for Nova 1938 in M14. Spectroscopic confirmation is needed since their object has rather odd colors, $(B-V)_o = 0.8 \pm 0.4$, $(U-B)_o = -0.3 \pm 0.4$, suggesting that the putative white dwarf has an evolved companion. A nova was also observed in M80 in the year 1860 but, in view of its proximity to the cluster center, will probably never be recovered (see further discussion in Trimble 1980).

To the above list we can probably add the low luminosity x-ray sources observed in the direction of globular clusters (Hertz and Grindlay 1983). Krolik (1984) and Hertz and Wood (1985) have suggested that these are the high luminosity end of a population essentially similar to the field cataclysmic variables. The binaries are believed to be the result of encounters between main sequence stars and an ambient population of about 5000 white dwarfs per cluster. These observations are perhaps the best evidence that a significantly large number of white dwarfs inhabit the globular clusters. A cautionary note has been sounded by Margon and Bolte (1987) who were unable to identify plausible optical candidates for the five sources listed by Hertz and Grindlay (1983) in ω Cen.

(3) Direct Observations

We finally come to the holy grail of this subject, unambiguous evidence for the white dwarf cooling sequence in globular clusters. There are two parts to the observational problem: (i) identifying, through photometric studies, plausible candidates for cluster white dwarfs and (ii) obtaining some spectroscopic confirmation that we are indeed dealing with bonafide white dwarfs. We have yet to get convincingly past the first part.

A recent photographic study by Chan and Richer (1986) in M4 has revealed a surprisingly large population of blue objects whose spatial distribution, after background subtraction, appears to follow the cluster surface brightness profile. Calibrated three color photometry is available for a subset of these objects and allows a further discrimination between background QSO's and potential cluster white dwarfs. Among the white dwarf candidates, there appears to be two groups separated in color (they are shown in Figure 2). The bluest group was identified with cluster white dwarfs and the redder group, with foreground white dwarfs. The cluster white dwarf candidates, it will be noted, are rather luminous with $M_V \leq 9.0$. Given the Lee

(1976b) counts of HB stars in M4, we would expect only 5 white dwarfs brighter than M_V=9.0 in the entire cluster. The five objects shown in the figure are certainly not a complete sample and therefore either there are many more luminous white dwarfs than expected or the observed objects are something else. The same problem, too many too bright candidates, also applies to an earlier study of NGC 6752 reported by Richer (1978).

The use of small field CCD's has largely supplanted photography and has been extensively used for deep photometric studies in globular cluster fields. Taking advantage of the superb imaging capability of the CFHT, we have made a detailed study of the relatively nearby cluster M71 using deep U,B,V exposures specifically to find the white dwarf cooling sequence (Richer and Fahlman 1988a). In that work we identified two groups of blue stars as shown in Figure 1.

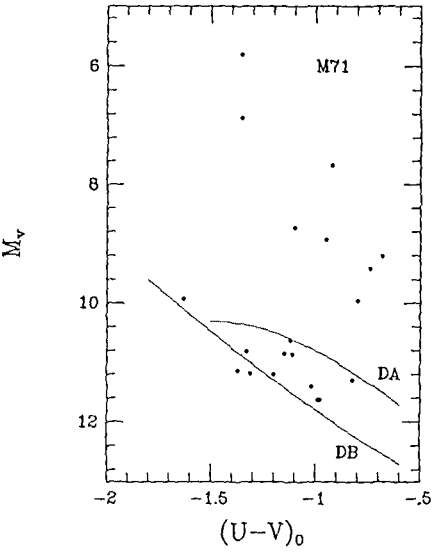

Figure 1. *The blue stars in M71 from Richer and Fahlman (1988a) are plotted. The lines show the DA and DB (He) sequences defined by the regression curves of Greenstein (1988).*

The fainter group looks very much like a white dwarf cooling sequence. With our adopted distance modulus of 13.7, the sequence does not match the locus of the field DA stars but instead appears to be in better agreement with the field DB sequence. An alternate explanation is that the sequence members are DA's but more massive (by about $0.1M_\odot$) than the field stars. Unfortunately these objects are still beyond spectroscopic study and so the issue remains open.

Recently Ortolani and Rosino (1987) have claimed that they have detected white dwarfs in their deep V, B-V CMD of ω Cen. Taken at face value, their objects appear to be a mixture of DA and DB stars. However, in view of the large scatter apparent at the faint end of their diagram, there is a need for further photometric study, particularly with U, to confirm the reality of these candidates.

In addition to the possible white dwarfs, there is another 'sequence' of blue objects in M71 which is clearly seen in Fig. 1. These stars are far too bright to

be cluster white dwarfs and too numerous to be foreground objects. Their colors are similar to those of field cataclysmic variables and we suggested that they may be cluster analogues of that group of objects. That this is no longer a viable explanation will be made clear shortly.

For convenience, the Chan-Richer objects found in M4 and the M71 blue stars are plotted together in Figure 2. Also shown are three hot sdO stars discovered by Drilling (1983) and analysed by Schönberner and Drilling (1984), and a group of 10 faint ($M_V \geq 6.0$) sdB stars discovered by Downes (1986). This diagram raises the interesting possibility that the three bright blue objects in M71 may be related to the sdO/sdB stars. The remaining bright blue objects in M71 seem to be similar in color to the 'foreground' group seen in M4. Finally, the faintest of the Schönberner-Drilling stars, LSE 21, which they note is close to the transition point between sdO's and the white dwarfs, is located near the luminous M4 candidates.

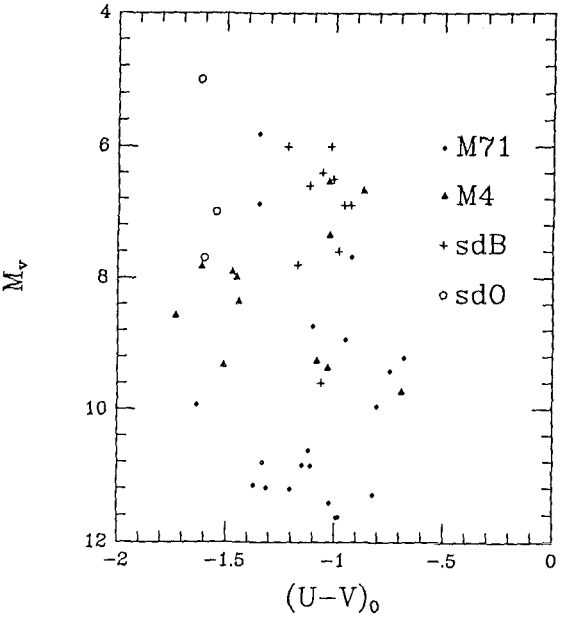

Figure 2. *The M71 blue stars, and the M4 white dwarf candidate from Chan and Richer (1986) are plotted together with a slection of 3 sdO stars and 10 sdB stars.*

Very recently, we were able to obtain low dispersion spectroscopic observations at the CFHT of the three bright blue stars in M71 and two stars in M4, one belonging to the 'foreground' group and the other belonging to the 'cluster' group. The data has not been fully analysed and so only very preliminary results can be discussed here.

The best data, naturally enough, was obtained for the brightest blue star in M71. A calibrated spectrum of this star is shown in Fig. 3 together with a spectrum of the standard sdB star F108. The Balmer lines, while noisy, are

clearly evident, He II lines cannot be convincingly identified and the general shape of the continuum suggests that the candidate is somewhat cooler than F108. It appears to be an sdB star. We emphasize that this data is a 'quick look' and will very likely be improved upon with further processing. The spectra of the other two M71 candidates are essentially similar but, as yet, too noisy to identify absorption lines with any confidence. However, they too are likely to be sdB stars.

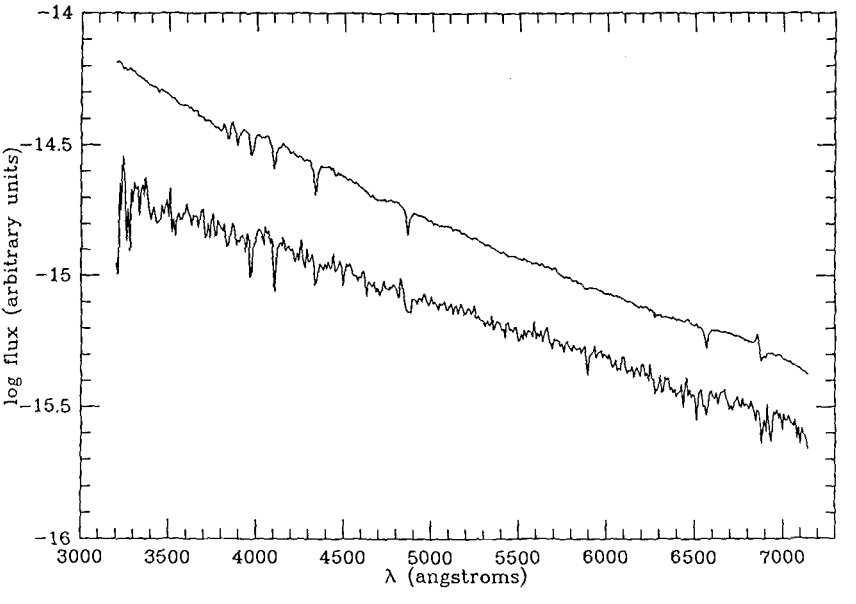

Figure 3. *The spectrum of the brightest blue star in M71 is shown together with the spectrum of the sdB standard star Fiege 108.*

The cluster membership of these stars is questionable. Downes (1986) finds that the space density of sdB's is about 2 x 10^{-6} pc^{3}. Given the distance to M71, 3.7 kpc, and the area of the sky surveyed, 24', we expect to see only 0.07 sdB stars in the foreground. However, the three stars could be in the background. The nearest would be at a distance of about 8.3 kpc and, if identified with the brightest star, have $M_V \simeq 4.0$, somewhat brighter than the mean magnitude of Downes' (1986) sample. The only mitigating factor is that the height of the object above the plane, at 660 pc, is higher than the sdB scale height of 325 pc found by Green, Schmidt and Liebert (1986).

The spectrum of brighter and redder M4 star, Chan-Richer #774, was poor because of some moonlight contamination but nevertheless it is clearly not the spectrum of a white dwarf. The bluer M4 candidate, CR-831, appears to be rather flat and featureless. For now its true nature remains unknown.

The bottom line is that we have not yet clearly identified a <u>single</u> white dwarf in any of the galactic globular clusters.

V Concluding Remarks

Where do we go from here? There is still very useful work to be done on the ground. The present generation of 4-m class telescopes, equipped with CCD detectors, is capable of identifying white dwarf candidates with deep broad band photometry in the nearer globular clusters. It is clear, however, that a convincing delineation of a white dwarf cooling sequence requires a dedicated effort, both to survey a sufficiently large area and to beat down the photometric errors. While expensive in terms of telescope time, such programs are far cheaper than the cost of making similar observations from space. When the planned new generation of large telescopes come on stream, deeper surveys will be possible and spectroscopic confirmation will become feasible. Of course, when HST (or perhaps its successor) is finally operational, many of the issues discussed here will be settled.

This research is supported with operating grants from the Natural Sciences and Engineering Research Council of Canada. The CFHT is operated by the National Research Council of Canada, the Centre National de la Recherche Scientifique de France and the University of Hawaii.

References

Adams, S., Seaton, M.J., Howarth, I.D., Auriere, M. and Walsh, J.R. 1984, M.N.R.A.S. 207, 471.
Bailyn, C.D., Grindlay, J.E., Cohn, H. and Lugger, P.M. 1988, 'The Harlow Shapely Symposium on Globular Cluster Systems in Galaxies', eds. J.E. Grindlay and A.G.D. Philip (Dordrecht:Reidel), p.679.
Buonanno, R., Corsi, C.E. and Fusi Pecci, F. 1985, Astr. Ap. 145, 97.
Buzzoni, A., Fusi Pecci, F., Buonanno, R. and Corsi, C.E. 1985, Astr. Ap. 128, 94
Caloi, V. et al 1986, M.N.R.A.S. 222, 55.
Chan, E. and Richer, H.B. 1986, Ap. J. 302, 257.
Clegg, R.S. 1987, 'Stellar Evolution and Dynamics in the Outer Halo of the Galaxy', eds. M.Azzopardi and F. Matteucci (ESO), p.543.
Crocker, D.A., Rood, R.T. and O'Connell, R.W. 1986, Ap.J. (Lett), 309, L23.
de Boer, K.S. 1985, Astr. Ap. 142, 321.
Downes, R.A. 1986, Ap.J. Suppl. 61, 569.
Drilling, J.S. 1983, Ap.J. (Lett), 270. L13.
Drukier, G.A., Fahlman, G.G., Richer, H.B. and VandenBerg, D.A. 1988, A.J. 95, 1415.
Elson, R., Hut, P. and Inagaki, S. 1987, Ann. Rev. Astr. Ap. 25, 565.
Fusi Pecci, F. 1986, ' Spectroscopic and Photometric Classification of Population II Stars', ed. A.G.D. Philip (Schenectady:L. Davis Press), p.83.
Green, R.F. 1980, Ap.J. 238, 685.
Green, R.F., Schmidt, M. and Liebert, J. 1986, Ap.J. Suppl. 86, 305.
Greenstein, J. 1988, P.A.S.P. 100, 82.
Heap, S. and Augensen, H.J. 1987, Ap.J. 313, 268.
Heber, U., Kruditzki, R.P., Caloi, V.,Castellani, V. and Danziger, J. 1987, 'Stellar Evolution and Dynamics in the Outer Halo of the Galaxy', eds. M.Azzopardi and F. Matteucci (ESO), p.407.
Hesser, J.E. et al 1987, P.A.S.P. 99, 739.
Hertz, P. and Grindlay, J.E. 1983, Ap.J. 275, 105.
Hertz, P. and Wood, K.S. 1985, Ap.J. 290, 171.
Iben I. Jr. and Renzini, A. 1983, Ann. Rev. Astr. Ap. 21, 271.
Iben I. Jr. and Tutukov, A.V. 1986, Ap.J. 311, 742.
Illingworth, G. 1976, Ap.J. 204, 73.
King, I. 1966, A.J. 71, 64.
Krolik, J.H. 1984, Ap.J. 282, 452.

Lee, S.W. 1977a, Astr. Ap. Suppl. 27, 367.
Lee, S.W. 1977b, Astr. Ap. Suppl. 27, 381.
Lee, S.W. 1977c, Astr. Ap. Suppl. 28, 409.
Lee, Y.-W., Demarque, P. and Zinn, R.J. 1988, 'Second Conference on Faint Blue Stars', ed. A.G.D. Philip (Schenectady:L. Davis Press).
Margon, B. and Bolte, M. 1988, Ap.J. (Lett) 321, L61.
Margon, B. and Downes, R.A. 1983, Ap.J. (Lett) 274, L31.
Margon, B., Downes, R.A. and Gunn, J.E. 1981, Ap.J. (Lett) 247, L89.
McClure, R.D. et al 1986, Ap.J. (Lett) 307, L49.
Mendez, R.H., Groth, H.G., Husfeld, D., Kudritzki, R.P. and Herrero, A. 1988, Astr. Ap. 197, L172.
Meylan, G. 1987, 'Stellar Evolution and Dynamics in the Outer Halo of the Galaxy', eds. M.Azzopardi and F. Matteucci (ESO), p.665.
Meylan, G. 1988, Astr. Ap. 191, 215.
Murphy, B.W. and Cohn, H. 1988, M.N.R.A.S. 232, 835.
Nemec, J.N. and Harris, H.C. 1987, Ap.J. 316, 172.
Ortolani, S. and Rosino, L. 1987, Astr. AP. 185, 102.
Peterson, R.C. and Latham, D.W. 1986, Ap. J. 305, 645.
Pryor, C., Smith, G.H., McClure, R.D. 1986, A.J. 92, 1358.
Pryor, C., McClure, R.D., Fletcher, J.M., and Hesser, J.E. 1988, 'The Harlow Shapely Symposium on Globular Cluster Systems in Galaxies', eds. J.E. Grindlay and A.G.D. Philip (Dordrecht:Reidel), p.661.
Renzini, A. 1977, ' Advanced Stages Of Stellar Evolution', eds. P.Bouvier and A. Maeder (Geneva Obs.), p.149.
Renzini, A. 1985a, Astronomy Express 1, 177.
Renzini, A. 1985b, 'Horizontal Branch and UV-Bright Stars', ed. A.G.D. Philip (Schenectady:L. Davis Press), p.19.
Renzini, A. 1988, 'The Harlow Shapely Symposium on Globular Cluster Systems in Galaxies', eds. J.E. Grindlay and A.G.D. Philip (Dordrecht:Reidel), p.443.
Renzini, A., and Buzzoni, A. 1986, 'Spectral Evolution of Galaxies', ed. C. Chiosi and A. Renzini (Dordrecht:Reidel), p.135.
Renzini, A., and Fusi Peci, F. 1988, Ann. Rev. Astr. Ap. 26.
Richer, H. B. 1978, Ap.J.(Lett) 224, L9.
Richer, H. B. and Fahlman, G. G. 1988a, Ap.J. 325, 218.
Richer, H. B. and Fahlman, G. G. 1988b, Ap.J., in press.
Richer, H. B., Fahlman, G. G. and VandenBerg, D.A. 1988, Ap.J. 329, 187.
Schönberner, D. 1983, Ap.J. 272, 708.
Schönberner, D. 1987, 'Stellar Evolution and Dynamics in the Outer Halo of the Galaxy', eds. M.Azzopardi and F. Matteucci (ESO), p.519.
Schönberner, D. and Drilling, J.S. 1984, Ap.J. 278, 702.
Shara, M., Moffat, A.F.J., Potter, M., Hogg, H.S. and Whelau, A 1986, Ap.J. 311, 796.
Trimble, V. 1980, 'Star Clusters', ed. J.E. Hesser (Dordrecht:Reidel), p.259.
VandenBerg, D. A. and Bell, R..A. 1985, Ap.J. Suppl. 58, 561.
Webbink, R.F. 1985, 'Dynamics of Star Clusters', eds. J.Goodman and P. Hut (Dordrecht:Reidel), p.541.
Weidemann, V. 1984, Astr. Ap. 134, L1.
Weidemann, V. 1987, 'Late Stages of Stellar Evolution', eds. S. Kwok and S.R. Pottasch (Dordrecht: Reidel), p. 347.
Weidemann, V. and Koester, D. 1983, Ast. Ap. 121, 77.

TOWARD A DETERMINATION OF THE HELIUM ABUNDANCE IN COOL DA WHITE DWARFS

P. Bergeron, F. Wesemael, and G. Fontaine
Département de Physique, Université de Montréal

Convective mixing between the thin superficial hydrogen layer and the more massive and deeper helium layer is generally believed to be responsible for the increased number of non-DA white dwarfs relative to the number of DA below 10000K (see Sion 1984 and references therein). However, because of the spectroscopic invisibility of the helium lines at effective temperatures below 13000K, the true atmospheric composition of these cool stars remains somewhat uncertain. On theoretical grounds, studies of the evolution of white dwarfs on the cooling sequence have shown that if the hydrogen layer is thicker than $\sim 10^{-6} M_{\odot}$, convective mixing does not occur (Tassoul, Fontaine, and Winget 1988). Furthermore, the exact amount of helium pollution is very sensitive to the thickness of the hydrogen layer. It seems therefore imperative to evaluate to what extent DA stars below 13000K truly are hydrogen-rich. In line with our previous efforts geared toward an understanding of the atmospheric properties of the cool DA white dwarfs, we present new insights into the spectroscopic modelling of these cool stars, and also demonstrate, for a particular object, how the helium abundance might be determined.

Despite its spectroscopic invisibility, the helium abundance can be inferred from its effect on the Balmer lines through increased pressure ionization (Wehrse 1977; Liebert and Wehrse 1983; Bergeron, Wesemael, and Fontaine 1987, Paper I hereafter). In order to evaluate properly this spectroscopic diagnostic, a detailed model of pressure ionization is required. As discussed briefly in Paper I, Hummer and Mihalas (1988) have recently developed such a model where the pressure ionization is treated with an occupation probability formalism. For each atomic level of the hydrogen atom, an occupation probability w is assigned: the electron has a probability w of being bound to the atom, and a probability 1-w of being ionized. In the Hummer-Mihalas formalism, this occupation probability is governed by two

different types of perturbers: the charged and neutral particles. The combined occupation probability can be expressed as the product of both perturbations, $w=w_{charged}w_{neutral}$.

Within this occupation probability framework, some care must be taken in calculating the bound-bound opacity, or the bound-free opacity from dissolved atomic levels (Däppen, Anderson, and Mihalas 1987). In particular, these dissolved levels will produce a smooth pseudo-continuum opacity similar to the Inglis-Teller prescription. The inclusion of the Hummer-Mihalas formalism in the context of the spectroscopy of cool DA white dwarfs is illustrated in Figure 1, where synthetic spectra of two characteristic models at log g=8.0 are displayed.

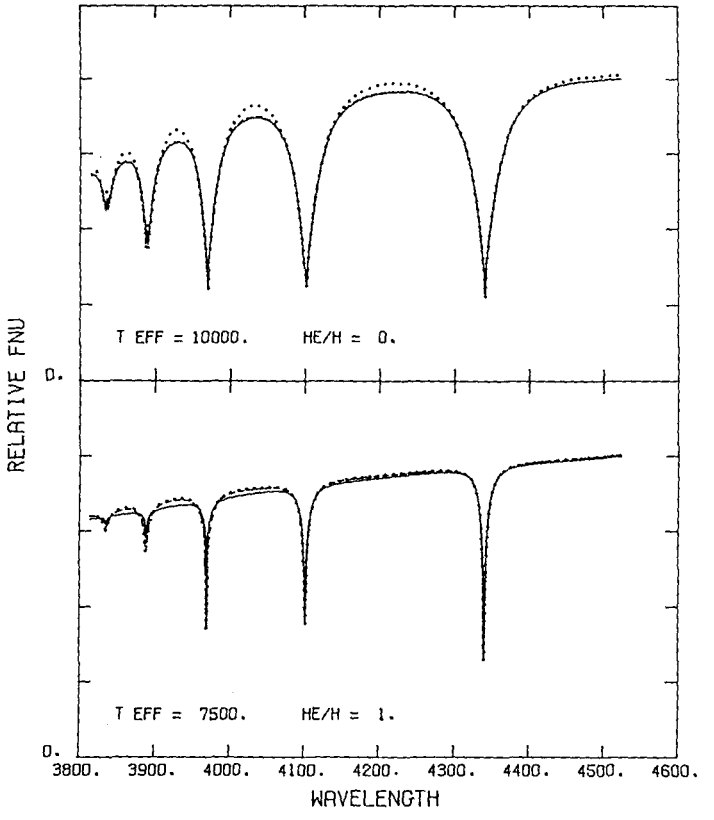

Fig. 1. Comparison of synthetic spectra using an occupation probability unity (dotted line), the full occupation probability including perturbations from both charged and neutral particles (solid line), and from charged particles only (dashed line).

Spectra at both temperatures have been calculated with different versions of the occupation probability. The dotted line is calculated with an occupation probability unity for each atomic level. This approximation corresponds to a large extent to previous spectroscopic analyses. The solid line represents the calculation obtained with the full occupation probability w, while the dashed line takes into account only the contribution from the charged particles (e.g. $w_{neutral}=1$).

In the hotter pure hydrogen model (top panel), the solid and dashed lines are superposed, thus showing that the main contribution to the occupation probability comes from the charged particles. The neutral particle density of hydrogen is too low to modify significantly w. We note also that the full occupation probability treatment does not affect the line centers, even for the higher Balmer lines. What is dramatically modified however, is the increased contribution of the pseudo-continuum opacity produced by dissolved upper atomic levels, in spectral regions where the line opacity is relatively unimportant. Spectroscopic analyses of DA stars using this newer formalism, particularly *in the region of ZZ Ceti stars*, could shift temperatures to higher values than estimated from previous studies (e.g. Daou *et al.* 1988).

In the cooler model with an increased helium abundance (lower panel), the contribution from the charged particles is completely negligible (the dashed and dotted lines are superposed). Once again, the pseudo-continuum between the Balmer lines is affected by the Hummer-Mihalas formalism but, this time, through the perturbations from the neutral particles. However, in cool pure hydrogen models where the photospheric pressure and the neutral particle density are decreased, the pseudo-continuum contribution is significantly reduced, and does not affect the determination of effective temperatures (Bergeron *et al.* 1988). In the particular model presented on the lower panel, the helium signature is clearly noticeable from a close examination of the higher Balmer lines, when the perturbation from the neutral particles is included.

These considerations can be used to infer the helium abundance, as first suggested by Wehrse (1977), and Liebert and Wehrse (1983). The sensitivity of the predicted line profiles on the helium abundance is clearly illustrated in Figure 2 where the spectrum of the DA white dwarf GD25 (Gr312) is displayed, along with three synthetic spectra at log g=8.0 and different helium to hydrogen ratios. For

each model, the effective temperature was obtained from the best fit to H_γ and H_δ as these lines are less sensitive to the presence of helium (or to a variation of gravity) than H_ϵ or higher Balmer lines. It is obvious that a fit to the whole spectrum requires a helium to hydrogen ratio in GD25 of the order of ~1.

One particular aspect that has not been considered yet is the effect of the assumed surface gravity. Despite the analytical arguments considered by Liebert and Wehrse (1983), a careful reanalysis (Bergeron, Wesemael, and Fontaine 1989) clearly demonstrates that *helium abundance and gravity effects cannot be separated*; this conclusion is independent of the exact treatment of the occupation probability. Therefore, the GD25 spectrum could as well be fit with a pure hydrogen spectrum, but with an increased surface gravity. One way of avoiding this uncertainty is to look at a large sample of cool DA white dwarfs, and assume a mean surface gravity of log g=8.0. Such a large sample of objects is currently under investigation using this technique.

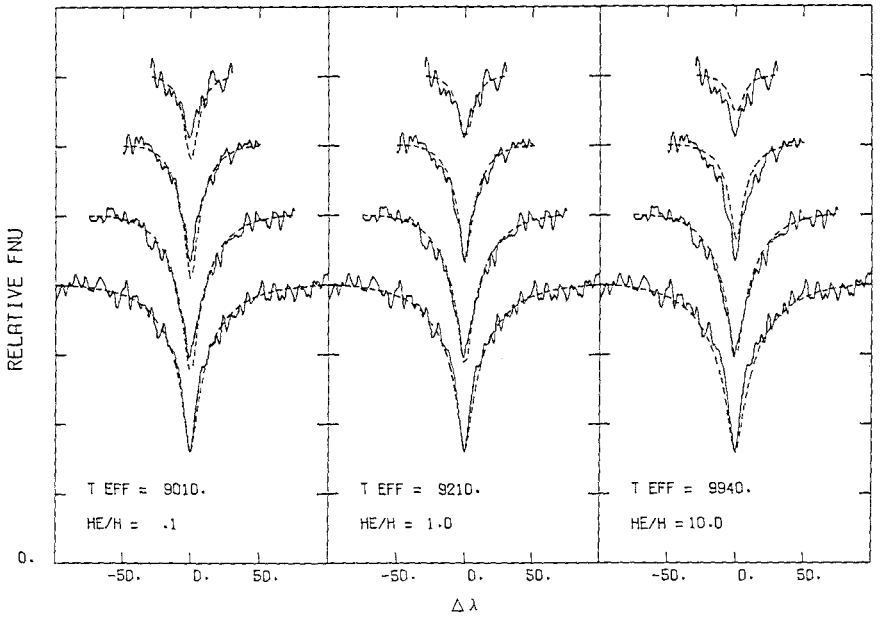

Fig. 2. Comparison of the spectrum of GD25 (from top to bottom H_β to H_γ) with our best fit at different helium to hydrogen ratios.

Preliminary results indicate that the fit obtained for GD25 is not a unique occurence, and that a fair number, and probably most of the cool DA white dwarfs below ~10000K are best fit with atmospheres with helium abundances He/H~0.1, with a few objects as high as He/H~10. Because the surface gravity distribution of DA white dwarfs is expected to be very narrow (Weidemann and Koester 1984), this result opens up the tantalizing possibility of actually measuring the thickness of the hydrogen layer in DA stars through abundance analyses.

This work was supported in part by the NSERC Canada, and by a E.W.R. Steacie Fellowship to one of us (GF).

Bergeron, P., Wesemael, F. and Fontaine, G. 1987, in IAU Colloquium 95, The Second Conference on Faint Blue Stars, eds. A.G.D. Philip, D.S. Hayes and J. Liebert, (Schenectady: L. Davis Press), p.661 (Paper I).

Bergeron, P., Wesemael, F. and Fontaine, G. 1989, in preparation.

Bergeron, P., Wesemael, F., Liebert, J., Fontaine, G. and Lacombe, P. 1988, these Proceedings.

Daou, D., Wesemael, F., Bergeron, P., Fontaine, G. and Holberg, J.B. 1988, these Proceedings.

Däppen, W., Anderson, L. and Mihalas, D. 1988, *Astrophys. J.*, **319**, 195.

Hummer, D.G. and Mihalas, D. 1988, *Astrophys. J.*, **331**, 794.

Liebert, J. and Wehrse, R. 1983, *Astron. Astrophys.*, **122**, 297.

Sion, E.M. 1984, *Astrophys. J.*, **282**, 612.

Tassoul, M., Fontaine, G. and Winget, D. 1988, in preparation.

Wehrse, R. 1977, *Mem. Soc. Astron. Italiana*, **48**, 13.

Weidemann, V. and Koester D. 1984, *Astron. Astrophys.*, **132**, 195.

CONSTRAINTS ON THE ATMOSPHERIC PARAMETERS OF THE BINARY DA WHITE DWARF L870-2 (EG11)

P. Bergeron, F. Wesemael
Département de Physique, Université de Montréal
J. Liebert
Steward Observatory, University of Arizona
G. Fontaine, P. Lacombe
Département de Physique, Université de Montréal

The recent discovery that the cool DA white dwarf L870-2 (EG11, WD0135-052) is a double-lined spectroscopic binary composed of a detached pair of DA white dwarfs (Saffer, Liebert, and Olszewski 1988, SLO hereafter) has raised some challenging problems for stellar evolution theories of such binary systems. One first important step in the understanding of this short-period system is to establish the atmospheric parameters of each component. SLO have argued from previous determinations of the effective temperature and absolute magnitude of the system, and also from their own study of the composite H_α profile, that the two components should be similar. We wish here to reexamine this assertion by taking a new look at the constraints on the two components brought about by the available observational data.

As first pointed out by SLO, L870-2 has widely been used as a photometric standard. In particular, several spectra of L870-2 at 2.25 Å resolution have been obtained with the Steward Observatory 2.3m reflector and blue photon-counting Reticon in the course of our current study of the atmospheric properties of cool DA white dwarfs (e.g. Lacombe *et al.* 1983; Bergeron, Wesemael, and Fontaine 1987, 1988). The average optical spectrum covering the high Balmer lines is displayed on Figure 1 together with the spectrum of G74-7 (EG168), a DAZ white dwarf with similar effective temperature and discussed by Lacombe *et al.* (1983). From this comparison alone, L870-2 does not appear to differ much from other garden variety hydrogen-line stars at that temperature. A particularly noteworthy fact is that this combined

optical spectrum can be fit by a single component spectrum. Using a newly developed grid of model atmospheres appropriate to the study of cool DA white dwarfs (Bergeron, Wesemael, and Fontaine 1987, 1988), we obtain for L870-2 an effective temperature of 7240K±75K, with a surface gravity of 7.8±0.1. The resulting fit is displayed on Figure 2. Our effective temperature is in good agreement with those previously obtained under similar assumptions by Koester, Schulz, and Weidemann (1979, T_e=7254K), Shipman (1979, T_e=7300K), and Schulz and Wegner (1981, T_e=7500K). A comparison of surface gravities determined by these authors is not appropriate here, since all have used the measured parallax to first constrain the radius of the purported single star. However, the surface gravity obtained by Schulz and Wegner (1981) from equivalent widths *alone*, yields a value near log g=7.9, entirely consistent with our determination. Thus, a first constraint can already be imposed from this spectroscopic evidence, namely that *the summed spectra from both components must be fit by a single spectrum at T_e=7240K and log g=7.8.*

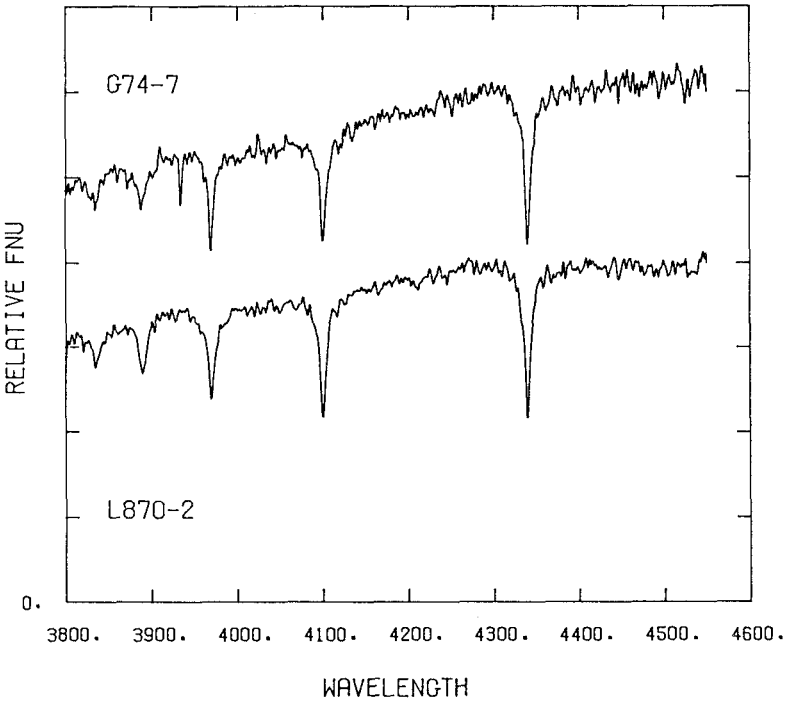

Fig. 1. Comparison of the spectrum of L870-2 with the spectrum of G74-7, a single DAZ white dwarf with similar effective temperature.

A second constraint is obtained from the study of the kinematics of the binary system. SL0 have estimated the radial velocity semiamplitude for each component as K_1=77.6 km s^{-1} and K_2=69.6 km s^{-1}, which corresponds to a mass ratio of $q=\frac{M_2}{M_1}=1.115$. Our second constraint is thus that *the surface gravities of both components be consistent with a mass ratio of 1.115*.

A third constraint comes from the Strömgren photometry. Because (u-b) ceases to be gravity sensitive at the low effective temperature of L870-2 (Fontaine *et al.* 1985), not much can be learned from this particular color index. The color index (b-y), however, is temperature sensitive. Fontaine *et al.* (1985) have measured (b-y)=0.274±0.019 for L870-2 which agrees with other values quoted in McCook and Sion (1987). The Strömgren photometry thus imposes that *the (b-y) obtained from the sum of spectra of both components yield a value consistent with the measured value of 0.274*.

Finally, a fourth constraint is obtained from the measured luminosity excess. Greenstein (1985) has determined from measurement of m_V and from an accurate trigonometric parallax, that L870-2 has a luminosity excess of 1.1 magnitude from its mean (G-R)-M_V relation (or equivalently (b-y)-M_V). This result can be translated into total luminosity if, as we argue below, the two components have similar effective temperatures. Accordingly, the binary system has a total luminosity ~2.75 times larger than that of a single star which would have the same color ((G-R) or (b-y)) as L870-2 but at log g=8.0, the gravity most appropriate to the mean relation defined by Greenstein. From our (b-y)-T_e calibration, we obtain for (b-y)=0.274 an effective temperature of 7280K, completely consistent with the previous estimate of the spectroscopic temperature. We thus express the fourth constraint by requiring that *the sum of the individual luminosities from each component be equal to the observed total luminosity*.

In order to reconcile all these constraints, we use the following procedure. Firstly, for a given set of surface gravities (g_1, g_2), consistent with the estimated mass ratio of 1.115 (second constraint), we add the surface fluxes (weighted by the respective radii assuming a carbon core composition) for a large set of effective temperature couples (T_1, T_2). A grid at log g=7.8 (first constraint) is then used to fit these spectra in terms of a single star and to determine the best-fitting temperature for each of these combined spectra. The locus of spectra which yield a

spectroscopic effective temperature of 7240K is then plotted on a (T_1, T_2) diagram. An example of such a diagram is shown on Figure 3 where the solid line represents the desired locus of model combinations: on this line, the combined optical spectra are all rigorously equivalent and can be fit by a single DA star at 7240K, log g=7.8. However, we should point out that this *best* fit does not represent necessarily a *good* fit to the observed spectrum. Secondly, we follow the same procedure but this time, calculate the Strömgren color index (b-y) and define in the (T_1, T_2) diagram the locus of constant (b-y)=0.274, consistent with the third constraint (dashed line). Finally, we plot on the same diagram the locus of models with the appropriate overluminosity, according to the fourth constraint (dash-dotted line).

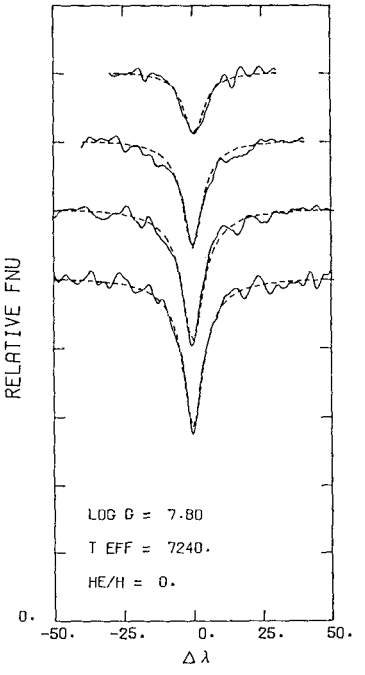

Fig. 2. Comparison of the spectrum of L870-2 (from top to bottom, H_β to H_γ) with our best fit, under the assumption of a single DA star.

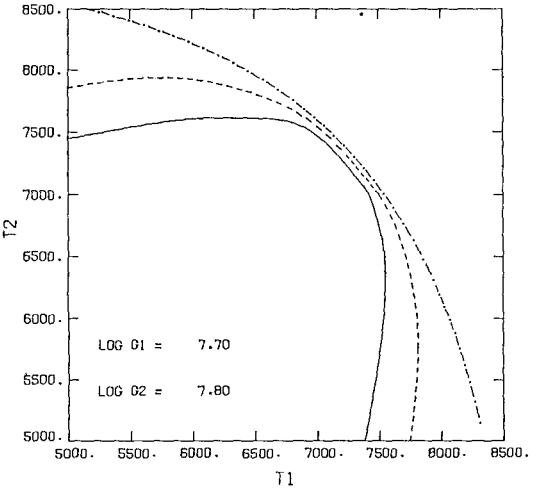

Fig. 3. Fitting diagram for the temperature of each component, constrained by spectroscopy (solid line), photometry (dashed line), and luminosity (dash-dotted line). The solution shown also satisfies the constraint imposed on the mass ratio of the components.

For the binary system L870-2, components with surface gravities of log g_1=7.7 and log g_2=7.8 represent the best estimated fit (Figure 3). From the mass-radius relation for a *carbon core composition* (Winget, Lamb, and Van Horn 1988), the corresponding masses are M_1=0.42$M_\odot$ and M_2=0.47$M_\odot$. As can be seen, in order to match the Strömgren photometry and luminosity requirements, the effective temperatures of both components cannot differ significantly. A conservative estimate of the range of effective temperatures varies from T_1=6750K, T_2=7585K to T_1=7470K, T_2=6830K, with all the intermediate cases equally acceptable. This conclusion is also consistent, as pointed out by SLO, with the observation that the H_α profiles at quadrature differ in depth by only ~30%. In principle, these H_α profiles could serve as another observational constraint to further narrow the temperature and/or gravity range of the system components. Clearly, this work represents only an exploratory investigation of this exciting system. Further studies of the uncertainties associated with the overluminosity and with the assumed core composition of both components are now underway.

This work was supported in part by the NSERC Canada, by the NSF grant AST 85-14778, and by a E.W.R. Steacie Fellowship to one of us (GF).

Bergeron, P., Wesemael, F. and Fontaine, G. 1987, in IAU Colloquium 95, The Second Conference on Faint Blue Stars, eds. A.G.D. Philip, D.S. Hayes and J. Liebert, (Schenectady: L. Davis Press), p.661.

Bergeron, P., Wesemael, F. and Fontaine, G. 1988, these Proceedings.

Fontaine, G., Bergeron, P., Lacombe, P., Lamontagne, R. and Talon, A. 1985, *Astron. J.*, **90**, 1094.

Greenstein, J.L. 1985, *P.A.S.P.*, **97**, 827.

Koester, D., Schulz, H. and Weidemann, V. 1979, *Astron. Astrophys.*, **76**, 262.

Lacombe, P., Liebert, J., Wesemael, F. and Fontaine, G. 1983, *Astrophys. J.* **272**, 660.

McCook, G.P. and Sion, E.M. 1987, *Astrophys. J. Suppl.*, **65**, 603.

Saffer, R.A., Liebert, J. and Olszewski, E.M. 1988, *Astrophys. J.*, in press.

Schulz, H. and Wegner, G. 1981, *Astronom. Astrophys.*, **94**, 272.

Shipman, H.L. 1979, *Astrophys. J.*, **228**, 240.

Winget, D.E., Lamb, D.Q. and Van Horn, H.M. 1988, in preparation.

THE WHITE DWARF MASS AND ORBITAL PERIOD DISTRIBUTION IN ZERO-AGE CATACLYSMIC BINARIES

M. Politano and R. F. Webbink
University of Illinois at Urbana-Champaign

I. INTRODUCTION

A zero-age cataclysmic binary (ZACB) we define as a binary system at the onset of interaction as a cataclysmic variable. We present here the results of calculations of the distributions of white dwarf masses and of orbital periods in ZACBs, due to binaries present in a stellar population which has undergone continuous, constant star formation for 10^{10} years.

II. METHOD

Distributions of ZACBs were calculated for binaries formed t years ago, for log t = 7.4 (the youngest age at which viable ZACBs can form) to log t = 10.0 (the assumed age of the Galactic disk), in intervals of log t = 0.1. These distributions were then integrated over time to obtain the ZACB distribution for a constant rate of star formation. To compute the individual distributions for a given t, we require the density of systems forming (number of pre-cataclysmics forming per unit volume of orbital parameter space), $n_f(t)$, and the rates at which the radii of the secondary and of its Roche lobe are changing in time, $\dot{R}_s(t)$ and $\dot{R}_{L,s}(t)$, respectively. In calculating $n_f(t)$, we assume that the distribution of the orbital parameters in primordial (ZAMS) binaries may be written as the product of the distribution of masses of ZAMS stars (Miller and Scalo 1979), the distribution of mass ratios in ZAMS binaries (cf. Popova, *et al.*, 1982), and the distribution of orbital periods in ZAMS binaries (Abt 1983). In transforming the the orbital parameters from progenitor (ZAMS) to offspring (ZACB) binaries, we assume that all of the orbital energy deposited into the envelope during the common envelope phase leading to ZACB formation goes into unbinding that envelope. $\dot{R}_{L,s}(t)$ is determined from orbital angular momentum loss rates due to gravitational radiation (Landau and Lifshitz 1951) and magnetic braking ($\gamma = 2$ in Rappaport, Verbunt, and Joss 1983). We turn off magnetic braking if the secondary is completely convective.

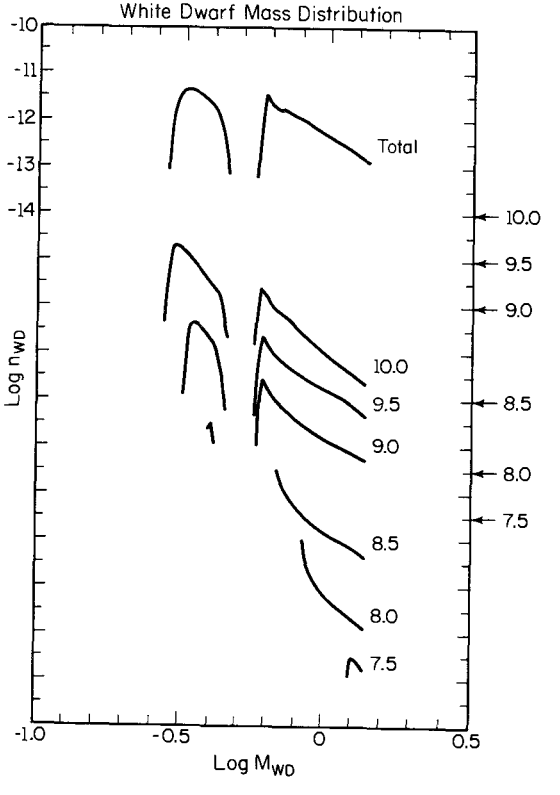

Fig1: The distribution of the white dwarf masses in ZACBs resulting from a constant stellar birthrate over 10^{10} years (curve labeled "total"), and the contributions to this distribution from systems formed "t" years ago for several values of t (curves labeled by values of log t). M_{WD} is the mass of the white dwarf in solar masses and n_{WD} is the number of CVs forming per year per log white dwarf mass per unit area of the Galactic plane (in pc^2). An absolute scale is provided for the total distribution. The distributions for individual values of log t are plotted on a relative scale having the same spacing as the absolute scale. For the purposes of comparison, log n_{WD} = -10 for each distribution is indicated on the right-hand scale by an arrow labeled with the corresponding value of log t.

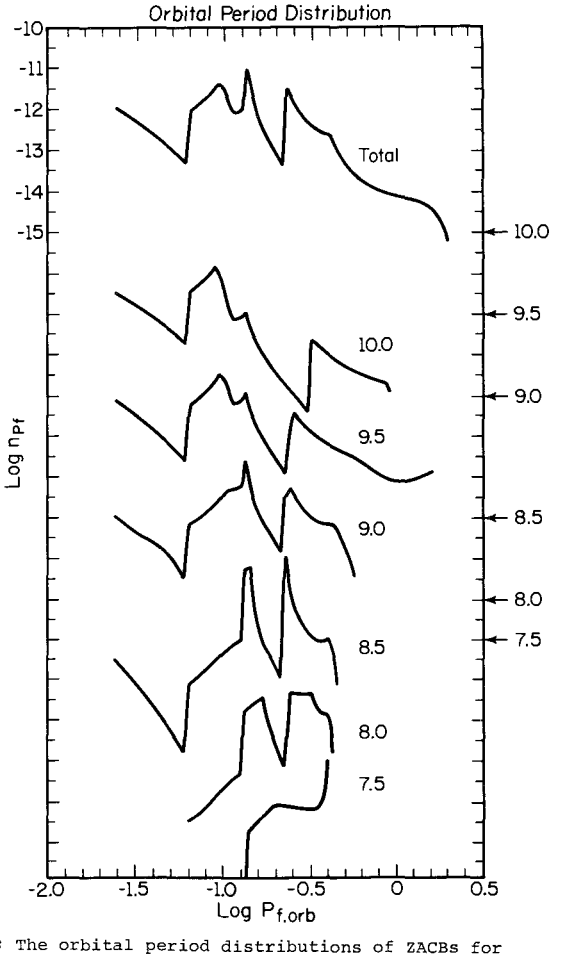

Fig. 2: The orbital period distributions of ZACBs for the same cases as in Fig. 1 $P_{f,orb}$ is the orbital period in days and n_{pf} is the number of CVs forming per year per log orbital period per square parsec. The scale used on the y-axis is explained in the caption to Fig. 1.

III. RESULTS

Figures 1 and 2 show the results of these calculations. Our principal conclusions may be summarized as follows:

- Cataclysmic variables (CVs) first appear in a stellar population at an approximate age log t = 7.4 years. This is the smallest age at which close binaries leave white dwarf remnants.
- The distribution of white dwarf masses in ZACBs is not sufficient to account for the observed high white dwarf masses in CVs, emphasizing the possible importance of selection effects (Ritter and Burkert 1986; see also Politano, Ritter, and Webbink, these proceedings).
- The orbital period distribution identifies four main subsets of ZACBs: (1) short-period systems containing He white dwarfs (peak near log P = -1.1); (2) systems with CO white dwarfs whose secondaries are convectively stable against rapid mass transfer to the white dwarf (peak near log P = -0.9); (3) systems with CO white dwarfs whose secondaries are radiatively stable against rapid mass transfer (peak near log P = -0.65); and (4) long period systems with evolved secondaries (wing out to periods of roughly 2 days).
- The period distribution of ZACBs has a local minimum between 2 and 3 hours, due to the discontinuity in white dwarf masses between CVs containing He white dwarfs and systems containing CO white dwarfs (cf. Webbink 1979).
- CVs forming from binaries less than 10^9 years old do not contain He white dwarfs.
- The formation rate of CVs is maximized when the nuclear time scale of the initial primary is comparable to the time scale for angular momentum loss during the pre-CV state. In this case, pre-CV systems are brought into contact roughly as fast as they are formed (emerge from the common envelope phase).

This research was supported in part by NSF grant AST 86-16992.

REFERENCES

Abt, H. 1983, *Ann. Rev. Astron. Astrophys.* **21**, 343.

Landau, L., and Lifshitz, E. 1951, *The Classical Theory of Fields*, Addison-Wesley.

Miller, G.E., and Scalo, J.M. 1979, *Astrophys. J. Suppl.*, **41**, 513.

Popova, E.I., Tutukov, A.V., and Yungelson, L.R. 1982, *Astrophys. Space Sci.*, **88**, 55.

Rappaport, S., Verbunt, F., and Joss, P.C. 1983, *Astrophys. J.*, **275**, 713.

Ritter, H., and Burkert, A. 1986, *Astron. Astrophys.*, **158**, 161.

Webbink, R.F. 1979, in *IAU Colloq. No. 53, White Dwarfs and Variable Degenerate Stars*, H.M. Van Horn and V. Weidemann (eds.), Univ. of Rochester Press, p. 426.

THE OPTICAL SPECTRA OF V803 CEN*

S.O.Kepler
Instituto de Fisica
Universidade Federal do Rio Grande do Sul,

J.E.Steiner and F.Jablonski
Instituto Nacional de Pesquisas Espaciais, Brazil

ABSTRACT.

We obtained spectrophotometry of V803 Cen in both high state ($B \approx 13.5$) and low state ($B \approx 17$) from 3800 Å to 7100 Å and 5 Å resolution. Essentially all the observed absorption lines are due to He I. No emission lines in either high or low state were detected, as well as no significant departures from a Planck law distribution.

1. INTRODUCTION

V803 Cen, also named AE-1, was discovered by Elvius (1975) as a blue variable star with a 4 magnitude luminosity variation on a timescale of days. E.L.Robinson, on a literature search for stars similar to AM CVn (HZ29) and PG1346+082, both interacting binary white dwarfs (IBWD), suggested (private communication) AE-1 as a possible similar star, prompting a search for short timescale variations similar to the ones observed in AM CVn and PG1346+082 (Wood *et. al.* 1987). These short timescale variations were found by Kepler (1987) and O'Donoghue, Menzies and Hill (1987), demonstrating that V803 Cen was indeed similar to the IBWD PG1346+082.

Since all the spectral observations were obtained with V803 Cen in either high state or medium state, and also only observed in the blue (Elvius 1975, Westin 1980, and O'Donoghue, Menzies and Hill 1987), we decided to obtain spectrophotometry of the star from 3800 to 7100 Å to see if we could detect light from different components of the system, as well as to see if we could detect any emission line, especially on the low state.

Our observations show no evidence of emission lines or light from more than one component in the spectra at low or high state.

2. OBSERVATIONS

We obtained three spectra of V803 Cen at CTIO, using the '2D-Frutti' two- dimensional photon-counting detector on the Boller and Chivens spectrograph of the 1.0 m telescope, with a 300 lines mm^{-1} grating. The wavelenght coverage was from 3800 to 7100 Å , and the resolution was $\approx$ 5 Å (FWHM). A WG360 filter was used to minimize contamination by second- order blue light in the red, and the observations were done with a 5 arcsec slit. We observed at least one spectrophotometric standard every night.

Data reduction was done with IRAF, following a standard procedure; the two- dimensional images were first corrected for detector distortions using a calibration spectra of a tungsten lamp taken through a multihole decker and a long-slit HeAr lamp. After subtracting the dark current scaled by the exposure time, the images were divided by a normalized flatfield image obtained from dome-flat exposures. Sky-subtracted spectra were then obtained, rebinned onto a final linear wavelenght scale using the calibration derived from a HeAr lamp exposure taken at the position of the star, and corrected for extinction using the mean curve given by Stone and Baldwin (1983).

The three exposure obtained were:

1) d001, 1600 sec, on 26.06.86, UT 23:08
2) d002, 600 sec, on 02.07.86, UT 23:15
3) d003, 10800 sec, on 20.07.87, UT 0:59
   10800 sec, on 21.07.87, UT 0:55.

Exposure d003 is the sum of two exposures obtained on consecutive days in which the star stayed in low state.

---

* Based on observations obtained at Cerro Tololo Inter-American Observatory, National Optical Astronomy Observatories, operated by the Association of Universities for Research in Astronomy, Inc., under contract with the National Science Foundation.

Figure 1 Spectrophotometry of V803 Cen from high state ($B \approx 13.5$), to low state ($B \approx 17.2$).

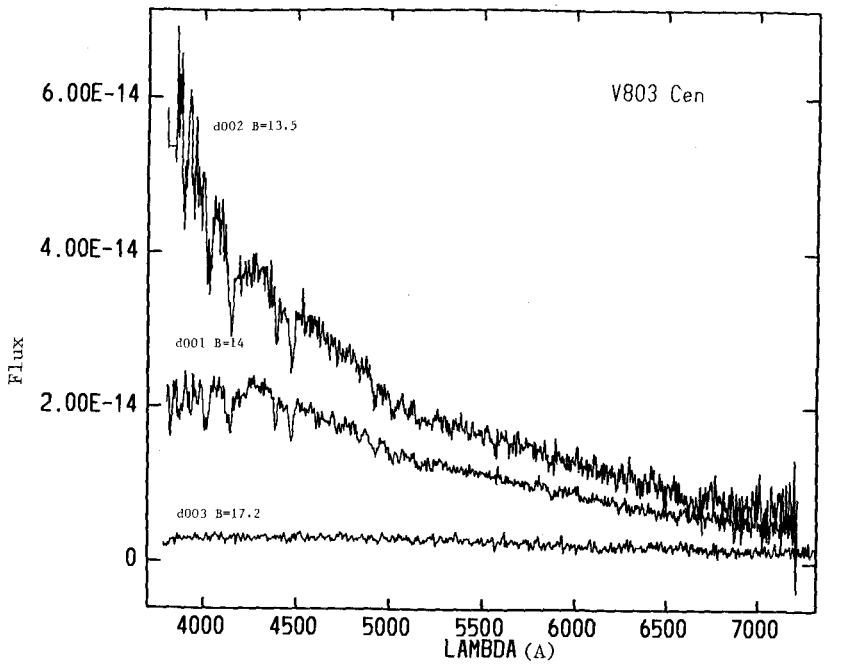

Figure 2 Line identification for the spectra of V803 Cen at high state (d001 - $B \approx 14$). All the lines identified bellow the spectra are He I lines. The lines within parenthesis are unidentified. The data has been smoothed with a 3 point boxcar average for presentation.

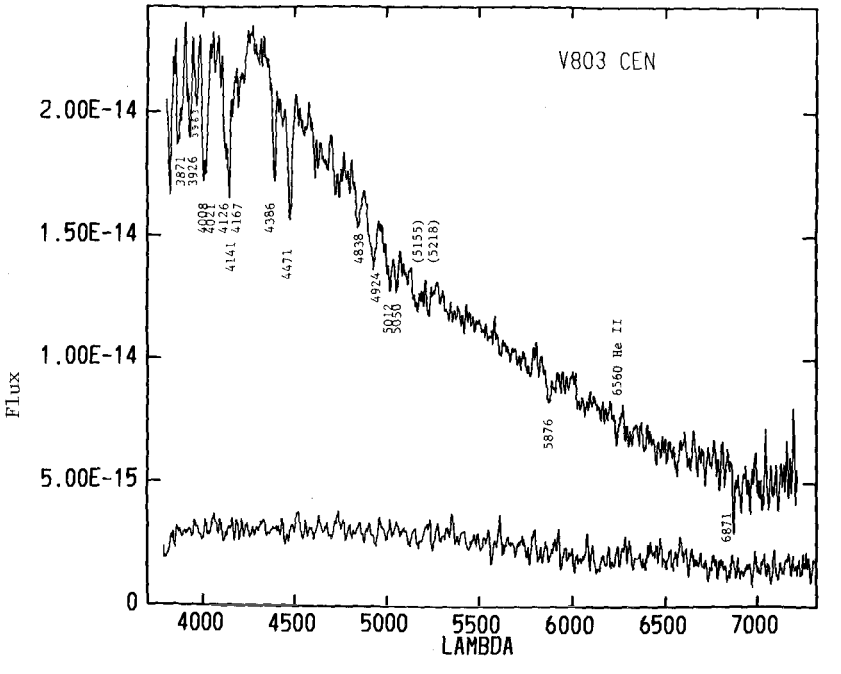

3. DATA ANALYSIS

The high state spectra contains only He I lines, with a possibility for a He II line at 6560 Å . A fit of a Planck function to the portion of the spectra redward of 4500 Å for d001, when the count rate corresponded to $B \approx 14$, gives an effective temperature of $T_{eff} = 17106 \pm 275K$. The curvature of the spectra blueward of 4500 Å could be caused by undercorrection with the spectrophotometric standard, since we only observed one standard that night, or possibly by a strong blanketing effect due the He I lines. There is no evidence for either a blue or red excess continuum emission.

For d002, at a high state around $B \approx 13.5$, a fit of a Planck function from 3900 Å to 7100 Å gives $T_{eff} = 25776 \pm 682K$, and also shows no evidence of excess continuum. The temperatures at high state ($T_{eff} \leq 30000K$) are still consistent with the absence of strong He II lines, especially $\lambda 4686$.

The low state spectra d003, at $B \approx 17.2$, unfortunately of low S/N due to the small size of the telescope (obtained with a small telescope because we cannot predict what will be the magnitude of the star at any given period), shows no evidence for lines, either in absorption or emission. A Planck function fit to the whole spectrum gives an effective temperature of $T_{eff} = 7315 \pm 73K$. The low state spectra also does not show any evidence for multiple components.

In conclusion, the observed spectra of V803 Cen shows essentially only He I lines, shallow in comparison with that of a DB white dwarf, and does not show any evidence for multiple components. The observations are therefore consistent with the model for the interacting double degenerate star, with two Helium white dwarfs and an optically thick accretion disk. The 4 magnitude luminosity variations detected in the star can, in the IBDW model, be explained by mass transfer between the two white dwarfs. The absence of multiple components in the observed spectra indicates that all the optical light comes from the accretion disk. The absence of emission lines even at low state implies that, unless we are seeing a 7300K white dwarf, the disk must be optically thick even in faint state.

This work was partially supported by grants from CNPq and FINEP - Brazil.

REFERENCES

Elvius, A. 1975, *Astr. Astrophys.*, **44**, 117.
Kepler, S.O. 1987, *IAU Circular No. 4332.*
O'Donoghue, D., Menzies, J.W., and Hill, P.W. 1987, *Mon. Not. R. Astr. Soc.*, **227**, 347.
Stone, R.P.S., and Baldwin, J.A. 1983, *Mon. Not. R. Astron. Soc.*, **204**, 347.
Westin, B.A.M. 1980, *Astr. Astrophys.*, **81**, 74.
Wood, M.A., Winget, D.E., Nather, R.E., Hessman, F.V., Liebert, J., Kurtz, D.W., Wesemael, F., and Wegner, G. 1987, *Astrophys. J.*, **313**, 757.

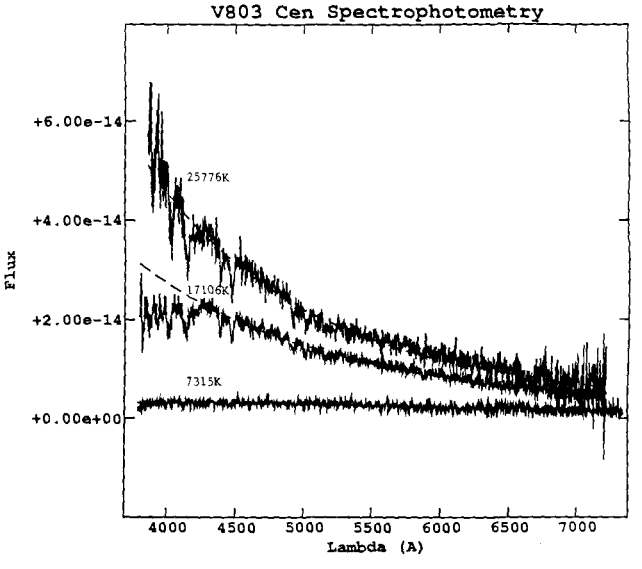

Figure 3 Planck function fits to the spectra of V803 Cen. The dashed line is a plot of only one Planck function to each spectrum. The curvature blueward of 4500 Å in d001 is probably instrumental.

THE PERIOD PROBLEM OF THE INTERACTING BINARY WHITE DWARF SYSTEM AM CVn

J.-E. Solheim
University of Tromsø
Institute of Mathematical and Physical Sciences
Tromsø, Norway

ABSTRACT

A short review is given of the searches for an orbital period of this (believed to be) interacting binary white dwarf system. Today, 3 or 4 periods are known. A polar ring accretion model is proposed to explain the observations - at least partly.

THE PHOTOMETRIC PERIOD

Periodic variability of this star was first detected by Smak (1967). He found a period of 17.5 minutes. The star was proclaimed to be the shortest period binary system then known. Many theories for the system were proposed, but rapid flickering in the light curve and no strong X-ray emission, eliminated all models except the interacting binary white dwarf system (Faulkner et al., 1972). In this model a low mass white dwarf orbits a normal mass white dwarf in a close orbit. Mass is transferred from the low mass star, which is peeled off matter layer by layer. Later, 3 other objects of the same type were discovered. AM CVn may still have the shortest orbital period of this group of stars.

Since only helium is detected in the optical spectrum, the mass losing star must be a helium white dwarf. An ultrashort period binary system will lose angular momentum by gravitational radiation. Detection of the secular changes in the period may therefore be a test of the theory of General Relativity or other theories of gravitation (Krisher, 1985). Assuming that gravitational radiation is the only way of removing angular momentum, GR predicts a rate of increase in the otbital period between 3.6 and 7.3×10^{-13}. Extensive observations by Patterson et al. (1979) showed an increase in the orbital period 1000 times this prediction.

The times of minima in the light curve arrive rather unprecisely. They can arrive up to 0.2 of the period too early or too late. Some-

times one minimum is shallower than the other - or even missing for a few cycles. From one night to the next it is easy to commit a cycle count error, which may lead to calculation of a wrong period. Solheim et al. (1984) observed the system in 1982-83 and collected all times of minima published. It was shown that if one did not make a distinction between primary and secondary minima, and avoided cycle count errors, all observations could fit one period: 1051.04 s or exactly half of that. A secular decrease in the period was found to be 3.2×10^{-12}. This is a factor of 100 less than found by Patterson et al. (1979), but with an opposite sign with respect to the value predicted by General Relativity. This period was interpreted as a period of rotation, and it was shown that the spinning up of the accreator easily could be explained by the transfer of angular momentum in the accreation process. The orbital period became unknown.

At the same time, SFT analysis of long strings of old data (Kepler, 1984) showed periods of 1011.5, 525.6, and 350.4 s. No power was found at the period of 1051 s. This means that if the observing period is long enough there is no feature in the light curve that repeats with 1051 s period. The period can still be 1051 s, but only the higher harmonics are observed. The new period of 1011 s could then cause much of the changes observed in the light curve, making one minimum disappear, or arrive too late or too early, explaining some of the timing irregularities of the system. If the 1051 s (525.5 s) period is related to rotation, then the new period of 1011 s might be related to the orbital period.

No polarization is observed for the system, and if this is interpreted as a sign of a weak magnetic field, some of the phasing irregularities in the light curve can be explained if accretion happens mostly in the polar regions. Accretion may take place in a polar ring area and then mostly on the "night" side with respect to the donator. This produces the orbital modulation of the light curve. Part of the phase jitter may then be related to the migration in longitude of the accreting areas just as we observe it in the auroral regions on the Earth (figure 1). If the magnetic axes is tilted with respect to the orbital axes, we should also expect rotational modulation of the light curve.

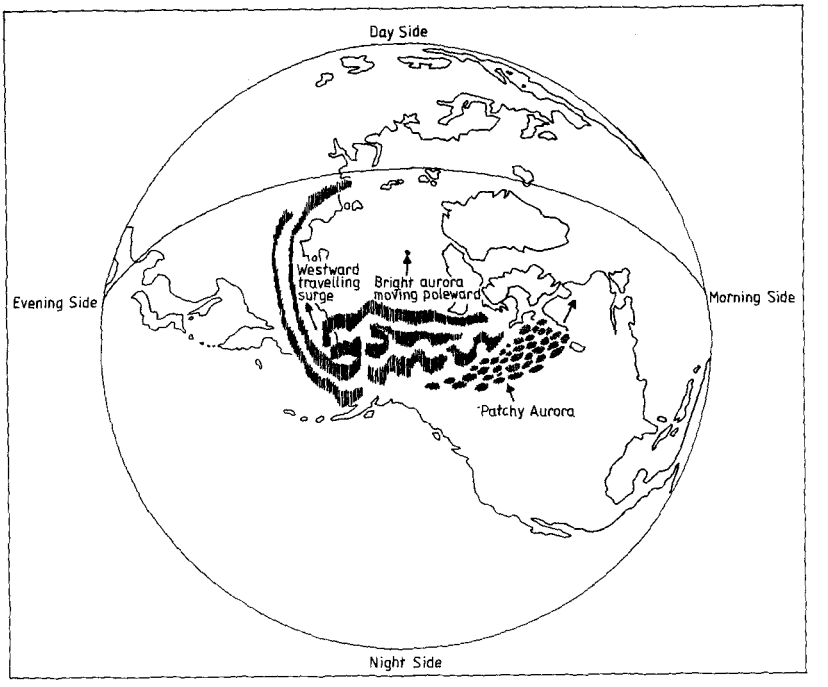

Figure 1: Basic auroral activities during an auroral substorm, when observed from above the north pole region.

SPECTROSCOPIC PERIODS

There has been 3 attempts to do high speed spectroscopy to determine the orbital velocity. Robinson and Faulkner (1975) did not find any secular variations or variations over the 17.5 min photometric period. They claimed to be able to detect sinusoidal variations with a semi-amplitude greater than 30 km s^{-1}. Voikhanskaya (1982) observed with the 6 m telescope, but did not succeed in detecting the 17.5 min period. Attempts made at La Palma in 1987 by Lazaro et al. (1988) will be reported at this meeting.

Observations of IUE spectra (Solheim and Kjeldseth-Moe, 1987) showed narrow absorption lines of C, N and Si which vary in intensity with time, always blueshifted. This is interpreted as a sign of an optically thick wind seen against a bright disk. There are only marginal signs of a P-Cygni profile now and then, and from line profile studies, it was concluded that the orbital inclination is less than 30 degrees.

This may explain the difficulty in making spectroscopical velocity studies.

FUTURE WORK

It is proposed to include this system in the whole Earth Telescope Project (Nather, 1988) to do as continuous observations as possible. This may solve the problem of the interpretation of the multiple periods observed, and also indicate if any of them are related to g- or r-mode pulsations, which also may be present in such a disturbed system as we believe AM CVn is.

REFERENCES

Faulkner, J., Flannery, B., and Warner, B.: 1972, Astrophys. J. 175, L79.
Kepler, S.O.: 1984 (private communication).
Krisher, T.P.: 1985 (preprint).
Lazaro, C., Solheim, J.-E., and Arevalo, M.J.: 1988, IAU coll. #114.
Nather, R.E.: 1988, IAU coll. #114.
Patterson, J., Nather, R.E., Robinson, E.L., and Handler, F.: 1979, Astrophys. J. 232, 819.
Robinson, E.L. and Faulkner, J.: 1975, Astrophys. J. 200, L23.
Smak, J.: 1967, Acta Astron. 17, 255.
Solheim, J.-E., Robinson, E.L., Nather, R.E., and Kepler, S.O.: 1984, Astron. Astrophys. 135, 1.
Solheim, J.-E. and Kjeldseth-Moe, O.: 1987, Astrophys. Space Sci. 131, 785.
Voikhanskaya, N.F.: 1982, Sov. Astron. 26, 558.

CRITICAL MASS FOR MERGING IN DOUBLE WHITE DWARFS

Izumi HACHISU[1] and Mariko KATO[2]
[1]Department of Aeronautical Engineering, Kyoto University
[2]Department of Astronomy, Keio University

I. INTRODUCTION

We examine whether or not double white dwarfs are ultimately merging into one body. It has been argued that such a double white dwarf system forms from some intermediate-mass binary stars and will merge due to the gravitational radiation which decreases the separation of binary. After filling the inner critical Roche lobe, the less massive component begins to transfer its mass to the more massive one. When the mass transfer rate exceeds a some critical value, a common envelope is formed. If the common envelope is hydrostatic, the mass transfer is tuned up to be a some value which depends only on the white dwarf mass, radius, and the Roche lobe size. The mass transfer from the less massive to the more massive components leads the separation to increase. On the other hand, the gravitational radiation effect reduces the separation. Which effect wins determines the fate of double white dwarfs, that is, whether merging or not merging. Since the formula of the gravitational radiation effect is well known, we have studied the mass accretion rate in common envelope phase of double white dwarfs assuming the Roche lobe size is as small as 0.03 $R_\odot$ or 0.1 $R_\odot$.

II. CRITICAL MASS ACCRETION RATES IN COMMON ENVELOPE PHASE

When the mass transfer exceeds the so-called Eddington accretion rate, i.e.,

$$\dot{M}_{Edd} = L_{Edd}/[GM_{WD}/R_{WD} - GM_{WD}/R_{ph}], \qquad (1)$$

where L_{Edd} is the Eddington luminosity at the photosphere, i.e., $L_{Edd} = 4\pi cGM_{WD}/\kappa$, the accreted envelope expands to overfill the Roche lobe. Two pressures between the extended envelope and the mass-losing white dwarf balances with each other. Hydrostatic balance is reached in the common envelope. We assume that the envelope around the more massive

white dwarf just fills the same potential surface as the less massive one's surface. Assuming further that the envelope around the white dwarf is spherically symmetric, we have obtained the mass accretion rates.

The accreting matter releases the gravitational energy. In the equation of energy conservation, we include the homologous term, i.e.,

$$\frac{dL_r}{dM_r} = \varepsilon_g^{(h)} + \varepsilon_n, \qquad (2)$$

where M_r is the mass within the radius r, $\varepsilon_g^{(h)}$ the homologous term of ε_g (e.g., Sugimoto and Nomoto 1975; Nariai, Nomoto, and Sugimoto 1980), ε_n the nuclear energy generation per unit time and per unit mass. We implicitly assume that the entropy of the transferred matter is the same as the entropy of at the top of the extended envelope.

It is found that there is the minimum envelope mass for a given set of the white dwarf mass and the Roche lobe size. For the minimum envelope mass, the mass accretion rate is very close to the Eddington accretion rate defined by equation (1). The mass accretion rate decreases gradually until helium/carbon is ignited at the bottom of the envelope as the envelope mass is increased. For $M_{WD} \lesssim 0.8\ M_\odot$, however, helium is ignited before the envelope expands to $0.03\ R_\odot$ if the accreted matter is helium. For $M_{WD} > 1.1\ M_\odot$, carbon is ignited off-center before the envelope expands to $0.03\ R_\odot$ if the matter is carbon-oxygen mixture. The mass accretion rates are plotted in Figures 1 and 2.

III. CRITICAL MASS FOR MERGING

a) He-CO pair

When the white dwarf mass is larger than $0.8\ M_\odot$, helium is ignited before a common envelope is formed. After helium ignition, the structure of the envelope changes and the envelope expands to overfill the Roche lobe. Then a common envelope may be formed around the system. Then the mass transfer rate is given by the steady burning line in Figure 2a. The change in the separation may be determined by

$$\frac{\dot{a}}{a} = -2(1-q)\frac{\dot{M}_2}{M_2} + \frac{2}{J}\left(\frac{dJ}{dt}\right)_{GR} = \tau_M^{-1} - \tau_G^{-1}, \qquad (3)$$

if the total mass is conserved, where $\dot{a}$ is the increasing rates of the separation, $\dot{M}_2$ the mass transfer rates, and the second term in the middle means the decrease in the separation due to the loss of the orbital angular momentum by gravitational wave radiation, i.e.,

$$\frac{1}{J}\left(\frac{dJ}{dt}\right)_{GR} = -1.94\times10^{-2}\left(\frac{M_1}{M_\odot}\right)^3(1+q)q\ (a/10^9\mathrm{cm})^{-4}\ \mathrm{yr}^{-1}. \quad (4)$$

It is clear that if the time scale of the mass transfer τ_M is shorter than that of the gravitational wave radiation τ_G, two white dwarfs are separating from each other. If $\tau_M > \tau_G$, two stars are merging into one body.

Equating $\tau_M = \tau_G$, we obtain the critical masses for merging in common envelope phase as:

$$M_{cr}(\mathrm{He}) \sim 0.25\ M_\odot \quad \text{for } M_{CO} \sim 1\ M_\odot . \quad (5)$$

b) CO-CO or CO+ONeMg pair

Two white dwarfs are always merging into one body because $\tau_G >> \tau_M$ always holds.

c) He-He pair

When the total mass of the system is larger than $\sim 0.6\ M_\odot$, two white dwarfs are probably merging after helium is ignited off-center and the mass accreting helium white dwarfs expands to a few solar radii (Saio and Nomoto, private communication). The total mass is less than $0.6\ M_\odot$ and the less massive white dwarf mass is smaller than $0.2\ M_\odot$, two helium white dwarfs will not merge.

REFERENCES

Hachisu, I., and Kato, M. 1988, Ap. J., submitted.

Kato, M., Saio, H., and Hachisu, I. 1988, Ap. J., submitted.

Nariai, K., Nomoto, K., Sugimoto, D., 1980 Pub. Astr. Soc. Japan., 32, 473.

Sugimoto, D., and Nomoto, K. 1975, Publ. Astr. Soc. Japan, 27, 197.

figure captions

Fig. 1-The mass accretion rate is plotted against the envelope mass for various white dwarf core masses. Open triangles: maximum accretion rate in a static envelope. Open circles: mass accretion rate at the helium ignition. Filled circles: mass accretion (i.e., steady burning) rate of helium matter. Numbers attached are the core mass of white dwarfs in solar mass units. $R_{ph} = 0.1\ R_\odot$ is assumed.

Fig. 2-The mass accretion rates at the maximum accretion (denoted by "max"), at the helium ignition (denoted by "ignition"), and at the steady helium shell burning are plotted against the core mass for two cases of the Roche lobe sizes, i.e., $0.1\ R_\odot$ and $0.03\ R_\odot$ for (a) helium accretion and for (b) C+O accretion.

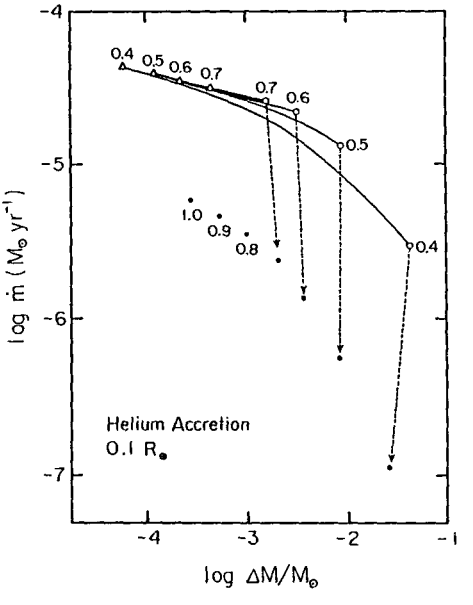

FIG. 1

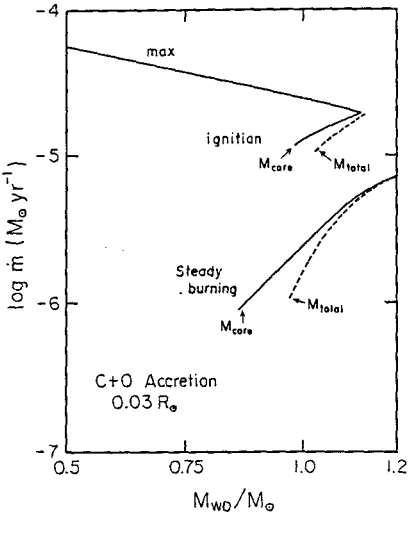

FIG.2b

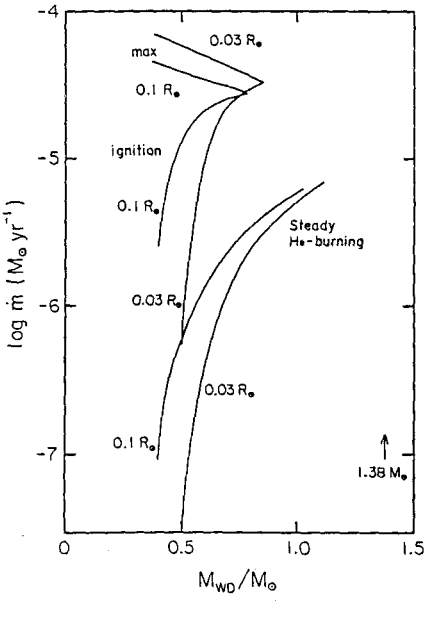

FIG.2a

ON THE SEPARATIONS OF COMMON PROPER MOTION BINARIES CONTAINING WHITE DWARFS

T.D. Oswalt
Dept. of Physics and Space Sciences
Florida Institute of Technology
Melbourne, Florida, USA 32901

E.M. Sion
Dept. of Astronomy and Astrophysics
Villanova University
Villanova, Pennsylvania, USA 19085

Luyten [1,2] and Giclas et al. [3,4] list over 500 known common proper motion binaries (CPMBs) which, on the basis of proper motion and estimated colors, are expected to contain at least one white dwarf (WD) component, usually paired with a late type main sequence (MS) star. Preliminary assessments of the CPMBs suggest that nearly all are physical pairs [5,6]. In this paper we address the issue of whether significant orbital expansion has occurred as a consequence of the post-MS mass loss expected to accompany the formation of the WDs in CPMBs.

Though the CPMB sample remains largely unobserved, a spectroscopic survey of over three dozen CPMBs by Oswalt [5] found that nearly all faint components of Luyten and Giclas color class "a-f" and "+1", respectively, or bluer were a WD. This tendency was also evident in a smaller sample studied by Greenstein [7]. Conversely, nearly all CPMBs having two components of color class "g-k" and "+3" or redder were MS+MS pairs. With the caveat that such criteria discriminate against CPMBs containing cool (but rare) WDs, they nonetheless provide a crude means of obtaining statistically significant samples for the comparison of orbital separations: 209 highly probable WD+MS pairs and 109 MS+MS pairs.

As a statistical measure of physical separation we define a separation index, log s/μ, where s is the angular separation (in ") of the pair and μ is its proper motion (in "/y). Frequency histograms for log s/μ are compared in Figure 1 for the WD+MS and MS+MS pairs. Evidently the mean separation indices of WD+MS systems are significantly larger than MS+MS pairs (labelled L+G in Table 1), implying nearly a factor of two difference in projected semimajor axis. The histograms also suggest that the dispersion in separations does not change much during post-MS mass loss; selection effects favoring the detection of one type of CPMB over the other would most likely result in different dispersions.

The lower half of Figure 1 displays F(ms), the fraction of CPMBs likely to be MS+MS pairs (expressed in logarithmic form for convenience), as a function of separation index, log s/μ (bins containing fewer than five CPMBs have been omitted). This plot suggests a monotonic decrease in the

fraction of MS+MS pairs with increasing separation-- contrary to the expectation that close pairs of contrasting colors (WD+MS) are more easily distinguished from those of similar color. There is also no discontinuity in either diagram which might be construed as the result of binary disruption dynamically induced by perturbations from the Galactic disk [8]. Curiously, $F(ms) \sim (s/\mu)^{-1/3}$ is consistent with the scatter in this plot; the physical significance, if any, has not yet been established.

Is the apparent difference in separation between WD+MS and MS+MS pairs an artifact of the criteria used by Luyten and Giclas in searching for WD binaries? We tested this hypothesis by selecting a random spatial distribution of CPMBs from the LDS catalog [9]. This sample yielded 210 probable MS+MS CPMBs and 26 probable WD+MS pairs. Since Luyten's criterion

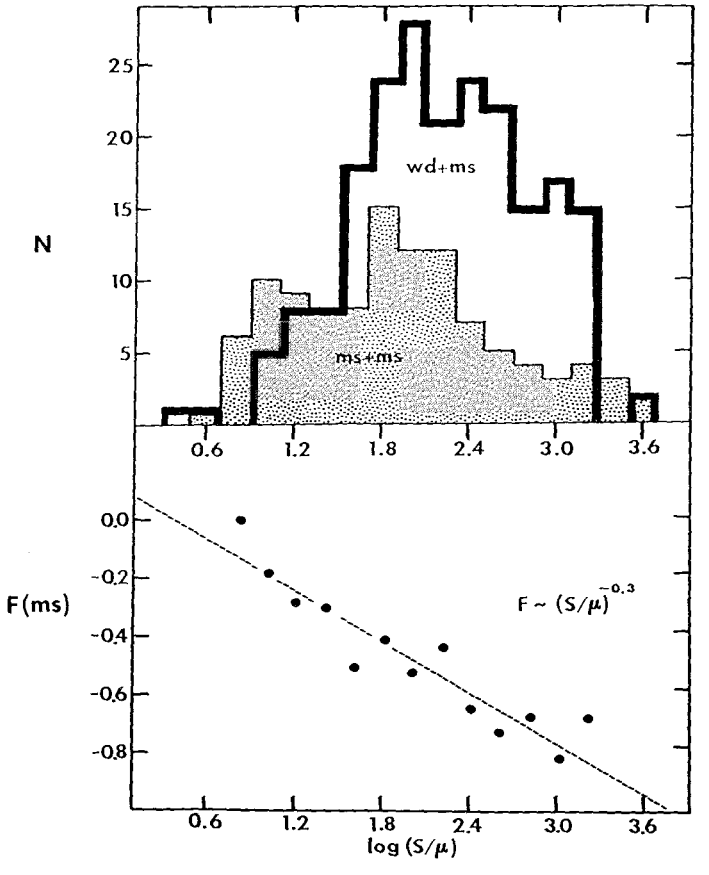

Figure 1. Top: Separation index log s/μ histograms of Luyten and Giclas CPMBs. Bottom: Fraction F(ms) of the sample likely to be MS+MS pairs plotted as a function of separation index.

Table 1.

Comparison of Binary Separation Indices

Sample	WD+MS pairs			MS+MS pairs		
	n	<log s/μ>	m.e.	n	<log s/μ>	m.e.
L+G	209	2.22	0.04	109	1.91	0.07
LDS	26	2.34	0.10	210	2.09	0.04
DA	52	2.11	0.07	-	-	-
nonDA	46	1.95	0.08	-	-	-
DQ	8	1.54	0.17	-	-	-

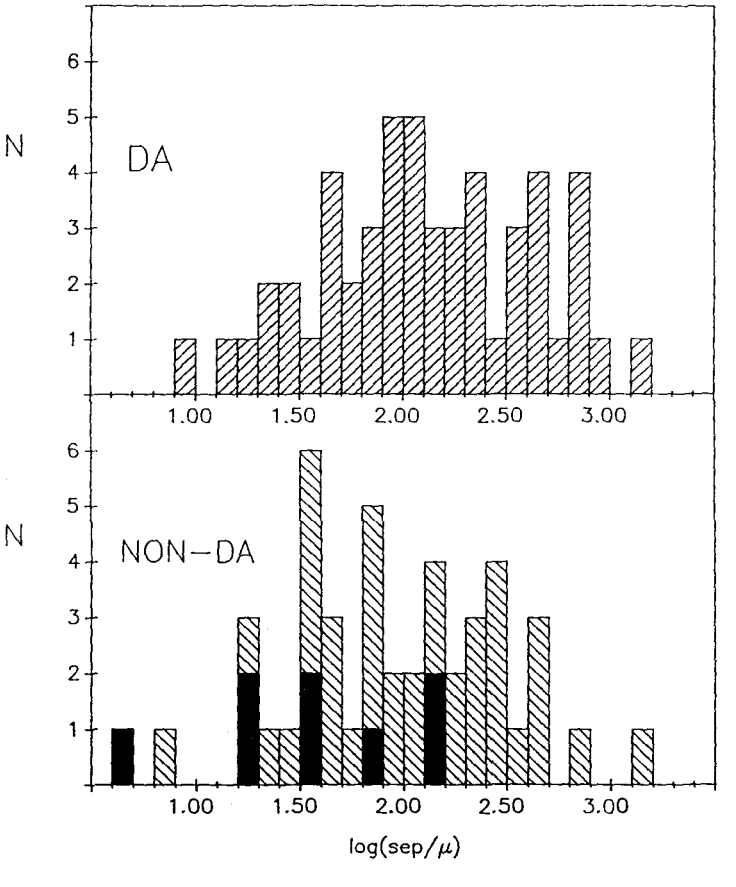

Figure 2. Comparison of separation index log s/μ histograms for CPMBs containing known DA (top) and nonDA (bottom) WDs. Both groups have MS companions. CPMBs with a DQ WD have been shaded in the nonDA histogram.

for inclusion in the LDS was solely identical proper motion, these samples should be fairly representative of the general distribution of CPMB transverse velocities. The mean separation indices derived for the LDS WD+MS and MS+MS pairs are given in Table 1. We again find that WD+MS pairs are nearly twice the physical separation of MS+MS pairs; however both LDS groups have separation indices larger than their counterparts in the Luyten and Giclas suspect WD binary lists. We tentatively ascribe this to the lower transverse velocities of the LDS pairs [10].

The frequency of helium-rich (i.e. nonDA) WDs is higher among CPMBs than among single stars [11]. Plausible explanations are that WDs found in CPMBs have different parent masses, angular momentum histories, and/or mass-loss compared to those of single WDs. Do the physical separations typical of DA and nonDA CPMBs differ? We culled a sample of 98 CPMBs containing spectroscopically identified WDs from the literature [12]. Figure 2 compares the separation index histograms for these DA and nonDA CPMBs. Although they may be marginally different (see Table 1), the heterogeneous nature of the sources of spectroscopic identifications admits the possibility that misclassified weak-lined WDs contaminate the sample. Possibly significant is the fact that the eight known CPMBs containing DQ WDs which are included in the "nonDA" histogram (shaded) have a mean separation one third that of most WD+MS pairs (see Table 1).

Clearly the potential of the Luyten and Giclas CPMBs as probes of post MS mass loss and orbital evolution has barely been tapped. Nevertheless, our preliminary results corroborate Greenstein's [7] assertion that significant orbital expansion is likely to have occurred among WD+MS pairs.

We gratefully acknowledge the able assistance of L. Roberts in the preparation of our extensive database on CPMBs. This paper was partially supported by a NASA grant administered by the American Astronomical Society (TDO) and NSF grants AST88-02687 (TDO) and AST88-02689 (EMS).

References

1. W.J. Luyten: "Proper Motion Survey with the 48-Inch Schmidt Telescope" 38 (Minneapolis: Univ. Minn. Press, 1974)
2. W.J. Luyten: "Proper Motion Survey with the 48-Inch Schmidt Telescope" 52 (Minneapolis: Univ. Minn. Press, 1979)
3. H.L. Giclas, R. Burnham, Jr., N.G. Thomas: "Lowell Proper Motion Survey, Northern Hemisphere" (Flagstaff: Lowell Obs., 1971)
4. H.L. Giclas, R. Burnham, Jr., N.G. Thomas: Lowell Obs. Bull. 164 (1978)
5. T.D. Oswalt: Ph.D. thesis, The Ohio State University (1981)
6. T.D. Oswalt, P.M. Hintzen, W.J. Luyten: Ap. J. Suppl. 66, 391 (1988)
7. J.L. Greenstein: A. J. 92, 85 (1986)
8. P. Hut, S. Tremaine: Ap. J. 90,1548 (1985)
9. W.J. Luyten: "Proper Motion Survey with the 48-Inch Schmidt Telescope" 29 (Minneapolis: Univ. Minn. Press, 1972)
10. R.B. Hanson: Mon. Not. R.A.S. 186, 875 (1979)
11. E.M. Sion, T.D. Oswalt: Ap. J. 326,249 (1988)
12. G.P. McCook, E.M. Sion: Ap. J. Suppl. 65, 603 (1987)

TIME RESOLVED SPECTROSCOPY OF AM CVn

C. Lázaro[1], J.-E. Solheim[2] and M.J. Arévalo[1,3]
1- Instituto de Astrofisica de Canarias, Spain
2- University of Tromsø, Norway
3- Dpto. Fisica, Universidad Politecnica de Canarias, Spain

ABSTRACT

The preliminary results of time resolved spectroscopy of the He White Dwarf system AM CVn are presented. We have searched for spectral variations at different photometric periods. These are found at different time scales although this does not particularly favour any of the searched periods.

INTRODUCTION

AM CVn (HZ 29) is a system whose photometric light curve shows variable minima (usually with a double hump) and (U-B), (B-V) color changes, with a periodicity of about 18 minutes (Smak, 1967; Warner and Robinson, 1972; Krzeminski, 1971). Rapid flickering, typical of the cataclysmic variables, has also been observed (Warner and Robinson, 1972).

In its optical spectra there are no hydrogen lines, and only broad asymmetric absorption lines of He I are observed. These lines are wider and shallower than in ordinary BD White Dwarfs (Robinson and Faulkner, 1972). The line profiles may be partly filled up by emission cores with long term variations (Voikhanskaya, 1982).

Among different models proposed over the years, a model with two helium white dwarfs orbiting each other as proposed by Faulkner et al. (1972) is the most plausible. In this model a low mass lobe-filling white dwarf transfers mass to a more luminous primary - and an optical thick disk with a considerable wind outflow is created (Solheim and Kjeldseth-Moe, 1987).

One problem with the system is that no orbital period has been detected (Solheim, 1988). The first attempt of high speed photometry was done by Robinson and Faulkner (1972) with the Lick 120-inch telescope. No sinusoidal variations with a semi-amplitude of $\gtrsim 30$ km s^{-1} were detected at the photometric period of 1051 s.

Spectra were also taken by Voikhanskaya (1982), at the prime focus of the 6 m telescope. No significant changes in position or intensity of the He lines with the photometric period were observed, but she noted secular changes in the line profile.

Our time resolved observations of AM CVn have been carried out with the highest spectral and time resolution to date. This allows us to better estimate the limit of the radial velocity periodic variations and to study the line changes at different time scales.

OBSERVATIONS

The observations were made during three nights, 3th - 5th February 1987, at the Cassegrain focus of the 2.5 m Isaac Newton telescope at the Observatorio del Roque de los Muchachos, La Palma, Canary Islands. The spectrograph used was the IDS (Intermediate Dispersion Spectrograph) with the IPCS camera. The spectra covered the range 3950-4450 Å with a spectral resolution of 0.25 Å per channel. We took 485 short exposures of one minute duration each, in order to allow a coadding in phase for any desired period. As the detector is photon-counting limited, it allowed us to make short exposures without degrading the S/N of the individual spectra.

SPECTROSCOPIC VARIABILITY

The data reduction process was carried using STARLINK programmes. For every selected period we added the spectra in eight phase intervals. Cross-correlations between the resultant spectra were made searching for Doppler shifts, in addition to a search for variations in equivalent width for the three absorption He I lines within our range (4026 Å, 4144 Å, 4388 Å). This period searches were made for different periods arising from high-speed photometric studies: 525 s, 1011 s, 2022 s and 1051 s.

In a preliminary analysis we do not find significant changes which could be interpreted as orbital variations at these periods. However, changes in both depth and profile of the He I lines are found for all the searched periods. As an example, Figure 1 shows the behaviour of two of the He I lines for the 1051 s period. This implies that AM CVn presents spectral variations in time intervals as short as a few minutes.

As we did not find a clear periodicity, we searched for time variations adding spectra within time intervals from 15 minutes to one night. Figure 2 shows the added spectra for every hour in three nights. Variations in the asymmetry and depth of the He I lines are noticeable above the noise. A specially interesting event seems to have occurred at the end of the 3-4 Feb. night, with sudden intensity changes at the longer wavelength end of our spectral window, including the He I 4388 Å line. A more detailed analysis will be published elsewhere.

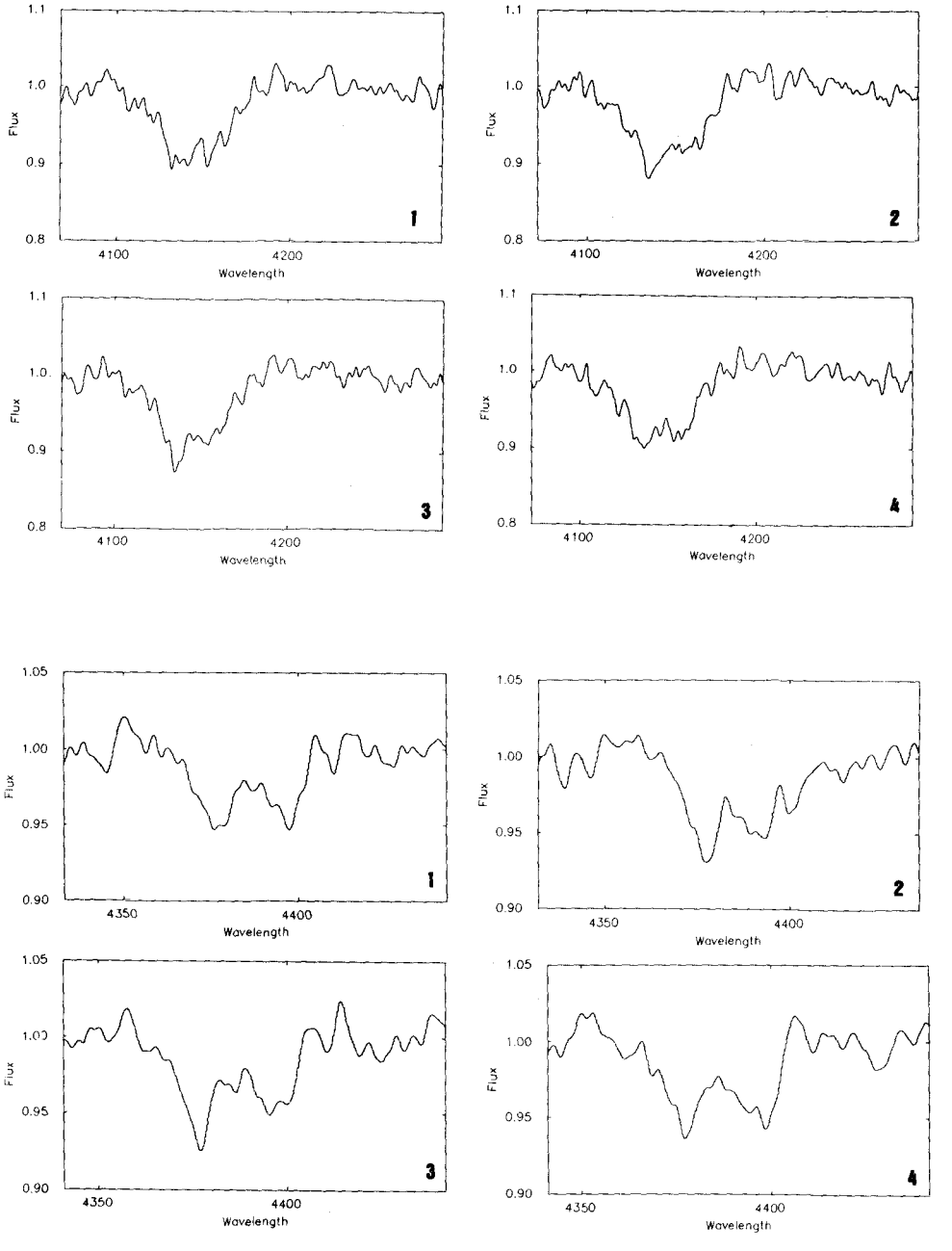

Figure 1: a) Line He I 4144 Å with spectra coadded in phase intervals: 0.875-0.125 (1); 0.375-0.625 (2); 0.12-0.375 (3); 0.625-0.875 (4). b) The same for the He I 4388 Å line.

REFERENCES

Faulkner, J., Flannery, B., and Warner, B.: 1972, Ap. J. (Letters) 125, L79.
Krzeminski, V.: 1971, Remeis-Sternw. Bamberg 9, 178.
Robinson, E.L. and Faulkner, J.: 1972, Ap. J. (Letters) 200, L23.
Smak, J.: 1967, Acta Astron. 17, 225.
Solheim, J.-E.: 1988, IAU Coll. # 114.
Solheim, J.-E. and Kjeldseth-Moe, O.: 1987, Astrophys. Space Sci. 131, 785.
Voikhanskaya, N.F.: 1982, Sov. Astron. 26, 558.
Warner, B. and Robinson, E.L.: 1972, Mon. Not. R. astro. Soc. 159, 101.

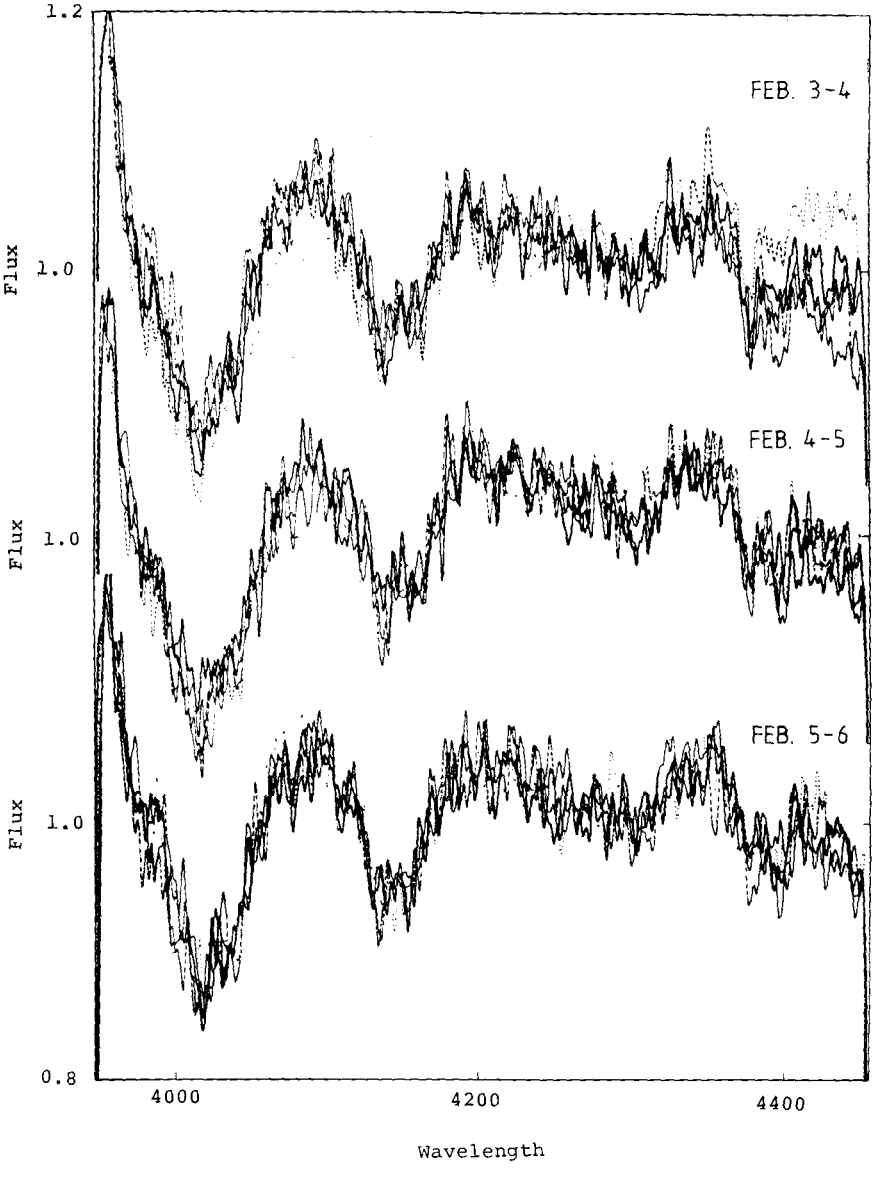

Figure 2: Added spectra in one hours interval for each night.

HIGH FREQUENCY OSCILLATIONS IN SS CYGNI

M.J. Arévalo[1,2], J.E. Solheim[3] and C. Lázaro[1]
1- Instituto de Astrofisica de Canarias, Spain
2- Dept. Fisica, Universidad Politecnica de Canarias, Spain
3- University of Tromsø, Norway

INTRODUCTION

Because of its relative brightness (m_v about 11.8 in quiescence and m_v about 8.6 in outburst), SS Cygni is the Dwarf Novae most extensively studied since 1896 (Mattei et al., 1985; Bath and van Paradijs, 1983).

Concerning its long-term behaviour, SS Cygni has *short*, *long* and *anomalous* outbursts. Correlations between outburst characteristics and periodicities have been studied by van Paradijs (1983), Campbell (1934), and Sterne and Campbell (1934).

SS Cygni, as any cataclysmic variable, also presents rapid variations. Since the discovery of this variability (Warner and Robinson, 1972) many long runs of high-speed photometry have been performed for different Dwarf Novae, both during outbursts and in quiescence stages. Regarding to SS Cygni we can summarize these variations as:

Flickering: Irregular oscillations in brightness which are attributed to variations in the luminosity of the bright spot. The typical timescale is of a few minutes, and it is completely random and unpredictable (Robinson and Nather, 1979). The amplitude is about 0.1 mag, and the power spectrum shows a smooth decrease from low to high frequencies.

Quasi periodic oscillations: Periods of 31.5 s have been reported (Robinson and Nather, 1979) at maximum eruption. These decline in time periods of 150 s and the mean amplitudes are 0.003 mag. It is assumed that they are associated to the accretion disk. Patterson (1981) found 32 and 36 s QPO's in outbursts.

Coherent oscillations: discovered by Patterson et al. (1978) have a mean amplitude of 0.005 mag and a determined period of about 10 s which can change rapidly (Robinson and Nather, 1979). These oscillations are only present some times during outburst with variable amplitudes and period correlated with the magnitude. They have been related (Hildebrand et al., 1981) with the soft X-ray 9 s pulsations found by Cordoba et al. (1980, 1984), and may be due to damped oscillations on the surface of the white dwarf or to material orbiting close to the dwarf (Hildebrand et al., 1981).

It is also interesting to mention the periodicity of 12.18 minutes found by

Bartolini et al. (1985) and detected mainly in the red bands R and I, that they take as support to the hypothesis that SS Cygni belongs to the intermediate polars group.

OBSERVATIONS AND RESULTS

We monitored SS Cygni during an extensive observing programme as part of an organized international campaign (Honey et al., 1988). The observations were carried out at the Observatorio del Roque de Los Muchachos (La Palma, Canary Islands), from September 9th to October 10th 1985. We used the 60 cm Swedish telescope and a one channel photometer modified by the Tromsø Astrophysics Group for continuous photometry, with a Johnson V-filter. The integration times were 5 s and 10 s in outbursts and quiescence respectively. Each run was occasionally interrupted for observations of the sky background and two nearby comparison stars. Two samples of the data are shown in Figure 1.

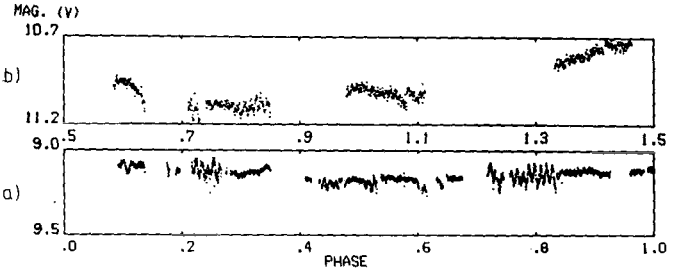

Figure 1: Two samples of the light curve observed. a) Sept. 10-11, (variations around phase .8 are due to telescope drive). b) Sept. 25-26.

The data reduction was carried out using a FT program at the University of Tromsø. The runs of both comparison stars were analyzed in order to exclude instrumental frequencies. During our observations SS Cygni had one eruption followed by a long quiescence period as shown in Figure 2.

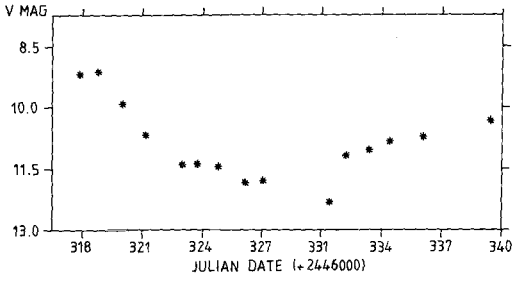

Figure 2: V-magnitude of SS Cygni during our observing period.

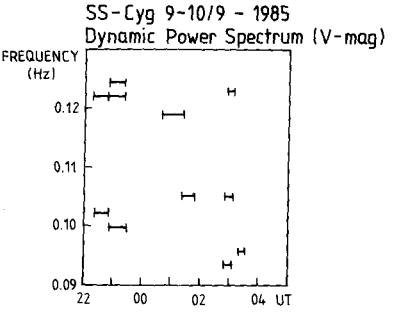

Figure 3: A dynamic power spectrum during the night Sept. 9-10 1985.

a) The highest frequency oscillations (8-10 s) were observed during the four nights at outburst, when the sampling rate was high enough. Figure 3 shows a dynamic power spectrum for one night. Two frequencies are present most of the time with some frequency drift towards slightly higher and lower frequencies. A consistent frequency increase with flux like that observed in the X-ray spectral range is not seen.

b) For the remaining of the observing nights we have searched for lower frequency oscillations in the range 0.4-60 min. We find several periods with significant power even if they are not present for all the observing dates. Oscillations with periods in the range 30-33 s are present every night, with amplitudes reaching 0.003 mag, also well into the quiescent stage.

The complete results will be presented elsewhere.

REFERENCES

Bartolini, C., Guarnieri, A., Lolli, M., Piccioni, A., Giovannelli, F., Gaudenzi, S., and Lombardi, R.: 1985, "Multifrequency Behaviour of Galactic Accreting Sources", 50. Proceedings of the Frascati Workshop 1984, Ed. F. Giovannelli.

Bath, G.T. and Van Paradijs, J.: 1983, Nature 305, 33.

Campbell, L.: 1934, Ann. Harvard Coll. Obs. 90, 93.

Cordoba, F.A., Chester, T.J., Tuohy, J.R., and Garmine, G.P.: 1980, Ap. J. 235, 163.

Cordoba, F.A., Chester, T.J., Mason, K.O., Kahn, S.M., and Garmire, G.P.: 1984, Ap. J. 278, 739.

Hildebrand, R.H., Spillar, E.J., and Stiening, R.F.: 1981, Ap. J. 243, 223.

Honey, W.B., Bath, G.T., Charles, P.A., Whitehurst, R., Jones, D.H.P., Echevarria, J., Arevalo, M.J., Solheim, J.E., Tovmassian, G., and Takagishi, K.: submitted to M.N.R.A.S.

Mattei, J.A., Saladya, M., Waagen, E.O., and Janes, C.M.: 1985, AAVSO Monograph No. 1.

Patterson, J.: 1981, Ap. J. Suppl. Ser. 45, 517.

Patterson, J., Robinson, E.L., and Kiplinger, A.L.: 1978, Ap. J. 226, L137.

Robinson, E.L. and Nather, R.E.: 1979, Ap. J. Suppl. Ser. 39, 461.

Van Paradijs, S.J.: 1983, Astron. Ap. 125, L16.

Warner, B. and Robinson, E.L.: 1972, Nature Phys. Sci. 239, 2.

THE MASS SPECTRUM OF THE WHITE DWARFS IN CATACLYSMIC BINARIES

M. Politano[1], H. Ritter[2], and R. F. Webbink[1]
[1] University of Illinois at Urbana-Champaign, U.S.A.
[2] Universitäts-Sternwarte München, F.R.G.

ABSTRACT

Using the theoretically predicted mass spectrum of the white dwarfs (WDs) in zero-age cataclysmic binaries (ZACBs) by Politano and Webbink (1988), we examine to what extent observational selection can account for the observed high masses of the WDs in cataclysmic binaries (CBs).

I. INTRODUCTION

It has long been suspected that the high masses of the WDs observed in CBs (for a compilation of WD masses in CBs see, *e.g.*, Ritter 1987a; for a discussion, Ritter 1987b) are due to some selection effect. That observational selection could, in fact, be the answer to the puzzle of the WD masses in CBs has first been shown by Ritter and Burkert (1986), Ritter and Özkan (1986), and Ritter (1986), hereafter referred to respectively as papers I, II and III. In these papers it was shown that flux limitation introduces a very strong bias in favor of observing CBs with high-mass WDs. Whereas the strength of the selection effect, expressed in terms of the selection function defined in paper I, is independent of the intrinsic distribution of the WD masses, $p_{1,i}$, the corresponding mass spectrum of a flux-limited sample, $p_{1,0}$, does of course depend on $p_{1,i}$. Therefore, the question whether the selection effect is strong enough cannot be answered without knowing $p_{1,i}$. The estimates made in papers I and II using the mass spectrum of single white dwarfs, i.e., $p_{1,i} = p_{SWD}$, showed that the selection effect is in fact strong enough to account for the observed WD masses in CBs if $p_{1,i}$ is not too different from p_{SWD}.

In the meantime, work done by Politano and Webbink (1988) provides, for the first time, a detailed and self-consistent theoretical prediction of the intrinsic mass distribution of the WDs in ZACBs, p_{ZACB}. In this paper we use p_{ZACB} in place of p_{SWD} to examine to what extent earlier conclusions about the importance of observational selection remain valid.

II. THE INTRINSIC MASS SPECTRUM OF THE WHITE DWARFS

Politano and Webbink (1988) compute the distribution functions of the orbital parameters, *i.e.*, of the WD mass M_1, the mass ratio $q = M_2/M_1$, and the orbital period P, for ZACBs that form after a time t of constant star formation. However, the selection problem does not directly involve the distribution functions for newly formed CBs, but rather the intrinsic mass spectrum $p_{1,i}$ of the WDs of the present, secularly evolved, CB population. The distribution functions characterizing the ZACBs and $p_{1,i}$ are related in a rather complicated way. However, under three not unreasonable assumptions, this relation simplifies considerably. The assumptions are: 1) Observational selection through flux-limitation is insensitive to the intrinsic mass spectrum of the secondaries of ZACBs. Computations in paper I showed this to be the case. 2) The time scale for the secular evolution of a typical CB is short compared to the time scale on which p_{ZACB} changes. Since the intrinsically brightest systems, which are predominantly seen in a magnitude-limited sample, are also the youngest, *i.e.*, at most a few 10^8 yr past the ZACB stage, this assumption is also reasonably well fulfilled. 3) White dwarf masses in CBs are negligibly affected by secular evolution. With these assumptions, it follows that $p_{1,i}$ is well-approximated by the current distribution p_{ZACB}. We take for the latter the distribution p_{ZACB} after 10^{10} yr of constant star formation.

TABLE 1: Main characteristics of the intrinsic WD mass spectra $p_{ZACB}(10^{10}$ yr) and p_{SWD}

		this paper	Ritter and Burkert (1986)
mass spectrum $p_{1,i}$		p_{ZACB}	p_{SWD}
Helium WDs	relative number	0.60	0.0
	mean mass	0.34 $M_\odot$	-
CO WDs	relative number	0.40	1.0
	mean mass	0.75 $M_\odot$	0.62 $M_\odot$

The main properties of $p_{ZACB}(10^{10}$ yr) and of p_{SWD} are listed in Table 1. The most important difference between p_{ZACB} and p_{SWD} is the presence and dominance of helium WDs in p_{ZACB}. However, it is important to note that for $M_1 \geq 0.6\ M_\odot$, p_{ZACB} and p_{SWD} agree to within a factor of ~2, and that p_{SWD} is flatter than p_{ZACB} for $M_1 \geq 0.85\ M_\odot$.

III. THE METHOD

We compute the mass spectrum $p_{1,0}$ and the expectation value of the WD mass $\langle M_1 \rangle$ for a number of flux-limited samples of CBs (defined in Table 2), using $p_{1,i} = p_{ZACB}(10^{10}$

yr). Because of the definition of the selection function S_1 (see paper I), we have

$$p_{1,0} = S_1 p_{1,i} \tag{1}$$

and

$$\langle M_1 \rangle = \int M p_{1,0} dM \quad . \tag{2}$$

Since selection is independent of $p_{1,i}$, we may use for S_1 the selection functions computed in papers I and II.

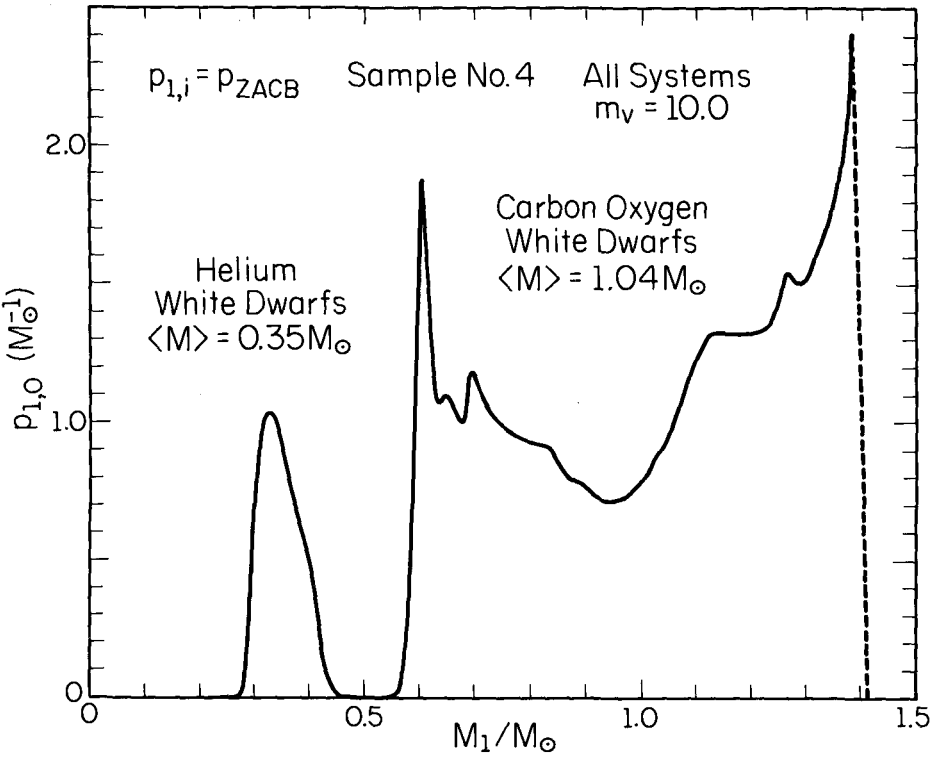

Figure 1: Normalized mass spectrum $p_{1,0}(M_1)$ of the WDs of sample No. 4 defined in Table 2.

IV. RESULTS

Table 2 lists the defining characteristics and the resulting properties of $p_{1,0}$ of 5 different magnitude-limited samples computed with $p_{1,i} = p_{ZACB}$. For comparison, we list also the corresponding results obtained in paper I using $p_{1,i} = p_{SWD}$. In order to illustrate the strength of the selection effect, we show in Fig. 1 the function $p_{1,0}$ for sample No. 4 of Table 2. The corresponding function $p_{1,i} = p_{ZACB}$ may be

TABLE 2: Defining and resulting characteristics of selected magnitude-limited samples. (Sample numbers refer to the samples defined and discussed in more detail in paper I.)

Defining characteristics of magnitude-limited samples			$p_{1,i} = p_{ZACB}$				$p_{1,i} = p_{SWD}$
			He white dwarfs		CO white dwarfs		CO white dwarfs
No.	limiting m_v	range of orbital periods	relative number	$\frac{\langle M_1 \rangle}{M_\odot}$	relative number	$\frac{\langle M_1 \rangle}{M_\odot}$	$\frac{\langle M_1 \rangle}{M_\odot}$
4	10.0	all systems	0.09	0.35	0.91	1.04	0.98
12	10.0	below the gap	0.23	0.35	0.77	0.89	0.78
13	10.0	above the gap	0.00	0.40	1.00	1.10	1.12
15	12.5	all systems	0.12	0.35	0.88	0.98	0.90
16	15.0	all systems	0.20	0.35	0.80	0.90	0.78

found in Politano and Webbink (1988), and the selection function in paper I. The main results may now be summarized as follows (see also Table 2):

- The selection effects introduced through flux-limitation are strong enough to account for the observed high masses of the WDs.
- Using $p_{1,i} = p_{ZACB}$, the results concerning the CO-WDs are qualitatively the same as, and quantitatively similar to, those obtained in papers I and II. Selection is strongest for $M_1 \geq 0.6\ M_\odot$, where p_{ZACB} is very similar to p_{SWD}.
- The mean mass of the CO WDs decreases with increasing limiting magnitude m_v.
- No CBs containing a helium WD are expected above the period gap ($P \geq 3^h$).
- At $m_v = 10$, about 25% of the CBs below the period gap ($P \leq 2^h$) should contain helium WDs.
- The mean mass of the helium WDs in CBs below the gap is $\langle M_1 \rangle \approx 0.35\ M_\odot$, and is insensitive to selection effects.
- The fraction of CBs containing helium WDs increases with increasing m_v.

This research was supported by grants from the NSF (AST 86-16992), DFG, and NATO.

REFERENCES

Politano, M., Webbink, R.F. 1988, this volume.

Ritter, H. 1986, *Astron. Astrophys.* **168**, 105 (paper III).

Ritter, H., Burkert, A. 1986, *Astron. Astrophys.* **158**, 161 (paper I).

Ritter, H., Özkan, M.T. 1986, *Astron. Astrophys.* **167**, 260 (paper II).

Ritter, H. 1987a, *Astron. Astrophys. Suppl.* **70**, 355.

Ritter, H. 1987b, in: *Physical Processes in Comets, Stars and Active Galaxies*, W. Hillebrandt, E. Meyer-Hofmeister, and H.-C. Thomas (eds.), Springer Verlag, p. 143.

Evolution of Low-Mass Helium Dwarfs in Interacting Binaries: Application to 4U1820-30

Lorne A. Nelson
CITA, University of Toronto, Toronto, Ontario, Canada

Paul C. Joss and Saul Rappaport
Center for Theoretical Physics, MIT, Cambridge, Mass., USA

1. Introduction

A number of evolutionary scenarios have been proposed that lead to the formation of binary systems consisting of a degenerate dwarf in orbit with a neutron star. In fact, most degenerate dwarfs in close-binary systems are probably the cores of evolved stars whose envelopes have been stripped by one or more episodes of common-envelope evolution. Once the envelope has been removed, the newly exposed core of the giant will have an effective temperature and radius that are considerably larger than the corresponding quantities in an older, highly degenerate dwarf. It is important for at least two reasons to evaluate the subsequent cooling history of such objects: (i) For *detached* binaries, we want to be able to infer from the current effective temperature and luminosity of the degenerate dwarf the elapsed time since the core of its progenitor giant was exposed. (ii) For *semi-detached* binaries, we must know the evolution of the radius of the degenerate dwarf in order to compute important relationships among the orbital period and its rate of change, the mass of the degenerate dwarf, and the mass-transfer rate.

One example of a system for which this type of analysis can be applied is the globular cluster X-ray burst source 4U1820-30. Recently, Stella, Priedhorsky, and White (1987) discovered a stable 685 s periodicity in the X-ray flux from this source. Using archival satellite data dating back to 1976, Morgan, Remillard, and Garcia (1988) confirmed the 685 s periodicity and set an upper limit on the fractional rate of change in the period of $\dot{P}/P < 2.7 \times 10^{-7}$ yr^{-1}. This high degree of stability provides convincing evidence that the periodic modulation in the X-ray intensity results from binary orbital motion. If the orbital period of 4U1820-30 is indeed 685 s, then it is the most compact binary yet discovered. Based on the recurrence times of the type I X-ray bursts that are observed and given our understanding of these events as thermonuclear flashes on neutron stars (see, e.g., Joss 1978), we can conclude that this system contains a neutron star that is accreting helium-rich matter. Moreover, the mean density of the Roche lobe-filling companion star can be inferred from the orbital period to be $\sim 3100\,\mathrm{g\,cm^{-3}}$. This density is indicative of a low-mass dwarf ($\lesssim 0.1\,M_\odot$) that is at least partially degenerate.

2. Evolution of the Semi-Detached Binary

In order to examine the present evolutionary status of 4U1820-30, we assume that it is a semi-detached binary system consisting of a neutron star of mass M_1 in a circular orbit with a low-mass secondary of mass M_2. Systemic angular momentum losses drive the mass transfer and can include (1) gravitational radiation losses as specified by the Einstein quadrupole formula ($\dot{J}_{GR} < 0$), and (2) angular momentum that is carried away by any matter that may be ejected from the binary system. By including both of these possibilities, a general expression for the

mass-transfer rate $\dot{M}_2$ was derived by Rappaport, Verbunt, and Joss (1983):

$$-\frac{\dot{M}_2}{M_2} = \frac{\frac{1}{2}\dot{R}_{TH}/R_2 - \dot{J}_{GR}/J}{\left[(5/6 + \xi_{ad}/2) - \frac{(1-\beta)}{3(1+q)} - \frac{(1-\beta)\alpha(1+q)+\beta}{q}\right]} \quad . \tag{1}$$

Here $(\dot{R}_{TH}/R_2)^{-1}$ is the thermal contraction time scale of the secondary (R_2 being the radius of the secondary), J is the orbital angular momentum, ξ_{ad} is the "adiabatic stellar index" (i.e., $\xi_{ad} = d\ln R_2/d\ln M_2$ evaluated at constant internal specific entropy), and $q \equiv M_1/M_2$. The parameters α and β describe angular momentum losses due to possible systemic mass loss (see Rappaport *et al.* 1983 for details). Since the secondary must fill its Roche lobe, the orbital period can be related to the secondary's mass and radius by the well-known relation $P = 9\pi(2G)^{-1/2}R_2^{3/2}M_2^{-1/2}$. Thus the fractional rate of change in the orbital period can be expressed as

$$\frac{\dot{P}}{P} = -\frac{1}{2}\frac{\dot{M}_2}{M_2} + \frac{3}{2}\frac{\dot{R}_2}{R_2} \quad . \tag{2}$$

Equations (1) and (2) can be integrated to obtain the systemic evolution once the response of the secondary to mass loss has been ascertained. For the low-mass secondaries of interest here, the thermal contraction time scale is generally much larger than the gravitational radiation time scale (see §3), so that the star responds almost adiabatically. Hence, ξ_{ad} can be determined to a good approximation from the mass-radius relationship for zero-temperature stars. Specifically, we have taken the radius of the secondary to be $R_2 = fR_{ZS}(M_2; X, Z)$, where R_{ZS} is the radius of a zero-temperature star as defined by Zapolsky and Salpeter (1969) and X and Z are the standard composition parameters for the secondary (which we have assumed to be chemically homogeneous). The factor $f(\geq 1)$ accounts for thermal contributions to the equation of state and is assumed to be constant in any given evolutionary calculation (see §III). We note that while the inferred values of ξ_{ad} may not be highly accurate when f exceeds unity, our results are rather insensitive to small variations in ξ_{ad}.

3. Cooling Evolution of Helium Dwarfs

We have determined the thermal contraction time scales of low-mass ($\lesssim 0.2\ M_\odot$) helium dwarfs by calculating their evolutionary cooling histories. Very little previous work has been carried out on the cooling of low-mass helium or CO degenerate dwarfs (but see D'Antona, Magni, and Mazzitelli 1972 for a detailed study of the evolution of a 0.15 $M_\odot$ helium dwarf). We are particularly interested in determining at what point during the evolution the thermal contraction time scale, $\tau_{TH} \equiv R_2/\dot{R}_{TH}$, becomes longer than the gravitational radiation time scale, $\tau_{GR} \equiv J/\dot{J}_{GR}$. For all times during the binary evolution when $\tau_{TH} >> \tau_{GR}$, we are justified in neglecting the $\dot{R}_{TH}/R_2$ term in equation (1). It can also be shown that $f \simeq$ *constant* when this criterion is satisfied. In this way, the thermal evolution is decoupled from the mass-transfer evolution.

We have followed the cooling of the degenerate dwarf using a version of a Henyey-type code that has previously been used to study the evolution of very low-mass stars in cataclysmic variables (see Nelson, Chau, and Rosenblum 1985 for further details). We incorporated extensive improvements to the evaluation of the equation of state and the radiative and conductive opacities. Specifically, we implemented the Magni and Mazzitelli (1979) description of the equation of

state for pure helium. The radiative and electron conduction opacity coefficients were interpolated from the Cox-Stewart (1970) and Hubbard and Lampe (1969) opacity tables, respectively. Extrapolations beyond the limits of the opacity tables were sometimes required but usually occurred in regions of the star that were unstable against efficient convection, so that the numerical accuracy of the opacities was not overly important. Since 4U1820-30 is located in the globular cluster NGC 6624, for which the metallicity Z is reasonably well known, we adopted the observationally inferred value ($Z \simeq 0.003$). We did not attempt to include the effects of chemical diffusion in this study, since they are thought to be unimportant (Alcock and Illarianov 1982).

In Figure 1 we compare the magnitudes of the thermal contraction and gravitational radiation time scales for three representative stellar masses as functions of f (the ratio of the stellar radius to the radius of a completely degenerate star of the same mass and composition). We have taken the mass of the neutron-star primary to be 1.4 $M_\odot$. As can be seen in the figure, the thermal contraction time scale is always much longer than the gravitational radiation time scale for $f \lesssim 1.8$. Values of f larger than ~ 1.8 correspond to stellar ages of less than $\sim 3 \times 10^8$ yr. Hence, we can reasonably conclude that if the progenitor binary (after an assumed phase of common-envelope evolution) took at least 3×10^8 yr to enter into a semi-detached state, then we are justified in neglecting the $\dot{R}_{TH}/R_2$ term in equation (1) and in taking f to be constant. We also find that none of our models underwent crystallization, even at late ages ($\sim 10^{10}$ yr).

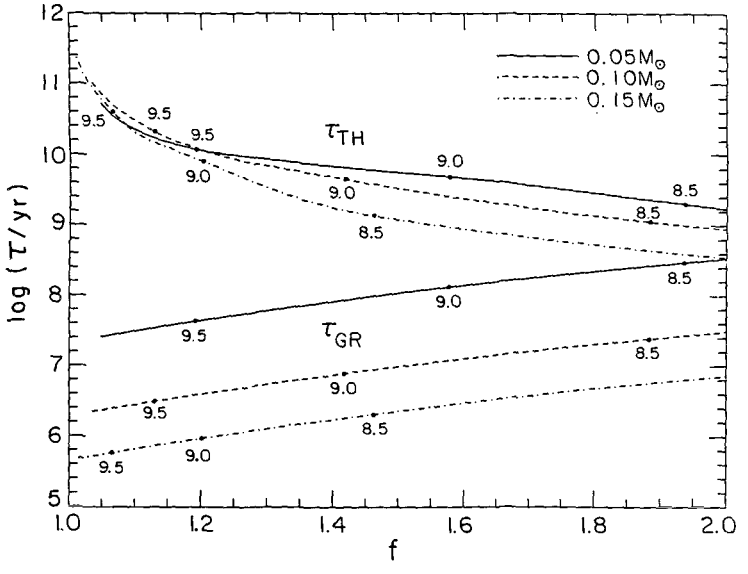

Figure 1. Calculated thermal evolution of a low-mass helium degenerate dwarf. The upper set of curves shows the thermal time scale, τ_{TH}, as a function of f (the ratio of the stellar radius to the radius of a completely degenerate star of the same mass and composition). The legend indicates which stellar mass has been used in each calculation. The numbers next to the heavy dots on the curves are the logarithms of the elapsed evolutionary times. The lower set of curves shows, for comparison, the gravitational-radiation time scale, τ_{GR}, of a semi-detached binary as a function of f, under the assumptions that the helium star is the lobe-filling secondary and that the primary has a mass of 1.4 $M_\odot$ (see text).

4. Discussion

Under the assumptions that the 4U1820-30 system consists of a neutron star with a mass of $1.4\,M_\odot$ and a radius of 10 km in a 685-s orbit with a fully degenerate ($f = 1$), helium-dwarf companion, and that no mass is being lost from the system during the mass-transfer process, it is possible to derive M_2, $\dot{P}/P$, and the observed X-ray luminosity L_x. The nominally predicted values for the system observables are $\dot{P}/P \simeq 1.1 \times 10^{-7}\mathrm{yr}^{-1}$, $L_x \simeq 8 \times 10^{37}\mathrm{ergs\ s}^{-1}$, and $M_2 \gtrsim 0.057\,M_\odot$. The calculated value of $\dot{P}/P$ is entirely consistent with the observed upper limit (see §1), and the calculated value of L_x is just consistent with the high end of the range of measured values of L_x. We conclude that the measured and inferred properties of the 4U1820-30 system can be readily accounted for in an evolutionary scenario that invokes conservative mass transfer driven by the emission of gravitational radiation. Since the measured upper limit on $\dot{P}/P$ is only about a factor of two higher than the value predicted for our standard model, we expect that the rate of change of the orbital period will be detectable within the next few years. Hence, 4U1820-30 could be the first mass-transfer system where the rate of change of orbital period resulting from gravitational radiation reaction can be measured directly.

We can also utilize the observationally inferred range of values for L_x and the upper limit on $\dot{P}/P$ to set quantitative constraints on some of the system parameters. In particular, we find that for $M_1 = 1.4\ M_\odot$ and conservative mass-transfer, f must be no greater than ~ 1.2. Assuming that the initial value of M_2 is $\leq 0.1\,M_\odot$, and given that f is approximately constant during the mass-transfer evolution, we see from Fig. 1 that at least $\sim 3 \times 10^9$ yr must have elapsed between the formation of the dwarf-star/neutron-star binary and the start of the mass-transfer phase (i.e., during the detached phase). (If the secondary retained a thin hydrogen-rich envelope after the spiral-in phase, the cooling time would only be increased.) Thus, this system might well have formed at a much earlier epoch in the history of the globular cluster NGC 6624, when the masses of the cluster giants would have been substantially higher than at the present time.

An earlier version of portions of this paper was published by Rappaport *et al.* (1987). This work was supported in part by the National Science Foundation under grant AST-8419834, by the National Aeronautics and Space Administration under grant NSG-7643, and by the Natural Sciences and Engineering Research Council (NSERC) of Canada.

References

Alcock, C., and Illarionov, A. 1980, *Ap. J.*, **235**, 534.
Cox, A. N., and Stewart, J. N. 1970, *Ap. J. Suppl.*, **19**, 243.
D'Antona, F., Magni, G., and Mazzitelli, I. 1972, *Astrophys. Sp. Sci.*, **19**, 151.
Hubbard, W. B., and Lampe, M. 1969, *Ap. J. Suppl.*, **18**, 297.
Joss, P. C. 1978, *Ap. J. (Letters)*, **225**, L123.
Magni, G., and Mazzitelli, I. 1979, *Astr. Ap.*, **72**, 134.
Morgan, E. H., Remillard, R. A., and Garcia, M. R. 1988, *Ap. J.*, **324**, 851.
Nelson, L. A., Chau, W. Y., and Rosenblum, A. 1985, *Ap. J.*, **299**, 658.
Rappaport, S., Nelson, L. A., Ma, C. P., and Joss, P. C. 1987, *Ap. J.*, **322**, 842.
Rappaport, S., Verbunt, F., and Joss, P. C. 1983, *Ap. J.*, **275**, 713.
Stella, L., Priedhorsky, W., and White, N. E. 1987, *Ap. J. (Letters)*, **312**, L17.
Zapolsky, H. S., and Salpeter, E. E. 1969, *Ap. J.*, **158**, 809.

BINARY, PULSATING, AND IRREGULAR VARIABLES AMONG PLANETARY NUCLEI

Howard E. Bond
Space Telescope Science Institute

Robin Ciardullo
Kitt Peak National Observatory

1. CCD Photometry of Planetary Nuclei

For the past two years, the authors have been carrying out a program of CCD photometry of planetary-nebula nuclei (PNNs), using the 0.9-m telescopes at Kitt Peak National and Cerro Tololo Inter-American Observatories. The aim of this program is to investigate the variability of PNNs on timescales of minutes to days, in order to search for close binaries and pulsators, as well as unexpected new classes of variable stars.

The program represents an extension of the photoelectric photometry of PNNs carried out by Bond and Grauer (1987). Use of the two-dimensional CCD detector allows us to model and subtract the nebulosity surrounding a PNN, in addition to providing exactly simultaneous observations of the PNN and several nearby comparison stars. The latter allow us to compensate for variable atmospheric transparency, permitting accurate differential photometry to be obtained even when the observing conditions are not photometric.

2. Close-Binary Nuclei

One of us has recently reviewed the subject of close-binary PNNs (Bond 1988*a*). That review lists the seven PNNs that are photometrically confirmed close binaries with orbital periods less than one day. Two of these objects—the nuclei of Abell 46 and Abell 63—are eclipsing binaries. For the remaining five systems, the light variability is due only to heated hemispheres on the main-sequence companions of the very hot primary stars. An example of the latter type of binary is the central star of Kohoutek 1-2, which has an orbital period of 16.2 hours. A complete B light curve, obtained with a CCD at CTIO, is shown below. The amplitude of the variation in the optical band is enormous, 1.2 mag peak-to-peak, because of the fact that the primary star radiates mainly in the ultraviolet, while the considerably cooler heated hemisphere radiates mainly in the optical. The central star of HFG 1 shows a nearly identical light curve, at an orbital period of 14.0 hours (Bond *et al.* 1988).

As discussed by Bond (1988*a*), the results of photometric searches for close-binary PNNs by several authors indicate that the fraction of binaries with $P \lesssim 1$ day among PNNs is about 15%. If we adopt the scenario suggested by Paczynski (1976), in which a wide binary drastically reduces its orbital separation by first entering a "common-envelope" stage, and then ejecting the envelope, it becomes clear that *a substantial fraction of planetary nebulae are ejected by binary interactions*, rather than in the normal course of single-star evolution.

The fraction of planetary nebulae ejected from binary PNNs could be much higher if many of the nuclei are binaries with periods of days to weeks. Such binaries would have been difficult to detect in existing surveys. We are now making a special effort to monitor PNNs over multi-night intervals, and there are already suggestions that many longer-period binaries may indeed exist. Two new examples are the nucleus of Sp 1, which we find to vary by about 0.1 mag with a period of about 3 days (a composite spectrum had already been noted by Méndez *et al.* 1988), and the nucleus of Sh 2-71, which varies by 0.4 mag with a period of approximately 2 weeks (the variability having been noted earlier by Kohoutek 1979).

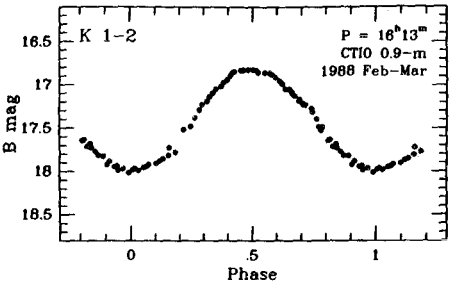

B light curve for the binary nucleus of K 1-2, obtained with a CCD detector on the CTIO 36-inch telescope in February-March 1988. The orbital period is 16.2 hours, and the variations are due only to a heated hemisphere on the main-sequence secondary star; no true eclipses occur.

During its subsequent evolution, a close-binary PNN will appear first as a detached white-dwarf/red-dwarf binary (such as V471 Tau), and ultimately, when magnetic braking and/or gravitational radiation force the stars close enough together for mass transfer, as a cataclysmic variable. A discussion of the birth rate for close-binary PNNs (Bond 1988*a*) shows that it is, if anything, more than enough to account for the origin of *all* cataclysmic binaries in the solar neighborhood.

3. Pulsating Nuclei

Grauer and Bond (1984) discovered the first known *pulsating* PNN, the central star of Kohoutek 1-16. Its spectroscopic properties—strong features of He II, C IV, and O VI—are shared by the four known pulsating GW Vir (PG 1159−035) white dwarfs, and both the white dwarfs and the PNN are multiperiodic, *g*-mode pulsators. It thus seems probable that all of these objects share a common instability mechanism, possibly cyclical ionization of C and/or O in a hydrogen-deficient envelope (Starrfield *et al.* 1984, 1985; see critical discussion by Kawaler 1988).

The nucleus of the southern planetary nebula Longmore 4 shows strong He II and C IV absorption, without detectable Balmer absorption (Méndez *et al.* 1985). It was therefore an obvious candidate for photometric monitoring, and CCD photometry obtained at CTIO has now confirmed that Lo 4 is the second known pulsating PNN (Bond 1988*b*). A typical light curve is shown below; the dominant periodicity, as in K 1-16, is near 30 minutes, but the strong beating shows that several additional modes are present.

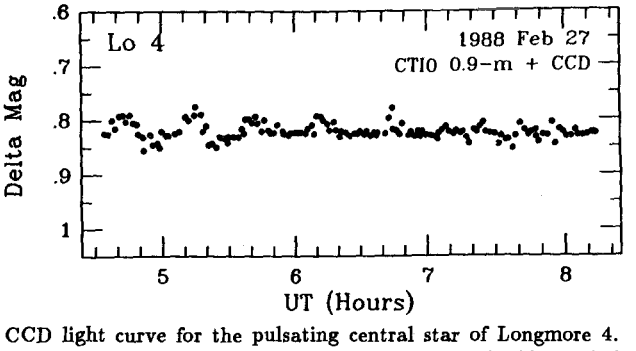

Typical CCD light curve for the pulsating central star of Longmore 4. There is a strong periodicity near 30 min, with beating due to several additional closely spaced frequencies.

The pulsation periods are considerably shorter (~6–10 min) in the four known GW Vir white dwarfs, in accordance with the view that they are somewhat more evolved, more compact stars. We presume that they were recently surrounded by planetary nebulae that have now dissipated. Continued monitoring of Lo 4 is planned, in an attempt to detect the period changes that are expected to be produced by the evolutionary contraction of this pre-white-dwarf star (*cf.* the study of GW Vir itself by Winget *et al.* 1985).

Preliminary analysis of our photometry of the central star of NGC 1501, a member of the "O VI" class of PNNs, suggests that it is another pulsator; if so, its light curve is unusually chaotic, implying a very rich mode spectrum.

4. Irregularly Variable Planetary Nuclei

Our monitoring program has revealed several members of a new class of non-periodic, low-amplitude variables. These objects show variations of a few hundredths of a magnitude over timescales of several hours, and/or show differences in light level by such amounts from night to night. A typical light curve, for the central star of IC 4593, is shown below.

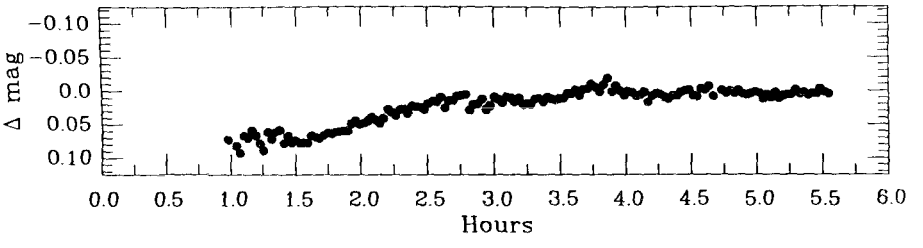

CCD light curve for the irregularly variable central star of IC 4593. During this night, the star brightened by nearly 0.1 mag over about 3 hr, and was then nearly constant for another 1.5 hr. On other nights, the PNN varied irregularly about levels that were 0.02–0.05 mag brighter.

Other members of this class are the nuclei of Hu 2-1, IC 3568, NGC 6543, and possibly NGC 40. Similar photometric behavior has been reported for the central star of IC 418 by Méndez *et al.* (1983), and seems to be present in photoelectric photometry of IC 2149 (Bond and Grauer, unpublished).

One obvious characteristic that these variables share is the presence of a high-surface-brightness nebula, suggesting that they are nuclei of relatively young planetaries. An even more striking characteristic is that *all of them are known to have strong stellar winds*, as revealed by *IUE* observations (Castor *et al.* 1981; Cerruti-Sola and Perinotto 1985).

The strong correlation of low-amplitude optical variability with presence of a stellar wind suggests either that the light variability is due to a variable mass-loss rate, or that both the variability and the mass loss arise from some common (but presently unknown) underlying physical mechanism. Further exploration of this new phenomenon will require simultaneous photometry and UV or optical spectroscopy.

5. References

Bond, H.E. 1988*a*, in *Proceedings of IAU Symp. No. 131, Planetary Nebulae*, in press.

_____. 1988*b*, *Bull. A.A.S.*, **20**, 735.

Bond, H.E., Ciardullo, R., Fleming, T.A., and Grauer, A.D. 1988, in *Proceedings of IAU Symp. No. 131, Planetary Nebulae*, in press.

Bond, H.E., and Grauer, A.D. 1987, in *Proceedings of IAU Colloq. No. 95, The Second Conference on Faint Blue Stars*, eds. A.G.D. Philip, D.S. Hayes, and J.W. Liebert (Schenectady: L. Davis Press), p. 221.

Castor, J.I., Lutz, J.H., and Seaton, M.J. 1981, *M.N.R.A.S.*, **194**, 547.

Cerruti-Sola, M., and Perinotto, M. 1985, *Ap. J.*, **291**, 237.

Grauer, A.D., and Bond, H.E. 1984, *Ap. J.*, **277**, 211.

Kawaler, S. 1988, these proceedings.

Kohoutek, L. 1979, *IAU Inf. Bull. Var. Stars*, No. 1672.

Méndez, R.H., Verga, A.D., and Kriner, A. 1983, *Rev. Mexicana Astr. Ap.*, **8**, 175.

Méndez, R.H., Kudritzki, R.P., and Simon, K.P. 1985, *Astr. Ap.*, **142**, 289.

Méndez, R.H., Kudritzki, R.P., Herrero, A., Husfeld, D., and Groth, H.G. 1988, *Astr. Ap.*, **190**, 113.

Paczynski, B. 1976, in *IAU Symposium No. 73, Structure and Evolution of Close-Binary Systems*, eds. P. Eggleton, S. Mitton, and J. Whelan (Dordrecht: Reidel), p. 75.

Starrfield, S., Cox, A.N., Kidman, R.B., and Pesnell, W.D. 1984, *Ap. J.*, **281**, 800.

_____. 1985, *Ap. J. (Letters)*, **293**, L23.

Winget, D.E., Kepler, S.O., Robinson, E.L., Nather, R.E., and O'Donoghue, D. 1985, *Ap. J.*, **292**, 606.

ON THE FORMATION OF CLOSE BINARY WHITE DWARFS

Icko Iben, Jr. and Ronald F. Webbink
University of Illinois

I. INTRODUCTION

Single stars of initial main-sequence mass larger than about $0.8\text{-}1.0M_\odot$ and less than approximately $6\text{-}8M_\odot$ evolve into carbon-oxygen white dwarfs of mass in the range $0.55\text{-}1.1M_\odot$ in less than the Hubble time. Single stars do not make helium white dwarfs in a Hubble time. These statements are based on both observational and theoretical considerations. It is not yet established, but there are suspicions that single stars of initial mass in the range $8\text{-}10M_\odot$ may evolve into oxygen-neon white dwarfs of mass in the range $1.1\text{-}1.4M_\odot$. As a single star of the appropriate initial mass develops a hot, electron-degenerate core composed of carbon and oxygen or of oxygen and neon, it becomes large ($R > 200R_\odot$) and luminous ($L > 6000L_\odot$), with the luminosity being generated most of the time by hydrogen burning, interrupted quasiperiodically by a helium shell flash. The star is said to be an asymptotic giant branch (AGB) star. Within $10^5\text{-}10^6$yr after arriving on the AGB, an envelope instability, whose nature is still being explored observationally and theoretically, leads to the ejection of most of the hydrogen-rich envelope of the star. The remnant shortly becomes the central star of a planetary nebula composed of the ejected material, and then cools into a white dwarf configuration.

In a close binary, the process of white dwarf formation can be radically different, as mass can be stripped from either star in a Roche-lobe overflow event and either transferred to the other star or lost from the system or both. Thus, the mass of the star which ultimately becomes a white dwarf can be quite different from that of the initial main-sequence progenitor, and the evolution of the white dwarf remnant of each Roche-lobe overflow event can be quite different from that of a single star of the same initial mass. Hence, the mapping between final white dwarf mass and composition and the main-sequence mass of the progenitor in a close binary is not the same as the mapping for single stars. For example, one can envision systems which form helium white dwarfs with masses in the range $\sim 0.1\text{-}0.5M_\odot$, something which single stars cannot do in a Hubble time. The upper limits on the masses of progenitors which can form carbon-oxygen and oxygen-neon white dwarfs is also influenced by presence in a close binary.

The evolution of white dwarfs formed in a close binary can also be different from the evolution of single white dwarfs. For example, the thicknesses of the hydrogen and helium layers in binary white dwarfs will be different from those of single white dwarfs because the mechanism of envelope ejection is different in the

two cases. This can affect cooling rates (through opacity) and spectral evolution (through diffusion, radiative levitation, and convective mixing). Due to frictional forces that arise in the common envelope which may be formed in Roche-lobe overflow events, the orbital separation of a binary white dwarf pair may be much smaller than the orbital separation of the progenitor main-sequence binary pair. If the white dwarfs are formed at a sufficiently small separation ($< 3R_{\odot}$), they will move once again into Roche lobe contact in less than the Hubble time due to the loss of orbital angular momentum by gravitational wave radiation. If the lighter white dwarf is sufficiently lighter than the heavier white dwarf, the net result may be a simple mass transfer with the ultimate dissolution of the secondary on a long time scale. GP Com may be an example of such evolution in progress (Nather, Robinson, and Stover 1981), and 40 Eridani B may be an example of the final result (Iben and Tutukov 1986). If the two white dwarfs are composed of helium and are initially of comparable and of sufficiently high mass, the immediate result of merger may be an sdO or sdB star (Webbink 1984; Iben and Tutukov 1985, 1986). If one of the dwarfs is made of carbon and oxygen and the other of helium, the immediate result of merger may be a hot helium deficient star or an R CrB star (Webbink 1984; Iben and Tutukov 1985). If both white dwarfs are composed of carbon and oxygen and the total mass of the pair exceeds the Chandrasekhar mass of $1.4M_{\odot}$, the net result of the merger may be a type Ia supernova (Iben and Tutukov 1984a; Webbink 1984). Finally, if the heavier white dwarf is made of oxygen and neon, the net result may be the formation of a neutron star without a very spectacular accompanying explosion (Iben 1986).

II. ROCHE-LOBE OVERFLOW, COMMON ENVELOPES, AND CONSERVATIVE MASS TRANSFER

Consider a close pair of intermediate mass ($2\text{-}8M_{\odot}$) main-sequence stars neither of which fills its Roche lobe until after it has exhausted hydrogen at its center. The primary evolves due to the transformation of lighter into heavier particles in its core. The core shrinks because (a) the pressure at any point is proportional to the number density of particles (which, without shrinkage, would decrease) at that point and (b) the gravitational force at any point is proportional to the mass interior to that point and, without shrinkage, this force would remain constant. Shrinkage of the core releases gravitational potential energy which is converted into heat. The increase in core temperatures causes the rate of nuclear energy production, which is proportional to a high power of the temperature, to increase. The increased flux of radiant energy through the envelope of the star causes this envelope to expand. Once hydrogen is exhausted at the center, this process of core shrinkage and envelope expansion accelerates, not to be halted until helium is ignited in the core.

If the primary fills its Roche lobe shortly after it exhausts central hydrogen and if the primary and secondary are initially of comparable mass, the time scale for mass transfer from primary to secondary will not be too different from the thermal

response time scale of the envelope of the secondary and the secondary may accrete most of the matter proferred by the primary. It is thought that this may be the way that relatively massive Algols are formed. During the final phase of mass transfer, the primary is a subgiant and the secondary is a brighter and hotter main sequence star. Even though Roche-lobe filling will be maintained in any case by nuclear evolution of the subgiant, the mass-transfer rate may be augmented by a magnetic stellar wind (e.g., Iben and Tutukov 1984b).

If the primary does not fill its Roche lobe until it is about to ignite helium, the rate of envelope expansion is so large that the timescale for mass transfer will be much smaller than the thermal response time scale of the secondary, and it is expected that the matter impinging on the secondary will form an expanding envelope which itself ultimately overflows the Roche lobe of the secondary. A "common envelope" (Paczynski 1976, Meyer and Meyer-Hofmeister 1979) then forms and the matter pushed into this envelope by the primary is thereafter presumably lost from the system. One may think of the common envelope as a viscous medium within which the binary evolves and this image points up the fact that frictional forces must abstract energy and angular momentum from the orbital motion (Bodenheimer and Taam 1984; Livio and Soker 1988; Livio 1988). The initial mass transfer rate will be even larger and the propensity to form a common envelope will be even further enhanced if the initial mass of the primary is much larger than the mass of the secondary. It is thought that classical cataclysmic variable systems and close binary central stars found in several planetary nebulae may be formed in this way (e.g., Paczynski 1976; Webbink 1979; Livio, Salzman, and Shaviv 1979).

The common envelope phenomenon continues until the amount of hydrogen-rich matter that remains on the surface of the primary drops below a critical value which depends on the mass and composition of the primary. This critical value is given roughly by the thickness of the hydrogen-burning shell and thus is larger for smaller primary masses. At the surface of the remnant, which has now contracted within its Roche lobe, matter which has undergone some CNO cycling has been exposed. The remnant continues to contract until helium is ignited at its center. At this time, its position in the H-R diagram lies between the main sequence and the white dwarf sequence, near the position occupied by homogeneous models of pure helium which are burning helium quiescently in their cores (the so-called helium main sequence).

The mass of the remnant is typically much smaller than the mass of its progenitor. For example, a $10M_{\odot}$ main sequence model of population I composition evolves into a core helium burning star of mass $2M_{\odot}$ and a $5M_{\odot}$ model evolves into a helium star of mass $0.77M_{\odot}$. Note that, in a binary system, the mass of a star which will ultimately evolve into a white dwarf can be larger than the maximum mass of a single star which can evolve into a white dwarf of the same composition. The numerical values quoted here and in the following are usually from the calculations of Iben and Tutukov (1985). Other choices of composition and input physics will lead to somewhat different values.

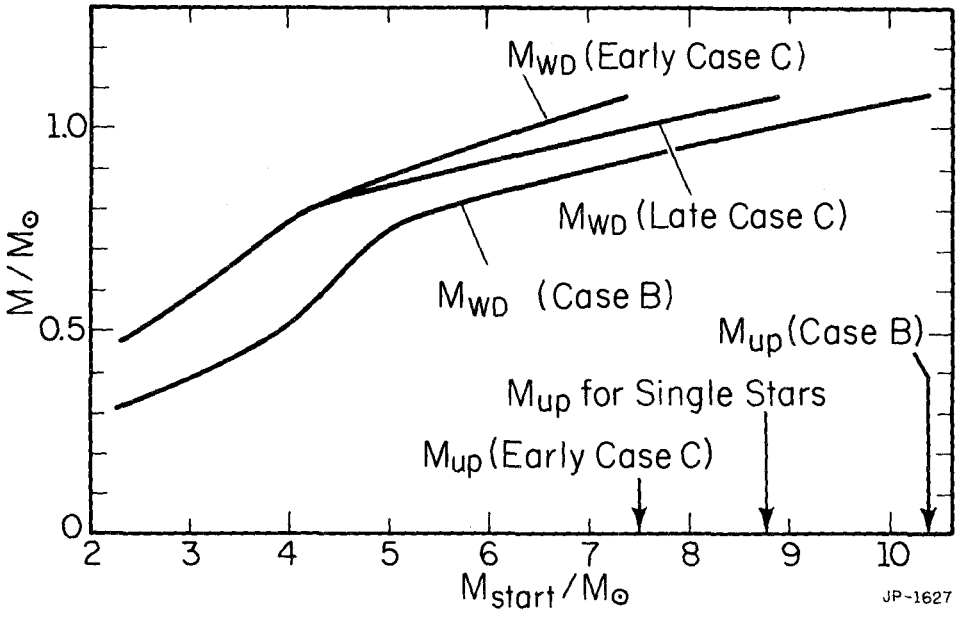

Figure 1. Transformations between progenitor mass and final white dwarf mass for case B and case C Roche-lobe overflow events.

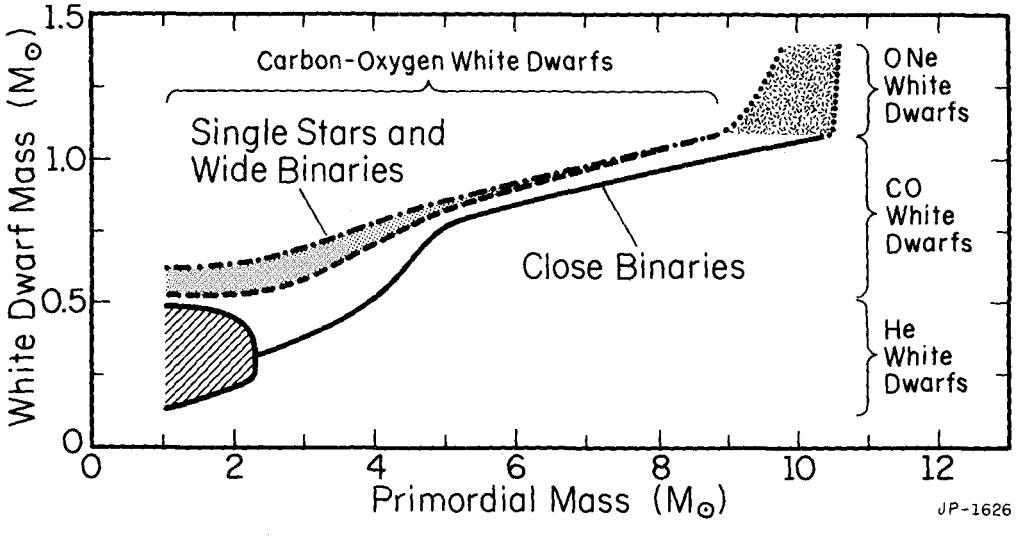

Figure 2. Transformation between initial progenitor mass and final white dwarf mass for single stars and binary stars in case B Roche-lobe overflow events.

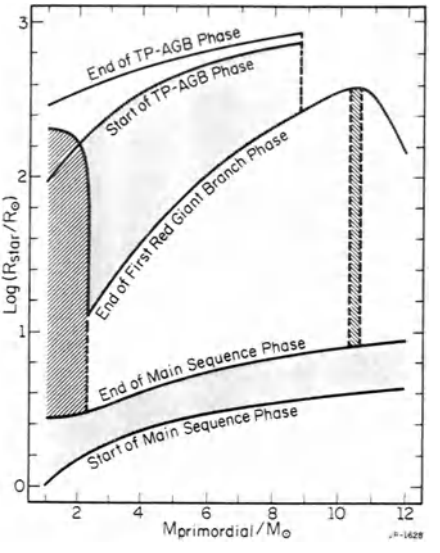

Figure 3. Radius versus initial stellar mass for various evolutionary stages of single stars.

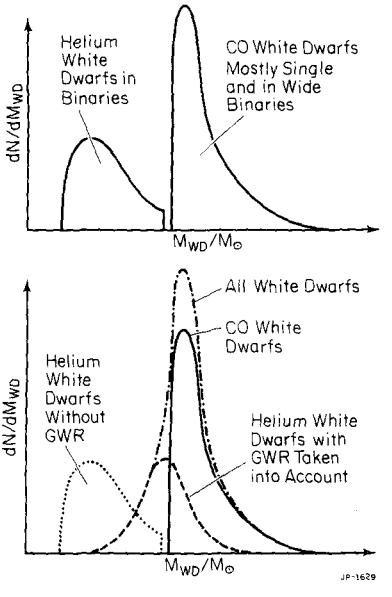

Figure 4. The top panel gives the birth rate of white dwarfs as estimated by Iben and Tutukov (1986). The lower panel is a schematic giving an impression of how the observed white dwarf mass distribution function may be built up from the estimated birth rate function when gravitational radiation is taken into account, forcing the merger of the lowest mass binary white dwarfs. The contribution of merged binaries has been overestimated by a factor of two, as we overlooked the fact that each merger reduces by one the number of white dwarfs surviving until the present.

If its mass is between ~0.75$M_\odot$ and ~2.5$M_\odot$, a helium star will expand again to fill its Roche lobe after exhausting central helium. It will begin and continue to lose mass until the mass of the helium layer remaining near its surface (its core has been converted into carbon and oxygen) has been reduced below a critical value. In this way the 2$M_\odot$ remnant of the first mass exchange event becomes ultimately a 1.05$M_\odot$ CO white dwarf and the 0.77$M_\odot$ remnant becomes a 0.75$M_\odot$ white dwarf.

If its mass is less than ~0.75$M_\odot$, the helium star remnant of the first common envelope event will not expand sufficiently on exhausting central helium to fill its Roche lobe for a second time. Instead, it will go on to become a white dwarf without losing any more mass.

If the mass of the progenitor is somewhere in the range 10-11$M_\odot$, the white dwarf formed will be of the oxygen-neon variety, with a mass in the range 1.1-1.4$M_\odot$. For more massive progenitors, evolution becomes more complicated, and the exact outcome of the Roche-lobe overflow episode has yet to be sorted out.

When a star fills its Roche lobe after having exhausted hydrogen at the center but before having ignited helium, we speak of a case B Roche-lobe overflow event. If the overflow event occurs before the star has crossed the Hertzsprung gap and developed a deep convective envelope (early case B event), much of the mass lost by the primary will be gained by the secondary. If orbital angular momentum is also partially conserved, the orbital separation may increase during the mass-transfer process. If the overflow event occurs after the primary has developed a deep convective envelope (late case B event), a common envelope is expected to be formed and the orbital separation is expected to be considerably reduced.

If Roche-lobe filling is delayed until the primary has exhausted helium at its center and has developed an electron-degenerate CO core, we speak of a case C event. If Roche-lobe filling occurs before thermal pulses begin (early case C event), the mass of the resultant white dwarf will be nearly the same as the CO core mass of a single star when it first begins to thermally pulse. Since mass loss can abort the "second" dredge up process (which occurs in population I stars for initial masses larger than ~5$M_\odot$) before the CO core is reduced to below 1.1$M_\odot$, the maximum mass of a progenitor which can produce a CO white dwarf is reduced by ~1$M_\odot$ relative to the maximum mass for single stars. If Roche-lobe filling is delayed until thermal pulses have begun (late case C event), the mass of the white dwarf which will be formed depends on how long the progenitor has remained in the thermally pulsing phase before Roche-lobe filling occurs. For progenitor masses less than ~2$M_\odot$, the mass of the white dwarf remnant can be anywhere between the mass of the CO core of the progenitor when thermal pulses begin and something approximately 0.1$M_\odot$ larger. For progenitor masses larger than this, the mass of the resultant white dwarf is essentially the same as the mass of a white dwarf formed by a single star. Because of the strong winds experienced by AGB stars, the mass of the primary could well be less than the mass of the secondary when Roche-lobe filling occurs. The result is that, in many late case C events, the initial rate of mass transfer might be considerably less than

would otherwise be expected, and that may reduce the tendency toward common envelope formation.

The mapping between progenitor initial mass and final white dwarf mass for the various types of Roche-lobe overflow events, as found in one set of calculations for one set of input physics (Iben and Tutukov 1985, Iben 1986) is shown in Figure 1. It is to be emphasized that these results are not definitive; any number of variations in the input physics could alter the mapping significantly.

III. MAPPING PROGENITOR BINARIES INTO WHITE DWARF BINARIES

The mapping between the masses and orbital separation of a main-sequence binary and the masses and orbital separation of the white dwarf binary (immediately following the formation of the second white dwarf) depends on which cases of Roche-lobe overflow are appropriate and on a number of other assumptions about the nature of the several mass-loss, mass-transfer interactions; very few of these assumptions are founded on first principles.

Of crucial importance is the evolutionary state of each star when it first fills its Roche lobe. Figure 2 gives curves in the radius-(initial)mass plane which mark where significant changes in the evolutionary state of single stars occur if they are of population I composition (Iben and Tutukov 1985).

When the first Roche-lobe overflow event is of the early case B variety and component masses are comparable, it has long been the practice to suppose that both the total mass and the total angular momentum of the system are conserved. Given a mapping between initial primary mass and resultant white dwarf mass, the assumption of conservation of total angular momentum and total mass then leads to a unique determination of the masses and orbital separation of the intermediate system, now consisting of a white dwarf and a main-sequence secondary which is more massive than the initial primary.

If the first Roche-lobe overflow event is of the late case B or of the case C variety or if the initial secondary is much less massive than the initial primary, it is commonly supposed that a common envelope will be formed. A convenient way of parameterizing the degree of orbital shrinkage which occurs in a common envelope event is (Iben and Tutukov 1984a)

$$G\, M_1^{\,2}/A_0 \sim \alpha\, GM_{1R}M_2/A_f, \qquad (1)$$

where M_1 and M_2 are the masses of the primary and secondary, respectively, M_{1R} is the mass of the remnant of the primary after the common envelope event, A_f and A_0 are the final and initial orbital separation, and α is a parameter which in some cases can be estimated theoretically but, in general must be determined from the observations. The expression on the left hand side of equation (1) is a crude measure of twice the energy required to drive off the common envelope when the mass lost from the system is large compared with the mass of the primary remnant and large compared with the mass of the secondary. The expression multiplying α on the right hand side of the

equation is a crude measure of twice the release in orbital binding energy for systems in which the degree of orbital shrinkage is large enough to neglect the initial orbital binding energy. When the masses of the two interacting stars are comparable, α in equation (1) should be divided by 4. With this understanding, an α of ~1 means that orbital energy is converted into the energy to drive off the common envelope with 100% efficiency. An α large compared with 1 means that some source of energy other than orbital has been tapped to drive off the common envelope. An α small compared with 1 means that only a fraction of the orbital energy has been used up in driving off the common envelope, the remaining fraction going into heating the escaping matter and supplying it with greater than escape velocities, or into radiative losses, or both.

Two and three dimensional hydrodynamical simulations of common envelope events (Livio and Soker 1988; Taam and Bodenheimer 1988) suggest an α of the order of 0.3-0.6. Livio and Soker find some evidence that, the larger the initial orbital separation, the greater the tendency for the stellar cores to spin up the common envelope, and therefore the less efficient the transfer of energy between the orbital energy and the expanding common envelope will be. In any case, one can understand the formation of cataclysmics by this kind of scenario. For example, suppose that the primary and the secondary are of initial mass ~$10M_\odot$ and ~$0.5M_\odot$, respectively, and that the primary fills its Roche lobe in a late case B event to become a white dwarf of mass ~$1.05M_\odot$. Inserting these numbers as well as $\alpha \sim 0.3$ in equation (1) gives $A_f \sim A_0/634$. For the chosen initial mass ratio, the radius of the Roche lobe of the primary is initially $R_{1L} \sim A_0/2$ and the radius of the Roche lobe of the secondary after the common envelope event is $R_{2L} \sim 0.3A_f$. Hence $R_{2L} \sim R_{1L}/1057$. But the secondary now has a radius of ~$0.5R_\odot$, and it presumably did not fill its Roche lobe until long after the common envelope event, when angular momentum loss by a magnetic stellar wind established contact. This means that $R_{1L} > 630R_\odot$. From Figure 2 it is obvious that our assumption of a case B event is inappropriate. A more consistent scenario requires choosing a slightly less massive primary and assuming a late case C event. Had we chosen $\alpha \sim 0.6$, the original scenario of a case B Roche-lobe overflow event would have been viable.

The main point of the exercise is to show that quite dramatic orbital shrinkages are implied by the assumption that orbital energy is the only source of energy for driving off the common envelope and that, the smaller the efficiency of conversion, the more dramatic is the shrinkage. We shall return to a discussion of this point in section V.

After the first white dwarf has been formed, if the secondary is massive enough to evolve off the main sequence in a Hubble time and if it fits well within its Roche lobe during its main-sequence lifetime, a second common envelope event will usually follow when the secondary exhausts a nuclear fuel at its center and expands to fill its Roche lobe. This is because the large ratio of donor mass to receiver mass ensures a mass transfer time scale much shorter than the thermal time scale of the

donor and because, not only is the thermal response time scale of the white dwarf much larger than the mass-transfer time scale, but hydrogen-burning may be ignited near the surface of the accreting white dwarf, causing the regeneration of a red giant (common) envelope, much as in the case of novae. The role of hydrogen burning is not absolutely certain since the mean densities in the common envelope may be much less than in the red giant envelope of a single star. In any case, due to frictional dissipation, orbital shrinkage will again occur and, when the two white dwarf remnants emerge from the common envelope, the orbital separation may be quite small. If the separation is less than several solar radii, gravitational wave radiation will lead to a merger of the pair in less than a Hubble time.

IV. LOW MASS BINARIES AND HELIUM WHITE DWARF PAIRS

Conventional theory suggests that a single star which is initially massive enough to evolve off the main sequence in less than a Hubble time can make a white dwarf no lighter than $\sim 0.5 M_\odot$ and that this white dwarf is made of carbon and oxygen (or of neon and oxygen in a small fraction of cases). On the other hand, if the primary in a low mass binary is less massive than about $2M_\odot$, it will develop an electron-degenerate core composed of helium as it leaves the main sequence, and, if it fills its Roche lobe before igniting helium, mass loss will transform it into the compact central star of a planetary nebula; after it has burned much of the hydrogen remaining in its envelope, it will evolve into a helium white dwarf capped by a very thin "skin" of hydrogen. The mass M_{He} of the white dwarf so formed is related to the effective radius R_L of the Roche-lobe when mass transfer begins by

$$R_L \sim 10^{3.5} M_{He}^{\,4}. \qquad (2)$$

If the primary and secondary are of comparable mass, and if the Roche-lobe radii are small enough (say, $R_L < 12R_\odot$, corresponding to $A_0 < 32.5R_\odot$ and orbital period $P < 12$ days) that the primary has not developed too deep a convective envelope before filling its Roche lobe, one might suppose that the mass transferred from the primary to the secondary will stick to the secondary. The primary will develop a deep convective envelope as it evolves to the giant branch, and an observer would see an Algol type binary. The primary will surely be tidally torqued so that it spins at nearly the orbital frequency, and one may further suppose that the agency which drives mass transfer is angular momentum loss by a magnetic stellar wind (MSW). If the time scale for mass transfer is short compared with the nuclear burning time scale $\tau_{nuc} = M_{He}/\dot{M}_{He}$, then the primary will shrink within its Roche lobe before M_{He} has grown appreciably and the Roche lobe of the primary will remain essential fixed during the entire mass-transfer phase. The orbital separation of the system after Roche-lobe detachment will be determined by solving

$$R_{iL} \sim 0.52(M_i/M_t)^{0.44} A, \qquad (3)$$

in conjunction with equation (2). In equation (3), R_{iL} is the Roche-lobe radius of the i^{th} component and M_i is its mass; M_t is the total mass of the system and A is the

orbital separation. There are more accurate expressions for the relationship between R_{iL}, M_i, M_t, and A, but for our purposes, expression (3) is quite accurate enough and it has the virtue of being simple to use.

Using equations (2) and (3) with the requirement that the radius of the Roche lobe is the same before and after the mass-transfer event, we have that

$$A_f = (M_1/M_{1R})^{0.44} A_0, \tag{4}$$

where A_0 and A_f are the orbital separation before and after the mass-transfer event and M_{1R} is the mass of the helium white dwarf remnant of the primary. Thus, A_f is typically a few times larger than A_0.

A reverse phase of mass transfer follows when the secondary grows to fill its Roche lobe. Since it will be a larger subgiant than was the primary when it filled its Roche lobe, the secondary will have a deeper convective envelope than did the primary as a subgiant. Furthermore, the accretor will now be a very compact object with a long thermal response time scale and probably capable of igniting the accreted fuel and regenerating its own extended envelope. The second mass transfer episode is therefore likely to lead to the formation of a common envelope, with all of the mass lost by the secondary being lost from the system. We therefore use equation (1) with $M_2 = M_{2R}$, $M_1 = M_2+(M_1-M_{1R}) = M_t-M_{1R} = M_{2f}$ = mass of secondary after the first mass transfer episode, $A_0 = A_f$, and $A_f = A_{ff}$ = final orbital separation to obtain:

$$A_{ff} = \alpha\, A_f (M_{1R}/M_{2f})(M_{2R}/M_{2f}). \tag{6}$$

Equations (2) and (3) can also be used to establish a relationship between the mass M_{2R} of the helium white dwarf remnant of the secondary and M_{1R}:

$$M_{2R} = M_{1R}(M_t/M_{1R}-1)^{0.11}. \tag{5}$$

The modest increase in orbital separation during the first mass-transfer/mass-loss episode thus implies that the second white dwarf is slightly more massive than the first. This is a general property of quasiconservative mass-transfer scenarios.

As an example, let us suppose that $M_1 = 1.5$, $M_2 = 1.0$, and $M_{1R} = 0.25$. Then, $M_{2R} = 0.32$, $A_0 = 29.7$, $A_f = 2.20A_0 = 65.4$, and $A_{ff} = 1.70\alpha$. An upper limit on the time required by the white dwarf pair to move into final Roche-lobe contact comes from assuming that the only way in which orbital angular momentum is lost is by the radiation of gravitational waves. This upper limit is given by

$$\tau_{GWR}(\mathrm{yr}) = 10^{8.175} A_{ff}{}^4/(M_{1R}M_{2R}M_{tR}), \tag{7}$$

where $M_{tR} = M_{1R}+M_{2R}$. Of course, if the orbital separation is comparable to the radii of the white dwarfs, tidal torques will cause heating and serve to shorten the time scale for moving into contact. Using $A_{ff} = 1.7\alpha$ in (7), we have that the helium white dwarf pair in our example will move into Roche-lobe contact in less than $\tau_{GWR} = 2.75\times10^{10}\alpha^4$ yr. Choosing $\alpha \sim 0.3$, $\tau_{GWR} \sim 2.2\times10^8$ yr.

One may repeat this exercise for many different combinations of initial (low) masses, only to find similar results: if the first-formed white dwarf is less massive than $\sim 0.3M_\odot$, the ultimate result is two helium white dwarfs which merge in less than a Hubble time. If the total mass of the two white dwarfs is less than some critical value of the order of $0.4\text{-}0.5M_\odot$, merger will lead to a white dwarf of mass equal to

the sum of the masses of the white dwarfs prior to merger. If the total mass of the merging pair is larger than this critical value, the immediate result of merging may well be an sdO or sdB star. But this star will ultimately evolve into a CO white dwarf.

If the initial orbital separation is large enough to permit the primary to reach the base of the giant branch (see Figure 2), it will have developed such a deep convective envelope that, when Roche-lobe filling first occurs, mass transfer takes place on a dynamical time scale, and a common envelope will be formed also in the first mass-transfer episode. If this is the case, then orbital shrinkage also occurs, with the consequence that the effective radius of the Roche lobe of the secondary becomes smaller than the effective radius of the Roche lobe of the primary (when the first mass-transfer episode begins). This means that the mass of the helium white dwarf formed by the secondary will be less than the mass of the first-formed helium white dwarf.

Using equations (1), (2), and (3) for each assumed common envelope event, we obtain:

$$M_{2R} = \alpha_1^{0.25}(M_2/M_1)^{0.36}(M_{1R}/M_1)^{0.25}(M_1+M_2/M_{1R}+M_2)^{0.11} \quad (9)$$

and

$$A_{ff} = \alpha_2\alpha_1 10^{3.784}(M_1+M_2/M_1)^{0.44}M_{1R}{}^4(M_{1R}/M_1)^2(M_{2R}/M_2) \quad (10)$$

for the mass of the second white dwarf and the final orbital separation in terms of the mass of the first white dwarf, respectively. Here we take into account the possibility that the parameter α could be quite different in the two common envelope events. Setting $M_1 = 1.5$, $M_2 = 1.0$, and $M_{1R} = 0.25$, we have $M_{2R} = 0.22\alpha_1^{0.25}$ ($= 0.16$ if $\alpha_1 = 0.3$) and $A_{ff} = 0.22\alpha_2\alpha_1^{0.25}R_\odot$ ($= 0.05R_\odot$ if $\alpha_1 = \alpha_2 = 0.3$) Equation (8) then gives $\tau_{GWR} \sim 1.36\times10^7\alpha_2{}^4\alpha_1{}^5$yr ($= 267$ yr, if $\alpha_1 = \alpha_2 = 0.3$). The same exercise for $M_{1R} = 0.35$ gives $M_{2R} = 0.30\alpha^{0.25}$ ($= 0.22$ if $\alpha_1 = 0.3$), $A_{ff} = 2.23\alpha_2\alpha_1^{1.25}R_\odot$ ($= 0.5R_\odot$ if $\alpha_1 = \alpha_2 = 0.3$), and $\tau_{GWR} = 5.4\times10^{10}\alpha_2{}^4\alpha_1{}^5$yr ($= 10^6$yr if $\alpha_1 = \alpha_2 = 0.3$). Note that typically $M_{2R} \sim 0.6M_{1R}$ (because $M_{1R}/M_1 \sim 0.16$ in equation 9). Only for values of M_{1R} larger than $\sim 0.45M_\odot$ will it take longer than a Hubble time for a merger to occur.

From these considerations it is evident that only the most massive helium white dwarfs are born at sufficiently wide separation that they can avoid merger in a Hubble time. This has interesting consequences for future searches for gravitational wave radiation from space detectors (e.g., Lipunov, Postnov, and Prokhorov 1986; Evans, Iben, and Smarr 1987; Hils, Bender, Faller, and Webbink 1988). It also explains why the observed white dwarf distribution function contains so few white dwarfs less massive than $\sim 0.5M_\odot$, despite the expectation that of the order of 10 percent of all stars are born in binaries with initial masses and separations such that they should go through the sort of evolution we have just sketched.

In Figure 4a we present an estimate (Iben and Tutukov 1986) of the birth rate of white dwarfs as a function of white dwarf mass. All of the white dwarfs in the low-mass hump of the two-humped distribution are helium white dwarfs in binaries. Most of the white dwarfs in the second hump are CO white dwarfs which are single or in

wide binaries. If, as our estimates suggest, all but the most massive helium white dwarf pairs merge in much less than the Hubble time, then, integrating over the lifetime of the galactic disk, the current white dwarf distribution function should look like what we have sketched in Figure 4b. That is, mergers shift all but the most massive helium white dwarf pairs made in binaries into the single star distribution and there are very few white dwarfs less massive than about $0.3M_{\odot}$.

V. THE CLOSE BINARY WHITE DWARF L870-2

Saffer, Liebert, and Olszewski (1988) have discovered that the star L870-2 is actually a pair of DA white dwarfs with a period of 1.6d. The two white dwarfs are very nearly of the same luminosity and surface temperature, implying that they are of very similar mass and age. However, the slight differences in global characteristics translate into finite differences in mass and cooling age which, though small, have a profound significance for unravelling the prior history of the system and for understanding the physics of mass transfer events in close binaries. We (Webbink and Iben 1988) have analysed data kindly provided by these authors in conjunction with theoretical evolutionary tracks in the HR diagram of cooling white dwarfs (Iben and MacDonald 1986) to estimate the masses of the white dwarfs to be $M_{1R} \sim 0.605$ and $M_{2R} \sim 0.54$. The mean cooling age of the white dwarfs is $\sim 10^9$yr, but the more massive white dwarf is older than the lighter white dwarf by $\sim 10^8$yr (adopting the mass-dependence of the cooling curves given by Winget et al. 1987). This means that the more massive white dwarf must be derived from the initially more massive of the main-sequence progenitor pair.

We shall explore several scenarios for the history of the system, showing how the properties of the current system place a constraint on the product of the two α's used to parameterize the degree of orbital shrinkage in common envelope events. Suppose, first, that the initial primary filled its Roche lobe after having exhausted central hydrogen, but before having ignited helium (a case B event). From Figure 1, we can estimate the mass of the primary to be $M_1 \sim 4.3M_{\odot}$. The main-sequence lifetime of such a star is $\tau_{MS} \sim 1.0 \times 10^8$yr. If the case B event was of the early variety, we might expect there to have been some orbital expansion and we might guess that the secondary was able to delay Roche-lobe filling until it had developed an electron-degenerate CO core, filling its Roche lobe eventually in a case C event. From Figure 2, we see that the mass of the secondary must be $M_2 \sim 2.7M_{\odot}$ when it first filled its Roche lobe. The main sequence plus core helium burning lifetime of such a star is $\tau_{MS+He} \sim 3.5 \times 10^8$yr. Since this is 2.5×10^8yr longer than the main sequence lifetime of the primary, and since the cooling ages of the current white dwarfs differ by only $\sim 10^8$yr, we exclude this scenario. Let us suppose next that the first mass-transfer event was of the late case B variety, thus presumably leading to orbital shrinkage in a common envelope; this requires that the second mass-transfer event also be of the case B variety. Again from Figure 2, we have that $M_2 \sim 4.1M_{\odot}$. The main-sequence

lifetime of such a star is $\tau_{MS} \sim 1.1 \times 10^8$yr, or only 10^7yr longer than the main-sequence lifetime of the primary. We therefore exclude this scenario as well.

Next, suppose that the primary undergoes a case C Roche-lobe overflow event. Its mass must have been $M_1 \sim 3.1 M_\odot$ and its main sequence plus core helium burning lifetime was $\tau_{MS+He} \sim 2.6 \times 10^8$yr. The secondary could not have undergone a case B Roche-lobe overflow event because its mass just prior to this event must have been, at $4.1 M_\odot$, larger than M_1, implying that it had gained at least $1 M_\odot$ from its companion. This contradicts our assumption that the first mass transfer event led to the formation of a common envelope, with all of the mass lost by the primary being lost from the system.

The last option, then, is that both Roche-lobe overflowing events were of the case C variety. Remarkably, but perhaps fortuitously, the main-sequence plus core helium burning lifetime of the $2.7 M_\odot$ secondary, $\tau_{MS+He} \sim 3.5 \times 10^8$yr, is longer than that of the primary by precisely the difference in the cooling ages of the white dwarfs.

The period of L870-2 combined with our estimates of component masses imply that the current orbital separation is $A_{ff} \sim 5.8 R_\odot$ and we may use this to make statements about the degree of orbital shrinkage in each mass-loss event. From equation (1) with $\alpha = \alpha_1$, we have $A_f = 0.17 \alpha_1 A_0$. For the second mass- transfer event we rewrite equation (1) as

$$G M_2^2 / A_f \sim \alpha_2 \, G M_{1R} M_{2R} / A_{ff} \qquad (1')$$

and solve for $A_f = 130.5/\alpha_2$. From equation (3), we have that the Roche lobe radius about the primary <u>after</u> the first mass-loss event is $R_{1L,f} = 0.25 A_f = 32 R_\odot/\alpha_2$. With $\alpha_2 = 0.3$-0.6, $A_f = (435$-$217) R_\odot$ and $R_{1L,f} = (106$-$53) R_\odot$. from the two relationships involving A_f, we find $A_0 = 768/\alpha_1\alpha_2$ and from equation (3) we find the radius of the Roche lobe about the primary <u>before</u> the first mass-transfer event to be $R_{1L,0} = 0.395 A_0 = 303 R_\odot/\alpha_1\alpha_2$ From Figure 2 it is evident that $25 < R_{1L,0}/R_\odot < 500$ and this means that $0.6 < \alpha_1\alpha_2 < 12$. But, with $\alpha_2 \sim 0.3$-0.6, $\alpha_1 > 1$-2.

Recall that, when the component masses are comparable, as is the case prior to the first mass-loss event, GM_2M_{1R}/A_f overestimates (two times) the binding energy release by approximately a factor of 4. Hence, our scenario and the observational constraints tell us that orbital energy provided only one-eighth to one-fourth of the energy needed to drive off the common envelope. This result has profound ramifications for our understanding of the physics of the common envelope process. If one is used to thinking that the only source of energy for driving off the common envelope is orbital binding energy and that only a portion of the binding energy release is available for this purpose, then an α smaller than unity makes sense, but an α larger than unity is nonsense.

However, we know that single stars that reach the AGB eject their hydrogen-rich envelopes in only a matter of 10^4-10^5 yr. Is it not possible that, in the case of L870-2, the primary reached the thermally pulsing AGB stage before it filled its Roche lobe, and that the main driving force which ejected its hydrogen-rich envelope

was exactly the same as that which drives off the envelope of a single AGB star? It could be that the modification of the gravitational potential caused by the presence of a close companion speeds up the process of mass loss to a time scale of only few times 10^3 yr (cf. Eggleton 1985). The high densities in the wind from the primary and the differential velocities between the main-sequence companion and the wind would mean that there will be dissipation that causes orbital shrinkage, but shrinkage on a much more moderate scale than we are used to thinking of in terms of common envelopes (see Livio 1988 for a further discussion of this point).

At this conference, a poster paper by Bergeron, Wesemael, Liebert, Fontaine, and LaCombe (1988) suggests that the white dwarfs in L870-2 have masses $M_{1R} = 0.47$ and $M_{2R} = 0.42$. (The difference between these mass estimates and our own is almost wholly due to differences in the adopted mass-radius relationships for cooling white dwarfs). It is not feasible here to examine all of the possible scenarios which might produce these masses at the current separation. We explore one.

Suppose that both stars are helium white dwarfs that derive from low-mass progenitors after the fashion described in section IV. The white dwarf masses are large enough that we expect a common envelope to be formed in each mass-loss episode. If the constraint of 10^8yr as the difference between the cooling ages of the white dwarfs still holds, even approximately, we must assume that both main-sequence progenitors are almost identical in mass ($\tau_{MS} \sim 10^{10}\text{yr} \times M_i^{-3.5}$ and $M_i < 2M_\odot$). From equations (2) and (3), we have $R_{1L,0} = 155R_\odot = 0.38A_0$, or $A_0 \sim 400R_\odot$. From equation (1) with $M_2 \sim M_1$, $A_f \sim 400R_\odot\alpha_1 M_{1R}/M_1 = 188R_\odot\alpha_1/M_1$. But, we also have, from equations (2) and (3) that $R_{2L,f} = 98R_\odot \sim 0.5A_f$, giving $A_f \sim 196R_\odot$. The two expressions for A_f yield $\alpha_1 \sim M_1$, and, since both M_1 and M_2 must be at least as large as $1M_\odot$ if the evolution to the current configuration takes place in less than a Hubble time, $\alpha_1 > 1$. Once again, since the two main sequence progenitors are of comparable mass, this means that only a quarter (if $M_1 \sim 1M_\odot$) to one eighth ($M_1 \sim 2M_\odot$) of the energy needed to drive off the common envelope can have come from the release of orbital binding energy. Unfortunately, there is no simple mechanism to which one can point to provide the extra energy.

We can also make a statement about α_2. Using equation (1′) and $A_{ff} = 4.9R_\odot$, we have $\alpha_2 = 0.13M_2^2$. Since $1 < M_2/M_\odot < 2$, $\alpha_2 \sim 0.13\text{-}0.52$, and these values are consistent with the estimates of Livio and Soker (1988) and Taam and Bodenheimer (1988).

This example points up a difficulty repeatedly encountered in trying to construct a scenario for the progenitor of L870-2. Whatever the scenario, the immediate progenitor of this system must have had an orbital separation of ~200-$400R_\odot$. At this separation, the binary cannot have avoided a preceding phase of mass exchange; yet, to have preserved such a wide system, the first mass transfer episode must have succeeded in dispelling most of the envelope of the initial primary with very little loss of angular momentum. Common envelope evolution alone does not appear capable of fulfilling this requirement -- the dissipation of enough orbital

energy to eject the common envelope necessarily involves the dissipation of a great deal of orbital angular momentum as well. Nevertheless, at so large a separation, it is difficult to avoid the conditions at the first episode of mass transfer that would have led to common envelope evolution. One must mitigate this tendency by appealing to other, more benign forms of systemic mass loss, such as stellar winds, or perhaps by tapping the ionization energy of the relatively weakly bound first common envelope. To produce yet more widely separated close binary white dwarfs taxes the imagination. We therefore expect L870-2 to be among the longest period close binary white dwarfs created by any scenario.

This paper is supported in part by NSF grants AST 84-13371 and AST 86-16992.

REFERENCES

Bergeron, P., Wesemael, F., Liebert, J., Fontaine, G., and LaCombe, P. 1988. In I. A. U. Colloq. 114, White Dwarfs, ed G. Wegner (Berlin: Springer-Verlag), in press.

Bodenheimer, P., and Taam, R. E. 1984. Ap. J., **280**, 771.

Eggleton, P. P. 1985. In Interacting Binary Stars, eds. J. E. Pringle and R. A. Wade (Cambridge: Cambridge University Press), p. 21.

Evans, C., Iben, I. Jr., and Smarr, L. 1987. Ap. J., **323**, 129.

Hils, D., Bender, P. L., Faller, J. E., and Webbink, R. F. 1988. In preparation.

Iben , I. Jr. 1986. Ap. J., **304**, 201.

Iben, I. Jr., and MacDonald, J. 1986. Ap. J., **301**, 164.

Iben, I. Jr., and Tutukov, A. V. 1984a. Ap. J. Suppl., **54**, 335.

----------1984b. Ap. J., **284**, 719.

----------1985. Ap. J. Suppl., **58**, 661.

----------1986. Ap. J., **311**, 753.

Lipunov, V. M., Postnov, K. A., and Prokhorov, M. E. 1986. Astr. Ap., **176**, L1.

Meyer, F., and Meyer-Hofmeister, E. 1979. Astr. Ap., **78**, 167.

Paczynski, B. 1976. In I. A. U. Symp. 73, Structure and Evolution of Close Binary Stars, eds. P. Eggleton, S. Mitton, and J. Whelan (Dordrecht: Reidel), p. 75.

Livio, M. 1988. In I. A. U. Colloq. 107, Algols, ed. A. Batten (Dordrecht: Kluwer), in press.

Livio, M., Salzman, J., and Shaviv, G. 1979. M. N. R. A. S., **188**, 1.

Livio, M., and Soker, N. 1988. Ap. J., **329**, 764.

Nather, R. E., Robinson, E. L., and Stover, R. J. 1981, Ap. J., **244**, 269.

Saffer, R. A., Liebert, J. W., and Olszewski, E. 1987. B. A. A. S., **19**, 1041.

Taam, R. E., and Bodenheimer, P. 1988. Ap. J., in press.

Webbink, R. F. 1979. In I. A. U. Colloq. 46, Changing Trends in Variable Star Research, eds. F. M. Bateson, J. Smak, and I. H. Urch (Hamilton, NZ: University of Waikato Press), p. 102.

----------1984. Ap. J., **277**, 355.

Webbink, R. F., and Iben, I. Jr. 1988. In preparation.

Winget, D. E., Hansen, C. J., Liebert, J., Van Horn, H. M., Fontaine, G., Nather, R. E., Kepler, S. O., and Lamb, D. Q. 1987. Ap. J. Lett. **315**, 177.

A LIMIT ON THE SPACE DENSITY OF SHORT-PERIOD BINARY WHITE DWARFS

Edward L. Robinson and Allen W. Shafter
Department of Astronomy, University of Texas at Austin
Austin, Texas 78712

We infer that detached binary white dwarfs with orbital periods of a few hours exist because we observe both their progenitors and their descendents. The binary LB 3459 has an orbital period of 6.3 hr and contains a pair of hot subdwarfs that will eventually cool to become white dwarfs (Kilkenny, Hill, and Penfold 1981). L870-2 is a pair of white dwarfs and, given enough time, its 1.55 d orbital period will decay to shorter periods (Saffer, Liebert, and Olszewski 1988). GP Com, AM CVn, V803 Cen, and PG1346+082 are interacting binary white dwarfs with orbital periods between 1051 s for AM CVn and 46.5 min for GP Com (Nather, Robinson, and Stover 1981; Solheim *et al.* 1984; Wood *et al.* 1987; O'Donoghue and Kilkenny 1988). These ultra-short period systems must be descendents of detached pairs of white dwarfs. We also expect short-period binary white dwarfs to exist for theoretical reasons. All calculations of the evolution of binary stars show that main-sequence binaries can evolve to binary white dwarfs (*e.g.*, Iben and Tutukov 1984). Among Population I stars, 1/2 to 2/3 of all main-sequence stars are binaries and about 20% of these binaries should become double white dwarfs with short orbital periods (Abt 1983, Iben and Tutukov 1986). Thus, about 1/10 of all white dwarfs could be close binaries (Paczynski 1985). Nevertheless, no detached binary white dwarfs with extremely short periods have yet been found.

The space density of short-period binary white dwarfs is worth measuring for several reasons. Most generally, the space density is a test of modern theories for the evolution of binary stars. In addition, short-period binary white dwarfs should be the dominant source of gravitational radiation at periods between about 0.5 min and 1 hour (*e.g.*, Clark and Epstein 1979, Evans, Iben and Smarr 1987). Plans to build detectors of gravitational radiation at these periods using space-based interferometers are now being seriously considered and this new generation of detectors should be sensitive enough to detect binary white dwarfs (Faller and Bender 1984). Finally, in the most commonly discussed model for Type Ia supernovae, the progenitor of the supernova is a short-period binary consisting of two white dwarfs with a total mass greater than the Chandrasekhar limit (Webbink 1979; Tutukov and Yungelson 1979; Iben and Tutukov 1984; Paczynski 1985; Tornambè and Matteucci 1986). Gravitational radiation drives the binary to shorter orbital periods and ultimately disrupts the lower mass white dwarf. If enough mass accretes onto the higher-mass white dwarf, its mass will exceed the Chandrasekhar limit and it will collapse

catastrophically. The space density of short-period binary white dwarfs is a direct test of this model.

We undertook, therefore, a search for binary white dwarfs among spectroscopically identified DA and DB white dwarfs (Robinson and Shafter 1988). As our primary goal was to test binary white dwarf models for Type Ia supernovae, we designed the survey to be sensitive to extremely short periods. Our basic method was to look for orbital radial velocity variations in the white dwarfs, although we chose an unusual instrumental technique for measuring the velocity variations. We used a high-speed photometer equipped with narrow band filters whose bandpasses lay in the wings of an absorption line, the Hγ line for DA white dwarfs or the He I λ4471 line for DB white dwarfs. If the radial velocity of the white dwarf varies, the center of the absorption line moves toward or away from the filter bandpass, decreasing or increasing the flux of light through the filters. Orbital radial velocity variations can be detected from periodic variations in the filtered light curve. The amplitude of the flux variations can be converted to the amplitude of the radial velocity variation once the slope of the spectrum in the wing of the absorption line is known. Since all white dwarfs have surface gravities near $\log g = 8$ and since the slopes do not depend strongly on the temperature of the white dwarf over the temperature range in which most white dwarfs are found, we used a typical value for the slopes to convert the flux variations to radial velocity variations. The slopes were taken from the theoretical line profiles calculated by Koester (1980) for the DB white dwarfs and by Wickramasinghe (1972) for the DA white dwarfs.

We observed 44 DA and DB white dwarfs chosen from the Villanova catalogue of spectroscopically identified white dwarfs (McCook and Sion 1987). The sample of stars consisted of white dwarfs that are brighter than $V = 14.5$, do not have close visual companions, and are observable from McDonald Observatory. There were no other selection criteria. We did not detect any binaries.

There are three significant limitations to our survey. First, because the temperatures of the narrow band filters were not actively controlled, their central wavelengths slowly drifted as the ambient temperature in the telescope dome changed, introducing systematic errors into the measured intensities. These errors became significant on time scales longer than three hours and, therefore, we limited our survey to orbital periods less than three hours. The short-period limit was 30 s and was set by the sampling interval in the flux measurements. Second, the fluxes through the narrow band filters were low, limiting our ability to detect small flux and radial velocity variations. Finally, if the two stars in a binary have similar brightness, our sensitivity to radial velocity variations decreases. If the spectral types of the two stars are different, the absorption line being measured is diluted by the continuum light from the other star and the slope of its wings and the flux variations are reduced. If the spectral types of the two stars are the same, the detected flux variations correspond to the weighted average of the radial velocity variations of the two stars. Since the radial

velocities of the two stars have different signs, the averaging can reduce the flux variations and thus our sensitivity to radial velocity variations greatly.

It is impossible to know the exact effect of these various limits on our sensitivity to short-period binaries without knowing the distribution of orbital periods, spectral types, and masses of the binary white dwarfs, which is precisely what we do not know. The upper limits to the semi-amplitudes of the radial velocity variations are less than 70 km s^{-1} for 34 of the stars we observed and between 70 and 100 km s^{-1} for the remaining 10 stars. We have estimated the probability that we would have missed any binaries in our sample given these velocity limits by examining types of binaries that would be pathologically difficult to detect, generally binaries with periods at the long-period limit containing white dwarfs of nearly equal luminosities. We find that we should have detected more than half of even the most difficult cases. Although there is a finite probability that we have missed some binaries in our sample, we believe that our sensitivity is good enough to have detected a large fraction, perhaps 90%, of all binaries in our sample.

Our null result implies that the fraction of field white dwarfs that are binaries with periods less than 3 hours is less than 1/20 with a probability of 0.9. Since the properties of the white dwarfs in our sample are roughly similar to the properties of the white dwarfs in the sample used by Fleming, Liebert and Green (1986) to determine the space density and birth rates of white dwarfs, we can scale their results to obtain limits on the space density of binary white dwarfs. We find that the space density of binary white dwarfs with periods less than 3 hours and with $M_V < 12.75$ is less than 3.0×10^{-5} pc^{-3} with a probability of 0.9.

We test the binary white dwarf model for the progenitors of Type Ia supernovae by comparing the observed limit on the space density of binary white dwarfs to the space density required to produce the observed rate of Type Ia supernovae. If the observed rate of Type Ia supernovae per unit volume in the Galaxy is R and if the orbital periods of the progenitor binary white dwarfs decay at a rate dP/dt, the distribution of binary white dwarfs in period is

$$n(P) = R\left(\frac{dP}{dt}\right)^{-1} .$$

We assume that the only mechanism causing the orbits to decay is gravitational radiation and that most of the binary white dwarfs first emerge from their common envelope evolution at periods longer than 3 hours. The required space density of binary white dwarfs with orbital periods less than 3 hours is given by the integral of $n(P)$ over orbital periods between 0 and 3 hours.

The rate of Type Ia supernovae in the galaxy is not well known. Using the historical supernovae, Tammann (1982) derives a rate of 0.027 yr^{-1} for the entire Galaxy. Using a subset of the historical supernovae, van den Berg (1983) and van den Berg, McClure, and Evans (1987) derive a rate of 0.022 yr^{-1} for all supernovae.

Somewhat over half of this rate is due to Type I supernovae, from which we can derive a rate of roughly 0.012 yr^{-1} for Type I supernovae alone. Note that the observed ratio of Type I to Type II supernovae in the Galaxy is not the same as the ratio in other galaxies, almost certainly because many Type II supernovae in the Galaxy have been missed. We convert the total rate to a volume rate by the usual method. The effective area of the Galactic disk is 10^9 pc^3 (Miller and Scalo 1979). According to Tammann (1982) the observed scale height of Type I supernovae about the Galactic disk is about 200 pc. Alternatively, if we assume that Type Ia supernovae belong to an extremely old disk population, a scale height as large as 400 pc may be more appropriate. The value of R could, then, reasonably lie anywhere between 1.5×10^{-14} and 6.8×10^{-14} yr^{-1} pc^{-3}. The latter value is the one given by Tammann (1982). We adopt $R = (4.0 \pm 2.5) \times 10^{-14}$ yr^{-1} pc^{-3}.

We this choice of R, the required space density of binary white dwarfs that will become Type Ia supernovae is $(1.6 \pm 1.0) \times 10^{-5}$ pc^{-3}. On theoretical grounds we expect that only about 1/10 of all binary white dwarfs are pairs of Carbon-Oxygen white dwarfs with total masses high enough to become Type Ia supernovae (Iben and Tutukov 1986) and, therefore, the required space density of progenitors for Type Ia supernovae must be multiplied by 10 to give the a required space density of all short-period binary white dwarfs. The number that is to be compared to our observed limit is, then, $(1.6 \pm 1.0) \times 10^{-4}$ pc^{-3}. The required space density is a factor of 5 ± 3 greater than our observed limit.

Our result is evidence that there is something amiss in the simplest binary white dwarf models for the progenitors of Type Ia supernovae. There are several possibilities for what could be wrong; among them:

1) The measured rate of Type Ia supernovae in the Galaxy may be too high. The rate is based on a small number of historical supernovae in the galaxy, 7 in Tammann's sample and 3 in van den Berg's sample, and requires uncertain corrections for incompleteness. A large error in the rate would, nevertheless be surprising because with reasonable choices for the luminosity of the Galaxy and for the Hubble constant the galactic rate now agrees with the rate for external galaxies (van den Berg, McClure, and Evans 1987).
2) Binary white dwarfs may be only one of several different progenitors for Type Ia supernovae. Iben and Tutukov (1984) have catalogued the possible alternative progenitors. One alternative, interacting helium star-white dwarf pairs, is particularly attractive as these systems could have a high enough birth rate to account for Type Ia supernovae if a large fraction of these systems become Type Ia instead of Type Ib supernovae (Iben and Tutukov 1987; Iben, Nomoto, Tornambè, and Tutukov 1987).
3) We have assumed that binary white dwarfs all form at orbital periods longer than 3 hours. Theoretical calculations (*e.g.*, Webbink 1984) suggest that some fraction of the binaries should form at periods less than 3 hours. Because binaries formed at shorter periods have shorter lifetimes, the space density of these short period

systems would be low. The fraction of systems that are formed at periods less than 3 hours is uncertain because the physics of common-envelope evolution is uncertain, but a fraction larger than one-half may require a major revision in our understanding of common envelope evolution.

4) If the binaries have special properties, they could have been missed because of the way we selected the stars to observe. A magnitude limited survey like ours is biased towards intrinsically bright stars. If most of the progenitors of Type Ia supernovae have absolute visual magnitudes fainter than about 13.0 they will be under-represented in our sample. Also, if the progenitors are pairs of DC white dwarfs, they would not be included in our sample.

5) Finally, some technical problems could arise in comparing the space density of binary white dwarfs to the birth rate for Type Ia supernovae. If any mechanism for removing orbital angular momentum from the system besides gravitational radiation is operating, the orbits will decay faster and the required space density of binary white dwarfs will be reduced. No reasonable alternative to gravitational radiation has been suggested, however. We have adopted a value of 1/10 for the ratio of the number of binary white dwarfs with total mass large enough to make supernovae to the number with mass too small to make supernovae. It would be necessary to invoke a peculiar IMF at early times to change the ratio by a large factor. If the distribution of binary white dwarfs in orbital periods is not in a steady state, the relation between $n(P)$ and R that we have adopted is not correct. This could happen if the star formation rate in the galaxy (or at least in the neighborhood of the sun) has been far from uniform.

This research was supported in part by NSF Grant AST-8704382.

References

Abt, H. A. 1983, *Ann. Rev. Astr. Ap.*, **21**, 343.
Clark, J.P.A., and Epstein, R. 1979, in *Sources of Gravitational Radiation*, ed. L. L. Smarr (Cambridge: Cambridge University Press), p. 482.
Evans, C. R., Iben, I., and Smarr, L. 1987, *Ap. J.*, **323**, 129.
Faller, J. E., and Bender, P. L. 1984, in *Precision Measurement and Fundamental Constants II*, ed. by B. N. Taylor and W. D. Phillips (NBS Spec. Pub. 617).
Fleming, T. A., Liebert, J., and Green, R. F. 1986, *Ap. J.*, **308**, 176.
Iben, I., Nomoto, K., Tornambè, A., and Tutukov, A. V. 1987, *Ap. J.*, **317**, 717.
Iben, I., and Tutukov, A. V. 1984, *Ap. J. Suppl.*, **54**, 335.
Iben, I., and Tutukov, A. V. 1986, *Ap. J.*, **311**, 753.
Iben, I., and Tutukov, A. V. 1987, *Ap. J.*, **313**, 727.
Kilkenny, D., Hill, P. W., and Penfold, J. E. 1981, *M.N.R.A.S.*, **194**, 429.
Koester, D. 1980, *Astr. Ap. Suppl.* , **39**, 401.
McCook, G. P., and Sion, E. M. 1987, *Ap. J. Suppl.*, **65**, 603.
Miller, G. E., and Scalo, J. H. 1979, *Ap. J. Suppl.*, **41**, 513.
Nather, R. E., Robinson, E. L., and Stover, R. J. 1981, *Ap. J.*, **244**, 269.

O'Donoghue, D., and Kilkenny, D. 1988, *M.N.R.A.S.*, in press.
Paczynski, B. 1985, in *Cataclysmic Variables and Low-Mass X-Ray Binaries*, ed. D. Q. Lamb and J. Patterson (Dordrecht: Reidel), p. 1.
Robinson, E. L., and Shafter, A. W. 1987, *Ap. J.*, **322**, 296.
Saffer, R. A., Liebert, J., and Olszewski, E. W. 1988, *Ap. J.*, in press.
Solheim, J. E., Robinson, E. L., Nather, R. E., and Kepler, S. O. 1984, *Astr. Ap.*, **135**, 1.
Tammann, G. A. 1982, in *Supernovae: A Survey of Current Research*, ed. M. J. Rees and R. J. Stoneham (Dordrecht: Reidel), p. 371.
Tournambè, A., and Matteucci, F. 1986, *M.N.R.A.S.*, **223**, 69.
Tutukov, A. V., and Yungelson, L. R. 1979, *Acta Astr.*, **29**, 665.
van den Berg, S. 1983, *P.A.S.P.*, **95**, 388.
van den Berg, S., McClure, R. D., and Evans, R. 1987, *Ap. J.*, **323**, 44.
Webbink, R. F. 1979, in *IAU Colloquium No. 53, White Dwarfs and Variable Degenerate Stars*, ed. H. M. Van Horn and V. Weidemann (Rochester: University of Rochester), p. 426.
Webbink, R. F. 1984, *Ap. J.*, **277**, 355.
Wickramasinghe, D. T. 1972, *Mem. R. A. S.*, **76**, 129.
Wood, M. A., Winget, D. E., Nather, R. E., Hessman, F. V., Liebert, J. W., Kurtz, D. W., and Wesemael, F. 1987, *Ap. J.*, **313**, 757.

ON THE MASSES OF THE WHITE DWARFS IN CLASSICAL NOVA SYSTEMS

James W. Truran
University of Illinois

and

Mario Livio
Department of Physics, Technion

I. INTRODUCTION

Significant progress in our understanding of the nature of the outbursts of the classical novae has occurred over the past two decades (see, e.g., reviews by Truran 1982; Starrfield 1986). Their outbursts are now understood to be driven by thermonuclear runaways proceeding in the accreted hydrogen-rich shells on the white dwarf components of close binary systems. Critical parameters which serve to dictate the varied characteristics of the observed outbursts include the intrinsic white dwarf luminosity, the rate of mass accretion, the composition of the envelope matter prior to runaway, and the white dwarf mass.

Our concern in this paper is specifically with the question of the white dwarf mass. The expected average mass of isolated white dwarfs in the interstellar medium is $\sim 0.6 - 0.7\ M_{\odot}$; this follows straightforwardly from the assumption of a Salpeter (1955) stellar mass function and standard stellar evolution theory, and is confirmed by observations (Koester, Schulz, and Weidemann 1979). The question arises as to whether white dwarf masses in this range should be typical of the white dwarfs in close binary systems. We seek to provide a partial answer to this question, for the specific case of classical nova systems, on the basis of observations of the dynamical evolution of novae in outburst (Section II) and of the abundances in nova nebular ejecta (Section III). We then provide an estimate of the average mass of the white dwarf component of observed classical nova systems (Section IV), on the basis of theoretical arguments concerning the critical envelope mass necessary to trigger runaway on a white dwarf of specified mass. Finally, we review existing mass estimates for novae and discuss these in the light of theoretical models.

II. DYNAMICAL INDICATIONS

There exists a large number of observations which point towards a very dynamical nature of many nova outbursts. These dynamical indicators can, in turn, be related to a relatively high mass for the white dwarf. We shall now review some of these observation and their implications.

(i) Speed class

Out of 65 galactic novae listed by Payne-Gasposchkin (1957), 39 can be classified as "fast" or "very fast" novae, in the sense that their rate of decline from maximum exceeds 0.08 magnitudes per day.

(ii) Super-Eddington luminosity

The Eddington luminosity for a Chandrasekhar-mass white dwarf is of the order of 5.3×10^4 $L_\odot$, corresponding to an absolute bolometric magnitude $M_{bol} = -7.1$. It is interesting to note in this regard that de Vaucouleure (1978) finds that twelve out of fifteen novae for which the distance has been determined, using expansion parallaxes or interstellar line intensities, reach absolute magnitudes brighter than -7.1. Therefore, 12 out of the 15 systems reached super-Eddington luminosities (see Truran, Shankar, Livio, and Hayes (1988), for a discussion of this point). Moreover, all of the novae designated as "fast novae" by Payne-Gaposchkin (1957) reached absolute visual magnitudes brighter than -7.1.

(iii) High expansion velocities

In a number of novae for which expansion velocity measurements exist, high velocities were indicated. A few examples are: V1500 Cyg (1975) for which a velocity of $V_{exp} = 1600$ km s^{-1} was measured (e.g. Ferland 1978; Ferland and Shields 1978), CP Lac (1936) where $V_{exp} = 1300$ km s^{-1} (e.g. Pottasch 1959; Ferland 1979), DK Lac (1950) with $V_{exp} = 870$ km s^{-1} (Collin-Souffrin 1977), IV Cep (1971) with $V_{exp} = 1000$ km s^{-1} (Pacheco 1977; Ferland 1979) and V1668 Cyg (1978) with $V_{exp} = 740$ km s^{-1} (Stickland et al. 1981).

We shall now argue that all of these observations (in addition to others discussed in the next sections) point towards high white dwarf masses in the observed novae. The main point to note here is that the observations described in (i) - (iii) above outline a very dynamical nature of the outburst.
Specifically: (a) High expansion velocities are clearly the signature of a dynamical event. (b) Super-Eddington luminosities can be obtained only in a configuration departing from hydrostatic equilibrium and (c) a rapid return to minimum indicates rapid expansion (which leads to cooling) and a short timescale for nuclear burning. All of these, in turn, can be obtained for relatively small envelope masses. We will now show that the theory of hydrogen shell flashes on the surface of accreting white dwarfs demonstrates that the more massive the white dwarf, the lower the mass it needs to accrete for a thermonuclear runaway (TNR) to occur. Both semi-analytical estimates (Fujimoto 1982, MacDonald 1983) and detailed numerical calculations (e.g. Prialnik et al. 1982, Starrfield, Sparks and

Truran 1985) have demonstrated that the strength of the outburst is determined largely by the pressure at the base of the accreted envelope. This pressure is given approximately by

$$P_b \doteq \left(GM_{WD}\Delta M_{acc}\right)/\left(4\pi R_{WD}^4\right) \qquad (1)$$

where ΔM_{acc} is the accreted mass. A TNR occurs when P_b exceeds some critical value, $P_{crit} \sim 2 \times 10^{19}$ dyne cm^{-2} (Truran and Livio 1986). Consequently, we find that ΔM_{acc} is proportional to R^4_{WD}/M_{WD}, which is a strongly decreasing function of the white dwarf mass. Therefore, massive white dwarfs ensure a low envelope mass at the time of the runaway. We would like to note, in this respect, that in the few cases in which the mass of the ejected nebula has been determined from observations (e.g. V1500 Cyg, CP Lac, IV Cep) masses of the order of 10^{-5} - 10^{-4} $M_\odot$ were found (admittedly with large uncertainties). These values are consistent with $M_{WD} \gtrsim 1\ M_\odot$ (Truran and Livio 1986). High white dwarf masses are associated also with higher expansion velocities, simply by the fact that the escape velocity (which the expansion velocity must exceed) is higher for higher white dwarf masses. Finally, we would like to point out that an optically thick wind, which can be responsible for large mass loss, also occurs only for relatively massive white dwarfs ($M_{WD} > 0.8\ M_\odot$; Kato and Hachisu 1988a,b). This is a consequence of the fact that the wind phase is obtained only following a large envelope expansion (which is obtained for massive white dwarfs, as explained above). Significant mass loss is essential in order to obtain nuclear burning timescales (and timescales for return to minimum) which are not excessively long (compared to observations).

We can therefore conclude that the most direct observations of nova outbursts, the light curve and expansion velocities, point towards relatively massive white dwarfs in many classical nova systems.

III. ABUNDANCE INDICATIONS

Spectroscopic studies of nova ejecta provide further support for the view that rather massive white dwarfs are common occurrences in classical nova systems. Element abundance data are now available for a number of novae. The available heavy element data, reviewed most recently by Truran (1985a,b) and Williams (1985), are presented in Table 1. Here we present specifically the mass fractions in the form of hydrogen, helium, carbon, nitrogen, oxygen, neon, sodium, magnesium, aluminum, silicon, sulphur, and iron. The available information concerning both helium and heavy-element abundances (total mass fraction Z) is collected in Table 2. For purposes of comparison, we note that solar system matter is characterized by a ratio He/H = 0.08 and a heavy-element mass fraction 0.019 (Anders and Ebihara 1982; Cameron 1982). Following Truran and Livio (1986), this table also indicates the fraction of the ejecta in the form of helium and/or heavy-element enriched matter for these 13 well-studied novae.

TABLE 1

Heavy-Element Abundances in Novae

Object	Mass Fractions									
	H	He	C	N	O	Ne	Na	Mg	Al	Si
RR Pic[1]	0.53	0.43	0.0039	0.022	0.0058	0.011	...	...	...	...
HR Del[2]	0.45	0.48	...	0.027	0.047	0.0030	...	...	...	...
T Aur[3]	0.47	0.40	...	0.079	0.051	...	...	...	...	...
V1500 Cyg[4]	0.49	0.21	0.070	0.075	0.13	0.023	...	...	...	...
V1668 Cyg[5]	0.45	0.23	0.047	0.14	0.13	0.0068	...	...	...	...
V693 Cr A[6]	0.29	0.32	0.0046	0.080	0.12	0.17	0.0016	0.0076	0.0043	0.0022
DQ Her[7]	0.34	0.095	0.045	0.23	0.29	...	...	...	...	...
V1370 Aql[8]	0.053	0.085	0.031	0.095	0.061	0.47	...	0.0092	...	0.0012

References. – (1) Williams and Gallagher 1979. (2) Tylenda 1978. (3) Gallagher et al. 1980. (4) Ferland and Shields (1978). (5) Stickland et al. 1981. (6) Williams et al. (1985). (7) Williams et al. 1978. (8) Snijders et al. 1984.

Several important conclusions can be drawn from the abundance data collected in these tables. (1) High helium to hydrogen ratios are characteristic of nova ejecta: the average for the 13 novae in Table 2 is He/H = 0.19. (2) High abundances of heavy elements, both the CNO group elements and the ONeMg group elements, characterize the ejecta particularly of the faster novae: V1500 Cyg, V1668 Cyg, V693 CrA, and V1370 Aql. (3) Substantial fractions of enriched matter are typical of both fast and slow novae: the average value for the novae listed in Table 2 is 0.38.

The presence of these abundance enrichments holds important implications with respect to the typical white dwarf masses in these systems. The critical question here is how such concentrations can arise. Possible sources of these heavy-element abundance enrichments include (i) mass transfer from the secondary, (ii)

TABLE 2

Abundances in Novae

Nova	Date	He/H	Z	Reference	Enriched Fraction
T Aur	1891	0.21	0.13	1	0.36
RR Pic	1925	0.20	0.039	2	0.28
DQ Her	1934	0.08	0.56	2	0.55
CP Lac	1936	0.11±0.02	...	2	0.08
RR Tel	1946	0.19	...	2	0.24
DK Lac	1950	0.22±0.04	...	2	0.30
V446 Her	1960	0.19±0.03	...	2	0.24
V533 Her	1963	0.18±0.03	...	2	0.23
HR Del	1967	0.23±0.05	0.077	2	0.35
V1500 Cyg	1975	0.11±0.01	0.30	2	0.34
V1668 Cyg	1978	0.12	0.32	3	0.38
V693 Cr A	1981	0.28	0.38	4	0.61
V1370 Aql	1982	0.40	0.86	5	0.93

References – (1) Gallagher et al. 1980. (2) Ferland 1979. (3) Stickland et al. 1981. (4) Williams et al. 1985; Williams 1985. (5) Snijders et al. 1984.

nuclear transformations accompanying the outburst, and (iii) outward mixing of matter from the underlying white dwarfs. Truran (1985b) and Truran and Livio (1986) have scrutinized these possibilities and concluded that neither mass transfer nor nuclear reactions accompanying the outburst are capable of explaining the observed anomalies.

It would appear, rather, that some fraction of the envelope matter and ejecta represents material which has somehow been dredged up from the core of the underlying white dwarf. Such envelope contamination can result, in principle, from shear-induced turbulent mixing between the white dwarf and the accreted material (Livio and Truran 1987), from diffusion induced convection (Kovetz and Prialnik 1985), or from convective overshooting subsequent to the runaway (Woosley 1987). Whatever the mechanism, the character of such enrichments is a function of the underlying white dwarf structure and composition. High He/H ratios can result when the accreted hydrogen-rich matter mixes with helium-shell matter on white dwarfs, but the observed enrichments of CNO and ONeMg nuclei must arise from the deeper regions of the core. This demands the presence, respectively, of carbon-oxygen and oxygen-neon-magnesium white dwarfs (Law and Ritter 1983; Williams et al. 1985). We note, in particular, that such ONeMg white dwarfs are the expected products of the evolution of stars in the mass range ~ 8 - 12 $M_\odot$ and are predicted to have masses ~ 1.2 - 1.4 $M_\odot$. The fact that two of the eight novae for which detailed heavy element abundance analyses have been performed are enriched in the ONeMg element group (with Nova Vul 1984 II being a third possible candidate) strongly suggests that a significant population of massive white dwarfs is to be found in observed classical nova systems. Selection effects which help us to understand this result are reviewed in the next section.

IV. RELATIVE FREQUENCY OF OCCURRENCE OF WHITE DWARF MASSES

In a recent work, Truran and Livio (1986) estimated the relative frequencies of occurrence of different white dwarf masses in observed classical nova systems. In order to obtain these estimates, they made the following assumptions:

(i) The TNR occurs when the pressure at the base of the accreted envelope reaches a critical value (Section 2, eq. 1).

(ii) The initial mass function for the progenitors of the white dwarf is given by the Salpeter (1955) mass function (see the discussion below of the effect of using different mass functions).

(iii) The relation between the progenitor mass and the white dwarf mass provided by Iben and Truran (1978), is assumed to hold throughout the white dwarf mass range. (Using a different relation for high mass white dwarfs changes the estimates somewhat, but not the conclusions.)

The relative frequencies obtained, based on these assumptions, as well as the recurrence time (for an assumed accretion rate $\dot{M}_{acc} = 10^{-9}\ M_\odot\ yr^{-1}$), are presented

in Table 3. The first two things to note in the table are: (i) about one third of all observed novae should contain very massive ($M_{WD} \sim 1.35\ M_\odot$) white dwarfs (this is fully consistent with the observations of ONeMg white dwarfs, Section III) and (2) the average mass of the white dwarfs in observed classical nova systems is $\bar{M}_{WD} = 1.14\ M_\odot$. In fact, if instead of a Salpeter mass function (assumption (ii) above) we use the estimates of ranges of initial main-sequence masses in binary systems obtained by Iben and Tutukov (1985), we find $\bar{M}_{WD} = 1.23\ M_\odot$. On the other hand, the white dwarf mass spectrum of Politano and Webbink (1988) would result in a somewhat lower average mass. We can therefore conclude that relative frequency of occurrence arguments predict an average white dwarf mass of about $1.1 - 1.2\ M_\odot$.

Table 3 has another important consequence. The mean recurrence time between outbursts (for an assumed accretion rate of $10^{-9}\ M_\odot\ yr^{-1}$) is 8900 yr. Recently, Livio (1987) has suggested that the accretion rate can be somewhat higher ($\sim 10^{-8}\ M_\odot$/yr) for a period of about 50-300 years both before and after the outburst. Thus, the mean recurrence time can be of the order of 3000-4000 yrs. For such relatively short recurrence timescales, the discrepancy between the space density of classical novae as obtained by Patterson (1984) and Duerbeck (1984), and the Bath and Shaviv (1978) estimate, largely disappears.

TABLE 3

Relative Frequencies and Recurrence Time Scales

M_{WD}	T_{rec} (yr)	$f(M_{WD})$
CO White Dwarfs:		
0.6	1.29×10^6	0.103
0.7	7.31×10^5	0.053
0.8	4.16×10^5	0.042
0.9	2.36×10^5	0.040
1.0	1.20×10^5	0.046
1.1	6.39×10^4	0.062
1.2	2.81×10^4	0.100
1.3	9.02×10^3	0.232
ONeMg White Dwarfs:		
1.35	3.98×10^3	0.322

V. OBSERVATIONS OF WHITE DWARF MASSES IN CLASSICAL NOVA SYSTEMS

The masses of the white dwarfs in classical nova systems are extremely poorly known. Table 4 (compiled from Ritter's 1988 catalog) lists all the cases for which some estimates for the mass exist. Even in this table, the masses for HR Del and RR Pic are highly uncertain. In this list, V603 Aql and GK Per are fast novae. We would also expect the mass of the white dwarf in the case of the fast nova V603 Aql to be considerably higher than the quoted value, although the possible presence of a magnetic field may complicate matters (Haefner and Metz 1985). Observations of this object in an attempt to determine the white dwarf mass are thus strongly encouraged (although this is not an easy task for a system

with an inclination of 17°). In general, observations aimed at determining more white dwarf masses in nova systems (e.g. BT Mon is a good candidate) can be very valuable, as the present work has demonstrated.

TABLE 4

Masses of White Dwarfs in Classical Nova Systems

System	Orbital Period (days)	$M_{WD}(M_\odot)$	M secondary ($M_\odot$)
GK Per (1901)	1.996803	0.9±0.2	0.25
HR Del (1967)	0.214167 0.1775	0.9±0.1	0.58±0.01
DQ Her (1934)	0.193621	0.62±0.09	0.44±0.02
RR Pic (1925)	0.145026	0.95	0.4
V603 Aql (1918)	0.138154 0.144854	0.66±0.27	0.29±0.02

CONCLUSIONS

On the basis of the considerations reviewed in this paper, we are led to the conclusion that the typical masses of the white dwarfs in observed classical nova systems are significantly higher than the 0.6-0.7 $M_\odot$ range characteristic of single white dwarfs. This (in itself) does not imply that the average mass in close binary systems differs significantly from 0.6-0.7 $M_\odot$. Selection effects are extremely important here. We emphasize that the present work discusses the masses of the white dwarfs in nova systems that are actually observed to erupt and not in CVs in general. Therefore, the conclusion obtained here, that the masses of the WDs in observed nova systems is high, is not in conflict with other works discussing the distribution of WD masses in nova systems in general. For example, Hameury, King, Lasota, and Livio (1988) have found recently that the majority of the WDs in magnetic nova systems, should have a mass around 0.6-0.7 $M_\odot$, with a smaller group having a larger mass.

To be put even more strongly, the present work implies that the observed nova systems do not represent average CV systems (in terms of the WD mass) and cannot be assumed therefore to imply general properties of the CV population.

The estimates we provide of frequencies of occurrence of white dwarfs as a function of mass and of the average mass ~ 1.1-1.2 $M_\odot$ in active systems reveals the nature of the selection effect: more massive white dwarfs simply require less accreted matter to trigger an outburst. Dynamical arguments and abundance arguments both strongly support this conclusion. In general, we believe that the picture that emerges from our arguments concerning the role of massive white dwarfs in classical nova systems is entirely consistent with theoretical and observational constraints.

We also wish to call attention to the fact that the higher masses typical of observed classical novae serve to define rather tightly the range of luminosities and allow the possible use of their plateau luminosities as standard candles (Truran 1982). This arises from the fact that the bolometric luminosities of the hydrogen shell-burning remnants of nova eruptions essentially obey the Paczynski (1971) core-mass-luminosity relation for AGB stars with degenerate carbon-oxygen cores. The corresponding luminosity plateaus for dwarf masses 1.0 to 1.3 $M_\odot$ range from 2.8×10^4 to 4.6×10^4 $L_\odot$, with less than a factor two variation in luminosity and magnitude range $\Delta m \leq 1$. Novae thus represent potentially useful probes of the distance scale out to distances of order those of nearby clusters. Recognizing that very fast novae violate this condition at peak optical light, it is best to consider only moderately fast and slow novae.

This research has been supported in part by the US National Science Foundation under grant AST 86-11500 at the University of Illinois.

REFERENCES

Anders, E., and Eibhara, M. 1982, Geochim. Cosmochim. Acta., **46**, 2363.

Bath, G. T., and Shaviv, G. 1978, M.N.R.A.S., **183**, 515.

Cameron, A. G. W. 1982, in Essays in Nuclear Astrophysics, ed. C. A. Barnes, D. D. Clayton, and D. N. Schramm (Cambridge: Cambridge University Press), p. 23.

Collin-Souffrin, S. 1977, in Novae and Related Stars, ed. M. Friedjung (Dordrecht: Reidel), p. 123.

Duerbeck, H. W. 1984, Astrophys. Space Sci., **99**, 363.

Ferland, G. J. 1979, Ap. J., **231**, 781.

Ferland, G. J., and Shields, G. A. 1978, Ap. J., **226**, 172.

Fujimoto, M. 1982, Ap. J., **257**, 752.

Gallagher, J. S., Hege, E. K., Kopriva, D. A., Williams, R. E., and Butcher, H. R. 1980, Ap. J., **237**, 55.

Haefner, R., and Metz, K. 1985, Astr. Ap., **145**, 311.

Hameury, J.-M., King, A. R., Lasota, J.-P., and Livio, M. 1988, submitted to M.N.R.A.S.

Koester, D., Schulz, H., and Weidemann, V. 1979, Astr. Ap., **76**, 262.

Kovetz, A., and Prialnik, D. 1985, Ap. J., **291**, 812.

Law, W. Y., and Ritter, H. 1983, Astr. Ap., **123**, 33.

Livio, M. 1988, in IAU Colloq. 108, Atmospheric Diagnostics of Stellar Evolution, ed. K. Nomoto, in press.

Livio, M., and Truran, J. W. 1987, Ap. J., **318**, 316.

MacDonald, J. 1983, Ap. J., **267**, 732.

Pacheco, J. A. F. 1977, M.N.R.A.S., **181**, 421.

Paczynski, B. 1971, Acta. Astr., **21**, 417.

Patterson, J. 1984, Ap. J. Suppl., **54**, 443.

Payne-Gaposchkin, C. 1957, The Galactic Novae, (Amsterdam: North Holland).

Politano, M. J. and Webbink, R. F. 1988, poster paper this conference.

Prialnik, D., Livio, M., Shaviv, G. and Kovetz, A. 1982, Ap. J., 257, 312.

Salpeter, E. E. 1955, Ap. J., 121, 161.

Snijders, M. A. J., Batt, T. J., Seaton, M. J., Blades, J. C., and Morton, D. C. 1984, M.N.R.A.S., 211, 7P.

Starrfield, S. 1986, preprint.

Starrfield, S., Sparks, W. M. and Truran, J. W. 1985, Ap. J., 219, 136.

Stickland, D. J., Penn, C. J., Seaton, M. J., Snijders, M. A. J., and Storey, P. J. 1981, M.N.R.A.S., 197, 107.

Truran, J. W. 1982, in Essays in Nuclear Astrophysics, ed. C. A. Barnes, D. D. Clayton, and D. N. Schramm (Cambridge: Cambridge University Press), p. 467.

_____. 1985a, in Production and Distribution of CNO Elements, ed. I. J. Danziger (Garching: ESO), p. 211.

_____. 1985b, in Nucleosynthesis: Challenges and New Developments, ed. W. D. Arnett, and J. W. Truran (Chicago: University of Chicago Press), p. 292.

Truran, J. W., and Livio, M. 1986, Ap. J., 308, 721.

Truran, J. W., Shankar, A., Livio, M., and Hayes, J. 1988, in preparation.

Tylenda, R. 1978, Acta. Astr., 28, 333.

Williams, R. E. 1985, in Production and Distribution of CNO Elements, ed. I. J. Danziger (Garching: ESO), p. 225.

Williams, R. E., and Gallagher, J. S. 1979, Ap. J., 228, 482.

Williams, R. E., Sparks, W. M., Starrfield, S., Ney, E. P., Truran, J. W., and Wyckoff, S. 1985, M.N.R.A.S., 212, 753.

Williams, R. E., Woolf, N. J., Hege, E. K., Moore, R. L., and Kopriva, D. A. 1978, Ap. J., 224, 171.

Woosley, S. E. 1987, in Nucleosynthesis and Chemical Evolution, eds. E. Hauck, A. Maeder, and G. Meynet (Geneva: Geneva Observatory), p. 82.

GROWTH RATE OF WHITE DWARF MASS IN BINARIES

Mariko Kato
Department of Astronomy, Keio University
Kouhoku-ku, Yokohama 223 Japan

Hideyuki Saio
Department of Astronomy, University of Tokyo
Bunkyou-ku, Tokyo 113 Japan

and

Izumi Hachisu
Department of Aeronautical Engineering, Kyoto University
Sakyou-ku, Kyoto 606 Japan

ABSTRACT: The growth rate of a white dwarf which accretes hydrogen-rich or helium matter is studied. If the accretion rate is relatively small, unstable shell flash occurs and during which the envelope mass is lost. We have followed the evolutions of shell flashes by steady state approach with wind mass loss solutions to determined the mass lost from the system for wide range of binary parameters. The time-dependent models are also calculated in some cases. The mass loss due to the Roche lobe overflow are taken into account. This results seriously affects the existing scenarios on the origin of the type I supernova or on the neutron star formation induced by accretion.

Some neutron stars in low-mass X-ray binaries and binary radio pulsars are suggested to be formed through the accretion-induced collapse of white dwarfs (e.g., Taam and van den Heuvel 1986 and references therein). This accretion-induced collapse is based on the assumption that the accreting white dwarfs can grow to the Chandrasekhar mass. However, once a strong nova explosion occurs, a significant part of the envelope mass is ejected from the system (see, e.g., Prialnik 1986). When the mass accretion rate is higher than $\sim 2\times10^{-7}$ $M_\odot$ yr^{-1}, the hydrogen shell burning is stable but helium shell

burning is unstable. Therefore we studied whether white dwarfs can grow to the Chandrasekhar mass or not.

We have solved steady state equations with mass loss for the cases of nova and helium nova and obtain sequences of optically thick wind solutions. The wind is accelerated by continuum radiation. When the wind does not occur we solved static equations. The formulation of the wind and the basic envelope structures are explained in Kato (1983).

An evolutionary path of a nova can be followed by a sequence consisting of this static and steady state models with mass loss. Figure 1 shows that the mass loss solutions and static solutions for decay phase of nova for various white dwarf masses obtained by Kato and Hachisu (1988b). A complete cycle of nova for a 1.3 $M_\odot$ white dwarf is described in a similar way in Kato and Hachisu (1988a).

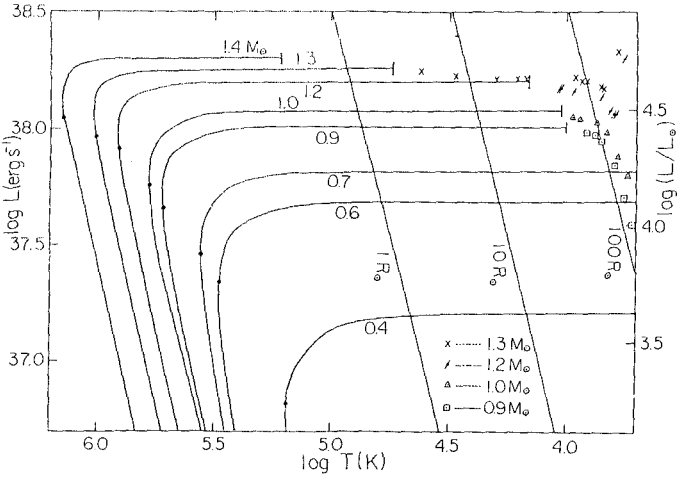

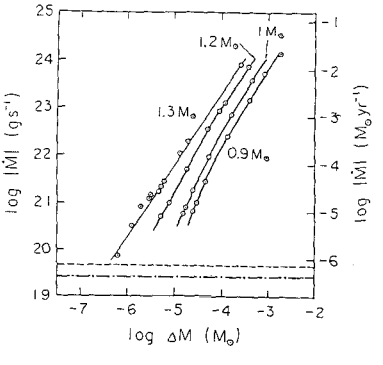

Fig. 1: The theoretical decay phase of novae. The wind solutions are denoted by the crosses or the other symbols. This wind ceases at the point with short vertical bar. Thin solid lines denote the constant radius lines.

Fig. 2: The mass loss rate of the steady mass-loss solution for nova against the envelope mass.

The mass loss rate of these wind solutions is plotted in Figure 2 against the hydrogen envelope mass ΔM. The mass loss rate is large when the photospheric temperature is low and it becomes smaller as the star moves blueward in the H-R diagram. Dashed and dot-dashed lines denote the mass decreasing rate due to the hydrogen burning for 1.3 and $0.9M_{\odot}$, respectively.

Figure 3 depicts evolutionary tracks of one cycle of helium nova. The terminology "helium nova" is used to stress the observational aspects of helium shell flashes on a white dwarf surface.

The evolutionary track in the rising phase depends on the ignition mass: three tracks are plotted for three ignition masses. The optically thick wind occurs at the filled circles and terminates at the point with the short vertical bar. Contrary to the initial phase, the evolutionary track in the decay phase is independent of the ignition mass, because the decay phase is assumed to be in the thermal equilibrium.

The mass loss rate of these solutions are plotted in figure 4. The mass decreasing rate due to nuclear burning is also shown.

We have also calculated time-dependent models These two results are in good agreement with each other.

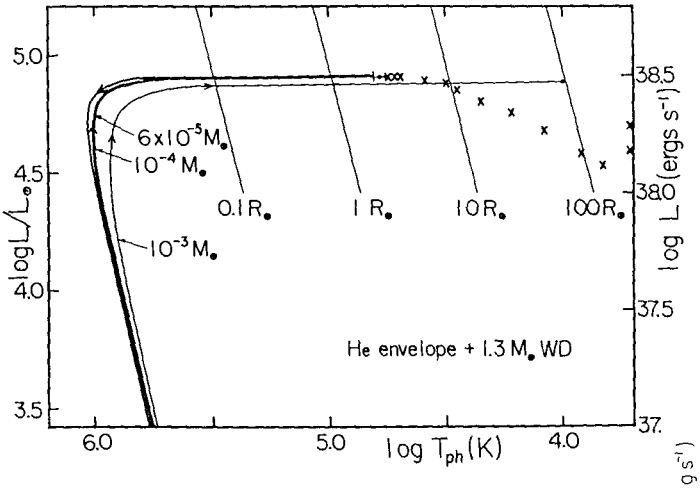

Fig. 3: The one cycle of helium nova in H-R diagram. The rising phase depends on the initial envelope mass which is attached to each curve. Wind mass loss begins at filled circles. The crosses denote the wind mass loss solutions in decay phase.

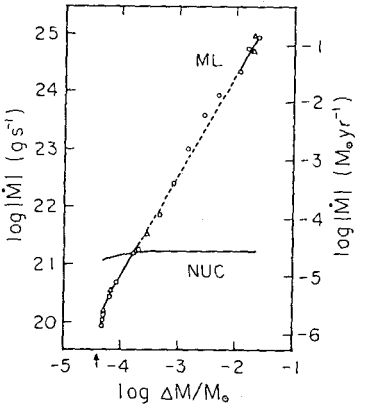

Fig. 4: The mass loss rate of the steady mass-loss solutions against the helium envelope mass for $1.3M_{\odot}$ white dwarf.

We have obtained how much mass is lost from the system or how much mass accumulates on the white dwarf. The mass accumulation ratio is calculated as follows. When the Roche lobe is large enough the envelope lose its mass due to the wind mass loss. We have mass loss rate during wind phase. The nuclear burning always produces processed matter which accumulate on the white dwarf surface except the first stage in which the convection prevents the production to accumulate. From these values (in figures 2 and 4) we have calculated the mass of the processed matter accumulated on the white dwarf. If the Roche lobe is small enough, the Roche lobe overflow is effectively occurs. We assumed that the matter outside of the Roche lobe is quickly removed.

Figure 5 shows that the mass accumulation ratio, i.e., the growth rate of the white dwarf mass. Figure 5a is for the nova case with large Roche lobe (For the small Roche lobe see Kato and Hachisu 1988a, b). Figure 5b shows for the growth rate of the $1.3M_{\odot}$ white dwarf. The crosses denote the results obtained from the time-dependent calculation in which $1R_{\odot}$ Roche lobe are assumed. Solid curves are from the steady state approach. (For detail see Kato, Saio, and Hachisu 1988).

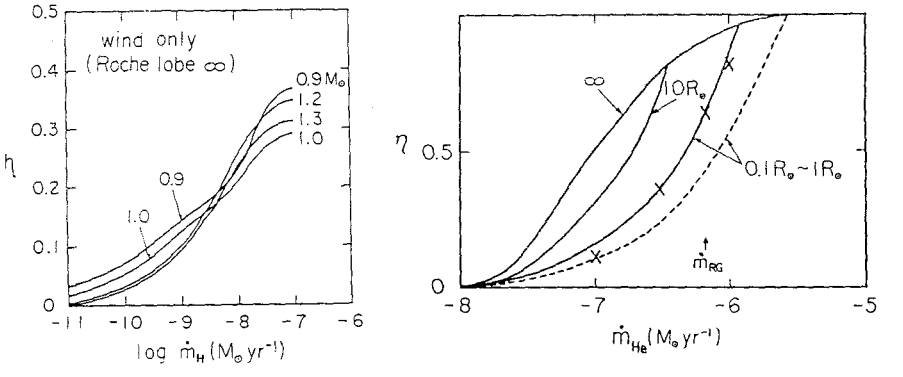

Fig. 5: The growth rate of the white dwarf is plotted against the accretion rate. a) Nova. b) Helium nova. The size of the Roche lobe are attached to each curve.

REFERENCES

Kato, M. 1983, Pub. Astr. Soc. Japan, 35, 507.
Kato, M., and Hachisu, I. 1988a, Ap. J., **329**, 808.
—— 1988b, Ap. J., submitted.
Kato, M., Saio, H., and Hachisu, I. 1988, Ap.J., submitted.
Prialnik, D., 1986 Ap.J.,**310**, 222.
Taam, R.E., and van den Heuvel, E.P.J. 1986 Ap.J., 305,235.

DYNAMIC MASS EXCHANGE IN DOUBLY DEGENERATE BINARIES. II. THE IMPORTANCE OF NUCLEAR ENERGY RELEASE

W. Benz and A.G.W. Cameron

Harvard-Smithsonian Center for Astrophysics
60 Garden Street, Cambridge, MA 02138

and

R. L. Bowers
Applied Theoretical Physics, X-10, MS B259
Los Alamos National Laboratory, Los Alamos, N.M. 87545

I. INTRODUCTION

The hypothesis that Type I supernova explosions originate in binary stars, in which the secondary overflows its Roche lobe and causes a white dwarf primary to pass a critical threshold for dynamical collapse, has gained in popularity over the last decade and a half (Truran and Cameron 1971; Whelan and Iben 1973; Wheeler 1982). During this period attention has also focussed on double-degenerate binary precursors of such systems, in which gravitational radiation of orbital angular momentum causes two white dwarf stars to spiral slowly together until the less massive of the stars begins to overflow its Roche lobe (Tutukov and Yungelson 1979; Webbink 1979; Iben and Tutukov 1984; Paczyński 1985). Cameron and Iben (1986) discussed the stability of such systems as the threshold of Roche lobe overflow was approached and for low mass ratios in which gravitational radiation can maintain a low rate of such overflow. Benz, Bowers, Cameron, and Press (1988, hereafter BBCP) computed the actual merging of a binary system composed of a $1.2M_\odot$ primary and a $0.9M_\odot$ secondary using a fully three-dimensional SPH code. Their simulation did not include the effect of nuclear energy release despite the fact that the temperature in the accretion shock reached the carbon ignition threshold, and therefore their conclusions about the structure of the merged object remained uncertain.

In this paper we present preliminary results for the merging of the same binary system as in BBCP, but we have included in the code a reduced nuclear reaction network and we have allowed for radiation pressure effects. The binary stars were, as in BBCP, assumed to be two zero temperature carbon-oxygen white dwarfs. Since BBCP describes in sufficient detail the equations solved and the numerical method, we will only concentrate here on the new physics that has been introduced into the code.

II. HYDRODYNAMIC EQUATIONS AND NUCLEAR REACTION NETWORK

The results reported below were obtained using a fully three-dimensional hydrodynamic code based on the SPH scheme, which includes self-gravity and which makes no assumptions whatsoever about the flow symmetry. The hydrodynamics is described by the momentum equation in its Lagrangian form:

$$\frac{d\mathbf{v}}{dt} = -\frac{\nabla \mathbf{P}_{tot}}{\rho} - \nabla\phi + \mathbf{S}_{visc} \tag{2.1}$$

where $\mathbf{S}_{visc}$ is the classical artificial viscous stress which is introduced to model kinetic energy

dissipation in shocks; and the gravitational potential ϕ is obtained from Poisson's equation

$$\nabla^2\phi = 4\pi G\rho. \tag{2.2}$$

The mass density is denoted by ρ, the gravitational constant by G, and $\mathbf{v}$ is the velocity of a mass element.

In BBCP the total fluid pressure did not include radiation effects; we now add this term by writing the total pressure to be equal to the sum of a degenerate electron pressure, a non-degenerate gas pressure, and a radiation pressure term:

$$P_{\mathbf{tot}} = P_{\mathbf{deg}} + P_{\mathbf{gas}} + P_{\mathbf{rad}} \tag{2.3}$$

In the degenerate regime, the pressure is obtained, as in BBCP, from the ideal, fully relativistic equation of state (Chandrasekhar 1939). The gas pressure is found from the perfect gas equation of state. The radiation pressure term has the usual form:

$$P_{\mathbf{rad}} = \frac{1}{3}aT^4 \tag{2.4}$$

In order to compute the gas and radiation pressure terms we first have to know the temperature. To obtain the temperature we solve for each particle the equation:

$$U_{\mathbf{non-deg}} = U_{\mathbf{rad}} + U_{\mathbf{therm}} = aT^4 + c_{\mathbf{v}}T \tag{2.5}$$

where $c_{\mathbf{v}}$ is the specific heat at constant volume and $U_{\mathbf{non-deg}}$ is the non-degenerate part of the total internal energy which is obtained by subtracting the degenerate energy from the total internal energy. The degenerate energy is only a function of density and can be readily obtained once ρ is known, and the total internal energy is given by solving the energy conservation equation.

As mentioned above, the high temperature reached in the accretion shock indicates that nuclear energy release should be included in the code. Of course, a full network coupled with the 3D hydro code would be impractical because of the computer time and storage that would be required. We therefore used the same reduced network as in Benz, Hills, and Thielemann (1988, hereafter BHT). This network, developed for the study of white dwarf collisions, was devised having two simplifications in mind. First, since the dynamics has to be modelled but not the detailed chemical composition, the network should only serve the purpose of reproducing the energy generation accurately. This energy release should also take place over the correct timescale. Second, the bulk composition of white dwarfs, generally a mixture of carbon and oxygen, with perhaps some helium, implies that "multiple alpha-particle" nuclei will dominate and that neutron- and proton-induced reactions can be neglected in a first approximation. For fast nuclear burning in which the principal products produced are not heavier than magnesium or silicon, as turned out to be the case here, a simple chain of these multiple alpha-particle nuclei, emitting and absorbing alpha-particles, gives an acceptable approximation to a larger network, and that is what was used here.

Further details about the equations, the nuclear reaction network, and the numerical method can be found in BBCP and in BHT.

III. RESULTS

Figure 1 shows a selected number of snapshots of the binary dissolution. The velocity vectors are plotted projected onto the orbital plane. The magnitude of the minimum and maximum

velocity vectors is indicated on the second line above each frame in units of 6363 km/s. Time is given on the upper line in units of 1.10 seconds and each frame is 5.6×10^9 cm on a side. The initial conditions were taken identical to those in BBCP, that is two initially non-rotating, zero temperature white dwarfs. The simulation begins with the secondary filling its Roche lobe. We further assume that angular momentum losses due to gravitational radiation can be neglected during the actual merging.

After a few seconds, mass transfer starts and very quickly grows to reach values as high as $0.0525M_\odot$/s. As expected, the dissolution of the binary proceeds in a very similar way to that reported in BBCP, and the secondary is again completely destroyed in about 60 seconds, i.e., three original orbital periods. We pointed out in BBCP that this extremely rapid merging is due to the fact that not only mass but a substantial amount of angular momentum is transferred into the disk orbiting the primary which results in the two stars moving closer rather than away from each other.

The resulting merged object, although more massive than a Chandrasekhar mass, does not collapse for the same reasons as found in BBCP. The inner part of the material added to the primary is no longer degenerate but is supported by thermal pressure, whereas the outer parts are supported by rotation. It will take at least one cooling time for the potential supernova event to take place.

As predicted, we find that the temperature rises high enough in the accretion shock to ignite carbon burning. However, the density and temperature only reach values for which carbon burns very slowly, and the amount of nuclear energy released only marginally affects the dynamics. The major effect of nuclear burning is to allow considerably more mass loss from the system. Although still a small amount, the mass lost, now $0.051M_\odot$, is about 9 times larger than was found in BBCP. Most of the ejected mass has been highly processed. ^{12}C has been reduced in abundance from 0.5 to 0.164, and ^{16}O at 0.5013 is slightly above the original abundance of 0.5. The major elements that have been produced are ^{24}Mg (0.184), ^{28}Si (0.138), and ^{32}S (0.012). The equivalent mass of the processed material ejected into the interstellar medium prior to the eventual explosion amounts to $0.0094M_\odot$ of ^{24}Mg and $0.0071M_\odot$ of ^{28}Si. This should not be enough to produce any visible signature later on when the ejecta from the supernova explosion runs into this earlier debris.

The chemical composition of the merged object is practically unchanged from its original value. Processed elements are only present in traces. The most abundant of them, again ^{24}Mg and ^{28}Si, have abundances of 0.0073 and 0.0054, respectively. All these processed elements are located in the hot envelope surrounding the original primary. Practically no burning took place involving material from the primary. The merging process will therefore leave no obvious signature, at least as far as the chemical composition of the supernova progenitor is concerned.

This work has been supported in part by NASA grant NGR 22-007-272. One of us (W.B.) also aknowledges partial support from the Swiss National Science Foundation and would like to express his gratitude to the Theoretical Astrophysics Group of the Los Alamos National Laboratory for their hospitality.

IV. REFERENCES

Benz, W., Bowers, R.L., Cameron, A.G.W, and Press, W.H., *Astrophys. J.*, submitted.

Benz, W., Hills, J.G., and Thielemann F.K., *Astrophys. J.*, in preparation.

Cameron, A. G. W., and Iben, I., Jr., *Astrophys. J.*, **305**, 228 (1986).

Chandrasekhar, S., *Introduction to the Study of Stellar Structure*, University of Chicago Press,

Chicago, Illinois, Chap. XI (1939).
Chandrasekhar, S., ***Classical Ellipsoidal Figures of Equilibrium***, Yale University Press (1969).
Iben, I., Jr., ***The Galaxy***, Ed. G. Gilmore, V. Carswell (Dordrecht: Reidel), p. 365 (1987).
Iben, I., Jr., ***Astrophys. J.***, **324**, 355 (1988).
Iben, I., Jr., and Tutukov, A. V., ***Astrophys. J. Suppl.***, **54**, 535 (1984).
Iben, I., Jr., and Webbink, R. F., in proceedings of the "second conference on faint blue stars", Ed. A. G. Davis-Philip, D. F. Hayes, J. W. Liebert (L. Davis Press), p. 401 (1988).
Paczyński, B., in ***Cataclysmic Variables and Low-Mass X-Ray Binaries***, Ed., D. Q. Lamb and J. Patterson (Dordrecht: Reidel), p. 1 (1985).
Truran, J. W., and Cameron, A. G. W., ***Ap. Space Sci.***, **14** 179 (1971).
Tutukov, A. V., and Yungelson, L. R., ***Acta Astr.***, **23**, 665 (1979).
Webbink, R. F., in ***White Dwarfs and Variable Degenerate Stars***, Ed. H. M. Van Horn and V. Weidemann (New York: University of Rochester Press), p. 426 (1979).
Webbink, R. F., Iben, I., Jr., in proceedings of the "second conference on faint blue stars", Ed. A. G. Davis-Philip, D. F. Hayes, G. W. Liebert, (L. Davis Press), p. 445 (1988).
Wheeler, J. C., in ***Supernovae: A Survey of Current Research***, Ed. M. J. Rees and R. J. Stoneham (Dordrecht: Reidel) p. 167 (1982).
Whelan, J. C., and Iben, I., Jr., ***Astrophys. J.***, **186**, 1007 (1973).

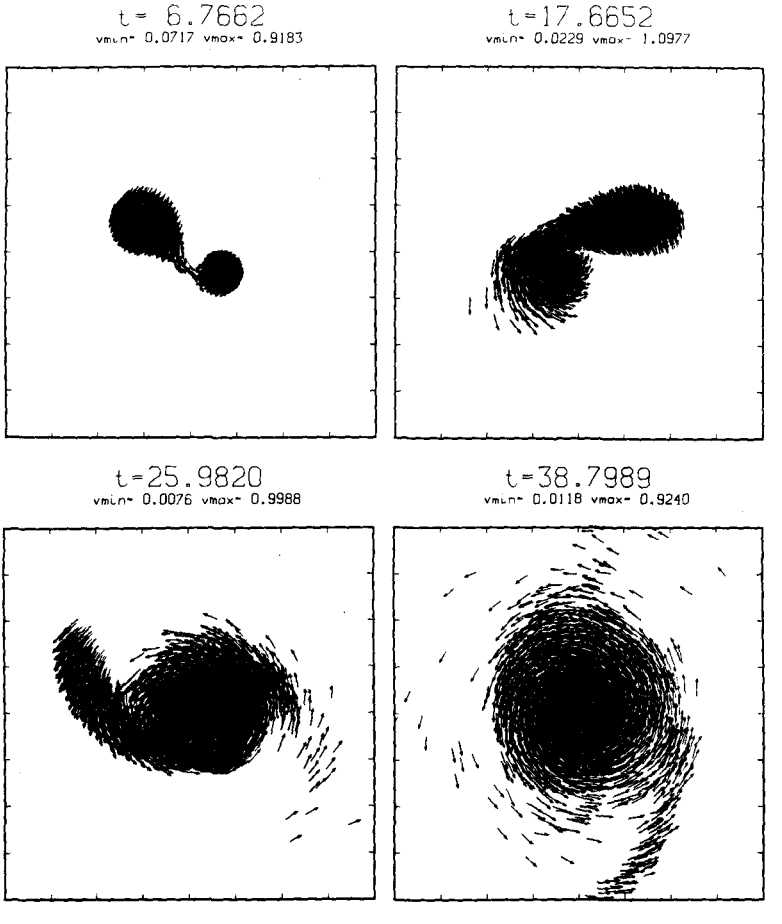

Figure 1

THE COALESCENCE OF WHITE DWARFS AND TYPE I SUPERNOVAE

Robert Mochkovitch[1] and Mario Livio[2]

[1]Institut d'Astrophysique de Paris, 98 bis Bd Arago, 75014 Paris, France

[2]Department of Physics, Technion, Haifa 32000, Israel

ABSTRACT: In the context of the white dwarf coalescence model for type Ia supernovae, we compute post-coalescence configurations involving a thick disk, rotating around a central white dwarf (the original primary), having the same total mass, angular momentum and energy as the initial system. We show that carbon ignition in rather low density material ($10^5 - 10^6$ g.cm^{-3}) can be triggered during the merging process itself or later, by dissipation due to turbulence in the disk. The evolution of the object following carbon ignition is very uncertain.

1. INTRODUCTION

Exploding white dwarfs are generally considered to be responsible for type Ia supernovae (SN Ia) for a number of observational and theoretical evidences: SNe Ia have progenitors belonging to the old galactic population and spectra without hydrogen lines; SN Ia light curves are nicely explained by the radioactive energy release of $0.5 - 0.7$ M$_\odot$ of ^{56}Ni resulting from the combustion of a fraction of the white dwarf to nuclear statistical equilibrium [1,2]; uncomplete nuclear burning in the outer layers produces intermediate mass elements and the resulting abundances together with the dynamics of the ejecta give synthetic spectra which fit rather well with the observations [3]; the burning front propagates from the center to the surface by a deflagration wave, with expansion velocities which can reach 20000 km.s^{-1} and leaving no compact remnant [4], in agreement with the absence of neutron star in the two historical SNe I Tycho and Kepler.

The carbon deflagration model therefore appears quite successfull in accounting for many of the observed features of SNe Ia but the main problem which remains is related to the presupernova evolution and can be summarized by the following two questions: (i) is it really possible to bring a white dwarf by accretion sufficiently close to the Chandrasekhar limit to allow central carbon ignition? (ii) if it is possible, does it occur in a large enough number of systems to explain the SN Ia rate, which is estimated to be of the order of 6.8 10^{-14} pc^{-3}.yr^{-1} in our Galaxy?

The answer to these two questions is very uncertain. It may indeed be difficult to reach the Chandrasekhar limit by accretion of hydrogen-rich material, due to periodic mass ejection by hydrogen shell flashes [5]. Accumulation of helium appears to be possible only for accretion rates larger than 10^{-8} M$_\odot$.yr^{-1}. However, even in this case, mass loss by a stellar wind during the reccurent helium shell flashes could also reduce the efficiency of accretion and prevent the white dwarf mass from growing [6]. For a discussion of point (ii), the evolution of close binaries must be followed from their birth (with an assumed IMF and distribution function of initial orbital

separation) until the eventual explosion of one of their components as a SN Ia. Such a study may include periods of non-conservative mass transfer, loss of angular momentum by magnetic breaking, accretion from a stellar wind, etc... In spite of uncertainties in the theoretical modelling of these proccesses, it seems that no (at least classical) evolutionary path can be found, which could bring a large enough number of systems to the SN Ia stage [7]. This has led to the search for (a priori) more "exotic" scenarios, such white dwarf coalescence [7,8]. Binary white dwarfs (BWD) are produced after the second period of mass transfer in systems of initial semi-major axis from a few tens to a few hundreds $R_\odot$ and with components of intermediate mass. If the white dwarfs are formed with a separation in the range $2 - 3\ R_\odot$, they can be brought in contact by the emission of gravitational radiation within a Hubble time or less. For two carbon-oxygen white dwarfs the total mass involved is often larger than the Chandrasekhar limit and some explosive outcome can be expected. Both observational [9] and theoretical [7,8,10] estimates of the BWD birthrate have been obtained, but the results are still contradictory so that no reliable comparison with the SN Ia rate can be made. We did not address this problem in the present work. We focused on the structure and possible evolution of post-coalescence configurations, assuming conservation of total mass, angular momentum and energy in the merging process. These assumptions have been confirmed by the very recent 3 D numerical simulation of Benz et al. [11].

2. COMPUTATIONAL METHOD

A post-coalescence configuration consists of a central white dwarf (the original primary) surrounded by a thick disk coming from its disrupted companion. To compute its structure, we used the classical self-consistent field approach for differentially rotating, self-gravitating systems [12]. If the material behaves as a barotrope, which is the case for the fully degenerate white dwarf interior and has been assumed for the partially or non-degenerate disk, the specific angular momentum must be constant along axial cylinders. We have then $j = j(\tilde{\omega})$, with the constaint that this distribution must satisfy the Rayleigh criterion $dj/d\tilde{\omega} > 0$, $\tilde{\omega}$ being the polar radial coordinate. For practical purposes, the mass coordinate $m(\tilde{\omega})$ has been adopted instead of $\tilde{\omega}$ and the following expression has been used for $j(m)$ in the disk

$$j(m) = j_o \cdot \frac{(m - M_1)}{M_1 + M_2 + b(m - M_1)} \cdot \tag{1}$$

M_1 and M_2 are respectively the mass of the central white dwarf and the mass of the disk. The constant j_o is determined for any b by the condition $\int_{M_1}^{M_1+M_2} j(m)dm = J$, where $J = J_{orb} + J_2$ is the sum of the orbital angular momentum (before coalescence) and the proper angular momentum of the disrupted white dwarf. We assume that the central white dwarf is non-rotating since it is less affected by tidal interaction due to its smaller radius (even in synchronized systems, its angular momentum remains moderate compared to J with therefore little effect on the final results).

We take into account the thermal contribution to the pressure by adopting a polytropic relation, $P = A\rho^\gamma$ with $\gamma < 5/3$ (i.e. smaller than the value for degenerate, non-relativistic electrons only), when the density goes below a given limit ρ_o. If we take for ρ_o the density at which the thermal and degenerate electron contributions are equal, this gives a transition temperature,

$T_o \approx 10^5 \rho_o^{2/3}$ K. The value of A is obtained from the continuity of pressure at $\rho = \rho_o$.

3. RESULTS AND DISCUSSION

We considered systems with a primary of mass 1 $M_\odot$ and 0.6 or 0.8 $M_\odot$ companions. We then searched for white dwarf plus thick disk configurations with distributions of angular momentum given by (1) and $\gamma = 1.4$. The central and transition densities ρ_c and ρ_o were adjusted so as to conserve mass and energy while angular momentum conservation is automatic when (1) is adopted. For infinite b, i.e. a uniform angular momentum distribution, no solution can be found, in agreement with the work of Hachisu et al. [13]. However, a uniform j disk is detached or just in contact with the central white dwarf, which is not the most likely configuration to be produced in the merging process. The primary occupies a large fraction of its Roche lobe before coalescence and the transferred material strikes it directly. We therefore believe that configurations in which the disk takes some pressure support on the central white dwarf are more probable. It is then possible to find solutions conserving mass, angular momentum and energy for $b < b_{max}$ ($b_{max} = 75$ for $M_2 = 0.6$ $M_\odot$, $b_{max} = 20$ for $M_2 = 0.8$ $M_\odot$). The solution with $b = b_{max}$ is entirely degenerate, while for $b < b_{max}$, the transition density and temperature increase, which corresponds to a growing lift of degeneracy in the disk. We also found that for $b < b_{ign}$ ($b_{ign} = 17$ for $M_2 = 0.6$ $M_\odot$, $b_{ign} = 5$ for $M_2 = 0.8$ $M_\odot$), the transition point (ρ_o, T_o) lies above the carbon ignition line which means that dissipation during coalescence has triggered carbon burning in the disk. We have represented in Fig. 1 an intermediate solution for the $M_2 = 0.8$ $M_\odot$ case, corresponding to $b = 12$.

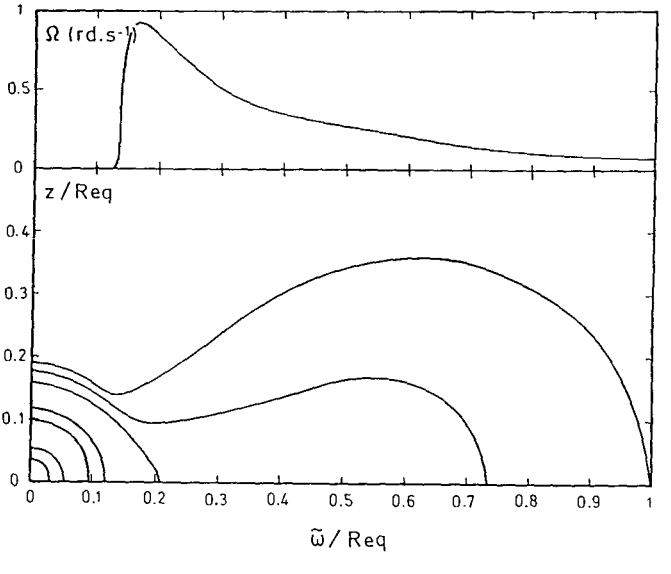

Figure 1: Equilibrium configuration after coalescence obtained with $\gamma = 1.4$ and $b = 12$. The total mass, central density, transition density and temperature and equatorial radius are respectively M $= 1.8$ $M_\odot$, $\rho_c = 4.5$ 10^7 g.cm^{-3}, $\rho_o = 2.5$ 10^5 g.cm^{-3}, $T_o = 3.7$ 10^8 K, $R_{eq} = 2.6$ 10^9 cm. The upper curve gives the distribution of angular velocity ($\Omega = 0$ in the inner 1 $M_\odot$) and the lower figure shows the shape of isodensity contours $\rho/\rho_c =$ 0.8, 0.5, 0.2, 0.1, 0.01, 0.001 and 0.

Even if such a model does not ignite carbon during coalescence, it will probably do it shortly after in the boundary layer and inner disk region where a very high shear is present and turbulence is likely to develop (the Richardson criterion for stability is strongly violated there). With an α–type prescription for the turbulent viscosity, values of ν_{turb} as large as $10^{11} - 10^{12}$ cm^2.s^{-1} are obtained, leading to a dissipation rate which can reach 10^{11} erg.g^{-1}.s^{-1} in the boundary layer and 10^9 erg.g^{-1}.s^{-1} in the inner disk.

We then conclude that carbon will be ignited off-center, in a relatively low density, partially or non degenerate material ($10^5 - 10^6$ g.cm^{-3}) either during the merging process itself, or later on in the just-formed disk. Such physical conditions cannot directly give a SN Ia explosion. It is not clear at all whether carbon burning (to O – Ne – Mg composition) will propagate inward into the white dwarf or outward in the disk (or both !) or if it will be rapidly quenched, for example by material expansion. In the first case, the O – Ne – Mg white dwarf which is formed can collapse to become a neutron star with only a weak explosion [14], while in the second case, the nuclear energy which is still available may not be large enough to power a SN Ia [15].

It finally appears that the evolution which follows carbon ignition remains very uncertain. Now that the possibility of dynamical merging has been confirmed [11], an important theoretical effort is still to be made to prove that a SN Ia can indeed result from white dwarf coalescence.

REFERENCES

[1] Colgate, S.A., McKee, C.: 1969, *Astrophys. J.* **157**, 623
[2] Arnett, W.D.: 1982, *Astrophys. J.* **253**, 785
[3] Branch, D., Doggett, J.B., Nomoto, K., Thielemann, F.K.: 1985, *Astrophys. J.* **294**, 619
[4] Nomoto, K., Thielemann, F.K., Yokoi, K.: 1984, *Astrophys. J.* **286**, 644
[5] MacDonald, J.: 1984, *Astrophys. J.* **283**, 241
[6] Saio, H., Kato, M., Hachisu, I.: 1987, in *Atmospheric Diagnostics of Stellar Evolution: Chemical Peculiarity, Mass Loss and Explosion*, I.A.U. Colloquium 108, to be published
[7] Iben, I., Jr., Tutukov, A.V.: 1984, *Astrophys. J. Supp.* **54**, 335
[8] Webbink, R.F.: 1984, *Astrophys. J.* **277**, 355
[9] Robinson, E.L., Shafter, A.W.: 1987, *Astrophys. J.* **322**, 296
[10] Tornambé, A., Matteuci, F.: 1986, *Monthly Notices Roy. Astron. Soc.* **223**, 69
[11] Benz, W., Bowers, R.L., Cameron, A.G.W., Press, W.H.: 1988, preprint and this conference
[12] Ostriker, J.P., Mark, J.W.K.: 1968, *Astrophys. J.* **151**, 1075
[13] Hachisu, I., Eriguchi, Y., Nomoto, K.: 1986, *Astrophys. J.* **308**, 161
[14] Nomoto, K., Iben, I., Jr.: 1985, *Astrophys. J.* **297**, 531
[15] Wheeler, J.C., Swartz, D., Li, Z.W., Sutherland, P.G.: 1987, *Astrophys. J.* **316**, 733

WHITE DWARF – ACCRETION DISK BOUNDARY LAYERS

Oded Regev
Department of Astronomy, Columbia University
New York, N.Y. 10027
on leave from:
Department of Physics, Technion
Israel Institute of Technology, Haifa 32000

ABSTRACT

The method of matched asymptotic expansions is used to calculate the detailed structure of white dwarf- accretion disk boundary layers. Both optically thick and thin boundary layers are investigated for various values of the relevant parameters, as long as the layer's vertical extension remains very much smaller than the white dwarf's radius. Detailed, self consistent solutions for the boundary layer's and disk's structure are calculated and used to find the amount of energy radiated onto the accreting white dwarf (recently recognized to be an important factor in nova outburst modelling).

INTRODUCTION

The importance of the accretion disk inner boundary layer (BL) is well established. However, since the pioneering work of Lynden-Bell & Pringle (1974), progress in trying to understand the BL structure has been rather limited. For a recent review, see Shaviv (1987). In cataclysmic variables the problem is particularly important. For example, it is clear that various observational characteristics of dwarf novae (in particular the X-ray emission) have to do with the BL (Pringle, 1977; Pringle & Savonije, 1979; Tylenda, 1981; Patterson & Raymond, 1985). Very recently it has been pointed out that the effect of BL heating on the pre-nova accreting white dwarf is of paramount importance in modelling the outburst (Shaviv & Starrfield, 1987).

Regev (1983) and Regev & Hougerat (1988) introduced the method of matched asymptotic expansions as a practical tool for obtaining the BL structure self consistently, and demonstrated its viability for the study of optically thin and thick BL's in cataclysmic variables. In this work I would like to report on the results of an extensive parameter space study in which self consistent BL solutions have been found. The parameters include (in addtion to the white dwarf's mass and radius) the angular velocity – Ω_* at the star's surface, $\dot{M}$ – the mass accretion rate and, in certain cases, the pressure (or the temperature) at the BL inner edge. It has to be pointed out that our method fails whenever some of the basic assumptions break down or another viscosity prescription in the BL is used. This may result in different BL structures with transition regions (Papaloizou & Stanley, 1986).

OUTLINE OF THE METHOD

I describe here only the essentials of the method. A full derivation is given in Regev (1983), hereafter R, for the optically thick case and in Regev & Hougerat (1988), hereafter RH, for optically thin BLs. Consider the r component (in cylindrical coordinates) of the momentum equation. In its non-dimensional form, assuming steady state and axial symmetry it is:

$$\epsilon^2 u\frac{\partial u}{\partial r}+\epsilon v\frac{\partial u}{\partial z}-\Omega^2 r=-\epsilon^2\frac{1}{\rho}\frac{\partial p}{\partial r}-\frac{1}{r^2}+\epsilon^2\frac{z^2}{r^4} \tag{1}$$

see R eq. 7. The symbols here have their usual meaning. Note the role of the small parameter, ϵ, defined to be $\tilde{v}_s/\Omega_{K*}R_*$. $\Omega_{K*}\equiv(GM_*/R_*^3)^{1/2}$ is the Keplerian angular velocity at the star's radius, R_*, and is used to scale Ω. $\tilde{v}_s$ is the sound velocity at a typical point. If $\epsilon\ll 1$, one can expand all the functions in ϵ, and the lowest order approximation should be satisfactory. Dropping terms of order ϵ and smaller in equation 1 one gets:

$$\Omega^2=\frac{1}{r^3} \tag{2}$$

which means that the Keplerian angular velocity is the lowest order solution. However, one now faces the obvious difficulty of being unable to satisfy the inner boundary condition for Ω which should be Ω_* and not 1 (Keplerian at $r=R_*$ in our units). Obviously, very near the boundary, in the BL, the above *outer solution* is invalid. The solution may be something of the type used in the so-called standard theory (Shakura & Sunyaev, 1973), but the price is the loss of consistency and the necessity to treat the BL somehow, separately. It is also quite disturbing that in such a treatment the disk structure does not depend at all on the inner boundary condition.

The remedy is to use *boundary layer methods*, i.e. to use another expansion (the inner expansion) very near the inner boundary. In order to do this the coordinates (here the r-coordinate) have to be stretched, i.e. one defines a new coordinate $r=1+\delta R$ with $\delta(\epsilon)$ very small. Changing variables in eq. 1, r to R, one gets a possible meaningful equation in lowest order only for a certain choice of δ as a function of ϵ. This is called the significant limit and it determines essentially the BL width. For details, see R and RH, as well as Bender & Orszag (1978) or Van Dyke (1964). While the basis for understanding the method can be found in these last two references, our case is considerably more complicated as it involves several equations in two space variables. We eliminate the z-dependence by vertically averaging and using the assumption that the disk, as well as the BL is geometrically thin. We then proceed as explained in R (or RH) when the BL is optically thick and dominated by gas pressure and free-free opacity (optically thin and dominated by radiation pressure and electron scattering opacity).

The decision which assumption to use is based on the following consideration. For each choice of the parameters (notably Ω_*, and $\dot{M}$) we look for an inner solution and try to match it to the outer solution (letting $\epsilon\to 0$). If matching is impossible, something must be wrong with the assumptions. If we can match, we check our solution for consistency – i.e. if the BL is still geometrically thin and if its optical depth is according to the assumption. In doing this we use ratios of relevant timescales and optical depth formulae similar to the ones of Pringle & Savonije (1979) and King & Shaviv (1984).

The outer solution we find is, of course, identical to the Shakura & Sunyaev (1973) solution. However we improve on it by trying to determine all integration constants from matching with the inner solution and not by new assumptions and approximations. Consider, in particular, the

angular momentum equation for the outer solution (eq. 17 in R). After integrating on z one gets the familiarly looking equation for the specific angular momentum transport caused by the gradient of visous stresses:

$$\dot{M}\frac{d}{dr}(r^2\Omega) = -\frac{\alpha}{\mu}\frac{d}{dr}\left(\nu\Sigma r^3\frac{d\Omega}{dr}\right). \tag{3}$$

See eq. 22 in R. This equation is again in nondimensional units. α and μ are constants, ν is the viscosity and Σ the surface density. Integrating, one needs a constant (call it C):

$$\dot{M}\left[(r^2\Omega) - C\right] = -\frac{\alpha}{\mu}\nu\Sigma r^3\frac{d\Omega}{dr}. \tag{4}$$

Obviously, C has to do with the ability of the BL to take up angular momentum. See the discussion in Katz (1987) (p. 199) on this matter. The assumption of $C = 1$ (see e.g. Pringle, 1981) allows one to decouple the disk structure from the BL in the manner explained above. Our method, however allows one to determine C from the matching (if at all possible) and construct a consistent approximation by composing it from the outer and inner expansions. In this way we obtain the structure of the accretion disk all the way down to the star. In additon various integral quantities depend on C. For example the disk luminosity is $L_d = L_{\rm acc}(\frac{3}{2} - C)$ and the BL luminosity is $L_{\rm BL} = L_{\rm acc}\left[C - \frac{1}{2}(1+\Omega_*^2)\right]$ giving together the total luminosity $L_T = L_{\rm acc}\left(1 - \frac{1}{2}\Omega_*^2\right)$, where $L_{\rm acc} \equiv GM_*\dot{M}/R_*$.

RESULTS

The optically thick BL differs from the optically thin one. Let us call them Case A and B respectively. We find that $\delta = \epsilon^2$ in Case A, and $\delta = \epsilon$ in Case B. It follows that the BL thickness (in the r direction) is $\sim \epsilon H_*$ in Case A and $\sim H_*$ in Case B, where H_* is the vertical extension of the BL. This supports the finding of Pringle & Savonije (1979) who based their argument on a somewhat different consideration.

For all the values of the relevant parameters for which a Case A solution exists and is consistent, we find values of $0.7 \gtrsim C \gtrsim 1.0$. In this case one has to solve a set of four coupled ODE's for the structure of the BL. The equations are given in R (eqs. 34–37). C is found from the matching provided the values of p (or T) and Ω are given on the surface. We use a numerical code for the solution of this boundary value problem, which allows to determine C as an eigenvalue. A relaxation method using quasilinearization (Henyey method) is quite effective if a good initial guess is known. Figure 1a is a typical example of Case A. In addition to the obvious departure from the standard solution (dashed curve) one sees also the effect of the BL on the disk up to $r \sim 2R_*$. This result is for $M_* = 1M_\odot$, $R_* = 9 \times 10^8$cm, $\Omega_* = 0.3\Omega_{K*}$, $\dot{M} = 5.5 \times 10^{-9}M_\odot$/yr. The value of C for this model is found to be $C = 0.71$.

In case B, as described in RH, we were able to find an analytical solution for the BL which can be matched to the outer solution if $C = 1$. Thus, the standard solution continues inward until it is smoothly matched with the BL solution. As expected, one gets in this case a much hotter BL (see figure 1b). This result is for the same white dwarf parameters but for a significantly lower value of $\dot{M}$: $\dot{M} = 3.5 \times 10^{-10}M_\odot$/yr.

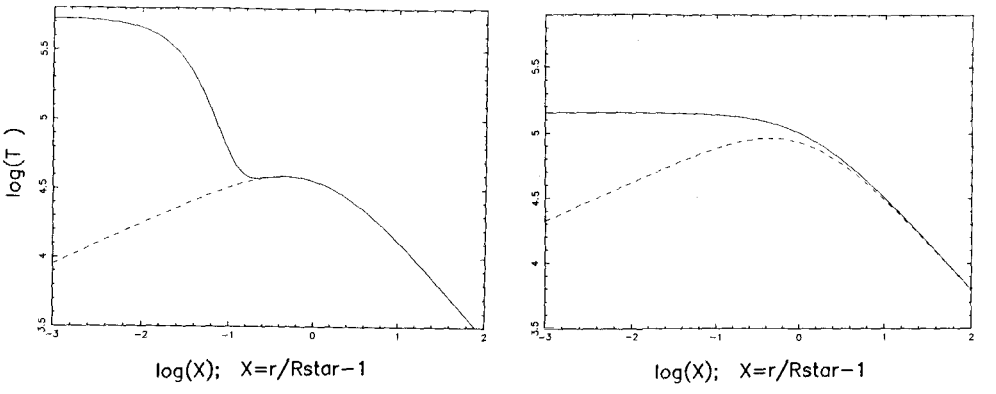

Figure 1: Log(T) (absolute temperature) as a function of position (distance from the white dwarf's edge) in the BL and the inner disk. The right panel (a) is Case A (optically thick) and the left one (b) is Case B (optically thin). The dashed curves are the standard (Shakura & Sunyaev) solutions for both cases.

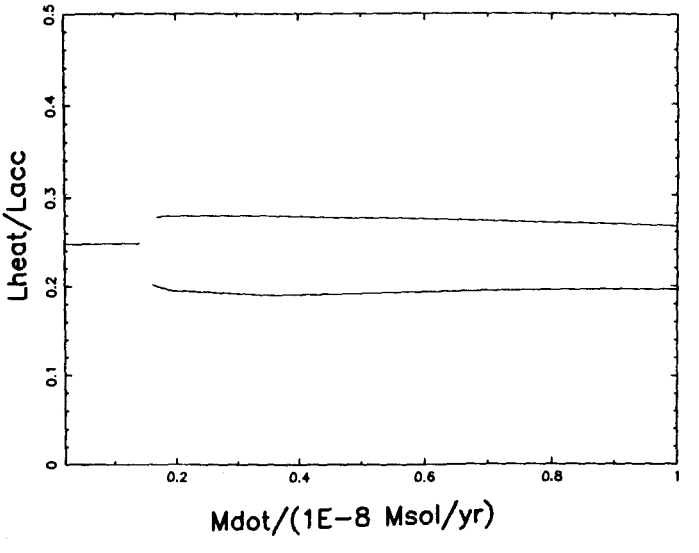

Figure 2: The heating of the white dwarf ($L_{\rm heat}$) in units of $L_{\rm acc} \equiv GM_*\dot{M}/R_*$ as a function of $\dot{M}$. The single curve on the left is in the case of an optically thin BL. The two curves on the right delineate the region for which optically thick BL solutions exist.

Finally, I present the results for the amount of radiation falling onto the white dwarf from the BL and the accretion disk. The effect of this heating on the accreting star and its implications for the nova outburst have recently been studied by Shaviv & Starrfield (1987). They point out that this heating can significantly affect the evolution to a thermonuclear runaway. The inclusion of this energy makes it more difficult to produce a nova outburst; specifically when $L_{\rm heat} \sim 0.25 L_{\rm acc}$,

the outburst is significantly less violent, and little or no mass is ejected.

Figure 2 depicts the amount of heating of the white dwarf for the same $1M_\odot$ star as before (with $R_* = 9 \times 10^8$cm and $\Omega_* = 0.3\Omega_{K*}$) as a function of $\dot{M}$. We calculate $L_{\rm heat}$ by adding the energy radiated into the star (calculated numerically in Case A) to the fraction of the disk and BL radiation which after being emitted from the surface falls on the WD. In the optically thin case a unique solution of $\alpha \equiv L_{\rm heat}/L_{\rm acc}$ equal to 0.248 is obtained. In the optically thick case an addtional free parameter (the temperature or pressure at the BL-white dwarf boundary) is needed. All the possible values of such a parameter which give a consistent matched solution fall between the two curves on the right side of figure 2. The temperature is lower for the upper limit curve (since then the gradient of T into the star is bigger and hence more energy is radiated inward).

I would like to thank Joe Patterson, Mike Shara and Giora Shaviv for discussions; Norman Baker for letting me use his computer code and the Astronomy Department at Columbia and the Space Telescope Science Institute (where a part of this work has been done) for their hospitality.

REFERENCES

Bender, C.M. & Orszag, S.A., 1978, *Advanced Methods for Scientists and Engineers,* McGraw-Hill.
Katz, J.I., 1987, *High Energy Astrophsyics*, Addison-Wesley.
King, A.R. & Shaviv, G., 1984, *Nature*, **308**, 519.
Lynden-Bell & Pringle, J.E., 1974, *M.N.R.A.S.*, **168**, 603.
Papaloizou, J.C.B. & Stanley, C.Q.G., 1986, *M.N.R.A.S.*, **220**, 593.
Patterson, J., & Raymond, J.C., 1985, *Ap.J.*, **292**, 535 and 550.
Pringle, J.E., 1977, *M.N.R.A.S.*, **178**, 195.
Pringle, J.E., 1981, *Ann. Rev. Astr. Ap.*, **19**, 137.
Pringle, J.E. & Savonije, G.J., 1979, *M.N.R.A.S*, **198**, 777.
Regev, O., 1983, *Astr. Ap.*, **126**, 146 (R).
Regev, O. & Hougerat, A.A., 1988, *M.N.R.A.S.*, **232**, 81 (RH).
Shakura, N.I. & Sunyaev, R.A., 1973, *Astr. Ap.*, **24**, 337.
Shaviv, G., 1987, *Ap. Sp. Sci.*, **130**, 303.
Shaviv, G. & Starrfield, S., 1987, *Ap.J.*, **321**, L51.
Tylenda, R., 1981, *Acta Astr.*, **31**, 127 and 267.
Van Dyke, M., 1964, *Perturbation Methods in Fluid Mechanics,* Academic Press.

HIGH RESOLUTION OPTICAL SPECTRA OF 120 WHITE DWARFS

David Tytler and Eric Rubenstein
Columbia University

ABSTRACT. High quality optical spectra of 120 white dwarfs have been obtained to search for double degenerate systems, some of which might become type I supernovae. No systems with high amplitude velocity variations have been found. However several exceptionally cool DA white dwarfs have been found to show weak Helium absorption lines, and four stars have split H-alpha line cores indicative of binary systems.

It is now widely believed (eg. Iben and Tutukov 1984) that short period double degenerate stars – binaries containing two white dwarfs – are the most likely progenitors of type I supernovae. Robinson and Shafter (1987) have obtained an upper limit on the space density of these systems by searching for variations in the flux measured in the wing of an absorption line. In common with Bragaglia *et al.* (1988 and these proceedings) and Foss (these proceedings), we are hoping to determine the frequency of occurrence of short period double degenerates by looking for radial velocity shifts in optical spectra.

The Palomar Observatory Hale 5m has been used with the Oke and Gunn double spectrograph to obtain simultaneous spectra of H-beta (4650-5060) and H-alpha (6250-6850). TI 800x800 CCDs were used with 35 kms^{-1} per pixel giving a resolution of 70 kms^{-1}. The wavelength ranges covered are sufficient to include the whole absorption line profile in all cases, while the resolution is just adequate to show the common sharp NLTE line cores. A signal to noise ratio of over 100 was usually obtained with integration times of about 20 minutes. Some 120 stars were observed two or three times each, giving a total of 600 spectra. By cross-correlating numerous spectra of four subdwarf flux standard stars we have found that our wavelength scale has an accuracy of 1 kms^{-1}. The velocities of the white dwarfs can be measured to an accuracy of about 1-10 kms^{-1}, depending on the strength of the line core. A preliminary analysis of about half of the spectra has not revealed any large velocity variations.

The spectra of eight stars which are of particular interest are shown below. The fluxes are only approximate, while the zero points for the spectra of 0501+527 and 1538+269 have been shifted up by 35000 and 30000 μJy respectively. One the left, from top to bottom, are the red spectra of stars which all show split H-alpha lines: 1036+433 (Feige 34, type sd O), WD0501+527 (G191-B2B, DA0), 2317-054 (Feige 110, sd O), and WD2256+249 (G245, DA4+dM). On the right are four stars with both H-alpha and He I λ6678.15 : WD1637+335 (L1491-027, DA5/DA6), WD1247+553 (GD319, sd B/DA4), WD1538+269 (Ton 245, sd B), and WD1430+427 (PG, DA3). These include the coolest DA stars known to show helium lines.

Bragaglia, A., Greggio, L., Renzini, A. and D'Odorico, S. 1988, *ESO Messenger*, **52**, 35.
Iben, I. and Tutukov, A.V. 1984, *Ap.J. Suppl.*, **54**, 335.
Robinson, E.L. and Shafter, A.W. 1987, *Ap.J.*, **322**, 296.

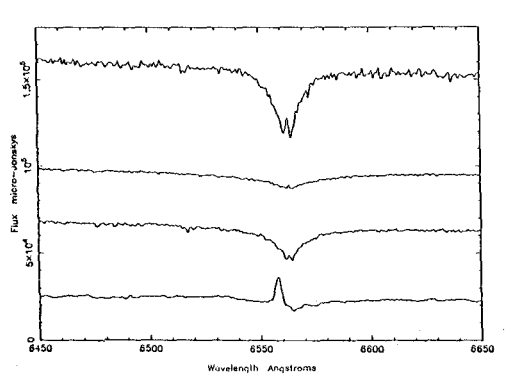

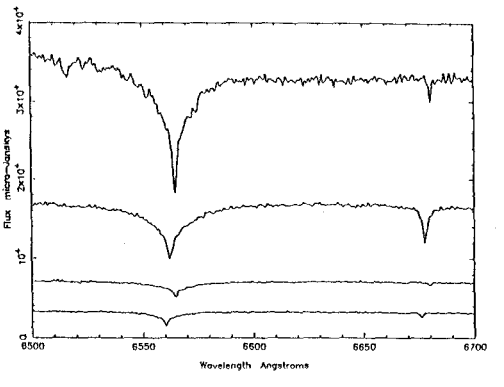

Lecture Notes in Mathematics

Vol. 1236: Stochastic Partial Differential Equations and Applications. Proceedings, 1985. Edited by G. Da Prato and L. Tubaro. V, 257 pages. 1987.

Vol. 1237: Rational Approximation and its Applications in Mathematics and Physics. Proceedings, 1985. Edited by J. Gilewicz, M. Pindor and W. Siemaszko. XII, 350 pages. 1987.

Vol. 1250: Stochastic Processes – Mathematics and Physics II. Proceedings 1985. Edited by S. Albeverio, Ph. Blanchard and L. Streit. VI, 359 pages. 1987.

Vol. 1251: Differential Geometric Methods in Mathematical Physics. Proceedings, 1985. Edited by P.L. García and A. Pérez-Rendón. VII, 300 pages. 1987.

Vol. 1255: Differential Geometry and Differential Equations. Proceedings, 1985. Edited by C. Gu, M. Berger and R.L. Bryant. XII, 243 pages. 1987.

Vol. 1256: Pseudo-Differential Operators. Proceedings, 1986. Edited by H.O. Cordes, B. Gramsch and H. Widom. X, 479 pages. 1987.

Vol. 1258: J. Weidmann, Spectral Theory of Ordinary Differential Operators. VI, 303 pages. 1987.

Vol. 1260: N.H. Pavel, Nonlinear Evolution Operators and Semigroups. VI, 285 pages. 1987.

Vol. 1263: V.L. Hansen (Ed.), Differential Geometry. Proceedings, 1985. XI, 288 pages. 1987.

Vol. 1265: W. Van Assche, Asymptotics for Orthogonal Polynomials. VI, 201 pages. 1987.

Vol. 1267: J. Lindenstrauss, V.D. Milman (Eds.), Geometrical Aspects of Functional Analysis. Seminar. VII, 212 pages. 1987.

Vol. 1269: M. Shiota, Nash Manifolds. VI, 223 pages. 1987.

Vol. 1270: C. Carasso, P.-A. Raviart, D. Serre (Eds.), Nonlinear Hyperbolic Problems. Proceedings, 1986. XV, 341 pages. 1987.

Vol. 1272: M.S. Livšic, L.L. Waksman, Commuting Nonselfadjoint Operators in Hilbert Space. III, 115 pages. 1987.

Vol. 1273: G.-M. Greuel, G. Trautmann (Eds.), Singularities, Representation of Algebras, and Vector Bundles. Proceedings, 1985. XIV, 383 pages. 1987.

Vol. 1275: C.A. Berenstein (Ed.), Complex Analysis I. Proceedings, 1985–86. XV, 331 pages. 1987.

Vol. 1276: C.A. Berenstein (Ed.), Complex Analysis II. Proceedings, 1985–86. IX, 320 pages. 1987.

Vol. 1277: C.A. Berenstein (Ed.), Complex Analysis III. Proceedings, 1985–86. X, 350 pages. 1987.

Vol. 1283: S. Mardešić, J. Segal (Eds.), Geometric Topology and Shape Theory. Proceedings, 1986. V, 261 pages. 1987.

Vol. 1285: I.W. Knowles, Y. Saitō (Eds.), Differential Equations and Mathematical Physics. Proceedings, 1986. XVI, 499 pages. 1987.

Vol. 1287: E.B. Saff (Ed.), Approximation Theory, Tampa. Proceedings, 1985–1986. V, 228 pages. 1987.

Vol. 1288: Yu. L. Rodin, Generalized Analytic Functions on Riemann Surfaces. V, 128 pages, 1987.

Vol. 1294: M. Queffélec, Substitution Dynamical Systems – Spectral Analysis. XIII, 240 pages. 1987.

Vol. 1299: S. Watanabe, Yu.V. Prokhorov (Eds.), Probability Theory and Mathematical Statistics. Proceedings, 1986. VIII, 589 pages. 1988.

Vol. 1300: G.B. Seligman, Constructions of Lie Algebras and their Modules. VI, 190 pages. 1988.

Vol. 1302: M. Cwikel, J. Peetre, Y. Sagher, H. Wallin (Eds.), Function Spaces and Applications. Proceedings, 1986. VI, 445 pages. 1988.

Vol. 1303: L. Accardi, W. von Waldenfels (Eds.), Quantum Probability and Applications III. Proceedings, 1987. VI, 373 pages. 1988.

Lecture Notes in Physics

Vol. 303: P. Breitenlohner, D. Maison, K. Sibold (Eds.), Renormalization of Quantum Field Theories with Non-linear Field Transformations. Proceedings, 1987. VI, 239 pages. 1988.

Vol. 304: R. Prud'homme, Fluides hétérogènes et réactifs: écoulements et transferts. VIII, 239 pages. 1988.

Vol. 305: K. Nomoto (Ed.), Atmospheric Diagnostics of Stellar Evolution: Chemical Peculiarity, Mass Loss, and Explosion. Proceedings, 1987. XIV, 468 pages. 1988.

Vol. 306: L. Blitz, F.J. Lockman (Eds.), The Outer Galaxy. Proceedings, 1987. IX, 291 pages. 1988.

Vol. 307: H.R. Miller, P.J. Wiita (Eds.), Active Galactic Nuclei. Proceedings, 1987, XI, 438 pages. 1988.

Vol. 308: H. Bacry, Localizability and Space in Quantum Physics. VII, 81 pages. 1988.

Vol. 309: P.E. Wagner, G. Vali (Eds.), Atmospheric Aerosols and Nucleation. Proceedings, 1988. XVIII, 729 pages. 1988.

Vol. 310: W.C. Seitter, H.W. Duerbeck, M. Tacke (Eds.), Large-Scale Structures in the Universe – Observational and Analytical Methods. Proceedings, 1987. II, 335 pages. 1988.

Vol. 311: P.J.M. Bongaarts, R. Martini (Eds.), Complex Differential Geometry and Supermanifolds in Strings and Fields. Proceedings, 1987. V, 252 pages. 1988.

Vol. 312: J.S. Feldman, Th.R. Hurd, L. Rosen, "QED: A Proof of Renormalizability." VII, 176 pages. 1988.

Vol. 313: H.-D. Doebner, T.D. Palev, J.D. Hennig (Eds.), Group Theoretical Methods in Physics. Proceedings, 1987. XI, 599 pages. 1988.

Vol. 314: L. Peliti, A. Vulpiani (Eds.), Measures of Complexity. Proceedings, 1987. VII, 150 pages. 1988.

Vol. 315: R.L. Dickman, R.L. Snell, J.S. Young (Eds.), Molecular Clouds in the Milky Way and External Galaxies. Proceedings, 1987. XVI, 475 pages. 1988.

Vol. 316: W. Kundt (Ed.), Supernova Shells and Their Birth Events. Proceedings, 1988. VIII, 253 pages. 1988.

Vol. 317: C. Signorini, S. Skorka, P. Spolaore, A. Vitturi (Eds.), Heavy Ion Interactions Around the Coulomb Barrier. Proceedings, 1988. X, 329 pages. 1988.

Vol. 319: L. Garrido (Ed.), Far from Equilibrium Phase Transitions. Proceedings, 1988. VIII, 340 pages. 1988.

Vol. 320: D. Coles (Ed.), Perspectives in Fluid Mechanics. Proceedings, 1985. VII, 207 pages. 1988.

Vol. 321: J. Pitowsky, Quantum Probability – Quantum Logic. IX, 209 pages. 1989.

Vol. 322: M. Schlichenmaier, An Introduction to Riemann Surfaces, Algebraic Curves and Moduli Spaces. XIII, 148 pages. 1989.

Vol. 323: D.L. Dwoyer, M.Y. Hussaini, R.G. Voigt (Eds.), 11th International Conference on Numerical Methods in Fluid Dynamics. XIII, 622 pages. 1989.

Vol. 324: P. Exner, P. Šeba (Eds.), Applications of Self-Adjoint Extensions in Quantum Physics. Proceedings, 1987. VIII, 273 pages. 1989.

Vol. 327: K. Meisenheimer, H.-J. Röser (Eds.), Hot Spots in Extragalactic Radio Source. Proceedings, 1988. XII, 301 pages. 1989.

Vol. 328: G. Wegner (Ed.), White Dwarfs. Proceedings, 1988. XIV, 524 pages. 1989.